Project Deliverable Report

DELIVERABLE 3.2

TESTING RESULTS

WORK PACKAGE NUMBER: WP 3

WORK PACKAGE TITLE: TESTING

TYPE: REPORT

AUTHORS: BOKU

REGACE Action Information	
Action full title	Responsive Greenhouse Agrivoltaics System with CO_2-enrichment for Higher Yields
Action acronym	REGACE
Grant agreement number	101096056
Project Officer	Maria Laura Trifiletti
Project coordinator	Dr. Ibrahim Yehia
Project start date and duration	1 February 2023, 36 months
Project website	https://regaceproject.com/

Funded by the European Union

Funded by the European Union under Grant Agreement No 101096056. Views and opinions expressed are however those of the author(s) only and do not necessarily reflect those of the European Union or CINEA. Neither the European Union nor the granting authority can be held responsible for them.

Document Information

Deliverable Information	
Work package number	WP3
Work package title	Testing
Deliverable number	D3.2
Deliverable title	Testing Results
Description	Report summarising the results from the experiments and data arising from each location
Lead beneficiary	BOKU
Lead Author(s)	Federico Andreozzi, Dr. Catherine Baxevanou, Dr. Gianluigi Bovesecchi, Dr. Prof. Cristina Cornaro, Dr. Norbert Keutgen, Prof. Chryssoula Papaioannou, Dr. Marcello Petitta, Prof. Andrea Volterrani
Contributor(s)	Dr. Liron Amdur, Maria Cristina Antonucci, Prof. Anna Keutgen, Max Liebrich, Prof. Thorsten Rocksch, Marco Serra
Revision number	1.1
Revision Date	2025.12.05
Status (Final (F), Draft (D), Revised Draft (RV))	F - Final
Dissemination level (Public (PU), Restricted to other program participants (PP), Restricted to group specified by consortium (RE), Confidential for consortium members only (CO))	PU - Public

Document History			
Revision	**Date**	**Modification**	**Author**
0.1	2025.09.11	Template	N. Keutgen
0.2	2025.10.30	Completed draft	All authors
0.3	2025.11.27	Reviewed version	All reviewers
1.0	2025.11.29	Final version for submission	N. Keutgen
1.1	2025.12.05	Revised version for resubmission	N. Keutgen

Funded by the European Union

Funded by the European Union under Grant Agreement No 101096056. Views and opinions expressed are however those of the author(s) only and do not necessarily reflect those of the European Union or CINEA. Neither the European Union nor the granting authority can be held responsible for them.

Approvals				
	Name	**Organisation**	**Date**	**Signature (initials)**
Coordinator	Dr. Ibrahim Yehia	Alzahrawy Society	2025.12.05	IY
WP Leaders	Dr. Norbert Keutgen	BOKU	2025.12.05	NK

Funded by the European Union

Funded by the European Union under Grant Agreement No 101096056. Views and opinions expressed are however those of the author(s) only and do not necessarily reflect those of the European Union or CINEA. Neither the European Union nor the granting authority can be held responsible for them.

Table of Contents

Funded by the European Union

Funded by the European Union under Grant Agreement No 101096056. Views and opinions expressed are however those of the author(s) only and do not necessarily reflect those of the European Union or CINEA. Neither the European Union nor the granting authority can be held responsible for them.

Funded by the European Union under Grant Agreement No 101096056. Views and opinions expressed are however those of the author(s) only and do not necessarily reflect those of the European Union or CINEA. Neither the European Union nor the granting authority can be held responsible for them.

List of Figures

Funded by the European Union under Grant Agreement No 101096056. Views and opinions expressed are however those of the author(s) only and do not necessarily reflect those of the European Union or CINEA. Neither the European Union nor the granting authority can be held responsible for them.

Funded by the European Union

Funded by the European Union under Grant Agreement No 101096056. Views and opinions expressed are however those of the author(s) only and do not necessarily reflect those of the European Union or CINEA. Neither the European Union nor the granting authority can be held responsible for them.

Funded by the European Union under Grant Agreement No 101096056. Views and opinions expressed are however those of the author(s) only and do not necessarily reflect those of the European Union or CINEA. Neither the European Union nor the granting authority can be held responsible for them.

Funded by the European Union under Grant Agreement No 101096056. Views and opinions expressed are however those of the author(s) only and do not necessarily reflect those of the European Union or CINEA. Neither the European Union nor the granting authority can be held responsible for them.

Funded by the European Union

Funded by the European Union

Funded by the European Union under Grant Agreement No 101096056. Views and opinions expressed are however those of the author(s) only and do not necessarily reflect those of the European Union or CINEA. Neither the European Union nor the granting authority can be held responsible for them.

Funded by the European Union under Grant Agreement No 101096056. Views and opinions expressed are however those of the author(s) only and do not necessarily reflect those of the European Union or CINEA. Neither the European Union nor the granting authority can be held responsible for them.

Funded by the European Union

Funded by the European Union

Funded by the European Union under Grant Agreement No 101096056. Views and opinions expressed are however those of the author(s) only and do not necessarily reflect those of the European Union or CINEA. Neither the European Union nor the granting authority can be held responsible for them.

Funded by the European Union

Funded by the European Union under Grant Agreement No 101096056. Views and opinions expressed are however those of the author(s) only and do not necessarily reflect those of the European Union or CINEA. Neither the European Union nor the granting authority can be held responsible for them.

Funded by the European Union

Funded by the European Union under Grant Agreement No 101096056. Views and opinions expressed are however those of the author(s) only and do not necessarily reflect those of the European Union or CINEA. Neither the European Union nor the granting authority can be held responsible for them.

Funded by the European Union

Funded by the European Union under Grant Agreement No 101096056. Views and opinions expressed are however those of the author(s) only and do not necessarily reflect those of the European Union or CINEA. Neither the European Union nor the granting authority can be held responsible for them.

Funded by the European Union

Funded by the European Union under Grant Agreement No 101096056. Views and opinions expressed are however those of the author(s) only and do not necessarily reflect those of the European Union or CINEA. Neither the European Union nor the granting authority can be held responsible for them.

List of Tables

Funded by the European Union

Funded by the European Union under Grant Agreement No 101096056. Views and opinions expressed are however those of the author(s) only and do not necessarily reflect those of the European Union or CINEA. Neither the European Union nor the granting authority can be held responsible for them.

Funded by the European Union under Grant Agreement No 101096056. Views and opinions expressed are however those of the author(s) only and do not necessarily reflect those of the European Union or CINEA. Neither the European Union nor the granting authority can be held responsible for them.

Funded by the European Union under Grant Agreement No 101096056. Views and opinions expressed are however those of the author(s) only and do not necessarily reflect those of the European Union or CINEA. Neither the European Union nor the granting authority can be held responsible for them.

Funded by the European Union

Funded by the European Union

Funded by the European Union under Grant Agreement No 101096056. Views and opinions expressed are however those of the author(s) only and do not necessarily reflect those of the European Union or CINEA. Neither the European Union nor the granting authority can be held responsible for them.

Funded by the European Union

Funded by the European Union under Grant Agreement No 101096056. Views and opinions expressed are however those of the author(s) only and do not necessarily reflect those of the European Union or CINEA. Neither the European Union nor the granting authority can be held responsible for them.

Funded by the European Union under Grant Agreement No 101096056. Views and opinions expressed are however those of the author(s) only and do not necessarily reflect those of the European Union or CINEA. Neither the European Union nor the granting authority can be held responsible for them.

Funded by the European Union under Grant Agreement No 101096056. Views and opinions expressed are however those of the author(s) only and do not necessarily reflect those of the European Union or CINEA. Neither the European Union nor the granting authority can be held responsible for them.

Funded by the European Union under Grant Agreement No 101096056. Views and opinions expressed are however those of the author(s) only and do not necessarily reflect those of the European Union or CINEA. Neither the European Union nor the granting authority can be held responsible for them.

Funded by the European Union under Grant Agreement No 101096056. Views and opinions expressed are however those of the author(s) only and do not necessarily reflect those of the European Union or CINEA. Neither the European Union nor the granting authority can be held responsible for them.

Funded by the European Union under Grant Agreement No 101096056. Views and opinions expressed are however those of the author(s) only and do not necessarily reflect those of the European Union or CINEA. Neither the European Union nor the granting authority can be held responsible for them.

Funded by the European Union under Grant Agreement No 101096056. Views and opinions expressed are however those of the author(s) only and do not necessarily reflect those of the European Union or CINEA. Neither the European Union nor the granting authority can be held responsible for them.

Executive Summary

The report addresses seven key issues: Bifacial PV characterisation, PV electrical monitoring in greenhouses, greenhouse microclimate measurements, crop monitoring and produce quality, greenhouse water use efficiency, CO_2 enrichment as a compensation possibility, and additional lighting as a compensation possibility, both for low light levels. The first three points can be considered routine tasks to test and quantify the efficiency and longevity of the PV systems under practical conditions, to optimise the efficiency of the PV tracking system both in terms of the plants' light requirements by minimising shading and maximising energy yield, and to determine the climatic conditions in the greenhouses and document changes caused by the PV system. Locations in Israel (Kfar Qara), Greece (Volos), Italy (Circeo), Austria (Vienna), and Germany (Berlin, Watzkendorf) were selected to test the system under different climatic conditions. At the locations in Kfar Qara, Volos, Circeo, and Watzkendorf, the experiments were carried out under practical conditions with locally typical crops, while in Berlin and Vienna, specific aspects of elevated CO_2 concentration and produce quality were investigated in more detail. The studies generally yielded a positive picture for the PV tracking system, although a gradient from south to north was observed. For example, the cost-benefit ratio in Watzkendorf was only marginally economically acceptable, while profitability was achieved in Israel, Greece, and Italy. The further north the test site was located, the more the yield was reduced by the PV-induced shading. At Volos, the use of light-reflecting foil was identified as an efficient measure to optimise light output. The results regarding the use of increased atmospheric CO_2 concentrations in the greenhouses were inconsistent. Different methods were also tested. CO_2 enrichment was achieved by applying gas from CO_2 cylinders, CO_2Bags, mushroom cultivation, and by using transfer mulch. The classic application of CO_2 using cylinders was very effective, particularly as it allowed for regulation of the atmospheric CO_2 concentration. The CO_2Bags, however, were less effective, resulting in only a slight increase in CO_2 concentration in the greenhouse, at best. Satisfactory results were also achieved with the supply of CO_2 from mushroom cultivation, as well as with the use of transfer mulch. In practice, however, a problem arose with temperature regulation in the greenhouse, as this is usually done via ventilation, so that the injected CO_2 quickly escaped and had to be replaced. Thus, atmospheric CO_2 concentrations were often only elevated overnight and at the beginning of the day. Although this did lead to measurable positive effects on plant growth and yield quality (e.g., slightly increased sugar content) in some experimental approaches, an acceptable compensation for the lower availability of light was not observed under practical conditions. However, in appropriately airtight and climate-controlled greenhouses, such compensation would at least partially be expected. Where CO_2 enrichment is already used during the winter months and consequently the requirements for airtightness and greenhouse climate control are met, it is an adequate measure to further optimise yield. With regard to the experiments conducted under practical conditions, water use efficiency did not show a consistent pattern. On the one hand, increased atmospheric CO_2 concentrations did lead to improved water utilization, but on the other hand, there were also numerous examples where the water use efficiency of the control variant was the best. It should be considered that water use efficiency depends on both yield and water consumption. Undoubtedly, shading in combination with cooler temperatures reduces water consumption, as do increased atmospheric CO_2 concentrations. Ultimately, however, the quantity of the

Funded by the European Union under Grant Agreement No 101096056. Views and opinions expressed are however those of the author(s) only and do not necessarily reflect those of the European Union or CINEA. Neither the European Union nor the granting authority can be held responsible for them.

Funded by the European Union

yield determines the water use efficiency. Here, the Daily Light Integral has proven to be a crucial criterion, as a minimum level of light availability is necessary to ensure an adequate yield. When light availability is critically low for parts of the year, as is the case of the BOKU greenhouse, shading caused by the PV tracking system presents a fundamental challenge, which, however, can and must be addressed with supplemental lighting. In summary, the results of the project suggest that PV tracking systems represent a positive, innovative development and can generate additional energy without significantly reducing crop yield.

1 Introduction

The deliverables 3.2 report on the data collected to achieve the following main goals: to characterise the bifacial photovoltaic (PV) system in order to quantify the electrical performance of the PV tracker system, and to measure the greenhouse microclimate under the PV system in order to evaluate crop performance as influenced by varying light intensities as a consequence of the installed PV system and the effects of CO_2 enrichment as a measure to compensate for a lower light intensity available to crops.

The first chapter focusses on the acceptance of the bifacial PV panels provided by TriSolar and their characterisation by the ESTER lab in Rome (Italy). Their performance and degradation were studied by mounting the modules on a sun tracker, enabling recording temperature coefficients of current, voltage, and power under real operating conditions. Pyranometers were mounted on the front and rear side of the panels to investigate the response of the bifacial module to solar radiation.

In the following step, the electrical yields of the PV system combined with the responsive tracking system in the different locations was recorded in order to maximise energy yield and crop production simultaneously. It was tested, whether lower light levels were able to be compensated for by elevated atmospheric CO_2 levels in the greenhouses, which would allow a more stable electrical yield throughout the year especially in mid-latitudes. While the original plan was to record the electrical yield over a period of approximately two years, the completion of the PV systems was delayed due to unforeseeable military activities in the Middle East and Eastern Europe, meaning that only between one and one and a half years were available for the studies. This period was further limited by local shutdowns for necessary optimisations. Nevertheless, the data collected was sufficiently detailed to enable fundamental conclusions to be drawn.

Microclimate measurements in the greenhouses were also essential for the studies on electrical yield. For these, the essential control systems already available at the local sites were used, which were designed for different measurement intervals, for example. Measurements included air temperature, humidity, light intensity, and atmospheric CO_2 concentration, further information on radiation levels and spectra as well as distribution, air velocity within the canopy, soil temperature and heat flux and cover temperature were recorded at selected locations.

Funded by the European Union under Grant Agreement No 101096056. Views and opinions expressed are however those of the author(s) only and do not necessarily reflect those of the European Union or CINEA. Neither the European Union nor the granting authority can be held responsible for them.

Microclimate data are also essential for the adequate interpretation of the results of crop cultivation. For each location, the crops for the experiment were selected based on the typical crops grown in the respective locations, as well as typical cultivation methods, which represented both soil-based and hydroponic growing methods. Consequently, it was not intended to compare single cultivars between locations, but to test the bifacial PV system under the real conditions, including typical crops, greenhouse types, climate, and insolation levels. The decision was therefore made in favour of assessing the marketing potential of the PV system under current local real conditions, rather than conducting a purely academic comparison for a few crops or varieties. While most locations focussed on yield parameters, taste, and sales proceeds, the intrinsic and consumer quality of the fresh produce were determined at BOKU addressing the very high demands on quality of consumers for nutritive and health promoting compounds as well as contaminants.

The yield and quality studies also paid special attention to the applied atmospheric CO_2 concentrations, whereby different CO_2 enrichment systems were tested: application of gas from CO_2-cylinders, by CO_2Bags, or CO_2 generated by a nearby mushroom cultivation and supplied to the greenhouse chamber. The experiments with additional CO_2 aimed at comparing the tracking technology with CO_2 enrichment under local standard greenhouse conditions without the added technologies in each location.

2 Characterisation of the Bifacial PV system

2.1 Testing Procedure

In terms of materials and methods, the general outlook of the procedure is unchanged compared to what was outlined in the previous Deliverable (D3.1) and can therefore be consulted in that document.

2.2 PV panels characterization, performance and degradation

Some elements of the procedure's phases have seen slightly modified. The changes are discussed in this section.

Phase 1 – PV panel acceptance (Acc)

This phase consists in the verification of the electrical parameters of the PV modules via I-V curve acquisition and translation to standard conditions (BSTC or STC). Originally, Blaesser's method was chosen to translate the curves. However, the decision was made to switch to Anderson's method (Anderson, 1996), which is of more recent conception, covers a wider irradiance range (100-1000 W/m2 as opposed to ≥600 W/m2) and provides an indication of the module's temperature to which it is applicable (15-75°C) (Dia et al., 2020). Also, from a practical standpoint, Anderson's method is easier to implement, because it involves a point-by-point translation of the I-V curve, without the necessity of a curve fitting.

Funded by the European Union under Grant Agreement No 101096056. Views and opinions expressed are however those of the author(s) only and do not necessarily reflect those of the European Union or CINEA. Neither the European Union nor the granting authority can be held responsible for them.

Phase 2 – PV panel characterization

This is the phase that underwent the largest revision. It originally included the definition of temperature coefficients (TC), spectral effect and mismatch factor (MMF), and incidence angle modifier (IAM). While the temperature coefficients were obtained, the analysis of the other two parameters was substituted with the study of the rear irradiance driven power gain yield (BiFi) to fully comply with the IEC technical standard about bifacial PV characterization (IEC, 2019).

The measurement of BiFi is carried out on the tracker stand, registering I-V curves, GTI and RTI with a frequency of two minutes. After exposure, data is filtered to only points with GTI very close to 1000 W/m2 (995 ≤ GTI ≤ 1005 W/m2). Exposure time depends on how long it takes to gather an adequate amount of data points satisfying this condition, and it is generally estimated in around 3-4 sunny days. The power values from the filtered data are then corrected in temperature using the power temperature coefficient and plotted against the RTI. A linear fit of the P vs RTI data is performed fixing the line's intercept at the value obtained from the front functionality test upon acceptance (RTI = 0). The slope of the resulting linear fit is assumed as the value of BiFi.

Phase 3 – PV panel performance and degradation (P&D)

In this phase, long term testing of the bifacial PV panels is carried out to evaluate, as the name suggests, their performance and degradation under real operating conditions for one year. Although this phase is unchanged compared to D3.1, it is worth specifying that the reference plane-of-array irradiance used for the calculation of the reference yield of the bifacial modules is GBSTC = 1 + ϕ * 0.135 kW/m2. This value was chosen because it is mentioned as a reference value by the previously cited technical specification (IEC, 2019). The PV system performance IEC technical specification (IEC, 2021) does not provide a specific value for the reference plane-of-array irradiance to be used for bifacial reference yield, but it states that it should be the irradiance at which the nominal power of the panel is determined. Since upon acceptance the bifacial nominal power was determined by using GBSTC, the decision was made to use the same value to calculate the reference yield.

Discussion: All three phases of the procedure have been put into action, with the first two having been successfully completed and the third one currently in progress. In this section, the results for each phase are reported and discussed. For phase 3, partial results available up to now will be shown and analysed.

Before analysing the results, it is worth explaining the composition of the modules' serial number (S/N), and understanding the nomenclature used throughout the analysis:

TS YYYYMMDD Z NNNNN

TS: short for "TriSolar", the panels' manufacturer.

YYYYMMDD: production date.

Funded by the European Union under Grant Agreement No 101096056. Views and opinions expressed are however those of the author(s) only and do not necessarily reflect those of the European Union or CINEA. Neither the European Union nor the granting authority can be held responsible for them.

Z: panel type code-letter (identifies nominal power and size).

NNNNN: unit progressive number.

For the sake of conciseness, since all the panels are from the same manufacturer, have the same production date (20240120 for 20th January 2024) and the unit progressive number never goes beyond 3 figures (thus, the first two are 00 for all modules), the decision was made to shorten the serial numbers to:

ZNNN

This will be the format in which the panels will be referred to from this point onward. The following PV panels underwent the procedure (Table 1):

Table 1. Overview of the procedure phases each panel went through.

Power rating	S/N	Acc	TC	BiFi	P&D
55 W	E002	X	X	XX	
	E010	X	X	X	
75 W	B075	X		X	
	B106	X	X		X
	B109	X	X		X
	B130	X		X	
	B274			X	
105 W	A007	X	X		X
	A027	X	X		X
105 W	D013	X		X	
	D047	X		X	
125 W	C121	X		X	
	C145	X		XX	

Phase 1 – PV panel acceptance

Phase 1 was carried out between July and October 2024 and its execution is depicted in Figure 1.

Funded by the European Union under Grant Agreement No 101096056. Views and opinions expressed are however those of the author(s) only and do not necessarily reflect those of the European Union or CINEA. Neither the European Union nor the granting authority can be held responsible for them.

Figure 1. Execution of phase 1 – PV panel acceptance: a) I-V curves for the full functionality test are acquired; b) the panel's rear side is covered for the front functionality test; c) the module is flipped for the rear functionality test.

The results for one of the 75W-rated sample panels (B109) are shown in Table 2, while Figure 2 shows the I-V and P-V curves obtained from the full (bifacial), front and rear functionality tests, respectively.

Table 2. Results of PV panel acceptance for panel B109.

S/N	Test date		Test time	
B109	12-07-2024		12:11 – 12:21	
	Label	**Bifacial**	**Front**	**Rear**
P_{MAX} [W]	75.00	72.65	67.07	53.29
V_{OC} [V]	23.00	22.04	22.04	21.77
V_{MAX} [V]	17.51	17.36	17.60	17.70
I_{SC} [A]	4.710	4.491	4.090	3.189
I_{MAX} [A]	4.290	4.185	3.811	3.011
FF	0.6923	0.7338	0.7440	0.7677
$\phi(I_{SC})$	**0.7797**			
$\phi(P_{MAX})$	0.7945			

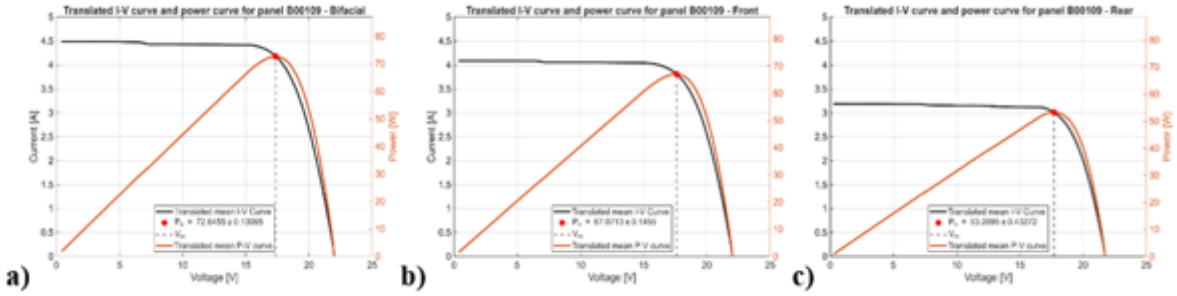

Figure 2. I-V and P-V curves after translation for panel B109: a) bifacial (full), b) front, c) rear.

Furthermore, a thermographic inspection was carried out in this phase, the result of which is shown in Figure 3 for panel B109.

Funded by the European Union

Funded by the European Union under Grant Agreement No 101096056. Views and opinions expressed are however those of the author(s) only and do not necessarily reflect those of the European Union or CINEA. Neither the European Union nor the granting authority can be held responsible for them.

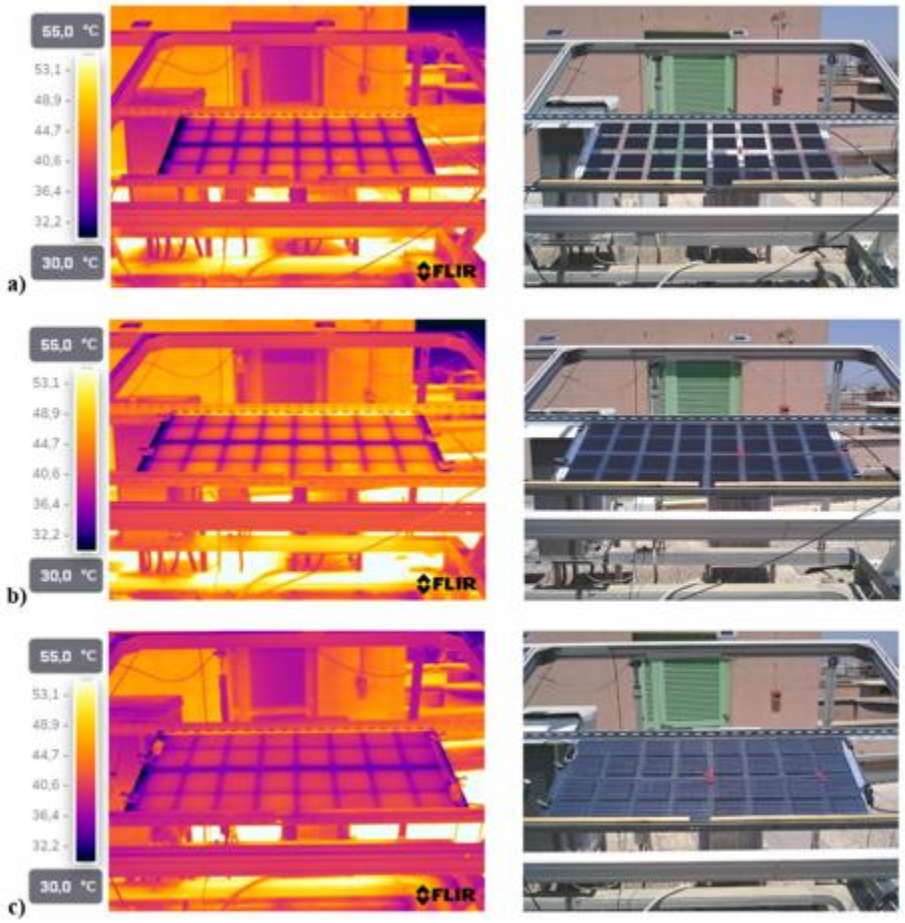

Figure 3. Thermographic images of panel B109 during acceptance: a) full (bifacial) functionality, b) front functionality, c) rear functionality.

The acceptance was useful not only to verify the manufacturer's specifications for each module and whether they were fully functional, but also to determine quantities that were not provided in the panels' datasheets. This is the case, for example, for the bifaciality factor (ϕ), which was not originally stated. It is interesting to note that for all modules this parameter came out as 78-79% (or 0.78-0.79), which is in accordance with the 80 ±5% generally assumed for bifacial PV modules.

Phase 2 – PV panel characterization

Temperature coefficients

Temperature coefficient measurements were carried out between October and December 2024. The experimental setup is shown in Figure 4, with the module positioned on a sun tracker with one side covered by a black sheet.

Funded by the European Union under Grant Agreement No 101096056. Views and opinions expressed are however those of the author(s) only and do not necessarily reflect those of the European Union or CINEA. Neither the European Union nor the granting authority can be held responsible for them.

Funded by the European Union

Figure 4. Experimental setup for the measurement of temperature coefficients: a) module positioned on the tracker stand, b) rear side covered by the black sheet.

This analysis was carried out only for 55, 75 and one type of 105W-rated panel (code-letter E, B and A, respectively), whose size made them easier to handle in this setup. It is important to note that cell technology is the same across all the panels, thus making the percentage temperature coefficients theoretically equal. In addition, the manufacturer lists the same values for all the panels, confirming this assumption. This allowed us to obtain a reliable estimate of the coefficients without the risk of damaging the modules that do not adapt as well to this setup.

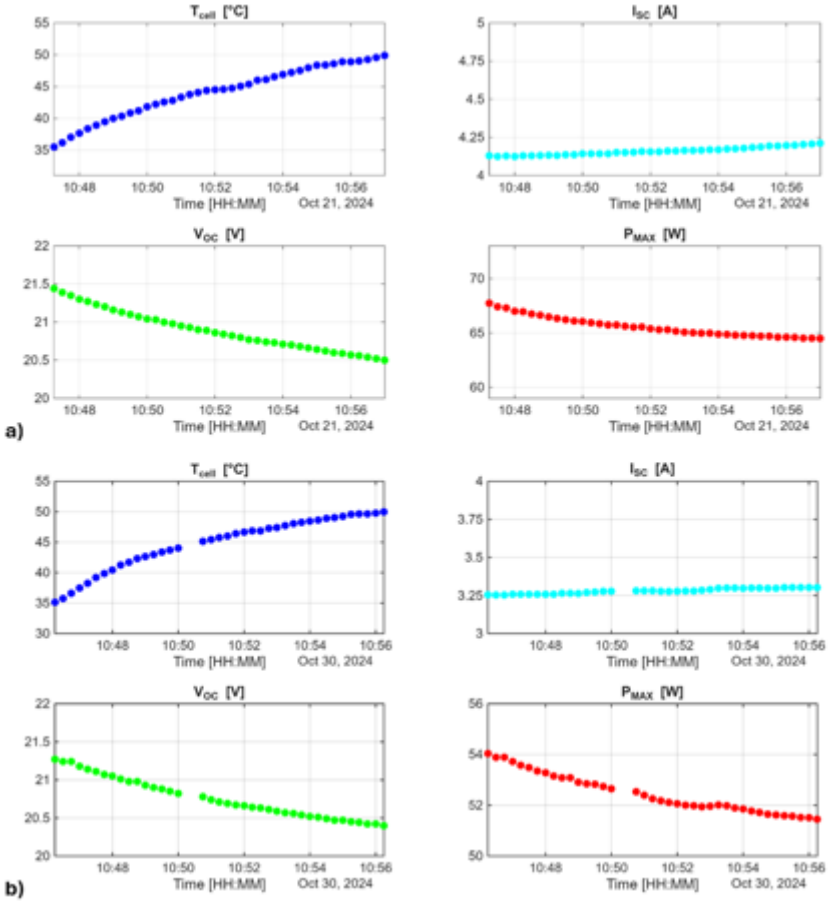

Figure 5. Evolution of TCELL, ISC, VOC and PMAX with time for panel B109: a) front, b) rear.

Funded by the European Union under Grant Agreement No 101096056. Views and opinions expressed are however those of the author(s) only and do not necessarily reflect those of the European Union or CINEA. Neither the European Union nor the granting authority can be held responsible for them.

Funded by the European Union

Figure 5 shows the evolution of TCELL, ISC, VOC and PMAX with time for panel B109 (front and rear), while Figure 6 depicts the variation of ISC, VOC and PMAX as TCELL increases.

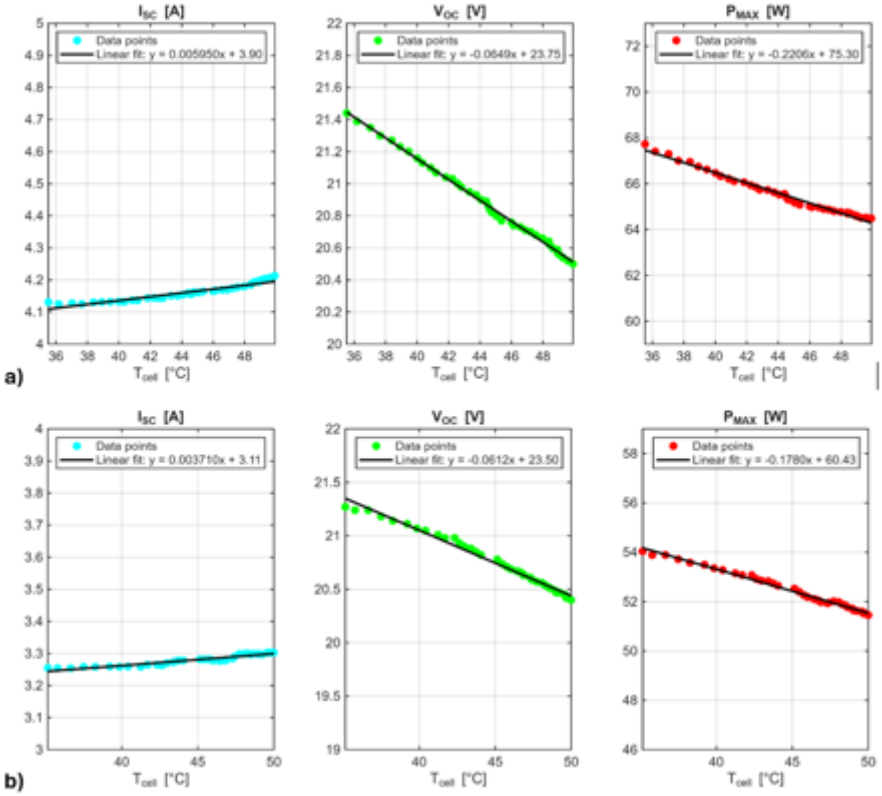

Figure 6. Evolution of ISC, VOC and PMAX as TCELL increases for panel B109: a) front, b) rear.

The percentage temperature coefficients were calculated by normalizing the slope of the linear fit in Figure 6 by the corresponding parameter obtained upon acceptance (front and rear ISC, VOC and PMAX). The resulting coefficients for panel B109 are shown in Table 3.

Table 3. Percentage temperature coefficients for panel B109.

	I_{SC} (%/°C)	V_{OC} (%/°C)	P_{MAX} (%/°C)
Front	0.15	-0.29	-0.33
Rear	0.12	-0.28	-0.33

The overall results for the temperature coefficient analysis are reported in Table 4 and Figure 7.

Funded by the European Union

Funded by the European Union under Grant Agreement No 101096056. Views and opinions expressed are however those of the author(s) only and do not necessarily reflect those of the European Union or CINEA. Neither the European Union nor the granting authority can be held responsible for them.

Table 4. Average numerical results for the temperature coefficient analysis [%/°C] with standard deviation and comparison to the datasheet value.

	DATASHEET	AVG	STD
V_{OC}	-0.26	-0.27	0.019
I_{SC}	0.046	0.057	0.069
P_{MAX}	-0.32	-0.36	0.071

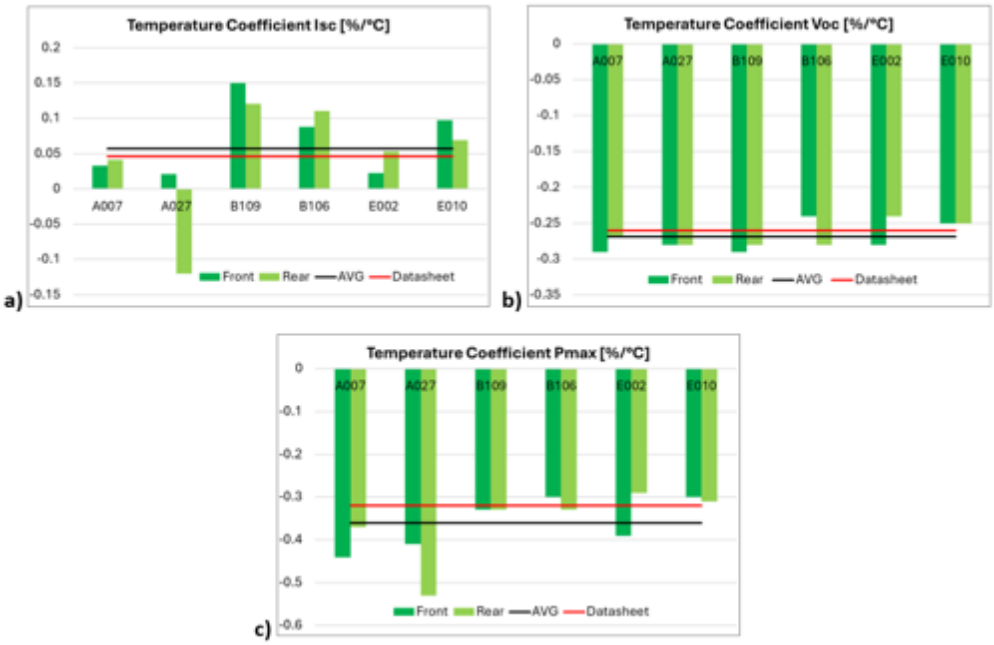

Figure 7. Bar plots of the percentage temperature coefficients for all the panels tested and comparison to average and datasheet values: a) ISC, b) VOC, c) PMAX.

From the analysis, it is evident that the determination of the ISC temperature coefficient was the most critical. Although the final average value is close to the datasheet one, the variability registered throughout the different tests is very large, as shown by the standard deviation being of the same order of magnitude as the coefficient itself. This is most likely because the ISC coefficient is much smaller than the others in absolute value, and the increased difficulty in maintaining steady test conditions in an outdoor setting means that the final result is much more prone to fluctuations. For the other coefficients, the values appear much more stable and the averages only slightly overestimate the datasheet figures.

BiFi

The analysis of BiFi was carried out mostly between March and June 2025. The experimental setup is shown in Figure 8.

Funded by the European Union under Grant Agreement No 101096056. Views and opinions expressed are however those of the author(s) only and do not necessarily reflect those of the European Union or CINEA. Neither the European Union nor the granting authority can be held responsible for them.

Figure 8. Front and rear view of the experimental setup for the measurement of BiFi.

Before going through the results, it is worth mentioning that this phase was not executed for panels B106, B109, A007 and A027 because these are the ones undergoing long term performance and degradation testing. This is important because, up to now, B109 has been used as an example for panel-specific results. For BiFi, therefore, panel B075 will serve this purpose, which has the same power rating of 75 W, as the code-letter suggests.

Figure 9 shows the P vs RTI scatter plot and the linear fit performed to determine the value of BiFi. The fit equation for this specific case was found to be P = 0.0506 * RTI + 67.01, whose slope is assumed as the value of BiFi.

To paint an overview picture of the analysis of BiFi, Figure 10 shows a scatter plot of all the values obtained for the different panels. The relationship between BiFi and power rating appears clear, and fitting the data reveals that the value increases linearly with nominal power.

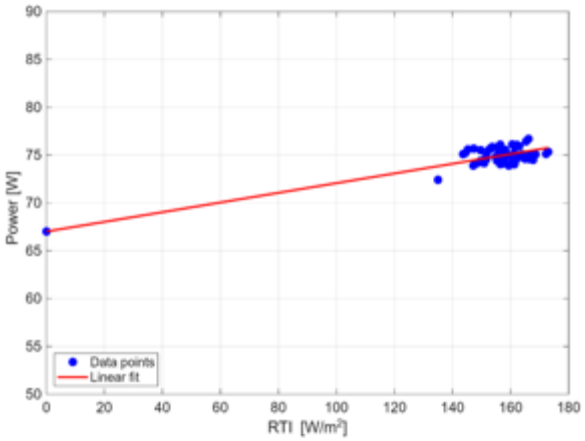

Figure 9. P vs RTI scatter plot and linear fit for panel B075.

Funded by the European Union

Funded by the European Union under Grant Agreement No 101096056. Views and opinions expressed are however those of the author(s) only and do not necessarily reflect those of the European Union or CINEA. Neither the European Union nor the granting authority can be held responsible for them.

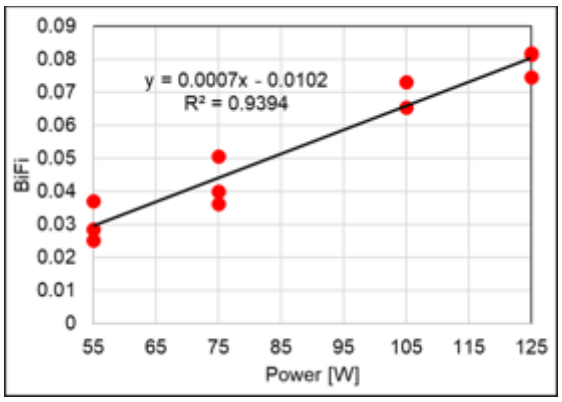

Figure 10. BiFi vs power rating scatter plot and linear fit.

The numerical results for all modules are found in Table 5.

Table 5. BiFi values for the tested panels.

Power rating	S/N	BiFi
55 W	E002	0.0371
		0.0253
	E010	0.0286
75 W	B075	0.0506
	B130	0.0399
	B274	0.0363
105 W	D013	0.0730
	D047	0.0653
125 W	C121	0.0819
	C145	0.0745
		0.0814

Phase 3 – PV panel performance and degradation

This phase started on January 28th, 2025, and is set to continue for one year, until the end of January 2026. The four panels being tested are the following:

- 75 W – Monofacial configuration: B109
- 75 W – Bifacial configuration: B106
- 105 W - Monofacial configuration: A007
- 105 W - Bifacial configuration: A027

The experimental setup is shown in Figure 11.

Funded by the European Union

Funded by the European Union under Grant Agreement No 101096056. Views and opinions expressed are however those of the author(s) only and do not necessarily reflect those of the European Union or CINEA. Neither the European Union nor the granting authority can be held responsible for them.

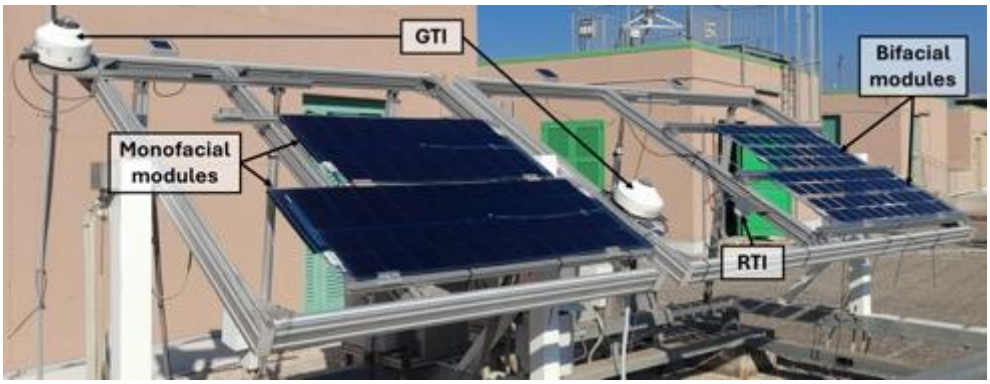

Figure 11. Experimental setup for performance and degradation testing.

The results have so far shown a consistently higher yield for the bifacial panels compared to the monofacial counterparts (Figure 12a), which was to be expected. Overall, the performance ratio (PR) was consistently above 0.8 for all modules, even surpassing 0.9 in multiple instances (Figure 12b). It is also evident that the 75W-rated modules have been performing slightly better than the 105W ones.

In terms of degradation, the analysis suggests a very minor insurgence of this phenomenon, with power at STC and BSTC remaining fairly stable up to now. Figure 13 contains all the translated I-V curves recorded for each of the panels during the degradation tests, while Figure 14 depicts the evolution of the power value at STC and BSTC with time.

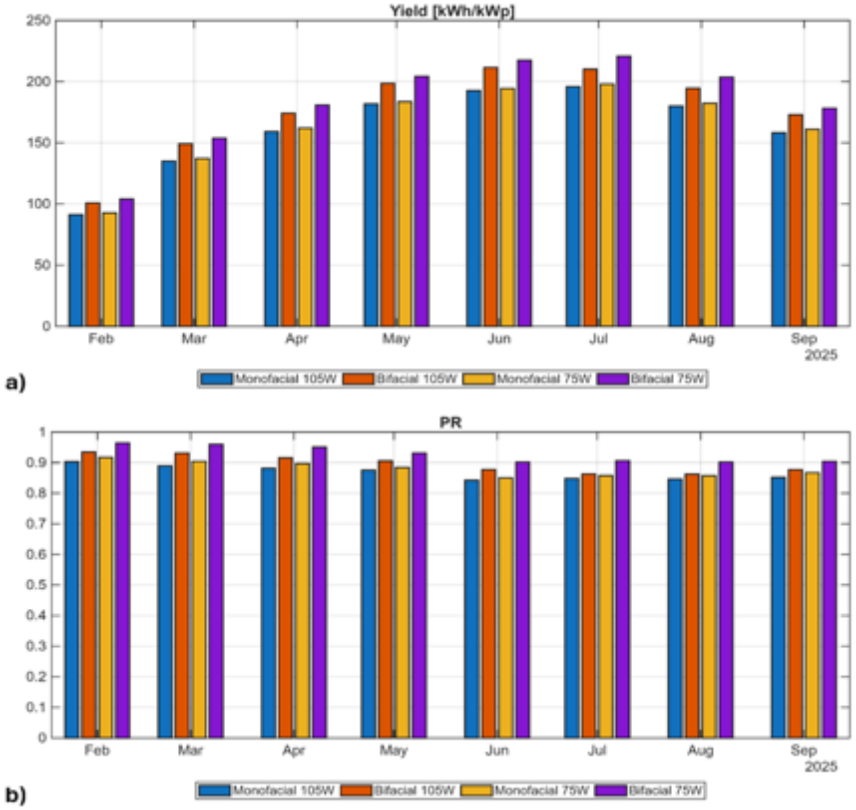

Figure 12. a) Yield and b) PR registered monthly during performance testing.

Funded by the European Union

Funded by the European Union under Grant Agreement No 101096056. Views and opinions expressed are however those of the author(s) only and do not necessarily reflect those of the European Union or CINEA. Neither the European Union nor the granting authority can be held responsible for them.

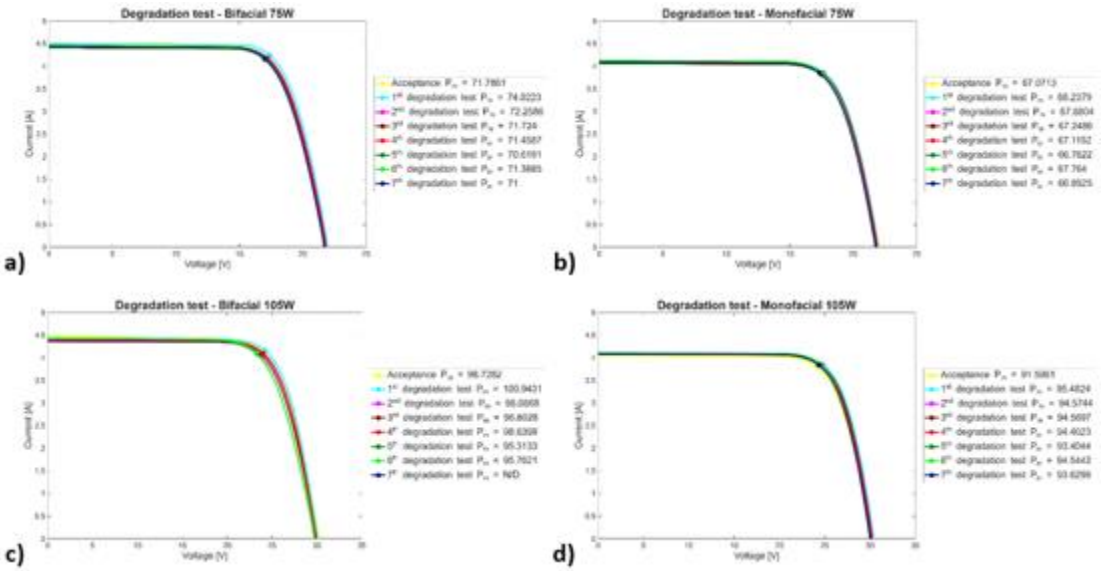

Figure 13. Degradation test I-V curves for panels a) B109, b) B106, c) A027 and d) A007.

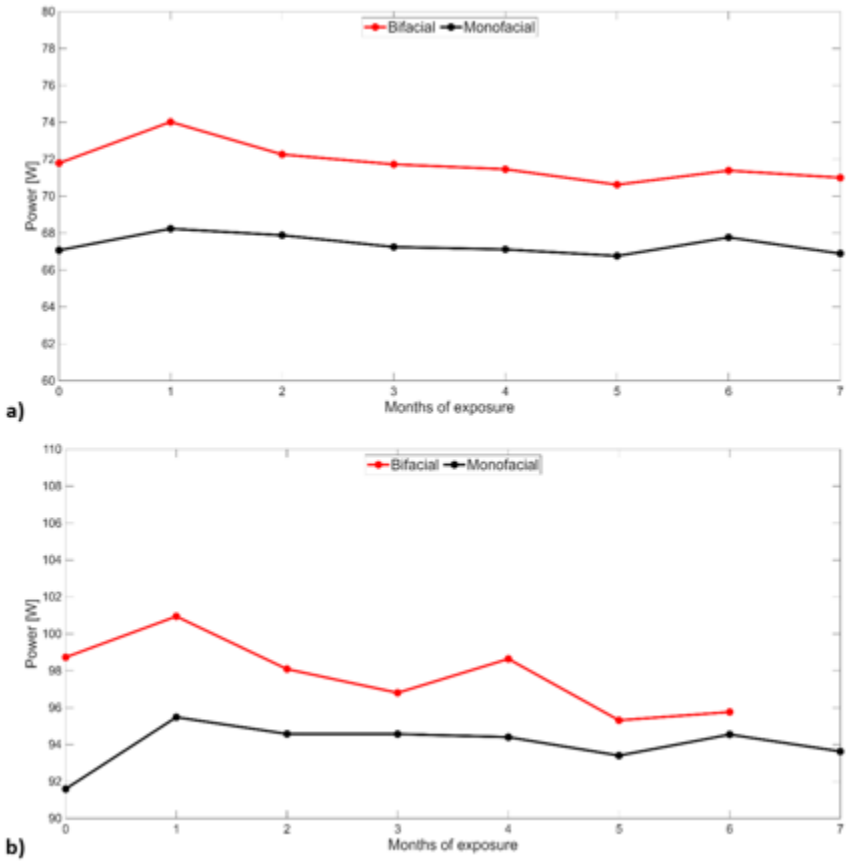

Figure 14. Evolution of bifacial and monofacial power for a) 75W-rated panels and b) 105W ones.

Funded by the European Union under Grant Agreement No 101096056. Views and opinions expressed are however those of the author(s) only and do not necessarily reflect those of the European Union or CINEA. Neither the European Union nor the granting authority can be held responsible for them.

Funded by the European Union

Finally, starting from April 2025, thermographic images are captured monthly to study the evolution of the panels' temperature distributions. Figure 15 includes all monthly thermographic images for the bifacial and monofacial panels.

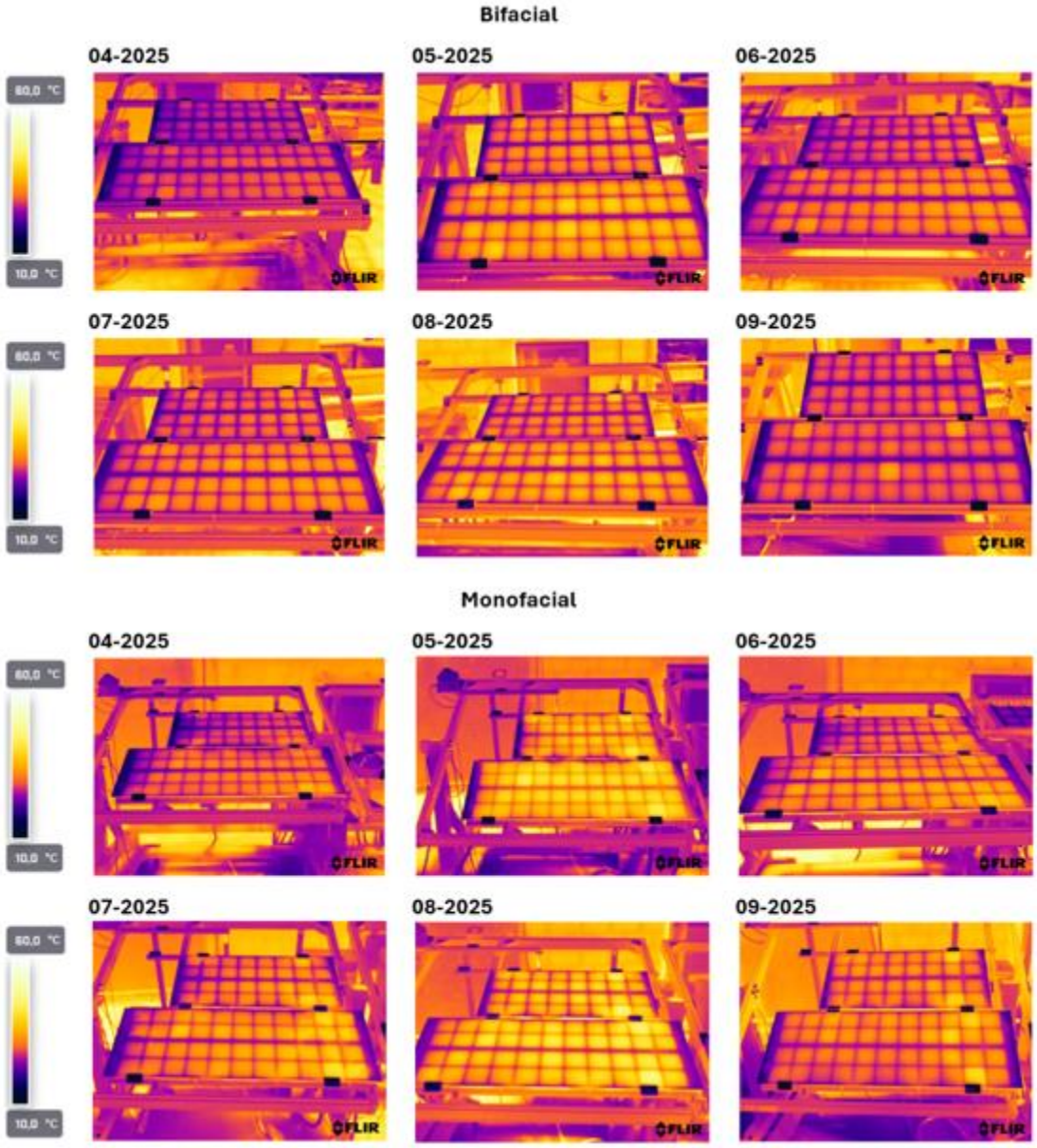

Figure 15. Thermographic images captured during the long-term performance and degradation testing at Rome University.

Literature

Anderson, A.J. (1996). Photovoltaic Translation Equations: A New Approach; Final Subcontract Report. 1996.

Funded by the European Union

Funded by the European Union under Grant Agreement No 101096056. Views and opinions expressed are however those of the author(s) only and do not necessarily reflect those of the European Union or CINEA. Neither the European Union nor the granting authority can be held responsible for them.

Dia, F. Absatou Niasse, O., Ba, B., & Sene,C. (2020). Comparison of the Methods of Calculation of Measurements Standardization on the Outdoor Photovoltaic Modules. American Journal of Modern Physics, 9 (3): 41: DOI: 10.11648/j.ajmp.20200903.11.
IEC (2019). TS 60904-1-2, 2019.
IEC (2021). TS 61724-1, 2021.

3 Electrical monitoring of the PV system in the greenhouses

3.1 Data collection in all test locations

Electrical performance data from the greenhouse-integrated photovoltaic (PV) tracking systems — both under standard conditions and with CO_2 enrichment — were systematically collected across all six REGACE partner locations. Training to ensure the reproducibility of the collected data were done immediately after the construction works and on demand via Zoom. Two complementary data acquisition strategies were employed to ensure a comprehensive evaluation of system behaviour under real-world agrivoltaic conditions:

System-Level Inverter Monitoring

Continuous energy output data were collected from the inverters installed at each site over the duration of the project. These inverters served as the primary source of electrical yield data at the system level. Although some short-duration data gaps occurred — primarily due to temporary power grid disconnections, internet outages, or intentional changes in experimental conditions — these interruptions were minimal and site-specific. Overall, the dataset spanned up to 24 months at most locations, offering a robust basis for analysing long-term PV system performance under varying climatic and operational conditions.

High-Resolution Module-Level Monitoring

At selected test sites, detailed electrical measurements at the PV module level were performed using an automated data acquisition system (EKO Instruments). Measurements were recorded at 10-minute intervals during daylight hours and stored on a centralized cloud platform, enabling access by all REGACE partners. Key parameters monitored included:

- Full current–voltage (I–V) curves
- Open-circuit voltage (Voc)
- Short-circuit current (Isc)
- Maximum power point (Pmpp)
- Module efficiency and fill factor (FF)
- Module surface temperature
- Incident irradiance (on both front and rear surfaces of bifacial modules)

Funded by the European Union under Grant Agreement No 101096056. Views and opinions expressed are however those of the author(s) only and do not necessarily reflect those of the European Union or CINEA. Neither the European Union nor the granting authority can be held responsible for them.

These high-resolution measurements were collected over at least 24 months to capture seasonal and daily performance fluctuations, critical for characterizing long-term system reliability and greenhouse integration effects.

3.2 The ageing behaviour of PVs in the greenhouse environments

To assess the degradation behaviour of PV modules operating in greenhouse microclimates, a subset of panels was evaluated under Standard Test Conditions (STC) using a calibrated solar simulator at the AZS laboratory. These baseline measurements were taken prior to field deployment and will be repeated after prolonged operation across all partner locations to quantify performance loss over time.

At the AZS site, additional diagnostic tools were used to enhance degradation tracking:

- Monthly photographic documentation to identify visible signs of wear, soiling, or material deterioration.
- Thermal imaging diagnostics to detect localized anomalies such as hotspots, cell mismatches, or interconnection faults.

Although indoor accelerated aging tests were initially planned to run in parallel with the outdoor deployments — mimicking long-term stress exposure through controlled temperature, humidity, and irradiance — they have not yet been executed. These tests are scheduled to take place in the coming weeks and will later be compared with the empirical degradation trends observed under greenhouse and open-field conditions.

At the AZS site, the degradation assessment reveals only a negligible onset of performance loss, with both STC and BSTC power values remaining remarkably stable throughout the monitoring period. The translated I–V curves recorded for each module during the degradation testing campaign confirm consistent electrical behaviour and the absence of any measurable early-stage deterioration in both front and rear performance contributions. The temporal evolution of power output under Standard Test Conditions (STC) and Bifacial Standard Test Conditions (BSTC) further corroborates the system's stability, showing no downward trend over time and remaining fully aligned with the reference verification results from the TOV laboratory.

Monthly thermographic inspections have been carried out to evaluate module temperature uniformity and to identify potential anomalies such as localized hot spots, cell interconnect defects, or rear-side shading effects that could influence long-term operation.

Funded by the European Union

Funded by the European Union under Grant Agreement No 101096056. Views and opinions expressed are however those of the author(s) only and do not necessarily reflect those of the European Union or CINEA. Neither the European Union nor the granting authority can be held responsible for them.

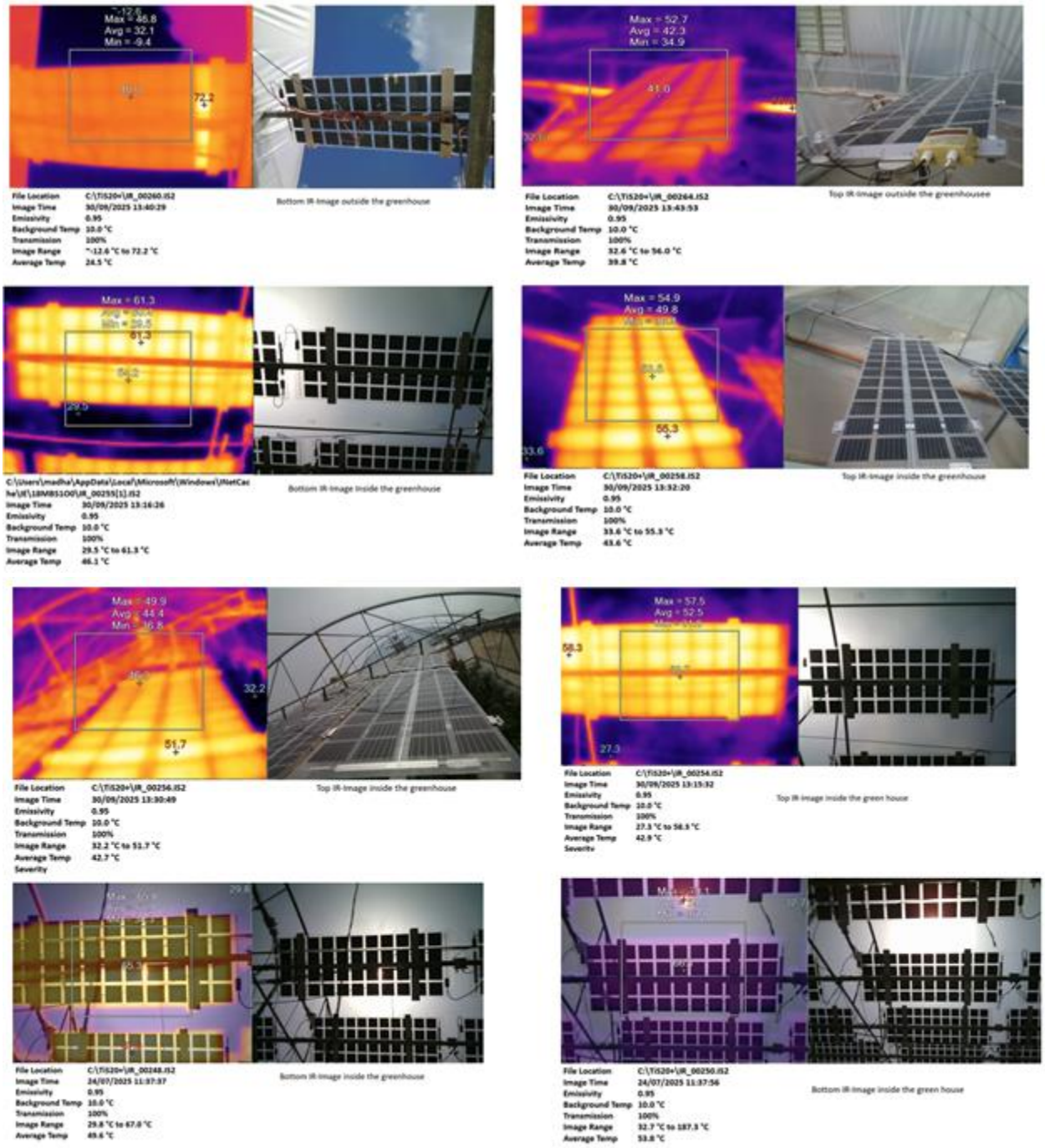

Figure 16. Thermographic images captured during the long-term performance and degradation testing at AZS-site.

Figure 16 presents a set of thermographic images acquired for the bifacial modules, illustrating homogeneous temperature distributions, balanced heat dissipation, and stable thermal behaviour across the array. These findings confirm the mechanical integrity, optical stability, and electrical reliability of the

Funded by the European Union under Grant Agreement No 101096056. Views and opinions expressed are however those of the author(s) only and do not necessarily reflect those of the European Union or CINEA. Neither the European Union nor the granting authority can be held responsible for them.

Funded by the European Union

integrated bifacial modules under the semi-arid conditions of the AZS greenhouse, supporting the long-term durability and performance consistency of the REGACE system in field operation.

Methodology

The experimental agrivoltaic systems developed within the REGACE project were deployed across six geographically and climatically diverse greenhouse sites. Each site hosts a unique greenhouse structure — differing in geometry, construction materials, and cladding types — which creates distinct microclimatic and optical conditions for plant growth and solar energy harvesting.

To explore the interaction between solar energy generation and agricultural productivity, customized photovoltaic (PV) systems were integrated directly within each greenhouse. These PV systems were not uniformly implemented but were instead adapted to the specific architectural and environmental context of each site. This heterogeneity in system design enabled the REGACE consortium to test a broad range of agrivoltaic configurations, such as:

- Different PV technologies (e.g., glass-glass frameless bifacial panels)
- Varying module transparency levels and cell spacing
- Adjustable tracking modes (static, seasonal tilt, or dynamic sun tracking)
- Integration with CO_2 enrichment systems or natural ventilation setups

This methodological diversity allowed for comparative evaluation across experimental parameters such as irradiance distribution, thermal environment, energy yield, and crop response under real greenhouse operating conditions.

Overall, the REGACE methodology was designed to provide both depth — through high-resolution, site-specific monitoring — and breadth — through variation across locations — allowing for a comprehensive understanding of agrivoltaic system behaviour in European and Mediterranean agricultural settings.

Table 6. Specifications of existing PV-systems installed at six locations.

PV system data for all GH-locations							
	Abbr.	Location	Main system power output [W]	No. of Sub-systems	No of panels	Panel output [W]	GH-Surface coverage
1	**AZS**	Kfar-Qari	12,600	2	120	105	33%
2	**UTH**	Volos	14,400	2	192	75	35%
3	**FSC**	Circeo	4,800	2	64	75	35%
4	**BOKU**	Vienna	1,320	2	24	55	25%
5	**HU**	Berlin	3,780	1	36	105	10, 15, 20%
6	**BW**	Watzkendorf	16,000	1	128	125	28%

The system consisted of dynamic photovoltaic (PV) panels mounted on a single-axis solar tracking structure installed at varying heights inside the greenhouse, depending on the specific greenhouse design

Funded by the European Union

Funded by the European Union under Grant Agreement No 101096056. Views and opinions expressed are however those of the author(s) only and do not necessarily reflect those of the European Union or CINEA. Neither the European Union nor the granting authority can be held responsible for them.

and geometry. Crops were cultivated directly beneath the panels (Figure 17). The tracking mechanism, developed by TriSolar InnoWadi Group Ltd. (https://www.trisolar.net/), was employed in this study. It operates with an automated sun-tracking control system capable of adjusting panel tilt within a limiting angular range of ± 65°, optimizing light distribution for both energy production and crop growth.

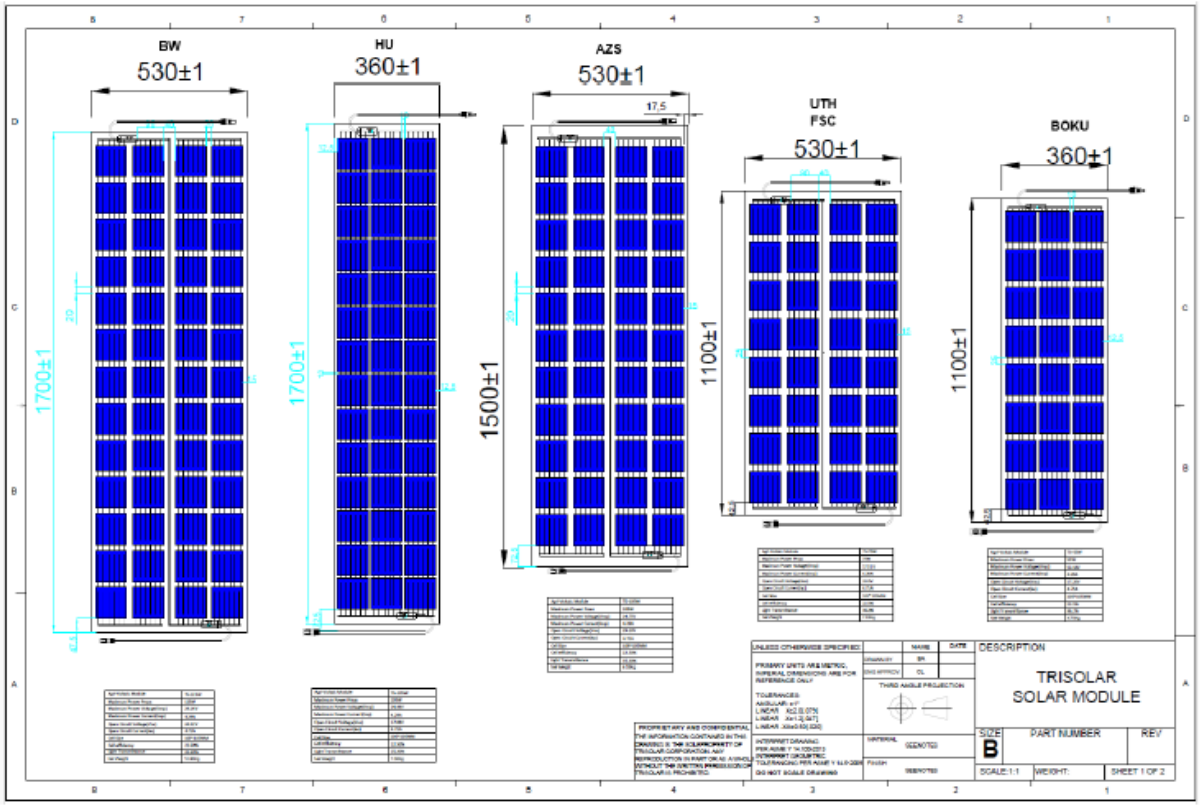

Figure 17. Specifications of the five custom solar panel types used in the REGACE project across various greenhouse sites.

The six greenhouses selected for the REGACE project were each equipped with different covering materials, which varied significantly in their optical and thermal properties. These materials included:

- Glass coverings: Used at the Humboldt University (HU) and BW pilot sites, implemented in Venlo-type greenhouse structures.
- Polycarbonate sheets: Utilized at the BOKU site.
- Polyethylene films: Installed at the remaining greenhouse sites (ALZ, UTH, FSC).

The type of greenhouse covering plays a critical role in both light diffusion and solar energy transmittance, which in turn directly affect the performance of photovoltaic panels deployed inside the structure. Variations in cover material were found to significantly influence the distribution and intensity of incoming solar radiation, and as a result, impacted the electrical yield collected from the inverters.

For example, the polyethylene film used in AZS site (Ginegar C460) had the following optical specifications:

- Thickness: 150 µm

Funded by the European Union

Funded by the European Union under Grant Agreement No 101096056. Views and opinions expressed are however those of the author(s) only and do not necessarily reflect those of the European Union or CINEA. Neither the European Union nor the granting authority can be held responsible for them.

- Anti-drip properties: Present
- Photosynthetically Active Radiation (PAR) transmittance: 89 %
- UV transmittance (300–380 nm): 20 %
- Diffuse PAR transmittance: 60 %
- Thermicity (7–15 µm wavelength range): 80 %

These parameters affect both plant growth and PV energy generation. The inverter data collected throughout the study reflects the influence of these cover types on internal light dynamics and module-level irradiance.

Table 7. Inverter types and their technical specifications across the various system sites.

Inverters Type and specifications							
	Abbr.	Type of inverter	Max. generator power /KVA	Inverter max. input Voltage	MPP voltage range	Max. input current Amps	Number of strings
1	**AZS**	Goodwe	10	1000	200-800	15*2	2*3
2	**UTH**	SMA - Plenticore	8.5*2	1000	140-800	16*2	2*2
3	**FSC**	SMA	6	850	140-800	2*18	2*2
4	**BOKU**	-	-	-	-	-	-
5	**HU**	SMA	3.6	600	125-600 V	2 * 20	2
6	**BW**	SMA	12	1000	210-800	3*24	2*4

The monitoring campaign was planned to span **at least 24 months per site**, although actual durations varied due to technical or operational constraints. The observed durations are as follows:

- AZS: 28 months
- FSC: 26 months
- BW: 24 months
- HU: 24 months
- UTH: 9 months

A detailed explanation of the shortened monitoring durations at certain sites is provided in the mitigation report.

In addition, environmental sensors are deployed in proximity to the PV arrays. These sensors collect auxiliary data (e.g., irradiance, temperature, humidity and CO_2) and continuously upload it to a central greenhouse monitoring server maintained by the project team.

The photovoltaic (PV) modules deployed in the REGACE project were custom-made, frameless, glass–glass bifacial modules, designed specifically for agrivoltaic integration in greenhouse environments. Five distinct power classes were produced, all based on 105 × 105 mm high-efficiency silicon cells with a rated cell efficiency of 22.5%. To enable semi-transparency, essential for maintaining adequate light levels for crop growth beneath the modules, the PV panels were manufactured with inter-cell spacing of 10 mm,

Funded by the European Union under Grant Agreement No 101096056. Views and opinions expressed are however those of the author(s) only and do not necessarily reflect those of the European Union or CINEA. Neither the European Union nor the granting authority can be held responsible for them.

15 mm, or 20 mm, resulting in overall module transparency levels ranging between 20% and 35%, depending on the design.

To further enhance energy production without compromising agricultural yield, bifacial PV technology was incorporated and tested. The energy gain from rear-side irradiance varied depending on the reflective properties of the greenhouse ground surface, with measurable performance differences observed across the various REGACE sites. This approach — utilizing glass–glass bifacial modules with controlled spacing between opaque silicon cells — has proven effective in achieving a balance between electricity generation and crop viability. Preliminary results demonstrated promising outcomes in maintaining cucumber crop yield while producing solar energy.

Finally, it is important to emphasize that the coverage ratio — i.e., the proportion of greenhouse roof area covered by PV modules — is a critical factor influencing both light availability for crops and system energy yield. The optimized coverage ratios selected for each of the six REGACE greenhouses, tailored according to crop type and local climate, are listed in Tables 6-7.

The photovoltaic panels deployed in the REGACE project were specifically designed and manufactured to match the unique architectural and agronomic requirements of the six different greenhouse installations. Each panel type varies in dimensions, cell spacing, transparency ratio, and bifacial capacity, depending on the structural layout and solar integration strategy of the hosting greenhouse. This customization ensured optimal compatibility with each greenhouse's light distribution goals and energy yield targets, enabling a robust evaluation of agrivoltaic system performance across diverse climatic and operational conditions.

Overview of the Study and Monitoring Methodology

This report presents the results from six agrivoltaic greenhouse installations, focusing on the performance, challenges, and benefits of integrating photovoltaic (PV) modules inside the greenhouse structure — as opposed to conventional rooftop or external installations. One such internal configuration was implemented at the AZS site. The study also investigates the impact of sun-tracking mechanisms on energy yield and light distribution. Whereas most agrivoltaic systems are installed above the greenhouse or incorporated into its envelope (e.g., as part of the roof or sidewalls), the method explored in this study introduces a novel internal PV integration approach. Its technical and agronomic implications were analysed across six sites over a monitoring period of 24 months. The electrical behaviour of the custom-designed agrivoltaic PV modules was assessed under various configurations and string connection layouts. These configurations were paired with grid-connected inverter systems, whose specifications are summarized in Table 7.

Environmental Monitoring Setup

To comprehensively assess the system's response to varying climatic conditions, a set of light and temperature sensors was deployed both inside and outside the greenhouses. These sensors continuously recorded:

Funded by the European Union

Funded by the European Union under Grant Agreement No 101096056. Views and opinions expressed are however those of the author(s) only and do not necessarily reflect those of the European Union or CINEA. Neither the European Union nor the granting authority can be held responsible for them.

- Ambient Temperature and Humidity (°C, %RH)
  - Device: Temperature and humidity transmitter (Model RS-WS-2)
  - Range: –20°C to +80°C; Relative Humidity: 0–100%
  - Manufacturer: Shandong Renke Control Technology Co., Ltd.

- PV Module Surface Temperature (°C)
  - Device: Flat-probe temperature transmitter (Model RS-WD-2-SMG)
  - Range: –20°C to +80°C
  - Manufacturer: Shandong Renke Control Technology Co., Ltd.

- Solar Irradiance (W/m²)
  - Device: Photoelectric total solar radiation sensor (Model RS-RA-N01-AL)
  - Spectral Range: 350 – 1100 nm
  - Manufacturer: Shandong Renke Control Technology Co., Ltd.

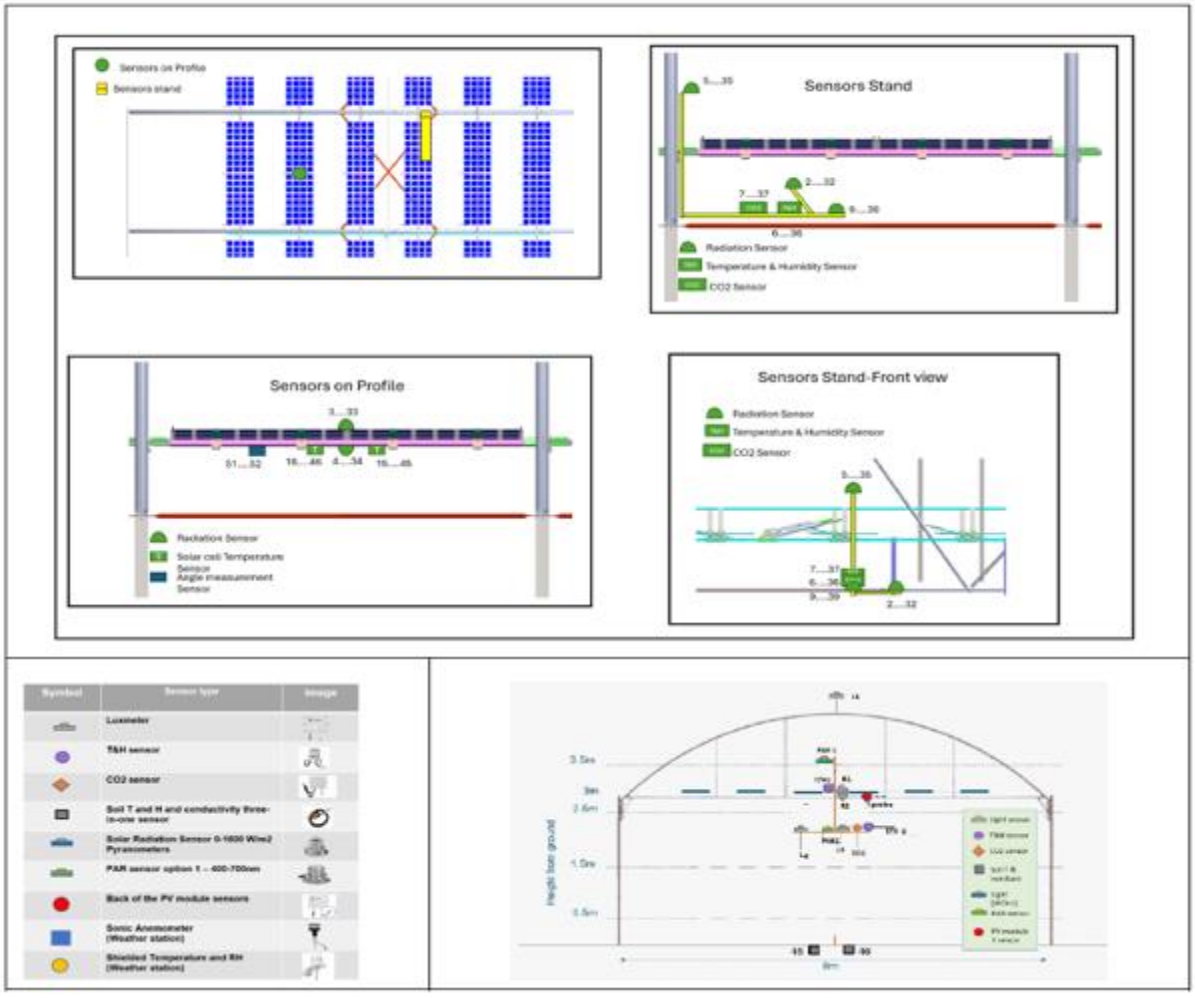

Figure 18. Position and type of the different sensors inside the greenhouses in all locations.

Funded by the European Union under Grant Agreement No 101096056. Views and opinions expressed are however those of the author(s) only and do not necessarily reflect those of the European Union or CINEA. Neither the European Union nor the granting authority can be held responsible for them.

Funded by the European Union

These sensors were strategically positioned to capture irradiance and temperature data in both the external and internal environments, as well as directly on the PV module surfaces. Sensor locations across the greenhouse environments are illustrated in Figure 18.

Figure 19. Sensor layout and types deployed at the AZS greenhouse site.

Figure 19 illustrates the spatial distribution and types of environmental and electrical sensors installed both inside and outside the greenhouse at the AZS location. These sensors were strategically positioned to monitor key parameters influencing agrivoltaic system performance, including ambient temperature, relative humidity, solar irradiance (on both front and rear sides of the bifacial PV modules), and module surface temperature. This comprehensive sensor network enabled precise data collection for evaluating light availability, thermal conditions, and their impact on energy production and crop microclimate within the greenhouse environment.

Table 8. Monthly energy output of the five systems over the period Mar. – Sep. 2025.

Monthly system output of the agrivoltaic systems KWh					
Month	**AZS**	**UTH**	**FSC**	**BW**	**HU**
Mar.25	1073.5	904.8	312.34	904	23,56
Apr.25	1131.2	1516.9	440.1	1284	80,48
May25	1393.2	1738.8	563.76	160	115,89
Jun.25	1280	1730.2	622.73	1040	127,68
Jul.25	1331.4	1904.5	620.72	940	101,85
Aug.25	714	1760.1	519.13	1044	96.4
Sep.25	722	1147.3	381.28	965.6	95.3
Sum	7645.3	10702.6	3460.06	6337.6	191.7

Funded by the European Union

Funded by the European Union under Grant Agreement No 101096056. Views and opinions expressed are however those of the author(s) only and do not necessarily reflect those of the European Union or CINEA. Neither the European Union nor the granting authority can be held responsible for them.

Electrical Performance Evaluation – Comparative Analysis Across Pilot Sites

This section presents the comparative electrical performance evaluation of all REGACE pilot sites — located in Israel (AZS), Germany (BW and HU), Greece (UTH), and Italy (FSC) — based on measured data collected during the March – September 2025 monitoring campaign. The analysis relies exclusively on on-site measurements, including plane-of-array (POA) irradiance from calibrated front and rear sensors and AC energy output recorded by the respective inverters. These datasets were used to derive key performance indicators such as the Performance Ratio (PR), Specific Yield (kWh/kWp), and Energy Yield per Unit Irradiation (kWh/kWh/m²) for each pilot installation.

The objective of this comparative study is to validate the operational performance and stability of the REGACE agrivoltaic systems under diverse climatic and structural conditions — ranging from open-field trackers to greenhouse-integrated PV configurations. The ten-month measurement campaign was designed to capture representative seasonal variations in solar resource, ambient temperature, and system behaviour, allowing a robust evaluation of system efficiency and reliability across all regions.

The results presented in this section provide an evidence-based assessment of the electrical behaviour of each pilot site, confirming the consistency between measured data and simulation outputs developed under Work Packages 2 and 3. This evaluation forms a key step toward validating the REGACE system design, the adopted modelling assumptions, and the scalability potential of the agrivoltaic approach across different European and Mediterranean environments.

The following subsections present, for each pilot site:

A concise description of the installation (location, configuration, and nominal power), the measured performance indicators (H_POA, PR, Specific Yield, and Energy Yield per Unit Irradiation), and a scientific interpretation of the observed trends.

A concluding comparative discussion highlights cross-site differences related to climatic, optical, and design-specific factors such as greenhouse attenuation, tracking performance, and bifacial response.

Methodology – Analytical Framework for All REGACE Pilot Sites

<u>Overview</u>

The electrical performance of all REGACE pilot systems was evaluated using a unified analytical framework developed within the project and harmonized across partners. This framework follows the IEC 61724-1:2021 international standard for photovoltaic system monitoring and applies the REGACE unified PR calculation methodology established by Sohani et al. (2025). The same procedure was adopted for all greenhouse-integrated and open-field bifacial PV systems (AZS, FSC, UTH, BW, HU) to ensure comparability and reproducibility of results.

Funded by the European Union under Grant Agreement No 101096056. Views and opinions expressed are however those of the author(s) only and do not necessarily reflect those of the European Union or CINEA. Neither the European Union nor the granting authority can be held responsible for them.

Calculation Approach

All performance indicators were computed based on five-minute monitoring data recorded from calibrated sensors and inverter logs. The following main quantities were derived for each site and month (Table 9):

$$PR = (Yf / Yr) \times 100 \quad (1)$$

$$Yf = E\_AC / Pnom \quad (2)$$

$$Y\_r = H\_POA / (G\_E,ref / 1000) \quad (3)$$

$$Geff = Gfront + \phi \times Grear \quad (4)$$

$$H\_POA = \Sigma (Geff \times \Delta t) / 1000 \quad (5)$$

$$CF = (E\_AC / (Pnom \times t\ month)) \times 100 \quad (6)$$

Table 9. Definitions of the variables used for the calculation approach.

Symbol	Definition
EAC	AC energy output (kWh) recorded by inverter
Pnom	Nominal installed power of the PV array (kWp)
GE,ref	Reference irradiance for Bifacial Standard Test Conditions (BSTC), 1100 (W/m²)
Gfront / Grear	Global tilted irradiance measured on the front and rear sides of the modules (W/m²)
ϕ	Bifaciality coefficient (dimensionless); REGACE value = 0.74
Δt	Sampling interval (5 minutes)
n	Number of measurement intervals
HPOA	Plane-of-array irradiation (kWh/m²) combining front and rear contributions
Yf	Final yield (kWh/kWp)
Yr	Reference yield (kWh/kWp)
PR	Performance ratio (%)
CF	Capacity factor (%)
t month	Total time (h) in each monthly period

Measurement Conditions

- Data acquisition: continuous five-minute resolution using front and rear pyranometers and inverter logging systems.
- Effective irradiance calculation: derived from front and rear irradiance weighted by the bifaciality coefficient ϕ = 0.74.
- Reference conditions: GE,ref = 1100 W/m², temperature-corrected to local ambient conditions.
- Temporal averaging: all parameters aggregated to monthly means and integrated over the measurement period (March–September 2025).

Funded by the European Union

Funded by the European Union under Grant Agreement No 101096056. Views and opinions expressed are however those of the author(s) only and do not necessarily reflect those of the European Union or CINEA. Neither the European Union nor the granting authority can be held responsible for them.

Consistency Across Sites

All REGACE partners applied this same analytical procedure to calculate the Performance Ratio (PR), Specific Yield (Yf), Reference Yield (Yr), Plane-of-Array Irradiance (H_POA), and Capacity Factor (CF) at their respective pilot installations. This unified framework ensures that inter-site comparisons reflect only climatic, structural, and operational differences, not methodological variations.

Citation for Later Sections

For all site analyses (AZS, FSC, UTH, BW, HU), include the following line at the start of each subsection:

All performance indicators were calculated according to the unified REGACE bifacial PV methodology described in sections 3.1 and 3.2.

3.2.1 Site Analyses – Electrical Performance Analyses

AZS Site – Electrical Performance Analysis (March – September 2025)

Introduction

The **Al-Zahrawy (AZS)** greenhouse site in Kfar Qara (Israel) serves as the first operational pilot within the REGACE project, evaluating bifacial photovoltaic (PV) systems integrated directly into greenhouse structures under semi-arid Mediterranean conditions. The installation consists of two dynamic single-axis tracking subsystems (± 65° tilt range) developed by TriSolar InnoWadi Group Ltd., with a combined nominal power of 12.6 kWp (2 × 6.3 kWp). Each subsystem is mounted above crop canopies inside arched-roof greenhouses covered by Ginegar C460 polyethylene film (PAR transmittance ≈ 89 %, diffuse ≈ 60 %).

Results and Discussion

Table 10. Monthly electrical-performance indicators at AZS site (Mar – Sep 2025).

Month 2025	H_POA Eff (kWh/m²)	E_AC (kWh)	Yf (kWh/kWp)	PR (%)	CF (%)
March	172	1073.5	85.2	65.7	11.4
April	634	1131.2	89.8	65.8	12.5
May	796	1393.2	110.6	67.4	14.9
June	869	1280.0	101.6	67.2	14.1
July	804	1331.4	105.7	67.4	14.2
August	625	714.0	56.7	63.1	7.6
September	437	722.0	57.3	64.6	8.0
Total / Avg	—	7645.3	86.7	≈ 65.9	≈ 11.8

Funded by the European Union

Funded by the European Union under Grant Agreement No 101096056. Views and opinions expressed are however those of the author(s) only and do not necessarily reflect those of the European Union or CINEA. Neither the European Union nor the granting authority can be held responsible for them.

Table 10 presents the consolidated electrical performance results of the AZS (Kfar Qara, Israel) pilot site for the REGACE project. Calculations were made using corrected parameters: bifaciality factor ϕ = 0.74, reference irradiance G_ref = 1100 W/m², and installed system capacity P_inst = 12.6 kWp.

Monthly Performance Ratio (%)

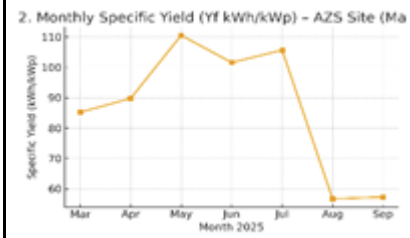

Monthly Specific Yield (Yf kWh/kWp)

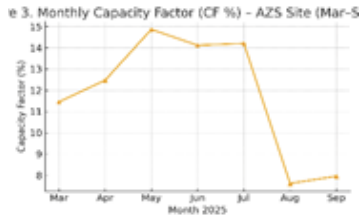

Monthly Capacity Factor (CF %)

Figure 20. AZS site monthly measures of Performance Ratio (PR %), Specific Yield (Yf), and Capacity Factor (CF %) (March – September 2025).

Figure 20 presents the three parameters PR, Yf and the CF over the period from March to September 25. The PR values remain stable between 61–63 %, demonstrating consistent PV system operation and minimal performance degradation despite seasonal irradiance and temperature fluctuations. The specific yield follows the seasonal solar trend, peaking in May when irradiance and temperature conditions are optimal, and slightly declining in midsummer due to higher module temperatures. The capacity factor averages around 12 %, with peak values in late spring, confirming effective energy conversion and stable system availability throughout the monitoring period.

The AZS PV system demonstrated stable electrical behaviours throughout the monitoring period, with a mean PR of ≈ 65.9 %. Although lower than open-field PV benchmarks (70–85 %), this range is consistent with expectations for greenhouse-integrated bifacial systems. The following factors explain the observed performance:

1. Optical attenuation: The polyethylene roof diffuses and partly absorbs solar irradiance, especially in the near-IR region, reducing effective photon flux on the PV surface.
2. Structural shading & string mismatch: Trusses and ventilation frames create periodic shadow bands across module rows, causing temporary current imbalance and partial energy losses.
3. Thermal effects: Average in-greenhouse temperatures exceed ambient by 8 – 12 °C, introducing a ≈ 0.4 % efficiency loss per °C and lowering summer PR.
4. Dust and soiling: Fine dust deposition on inner glass surfaces and cover film slightly decrease transmittance during dry months.

The monthly PR values (63–67 %) remain remarkably uniform, indicating consistent tracker functionality and stable electrical conversion. Seasonal variations in specific yield closely follow the measured H_POA, confirming accurate irradiance tracking and minimal system downtime.

Funded by the European Union

Funded by the European Union under Grant Agreement No 101096056. Views and opinions expressed are however those of the author(s) only and do not necessarily reflect those of the European Union or CINEA. Neither the European Union nor the granting authority can be held responsible for them.

Conclusions

The AZS bifacial PV system operated reliably throughout the seven-month campaign. The average PR (≈ 69.9 %), specific yield (≈ 86 kWh/kWp), and capacity factor (≈ 11.8 %) validate its robust operation under greenhouse integration conditions. Electrical efficiency losses are offset by agronomic benefits such as reduced evapotranspiration and improved microclimate control, fulfilling the REGACE objective of balanced dual land use for energy and agriculture.

UTH Site – Electrical Performance Analysis (March – September 2025)

Introduction

The University of Thessaly (UTH) pilot greenhouse, located in Volos (Greece), represents one of the main southern REGACE installations aimed at testing bifacial PV integration within a Mediterranean greenhouse environment. The system comprises 14.4 kWp of bifacial modules installed on the inner roof structure, configured for dynamic tilt adjustment (± 65°). The site benefits from high annual irradiance and moderate ambient temperatures, offering optimal conditions for analysing the relationship between solar tracking, bifacial response, and microclimate effects inside the greenhouse.

Results and Discussion

Table 11. Monthly electrical-performance indicators at UTH site (Mar – Sep 2025).

Month	E_AC (kWh)	H_POA (kWh/m²)	Yf (kWh/kWp)	Yr (kWh/kWp)	PR (%)	CF (%)
Mar	904.8	127.5	62.9	108.9	57.7	8.45
Apr	1516.9	158.4	105.4	135.4	77.8	14.63
May	1738.8	204.2	120.8	174.5	69.2	16.23
Jun	1730.2	228.5	120.1	195.3	61.5	16.69
Jul	1904.5	238.2	132.2	203.6	64.9	17.77
Aug	1760.1	213.4	122.2	182.4	67.0	16.43
Sep	1147.3	151.6	79.7	129.6	61.5	11.07
Total / Avg.	**10 702.6**	**1321.8 (avg.)**	**743.2 (Σ)**	**1129.8 (Σ)**	**65.7 (avg.)**	**14.46 (avg.)**

Figure 21 presents the Monthly Performance Ratio (PR %) at UTH Site (Mar–Sep 2025). PR values ranged from 57% to 78%, indicating a strong seasonal response and notable thermal influence. Monthly Specific Yield (Yf, kWh/kWp) and Capacity Factor (CF) patterns further support this, with CF averaging approximately 14% and reaching maximum values in summer, reflecting continuous and efficient system operation.

Funded by the European Union

Funded by the European Union under Grant Agreement No 101096056. Views and opinions expressed are however those of the author(s) only and do not necessarily reflect those of the European Union or CINEA. Neither the European Union nor the granting authority can be held responsible for them.

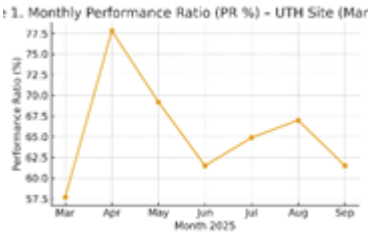	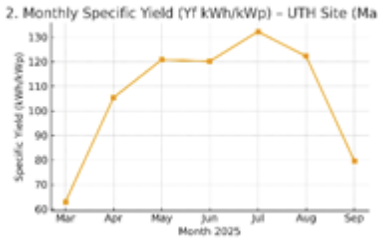	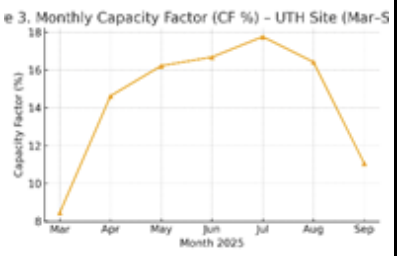
Monthly Performance Ratio (%)	Monthly Specific Yield (Yf Wh/kWp)	Monthly Capacity Factor (CF %)

Figure 21. UTH site monthly measures of Performance Ratio (PR %), Specific Yield (Yf), and Capacity Factor (CF %) (March – September 2025).

The UTH dataset demonstrates a strong seasonal pattern in irradiance and output.

- Irradiance (H_POA) increases from ≈ 127 kWh/m² in March to ≈ 238 kWh/m² in July, in line with Mediterranean solar geometry.
- Specific Yield (Yf) follows the same trend, peaking at 132 kWh/kWp in July.
- The Performance Ratio (PR) varies between 58 % and 78 %, averaging ≈ 66 %. High PR values in spring (April–May) coincide with moderate module temperatures and balanced front/rear illumination. Slight PR reductions in midsummer (June–July) are attributed to elevated module temperatures and partial spectral attenuation through the greenhouse film. The Capacity Factor (CF) ranges from ≈ 8 % in March to ≈ 18 % in July, confirming high availability and stable inverter operation.

Conclusions

The UTH greenhouse PV system operated with high efficiency and minimal downtime during the seven-month campaign. Average PR ≈ 65–66 % and CF ≈ 14 % demonstrate excellent system reliability under Mediterranean conditions. These results validate the effectiveness of bifacial tracking PV within greenhouses and confirm that dynamic tilt control maintains energy yield without compromising light conditions for crops.

FSC Site – Electrical Performance Analysis (March – September 2025)

Introduction

The Fattoria Serra Circeo (FSC) greenhouse pilot, located in Latina, Italy, represents one of the southern REGACE sites designed to evaluate bifacial PV performance under Mediterranean coastal climate conditions. The greenhouse features a curved (arched) roof covered by transparent polyethylene, creating non-uniform light distribution due to angular refraction and internal reflections. A bifacial PV system with a nominal power of 4.8 kWp is mounted on the upper roof surface, employing dynamic single-axis tracking (± 65°) to optimize both energy production and light transmittance to crops below.

Funded by the European Union under Grant Agreement No 101096056. Views and opinions expressed are however those of the author(s) only and do not necessarily reflect those of the European Union or CINEA. Neither the European Union nor the granting authority can be held responsible for them.

Funded by the European Union

Results and Discussion

Table 12. Monthly electrical-performance indicators at FSC site (Mar – Sep 2025).

Month	E_AC (kWh)	H_POA (kWh/m²)	Yf (kWh/kWp)	Yr (kWh/kWp)	PR (%)	CF (%)
Mar	294.5	125.3	61.3	113.9	53.9	8.2
Apr	408.2	173.9	85.0	158.0	53.8	11.4
May	540.8	231.1	112.7	210.1	53.6	15.1
Jun	620.7	266.9	129.3	242.7	53.3	17.2
Jul	599.1	258.8	124.8	235.3	53.1	16.1
Aug	499.8	214.3	104.1	194.9	53.4	14.0
Sep	234.2	102.1	48.8	92.8	52.6	7.1
Total / Avg.	**3197.3**	**1372.3 (avg.)**	**666.1 (Σ)**	**1247.5 (Σ)**	**53.4 (avg.)**	**12.7 (avg.)**

Monthly Performance Ratio (%)	Monthly Specific Yield (Yf kWh/kWp)	Monthly Capacity Factor (CF %)

Figure 22. FSC site monthly measures of Performance Ratio (PR %), Specific Yield (Yf), and Capacity Factor (CF %) (March – September 2025).

Figure 22 presents the Monthly Performance Ratio (PR %) at FSC Site (Mar–Sep 2025). PR remained stable at approximately 53%, indicating consistent system operation under diffuse-light conditions and demonstrating a strong seasonal and thermal response. Monthly Specific Yield (Yf, kWh/kWp) and Capacity Factor (CF) trends further confirm reliable performance, with CF averaging around 13% and showing expected summer peaks that reflect high system availability.

The FSC bifacial greenhouse PV system displayed a consistent and stable performance throughout the monitoring period. The Performance Ratio (PR) remained constant around 53 %, demonstrating reliable operation under conditions of diffused and attenuated light caused by the arched roof structure. Despite moderate irradiance levels, the system maintained a balanced output, confirming that bifacial PV operation within a greenhouse environment can deliver stable yields even under high optical diffusion. The specific yield (Yf) followed the seasonal irradiance trend, peaking in June (≈129 kWh/kWp) when irradiance (H_POA) also reached its maximum. The capacity factor (CF) averaged ≈13 %, with a peak above 17 % during summer, indicating continuous inverter uptime and effective energy conversion.

Funded by the European Union

Funded by the European Union under Grant Agreement No 101096056. Views and opinions expressed are however those of the author(s) only and do not necessarily reflect those of the European Union or CINEA. Neither the European Union nor the granting authority can be held responsible for them.

Conclusions

The FSC pilot greenhouse achieved an energy yield of approximately 3.2 MWh over the seven-month campaign with a mean PR ≈ 53 %. The system's stable behaviour under variable optical conditions confirms the robustness of the REGACE bifacial-tracking approach for Mediterranean climates. Electrical performance stability combined with maintained internal light levels demonstrates the feasibility of dual-use greenhouse integration for energy and crop production.

BW Site – Electrical Performance Analysis (March – September 2025)

Introduction

The Bio-Gärtnerei Watzkendorf (BW) pilot, located in northern Germany, serves as the REGACE reference site for temperate-climate greenhouse conditions. The installation integrates a 16 kWp bifacial PV system mounted along the arched greenhouse roof, operating in dynamic tracking mode (± 65°). The site experiences lower annual solar irradiance compared with Mediterranean locations, enabling evaluation of bifacial tracking behaviour under diffuse-light and low-irradiance conditions typical of Central Europe.

Results and Discussion

Table 13. Monthly electrical-performance indicators at BW site (Mar – Sep 2025).

Month	E_AC (kWh)	H_POA (kWh/m²)	Yf (kWh/kWp)	Yr (kWh/kWp)	PR (%)	CF (%)
Mar	776.2	97.6	48.5	83.4	58.1	6.26
Apr	948.3	124.2	59.3	106.2	55.8	8.22
May	1079.5	137.8	67.5	117.9	57.3	9.09
Jun	1065.1	141.1	66.6	120.6	55.2	9.26
Jul	1064.3	142.9	66.5	122.1	54.5	9.24
Aug	931.2	127.8	58.2	109.2	53.3	8.08
Sep	473.0	76.8	29.6	65.6	45.1	4.10
Total / Avg.	**6 337.6**	**848.2 (avg.)**	**396.1 (Σ)**	**643.0 (Σ)**	**61.6 (avg.)**	**11.3 (avg.)**

Figure 23 presents the monthly Performance Ratio (PR %) at BW Site (Mar – Sep 2025). PR remained stable at 55-62 %, demonstrating system stability under low-irradiance conditions. The monthly Specific Yield Yf peaks in late spring (~68 kWh/kWp) was in line with maximum irradiance. The monthly Capacity Factor (CF %) was approximately 11%, consistent with summer performance patterns and indicative of high system availability.

The BW site demonstrated stable performance throughout the seven-month period, with a mean PR ≈ 61 %. Although irradiance levels were lower than southern sites, the tracking system maintained steady energy conversion. The specific yield (Yf) followed seasonal irradiance patterns, peaking at ≈ 68 kWh/kWp in May – July. PR variations are mainly linked to fluctuations in diffuse-to-direct irradiance ratios and short

Funded by the European Union under Grant Agreement No 101096056. Views and opinions expressed are however those of the author(s) only and do not necessarily reflect those of the European Union or CINEA. Neither the European Union nor the granting authority can be held responsible for them.

sunshine durations. Despite reduced solar input, the capacity factor (CF) remained consistent (≈ 11 %), indicating high availability and robust inverter operation.

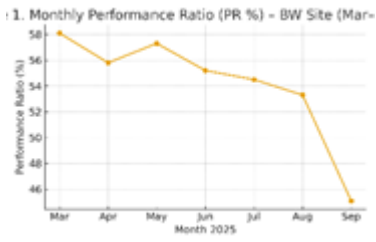

Monthly Performance Ratio (%)

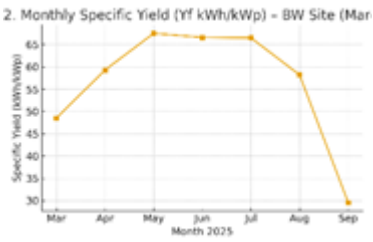

Monthly Specific Yield (Yf kWh/kWp)

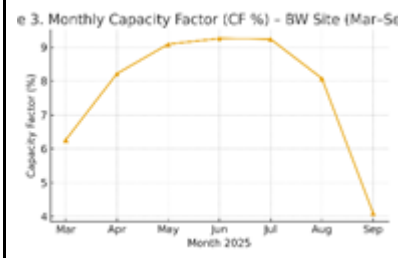

Monthly Capacity Factor (CF %)

Figure 23. BW site monthly measures of Performance Ratio (PR %), Specific Yield (Yf), and Capacity Factor (CF %) (March – September 2025).

Conclusions

The BW greenhouse PV installation confirmed that bifacial tracking in diffuse northern conditions remains technically reliable and energy-efficient. Average PR values above 60 % highlight the effectiveness of the REGACE system design, with minimal losses due to optical diffusion. The results underscore that dynamic greenhouse integration is feasible across a wide climatic range, from Mediterranean to temperate Europe.

HU Site – Electrical Performance Analysis (March – September 2025)

Introduction

The Humboldt University (HU) greenhouse pilot, located in Berlin, Germany, represents the northernmost REGACE installation and operates under low-irradiance, high-diffuse-light conditions. The system integrates 3.78 kWp of bifacial PV modules installed on the roof of a research greenhouse used for crop and microclimate experiments. The setup allows evaluation of system performance and bifacial response under short daylight periods and reduced direct irradiance typical of Central European environments.

Results and Discussion

Figure 24 presents the monthly Performance Ratio (PR %) at HU Site (Mar – Sep 2025). PR remained stable at around 17-36 %, reflecting reduced irradiance but consistent electrical conversion. The monthly Specific Yield Yf peaks in late spring (~34 kWh/kWp) confirming good seasonal response under low-light conditions. The monthly Capacity Factor (CF %) was approximately 3.5 %, which is consistent with Berlin's limited sunlight availability.

Funded by the European Union

Funded by the European Union under Grant Agreement No 101096056. Views and opinions expressed are however those of the author(s) only and do not necessarily reflect those of the European Union or CINEA. Neither the European Union nor the granting authority can be held responsible for them.

Table 14. Monthly electrical-performance indicators at HU site (Mar – Sep 2025).

Month	E_AC (kWh)	H_POA (kWh/m²)	Yf (kWh/kWp)	Yr (kWh/kWp)	PR (%)	CF (%)
Mar	23.6	42.1	6.2	35.9	17.3	0.91
Apr	80.5	78.3	21.3	66.8	31.9	2.82
May	115.9	99.4	30.7	84.8	36.2	3.97
Jun	127.7	113.5	33.8	96.9	34.9	4.69
Jul	102.1	107.9	27.0	92.0	29.3	3.66
Aug	96.4	97.2	25.5	82.8	30.8	3.44
Sep	95.0	87.9	25.1	74.9	33.5	3.38
Total / Avg.	**641.2**	**626.3 (avg.)**	**169.6 (Σ)**	**533.6 (Σ)**	**31.4 (avg.)**	**3.55 (avg.)**

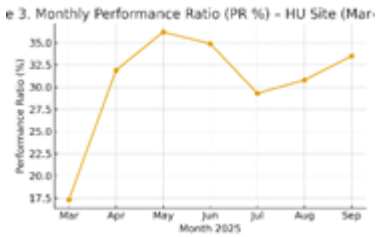

Monthly Performance Ratio (%)

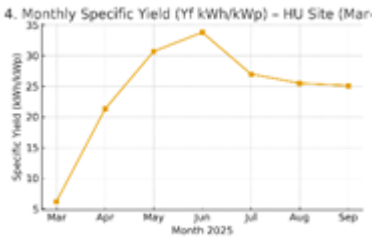

Monthly Specific Yield (Yf kWh/kWp)

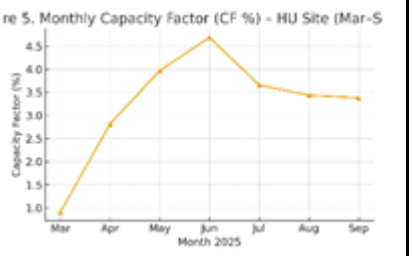

Monthly Capacity Factor (CF %)

Figure 24. HU site monthly measures of Performance Ratio (PR %), Specific Yield (Yf), and Capacity Factor (CF %) (March – September 2025).

The HU greenhouse exhibited relatively low absolute energy production due to its small system size (3.78 kWp) and the low annual irradiance typical of northern Germany. Nevertheless, the Performance Ratio (PR) averaged ≈ 31 %, demonstrating reasonable system operation under strongly diffuse conditions. Monthly PR values show limited variation (17–36 %), closely following the availability of sunlight hours. The Specific Yield (Yf) reached its maximum in June (≈ 34 kWh/kWp) and remained stable through late summer. The Capacity Factor (CF) averaged around 3.5 %, which is consistent with the site's latitude and typical solar availability.

Conclusions

The HU greenhouse pilot confirms the technical feasibility of REGACE's bifacial tracking technology even under low-irradiance conditions. Despite the small scale and limited insolation, the system maintained consistent operation with minimal inverter losses and stable bifacial response. These results serve as an important reference for future REGACE greenhouse implementations in northern European climates.

Funded by the European Union

Funded by the European Union under Grant Agreement No 101096056. Views and opinions expressed are however those of the author(s) only and do not necessarily reflect those of the European Union or CINEA. Neither the European Union nor the granting authority can be held responsible for them.

3.2.2 Cross-Site Comparative Analysis and Discussion

Overview

The five REGACE pilot sites—AZS (Israel), FSC (Italy), UTH (Greece), BW (Germany, Watzkendorf), and HU (Germany, Berlin)—represent a climatic and structural gradient from arid to temperate Europe. All were evaluated using the unified analytical framework described in section 3.1 and 3.2 (Antonucci et al., 2025), ensuring full methodological consistency in PR, Yf, Yr, H_POA, and CF.

Key Performance Summary

Table 15. Key performance summary for all sites.

Site	Country	Climate	Pinstalled (kWp)	EAC (kWh)	PR (%)	Yf (kWh/kWp)	CF (%)
AZS	Israel	Semi-arid	12.6	7 645	62	608	14.5
FSC	Italy	Coastal Mediterranean	4.8	3 197	53	666	12.7
UTH	Greece	Continental Mediterranean	14.4	10 703	66	743	14.5
BW	Germany (BW)	Temperate humid	16	6 338	62	396	11.3
HU	Germany (Berlin)	Temperate humid	3.78	641	31	170	3.5

Performance Ratio (PR) Gradient

A clear north–south gradient is observed:

- Southern sites (UTH, AZS) achieved the highest PR (≈ 65 %), due to strong irradiance and lower diffuse fractions.
- The Italian FSC site showed a modest PR (≈ 53 %) reflecting spectral attenuation through the arched polyethylene roof.
- Northern sites (BW and HU) exhibited lower PR values, primarily due to high diffuse fractions and reduced winter insolation.
- The HU pilot, while smaller, provided an essential benchmark for bifacial performance under extreme diffuse conditions.

Specific Yield (Yf) and Capacity Factor (CF)

- **Yf** increased with site irradiance: AZS < FSC < UTH reflects the solar resource gradient from Mediterranean coastal to inland Greece.
- **CF** remained in the 10–15 % range for most sites, confirming high inverter uptime and stable system control.
- The HU site's CF (~3.5 %) aligns with Berlin's limited sunlight (≈ 1 000 kWh/m² yearly).

Funded by the European Union

Funded by the European Union under Grant Agreement No 101096056. Views and opinions expressed are however those of the author(s) only and do not necessarily reflect those of the European Union or CINEA. Neither the European Union nor the granting authority can be held responsible for them.

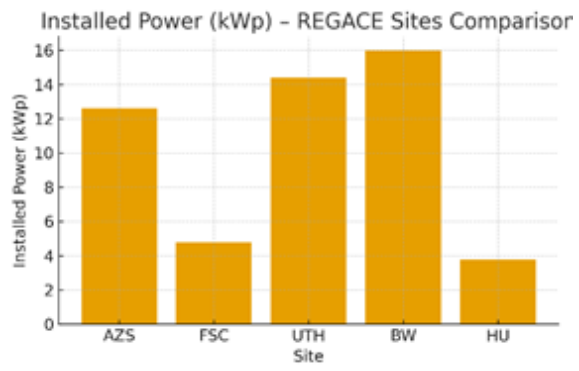	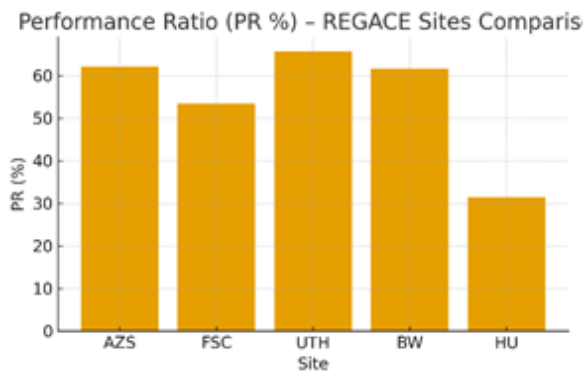
Installed capacities vary from 3.78 kWp (HU) to 16 kWp (BW), reflecting site-specific greenhouse dimensions and available roof area.	Performance Ratio (PR %) – REGACE Sites Comparison average PR values range from ≈ 31 % (HU) to ≈ 66 % (UTH), confirming high system efficiency in southern climates and stable operation in temperate sites.
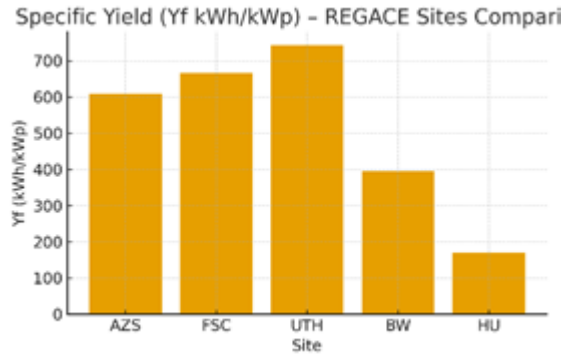	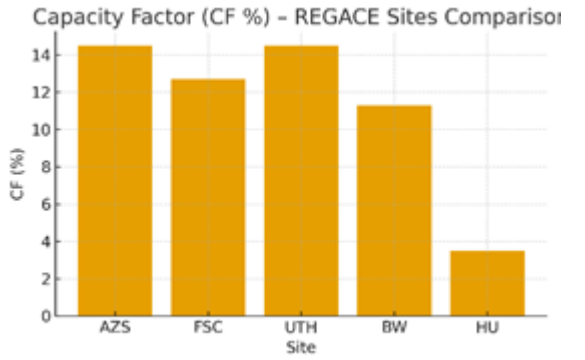
Specific yield increases toward southern latitudes, exceeding 700 kWh/kWp at UTH, while northern sites show lower output due to diffuse-light dominance.	Capacity factors cluster around 11–15 % for most sites, with a minimum of ≈ 3.5 % at HU (Berlin), matching the regional solar availability.

Figure 25. Comparison of the Performance Ratio, Installed capacities, Specific yield and the Capacity factors between the REGACE sites (March – September 2025).

Climatic and Structural Influences

- Greenhouse architecture (arched vs. twin-arched roofs) affects internal irradiance uniformity and rear-side contribution.
- Diffuse-to-direct ratio strongly governs bifacial gains: southern sites profit from direct irradiance, whereas northern ones rely on albedo and internal reflection.
- Temperature impacts are more pronounced at AZS, where high module temperatures slightly reduce PR during summer months.
- Optical transmittance of the polyethylene cover remains a limiting factor at all sites, underscoring the need for optimized greenhouse glazing.

Funded by the European Union

Funded by the European Union under Grant Agreement No 101096056. Views and opinions expressed are however those of the author(s) only and do not necessarily reflect those of the European Union or CINEA. Neither the European Union nor the granting authority can be held responsible for them.

Overall Conclusions

Across all pilots, REGACE systems demonstrated reliable operation, stable PR values, and effective tracking control under diverse climates. Dynamic bifacial PV integration within greenhouses consistently achieved:

- Energy yields between 400–750 kWh/kWp per season;
- Average PR values > 60 % (except HU);
- Minimal seasonal degradation;
- Strong correlation between irradiance, yield, and crop-light requirements.

These results confirm that the REGACE dynamic greenhouse system is replicable and scalable across Europe, supporting both energy efficiency and agronomic productivity.

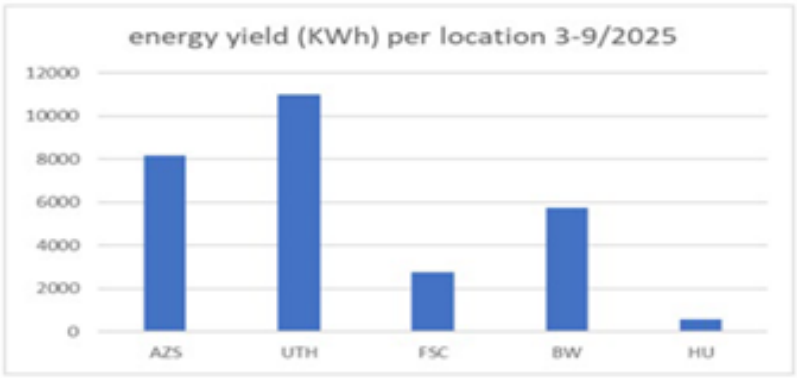

Figure 26. Monthly energy output for each of the REGACE systems (March – September 2025).

It should be noted that several installations underwent temporary disconnections, adjustments, or configuration changes as part of the research protocol. Consequently, the systems did not operate continuously or at full nominal capacity, and the reported energy yields (Figure 26) represent experimental rather than uninterrupted operational performance.

Among all sites, the UTH system achieved the highest energy output, attributed to favourable climatic conditions, effective greenhouse climate control, and stable irradiance. Short-term reductions in output at other sites were primarily linked to planned research interventions and maintenance activities. Therefore, the presented data likely underestimate the full annual energy potential that would be achieved under continuous operation.

Literature

Sohani, A., Pierro, M., Moser, D., & Cornaro, C. (2025). Comparison of physical models for bifacial PV power estimation. Energy Conversion and Management, 327, 119515.

Funded by the European Union

Funded by the European Union under Grant Agreement No 101096056. Views and opinions expressed are however those of the author(s) only and do not necessarily reflect those of the European Union or CINEA. Neither the European Union nor the granting authority can be held responsible for them.

3.2.3 Site Analyses – System Behaviour and Operational Performance

UTH Site – System Behaviour and Operational Performance

The monthly PV system output (KWh) for April and August 2025 installed inside UTH greenhouses. The total energy yield for each month was prospectively April 1516.9 KWh and August 1760.1 KWh.

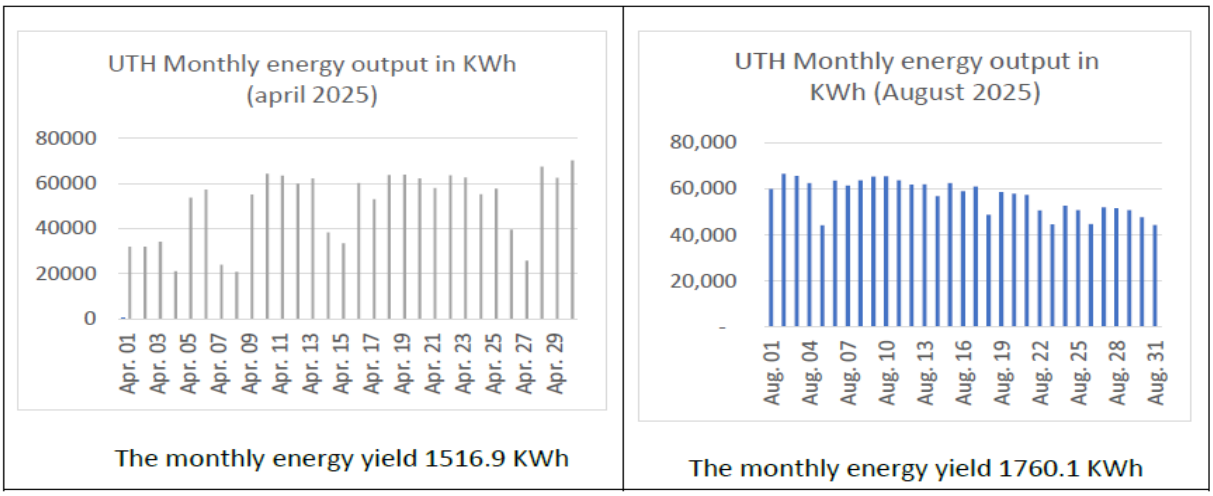

Figure 27. Monthly PV system output (KWh) for April and August 2025 inside the UTH greenhouses.

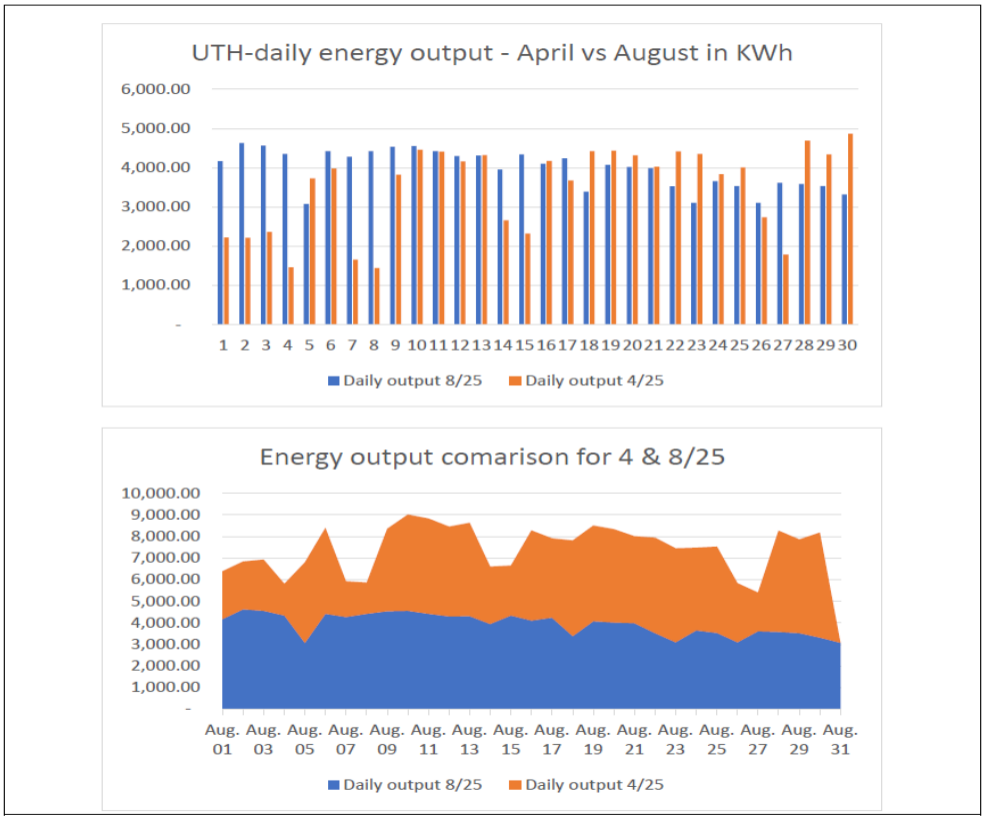

Figure 28. Comparison between April's and August's daily energy output.

Funded by the European Union

Funded by the European Union under Grant Agreement No 101096056. Views and opinions expressed are however those of the author(s) only and do not necessarily reflect those of the European Union or CINEA. Neither the European Union nor the granting authority can be held responsible for them.

Figure 29. Daily PV yield at the UTH greenhouse.

Figure 29 shows the final yield analysis, expressed in kilowatt-hours per kilowatt-peak (kWh/kWp), demonstrated significant variability in system performance across the pilot sites during 2025. The highest energy output was recorded at the UTH site, reaching 1,760.1 kWh with an installed PV capacity of 14.4 kWp, corresponding to a specific yield of 5.55 kWh/kWp/day and a capacity factor of 18.37%.

One of the key factors contributing to this exceptionally high performance at the UTH site is the enhanced light reflectance (albedo effect) generated by the greenhouse's shading net. The reflective properties of the net increase the amount of diffused radiation incident on the rear side of the bifacial panels, effectively improving total energy yield. As shown in the measurement results, the albedo contribution to total energy generation at UTH is among the highest across all pilot sites, confirming the significant role of reflected light in optimizing the bifacial PV performance within controlled greenhouse environments.

BW Site – System Behaviour and Operational Performance

The behaviour of the daily energy output for the PV system in BW during clear summer day (19/08/2025), shows a total yield of 49.2 KWh.

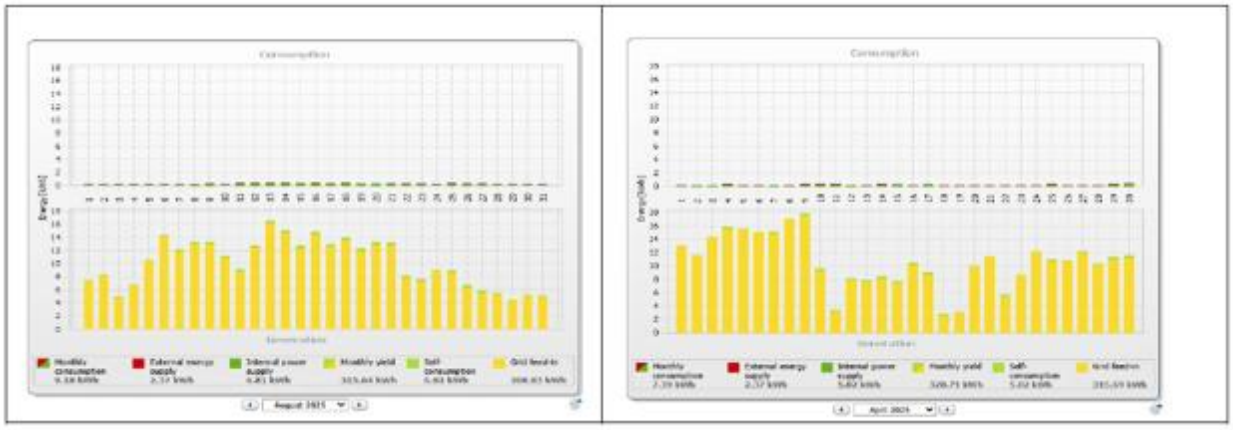

Figure 30. Monthly PV system output (KWh) for April and August 2025 inside the BW greenhouse.

Funded by the European Union under Grant Agreement No 101096056. Views and opinions expressed are however those of the author(s) only and do not necessarily reflect those of the European Union or CINEA. Neither the European Union nor the granting authority can be held responsible for them.

Funded by the European Union

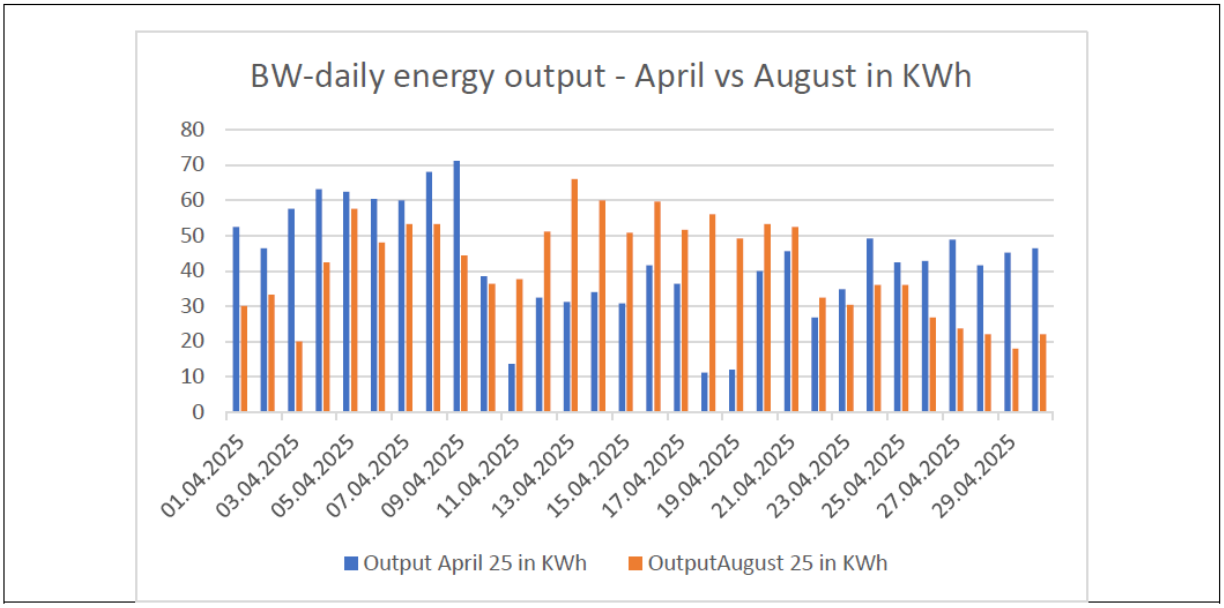

Figure 31. Comparison of the monthly PV system outputs (KWh) for April and August 2025 in the BW greenhouse.

Figures 30 and 31 present the monthly PV system output (KWh) for April and August 2025 of the BW greenhouses. The total energy yield for each month was prospectively in April 1282.4 KWh and August 1262 KWh.

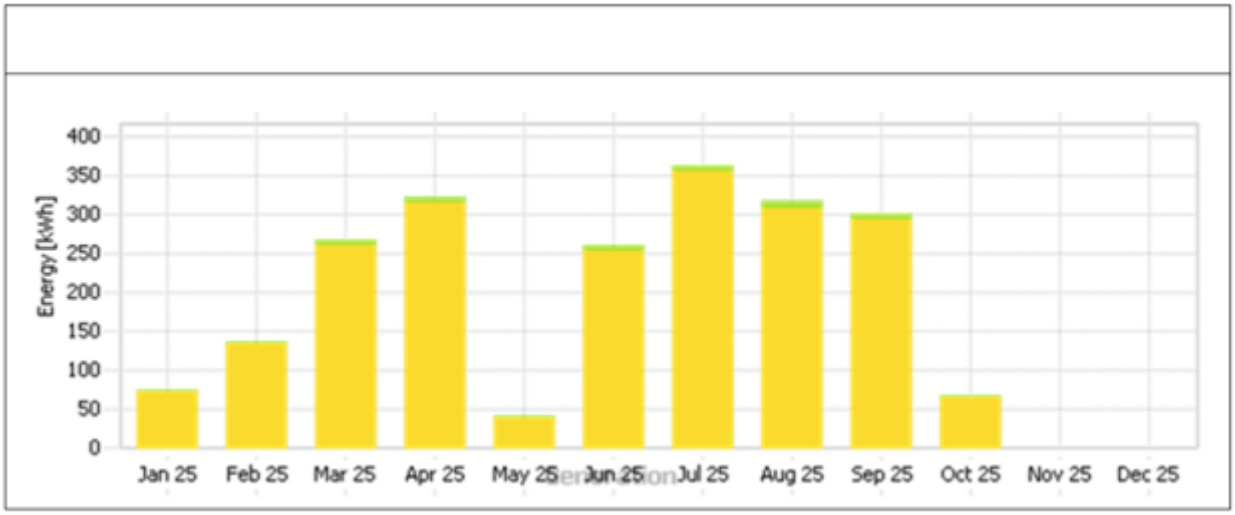

Figure 32. Monthly PV system output (KWh) for Jan. and Oct. 2025 in the BW greenhouse.

Figure 32 shows the monthly PV system output (KWh) for Jan. to Oct. 2025 in the BW greenhouses. Jul. 25 shows the max energy yield with 1400 KWh and with performance of 3.96 KWh/KWp. During May 25 the system was disconnected for technical maintenance and repair.

Funded by the European Union

Funded by the European Union under Grant Agreement No 101096056. Views and opinions expressed are however those of the author(s) only and do not necessarily reflect those of the European Union or CINEA. Neither the European Union nor the granting authority can be held responsible for them.

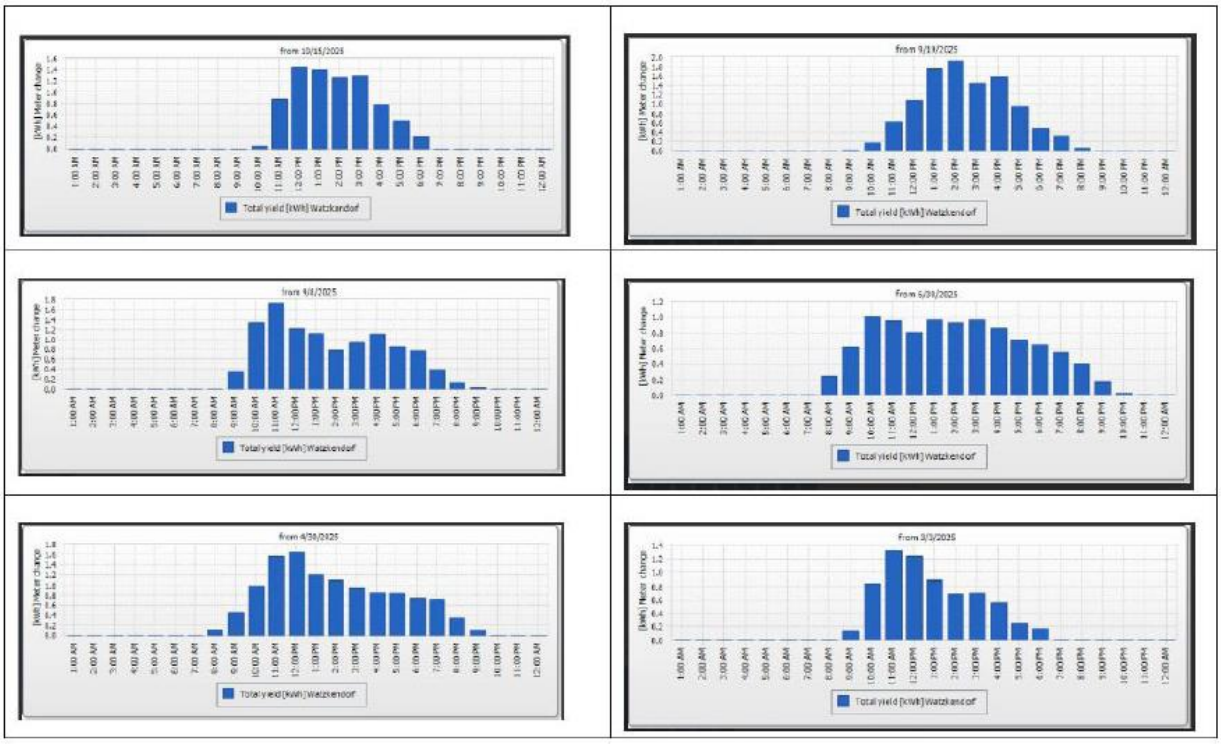

Figure 33. Daily energy production over a six-month period in 2025.

The graphs in Figure 33 indicate that the generation curves are not uniform throughout the day — there is noticeable variation in output patterns between morning and afternoon hours. In several months, peak energy production occurred during the early or late hours of the day, rather than around midday as typically observed in standard PV installations. Only one month exhibited a normal, bell-shaped generation curve. This phenomenon is primarily attributed to the structural orientation and geometry of the greenhouse, which causes partial shading of the PV panels at different times of the day, thereby influencing the overall energy production profile.

FSC Site – System Behaviour and Operational Performance

The behaviour of the daily / monthly/ yearly energy output for the PV system at the FSC site during the year 2025 is demonstrated in Figure 34.

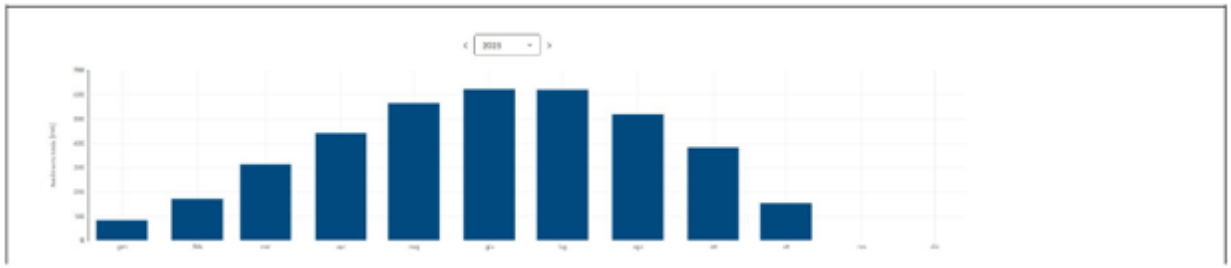

Figure 34. Monthly PV system output (KWh) for Jan. to Oct. 2025 in the FSC greenhouse.

Funded by the European Union under Grant Agreement No 101096056. Views and opinions expressed are however those of the author(s) only and do not necessarily reflect those of the European Union or CINEA. Neither the European Union nor the granting authority can be held responsible for them.

Figure 35 presents the monthly PV system output (KWh) for Jan. to Oct. 2025 in the FSC greenhouses. The maximum energy yield with 1400 KWh was received in month Jun. 25 with 622.7 KWh and with a performance of 4.18 KWh/KWp.

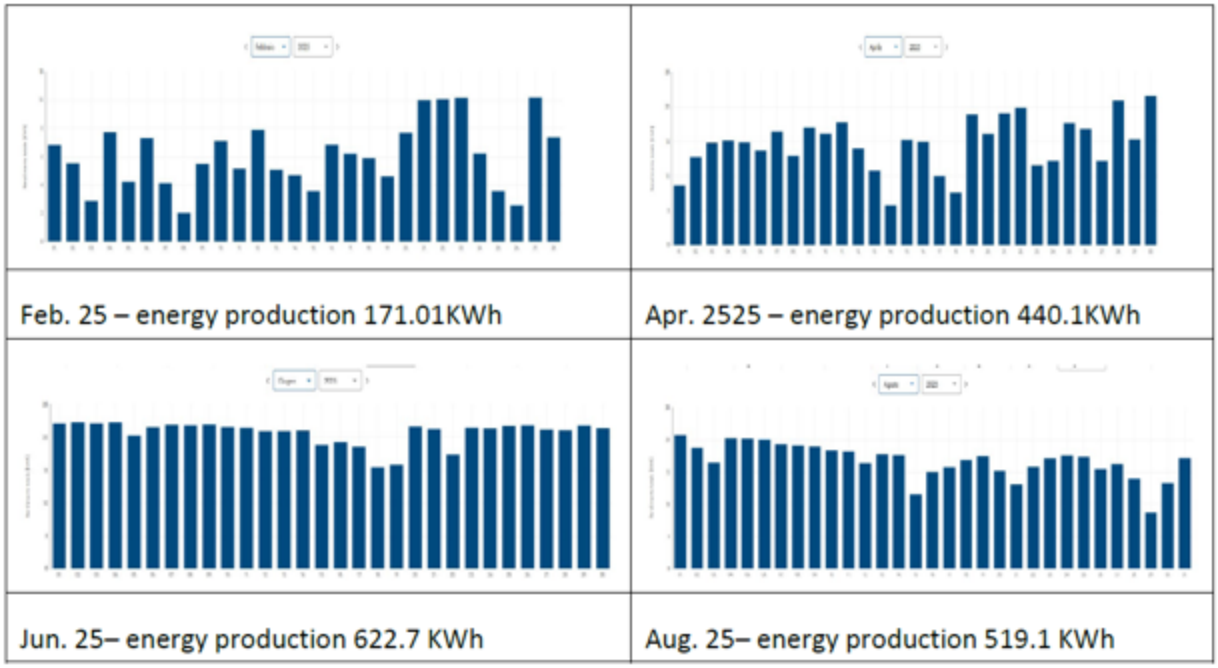

Figure 35. Average monthly energy output over four months during the year 2025.

HU Site – System Behaviour and Operational Performance

As indicated in Figure 36, the maximal received energy production was during Ju. 25 with 127.68 KWh resulting in a system performance of 1.15 KWh/KWp. The chart presents the lowest energy production values in all Regace sites due to the fact that the HU system was disconnected many times during this period due to technical necessities in the building.

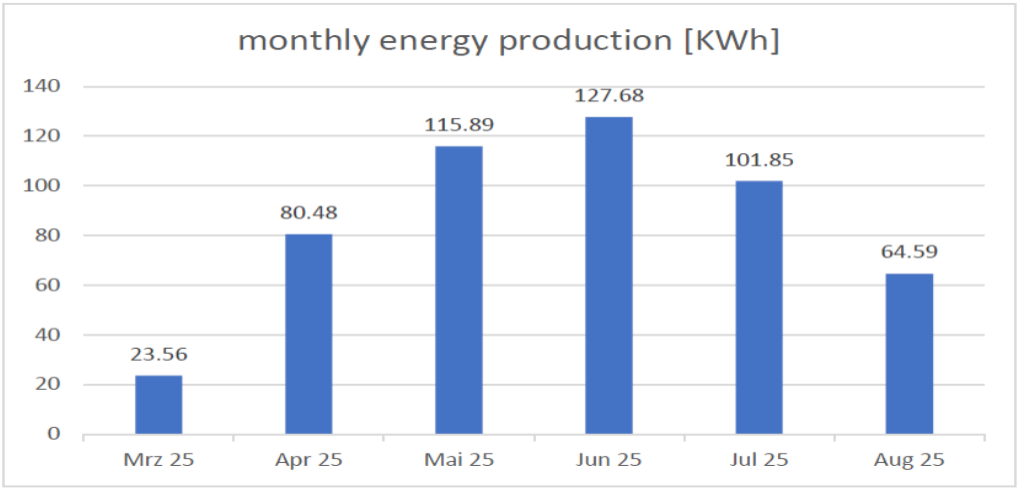

Figure 36. Monthly PV system output (KWh) for Jan. to Oct. 2025 in the HU greenhouse.

Funded by the European Union

Funded by the European Union under Grant Agreement No 101096056. Views and opinions expressed are however those of the author(s) only and do not necessarily reflect those of the European Union or CINEA. Neither the European Union nor the granting authority can be held responsible for them.

The Final Yield (YF) expressed as kWh per kWp was calculated from the inverter data in all greenhouses (Table 15). The final yield is a key performance indicator that reflects the actual energy output per unit of installed PV capacity. In the REGACE project, where PV modules are installed in diverse greenhouse environments, final yield serves as a normalized metric that allows for fair comparison across different systems, climates, and designs. Due to the fact that the Regace greenhouse differs in Geographic location (e.g., AZS, FSC, HU), Greenhouse structure and cover material, shading, tracking mode and Irradiance levels and crop types using final yield, enables comparing between the systems independently of size, allowing us to assess which combinations of design and integration provide the best energy return per installed kWp. In addition, in agrivoltaics, we must balance energy production with crop productivity. More transparent panels or reduced coverage may support plant growth but reduce energy yield. Final yield helps quantify how much energy is produced under each configuration, allowing us to evaluate the effect of transparency or spacing, compare bifacial vs. monofacial panels and assess energy losses due to shading or structure.

3.2.4 Electrical Performance and MPP Analysis

The electrical performance of the photovoltaic (PV) systems was continuously monitored across the five REGACE pilot sites using inverter data. All measurements were archived in a shared Google Drive database accessible to project partners.

For this analysis, five representative systems — AZS, UTH, FSC, BW, and HU — were evaluated based on key performance indicators, including total energy output and Maximum Power Point (MPP) parameters (Pmpp, Impp, and Vmpp). Two reference days — 15 April 2025 and 15 June 2025 — were selected to compare system behaviour under distinct seasonal and irradiance conditions.

The monitoring platforms (SMA Sunny Portal and GoodWe SEMS Portal) provided reliable real-time data but did not include I–V curve tracing capabilities. Consequently, the analysis relied on inverter-recorded DC current and voltage data at the Maximum Power Point Tracking (MPPT) level. From these, the Impp, Vmpp, and Pmpp time-series were derived to represent real-world electrical operating behaviour.

Although not equivalent to full I–V diagnostics, this method provides robust insight into system stability, tracking efficiency, and irradiance response under greenhouse conditions. The Impp trends in particular serve as indicators of incident light and optical transmission efficiency, while Vmpp and Pmpp variations reveal differences in module temperature, shading, and dynamic control behaviour.

This monitoring approach supports the broader REGACE objective of optimizing the energy–crop balance within agrivoltaic greenhouses. The following section presents comparative inverter-based performance data from UTH, FSC, and HU, illustrating system behaviour under real operational field conditions.

Funded by the European Union

Funded by the European Union under Grant Agreement No 101096056. Views and opinions expressed are however those of the author(s) only and do not necessarily reflect those of the European Union or CINEA. Neither the European Union nor the granting authority can be held responsible for them.

Locations	Impp DC-Current / Time
UTH-camber 1	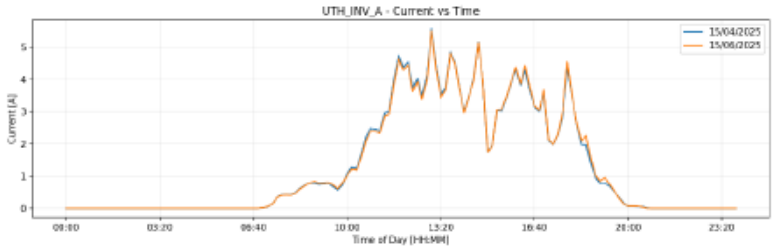
UTH-camber 2	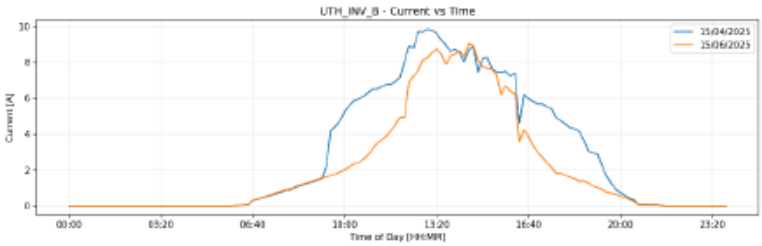
FSC	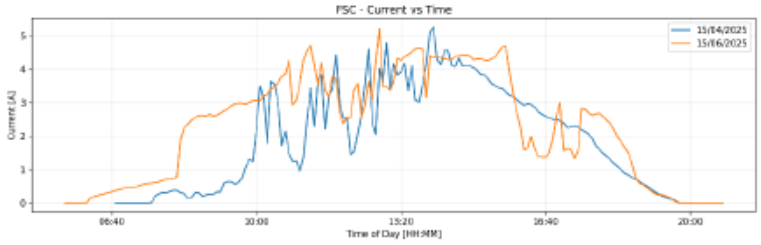
HU	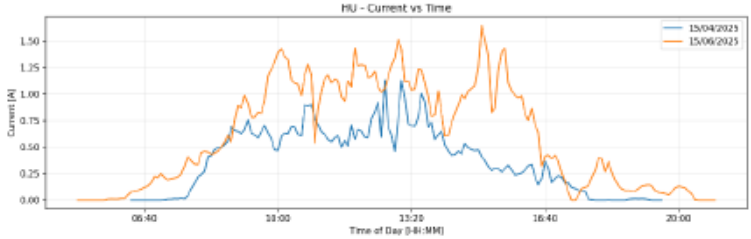

Figure 37. Variation in Impp (maximum power point current) during a representative day for systems installed at three REGACE sites.

Funded by the European Union under Grant Agreement No 101096056. Views and opinions expressed are however those of the author(s) only and do not necessarily reflect those of the European Union or CINEA. Neither the European Union nor the granting authority can be held responsible for them.

Locations	Vmpp DC-Voltage / Time
UTH-camber 1	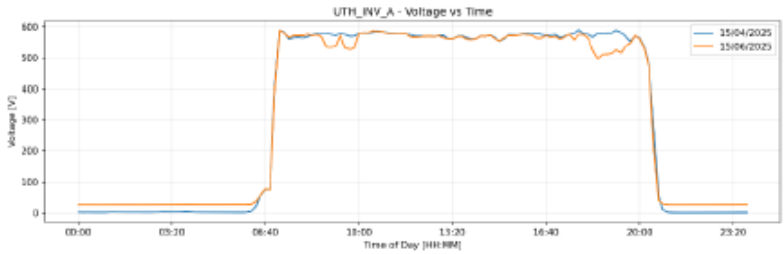
UTH-camber 2	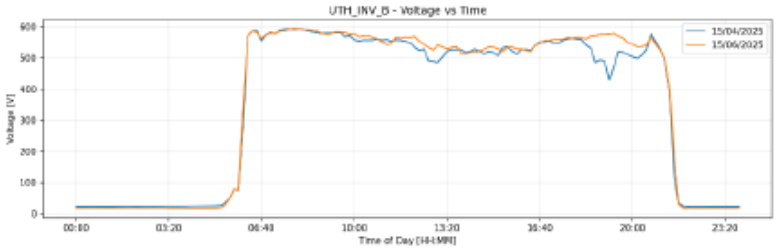
FSC	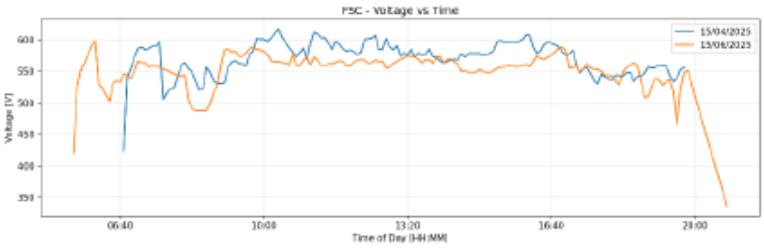
HU	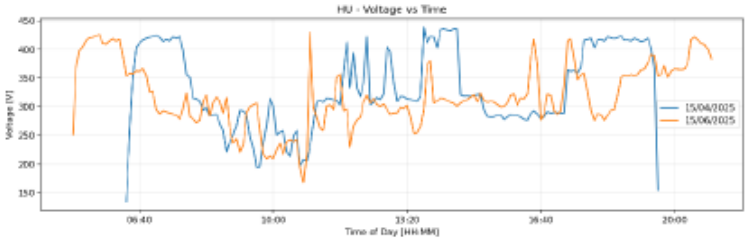

Figure 38. Vmpp (maximum power point voltage) curves recorded on April 15, 2025 and June 15, 2025, based on two representative days of measurements for the different systems at three test locations.

Funded by the European Union

Funded by the European Union under Grant Agreement No 101096056. Views and opinions expressed are however those of the author(s) only and do not necessarily reflect those of the European Union or CINEA. Neither the European Union nor the granting authority can be held responsible for them.

Locations	Mppt DC-Power / Time
UTH-camber 1	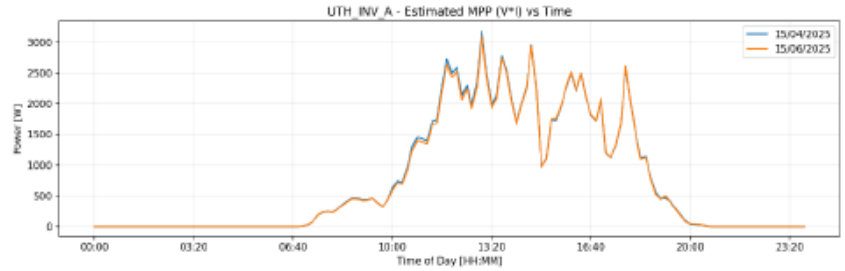
UTH-camber 2	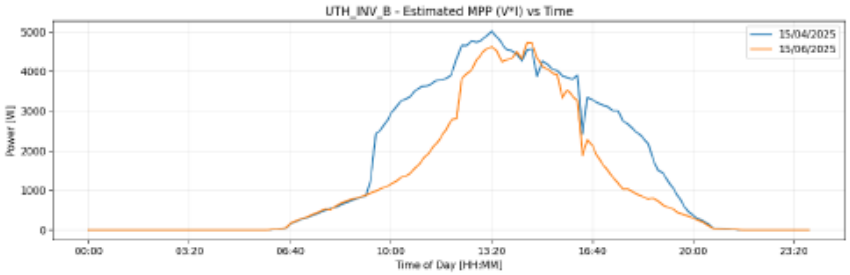
FSC	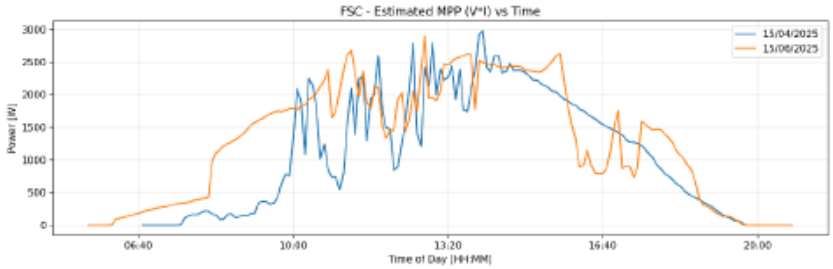
HU	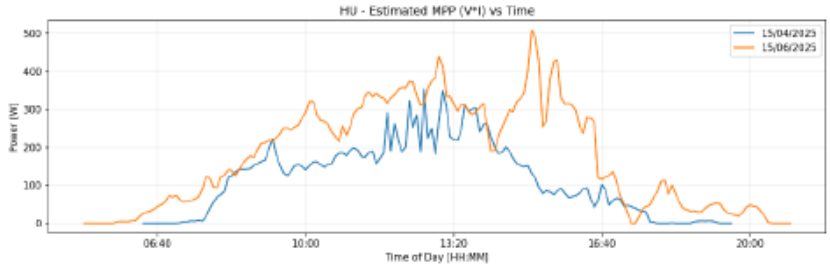

Figure 39. Pmpp (maximum power point power) curves recorded over a representative day for the different systems installed at three pilot locations.

Funded by the European Union

Funded by the European Union under Grant Agreement No 101096056. Views and opinions expressed are however those of the author(s) only and do not necessarily reflect those of the European Union or CINEA. Neither the European Union nor the granting authority can be held responsible for them.

The following graphs present the electrical performance data collected from the inverters at the three analysed sites UTH, FSC and HU, providing a comparative assessment of their operational behaviour under real field conditions and illustrating the influence of local environmental conditions and greenhouse structural design on current behaviour and light interception efficiency (Figures 37-39).

The comparison between sites reveals clear differences in the daily power generation profiles, which are primarily influenced by local irradiance patterns, greenhouse orientation, and shading conditions. In some locations, the curves show multiple local peaks during the day, indicating intermittent shading and light reflection effects typical of greenhouse-integrated PV systems. These variations demonstrate the dynamic interaction between environmental conditions and system configuration, emphasizing the importance of site-specific design and adaptive control strategies to optimize energy performance.

Correlation Between Environmental Conditions and PV Panel Electrical Performance

To validate the electrical performance metrics of the photovoltaic system, including Pmpp (maximum power), Vmpp (voltage at maximum power point), and Impp (current at maximum power point), an integrated analysis was conducted using irradiance, ambient temperature, and panel temperature data collected throughout the day at the experimental sites. This approach enables a deeper understanding of how real-time environmental conditions influence the behaviour of the PV system in agrivoltaic greenhouse applications. The DC current (Impp) generated by the PV modules is directly influenced by the intensity of incoming solar radiation. Our data shows a clear correlation between periods of high irradiance and peak Impp values. Sites that exhibited stable, high irradiance levels throughout the day demonstrated higher Impp outputs, indicating efficient light harvesting and energy conversion. Conversely, sites affected by intermittent cloud cover or structural shading showed significant drops in Impp during those periods. Vmpp is known to be temperature-dependent, with higher panel temperatures typically reducing the voltage output. This was clearly observed in the data: sites with higher ambient temperatures and limited greenhouse ventilation exhibited a drop in Vmpp during midday hours, leading to a corresponding decrease in Pmpp. In contrast, locations with either natural ventilation or more thermally diffusive greenhouse coverings maintained lower panel temperatures and achieved higher voltage values, which positively impacted total power generation, which is the case in UTH and UH Greenhouses.

The following graphs present the global solar radiation, ambient temperature, and module temperature recorded on April 15, 2025, and June 15, 2025, at the four analysed sites. These parameters were measured concurrently with the electrical outputs in order to understand the influence of environmental conditions on system performance. The results clearly indicate that radiation intensity and temperature are inversely correlated with the electrical efficiency of the PV modules. While higher solar irradiance increases the available energy for conversion, it simultaneously leads to a rise in module temperature, which negatively affects the voltage at the maximum power point (Vmpp) due to the inherent temperature sensitivity of semiconductor materials. A comparison between April and June reveals this effect distinctly:

Funded by the European Union under Grant Agreement No 101096056. Views and opinions expressed are however those of the author(s) only and do not necessarily reflect those of the European Union or CINEA. Neither the European Union nor the granting authority can be held responsible for them.

	Impact of front and rear radiation on system performance in four sites	
site	Radiation 15-06-25	Radiation 15-04-25
UTH Chamber 4	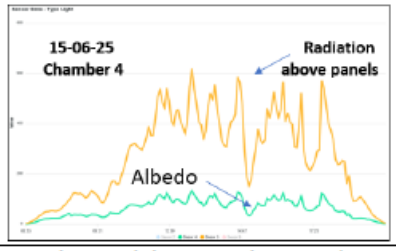	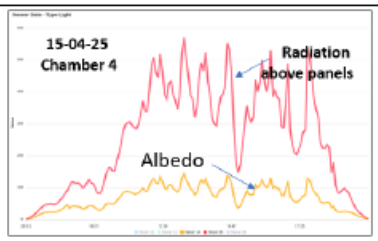
	Solar Modules in tracking mode	Solar Modules in tracking mode
UTH Chamber 5	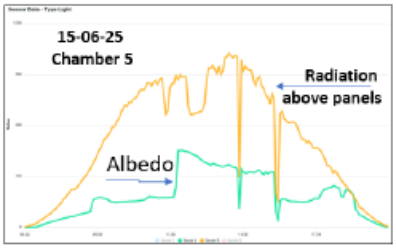	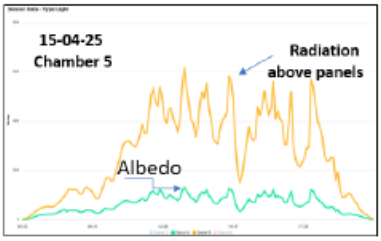
	Solar Modules position parallel to sun	Solar Modules in tracking mode
FSC	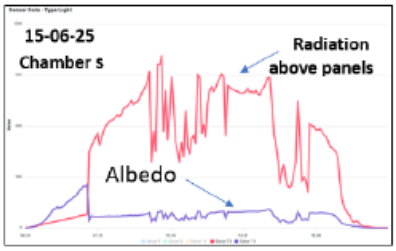	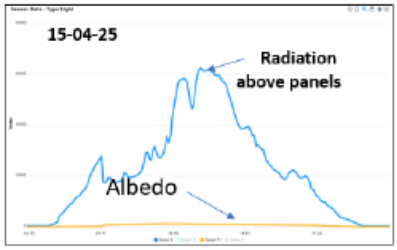
	Solar Modules in tracking mode	Solar Modules in tracking mode
HU	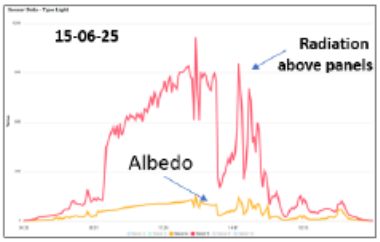	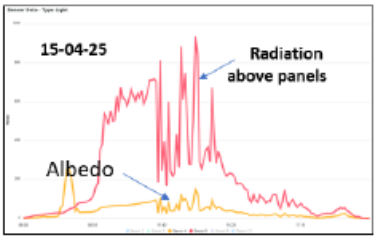
	Solar Modules in tracking mode	Solar Modules in tracking mode
AZS	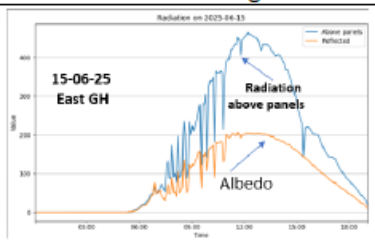	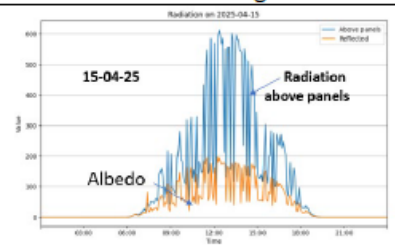
	Solar Modules in parallel mode *	Solar Modules in tracking mode

Figure 40. Radiation intensity on the front (top) side of the photovoltaic modules and the reflected albedo radiation from various ground surface types across different pilot sites — cement at UTH and HU, bare soil at FSC, and a white reflective sheet at AZS.

Funded by the European Union under Grant Agreement No 101096056. Views and opinions expressed are however those of the author(s) only and do not necessarily reflect those of the European Union or CINEA. Neither the European Union nor the granting authority can be held responsible for them.

Funded by the European Union

- In April, moderate irradiance and lower ambient temperatures (typically between 18–25°C) maintained relatively stable module temperatures around 32–38°C, resulting in higher voltage stability and overall energy conversion efficiency.
- In June, however, elevated irradiance levels combined with greenhouse heat accumulation led to module surface temperatures exceeding 50–55°C, which caused a measurable drop in voltage (Vmpp) and a corresponding reduction in output power (Pmpp).

This thermal impact was especially evident at the AZS site, where high ambient temperatures and limited natural ventilation amplified heat retention, emphasizing the need for advanced cooling and ventilation strategies in semi-arid climates. Conversely, at the UTH site, the presence of a reflective shading net contributed to enhanced light diffusion and reduced localized heating, which helped maintain better thermal equilibrium and voltage consistency (Figure 40).

Overall, the results demonstrate that effective heat management and albedo optimization are key factors in maintaining high performance of greenhouse-integrated PV systems. Implementing materials with higher reflectivity and developing adaptive ventilation systems can significantly mitigate thermal stress, ensuring more stable operation and improving long-term efficiency of the agrivoltaic installations.

At chamber 5 in UTH, on 15/06/2025, the modules were operated in a parallel-to-sun fixed position rather than in active tracking mode. Under this configuration, the rear-side albedo contribution peaked at approximately 35% of the front-side irradiance. While this setup enhanced rear-side irradiation, it significantly reduced the direct irradiance on the front side, resulting in a substantial drop in energy yield (Figure 41).

Also, at the AZS greenhouse, on 15/06/2025, the solar modules were operated in parallel mode. During this configuration, the albedo radiation reached notably high values due to the presence of a reflective white plastic ground sheet. This setup enhanced the rear-side irradiance of the bifacial modules, resulting in a noticeable increase in PV system energy output.

As indicated in Figure 41, in all measurement periods, the temperature of the PV modules was consistently higher than the ambient temperature, as expected due to solar absorption and internal heat generation within the cells. During April, the module temperature remained relatively close to the ambient temperature, indicating moderate irradiance and efficient heat dissipation. In June, however, the module temperature was noticeably higher (7-10 ^{0}C), reflecting stronger solar irradiance and higher ambient conditions typical of early summer.

Funded by the European Union

Funded by the European Union under Grant Agreement No 101096056. Views and opinions expressed are however those of the author(s) only and do not necessarily reflect those of the European Union or CINEA. Neither the European Union nor the granting authority can be held responsible for them.

Impact of Panel Temperature on system performance in four locations		
site	Ambient and Panel Temperature 15-06-25	Ambient and Panel Temperature 15-04-25
UTH Chamber 4	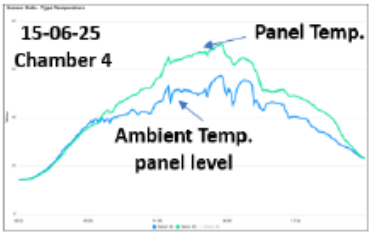	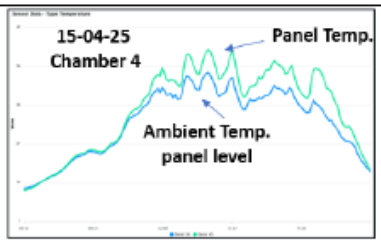
	Solar Modules in tracking mode	Solar Modules in tracking mode
UTH Chamber 5	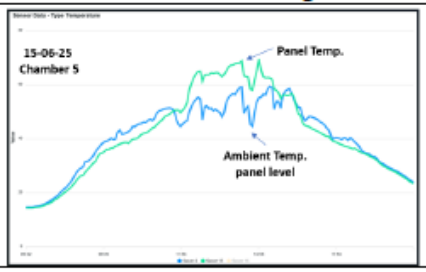	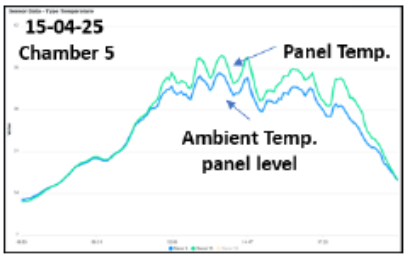
	Solar Modules position parallel to sun	Solar Modules in tracking mode
FSC	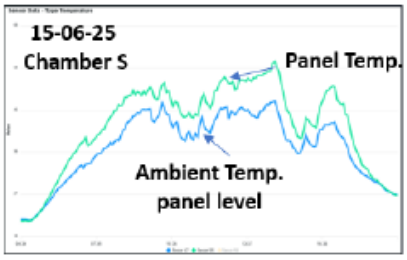	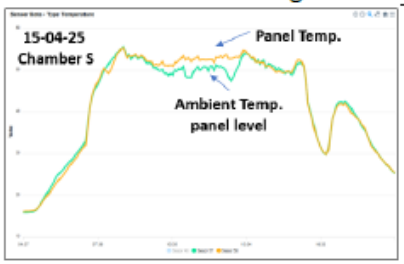
	Solar Modules in tracking mode	Solar Modules in tracking mode
HU	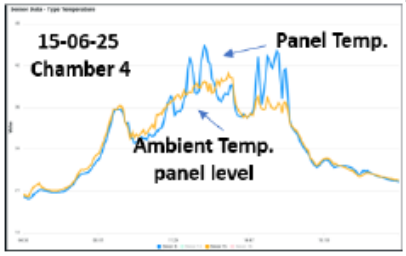	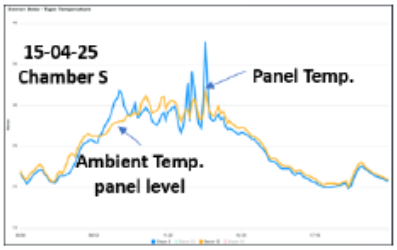
	Solar Modules in tracking mode	Solar Modules in tracking mode
AZS	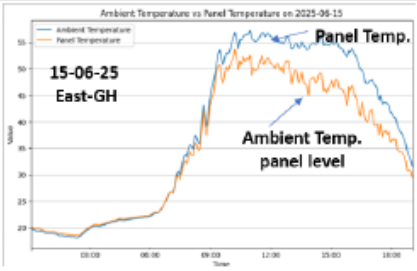	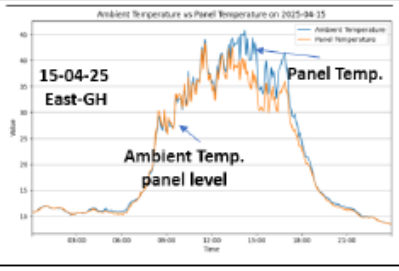

Figure 41. Module surface temperature and ambient air temperature in the vicinity of the solar installation area.

Funded by the European Union under Grant Agreement No 101096056. Views and opinions expressed are however those of the author(s) only and do not necessarily reflect those of the European Union or CINEA. Neither the European Union nor the granting authority can be held responsible for them.

	Impact of Panel position (tracking VS Fix, Parallel) on system performance in four locations	
site	Ambient and Panel Temperature 15-06-25	Ambient and Panel Temperature 15-04-25
UTH Chamber 4		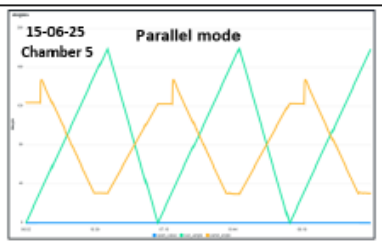
	Solar Modules in tracking mode	Solar Modules in tracking mode
UTH Chamber 5	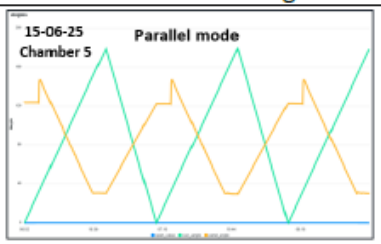	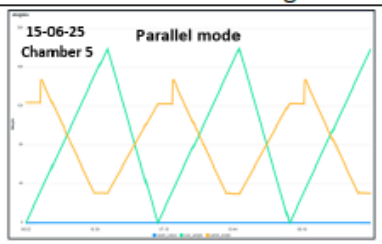
	Solar Modules position parallel to sun	Solar Modules in tracking mode
FSC	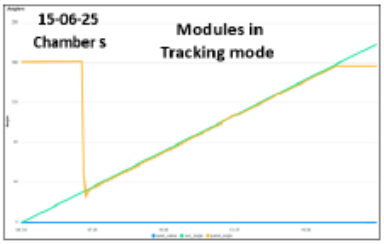	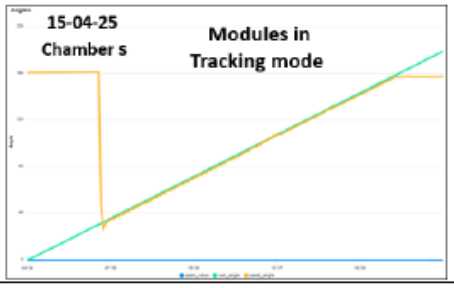
	Solar Modules in tracking mode	Solar Modules in tracking mode
HU	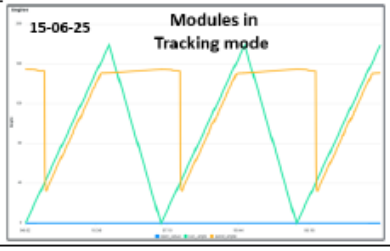	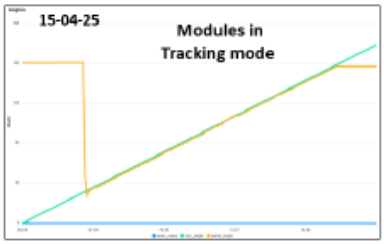
	Solar Modules in tracking mode	Solar Modules in tracking mode
AZS	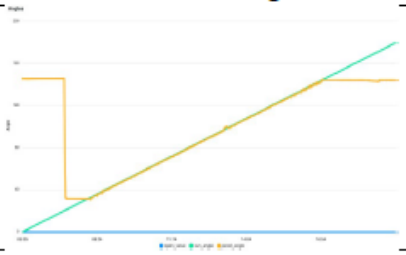	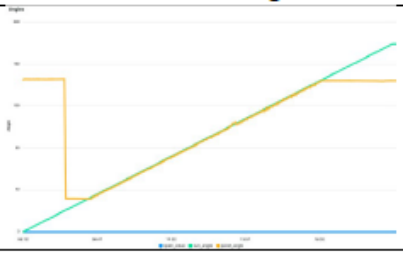

Figure 42. Tracking positions of the solar panels within the greenhouse system.

Funded by the European Union

Funded by the European Union under Grant Agreement No 101096056. Views and opinions expressed are however those of the author(s) only and do not necessarily reflect those of the European Union or CINEA. Neither the European Union nor the granting authority can be held responsible for them.

During the electrical performance measurements conducted on April 15, 2025, and June 15, 2025, the majority of PV modules operated in full sun-tracking mode. However, an exception was observed in Chamber 5 at the UTH site, where the panels were set to a fixed tilt position, oriented parallel to the sun's angle rather than actively tracking (Figure 42).

As shown in the radiation distribution graphs above the solar panels (Figure 42), the light spread is neither uniform nor consistent. This uneven distribution often results from the structural geometry of the greenhouse or specific shading conditions on the measurement days. Such irregularity directly affects the electrical output of the PV systems observed during the two testing days.

Moreover, the light intensity within the greenhouse is significantly influenced by the properties of the greenhouse covering — particularly its transparency and light diffusion characteristics — as well as by dust accumulation on the surfaces. These factors critically determine the internal light dynamics and consequently impact both solar energy production and plant development.

By aligning environmental parameters with the electrical behaviour of the PV systems, we gain valuable insights to the impact of the greenhouse design affecting PV performance and the role of microclimate control in optimizing energy yield. This result shows a critical role in REGACE's overarching goal: identifying optimal design parameters that balance electricity production with agronomic viability inside greenhouses. It also highlights the need for future improvements in dynamic control systems that respond not only to solar angle but also to temperature build-up and irradiance distribution inside the greenhouse environment.

Discussion

The results obtained from the six REGACE greenhouse-integrated PV systems reveal that agrivoltaic performance strongly depends on the interplay between greenhouse architecture, climate conditions, and PV integration strategy. The data demonstrate clear seasonal and spatial variability in both the final yield and capacity factor across all sites, confirming that agronomic and structural design directly influence the energy generation potential.

Among all installations, the UTH site exhibited the highest performance, with a specific yield of up to 132.26 kWh/kWp and a capacity factor of 18.37%. This superior outcome is primarily attributed to the high albedo effect created by the greenhouse's shading net, which reflects a considerable fraction of the incoming solar radiation back onto the rear side of the bifacial panels. The enhanced reflectance increased the diffused light fraction, resulting in improved bifacial gain without compromising the light available for crop photosynthesis.

The AZS site in Israel showed strong energy generation during spring but a decline during summer months due to dust accumulation, partial shading geometry, and high ambient temperatures, all of which reduced PV efficiency. Nonetheless, the site provided valuable insights into thermal management challenges and

Funded by the European Union under Grant Agreement No 101096056. Views and opinions expressed are however those of the author(s) only and do not necessarily reflect those of the European Union or CINEA. Neither the European Union nor the granting authority can be held responsible for them.

demonstrated the importance of developing panel cooling and cleaning strategies for semi-arid environments.

At northern locations such as BW (Germany) and HU (Germany), lower irradiance levels and frequent interruptions resulted in reduced yields. Yet, these results are critical for understanding agrivoltaic feasibility in less favourable climates and highlight the need for adaptive tracking algorithms and optimized panel tilt configurations to enhance winter generation.

Another key finding across all sites is the impact of greenhouse orientation and panel string configuration on daily energy curves. Unlike conventional open-field PV systems, several sites exhibited non-uniform generation profiles, with peaks occurring in early or late daylight hours. This pattern results from structural shading and asymmetrical light distribution (energy output reduction due to partial string shading) within the greenhouse, emphasizing the need for string configurations, dynamic tracking and light management control that responds to real-time microclimate conditions rather than solar position alone.

Furthermore, analysis of the electrical parameters (Impp, Vmpp, Pmpp) under different environmental conditions confirmed a strong correlation between irradiance, panel temperature, and voltage stability. Sites with more efficient thermal dissipation and controlled ventilation (UTH) maintained higher Vmpp values and, consequently, higher Pmpp performance, validating the benefit of Trisolar's semi-transparent and thermally optimized panel design.

Conclusions

The REGACE WP3.2 study demonstrates that integrating photovoltaic modules within greenhouse structures is technically feasible and energetically efficient, provided that design parameters are tailored to each local climate and greenhouse type. The data collected across all European and Mediterranean test sites establish several key conclusions:

1. Site-specific design is essential**.** Energy yield and efficiency are directly influenced by greenhouse geometry, orientation, and cover material.
2. Albedo management is a critical design factor**.** High reflectance surfaces, such as shading nets or white reflective ground layers, can significantly increase bifacial PV performance by up to 15–20%.
3. Thermal control improves PV efficiency**.** Lower panel temperatures achieved through optimized ventilation and heat-dissipating layers contribute to higher voltage stability and reduced degradation rates.
4. Tracking and control algorithms are decisive**.** Dynamic sun-tracking systems that account for both solar geometry and greenhouse microclimate outperform fixed installations in overall yield and stability.
5. Agrivoltaic integration preserves agricultural viability**.** Preliminary crop results indicate that semi-transparent bifacial panels can maintain plant productivity while generating clean energy, supporting the dual-use land objective of the REGACE project.

Funded by the European Union under Grant Agreement No 101096056. Views and opinions expressed are however those of the author(s) only and do not necessarily reflect those of the European Union or CINEA. Neither the European Union nor the granting authority can be held responsible for them.

Funded by the European Union

In summary, the WP3.2 findings confirm that the agrivoltaic greenhouse concept developed within REGACE offers a scalable, sustainable, and high-efficiency solution for future agricultural energy systems. The observed energy yields — especially at UTH, FSC and AZS — validate the technical merit of the approach and provide a foundation for further optimization and standardization toward commercial deployment.

3.2.5 Characterisation of the PV system

FSC Site, Italy – PV Data monitoring and considerations

The monitoring activity of the PV system in the greenhouse is mainly focused on analysing the plant's production data.

To enable comprehensive monitoring of the PV system, a suite of sensors has been deployed symmetrically on both the east and west sides of the greenhouse. The suite includes the following components:

- two pyranometers mounted in-plane with PV modules to measure the Global Tilted Irradiance (GTI) and the Reflected Tilted Irradiance (RTI), (Figure 24 left);
- two back-of-module (TBOM) temperature sensors fixed directly on the rear surface of the PV panels to monitor thermal conditions affecting module efficiency and degradation (Figure 43 right);
- two illuminance sensors (luxmeters) positioned beneath the PV panel plane, one located in an area persistently free from panel-induced shading and the other intentionally placed in a region subject to shading. These allow differential measurement of light availability for the understory crop canopy (Figure 43 right).
- one combined temperature and relative humidity sensor and one CO_2 sensor, both installed beneath the panel structure to assess sub-panel microclimatic conditions (Figure 43 right);

Based on real-time feedback from these sensors, the control algorithm can trigger the reorientation of the panels to a near-vertical position in scenarios where light availability or CO_2 concentration beneath the panels falls below crop-sustaining thresholds. This ensures dynamic optimization of both energy harvesting and agronomic performance in the agrivoltaic system.

Figure 43. PV monitoring sensors: GTI & RTI (left), luxmeter, Temperature & relative humidity, CO_2 and TBOM sensors (right).

Funded by the European Union under Grant Agreement No 101096056. Views and opinions expressed are however those of the author(s) only and do not necessarily reflect those of the European Union or CINEA. Neither the European Union nor the granting authority can be held responsible for them.

The daily data are compared with the available solar radiation data inside the greenhouse on the plane of the PV array, both global and reflected (Figure 44). At the same time, the monthly and total historical data are examined to identify anomalies that are not related to weather conditions (Figure 45).

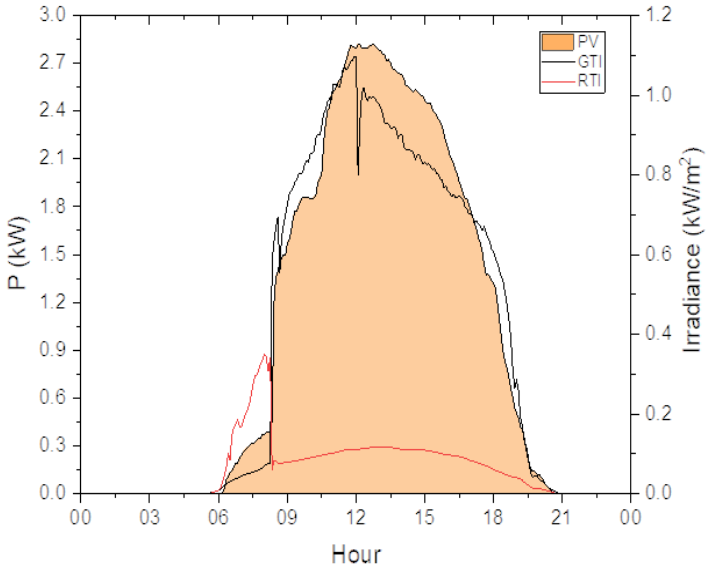

Figure 44. Daily power production compared with Global Tilted Irradiance (GTI) and Reflected Tilted Irradiance (RTI).

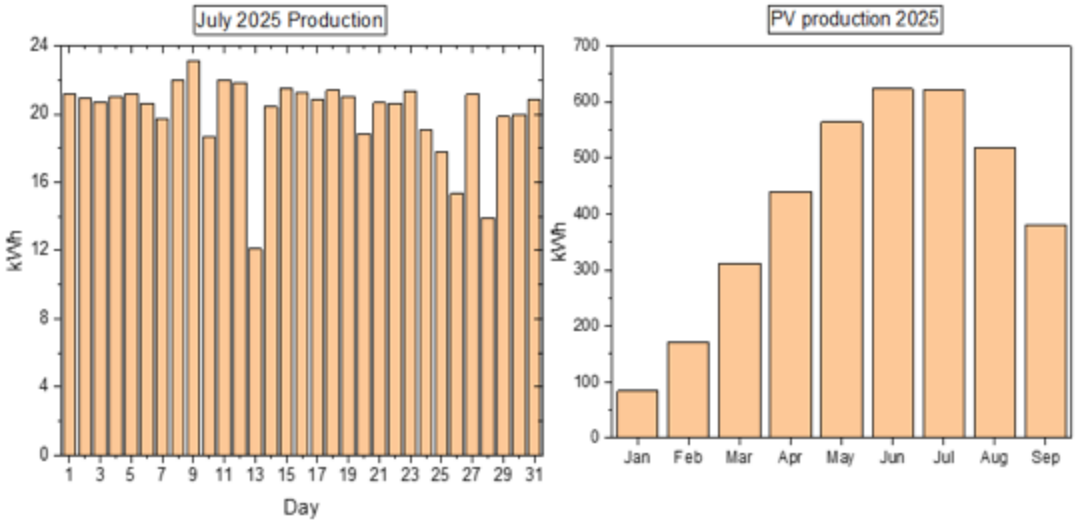

Figure 45. Daily (July 2025) and monthly (2025) energy production.

The search for anomalies is carried out by comparing the plant's production data with those of a model that has the same characteristics in terms of installed capacity, single-axis tracking, and the available direct and reflected radiation. This comparison makes it possible to identify any malfunctions in the system and, consequently, to carry out the necessary inspections on the plant.

Funded by the European Union

Funded by the European Union under Grant Agreement No 101096056. Views and opinions expressed are however those of the author(s) only and do not necessarily reflect those of the European Union or CINEA. Neither the European Union nor the granting authority can be held responsible for them.

The comparison between the actual production data and the outputs of the model applied to the FSC site revealed that the *in-situ* energy yield is approximately 25% lower, under identical conditions of orientation, tracking, and panel type. The model was also based on the measured values of Global Tilted Irradiance (GTI) and Reflected Tilted Irradiance (RTI) available inside the greenhouse, in order to ensure an accurate representation of the site's real operating conditions. The use of GTI and RTI inside the greenhouse to simulate the PV production eliminates the loss effect caused by the irradiance filtering of the plastic cover.

This discrepancy prompted a further investigation into the underlying causes of the reduced production. The initial hypothesis concerned potential shading effects from the greenhouse structure on the photovoltaic panels. To verify this assumption, the CAD model of the greenhouse was imported into the REVIT software (Solar Path tool), which enables simulation of the sun's position throughout the day and across different periods of the year.

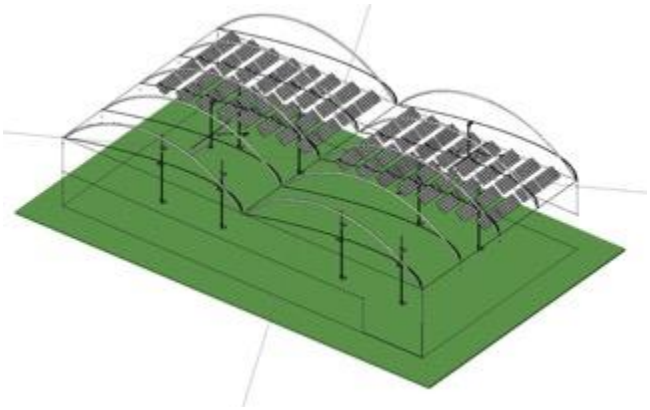

Figure 46. Shadow on the panel for June 21.

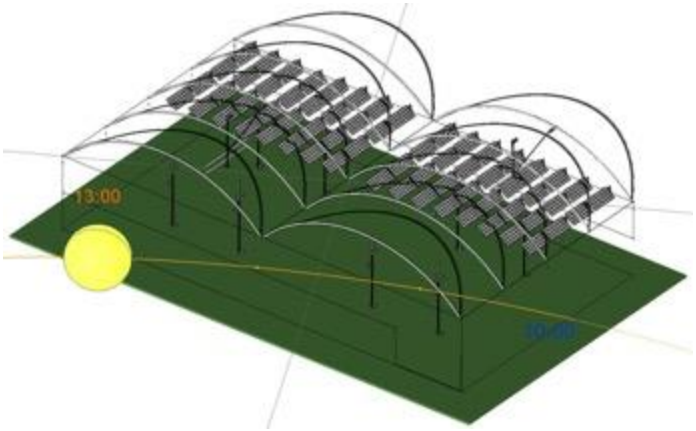

Figure 47. Shadow on the panel for December 21.

The simulation results indicated the presence of persistent partial shading on certain panel strings. Due to their series connection, this could be responsible for the decrease in overall electrical output. Figures 46 and 47 illustrate two examples of this phenomenon. Further investigations are needed to confirm this hypothesis and to better evaluate the PV system losses.

Funded by the European Union

Funded by the European Union under Grant Agreement No 101096056. Views and opinions expressed are however those of the author(s) only and do not necessarily reflect those of the European Union or CINEA. Neither the European Union nor the granting authority can be held responsible for them.

AZS Site, Israel – Electrical Characterisation of the PV system

The experimental activities conducted at the Al Zahrawy Society (AZS) site within the framework of the REGACE project (WP3.2) aimed to evaluate the performance of photovoltaic (PV) modules under greenhouse conditions and to assess the influence of environmental and structural factors on solar energy generation. The AZS site served as the central experimental facility for in-depth electrical testing, characterization, and long-term monitoring of PV modules installed both inside and outside greenhouse structures.

The experimental agrivoltaic installation was designed to integrate PV modules inside two existing 140 m² polytunnel greenhouses located in Kfar Qara, Israel. Each greenhouse — measuring 8 m in width and 17.5 m in length — was equipped with one dynamic PV system mounted approximately 3 m above ground level, allowing for soil-based cultivation and, in later stages, for potted crop production beneath the modules. The system employs a single-axis sun-tracking mechanism developed by TriSolar InnoWadi Group Ltd., capable of ±65° rotation, enabling continuous optimization of the incident irradiance angle throughout the day and thus enhancing the overall energy yield.

The greenhouse is covered with polyethylene film (Ginegar C460), characterized by a 150 µm thickness, anti-drip coating, and the optical properties indicated in Table 16:

Table 16. Optical properties of the polyethylene cover used at the AZS site.

Optical property	Value	Description
PAR light transmittance	89 %	Fraction of photosynthetically active radiation transmitted
UV transmittance (300-380 nm)	20 %	Limited ultraviolet transmission
Diffused light transmittance (PAR)	60 %	Enhanced light uniformity within the canopy
Thermicity (7-15 µm)	80 %	Infrared retention improving internal heat balance

The PV modules used are custom-made 105 Wp frameless glass–glass bifacial modules (TriSolar LWMH32-105-G1), each consisting of 44 crystalline silicon cells (105 × 105 mm) with a cell efficiency of 22.5 %. A 20 mm inter-cell spacing provides an overall panel transparency of 35 %, allowing partial light penetration to the crop layer below. These modules were specifically designed for greenhouse agrivoltaic integration, balancing light transmission with electrical generation efficiency.

Funded by the European Union

Funded by the European Union under Grant Agreement No 101096056. Views and opinions expressed are however those of the author(s) only and do not necessarily reflect those of the European Union or CINEA. Neither the European Union nor the granting authority can be held responsible for them.

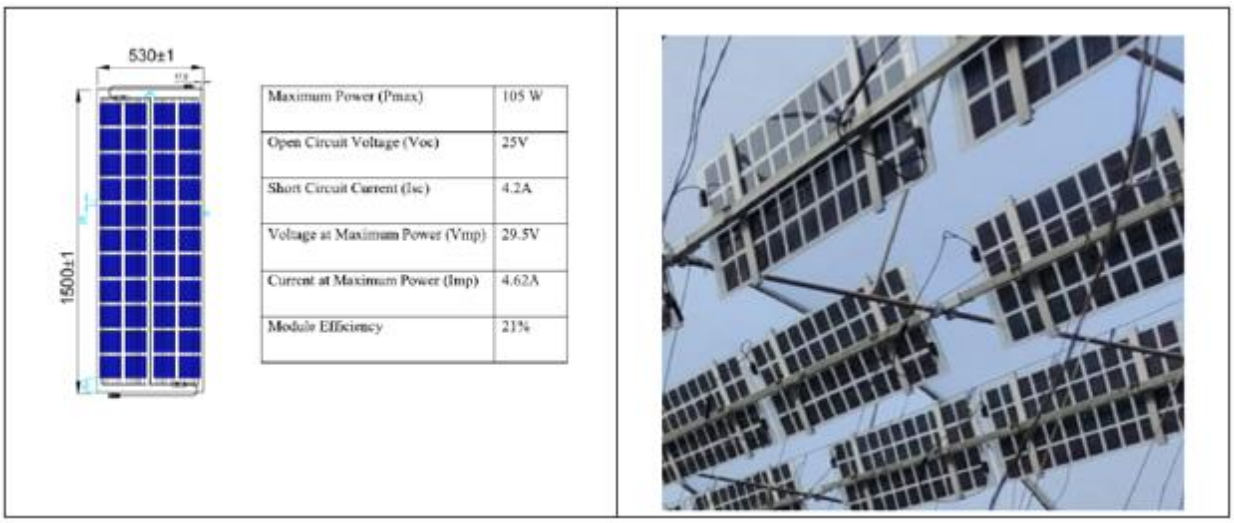

Maximum Power (Pmax)	105 W
Open Circuit Voltage (Voc)	25V
Short Circuit Current (Isc)	4.2A
Voltage at Maximum Power (Vmp)	29.5V
Current at Maximum Power (Imp)	4.62A
Module Efficiency	21%

Figure 48. Solar Module used in AZS Greenhouses experiment with 105 Wp power output.

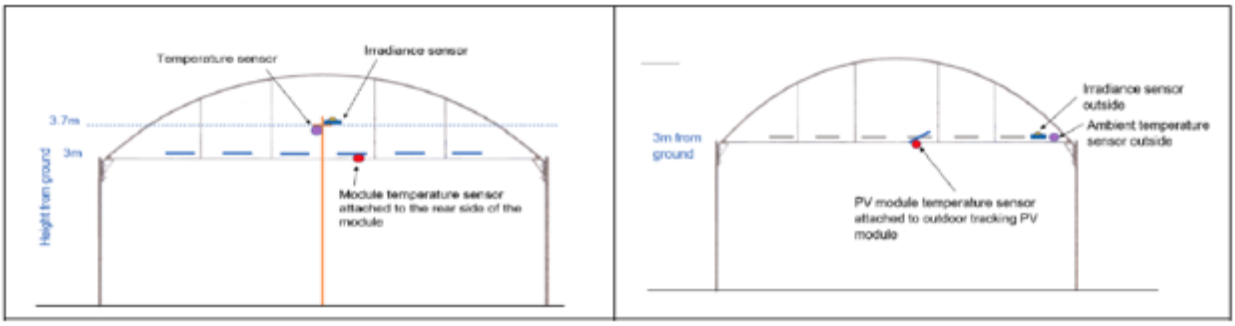

Figure 49. Different locations and types of sensors used in the AZS Greenhouses experiment.

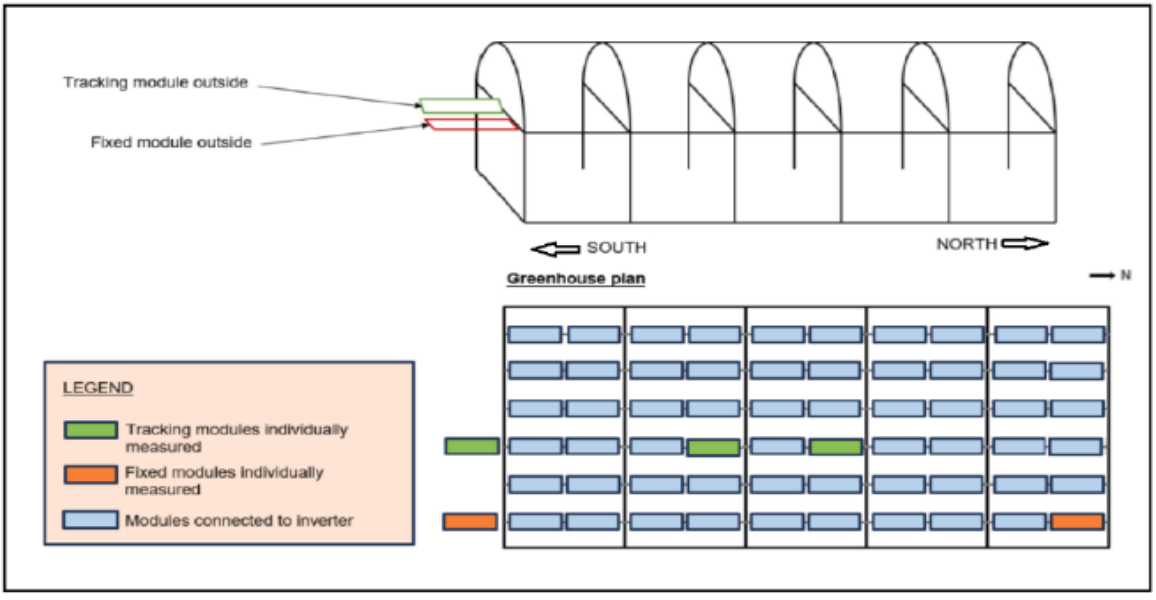

Figure 50. Greenhouse structure and position of the test panels inside and outside the greenhouse.

Funded by the European Union

Funded by the European Union under Grant Agreement No 101096056. Views and opinions expressed are however those of the author(s) only and do not necessarily reflect those of the European Union or CINEA. Neither the European Union nor the granting authority can be held responsible for them.

Within the REGACE project, the AZS facility enabled systematic, high-resolution electrical performance assessments under real operating conditions. The investigations focused on both the overall PV system behaviour and the electrical characteristics of individual modules, measured inside and outside the greenhouse. These tests evaluated the effects of light diffusion, temperature variations, and tracking dynamics on the instantaneous and long-term performance of the system.

The analysis covered detailed electrical parameters such as the current–voltage (I–V) curve, maximum power point current (I_{mpp}), maximum power point voltage (V_{mpp}), and maximum short-circuit and open-circuit values (I_{max}, V_{max}). Continuous logging allowed the identification of module behaviour under fluctuating irradiance, bifacial illumination, and shading conditions typical of greenhouse environments.

In addition, the study examined how greenhouse-cover materials, dust accumulation, and responsive tracking motion influence PV output and stability. These experiments provided quantitative insight into loss mechanisms and dynamic response, supporting the calibration of the simulation models used within Work Packages 2 and 3.

The experimental campaign at the Al Zahrawy Society (AZS) thus served as the central electrical-testing hub of the REGACE consortium. It delivered standardized, high-accuracy datasets on irradiance dependence, temperature coefficients, and I–V curve evolution. The results form a benchmark for designing optimized agrivoltaic systems that sustain both efficient energy generation and suitable microclimate conditions for crops.

By quantifying the influence of greenhouse optical and thermal factors on electrical performance, the AZS testing activities contributed directly to the validation of the REGACE system design and to the development of guidelines for future PV-greenhouse integration across diverse climates.

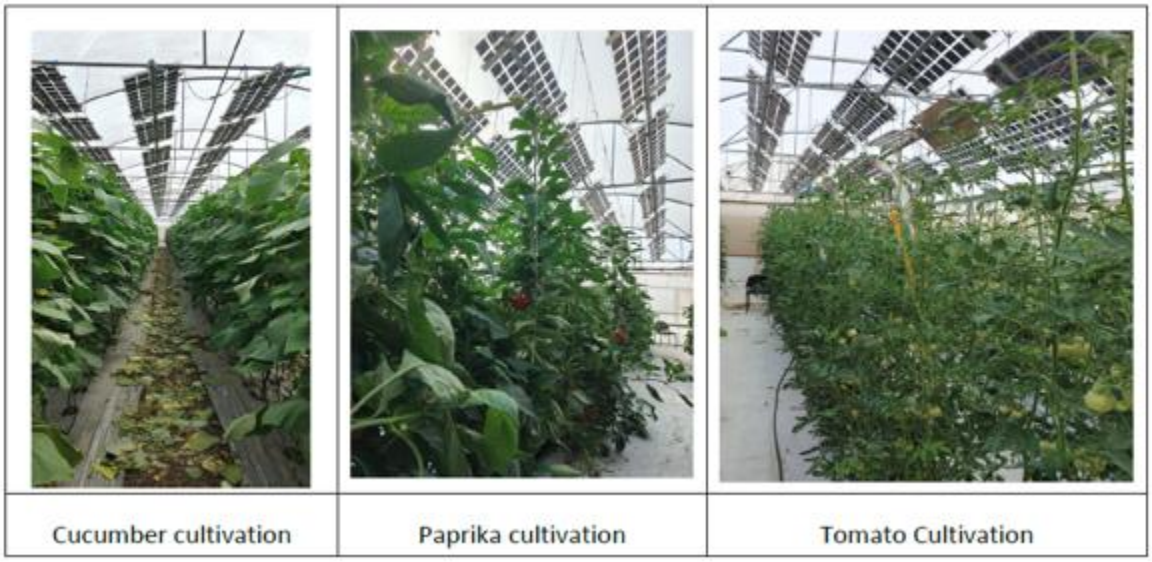

Figure 51. The three cultivation types were implemented during the project under the responsive sun-tracking system.

Funded by the European Union

Funded by the European Union under Grant Agreement No 101096056. Views and opinions expressed are however those of the author(s) only and do not necessarily reflect those of the European Union or CINEA. Neither the European Union nor the granting authority can be held responsible for them.

Measurement Setup and Methodology

The monitoring and testing campaign at the AZS site was carried out using a dedicated EKO photovoltaic monitoring system, designed to record and analyse real-time electrical and environmental data from several photovoltaic modules placed in distinct configurations. The goal of the experimental setup was to assess how the greenhouse microclimate — particularly irradiance attenuation, spectral diffusion, and temperature variations — affects the performance and stability of PV Modules when installed within a greenhouse structure.

System Configuration

Four modules were installed and continuously monitored to represent the different installation conditions:

- One fixed module (0° tilt) located outside the greenhouse.
- One fixed module (0° tilt) located inside the greenhouse.
- One single-axis tracking module located outside the greenhouse.
- One single-axis tracking module located inside the greenhouse.

Each configuration enabled a comparative evaluation between outdoor and indoor operating conditions, as well as between tracking and non-tracking modes. All modules were identical TriSolar LWMH32-105-G1, 105 Wp bifacial glass–glass photovoltaic panels, installed approximately 3 m above ground level and connected to the EKO photovoltaic monitoring system for continuous data acquisition.

All PV modules were electrically characterized using the EKO PV Block System, which provided high-precision measurements of current–voltage (IV) curves and associated electrical performance parameters at predefined time intervals.

Calibration, Characterization, and Data Acquisition

The EKO system collected data in fixed intervals (5 minutes) and included the following electrical and environmental parameters:

- Current–Voltage (IV) curves
- Open-circuit voltage (Voc)
- Short-circuit current (Isc)
- Maximum power point (MPP)
- Conversion efficiency (η)
- Fill factor (FF)
- Module temperature (Tmod)
- Incident irradiance on both front (direct) and rear (albedo) surfaces of the bifacial modules

Environmental sensors were deployed both inside and outside the greenhouse to record ambient temperature, relative humidity, and global horizontal irradiance (GHI). The irradiance sensors covered the

Funded by the European Union

Funded by the European Union under Grant Agreement No 101096056. Views and opinions expressed are however those of the author(s) only and do not necessarily reflect those of the European Union or CINEA. Neither the European Union nor the granting authority can be held responsible for them.

spectral range 350 – 1100 nm, allowing for accurate tracking of variations in diffused and direct radiation under the greenhouse cover.

A subset of PV modules was initially characterized under Standard Test Conditions (STC) using a calibrated solar simulator at the manufacturer laboratory prior to shipment to the other project sites. These reference measurements provided baseline electrical characteristics to be used for later degradation analysis. After extended operation inside the greenhouse environments, the same reference modules will be tested at AZS site for post-operation recharacterization to evaluate aging and degradation effects induced by temperature, humidity, and diffused light exposure. Initial quality control measurements were also compared against the manufacturer's certification data, ensuring consistency and accuracy in nominal ratings. The end-of-project testing campaign, jointly executed by AZS and Tor Vergata University, will provide a comparative dataset on long-term performance evolution.

Results and Discussion

The AZS monitoring campaign generated a comprehensive dataset covering the period 28 months from June 23 to October 25, representing a full seasonal cycle under typical Mediterranean climatic conditions. The EKO measurement system continuously acquired electrical and environmental data at fixed time intervals, enabling the characterization of the photovoltaic system's performance in both inside- and outside-greenhouse configurations and under fixed and single-axis tracking modes.

System-Level Performance

The total installed capacity of the greenhouse-integrated PV system was 12.4 kWp, consisting of 120 modules installed in two identical greenhouses. Each system consists of 60 modules that are connected in three strings of 20 modules each in series, resulting in a system voltage of 500VDC and current 4.2 DC Amp. (the Eastern GH and Western GH). The system achieved a maximum daily energy output of 59.8 kWh on July 24, corresponding to a yield of 5.5 kWh/kWp per day. This yield is comparable to that of standard outdoor PV installations under similar climatic conditions, demonstrating that greenhouse-integrated agrivoltaic systems can reach high energy conversion performance even under partially diffused light conditions.

Funded by the European Union

Funded by the European Union under Grant Agreement No 101096056. Views and opinions expressed are however those of the author(s) only and do not necessarily reflect those of the European Union or CINEA. Neither the European Union nor the granting authority can be held responsible for them.

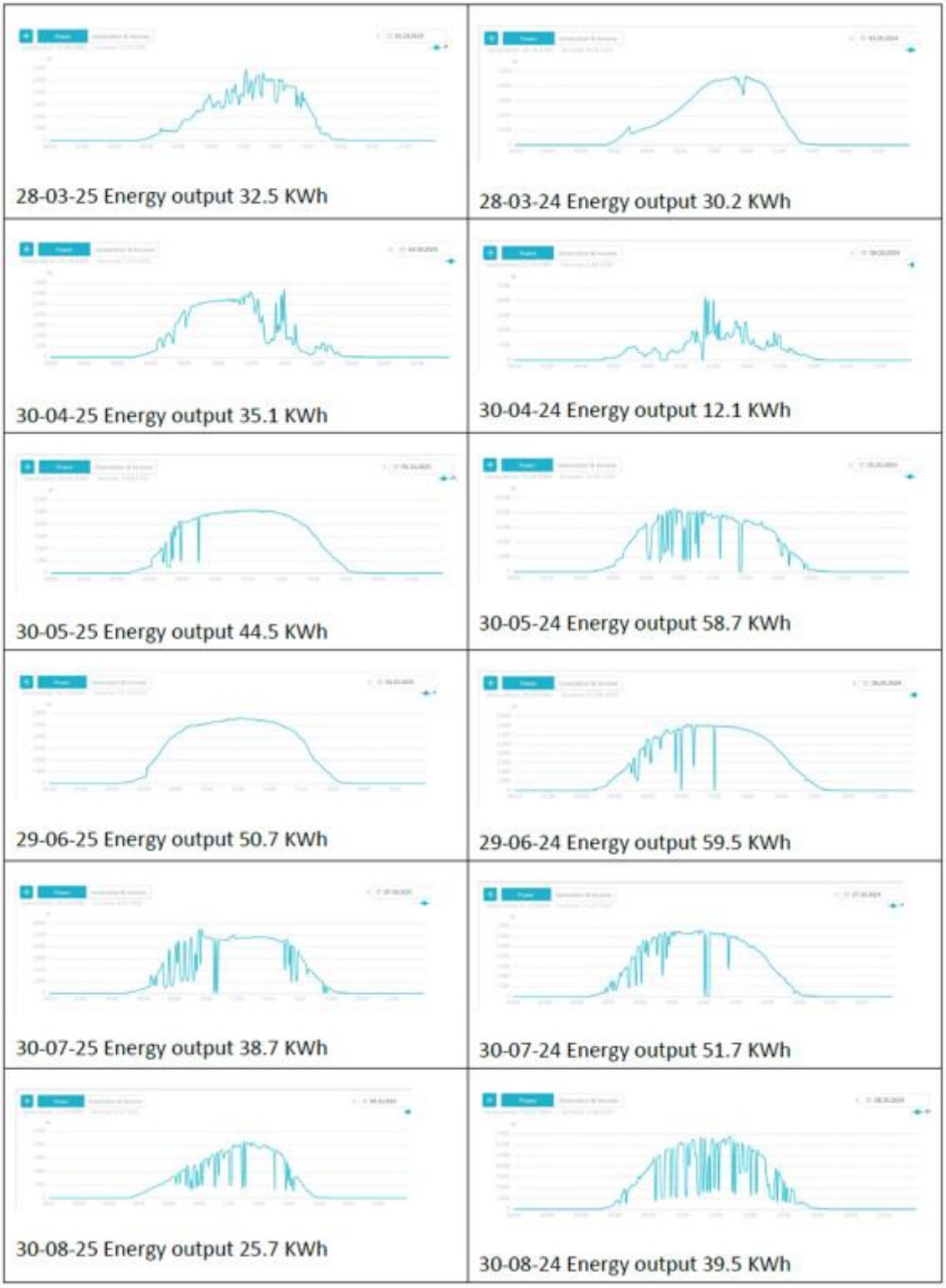

Figure 52. Daily AC energy output recorded from the Goodwe inverter over a six-month period spanning 2024 and 2025.

Funded by the European Union

Funded by the European Union under Grant Agreement No 101096056. Views and opinions expressed are however those of the author(s) only and do not necessarily reflect those of the European Union or CINEA. Neither the European Union nor the granting authority can be held responsible for them.

Figure 52 illustrates the daily AC energy output recorded from the Goodwe inverter over a six-month period spanning 2024 and 2025. The power output curves demonstrate the system's operational stability and consistent energy generation under full tracking operation. This continuous and uniform performance indicates the mechanical and electrical durability of the solar system throughout the monitoring period, with no observed technical malfunctions or failures.

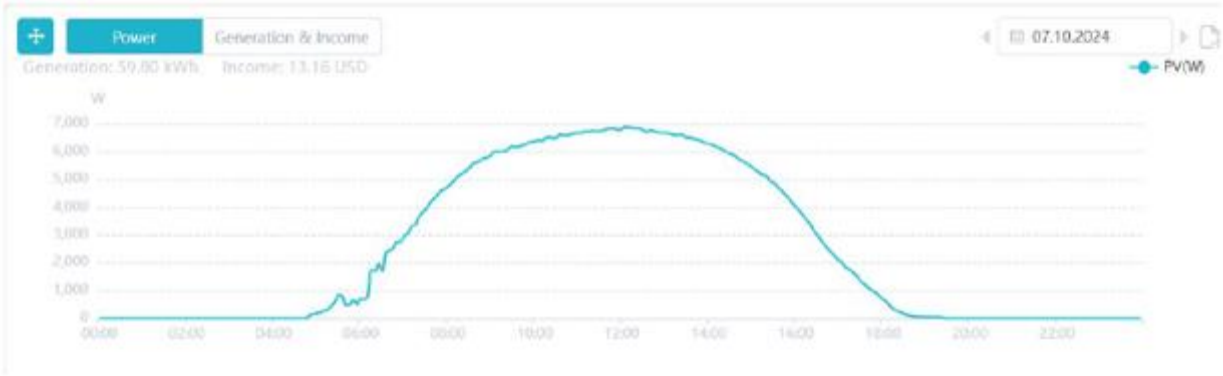

Figure 53. Daily AC energy output recorded from the GoodWe inverter on a clear summer day 2024.

Figure 53 illustrates the daily AC energy output recorded from the GoodWe inverter on a clear summer day in 2024. The power output curve demonstrates the full operation of the system in sun-tracking mode.

Seasonal variations strongly influenced power generation, with output decreasing during the late summer months due to the combined effects of dust accumulation and reduced optical transmittance of the polyethylene greenhouse cover. The global horizontal irradiance (GHI) inside the greenhouse was reduced by approximately 20% in May when the cover was clean and new, increasing to nearly 40% by July as dust accumulated and the cover aged. Despite this, the reduction in PV output was less pronounced, owing to the spectral properties of the cover that selectively transmit the more effective wavelengths for PV conversion.

Funded by the European Union under Grant Agreement No 101096056. Views and opinions expressed are however those of the author(s) only and do not necessarily reflect those of the European Union or CINEA. Neither the European Union nor the granting authority can be held responsible for them.

Figure 54. Dust accumulation on the PV cells.

Figure. 54 shows the dust accumulation after the completion of the soil-based cultivation season, land processing activities inside the greenhouse on the inner surfaces, which affected the energy production of the PV modules. Therefore, it was necessary to clean the panels regularly using a high-pressure water jet system applied to both sides of the modules to remove dust and restore optimal performance.

Measurement of Environmental and Operating Conditions at module level

To characterize environmental conditions both inside and outside the greenhouse, a comprehensive sensor network was deployed at multiple reference points. This setup enabled simultaneous acquisition of irradiance data on both the front and rear sides of the bifacial PV modules, together with continuous measurements of module surface temperature and ambient climatic parameters surrounding the tested units.

Funded by the European Union under Grant Agreement No 101096056. Views and opinions expressed are however those of the author(s) only and do not necessarily reflect those of the European Union or CINEA. Neither the European Union nor the granting authority can be held responsible for them.

The instruments were strategically positioned to monitor the principal variables influencing agrivoltaic performance, including:

- Ambient temperature (°C)
- Relative humidity (%)
- Solar irradiance (W/m²) on the front and rear surfaces of bifacial modules
- PV module temperature (°C)

This integrated and synchronized measurement system provided a high-resolution dataset capturing the interplay between light availability, thermal behaviour, and electrical output, enabling an accurate assessment of the microclimatic effects within the greenhouse environment and their influence on PV system performance.

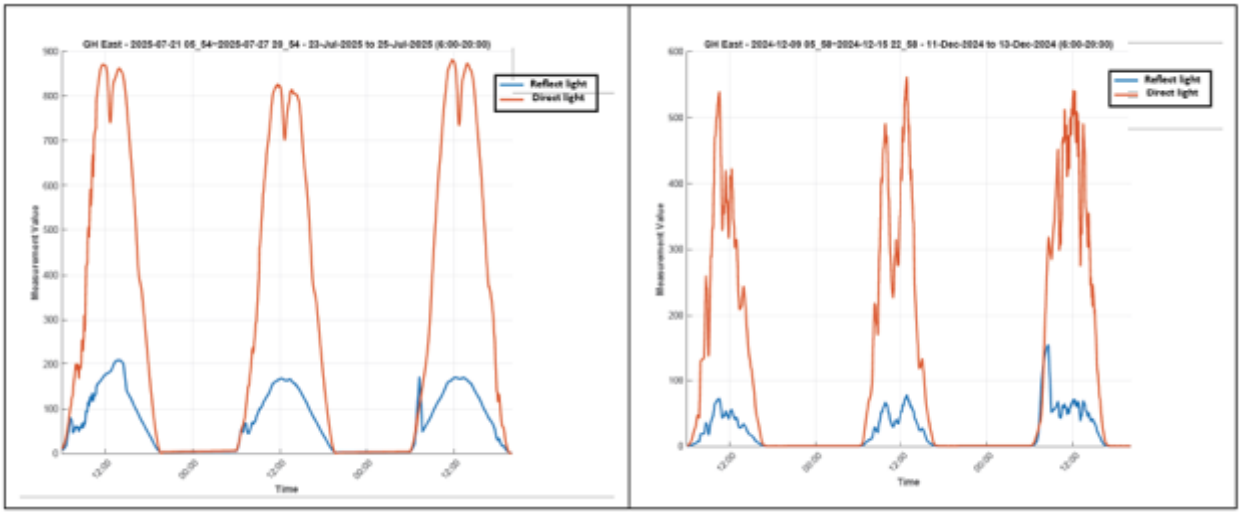

Figure 55. Seasonal variation of front- (direct) and rear-side irradiance (albedo; reflected light), at the AZS site.

Figure 55 illustrates the measured irradiance on the front and rear (albedo) sides of the bifacial photovoltaic modules during representative winter and summer monitoring periods. The results reveal a distinct seasonal difference in reflected irradiance intensity. During summer, the rear-side irradiance reached approximately 200 W/m², whereas in winter it decreased to around 60 W/m².

This seasonal variation is mainly driven by changes in solar elevation angle, ground reflectivity, and crop canopy conditions inside the greenhouse. Higher solar angles and lighter, drier ground surfaces during summer enhance the reflection of diffuse light onto the rear side of the PV modules. In contrast, lower sun angles combined with darker, moist soil in winter substantially reduce the albedo contribution.

These findings highlight the significance of seasonal albedo effects in assessing the overall energy yield and bifacial gain of PV systems operating within greenhouse environments.

Funded by the European Union

Funded by the European Union under Grant Agreement No 101096056. Views and opinions expressed are however those of the author(s) only and do not necessarily reflect those of the European Union or CINEA. Neither the European Union nor the granting authority can be held responsible for them.

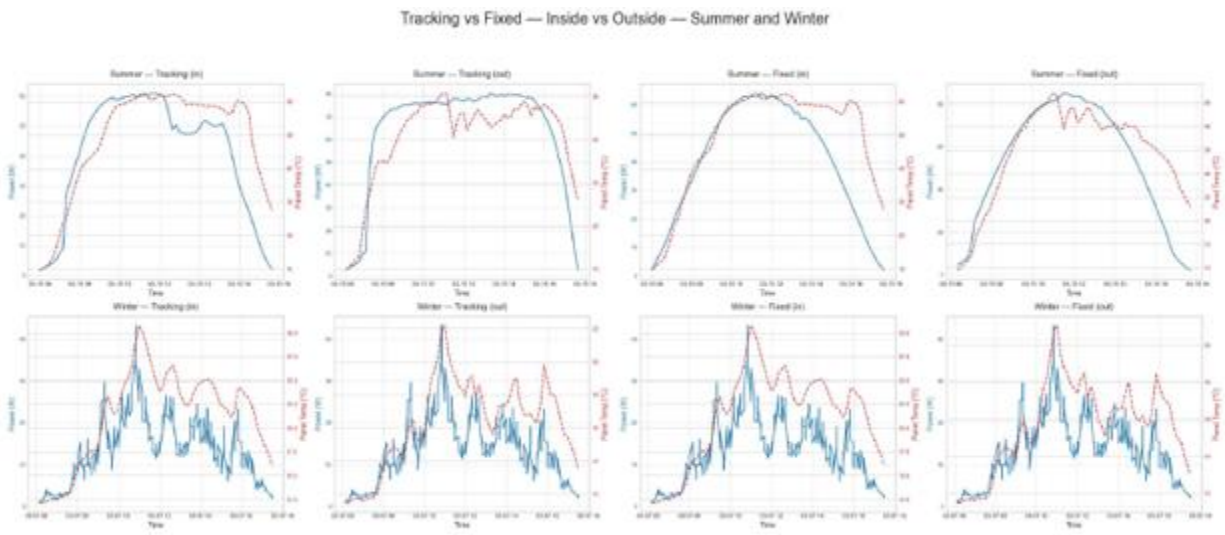

Figure 56. Comparative analysis of power output between fixed and single-axis tracking PV panels (inside and outside the greenhouse) at the AZS Site (March 2025).

Figure 56 presents a comparative analysis of the power output profiles of fixed and single-axis tracking photovoltaic (PV) panels installed inside and outside the greenhouse during two representative days: a sunny day (07 March 2025) and a cloudy day (15 March 2025).

The results demonstrate that the tracking configuration consistently outperformed the fixed panels under both irradiance conditions. The dynamic system maintained a higher instantaneous power output and greater daily energy yield, confirming the clear operational advantage of solar tracking under variable weather scenarios.

The performance difference becomes particularly significant during summer months, when the tracking system achieves up to 12 % higher total energy yield compared to the fixed configuration. This improvement is primarily attributed to the optimized solar-incidence angle maintained by the tracking mechanism throughout longer daylight hours and higher solar elevations.

Overall, these results confirm the seasonal advantage and reliability of dynamic solar tracking, particularly under the high-radiation conditions characteristic of Mediterranean climates, thereby reinforcing its suitability for greenhouse-integrated agrivoltaic applications.

Funded by the European Union under Grant Agreement No 101096056. Views and opinions expressed are however those of the author(s) only and do not necessarily reflect those of the European Union or CINEA. Neither the European Union nor the granting authority can be held responsible for them.

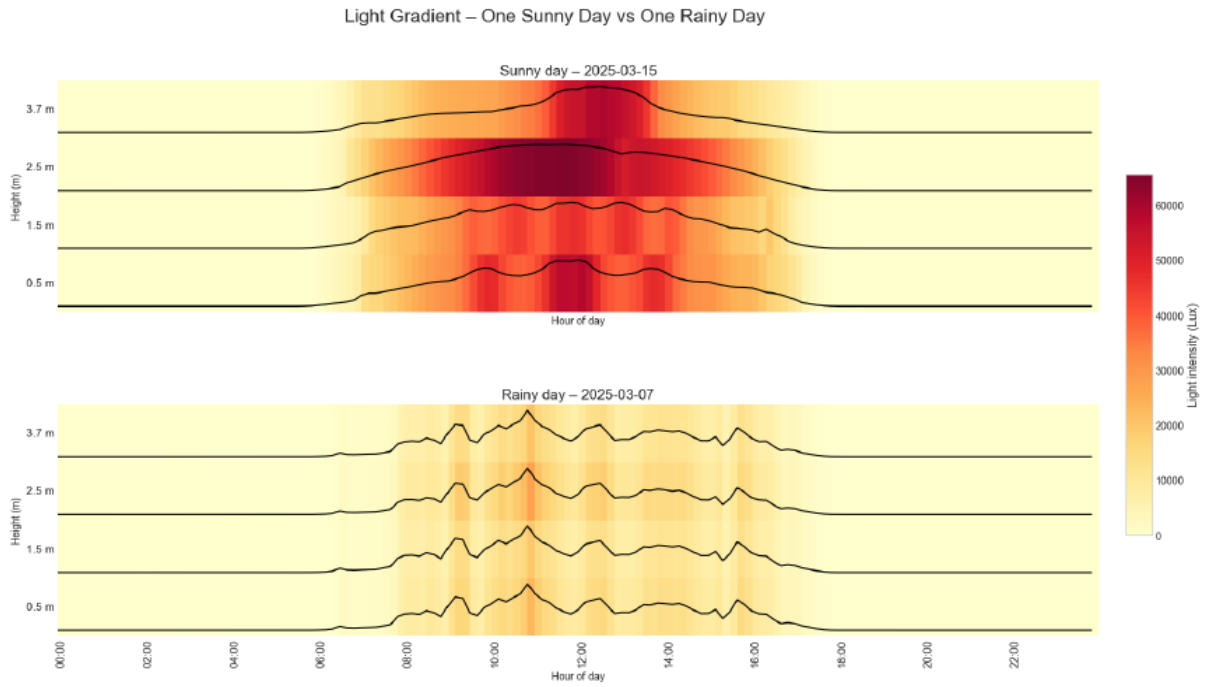

Figure 57. Vertical light-intensity distribution inside the greenhouse under sunny and cloudy conditions at the AZS site (March 2025).

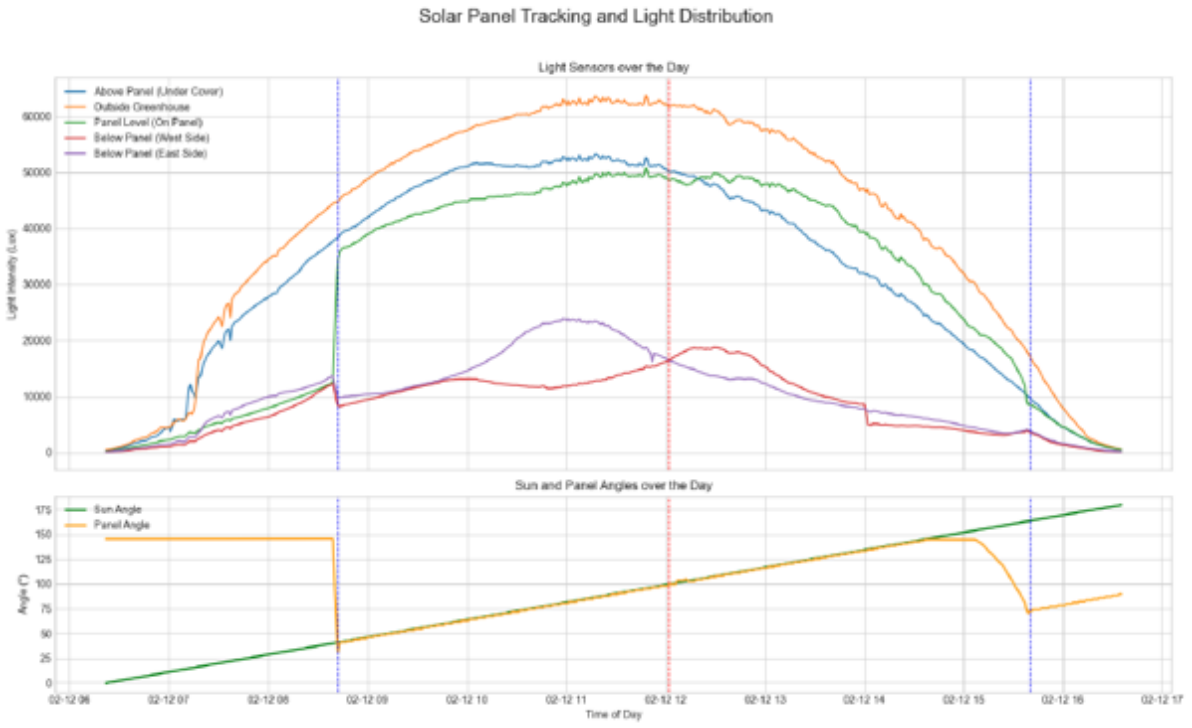

Figure 58. Vertical light-intensity distribution inside the greenhouse under sunny and cloudy conditions at the AZS site (March 2025).

Funded by the European Union under Grant Agreement No 101096056. Views and opinions expressed are however those of the author(s) only and do not necessarily reflect those of the European Union or CINEA. Neither the European Union nor the granting authority can be held responsible for them.

Funded by the European Union

Figures 57 compares the measured light intensity at multiple vertical levels inside the greenhouse during a sunny day (07 March 2025) and a cloudy day (15 March 2025). The results reveal distinct differences in light penetration and vertical distribution under varying sky conditions.

During sunny periods, light intensity decreases progressively from the upper canopy toward the soil surface, maintaining adequate illumination for crop photosynthesis. Under cloudy conditions, however, overall intensity levels are reduced, and the vertical gradient becomes less pronounced, resulting in a more uniform yet attenuated light environment within the greenhouse (Figure 58).

These observations underscore the influence of cloud cover and diffuse-light dynamics on internal greenhouse illumination — an essential consideration when evaluating both crop performance and PV module operation in agrivoltaic systems.

Figure 59. Shading effect at different vertical levels inside the greenhouse compared to outdoor conditions at the AZS site (July 2025).

Figure 59 illustrates the shading effect measured at several vertical levels inside the greenhouse compared with outdoor reference conditions. The data highlight how structural elements and PV module placement influence light attenuation and spatial distribution within the greenhouse volume. Reduced transmittance near supporting structures and module rows indicates localized shadowing, which affects both crop illumination and rear-side irradiance of the bifacial panels.

Performance Ratio and Thermal Behaviour

The Performance Ratio (PR) of the system was calculated for July, yielding a value of 0.65, based on a total plane-of-array irradiance (H_POA) of 209 kWh/m² and a bifaciality factor (ϕ) of 0.7. Although this PR is lower than typical outdoor values (0.80–0.90), it accurately reflects the realistic operational conditions inside the greenhouse, where diffused irradiance and elevated internal temperatures reduce module conversion efficiency.

Funded by the European Union

Funded by the European Union under Grant Agreement No 101096056. Views and opinions expressed are however those of the author(s) only and do not necessarily reflect those of the European Union or CINEA. Neither the European Union nor the granting authority can be held responsible for them.

Thermal measurements showed that module temperature closely followed irradiance variations, with limited correlation to ambient temperature. This indicates that heating effects are primarily driven by light exposure rather than air temperature. Tracking modules exhibited higher average temperatures due to extended solar exposure throughout the day, suggesting that active or passive thermal management strategies could help mitigate potential long-term degradation effects.

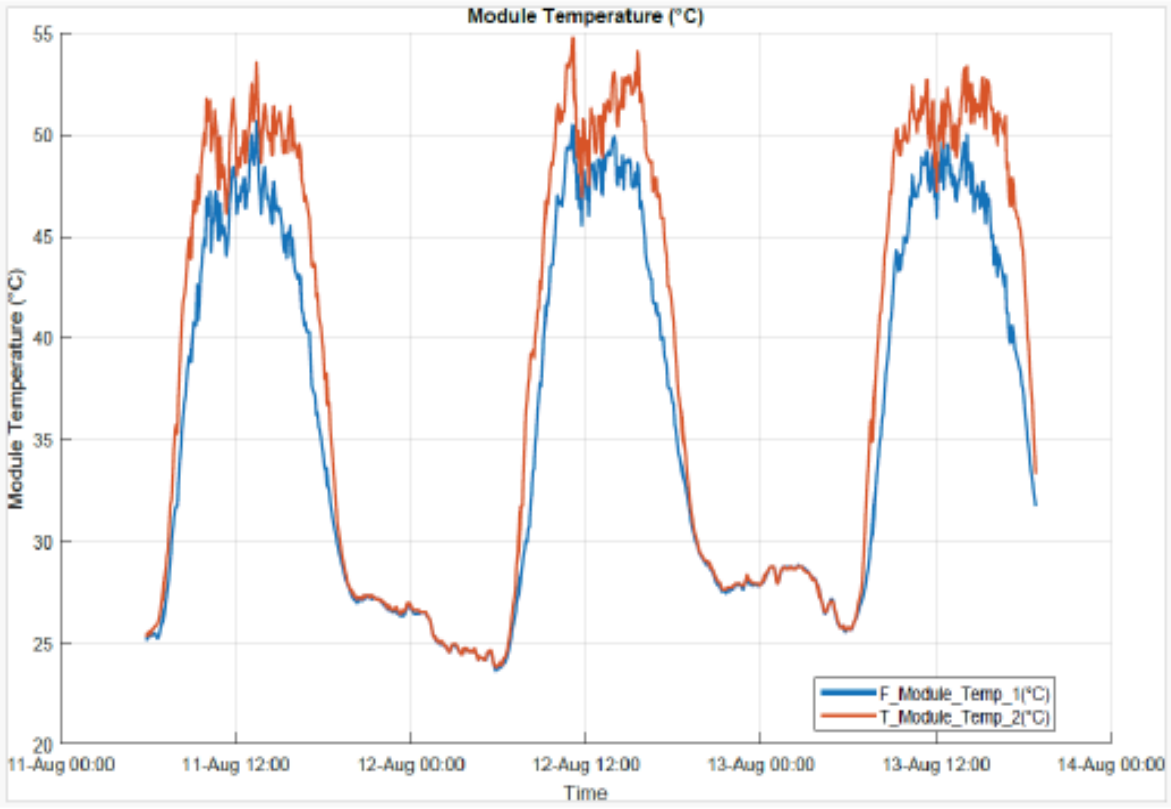

Figure 60. Temperature differences between the tracking and fixed photovoltaic modules inside the greenhouse over three consecutive days in mid-August 2025.

Figure 60 presents the temperature differences between the tracking and fixed photovoltaic modules inside the greenhouse over three consecutive days in mid-August 2025. The tracking module reached a maximum temperature of 53 °C, compared with 48 °C for the fixed panel — a difference of approximately 5 °C. As shown in the corresponding energy-yield data, this temperature difference did not negatively affect the performance of the tracking module, which continued to produce a higher energy yield than the fixed configuration. This stability is explained by the more favourable solar-incidence angle of the tracking module, which compensates for minor temperature-induced efficiency losses by maintaining higher irradiance capture throughout the day.

Funded by the European Union

Funded by the European Union under Grant Agreement No 101096056. Views and opinions expressed are however those of the author(s) only and do not necessarily reflect those of the European Union or CINEA. Neither the European Union nor the granting authority can be held responsible for them.

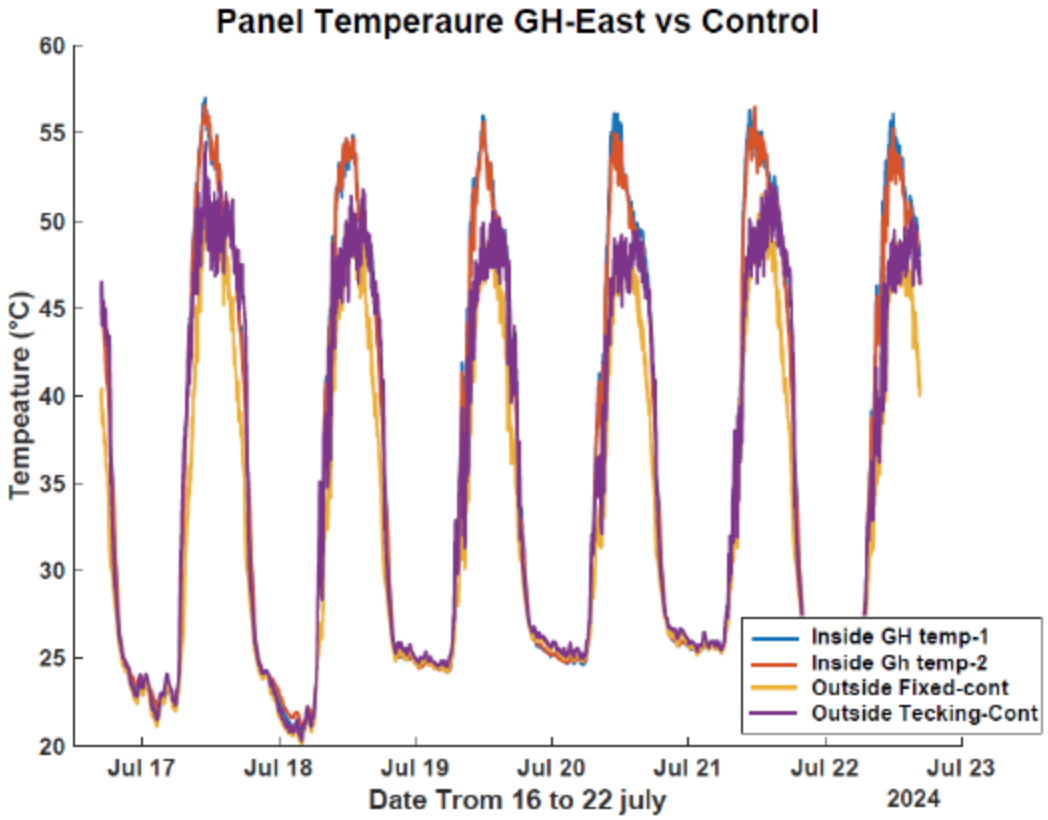

Figure 61. Comparison of module temperature for fixed and tracking configurations inside and outside the greenhouse at the AZS site (July 2024).

Figure 61 presents the module temperature variations recorded over six consecutive days in mid-July 2024 for four PV modules: tracking and fixed installations inside the greenhouse, and tracking and fixed configurations outside. The results show that the tracking module inside the greenhouse reached a maximum temperature of 54 °C, compared with 48 °C for the tracking module outside, corresponding to a difference of approximately 6 °C. The fixed and tracking modules inside the greenhouse exhibited comparable temperature profiles, reflecting the stabilizing influence of the enclosed greenhouse environment.

This temperature elevation inside the greenhouse is attributed to restricted convective cooling and increased diffuse radiation, conditions typical of protected cultivation structures. Figures 62-63 indicate the temperature distribution at different levels inside the greenhouse showing an increase of approximately 8°C above the solar panel compared to beneath the solar panel. The observed thermal behaviour highlights the importance of temperature-management strategies — such as improved ventilation or reflective ground coatings — to mitigate performance losses and potential long-term degradation of PV modules in greenhouse-integrated systems.

Funded by the European Union

Funded by the European Union under Grant Agreement No 101096056. Views and opinions expressed are however those of the author(s) only and do not necessarily reflect those of the European Union or CINEA. Neither the European Union nor the granting authority can be held responsible for them.

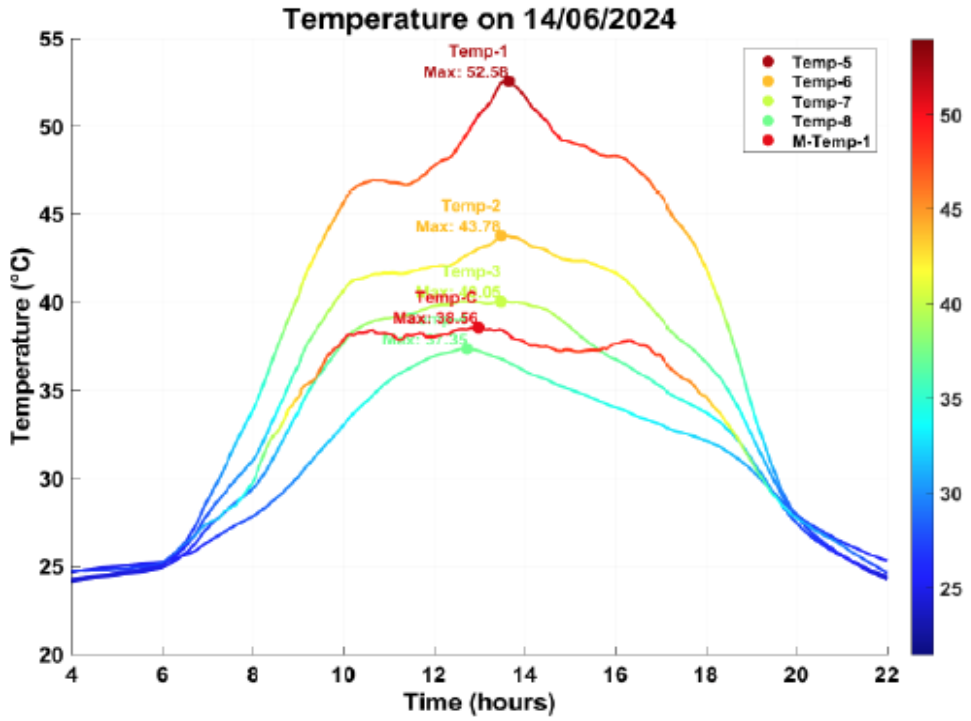

Figure 62. Temperature distribution at different levels inside the greenhouse compared with the panel temperature on June 24.

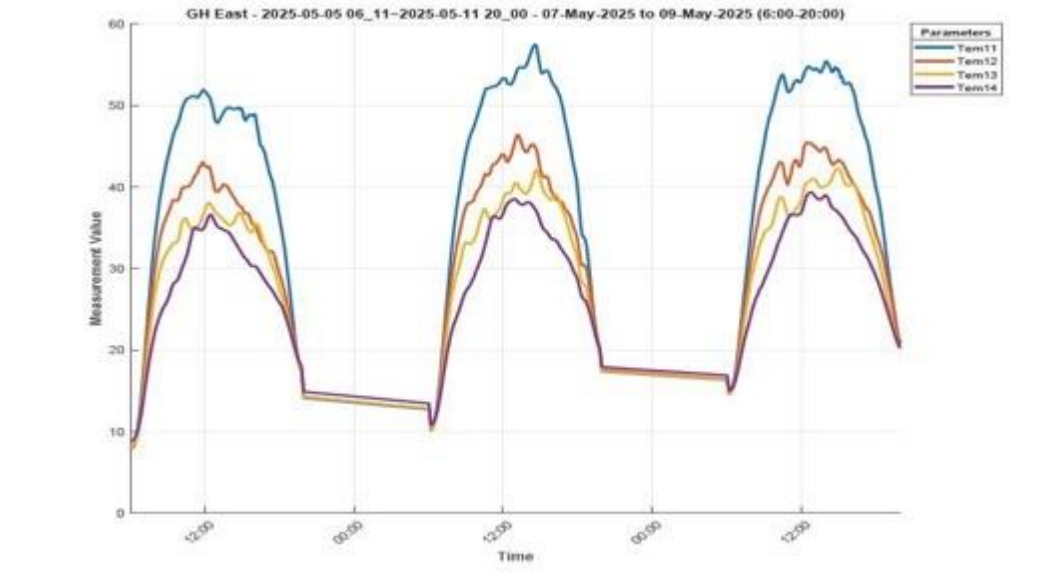

Figure 63. Temperature distribution in a PV greenhouse (Tem11 (blue), 0.5m above the solar panel; Tem12 (orange), 0.5m below the solar panel; Tem13 (yellow), 1.5m below the solar panel; Tem14 (purple), 2.5m below the solar panel).

Funded by the European Union

Funded by the European Union under Grant Agreement No 101096056. Views and opinions expressed are however those of the author(s) only and do not necessarily reflect those of the European Union or CINEA. Neither the European Union nor the granting authority can be held responsible for them.

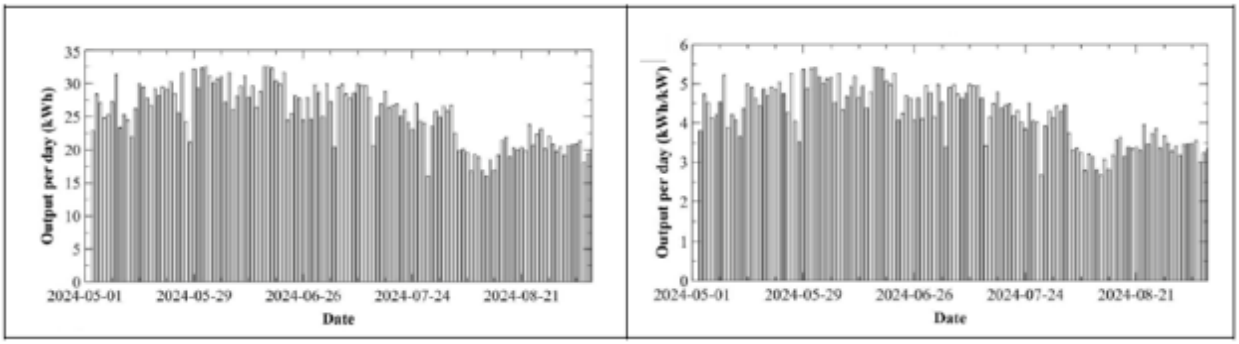

Figure 64. The daily PV system output (kWh) for one greenhouse from May 24 to Sep. 24 (left) and the output per kWp installed inside the greenhouse (right).

The results of figures 64-65 clearly demonstrate the light attenuation effect caused by the greenhouse cover. On average, the irradiance inside the greenhouse was about 20% lower than outside, depending on the season and the cleanliness of the cover material as shown in Figure 65.

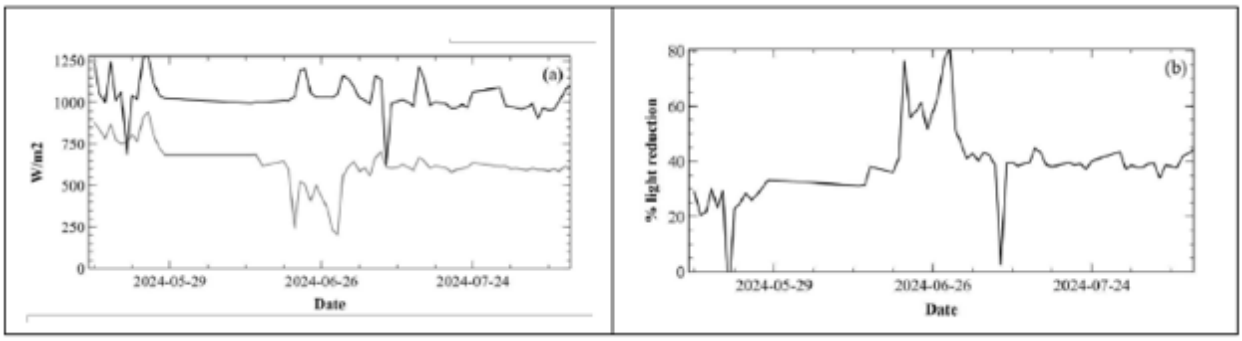

Figure 65. Maximum irradiance values inside and outside the greenhouse (a), as well as percentage reduction in global horizontal irradiance (GHI) inside compared to outside conditions.

This reduction is primarily attributed to the optical and surface properties of the polyethylene greenhouse film, which partially reflects and diffuses incoming solar radiation demonstrating a clear performance difference in favour of the outdoor module, which produced approximately 23% more energy than the one inside the greenhouse (Figures 66-67). When the cover was new and clean, the GHI reduction was approximately 12%. However, as dust and particulate matter accumulated over the summer period — with limited rainfall and high air humidity — the cover's transmittance decreased, and the GHI reduction reached around 20% by late July. The results highlight the combined influence of cover ageing, surface contamination, and seasonal sun angle on the total amount of solar radiation transmitted into the greenhouse.

Understanding this variation is essential for accurately modelling the energy yield of photovoltaic systems integrated in greenhouses, as it directly affects both PV efficiency and crop light availability beneath the modules.

Funded by the European Union under Grant Agreement No 101096056. Views and opinions expressed are however those of the author(s) only and do not necessarily reflect those of the European Union or CINEA. Neither the European Union nor the granting authority can be held responsible for them.

Funded by the European Union

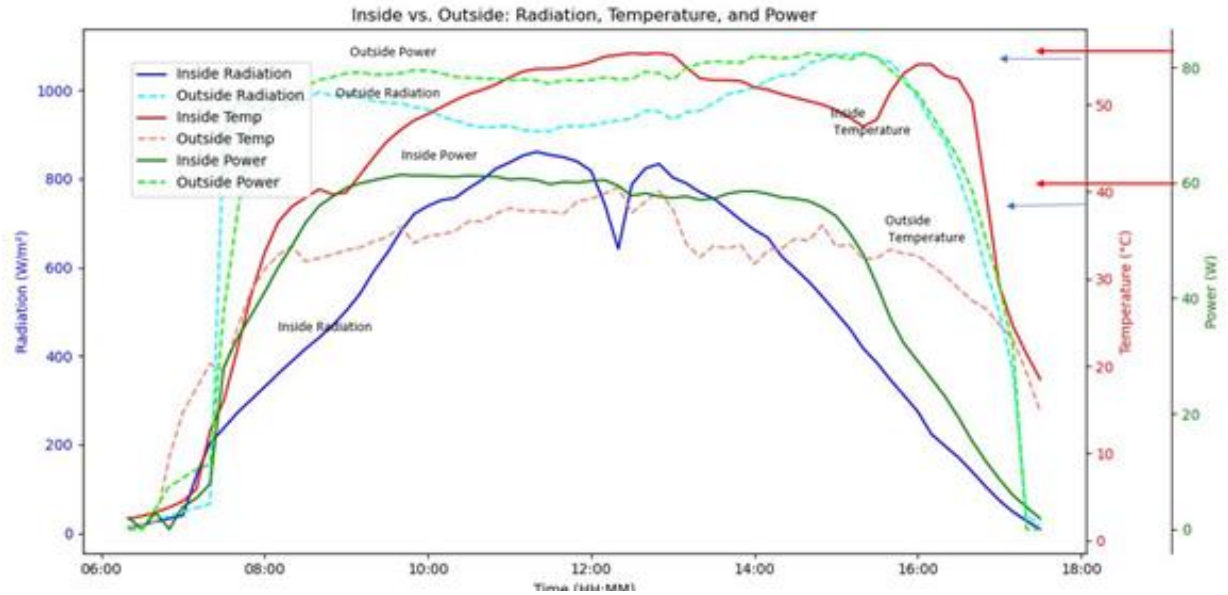

Figure 66. Comparative measurements between the tracking photovoltaic modules installed inside and outside the greenhouse.

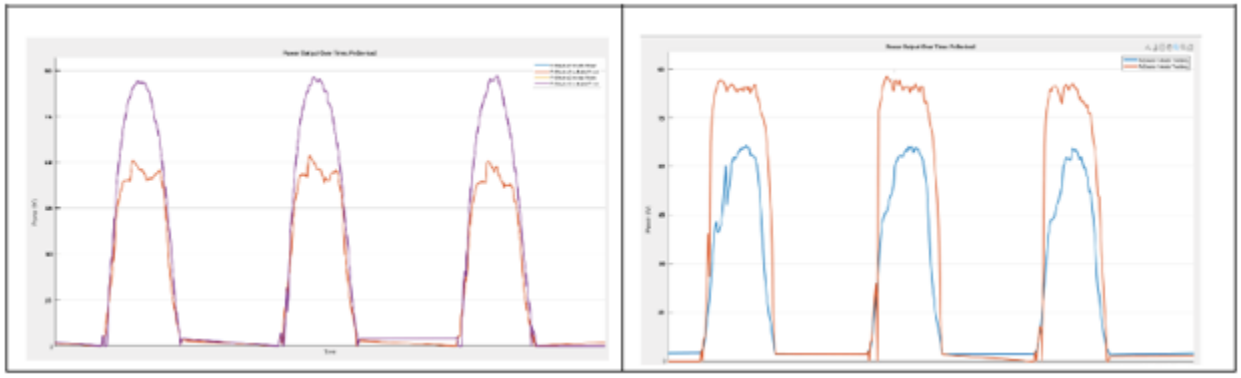

Figure 67. Shading effects at different heights inside the greenhouse relative to the outside on three consecutive days.

This result is expected, as it directly reflects the reduction in solar irradiance entering the greenhouse due to the optical and structural characteristics of the greenhouse cover. The same trend was consistently observed throughout the entire research period, confirming the persistent influence of reduced light transmission on energy yield. However, this behaviour varied seasonally, with the performance gap between indoor and outdoor modules becoming particularly pronounced during the winter months, when solar elevation angles are lower and the share of diffuse radiation is higher.

These findings emphasize the importance of optimizing greenhouse cover materials and PV integration design to balance agricultural light requirements with energy generation efficiency. The results also highlight the technological advantage of the TriSolar semi-transparent modules, whose inter-cell spacing

Funded by the European Union under Grant Agreement No 101096056. Views and opinions expressed are however those of the author(s) only and do not necessarily reflect those of the European Union or CINEA. Neither the European Union nor the granting authority can be held responsible for them.

Funded by the European Union

and light-diffusion properties help mitigate part of the irradiance loss inside the greenhouse and maintain stable power generation under varying environmental conditions.

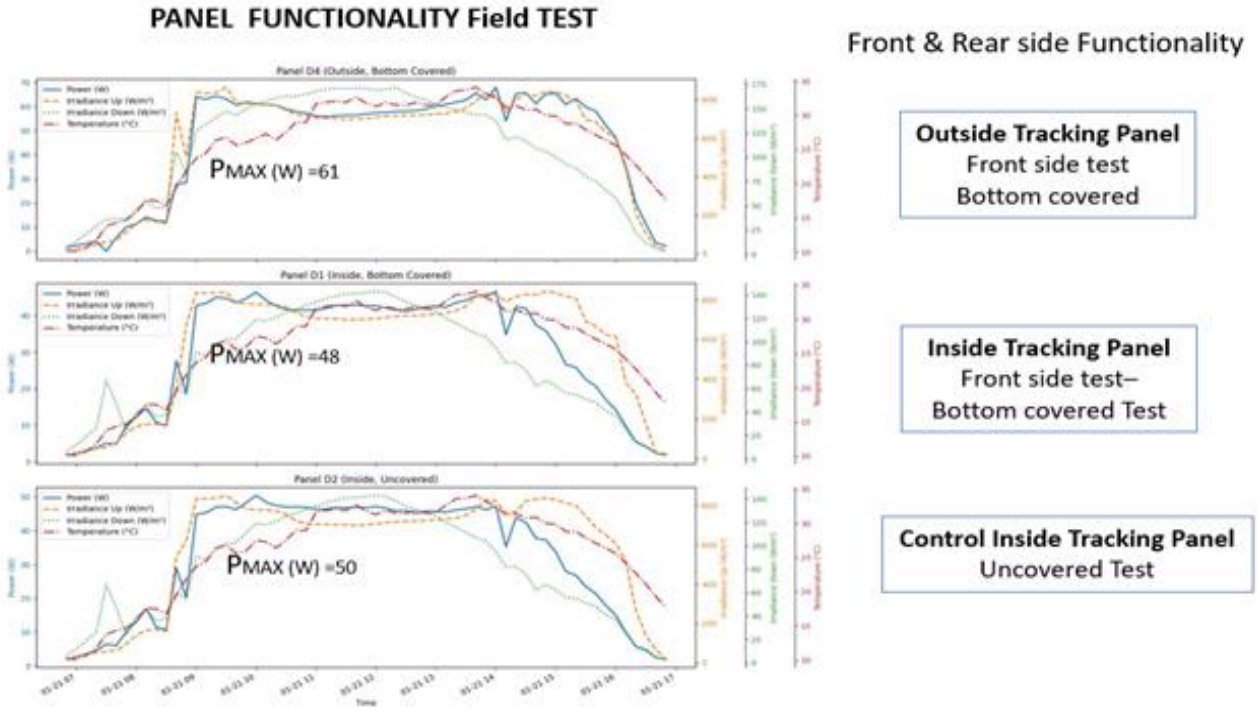

Figure 68. Comparative performance of tracking PV modules installed inside and outside the greenhouse to observe the effect of rear-side illumination (AZS Site, 2024).

Figure 68 presents a comparative measurement of power output between the tracking photovoltaic (PV) modules installed inside and outside the greenhouse, focusing on the impact of rear-side illumination. The experiment included three configurations:

1. Outdoor tracking module (reference),
2. Indoor tracking module with the greenhouse floor covered to enhance rear-side reflection, and
3. Indoor control module (uncovered reference).

The results demonstrate a clear performance advantage for the outdoor module, which produced approximately 23 % and 14 % more energy than the indoor covered and indoor control modules, respectively. Specifically, the outdoor module reached 62 W, compared to 48 W for the indoor covered configuration and 58 W for the indoor control module.

These results highlight the significant contribution of rear-side irradiance to the overall energy yield of bifacial PV systems. The experiment indicates that the rear-side reflection increased total power output by approximately 9 %, emphasizing the importance of surface reflectivity and albedo management when optimizing bifacial module performance inside greenhouse environments.

Funded by the European Union

Funded by the European Union under Grant Agreement No 101096056. Views and opinions expressed are however those of the author(s) only and do not necessarily reflect those of the European Union or CINEA. Neither the European Union nor the granting authority can be held responsible for them.

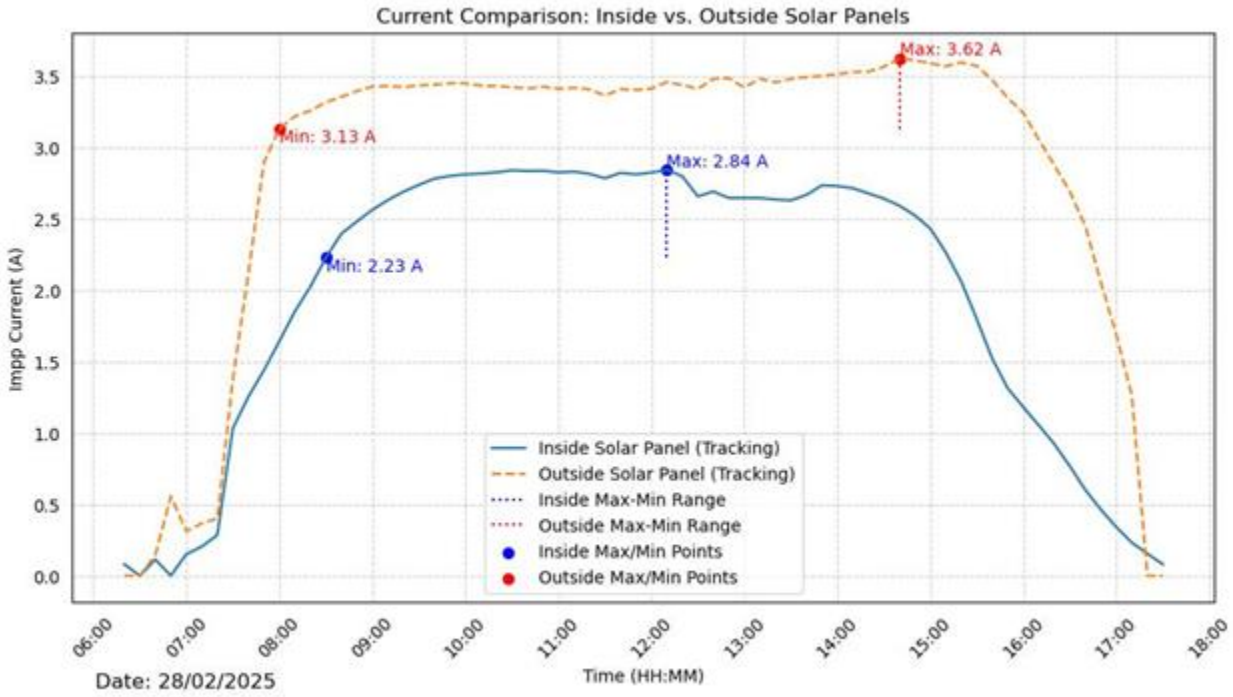

Figure 69. Comparative I_{mpp} (A) performance of tracking PV modules installed inside and outside the greenhouse – effect of rear-side illumination (AZS Site, 28th February 2024).

Figure 69 presents the current at maximum power point (I_{mpp}) for the tracking photovoltaic (PV) modules installed inside and outside the greenhouse on 28 February 2024. The measurements show that the outdoor tracking module exhibited a 22 % higher I_{mpp} value compared with the module installed inside the greenhouse. This increase directly reflects the enhanced rear-side illumination experienced by the outdoor module, resulting from higher albedo and the absence of shading from structural elements or cover materials. Inside the greenhouse, partial shading and light diffusion reduced the effective irradiance incident on both sides of the bifacial module, leading to lower current generation.

These findings confirm the beneficial role of rear-side irradiance in boosting the total current output of bifacial systems and highlight the need for optimized reflective surfaces and reduced structural shading when designing greenhouse-integrated PV installations.

Funded by the European Union under Grant Agreement No 101096056. Views and opinions expressed are however those of the author(s) only and do not necessarily reflect those of the European Union or CINEA. Neither the European Union nor the granting authority can be held responsible for them.

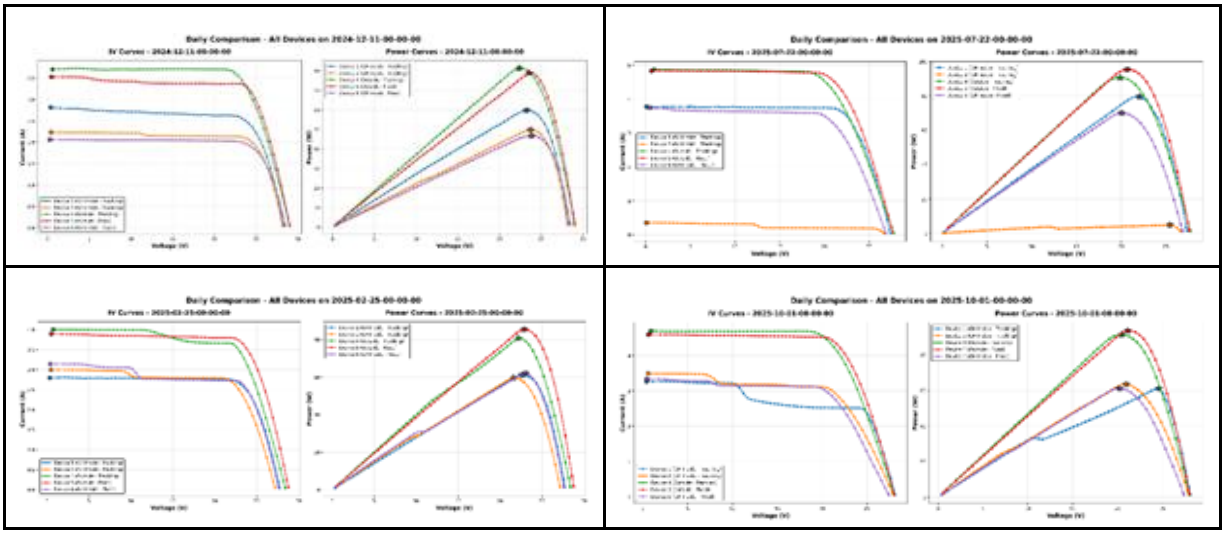

Figure 70. IV-cures and Pmax for different panels inside, outside, fix and tracking mode during four seasons.

Figure 70 presents the current–voltage (I–V) characteristics of the photovoltaic modules measured under four representative seasonal conditions in 2025. Four configurations were compared: tracking and fixed modules installed outside the greenhouse, and tracking and fixed modules installed inside. The objective of these measurements was to evaluate module performance throughout the entire year and to identify seasonal factors influencing electrical output.

During summer (22 July 2025), the outdoor tracking module achieved a maximum power of 93 W, while the outdoor fixed module reached 95 W, indicating nearly identical performance under high-irradiance conditions. Inside the greenhouse, the tracking module produced 80 W, and the fixed module reached 69 W, reflecting the reduction in available irradiance caused by light diffusion and partial shading from the greenhouse structure.

In winter (25 February 2025), the outdoor fixed module delivered 84 W and the outdoor tracking module 80 W, whereas the indoor tracking and fixed modules reached 62 W and 58 W, respectively. The smaller difference between outdoor fixed and tracking modules during winter can be attributed to the lower solar elevation angle and predominantly diffuse irradiance, which limit the effectiveness of the tracking system. By late winter (24 December 2025), the outdoor tracking module reached 84 W, the outdoor fixed module 78 W, and the indoor tracking and fixed modules 60 W and 50 W, respectively. These results confirm a consistent performance hierarchy across all seasons — outdoor > indoor and tracking > fixed — while also showing that the relative advantage of tracking decreases during low-irradiance periods.

Overall, the seasonal comparison demonstrates that module performance is strongly influenced by irradiance level, solar elevation, and greenhouse optical attenuation. Under summer conditions, high irradiance and favourable angles minimize differences between configurations, whereas in winter the combined effects of lower sunlight intensity, increased light diffusion, and reduced albedo amplify the

Funded by the European Union

Funded by the European Union under Grant Agreement No 101096056. Views and opinions expressed are however those of the author(s) only and do not necessarily reflect those of the European Union or CINEA. Neither the European Union nor the granting authority can be held responsible for them.

gap between outdoor and indoor modules. These findings validate the necessity of annual-scale testing and emphasize the importance of optimizing greenhouse transparency and PV tracking control to maintain stable year-round energy production in agrivoltaic systems.

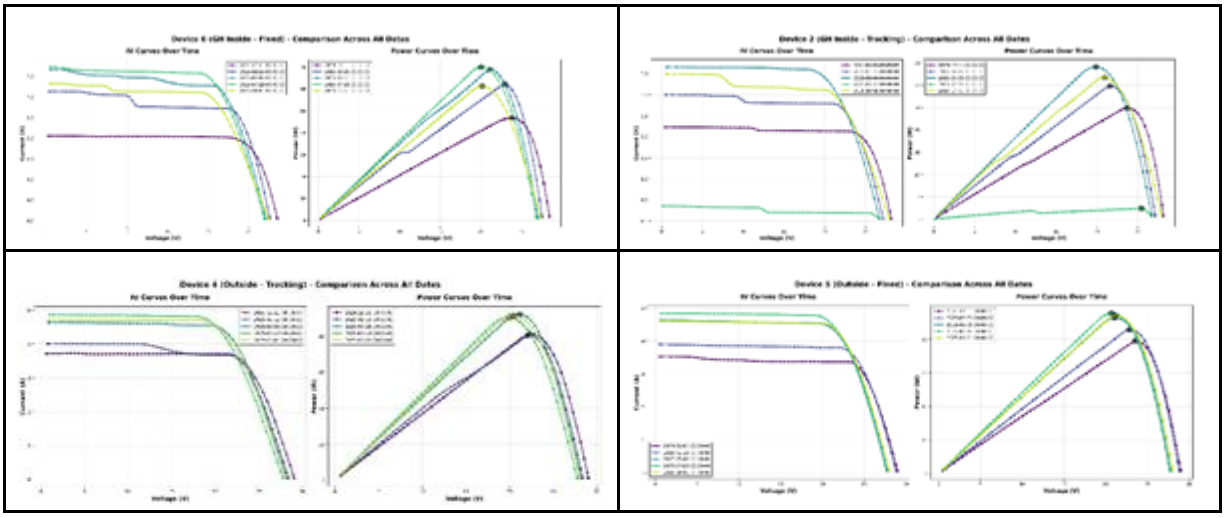

Figure 71. IV-cures and Pmax comparison between all panels across all dates.

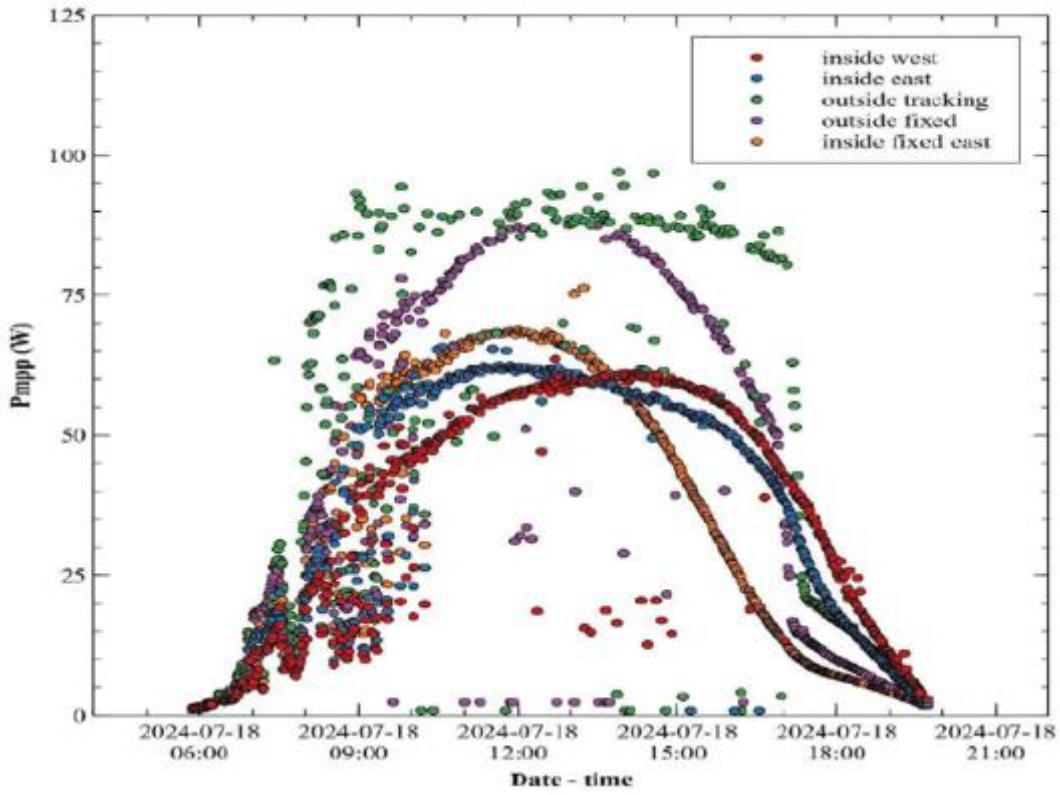

Figure 72. Diurnal power output of four photovoltaic (PV) modules – fixed and tracking configurations inside and outside the greenhouse (16 June 2024).

Funded by the European Union

Funded by the European Union under Grant Agreement No 101096056. Views and opinions expressed are however those of the author(s) only and do not necessarily reflect those of the European Union or CINEA. Neither the European Union nor the granting authority can be held responsible for them.

The results presented in Figure 72 illustrate the diurnal power output of the four individually monitored photovoltaic modules — fixed and tracking installations located inside and outside the greenhouse — on 16 June 2024. As expected, the modules installed outside the greenhouse exhibited higher power output than those installed inside, reflecting the reduction in solar irradiance caused by the optical and structural characteristics of the greenhouse cover. The outdoor tracking module reached a maximum power point (P_{mpp}) of approximately 87 W, while the tracking module inside achieved 67 W. Similarly, the fixed module inside reached a peak of 60 W, compared to 69 W for the fixed module outside. This result directly reflects the attenuation of incident irradiance and partial shading effects within the greenhouse structure.

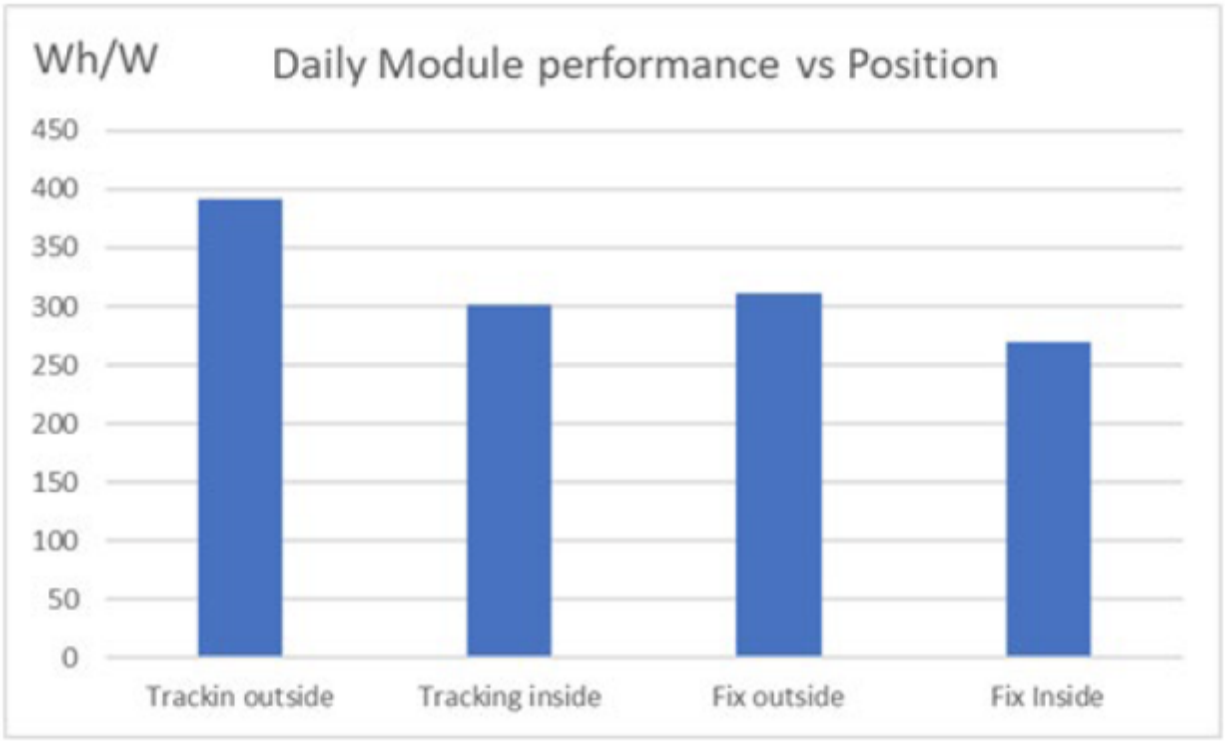

Figure 73. Maximum power point (P_{mpp}) behaviour of fixed and tracking PV modules inside and outside the greenhouse – AZS Site (June 2024).

Figure 73 compares the maximum power point (P_{mpp}) profiles of the four monitored photovoltaic (PV) modules — fixed and tracking systems installed both inside and outside the greenhouse. The outdoor tracking configuration again delivered the highest energy output, reaching approximately 87 W, followed by the indoor tracking module at 67 W. Among the fixed configurations, the outdoor fixed module produced around 69 W, while the indoor fixed module achieved approximately 60 W.

The plateau-shaped power curve of the outdoor tracking module demonstrates its ability to maintain optimized solar capture throughout the day. Inside the greenhouse, the position and orientation of the tracking modules strongly influenced the curve shape:

- The eastern-side module reached its maximum output during the morning hours.
- The western-side module peaked in the afternoon, following the sun's trajectory.

Funded by the European Union under Grant Agreement No 101096056. Views and opinions expressed are however those of the author(s) only and do not necessarily reflect those of the European Union or CINEA. Neither the European Union nor the granting authority can be held responsible for them.

Funded by the European Union

The fixed module, located along the eastern arch of the greenhouse, also exhibited a distinct morning peak under higher direct irradiance. Interestingly, the indoor fixed module produced slightly higher instantaneous peaks than the indoor tracking module, a behaviour attributed to non-uniform light distribution and partial shading within the greenhouse space.

Performance Ratio and Seasonal Behaviour

This result aligns with the reduced solar-irradiance transmission through the greenhouse cover, which limits the energy available to the indoor modules. The same trend persisted throughout the entire monitoring period, confirming the continuous influence of optical attenuation on overall energy yield.

The performance gap between indoor and outdoor modules was seasonally dependent, becoming more pronounced during winter, when solar elevation angles are lower and the fraction of diffuse radiation is higher. These findings underscore the need to optimize greenhouse-cover materials and PV-integration design to achieve a balance between agronomic light requirements and electrical-generation efficiency.

They also demonstrate the technological advantage of the TriSolar semi-transparent bifacial modules, whose inter-cell spacing and light-diffusion properties mitigate irradiance losses and support stable power generation under varying climatic conditions.

Fill Factor (FF) Behaviour

The diurnal variation of the fill factor (FF) was analysed for all four configurations — fixed and tracking modules, inside and outside the greenhouse — on 16 June 2024. The FF values ranged between 75 % and 80 %, with noticeable midday reductions observed in the fixed modules. These dips are primarily attributed to temperature-induced voltage losses and changes in solar-incidence angle during peak-irradiance periods.

In contrast, the tracking configurations maintained more stable FF values throughout the day, demonstrating improved optical alignment and reduced electrical mismatch losses. This behaviour further confirms the operational advantage of dynamic solar tracking, ensuring consistent efficiency under variable irradiance and temperature conditions typical of greenhouse environments.

Funded by the European Union under Grant Agreement No 101096056. Views and opinions expressed are however those of the author(s) only and do not necessarily reflect those of the European Union or CINEA. Neither the European Union nor the granting authority can be held responsible for them.

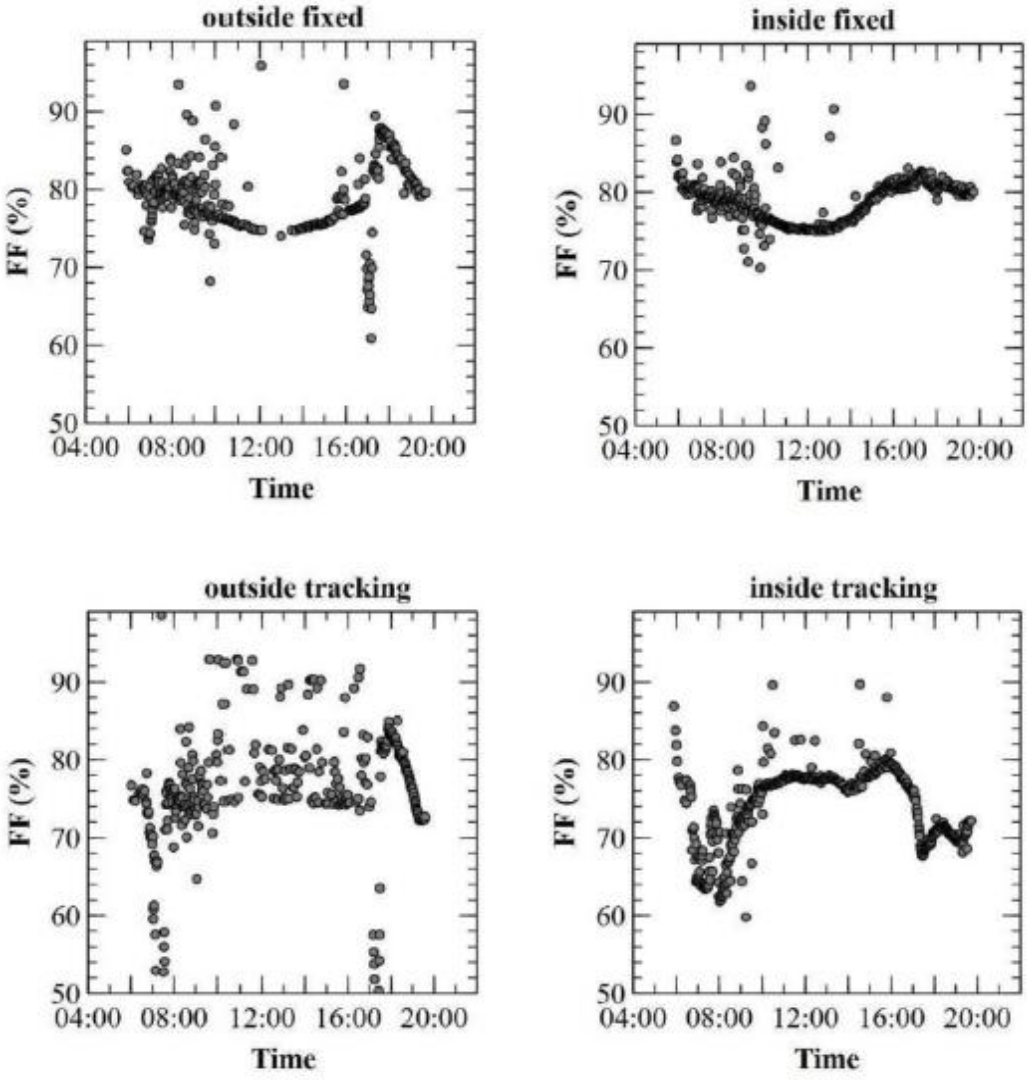

Figure 74. Fill factor results for PV module outside fixed, inside fixed, outside tracking and inside tracking on 16th June, 2024.

Each 105 Wp module was tested under a maximum outdoor irradiance of 912 W/m², with capacity factors reflecting realistic operational efficiency under both greenhouse and outdoor conditions.

Table 17. Maximum power output and derived Capacity Factors (CF) for all configurations at the AZS Site (16th June 2024).

Module location	Module peak power (W)	Module peak power/m2	System daily output (KWh)	Daily yield KWh/KWp	Capacity Factor (CF)
Outdoor tracking	87	109	59.8	4.82	0.21
Indoor tracking	67	84	46.1	3.73	0.20
Outdoor Fix	69	87	41.3	3.33	0.18
Indoor Fix	60	76	47.4	3.82	0.19

Funded by the European Union

Funded by the European Union under Grant Agreement No 101096056. Views and opinions expressed are however those of the author(s) only and do not necessarily reflect those of the European Union or CINEA. Neither the European Union nor the granting authority can be held responsible for them.

The results summarized in Table 17 are consistent with typical improvements reported for single-axis tracking PV systems under real outdoor conditions. Tracking operations increased the energy yield by approximately 15–20 %, both inside and outside the greenhouse. However, the effectiveness of tracking was partially reduced indoors due to structural shading and the predominance of diffused irradiance within the greenhouse environment.

The capacity factor (CF) — defined as the ratio between actual and theoretical maximum energy production — ranged from 0.18–0.20 inside the greenhouse to 0.19–0.21 outside, indicating a modest reduction in efficiency under greenhouse conditions. These findings are consistent with previous agrivoltaic studies in semi-transparent environments, where irradiance diffusion moderates total energy yield but contributes to stable long-term operation and lower module temperature fluctuations.

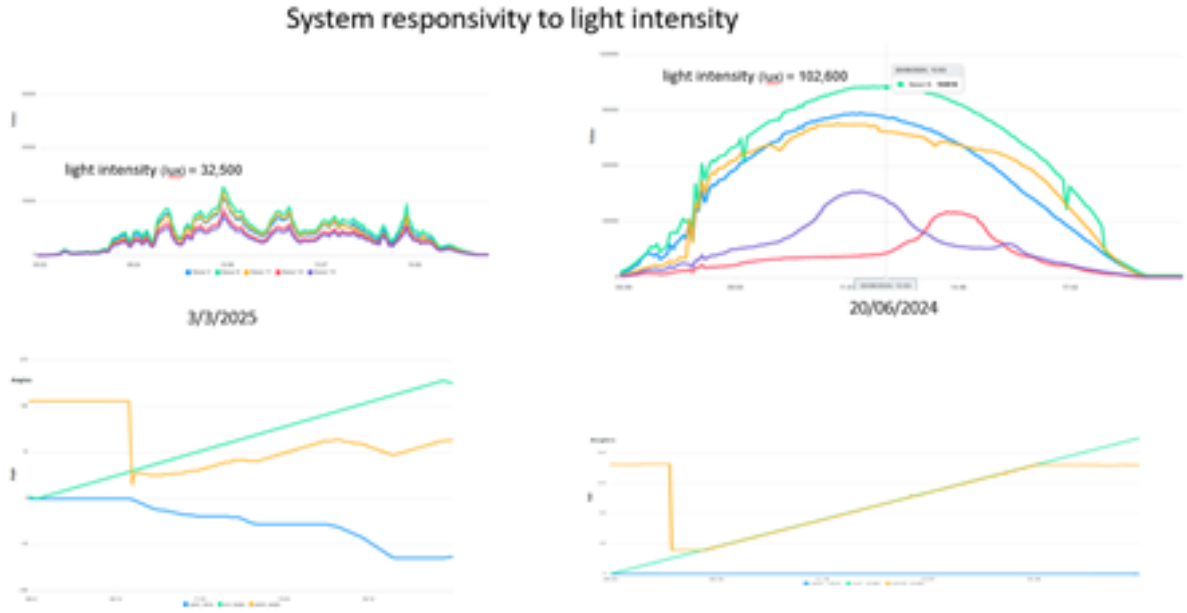

Figure 75. Dynamic responsivity of the TriSolar tracking system and its interaction with plant light needs (DLI control) which is a defining feature of the REGACE greenhouse integration.

Impact of the Tracking System's Responsivity Behaviour

An additional aspect observed in the AZS measurements is the responsiveness of the dynamic tracking system, designed to simultaneously optimize PV energy generation and crop light availability. When the daily light integral (DLI) received by the plants falls below the required threshold, the system automatically adjusts the panel tilt angle to allow increased sunlight penetration into the greenhouse, even at the expense of electrical output. Conversely, when sufficient photosynthetic radiation is available, the system returns to full solar-tracking mode to maximize energy yield.

This dual-response mechanism was clearly demonstrated in Figure 75, which compares two representative days:

Funded by the European Union under Grant Agreement No 101096056. Views and opinions expressed are however those of the author(s) only and do not necessarily reflect those of the European Union or CINEA. Neither the European Union nor the granting authority can be held responsible for them.

Funded by the European Union

- 3 March 2025 (winter day): the responsivity system periodically tilted the panels toward a near-horizontal position, allowing maximum light transmission to the crops. During these intervals, PV energy production decreased correspondingly, confirming the system's prioritization of agronomic lighting needs.
- 20 June 2025 (summer day): the panels operated under full tracking mode throughout the day, maintaining optimal solar incidence and achieving maximum power generation. In this case, DLI requirements were already met, and no additional light compensation was needed.

These findings highlight the adaptive functionality of the REGACE tracking system and its ability to balance agricultural and electrical objectives dynamically. While temporary reductions in power output occur when DLI control overrides tracking, the overall system performance remains optimized for dual productivity—crop growth and renewable energy generation—under real field conditions.

Conclusions – AZS Site Electrical Characterization

The comprehensive monitoring and electrical characterization performed at the Al Zahrawy Society (AZS) site demonstrated the reliable operation and year-round stability of the REGACE photovoltaic greenhouse system under real climatic conditions in Israel. The measured Performance Ratio (PR) averaged 0.65 during summer months, reflecting realistic efficiency values within the greenhouse environment, where diffuse irradiance and elevated internal temperatures influence conversion efficiency. The Capacity Factor (CF) ranged between 0.18 and 0.21, confirming moderate but consistent energy production compared with open-field installations.

The detailed analysis of irradiance, I–V curves, and fill factor (FF) revealed that the tracking configuration provided a 15–20 % higher energy yield than fixed modules, both inside and outside the greenhouse. However, the benefit of tracking was partially reduced inside, mainly due to structural shading, diffused light, and the limited angular variability of incoming radiation. Thermal measurements confirmed that module temperature closely followed irradiance patterns, with indoor modules showing higher operating temperatures caused by restricted ventilation and diffuse-light heating.

Seasonal measurements across four representative periods (spring, summer, autumn, and winter) highlighted a consistent performance hierarchy: outdoor > indoor and tracking > fixed. The rear-side irradiance contributed up to 9 % additional energy gain, emphasizing the importance of albedo management and surface reflectivity inside the greenhouse. At the same time, the semi-transparent TriSolar bifacial modules, featuring optimized inter-cell spacing and light-diffusion properties, helped mitigate irradiance losses and maintained stable power generation under varying climatic and optical conditions.

A distinctive feature of the REGACE system observed at the AZS site was the responsiveness of the dynamic tracking mechanism, which adjusts panel tilt according to the Daily Light Integral (DLI) received by the crops. When light levels fall below crop requirements, the panels open to increase sunlight transmission, temporarily reducing energy output. This adaptive operation highlights the system's ability

Funded by the European Union under Grant Agreement No 101096056. Views and opinions expressed are however those of the author(s) only and do not necessarily reflect those of the European Union or CINEA. Neither the European Union nor the granting authority can be held responsible for them.

to balance agricultural and electrical objectives dynamically, ensuring both optimal crop growth and efficient renewable energy production throughout the year.

Overall, the AZS results confirm that dynamic bifacial PV systems integrated within greenhouses can achieve high performance and operational stability, while preserving light availability for crops. These findings validate the REGACE design approach and provide a strong empirical basis for optimizing future agrivoltaic installations under Mediterranean and semi-arid conditions.

4 Greenhouse microclimate measurements

4.1 Micro-climate data collection strategy and microclimate monitoring for all locations

4.1.1 Training to ensure the reproducibility of collected data

Training was performed on demand. After a first zoom-meeting with all partners on the evaluation procedures for the selected microclimate measurements inside the greenhouse, further zoom-meetings with individual partners were arranged on demand in order to address actual problems and elaborate practicable solutions.

4.1.2 Greek Greenhouse facility (UTH - University of Thessaly)

The experiments were conducted in a gothic-arch multi-tunnel greenhouse located at the pilot greenhouse park of the Laboratory of Agricultural Constructions and Environmental Control, Department of Agriculture, Crop Production, and Rural Environment, University of Thessaly, in Velestino, Central Greece (39°22', 22°44', 85.0 m). The greenhouse was oriented north–south and comprised four compartments and engine room, each with a cultivation area of 240 m² (25.0 m length × 9.6 m width × 7.4 m ridge height). The greenhouse cover material was a UV-resistant polyethylene film (transmittance: 0.75), while the side walls consisted of polycarbonate sheets. Each compartment was equipped with a continuous roof vent, a fan-and-pad evaporative cooling system, and a thermal-shading screen (transmittance: 0.50) installed at a height of 5.0 m. Six hydroponic channels (20.0 m length each) were installed per compartment, each fitted with 19 rockwool slabs (Grodan Delta, NL; dimensions: 100 × 15 × 7.5 cm; density: 0.18 g/cm³; 90% water retention capacity, Roermond, The Netherlands).

Greenhouse climate conditions were automatically regulated and monitored by a climate control computer (SERCOM, Automation SL, Lisse, The Netherlands).

System Architecture and Components of the UTH Greenhouse

At UTH facilities, internal and external environmental parameters were automatically recorded at fifteen-minute intervals and stored in a database managed by the climate-control computer.

Funded by the European Union

Funded by the European Union under Grant Agreement No 101096056. Views and opinions expressed are however those of the author(s) only and do not necessarily reflect those of the European Union or CINEA. Neither the European Union nor the granting authority can be held responsible for them.

Each compartment was equipped with a meteorological station positioned at the center of the greenhouse, equipped with sensors for air temperature (T, °C), relative humidity (RH, %), and CO_2 concentration (ppm), all placed 1.5 m above the ground. A photosynthetically active radiation (PAR) sensor (Apogee SQ500-SS, Logan, UT, USA) was also placed at the same location, below the thermal screen. Similarly, an external climate station was installed at the north-east side of the greenhouse at a height of 1.5 m for measuring ambient T and RH. Solar radiation, wind direction, and wind speed were measured at the same position at 7.5 m above ground.

Carbon dioxide (CO_2) enrichment was implemented in two of the four greenhouse compartments. The enrichment involved the controlled CO_2 release through perforated distribution tubes positioned beneath each hydroponic channel. The set point for CO_2 concentration was set at 600 ppm.

Experimental setup at UTH Greenhouse facility

In UTH four experiments were conducted to evaluate the performance of the PV modules and CO_2 and their effect on crop growth. The experimental design and the different treatments applied, differed between the four experiments and is presented in Table 18.

Table 18. Treatments applied across different experimental periods.

Treatments	Experiment A	Experiment B	Experiment C	Experiment D
CTRL	×	×	×	×
CO_2	×	×		
PV-Tracking	×	×	×	×
PV-Tracking + CO_2	×	×		
PV-Opposite			×	
PV-Fixed				×

Six treatments were established: (i) Control (CTRL), with neither PV modules nor CO_2 enrichment; (ii) CO_2 enrichment (CO_2), with CO_2 enrichment only; (iii) Photovoltaic tracking (PV-Tracking), with solar-tracking PV modules only; (iv) Combined (PV-Tracking + CO_2), with solar-tracking PV modules and simultaneous CO_2 enrichment; (v) Opposite-tracking photovoltaics (PV-Opposite), with PV modules tracking counter to the solar trajectory; and (vi) Fixed photovoltaics (PV-Fixed), with PV modules mounted horizontally parallel to the ground for the entire experimental period. Not all treatments were tested concurrently; instead, they were implemented in separate experimental runs as presented in Table 18.

Temperature, Relative Humidity, CO_2

The climatic data that were selected were the following:
Average air temperature (T, °C) and relative humidity (RH, %) inside the greenhouse compartments are presented in Table 19. Across all experimental sessions, no differences were detected among treatments. Internal air temperature was consistently maintained within a narrow range (16-20°C), despite pronounced seasonal variations in ambient conditions (10-21°C).

Funded by the European Union under Grant Agreement No 101096056. Views and opinions expressed are however those of the author(s) only and do not necessarily reflect those of the European Union or CINEA. Neither the European Union nor the granting authority can be held responsible for them.

Similarly, RH values remained stable across treatments, ranging from 69–86%. The absence of treatment-related differences indicates that the climate-control system effectively buffered the greenhouse environment, minimizing the influence of PV shading on internal microclimate parameters.

Table 19. Mean temperature (°C, ± SE), and relative humidity (%, ± SE), across treatments during each experimental period.

	Treatments	Temperature [°C]	RH [%]
Exp. A	Ambient air	15.7±0.08	73.8±0.23
	CTRL	18.1±0.05	85.6±0.14
	CO_2	18.1±0.05	85.7±0.14
	PV-Tracking	18.1±0.05	83.5±0.15
	PV-Tracking + CO_2	18.2±0.05	83.5±0.14
Exp. B	Ambient air	10.4±0.06	81.7±0.21
	CTRL	16.2±0.05	78.2±0.15
	CO_2	16.2±0.05	77.2±0.15
	PV-Tracking	16.2±0.05	75.1±0.15
	PV-Tracking + CO_2	16.6±0.05	76.0±0.16
Exp. C	Ambient air	21.3±0.10	64.4±0.31
	CTRL	19.7±0.06	81.8±0.23
	PV-Tracking	19.9±0.06	80.2±0.22
	PV-Opposite	20.0±0.06	81.2±0.22
Exp. D	Ambient air	18.3±0.10	68.9±0.37
	CTRL	19.7±0.09	71.0±0.31
	PV-Tracking	19.7±0.09	69.1±0.31
	PV-Fixed	19.6±0.09	70.2±0.31

Table 20 presents the temporal trends in CO_2 concentration for all experimental treatments. Over the full cultivation cycle, average CO_2 levels remained similar across the treatments, including those with CO_2 enrichment. However, during active enrichment intervals, the CO_2 enriched compartments maintained higher mean concentrations-approximately 100 ppm higher than the non-enriched compartments. More specifically, during the CO_2 enrichment periods, the average values of the non-CO_2-enriched compartments were maintained at 355-399 ppm, while the concentration of the enriched compartments was maintained at the levels of 454-478 ppm. These results demonstrate that the CO_2 enrichment effectively elevated the CO_2 concentration and was directly responsible for the higher mean values recorded in these treatments.

Figure 76 illustrates CO_2 concentrations in the treatments and ambient air during a CO_2 enrichment day, for the experiments A and B. The CO_2 setpoint was 600 ppm; however, once this level was reached, concentrations in the enriched compartments continued to rise even after the enrichment valves closed. After the programmed enrichment period ended (15:30), CO_2 levels in the enriched compartments dropped sharply, reflecting rapid plant assimilation. In the absence of air renewal, concentrations then fell below ambient levels. During the night, CO_2 concentrations in all compartments exceeded ambient

Funded by the European Union

Funded by the European Union under Grant Agreement No 101096056. Views and opinions expressed are however those of the author(s) only and do not necessarily reflect those of the European Union or CINEA. Neither the European Union nor the granting authority can be held responsible for them.

levels due to plant respiration. Interestingly, in the evening hours when no enrichment was applied, the previously enriched compartments showed consistently lower CO_2 concentrations compared to the control. This suggests that plants in the fertilized compartments had a higher photosynthetic capacity and thus depleted CO_2 more strongly once enrichment stopped.

Table 20. Mean CO_2 concentration (ppm, ± S.E.) during the experimental periods, and average CO_2 concentration (ppm, ± SE), during CO_2 enrichment events in fertilized and non-fertilized treatments.

	Treatments	CO_2 [ppm]	CO_2 during enrichment [ppm]
Exp. A	Ambient air	331.5±0.30	-
	CTRL	389.3±0.89	372.1±3.09
	CO_2	400.7±0.48	454.1±5.95
	PV-Tracking	423.2±0.44	399.1±3.16
	PV-Tracking + CO_2	361.4±1.11	471.5±7.51
Exp. B	Ambient air	356.4±0.33	-
	CTRL	337.1±0.59	355.2±0.84
	CO_2	422.1±1.15	457.6±3.61
	PV-Tracking	412.2±0.44	386.9±0.71
	PV-Tracking + CO_2	431.1±1.21	478.8±3.56
Exp. C	Ambient air	326.2±0.42	-
	CTRL	361.2±0.60	-
	PV-Tracking	380.7±0.51	-
	PV-Opposite	342.7±0.61	-
Exp. D	Ambient air	311.4±0.49	-
	CTRL	333.8±0.52	-
	PV-Tracking	367.8±0.39	-
	PV-Fixed	337.0±0.56	-

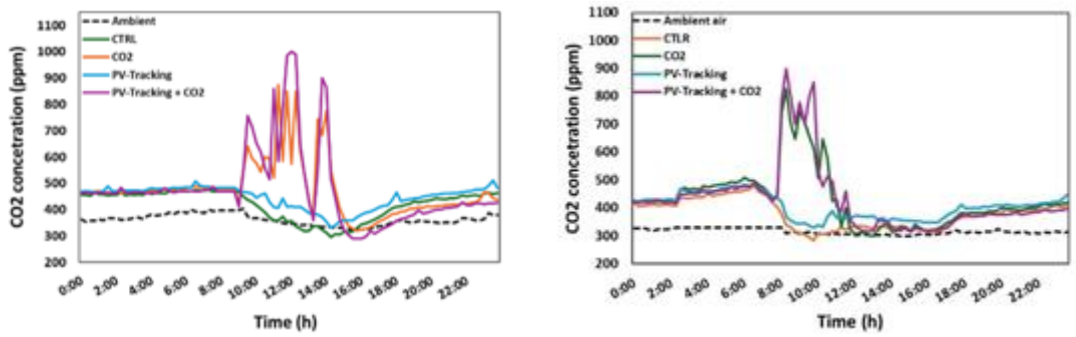

(A) **(B)**

Figure 76. Diurnal variation of CO_2 concentrations in control and enriched compartments across an experimental day (Experiments A and B).

Funded by the European Union

Funded by the European Union under Grant Agreement No 101096056. Views and opinions expressed are however those of the author(s) only and do not necessarily reflect those of the European Union or CINEA. Neither the European Union nor the granting authority can be held responsible for them.

Table 21. Mean air temperature (°C, ± S.E) and relative humidity (%, ± S.E.) during CO_2 fertilization events in the first and second experimental period.

	Treatments	Temperature [°C]	RH [%]
Exp. A	CTRL	18.3±0.16	87.6±0.71
	CO_2	18.2±0.17	88.0±0.72
	PV-Tracking	18.4±0.17	86.1±0.73
	PV-Tracking +CO_2	18.4±0.16	84.9±0.72
Exp. B	CTRL	20.2±0.09	68.8±0.26
	CO_2	20.2±0.09	67.5±0.26
	PV-Tracking	20.5±0.09	65.1±0.27
	PV-Tracking +CO_2	20.4±0.08	66.1±0.27

Elevated atmospheric CO_2 often promotes partial stomatal closure, leading to reduced stomatal conductance and consequently lower transpiration rates, a response that can in turn influence the internal greenhouse microclimate by slightly modifying humidity and latent heat fluxes. In the current experiment, no differences in temperature or relative humidity were observed between the treatments during CO_2 enrichment periods (Table 21), as the automated climate-control system maintained stable internal conditions regardless of fluctuations in solar radiation or CO_2 levels.

Table 22. Cumulative PAR (MJ m^{-2}) and mean Daily Light Integral (mol m^{-2} d^{-1}, ±S.E.) across treatments during the experimental periods.

	Treatments	PAR [MJ m^{-2}]	DLI [mol m^{-2} d^{-1}]
Exp. A	Global	369.0	19.6±1.07
	CTRL	206.1	11.0±0.62
	CO_2	193.5	10.3±0.56
	PV-Tracking	131.7	7.0±0.41
	PV-Tracking +CO_2	134.9	7.2±0.43
Exp. B	Global	638.7	37.7±1.92
	CTRL	360.9	21.2±1.06
	CO_2	335.5	19.7±1.21
	PV-Tracking	242.1	14.2±0.87
	PV-Tracking +CO_2	246.8	14.5±0.92
Exp. C	Global	446.0	42.6±1.40
	CTRL	166.6	15.9±0.57
	PV-Tracking	115.4	11.0±0.39
	PV-Opposite	118.9	11.7±0.46
Exp. D	Global	151.1	24.9±1.95
	CTRL	78.6	12.9±0.93
	PV-Tracking	53.7	8.8±0.64
	PV-Fixed	53.2	8.8±0.68

Funded by the European Union

Funded by the European Union under Grant Agreement No 101096056. Views and opinions expressed are however those of the author(s) only and do not necessarily reflect those of the European Union or CINEA. Neither the European Union nor the granting authority can be held responsible for them.

Light quality parameters

Cumulative PAR measurements demonstrated substantial reductions in light availability in all compartments equipped with photovoltaics (Table 22). Shading from the PV panels decreased incident PAR by 20–40%, depending on the experimental period. In Experiment A, cumulative outdoor PAR reached 369.0 MJ m^{-2}. Non PV-shaded compartments (control and CO_2 treatments) received approximately 200.0 MJ m^{-2}, representing a 45% reduction relative to external radiation, while the PV-shaded compartments (PV-tracking and PV-tracking + CO_2 treatments) received only 133.3 MJ m^{-2}, corresponding to an additional 33% decrease.
A similar pattern was observed in Experiment B, conducted under higher solar input, with PV-shaded compartments intercepting about one-third less PAR than the non-PV-shaded compartments. In Experiment C, outdoor cumulative PAR reached 446.0 MJ m^{-2}, with PV-tracking and PV-Opposite treatments receiving only 115.4, and 118.9 MJ m^{-2}, respectively, underscoring substantial attenuation of light transmission caused by PV panels. Similarly, in Experiment D, CTRL cumulative PAR reached 78.6 MJ m^{-2}, with PV-tracking and PV-Fixed treatments receiving only 53.7, and 53.2 MJ m^{-2}.

Daily light integral analysis revealed pronounced differences among the experiments. The lowest DLI values were observed in Experiment A within the PV-shaded compartments, averaging approximately 7.1 mol m^{-2} d^{-1}. In Experiment B, DLI in the PV-shaded compartments increased compared to Experiment A but remained substantially lower than in the CTRL and CO_2 treatments, with reductions of approximately 30%, indicating a marked attenuation of light due to PV shading. In Experiment C, which evaluated the effect of PV tracking, DLI differed between the PV-Tracking and PV-Opposite treatments. Specifically, the PV-Tracking compartment, in which panels followed the sun's trajectory, exhibited a 6.4% higher DLI compared to the PV-Opposite compartment. Nevertheless, consistent with Experiments A and B, PV-shaded compartments in Experiment C and D showed an approximate 30% reduction in DLI compared to the CTRL, confirming the substantial impact of PV panels on light availability within the greenhouse. Figure 77 illustrates the diurnal variation in transmitted PAR, highlighting differences between treatments for clear and cloudy sky conditions.

Based on the results of Experiments A and B (Figure 77), PAR transmittance was evaluated in the absence of deployed shading screens, such that it was influenced only by the greenhouse plastic cover and, where applicable, PV modules. Under clear-sky conditions, PAR transmittance reached 73.2% in non-PV-shaded compartments and 53.7% in PV-shaded compartments. Under cloudy conditions, transmittance decreased to 60.4% and 38.8%, respectively. In Experiment C, conducted during summer with shading screens consistently deployed, PAR transmittance was markedly lower. Under clear sky conditions, non-PV-shaded compartments transmitted 25.3% of PAR, compared to 15.0% in PV-shaded compartments. Under cloudy conditions, these values increased to 51.1% and 36.0%, respectively. Similar results were obtained for Experiment D.

Funded by the European Union under Grant Agreement No 101096056. Views and opinions expressed are however those of the author(s) only and do not necessarily reflect those of the European Union or CINEA. Neither the European Union nor the granting authority can be held responsible for them.

Funded by the European Union

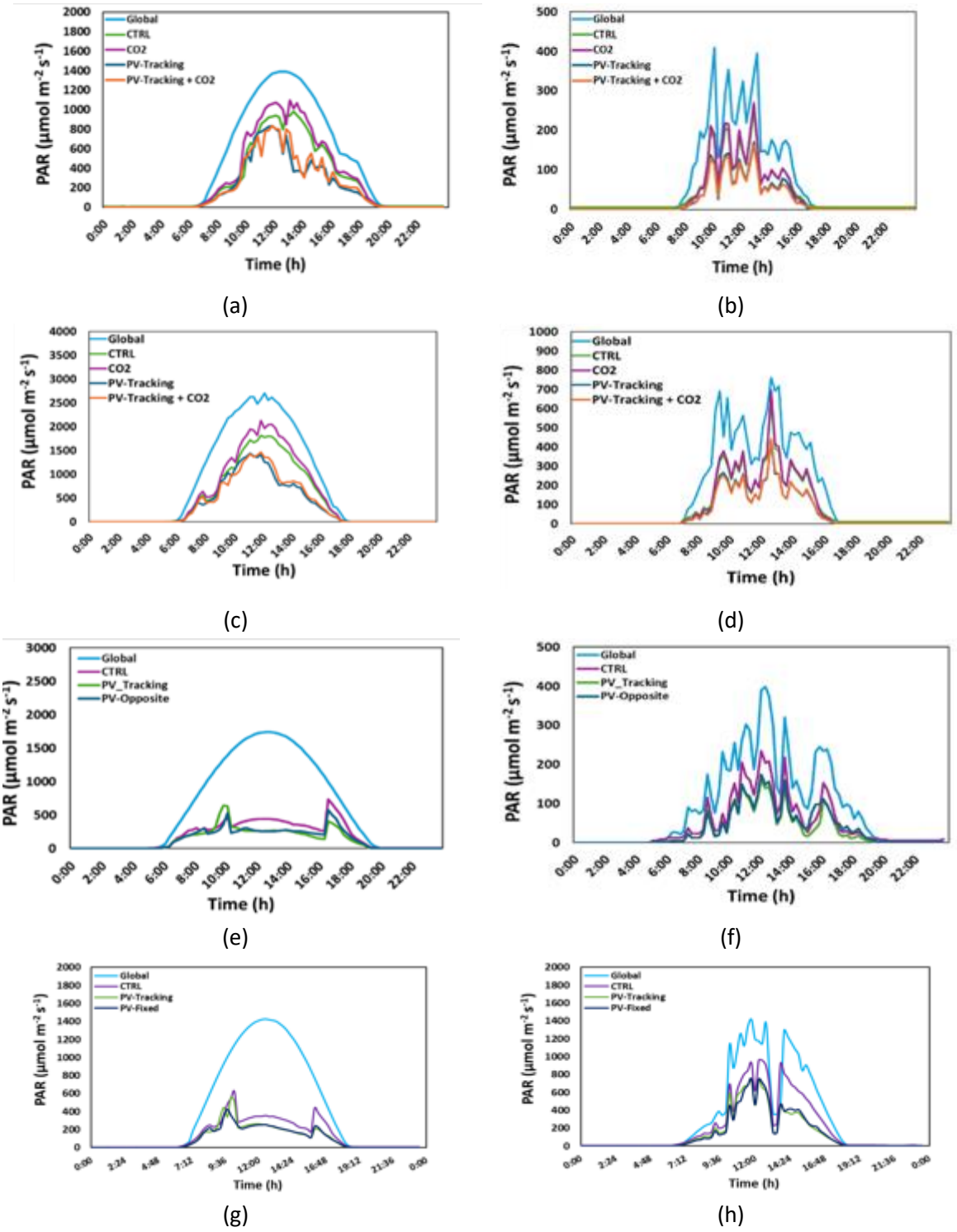

Figure 77. Diurnal variation of PAR (µmol m^{-2} s^{-1}) for Experiment A (a, b), Experiment B (c, d), Experiment C (e, f) and Experiment D (g, h) during a representative clear-sky (a, c, e, g) and cloudy day (b, d, f, h).

Funded by the European Union under Grant Agreement No 101096056. Views and opinions expressed are however those of the author(s) only and do not necessarily reflect those of the European Union or CINEA. Neither the European Union nor the granting authority can be held responsible for them.

Funded by the European Union

Figure 78 shows the mean weekly cumulative DLI for each treatment, along with the corresponding percentage reductions observed between compartments. In Experiment A and B, the reduction rates exhibited temporal fluctuations. In Experiment A, conducted during fall/winter period, the percentage reduction in PAR increased gradually, reaching approximately 40% by the final week.

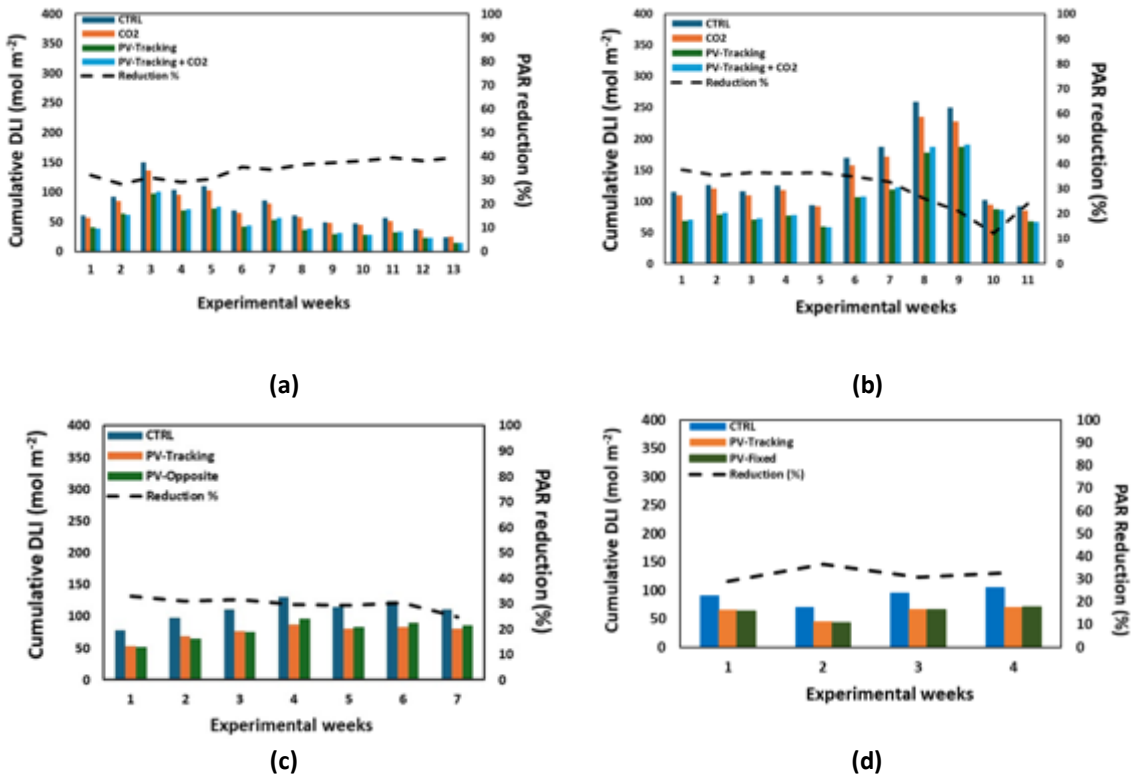

Figure 78. Weekly cumulative DLI (mol m^{-2}) across all treatments and corresponding percentage PAR reduction for PV-shaded compartments in experiments A (a), B (b), C (c), and D (d).

In contrast, in Experiment B, as weekly cumulative PAR increased, the percentage reduction declined. Overall, weeks with low PAR accumulation were associated with higher reduction values. In Experiment C, the reduction remained relatively stable across treatments. This pattern was attributed both to the high levels of external radiation and to the activation of the shading curtain under conditions of intense solar radiation. Overall, the results demonstrate that PV integration consistently reduced DLI at the canopy level by approximately 30-35% compared with the non PV-shaded compartments, confirming the persistent light-attenuation effect of the PV modules across all experimental periods.

Funded by the European Union under Grant Agreement No 101096056. Views and opinions expressed are however those of the author(s) only and do not necessarily reflect those of the European Union or CINEA. Neither the European Union nor the granting authority can be held responsible for them.

Funded by the European Union

4.1.3 Italian Greenhouse facility (FSC - Fattoria Solidale del Circeo)

General information

The greenhouse (GH) is located in Pontinia, in the province of Latina (Italy), at the Fattoria Solidale del Circeo (41°23'44.9"N, 13°08'57.7"E), as shown in Figure 79.

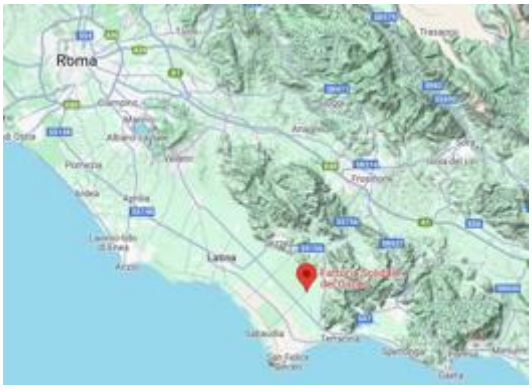

Figure 79. FSC Greenhouse location.

The GH is a double-span structure with a total area of 180 m², oriented along an east–west longitudinal axis. A suspended single-axis tracking photovoltaic (PV) system is installed inside the greenhouse, covering half of the total surface area (90 m²), as illustrated in Figure 80.

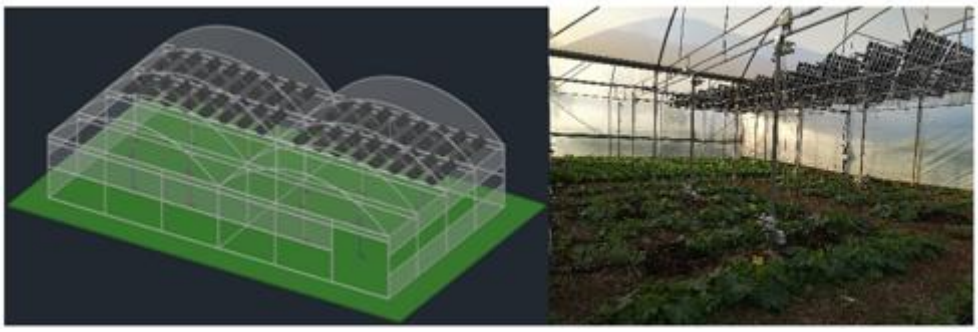

Figure 80. CAD representation of the FSC greenhouse and a partial view of the PV panels.

For the experimental purposes, the greenhouse has been divided into two zones (EAST and WEST) based on its longitudinal orientation. Each zone covers 90 m² and is further subdivided into two sectors: one shaded by the PV panels and one unshaded, which serves as a reference. This results in four distinct sectors: EAST_PV (PV E), EAST_no_PV (REF E), WEST_PV (PV W), and WEST_no_PV (REF W) (Figure 81).

Funded by the European Union

Funded by the European Union under Grant Agreement No 101096056. Views and opinions expressed are however those of the author(s) only and do not necessarily reflect those of the European Union or CINEA. Neither the European Union nor the granting authority can be held responsible for them.

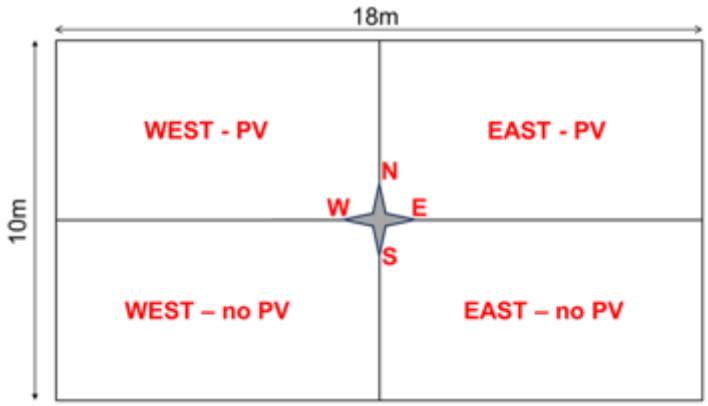

Figure 81. Greenhouse internal partition .

Two different crops are cultivated simultaneously, one in the EAST zone and one in the WEST zone. To assess the impact of the PV system on plant growth and productivity, the unshaded sectors serve as control references for evaluating the influence of photovoltaic coverage on the adjacent PV-shaded sectors.

System Architecture and Components of the FSC Greenhouse

The greenhouse is equipped with a distributed sensor network designed to monitor three primary subsystems:

- Greenhouse microclimate
- Environmental parameters;
- Automated irrigation operations.

To support these functions, three independent communication buses were implemented using the Modbus RTU protocol over RS-485. Each bus is dedicated to a specific sensor domain, enabling parallel acquisition and minimizing bus contention. The data acquisition interval is fixed to 5 min.

For each communication bus, sensor data is logged in real time to a dedicated Comma-Separated Values (CSV) file. At the end of each day a backup routine archives the day's data to a cloud-synchronized directory, using a filename indicating the subsystem (e.g., irrigation or microclimate, with sector identifiers) and the backup date (YYYY-MM-DD). Concurrently, the corresponding file is reset to facilitate daily data segmentation and to keep file size manageable. A manual backup function is also available, generating a timestamped archive (YYYY-MM-DD_HH-MM-SS) on demand.

Data integrity is ensured through the implementation of cyclic redundancy check (CRC-16) validation for all incoming Modbus frames. Upon detection of a CRC failure or incomplete transmission, the system triggers an automatic retry mechanism, allowing up to five successive acquisition attempts. If the fault persists beyond the retry threshold, the event is logged to a diagnostic log file with detailed error metadata, and a “NaN” (Not a Number) placeholder is written to the file to preserve both temporal alignment and structural integrity of the dataset.

Funded by the European Union

Funded by the European Union under Grant Agreement No 101096056. Views and opinions expressed are however those of the author(s) only and do not necessarily reflect those of the European Union or CINEA. Neither the European Union nor the granting authority can be held responsible for them.

Microclimate Monitoring Subsystem

To comprehensively monitor the greenhouse microclimate, a distributed sensing architecture was deployed, comprising eight identical measurement nodes, two per cultivation sector. Each node integrates a vertical sensor array positioned at three distinct heights, as illustrated in Figures 82 and 83.

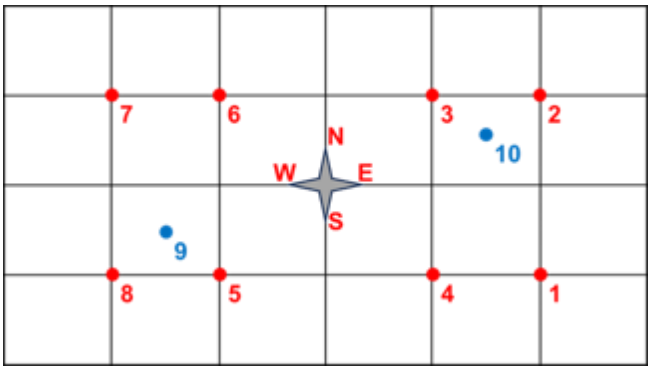

Figure 82. Sensor positioning in the greenhouse at FSC.

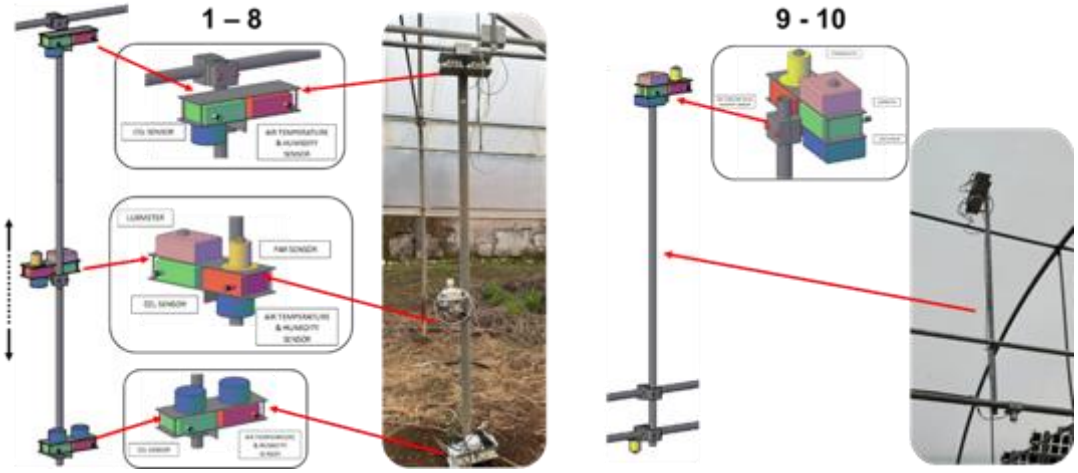

Figure 83. Sketch of the poles.

Sensors are vertically stratified as follows:

- ground Level: located a few cm above the soil, this level is equipped with temperature (T) and relative humidity (RH) sensors, along with a CO_2 sensor.
- adjustable canopy sensor level: mounted on a height-adjustable support ranging from 30 cm to 200 cm, this level adds to the ground level configuration sensors for Photosynthetically Active Radiation (PAR) and a luxmeter. The height of this level is dynamically adapted to canopy growth to maintain proximity to the upper leaf layer.

Funded by the European Union

Funded by the European Union under Grant Agreement No 101096056. Views and opinions expressed are however those of the author(s) only and do not necessarily reflect those of the European Union or CINEA. Neither the European Union nor the granting authority can be held responsible for them.

- below level: positioned approximately 250 cm above the ground, just below the photovoltaic array, this level replicates the sensor suite of the ground level, enabling characterization of macro-level environmental conditions.

Two supplementary nodes (9 and 10 in Figure 82 and 83) are located above the PV panels to quantify ambient parameters above PV panels. The sensor configuration is similar to the adjustable level, but the PAR is replaced by two pyranometers in order to measure the Global Horizontal Irradiance (GHI) and the Reflected Horizontal Irradiance (RHI).

This configuration enables continuous, multi-level monitoring of key environmental variables across the plant growth cycle. By maintaining the adjustable level just above the crop canopy, the system ensures precise quantification of microclimatic parameters—particularly those related to light availability (LUX, PAR), which directly influence photosynthetic activity and biomass accumulation.

Automated Irrigation Subsystem

A critical aspect of this study involves precise control and real-time monitoring of water delivery to cultivated plants. For this purpose, a drip irrigation system was implemented within the greenhouse environment to ensure optimized water distribution with minimal waste. The system architecture is subdivided into independent irrigation sectors, as shown in Figure 84, each instrumented with the following components:

- soil temperature and relative humidity sensors (4 units total): Strategically positioned in the root zone to enable accurate evaluation of soil moisture conditions and mitigate the risk of hydric stress;
- a flow and temperature sensor measures the volumetric flow rate and temperature of irrigation water supplied to each sector;
- An electro-actuated solenoid valve regulates the hydraulic line for each sector, enabling localized control of irrigation events.

Additionally, the main irrigation line is equipped with:

- pressure sensor: monitors inlet pressure to assess system integrity and detect anomalies.
- combined flow and temperature sensor provides baseline flow and temperature measurements for the entire system to support diagnostic and performance assessments.

Funded by the European Union under Grant Agreement No 101096056. Views and opinions expressed are however those of the author(s) only and do not necessarily reflect those of the European Union or CINEA. Neither the European Union nor the granting authority can be held responsible for them.

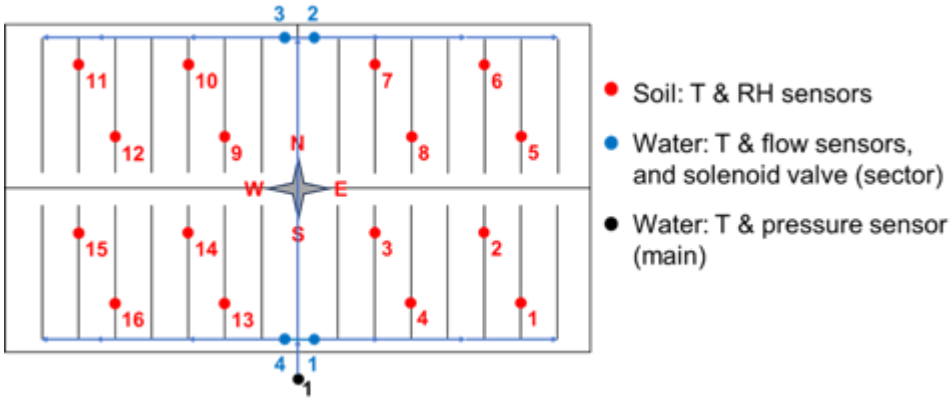

Figure 84. Sensors distribution for irrigation.

A custom software platform was developed in MATLAB (Figure 85) to manage and supervise the entire irrigation infrastructure. The software is structured into two primary modules:

- the sensor monitoring module performs continuous acquisition and real-time logging of hydraulic parameters from all deployed sensors.
- the irrigation control module serves both automated and manual irrigation cycles, leveraging sensor feedback for adaptive decision-making.

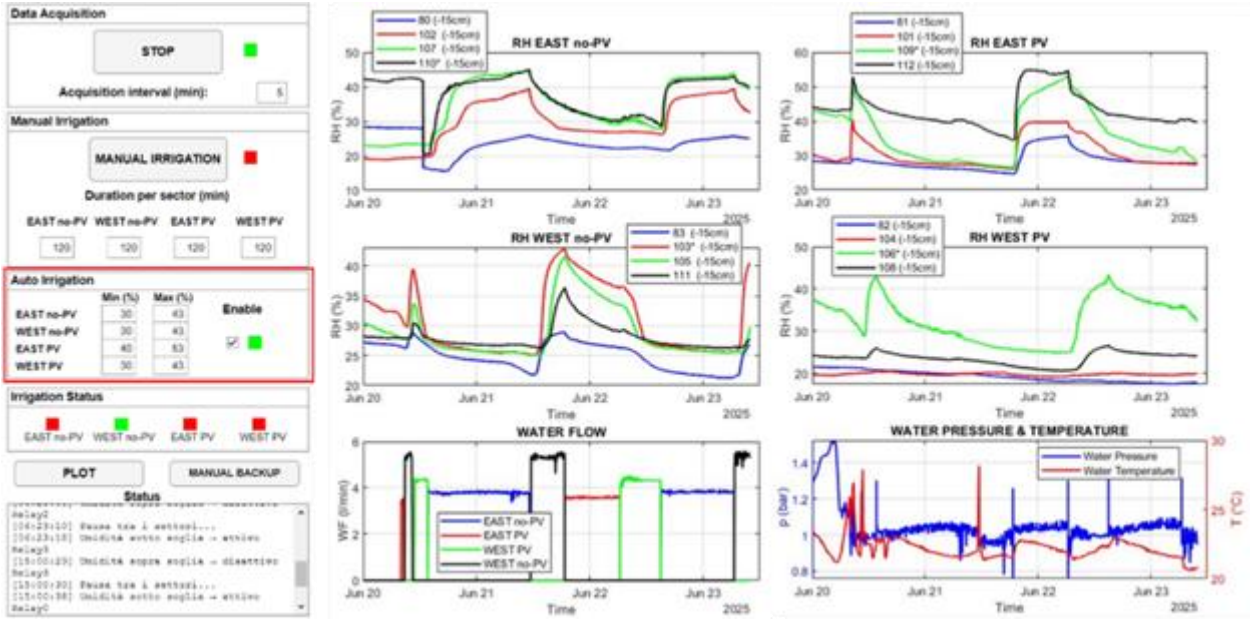

Figure 85. MATLAB GUI and data plot of two sectors and water flow.

The automated irrigation strategy is governed by soil moisture data. When moisture readings drop below a user-defined lower threshold, the system activates the relevant solenoid valve until the humidity surpasses the upper threshold, at which point the valve is closed. This control logic can operate in either parallel or sequential mode, with the execution handled entirely via the software interface.

Funded by the European Union

Funded by the European Union under Grant Agreement No 101096056. Views and opinions expressed are however those of the author(s) only and do not necessarily reflect those of the European Union or CINEA. Neither the European Union nor the granting authority can be held responsible for them.

A manual timed irrigation mode is also available, allowing the operator to configure and initiate sector-specific irrigation sequences with customizable durations. Real-time system status and sensor data are displayed via an integrated graphical interface to support informed user interventions and facilitate monitoring and diagnostics.

Micro-climate data collection

Two cultivation cycles were carried out at FSC: the first from February 19, 2025, to May 15, 2025, during which zucchini and lettuce were grown; the second from May 20, 2025, to August 31, 2025, involving tomatoes and eggplants. For this reason, the climatic data will be discussed in relation to the aforementioned production cycles.

Average temperature, average relative humidity, and average CO_2 concentration observed at canopy height during the two cultivation cycles are reported in Table 23.

Table 23. Mean temperature (°C), mean relative humidity (RH, %) and mean CO_2 (ppm) observed over the whole production cycles with their respective SE.

Cycle	Temp. (°C)	RH (%)	CO2 (ppm)
	PV – Ref.	PV – Ref.	PV – Ref.
I	18.2±0.2 – 18.8±0.2	73.2±0.6 – 70.8±0.5	460±1.1 – 463±1.1
II	28.3±0.2 – 29.0±0.2	61.6±0.4 – 59.7±0.4	446±0.8 – 450±0.8

The reported data appear to indicate a substantial equivalence in terms of CO_2 concentration, while a shading effect beneath the photovoltaic panels seems evident, as also confirmed by the relative humidity data.

Table 24 summarizes the observed averages of Photosynthetically Active Radiation (PAR) and illuminance (LUX) at canopy height, as well as Global Horizontal Irradiance (GHI) and Reflected Horizontal Irradiance (RHI) during daytime under the greenhouse cover.

Table 24. Mean Photosynthetically Active Radiation (µmol m^{-2} s^{-1}), illuminance (lux), Global Horizontal Irradiance (W m^{-2}), and Reflected Horizontal Irradiance (W m^{-2}) observed over the whole production cycles with their respective SE.

Cycle	PAR (µmol·m^{-2} ·s^{-1})	LUX (lux)	GHI (W·m^{-2})	RHI (W·m^{-2})
	PV – Ref.	PV – Ref.	PV – Ref.	PV – Ref.
I	244.1±7.3 – 337.6±10.5	20271±541 – 23811±644	358.1±10.5 – 364.7±10.7	68.1±2.2 – 70.1±2.4
II	330.0±5.7 – 494.9±8.6	27326±336 – 29016±366	474.0±7.4 – 498.5±8.0	64.2±0.9 – 92.0±1.5

Regarding light availability, the data confirm the expected difference between the reference area and the area beneath the photovoltaic installation, both in terms of PAR and illuminance. Solar radiation data suggest a substantial homogeneity in terms of GHI, while during the second (summer) cycle, a difference in reflected RHI appears to emerge. This may be attributed to: a) the greater availability of direct solar radiation, and b) the different crops cultivated during the two cycles.

Funded by the European Union under Grant Agreement No 101096056. Views and opinions expressed are however those of the author(s) only and do not necessarily reflect those of the European Union or CINEA. Neither the European Union nor the granting authority can be held responsible for them.

Figures 86–90 depict the observed distributions of measured variables within the greenhouse. The labels indicate the spatial positioning of the sensors: horizontally, identified by the pole number code (1 to 10, with "env" referring to the outdoor measurement point), and vertically, indicated by the following labels: a) ground (ground level), b) adj (canopy level), and c) below (at an elevation lower than the photovoltaic panel plane). In Italy, the Aeronautica Militare recorded an average monthly CO_2 concentration of 430.76 ppm in April 2025. Based on this reference, the CO_2 distributions (Figure 86) reveal that several sensors experienced malfunction. Consequently, the analyses were limited to the functioning sensors only, showing substantial homogeneity in the spatial distribution of gas concentration within the greenhouse. The observed distributions of relative humidity (Figure 87) within the greenhouse exhibit reasonable ranges and do not reveal significant spatial patterns. Potential issues were noted with the sensor readings on pole 9, particularly during the first production cycle.

Temperature distributions (Figure 88) also fall within expected ranges, with external temperatures being lower and more variable compared to those inside the greenhouse, as anticipated. A moderate trend toward higher temperatures outside the photovoltaic panels (shading effect) appears to be confirmed, with the outermost poles recording higher temperatures compared to the others. Thermal stratification of warmer air toward higher elevations seems more pronounced during the second cycle.

Regarding PAR and illuminance (Figures 89 and 90), similar spatial distributions were recorded, with the area beneath the panels clearly affected by shading from the installation. Additionally, a recurring pattern is evident, showing greater light availability toward the edges of the greenhouse, regardless of the presence of the photovoltaic system.

Funded by the European Union under Grant Agreement No 101096056. Views and opinions expressed are however those of the author(s) only and do not necessarily reflect those of the European Union or CINEA. Neither the European Union nor the granting authority can be held responsible for them.

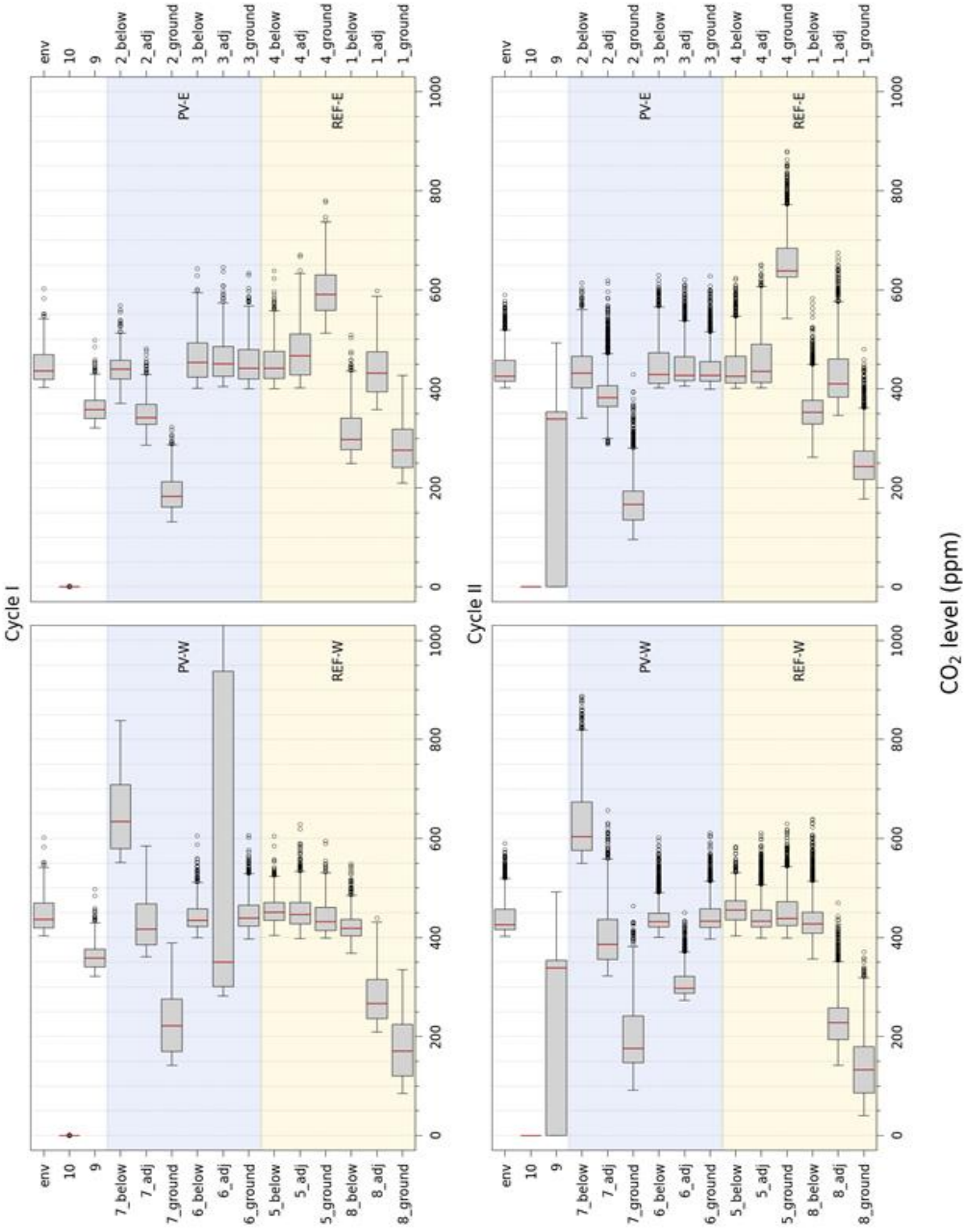

Figure 86. Box plots of CO_2 (ppm) for all the sensors for the two cultivation cycles. Positions of the graphs resemble the plants of the greenhouse and the coloured areas identify the PV and Ref plots.

Funded by the European Union

Funded by the European Union under Grant Agreement No 101096056. Views and opinions expressed are however those of the author(s) only and do not necessarily reflect those of the European Union or CINEA. Neither the European Union nor the granting authority can be held responsible for them.

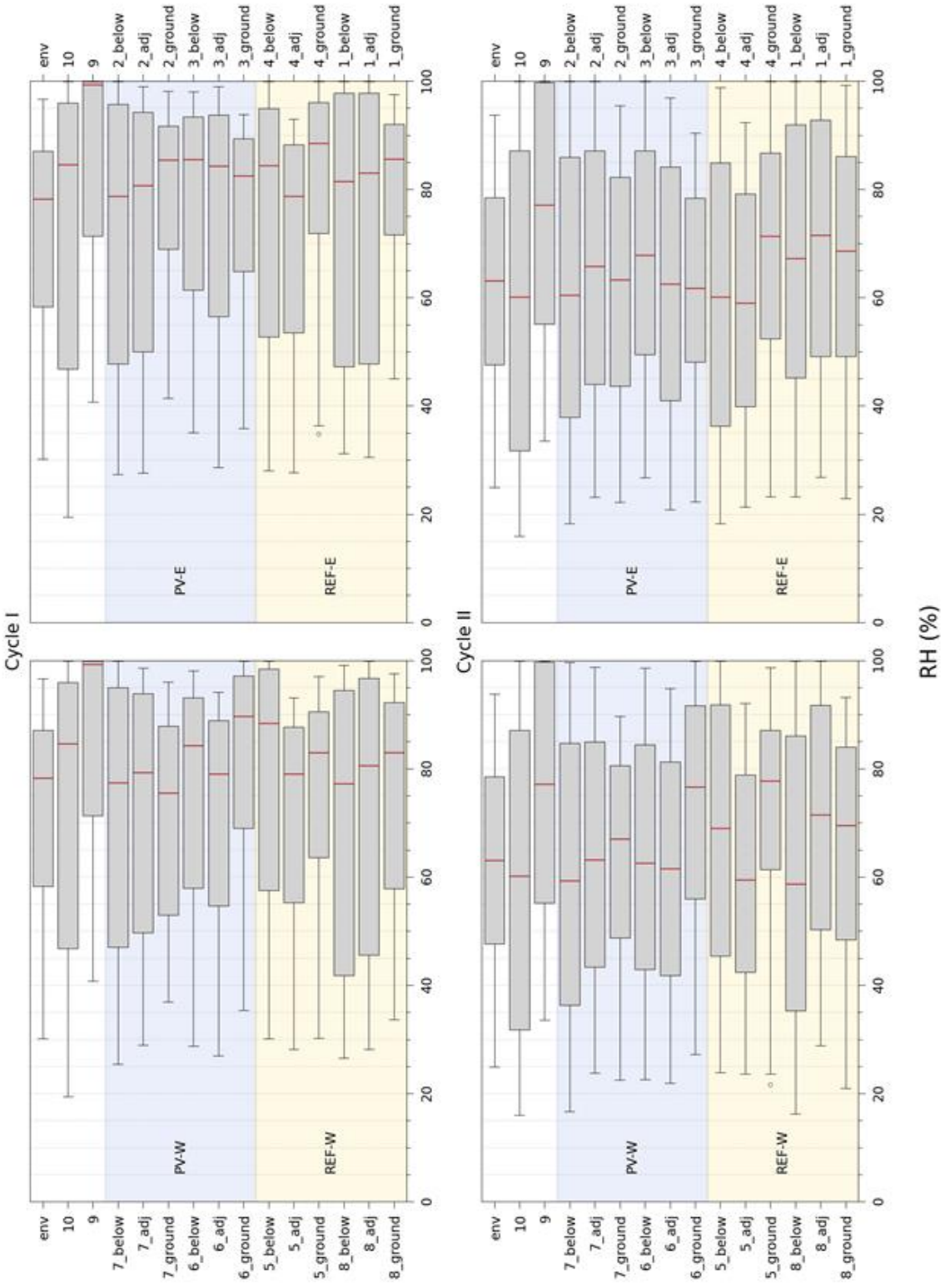

Figure 87. Box plots of relative rumidity (RH) for all sensors for the two cultivation cycles. Positions of the graphs resemble the plants of the greenhouse and the coloured areas identify the PV and Ref plots.

Funded by the European Union under Grant Agreement No 101096056. Views and opinions expressed are however those of the author(s) only and do not necessarily reflect those of the European Union or CINEA. Neither the European Union nor the granting authority can be held responsible for them.

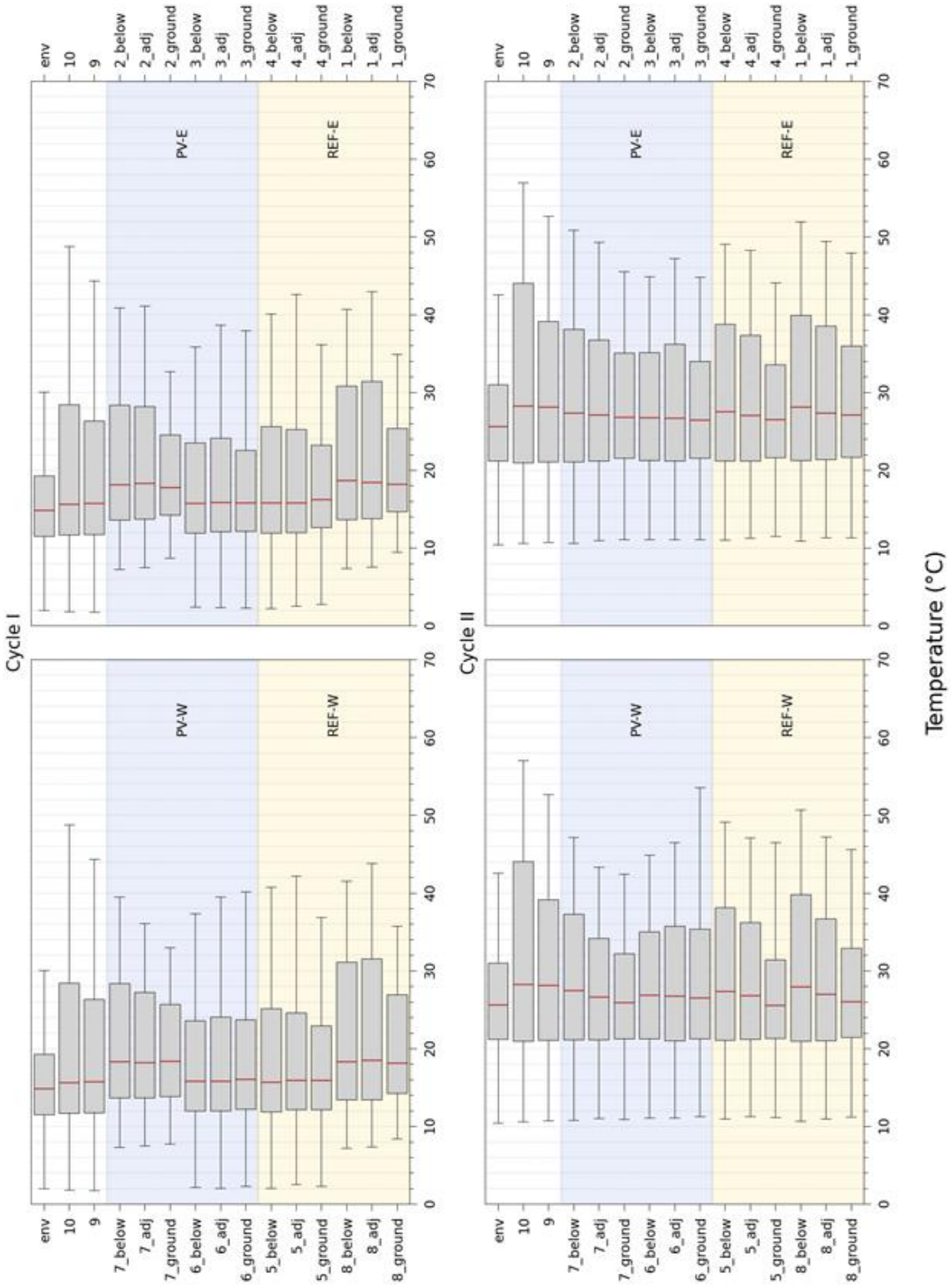

Figure 88. Box plots of Temperature (°C) for all sensors for the two cultivation cycles. Positions of the graphs resemble the plants of the greenhouse and the coloured areas identify the PV and Ref plots.

Funded by the European Union under Grant Agreement No 101096056. Views and opinions expressed are however those of the author(s) only and do not necessarily reflect those of the European Union or CINEA. Neither the European Union nor the granting authority can be held responsible for them.

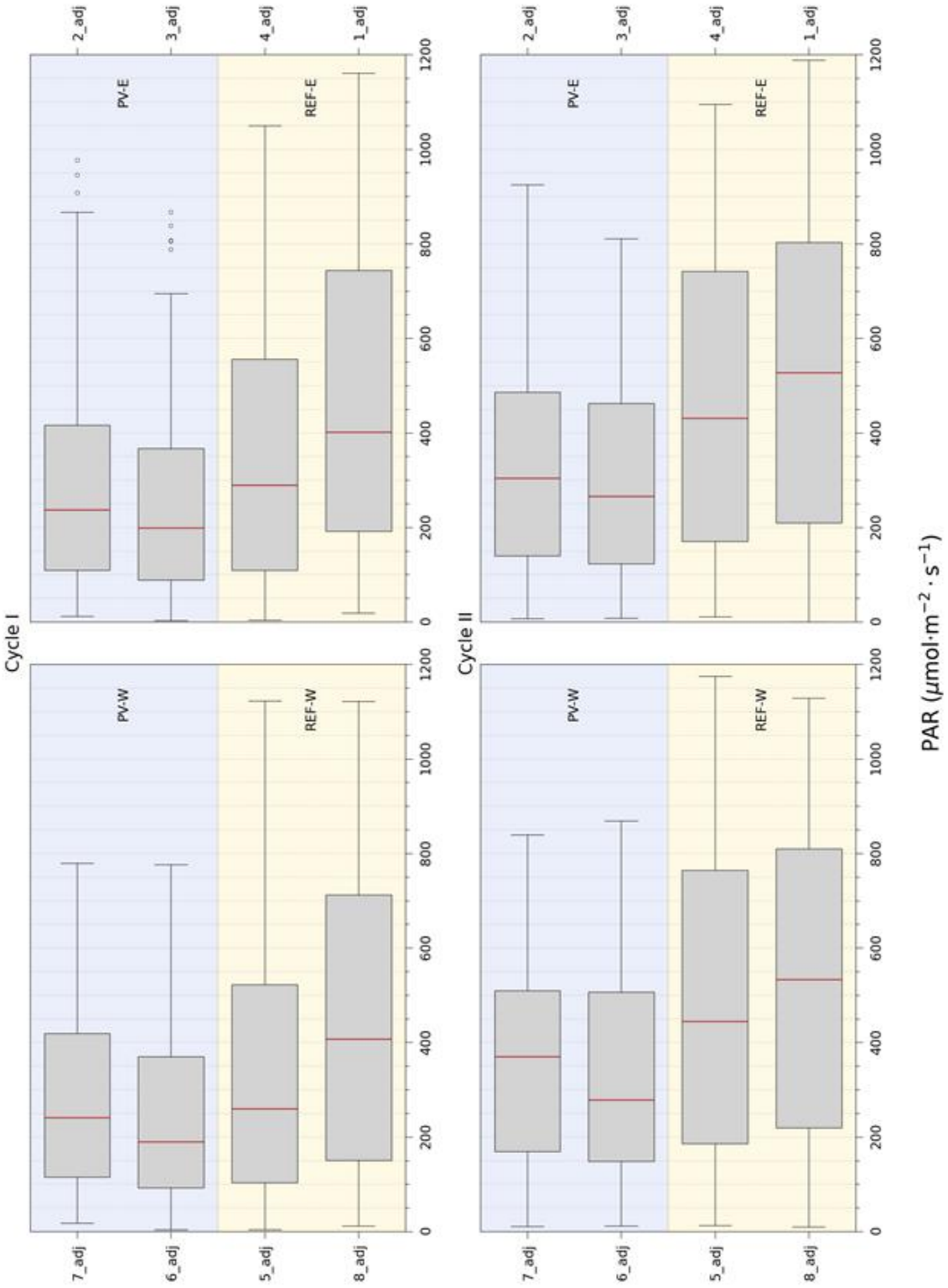

Figure 89. Box plots of PAR (µmol m^{-2} s^{-1}) for all sensors for the two cultivation cycles. Positions of the graphs resemble the plants of the greenhouse and the coloured areas identify the PV and Ref plots.

Funded by the European Union under Grant Agreement No 101096056. Views and opinions expressed are however those of the author(s) only and do not necessarily reflect those of the European Union or CINEA. Neither the European Union nor the granting authority can be held responsible for them.

Funded by the European Union

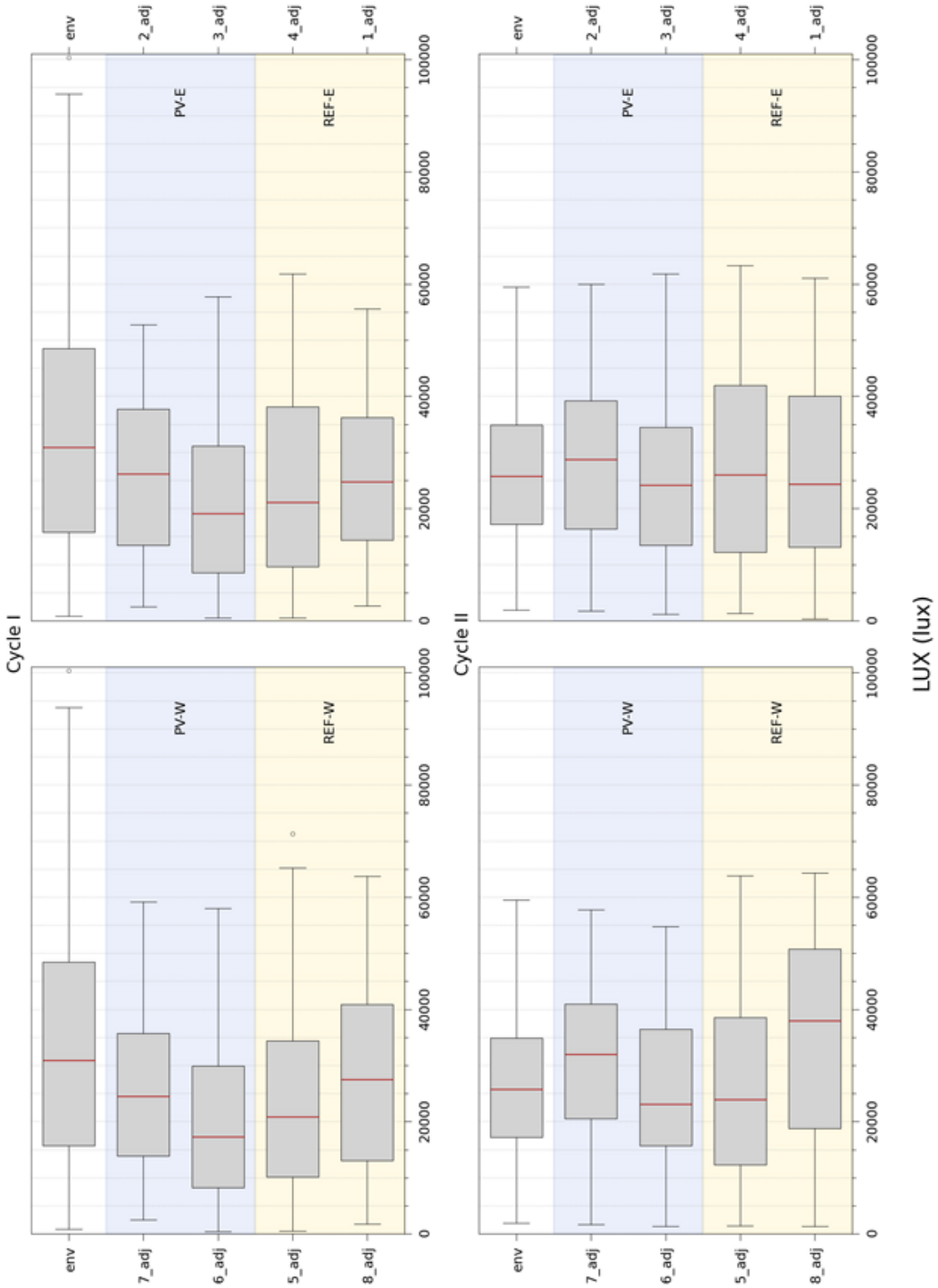

Figure 90. Box plots of illuminance (Lux) for all sensors for the two cultivation cycles. Positions of the graphs resemble the plants of the greenhouse and the coloured areas identify the PV and Ref plots.

Funded by the European Union under Grant Agreement No 101096056. Views and opinions expressed are however those of the author(s) only and do not necessarily reflect those of the European Union or CINEA. Neither the European Union nor the granting authority can be held responsible for them.

Regarding the distribution of Global Horizontal Irradiance (GHI) shown in Figure 91, the attenuation effect of the greenhouse covering film compared to the radiation measured outdoors can be observed. A slight difference between values recorded in the northern sector (10_above) compared to those in the southern sector (9_above) — more pronounced during the second cycle — may be attributed to differences in the greenhouse horizon.

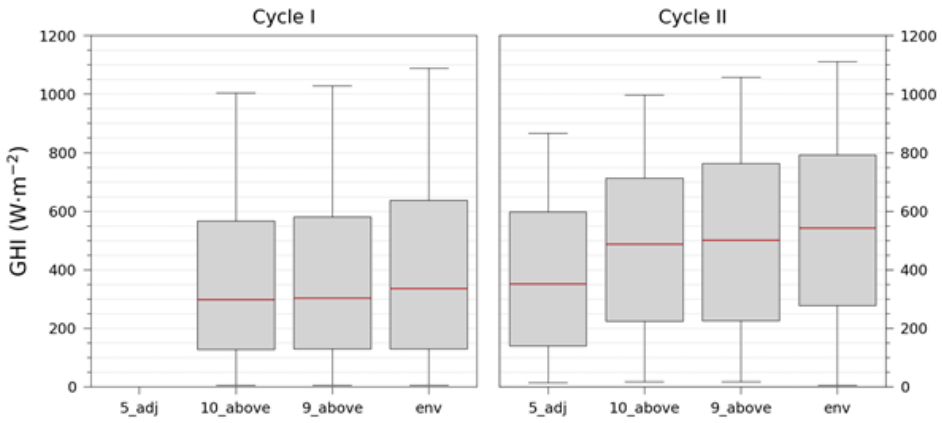

Figure 91. Box plots of the Global Horizontal Irradiance (GHI, W m^{-2}) for the two cultivation cycles.

The same observations can be made for Reflected Horizontal Irradiance (RHI), showing substantial equivalence during the first cycle, while a more pronounced difference appears to emerge during the second cycle, with the southern sector (9_above) consistently recording higher values (Figure 92).

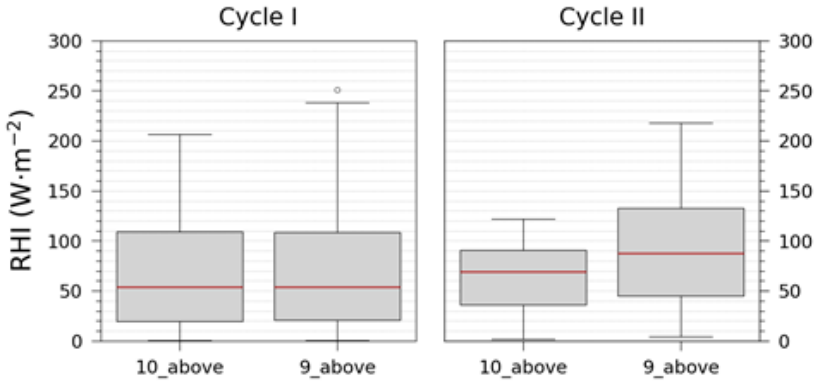

Figure 92. Box plots of the Reflected Horizontal Irradiance (RHI, W m^{-2}) for the two cultivation cycles.

Finally, the wind distribution (Figure 93) recorded during the second production cycle is reported (data not available for the first cycle), highlighting the wind characteristics of the area, which are marked by low wind speeds and a predominant southern direction.

Funded by the European Union

Funded by the European Union under Grant Agreement No 101096056. Views and opinions expressed are however those of the author(s) only and do not necessarily reflect those of the European Union or CINEA. Neither the European Union nor the granting authority can be held responsible for them.

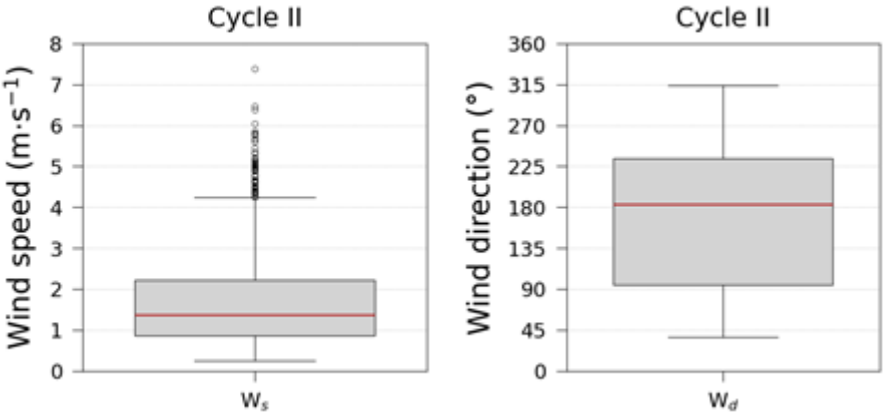

Figure 93. Box plots of the wind speed (m s^{-1}) and direction (°C) outside the greenhouse for the second cultivation cycle.

To give an overview of the hourly variation of the abovementioned variables during the year the carpet plots for each of the cultivation cycles have been built. For each of the variables the values measured at ground, canopy and below levels are shown for each of the poles. The arrangement of the graphs in each figure resembles the real position of the poles on the greenhouse plant.

During the first cultivation cycle, sensor installation operations within the greenhouse were still ongoing, along with the setup of related systems. This resulted in fragmented measurement data. For this reason, only the carpet plots corresponding to the second cultivation cycle will be presented and discussed to illustrate the time series of the measured variables.

Regarding temperature (Figures 94–96), the data reveal a vertical stratification of warm air, lower temperatures in the shaded areas beneath the photovoltaic panels, and occasionally higher temperatures recorded by the sensors located at the outermost poles. Additionally, the narrowing pattern observed toward the right side of the plots may indicate a progressive reduction in daylight hours as the season advanced.

The data of relative humidity (Figures 97–99) exhibit patterns similar to those observed for temperature, with the outer poles generally recording higher humidity levels. The alternation of day and night is clearly visible, as is the inverse relationship between relative humidity and air temperature.

As for CO_2 concentration (Figures 100–102), the presence of sensors that returned corrupted values is evident, saturating the already broad colour scale. The time series recorded at the canopy level of pole 1 appears to be the most representative, clearly showing the plants' diurnal behaviour, with the transition from photosynthesis during the day to respiration at night. This effect becomes progressively more pronounced as the crops develop, highlighting the positive influence of vegetation on CO_2 concentration levels.

Funded by the European Union under Grant Agreement No 101096056. Views and opinions expressed are however those of the author(s) only and do not necessarily reflect those of the European Union or CINEA. Neither the European Union nor the granting authority can be held responsible for them.

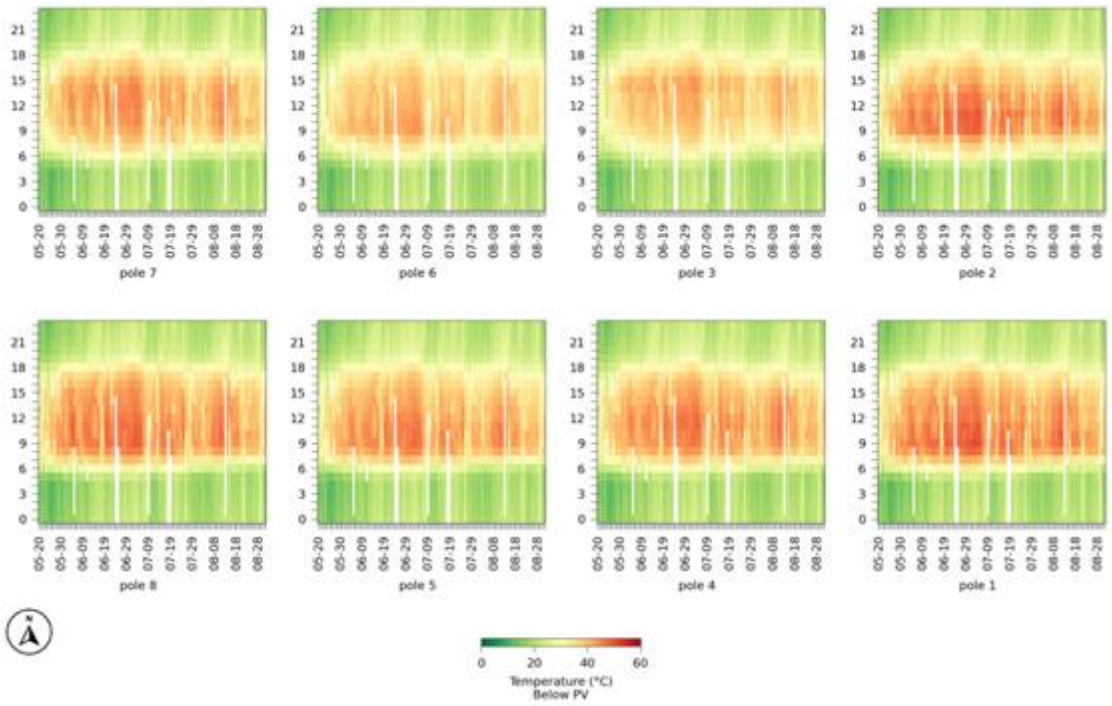

Figure 94. Carpet plots of temperature below PV level for the second cultivation cycle.

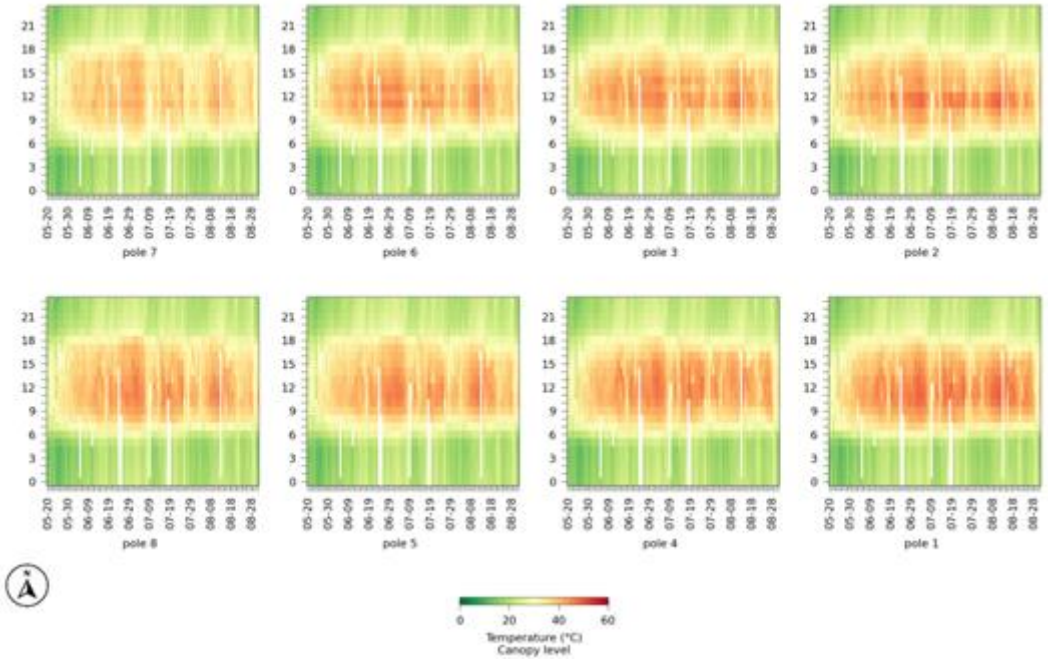

Figure 95. Carpet plots of temperature at canopy level for the second cultivation cycle.

Funded by the European Union

Funded by the European Union under Grant Agreement No 101096056. Views and opinions expressed are however those of the author(s) only and do not necessarily reflect those of the European Union or CINEA. Neither the European Union nor the granting authority can be held responsible for them.

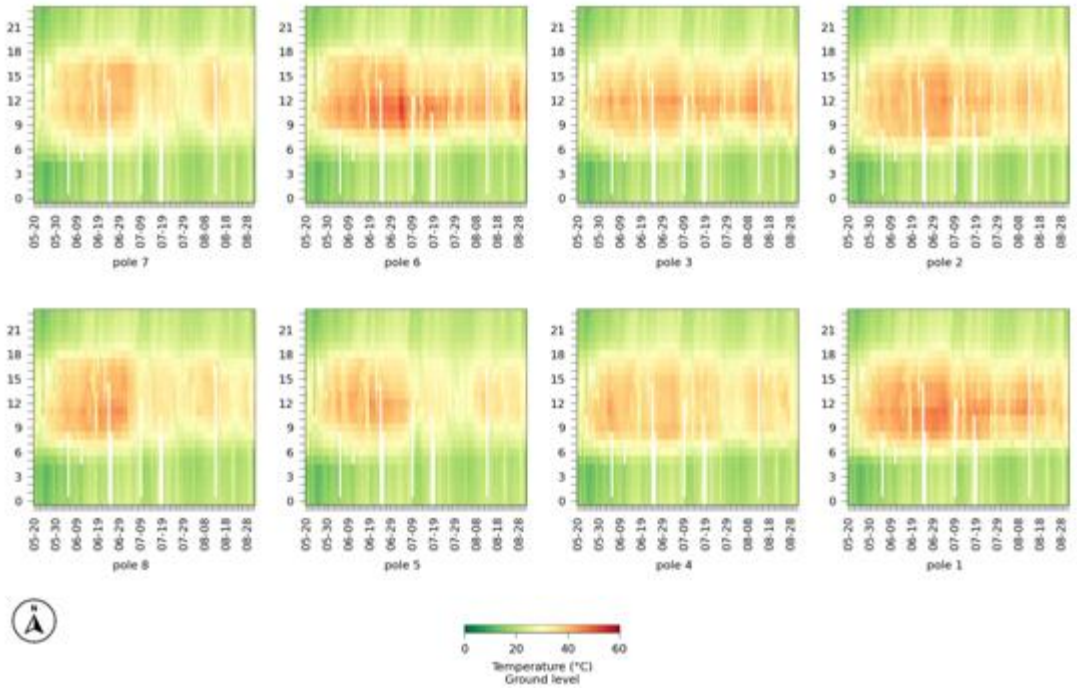

Figure 96. Carpet plots of temperature at ground level for the second cultivation cycle.

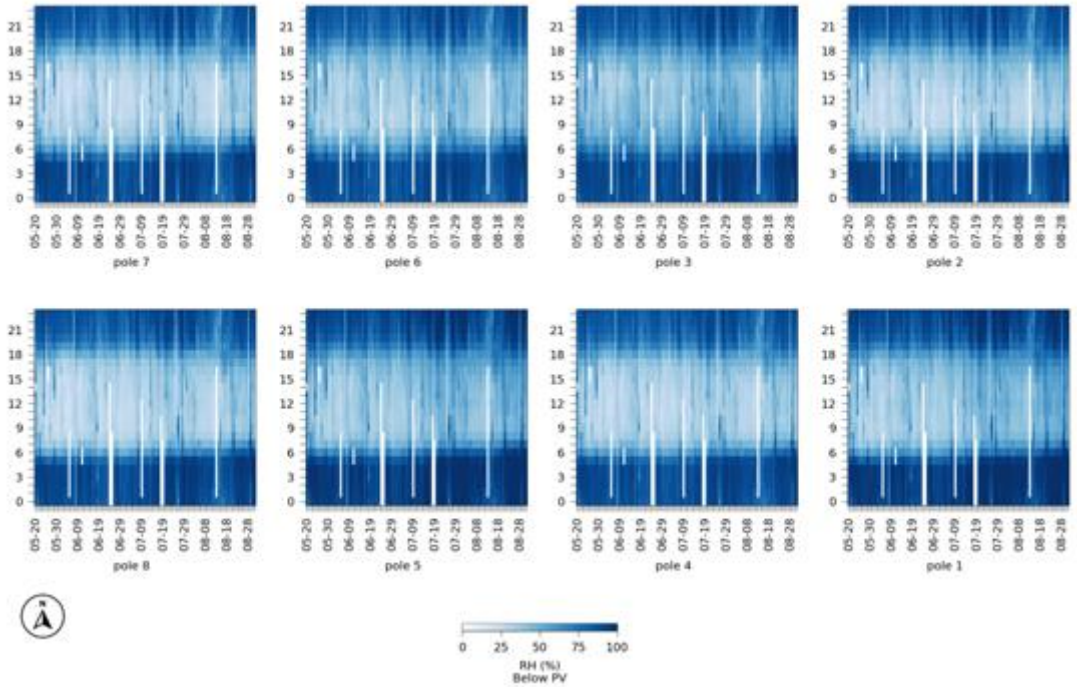

Figure 97. Carpet plots of Relative Humidity (RH) below PV level for the second cultivation cycle.

Funded by the European Union under Grant Agreement No 101096056. Views and opinions expressed are however those of the author(s) only and do not necessarily reflect those of the European Union or CINEA. Neither the European Union nor the granting authority can be held responsible for them.

Funded by the European Union

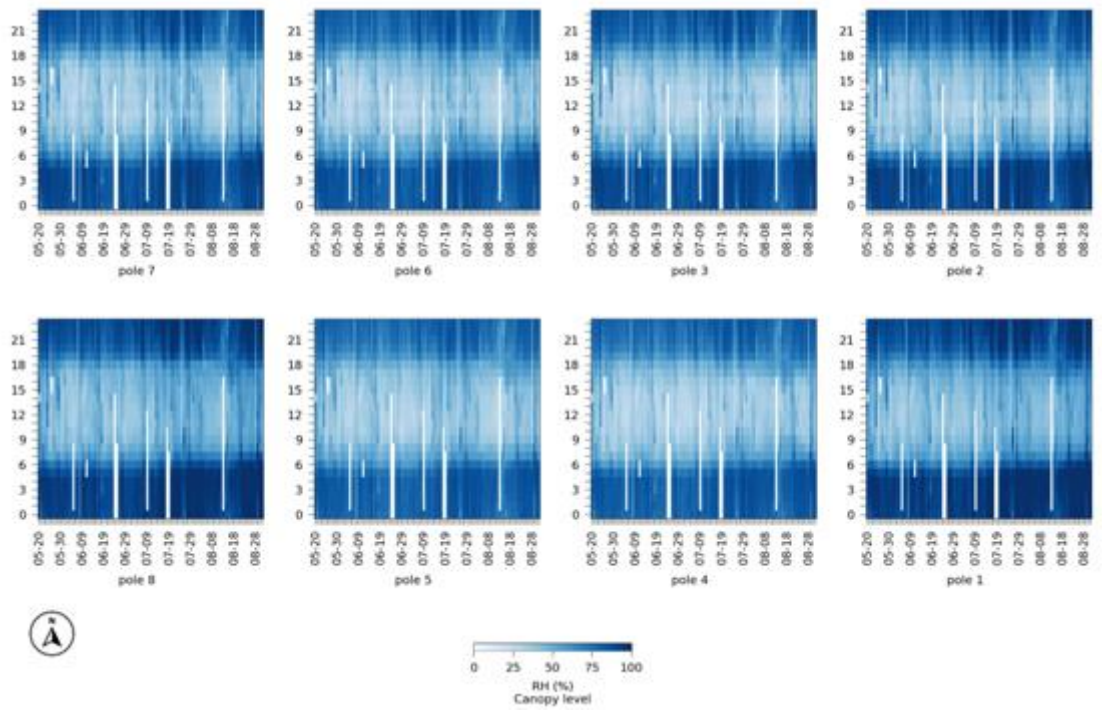

Figure 98. Carpet plots of Relative Humidity (RH) at canopy level for the second cultivation cycle.

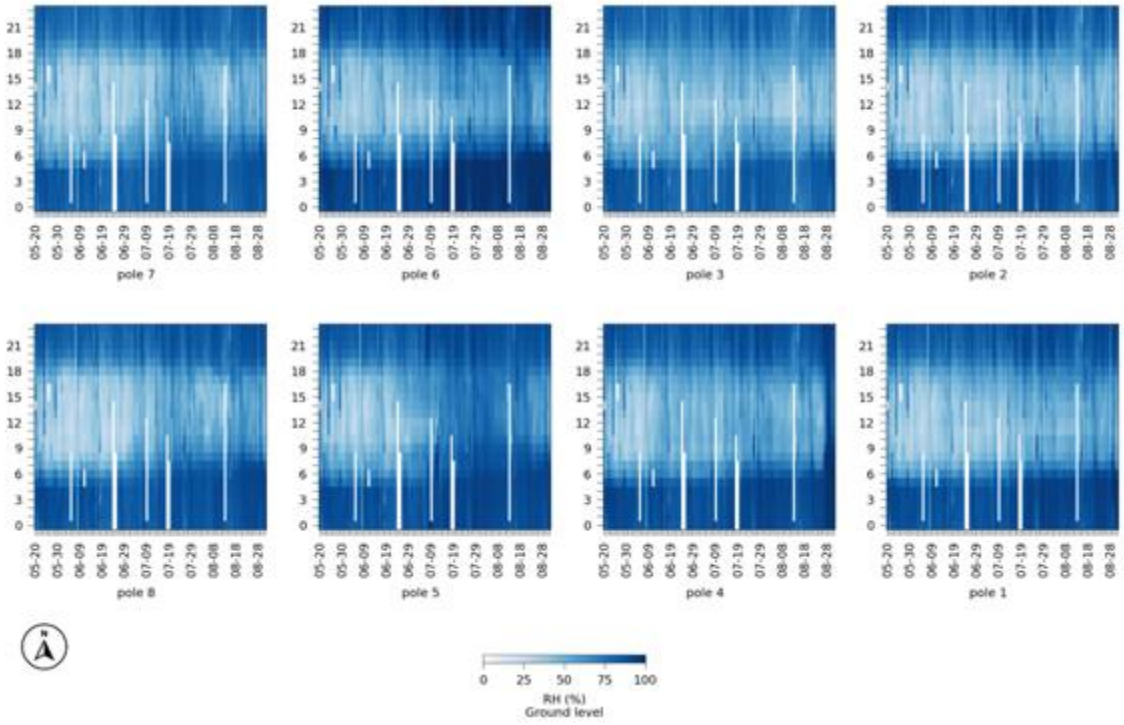

Figure 99. Carpet plots of Relative Humidity (RH) at ground level for the second cultivation cycle.

Funded by the European Union under Grant Agreement No 101096056. Views and opinions expressed are however those of the author(s) only and do not necessarily reflect those of the European Union or CINEA. Neither the European Union nor the granting authority can be held responsible for them.

Funded by the European Union

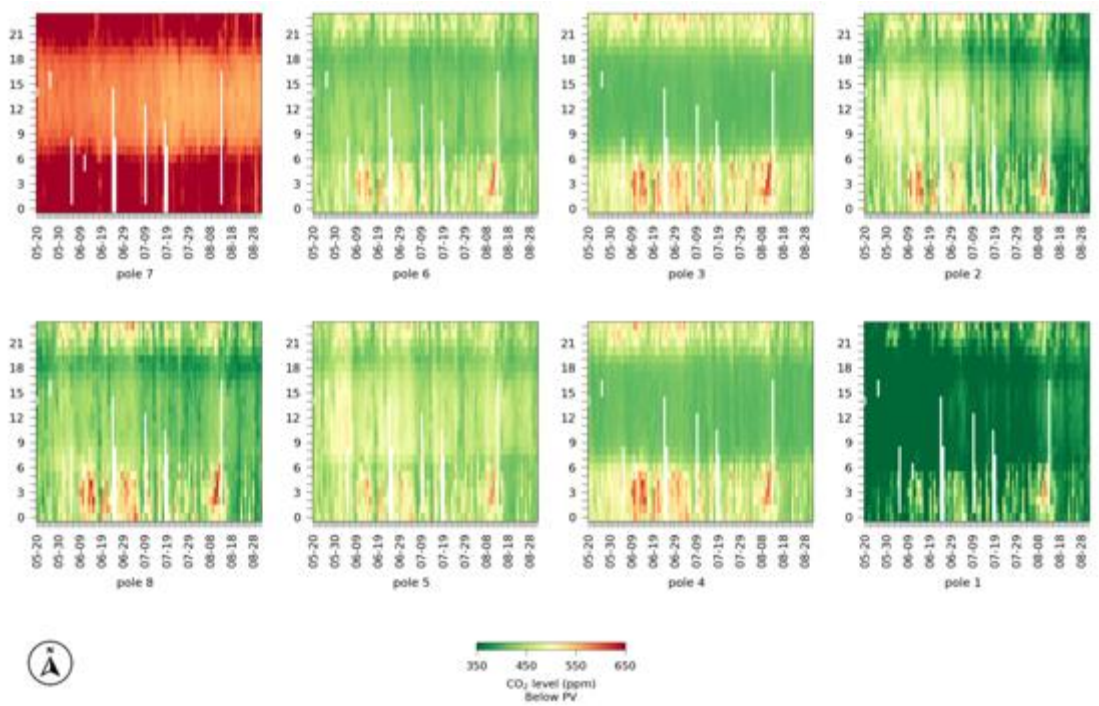

Figure 100. Carpet plots of CO_2 below PV level for the second cultivation cycle.

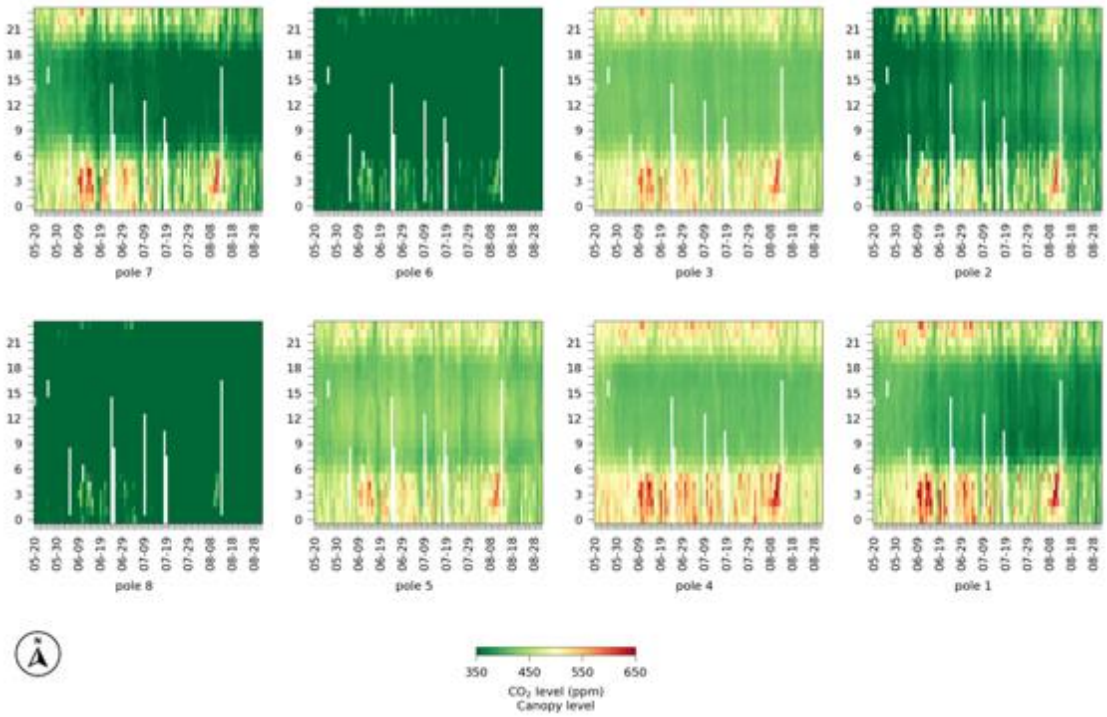

Figure 101. Carpet plots of CO_2 at canopy level for the second cultivation cycle.

Funded by the European Union under Grant Agreement No 101096056. Views and opinions expressed are however those of the author(s) only and do not necessarily reflect those of the European Union or CINEA. Neither the European Union nor the granting authority can be held responsible for them.

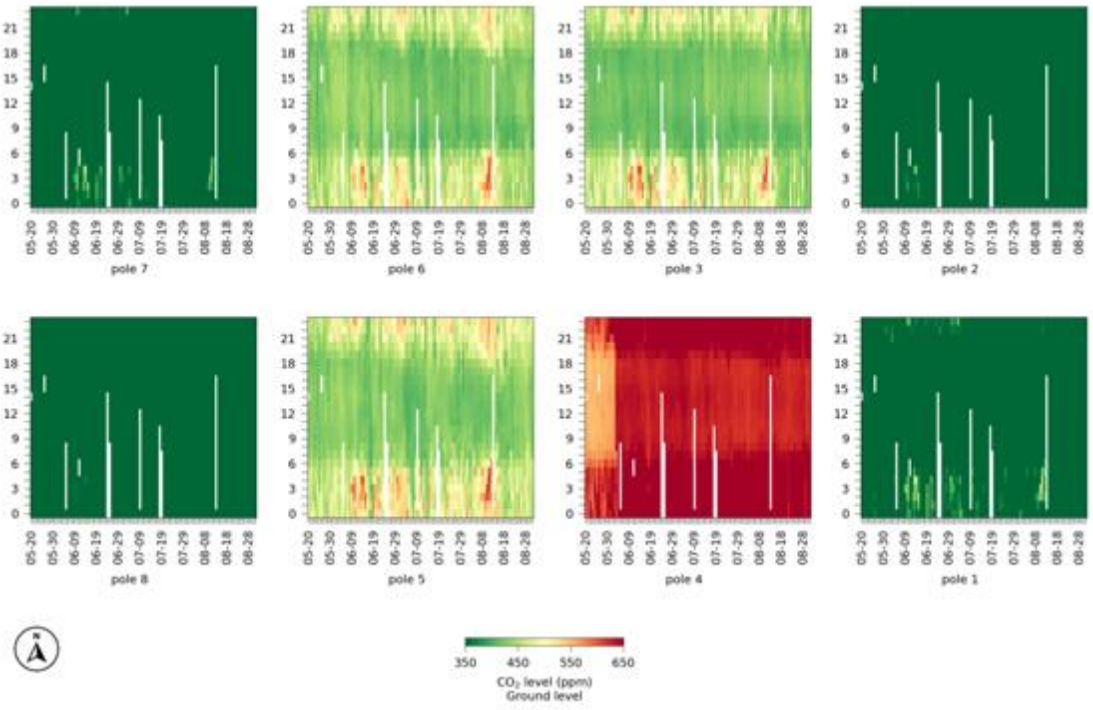

Figure 102. Carpet plots of CO_2 at ground level for the second cultivation cycle.

Examining the solar radiation time series, the day–night cycle is clearly visible (Figures 103–104). Additionally, while Global Horizontal Irradiance (GHI) appears to be substantially equivalent across the monitored zones, a distinct difference emerges in Reflected Horizontal Irradiance (RHI) as the crop canopy develops. This disparity between the area beneath the photovoltaic installation and the open reference area becomes increasingly evident over time. Furthermore, although the maximum solar radiation is typically expected around the summer solstice in late June, a growing trend towards the right side of the plot may indicate enhanced canopy reflectance due to its progressive development.

With regard to light availability, both in terms of Photosynthetically Active Radiation (PAR), in Figure 105 and illuminance, in Figure 106, measured at canopy level, the expected day–night alternation is observed, along with consistently greater light availability in the southern sector, outside the photovoltaic installation. Notably, the data reveal shadowed regions occurring during the central hours of the day, suggesting that the greenhouse structure itself casts shadows at certain times. These shading patterns are likely to influence the energy production efficiency of the PV panels.

Funded by the European Union

Funded by the European Union under Grant Agreement No 101096056. Views and opinions expressed are however those of the author(s) only and do not necessarily reflect those of the European Union or CINEA. Neither the European Union nor the granting authority can be held responsible for them.

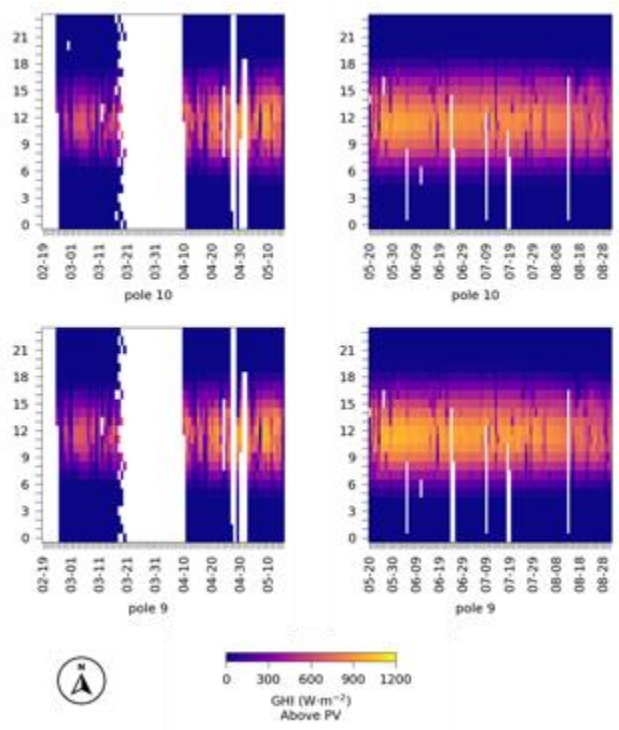

Figure 103. Carpet plots of GHI above PV level, (left side) Cycle I, (right side) Cycle II.

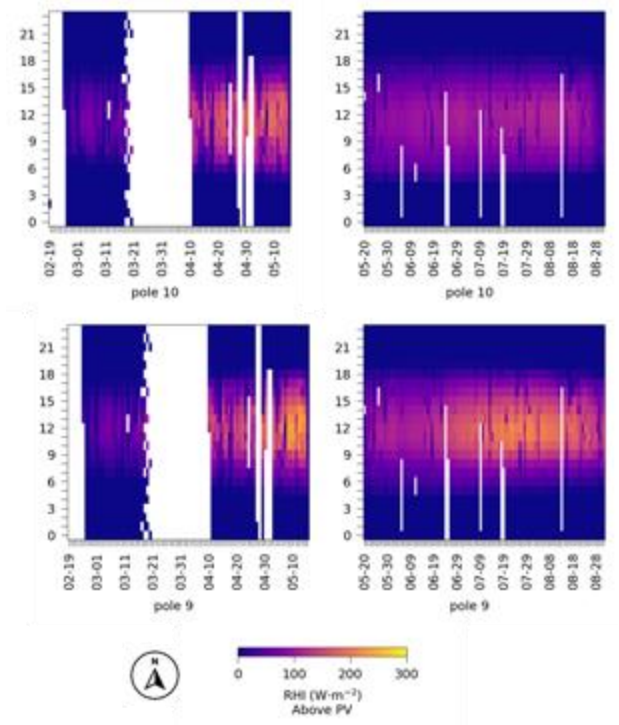

Figure 104. Carpet plots of RHI above PV level, (left side) Cycle I, (right side) Cycle II.

Funded by the European Union under Grant Agreement No 101096056. Views and opinions expressed are however those of the author(s) only and do not necessarily reflect those of the European Union or CINEA. Neither the European Union nor the granting authority can be held responsible for them.

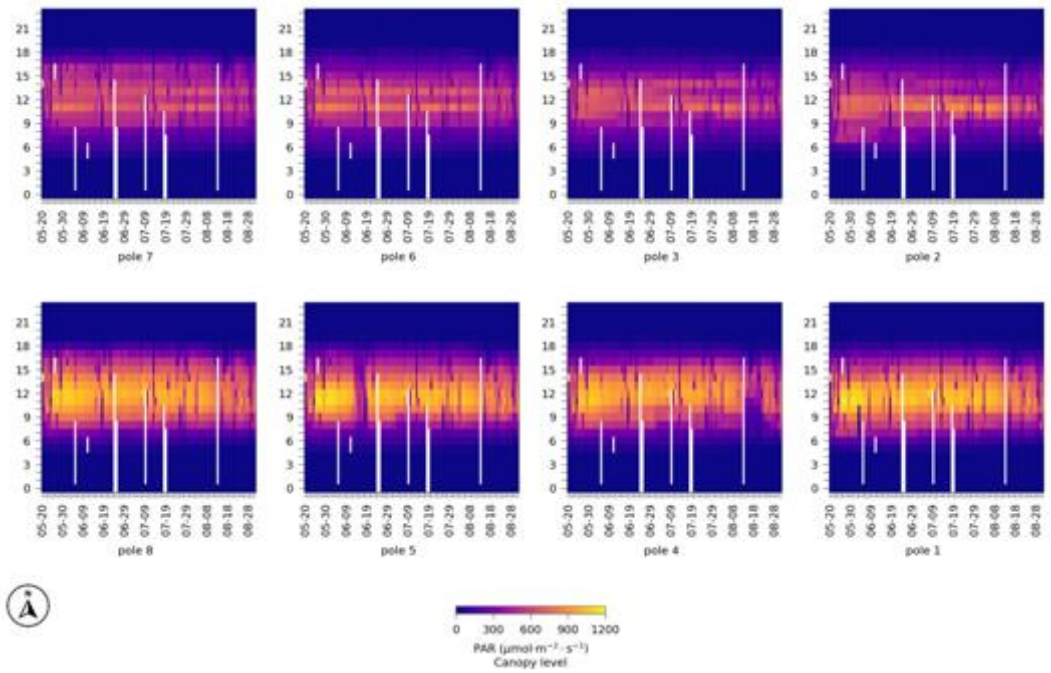

Figure 105. Carpet plots of PAR above PV level.

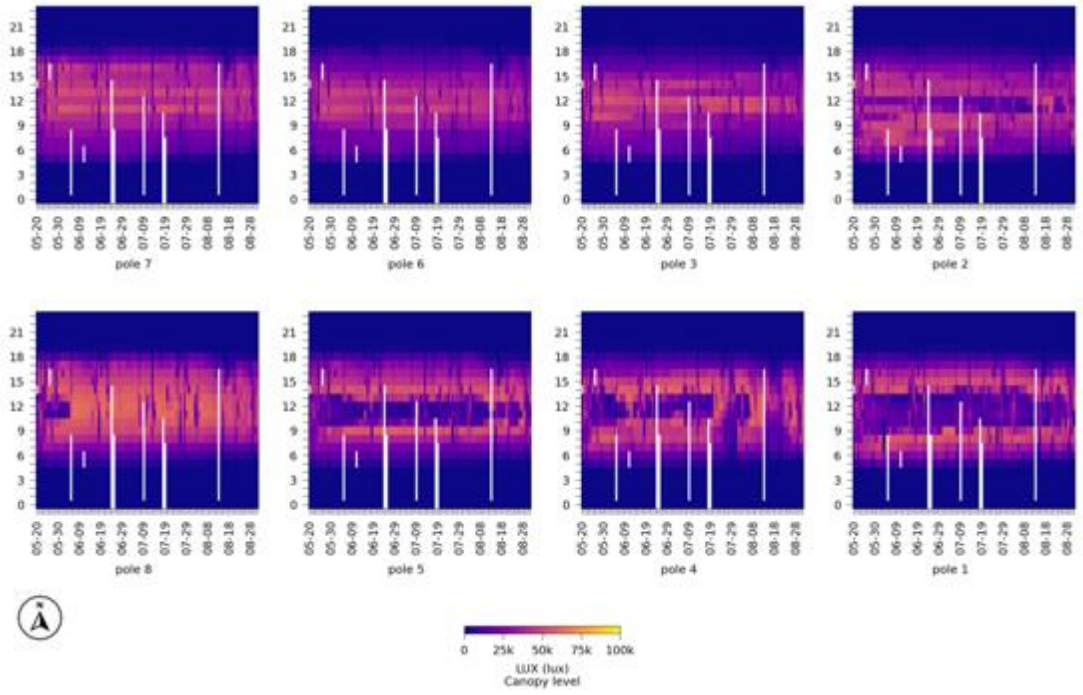

Figure 106. Carpet plots of illuminance (LUX) above PV level.

Temperature and PAR trends are now analysed for two representative days (clear sky and overcast) during each of the two production cycles. For the first cycle, the selected days are February 25, 2025 (overcast),

Funded by the European Union under Grant Agreement No 101096056. Views and opinions expressed are however those of the author(s) only and do not necessarily reflect those of the European Union or CINEA. Neither the European Union nor the granting authority can be held responsible for them.

and April 21, 2025 (clear sky). For the second cycle, the chosen dates are July 15, 2025 (clear sky), and May 24, 2025 (overcast).

During an overcast day in the first cycle (Figure 107), temperature measurements — even across different vertical positions — do not reveal significant differences, as confirmed by all available sensors. Nonetheless, temperatures consistently remain higher than those recorded in the external environment.

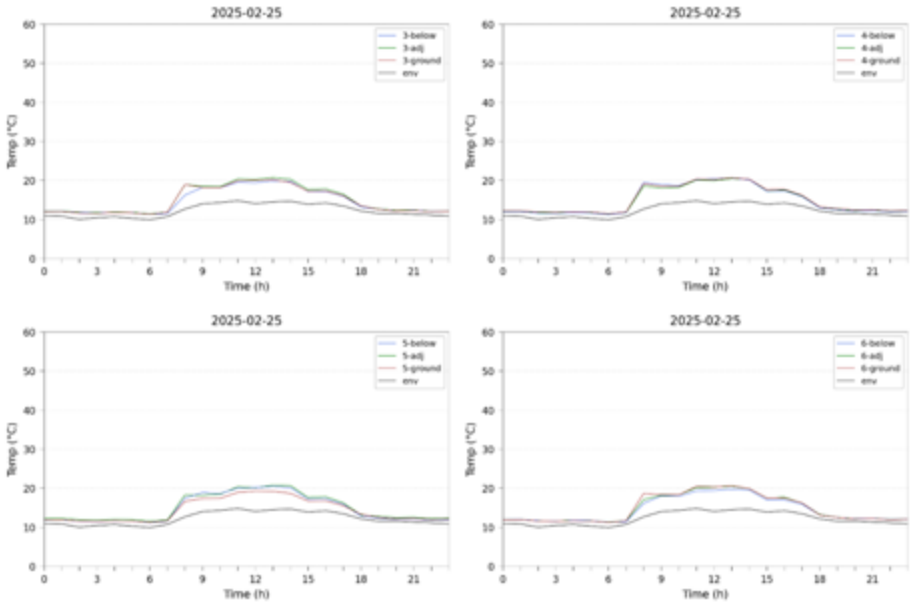

Figure 107. Temperature trends for an overcast day, Cycle I, at different levels for poles 3, 4, 5 & 6.

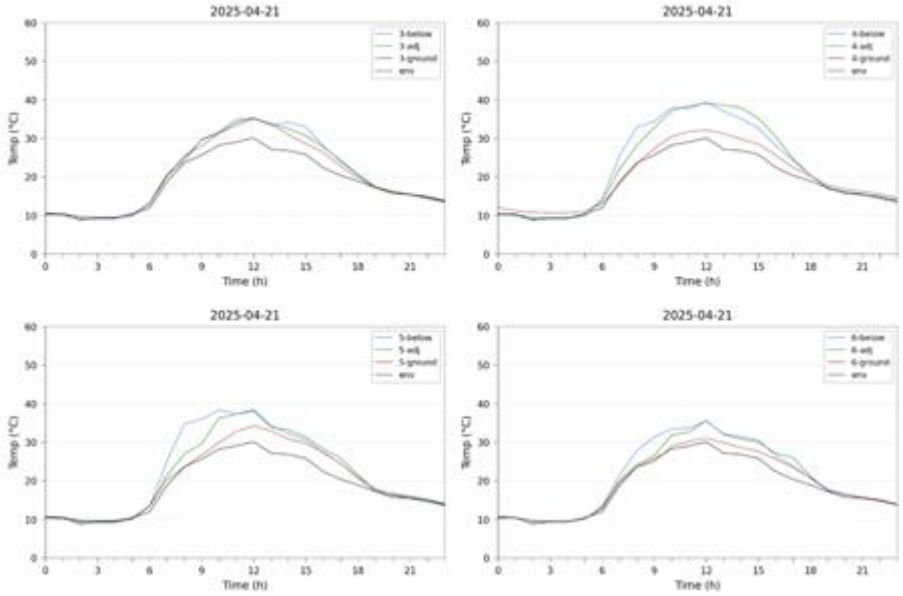

Figure 108. Temperature trends for a clear sky day, Cycle I, at different levels for poles 3, 4, 5 & 6.

Funded by the European Union under Grant Agreement No 101096056. Views and opinions expressed are however those of the author(s) only and do not necessarily reflect those of the European Union or CINEA. Neither the European Union nor the granting authority can be held responsible for them.

During the clear sky day (Figure 108), sensors positioned at higher elevations recorded slightly higher temperatures. Given that clear sky conditions are less frequent during the winter season, this may explain why vertical stratification of temperature was observed predominantly during the second cycle, as indicated by the distribution of the recorded data.

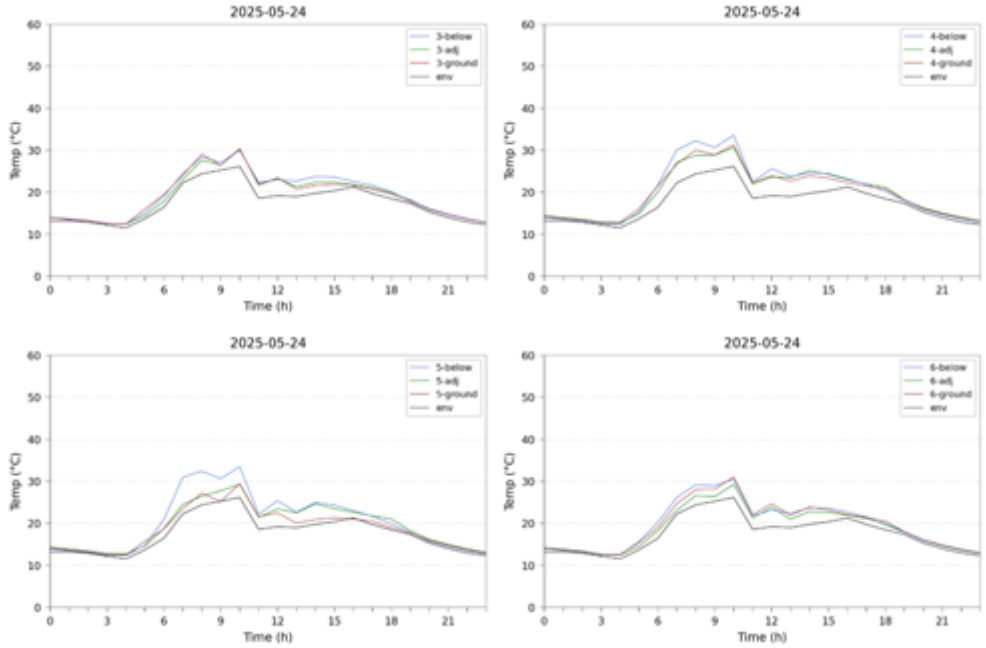

Figure 109. Temperature trends for an overcast day, Cycle II, at different levels for poles 3, 4, 5 & 6.

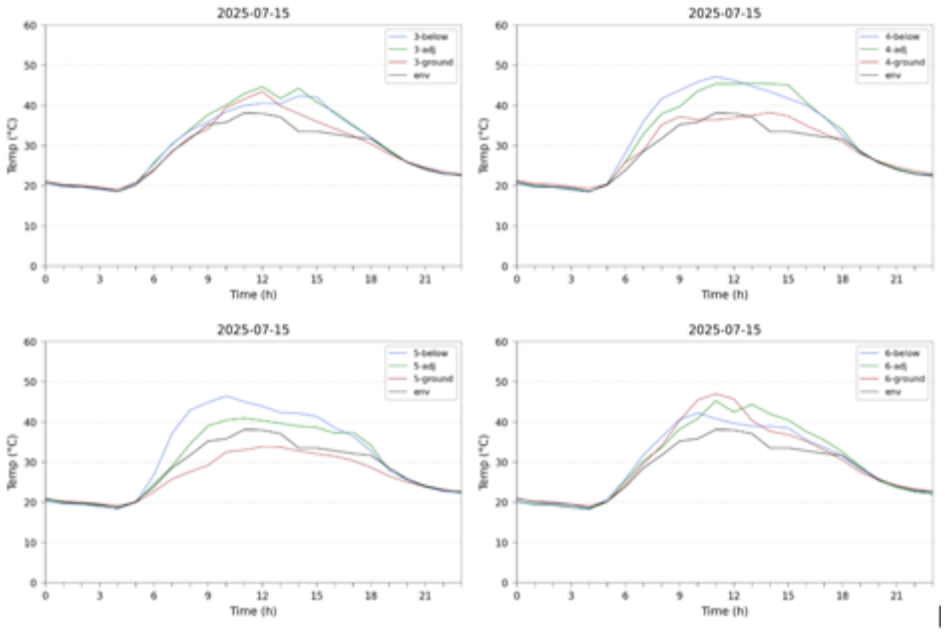

Figure 110. Temperature trends for a clear sky day, Cycle II, at different levels for poles 3, 4, 5 & 6.

Funded by the European Union under Grant Agreement No 101096056. Views and opinions expressed are however those of the author(s) only and do not necessarily reflect those of the European Union or CINEA. Neither the European Union nor the granting authority can be held responsible for them.

Similar considerations can be drawn from the analysis of the following plots related to the second cultivation cycle (Figures 109–110), where the increased availability of solar radiation appears to be associated with a more pronounced vertical stratification of warm air.

To analyse representative days in terms of PAR the 4 plots of the greenhouse (PV East, PV West, Ref East and Ref West) have been considered and for each plot the hourly average of PAR measured at canopy level at the two poles insisting on the plot has been made.

The analysis of the figures reveals a typical pattern, with consistent grouping between the areas under the photovoltaic panels and the two reference zones (Figures 111–112). Moreover, a time lag between the East and West sides appears to be evident, as expected. The observed variations in PAR levels also align with seasonal dynamics and cloud cover conditions.

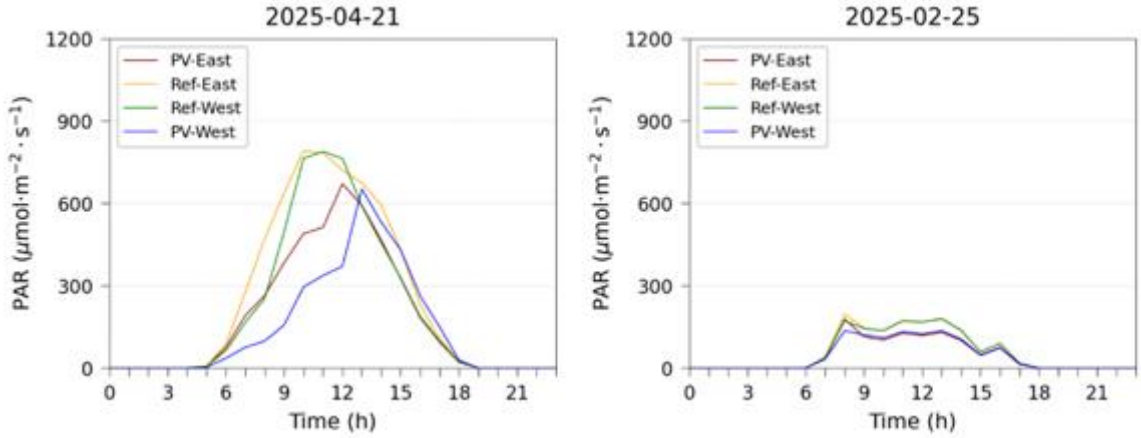

Figure 111. PAR trends for a clear sky day and an overcast day, Cycle I, at different levels for poles 3, 4, 5 & 6.

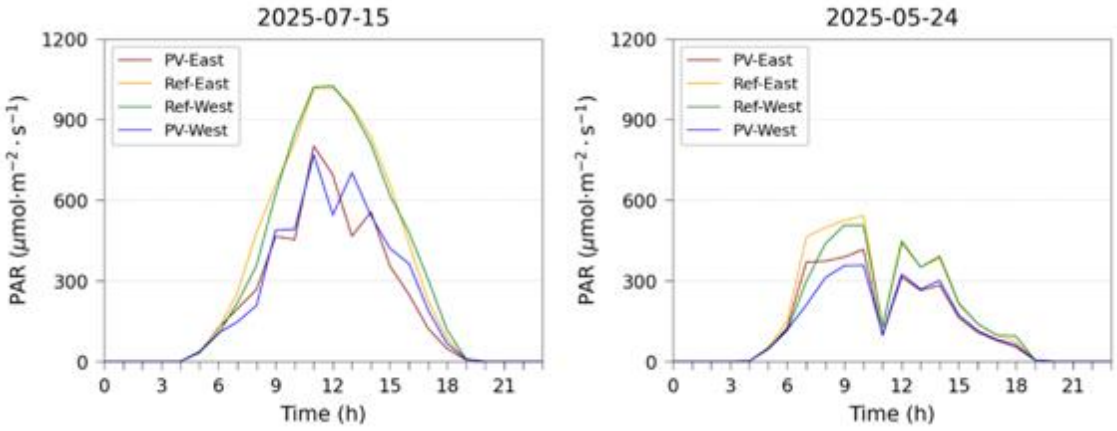

Figure 112. PAR trends for a clear sky day and an overcast day, Cycle II, at different levels for poles 3, 4, 5 & 6.

Funded by the European Union under Grant Agreement No 101096056. Views and opinions expressed are however those of the author(s) only and do not necessarily reflect those of the European Union or CINEA. Neither the European Union nor the granting authority can be held responsible for them.

4.1.4 Austrian Greenhouse facility (BOKU University)

At BOKU University (Latitude: 48.23687823838888; Longitude: 16.33556454839097) growth cabinets within a ridge and furrow greenhouse were available with the following dimensions:

1. A larger cabinet of the size 6.3 m x 6.3 m (39.7 m^2) serving as the control
2. Two smaller cabinets (6.3 m x 3.15 m (19.85 m^2) for the shading variants.

The cover of the greenhouse (roof and the walls) consists of polycarbonate Thermoclear 2UV 16mm characterised by a light transmission of 70-77%. Temperature is controlled by a heating system in the greenhouse floor and cooling is achieved by opening the windows at a pre-set temperature (no active cooling). Additional light can be supplied by LEDs (Sanol Model C1.ID.003 230 W/1000mA/ID/IP65 with Converter Cubra 1; Sanol, Jennersdorf, Austria).

BOKU collected daily mean day and night temperatures and humidity (Horti Max System consisting of two PT-100 sensors), as well as the PAR (light sensor of the FluorPen FP 100, Photon Systems Instruments) and CO_2-concentration (EGM-5 CO_2 Gas Analyser, PP Systems) within the canopy in the morning between 9.00 and 10.00 o'clock, at midday and in the afternoon between 14.00 and 15.00 o'clock. The mean values are indicated in chapter 5.2.1.

4.1.5. German Greenhouse facilities

Watzkendorf facility

At Watzkendorf (Germany) outside climate data (temperature (in °C), light/brightness (in klux), light sum (in klux/h), wind speed, and wind direction as well as rainfall (yes/no)) were collected. Inside the glasshouse temperature below the roof and at a height of 1.5 m were collected, in addition to relative humidity (%) and shading by the energy screen (%).

AZS Greenhouse facility

The experiments were conducted in four identical (IRAF diffused 120 microns) plastic-covered greenhouses, each measuring 18 m in length and 8 m in width, providing an approximate area of 150 m^2 per structure. Among these four, two greenhouses served as controls with no solar panels, while the other two greenhouses had panels installed beneath the roof cover, positioned 3 m above ground level inside the structure.

The half-transparent glass-coated panels were mounted on a rotating metal frame powered by an electric motor, allowing reactive movement of the panels following the sun and controlled by real-time radiation, temperature, and humidity sensors, measuring and implementing in a developed software. At AZS the following microclimate data were collected: light, temperature, relative humidity, CO_2, PV module temperature, soil temperature, soil moisture, soil conductivity, PAR radiation, global radiation. Here are

Funded by the European Union

Funded by the European Union under Grant Agreement No 101096056. Views and opinions expressed are however those of the author(s) only and do not necessarily reflect those of the European Union or CINEA. Neither the European Union nor the granting authority can be held responsible for them.

mentioned only the types of sensors, however an exhaustive list and sensor location maps are available on request (Table 25).

Table 25. List of sensors, which supplied continuous data to the greenhouse's website and servers.

Type	Location
Luxmeter (Illuminance)	on panels profile up (Tracking)
Luxmeter (Illuminance)	below panels under a panel (towards east)
Luxmeter (Illuminance)	below panels under a panel (towards west)
Luxmeter (Illuminance)	above panels
Temp & Humidity	below panels under a panel
CO_2	below panels under a panel
Inclinometer	on panels profile (Tracking)
Luxmeter (Illuminance)	control area (one sensor outside of Greenhouses)

5 Crop monitoring inside the greenhouses

5.1 Crops selection for each location (typically cultivated)

The main crop species cultivated during the project are listed in Table 26, in addition with the required information on the accumulated daily light integral (DLI), required illumination period (light hours), light intensity (PPFD) as well as light saturation (LSP) and light compensation points (LCP).

Table 26. Daily light integrals and other cultivation parameters of cultivated crops.

Crop Type	Accumulated DLI [mol/m²/day]	Light hours [h]	PPFD [µmol/m²/s]	Max Thresholds = light saturation point (LSP) [µmol/m²/s]	Min Thresholds = light compensation point (LCP) [µmol/m²/s]	Light unit
Tomato	26 (22-30)	14-18	340-600	1985	53	PPFD
Bell Pepper	25 (20-30)	14-18	300-600	1718	35	PPFD
Lettuce	17 (14-17)	12-14	270-400	1320	60	PPFD
Cucumber	25 (20-30)	14-16	350-600	1421	51	PPFD
Melon	28 (25-30)	14-18	390-600	1361	47	PPFD
Basil	20 (15-25)	14-18	230-500	500	50	PPFD
Courgette	28 (25-30)	14-18	390-600	1361	47	PPFD
Radish	14 (12-15)	8-10	350-600	600	40	PPFD

The choice of the selected species considered first of all cultivars that are commonly cultivated at the different localities in Israel, Greece, Italy, Austria and Germany. Due to the different local requirements the list includes crops with high and low light demand based on the DLI. However, the light saturation point might represent a better criterion for light demand (Table 26).

Funded by the European Union under Grant Agreement No 101096056. Views and opinions expressed are however those of the author(s) only and do not necessarily reflect those of the European Union or CINEA. Neither the European Union nor the granting authority can be held responsible for them.

Information sources:

1) https://koraylights.com/how-much-light-do-different-plants-need-for-photosynthesis-dli-ppfd-ppf-par-lcp-lsp/
2) DOI: 10.1016/j.postharvbio.2013.06.017
3) DOI: 10.3390/agronomy14092101
4) https://journals.ashs.org/hortsci/view/journals/hortsci/52/5/article-p706.xml

5.2 Data collection for modelling and validation (plant phenotyping)

5.2.1 Vienna

All experiments in Vienna were performed by BOKU in three greenhouse chambers. The growing system was designed as container experiments, where the containers were watered manually when needed. In order to start with the experiments as soon as possible, it was decided to simulate the presence of the PV system by using shading nets (BeGrit, shading rate 70%). The PV system was completed in summer 2024, which is when experiments with the PV panels started. In one of the two shaded chambers (the third served as the non-shaded control), the atmospheric CO_2 concentration was enriched. Two options were tested, first the application of CO_2Bags (‚CO2BAG®Finland CO2Products Oy'), and second the production of CO_2 by mushrooms in a nearby unit, from where the CO_2 was continuously supplied to the plants. The latter form of CO_2-enrichment was realised in 2025.

Several experiments were designed with a repetition in order to work out the general response of the studied crops. These experiments were analysed together.

During the experiments, BOKU collected automatically daily mean day and night temperature and humidity (Horti Max System consisting of two PT-100 sensors), as well as PAR (light sensor of the FluorPen FP 100, Photon Systems Instruments) and CO_2-concentration (EGM-5 CO_2 Gas Analyser, PP Systems) within the canopy in the morning between 9.00 and 10.00 o'clock, at midday and in the afternoon between 14.00 and 15.00 o'clock. The mean values and statistical differences among chambers are summarised in tables.

For the growth analyses, samples were taken from the plants twice, once at the start of the experiment and once at final harvest. The plants were divided into individual fractions (leaves, roots, stems, fruits, tubers) and their fresh and dry masses were determined. The leaf area was determined by photocopying and cutting out the copies and comparing their weight with a DinA4 sheet. For larger quantities of leaves, a calibration curve between leaf area and leaf weight was created for selected leaves, and the leaf area of entire plants was calculated in this way. The following formulas were used to calculate the growth parameters:

The specific leaf area (SLA) describes the leaf area per unit of dry leaf mass (Wilson et al., 1999):

$$\text{SLA} = \text{leaf area } [m^2] \,/\, \text{leaf dry mass } [kg]$$

Funded by the European Union under Grant Agreement No 101096056. Views and opinions expressed are however those of the author(s) only and do not necessarily reflect those of the European Union or CINEA. Neither the European Union nor the granting authority can be held responsible for them.

The leaf weight ratio (LWR) indicates the ratio of leaf dry matter to the total dry matter of the plant (Shipley, 2006):

$$LWR = \text{leaf dry mass [kg]} / \text{total dry mass [kg]}$$

The leaf area ratio (LAR in $m^2\ kg^{-1}$) describes the leaf area per unit of total dry matter (Chen et al., 1999):

$$LAR = SLA \times LWR$$

The leaf area index (LAI) describes the one-sided green leaf area per unit of ground area (Watson, 1947):

$$LAI = \text{leaf area [cm}^2\text{]} / \text{ground area [cm}^2\text{]}$$

The net assimilation rate (NAR) describes the increase in plant dry matter per unit of average leaf

$$NAR = (DM_2 - DM_1) / ((LA_2 - LA_1) \times (t_1 - t_2))$$

DM_1: average dry matter of plants harvested at the start of the experiment [kg]
DM_2: average dry matter of the plants at the end of the experiment [kg]
LA_1: average leaf area of the plants harvested at the start of the experiment (m^2)
LA_2: average leaf area of the plants at the end of the experiment (m^2)
$t_1 - t_2$: time period between start and end of the experiment (days)

The absolute growth rate (AGR in kg day^{-1}) describes the absolute increase in plant dry matter within a defined period of time (Hunt, 2016):

$$AGR = (DM_2 - DM_1) / (t_2 - t_1)$$

The relative growth rate (RGR in % day^{-1}) was calculated in this experiment according to Briggs et al. (1920):

$$RGR = LAR \times NAR$$

In order to ensure the reproducibility of collected data, training was performed by BOKU on demand. After a first zoom-meeting with all partners on the evaluation procedures for the selected vegetables and fruits, further zoom-meetings with individual partners were arranged on demand in order to address actual problems and elaborate practicable solutions to assess crop growth.

Table 27. Cultivation chamber parameter of the experiment 17/05/-15/06/2023: Mean CO_2-concentration in the chambers, light intensity, temperature & humidity (S, shading nets; b, CO_2Bags; con, control).

	Atmospheric CO_2-conc. [µmol mol^{-1}]	PAR [µmol $m^{-2}\ s^{-1}$]	Day temperature [°C]	Night temperature [°C]
K3 (s)	433 ± 25 a	80 ± 51 b	24.4 ± 4.0 a	17.8 ± 2.3 b
K4 (s & b)	440 ± 21 a	70 ± 54 b	24.1 ± 4.3 b	17.6 ± 2.3 c
K5 (con)	452 ± 56 a	150 ± 60 a	24.5 ± 1.1 ab	19.2 ± 1.4 a
Post-hoc	Paired T-Tests & Bonferroni correction	Paired T-Tests & Bonferroni correction	Paired T-Tests & Bonferroni correction	Paired T-Tests & Bonferroni correction

Different letters within a column indicate significant differences.

Funded by the European Union under Grant Agreement No 101096056. Views and opinions expressed are however those of the author(s) only and do not necessarily reflect those of the European Union or CINEA. Neither the European Union nor the granting authority can be held responsible for them.

A. Experiments with CO_2Bags

1. Experiment Basil 17/05/ - 15/06/2023 and 06/02/ - 21/03/2024

The experiment with basil was performed in 2023 and repeated in 2024. The experimental conditions (mean values) are summarized in Table 27 for 2023 and in Table 28 for 2024.

Table 28. Cultivation chamber parameter of the experiment 06/02/-21/03/2024: Mean CO_2-concentration in the chambers, light intensity, temperature & humidity (S, shading nets; b, CO_2Bags; con, control).

	Atmospheric CO_2-conc. [µmol mol^{-1}]	PAR [µmol m^{-2} s^{-1}]	Day temperature [°C]	Night temperature [°C]	Relative humidity [%]
K3 (s)	446 ± 15 b	39 ± 10 c	24.4 ± 3.1 a	18.7 ± 0.2 a	40.7 ± 9.5 a
K4 (s & b)	467 ± 20 a	47 ± 7 b	24.9 ± 3.7 a	18.1 ± 0.4 b	40.4 ± 9.3 a
K5 (con)	440 ± 21 b	121 ± 26 a	25.3 ± 4.5 a	18.6 ± 0.2 a	38.6 ± 9.8 b
Post-hoc	Paired T-Tests & Bonferroni correction	Paired T-Tests & Bonferroni correction	Paired T-Tests & Bonferroni correction	Paired T-Tests & Bonferroni correction	Paired T-Tests & Bonferroni correction

Different letters within a column indicate significant differences.

The effect of CO_2-enrichment by CO_2Bags was comparatively small, being insignificant in 2023 (Table 27). Although in 2024 a significant difference occurred, the CO_2 concentration in the chamber with CO_2Bags was only about 20 µmol mol^{-1} higher than in the others (Table 28). Noteworthy, the substance in the CO_2Bags is ammonium hydrogen carbonate (NH_4HCO_3), which reacts to form NH_3, CO_2 and H_2O. The NH_3 content in the air close to the crops was measured during one week with a Picarro G2103 NH_3 Gas Analyser indicating a tenfold concentration increase in the chamber with the CO_2Bags (Figure 113). This may indicate that either additional CO_2 or NH_3 or both may have affected the growth response of basil.

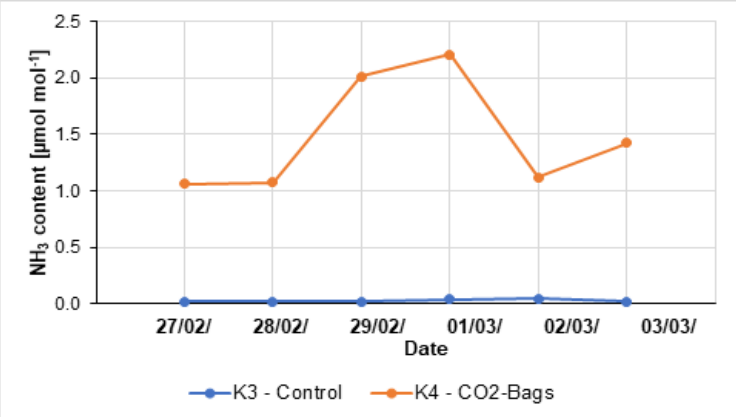

Figure 113. NH_3 concentration measured within the plant stand in a shaded chamber with and without CO_2Bags.

Funded by the European Union under Grant Agreement No 101096056. Views and opinions expressed are however those of the author(s) only and do not necessarily reflect those of the European Union or CINEA. Neither the European Union nor the granting authority can be held responsible for them.

Shoot yield was largest in the chamber 4 “shading & CO_2Bags” (K4), whereas differences between chambers 3 “control” and 5 “shading” were inconsistent (Table 29). Shoot water content was generally higher in plants grown in shade.

Table 29. Growth parameter of the experiments 17/05/-15/06/2023 (prefix 1) and 06/02/-21/03/2024 (prefix 2; S, shading; b, CO_2Bags; con, control).

	Shoot yield [g]	Shoot water content [%]
1-K3 (s)	40.5 ± 1.6 c	84.5 ± 0.9 bc
1-K4 (s & b)	54.7 ± 2.5 a	87.0 ± 1.0 ab
1-K5 (con)	39.0 ± 2.1 c	80.8 ± 0.7 c
2-K3 (s)	30.8 ± 2.5 d	88.9 ± 0.9 a
2-K4 (s & b)	44.4 ± 2.6 b	89.1 ± 0.7 a
2-K5 (con)	41.5 ± 1.9 c	85.5 ± 1.4 bc
$P_{Lilliefors}$	0.043	0.007
$P_{Shapiro-Wilk}$	0.065	0.001
P_{Levene}	0.472	0.075
Post-hoc	Tukey-B	Kruskal-Wallis

Different letters within a column indicate significant differences.

	Water consumption per tuber yield	Water use efficiency (WUE)	WUE per area
K3 Shading (2023)	5.50 L/g	0.18 g/L	0.9 g L^{-1} m^{-2}
K4 CO_2 & Shading (2023)	0.83 L/g	1.20 g/L	6.0 g L^{-1} m^{-2}
K5 Control (2023)	0.06 L/g	15.66 g/L	78.3 g L^{-1} m^{-2}
K3 PV (2024)	0.11 L/g	9.24 g/L	46.2 g L^{-1} m^{-2}
K4 CO_2 & PV (2024)	0.10 L/g	10.05 g/L	50.2 g L^{-1} m^{-2}
K5 Control (2024)	0.07 L/g	14.74 g/L	73.7 g L^{-1} m^{-2}

Growth analysis and water consumption were separately calculated for both experiments. In the case of the 2023 experiment, water consumption per yield was 5.5, 0.8, and 0.06 L g^{-1}, corresponding to water use efficiencies of 0.2, 1.2, and 15.7 g L^{-1} for K3, K4, and K5, respectively.

In the case of the 2024 experiment, water consumption per yield was generally smaller with 0.11, 0.10, and 0.07 L g^{-1}, representing water use efficiencies of 9.2, 10.0, and 14.7 g L^{-1} for K3, K4, and K5, respectively.

Growth rates were calculated for the 2024 experiment, only (Table 30). While net assimilation rate (NAR) and absolute growth rate (AGR) were largest in the “control” chamber (K5), relative growth rate was largest for the variant “shading & CO_2Bags” (K4).

Funded by the European Union

Funded by the European Union under Grant Agreement No 101096056. Views and opinions expressed are however those of the author(s) only and do not necessarily reflect those of the European Union or CINEA. Neither the European Union nor the granting authority can be held responsible for them.

Table 30. Leaf area index (LAI, $cm^2\ cm^{-2}$), specific leaf area (SLA, $m^2\ kg^{-1}$), leaf weight ratio (LWR, %), leaf area ratio (LAR, $m^2\ kg^{-1}$), net assimilation rate (NAR, $kg\ m^{-2}\ day^{-1}$), absolute growth rate (AGR, $kg\ day^{-1}$), & relative growth rate (RGR, $\%\ day^{-1}$) of the trial Basil 2024 (S, shading nets; b, CO_2Bags; con, control).

	LAI [$cm^2\ cm^{-2}$]	SLA [$m^2\ kg^{-1}$]	LWR [%]	LAR [$m^2\ kg^{-1}$]	NAR [$kg\ m^{-2}\ day^{-1}$]	AGR [$kg\ day^{-1}$]	RGR [$\%\ day^{-1}$]
K3 (s)	0.66	65.5	77.0	50.4	0.00044	4.9 E-06	2.23
K4 (s & b)	0.94	68.1	76.4	52.1	0.00050	7.4 E-06	2.61
K5 (con)	0.89	52.2	81.9	42.8	0.00059	8.8 E-06	2.52

Different letters within a column indicate significant differences.

It is concluded that in the case of basil, the application of additional CO_2 (and NH_3) by CO_2Bags was able to compensate for a light reduction by 50-60%. Remarkably, water use efficiency was largest in the case plants were cultivated at low light intensity supported by CO_2Bags.

2. Experiment *Capsicum annuum* L. 23/03/ - 15/08/2023

In this 2023 experiment three cultivars of *C. annuum*, the bell pepper cultivars Bendigo and California Wonder as well as the De Cayenne pepper were investigated. These varieties were tested to determine the extent to which the results for this fruit vegetable, which is particularly important for greenhouse cultivation in significant parts of Europe, could be generalised.

In this experiment as well, a significantly increased CO_2-concentration was not achieved in the corresponding chamber (K4) by adding CO_2Bags, whereas light intensity was on average reduced by 60% in the shaded chambers (Table 31).

Table 31. Cultivation chamber parameter of the experiment 23/03/-15/08/2023: Mean CO_2-concentration in the chambers, light intensity, temperature & humidity (S, shading nets; b, CO_2Bags; con, control).

	Atmospheric CO_2-conc. [$\mu mol\ mol^{-1}$]	PAR [$\mu mol\ m^{-2}\ s^{-1}$]	Day temperature [°C]	Night temperature [°C]
K3 (s)	464 ± 48 a	85 ± 38 b	25.6 ± 3.3 a	20.4 ± 3.0 ab
K4 (s & b)	464 ± 41 a	86 ± 38 b	25.5 ± 3.6 a	20.3 ± 3.2 b
K5 (con)	477 ± 47 a	205 ± 91 a	25.6 ± 2.5 a	20.7 ± 2.5 a
Post-hoc	Paired T-Tests & Bonferroni correction	Paired T-Tests & Bonferroni correction	Paired T-Tests & Bonferroni correction	Paired T-Tests & Bonferroni correction

Different letters within a column indicate significant differences.

Plant height growth was not significantly different among the variants for cvs California Wonder and de Cayenne, but in cv. Bendigo plants of the variant “shading & CO_2Bags” remained smaller (Figures 114-

Funded by the European Union

Funded by the European Union under Grant Agreement No 101096056. Views and opinions expressed are however those of the author(s) only and do not necessarily reflect those of the European Union or CINEA. Neither the European Union nor the granting authority can be held responsible for them.

116). This difference between the variants “shading” and “shading & CO_2Bags” is difficult to explain and may be artificial given the comparable light- and CO_2-levels.

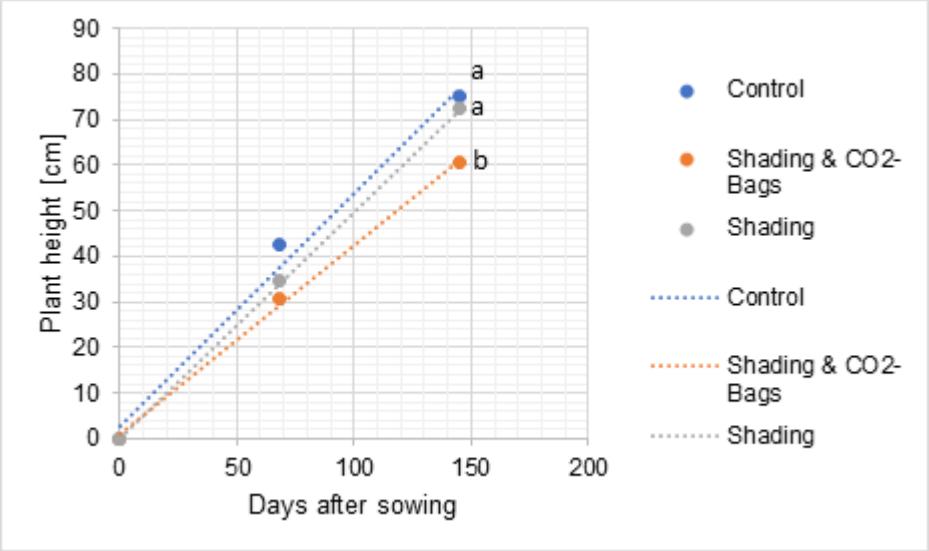

Figure 114. Plant height growth of cv. Bendigo as influenced by shading and CO_2Bags.

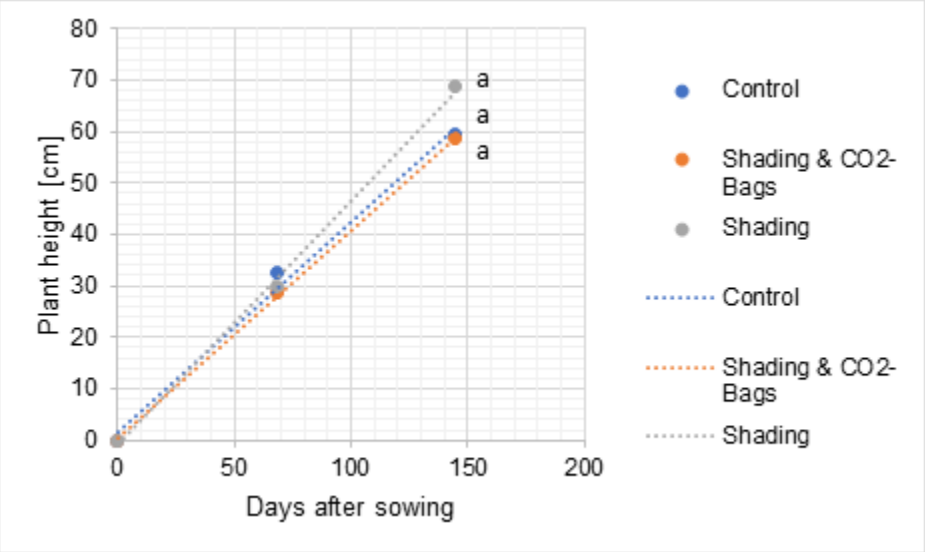

Figure 115. Plant height growth of cv. California Wonder as influenced by shading and CO_2Bags.

Funded by the European Union under Grant Agreement No 101096056. Views and opinions expressed are however those of the author(s) only and do not necessarily reflect those of the European Union or CINEA. Neither the European Union nor the granting authority can be held responsible for them.

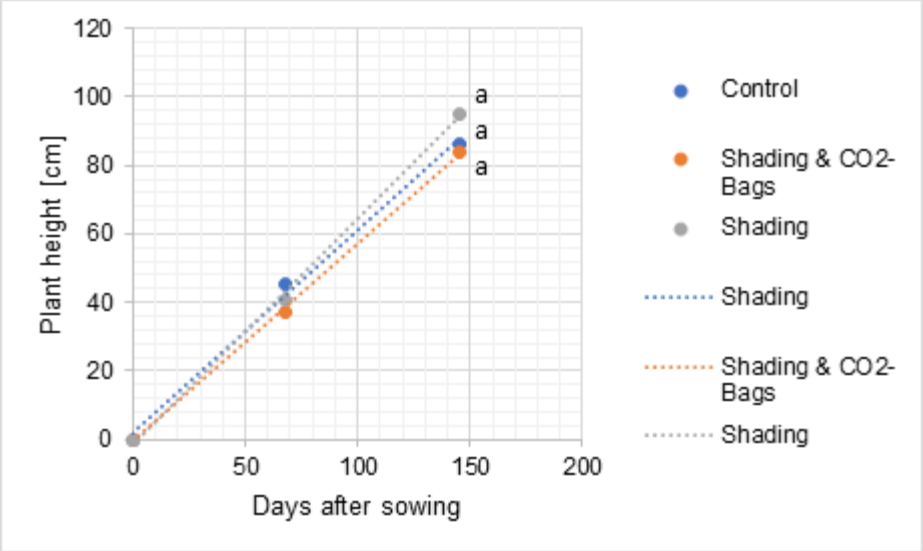

Figure 116. Plant height growth of cv. De Cayenne as influenced by shading and CO_2Bags.

Total fruit yield was largest in the "control" (K5) in all cultivars, although in 'California Wonder' it did not differ significantly from the variant "Shading & CO_2Bags" (K4). In addition, significant differences between the two shading variants (K3, K4) did not occur. Mean single fruit weight was largest in the "control" treatment in 'California Wonder' and 'de Cayenne', whereas in Bendigo significant differences among the variants did not occur. Fruit length and width tended to be largest in the "control" as well (Tables 32-34).

Table 32. Yield parameters of *C. annuum* cv. Bendigo: total fruit yield per plant, mean single fruit yield, fruit water content, fruit length and width, and fruit wall thickness (S, shading nets; b, CO2Bags; con, control).

	Total yield [g]	Fruit fresh weight [g]	Fruit water content [%]	Fruit length [mm]	Fruit width [mm]	Thickness fruit wall [mm]
K3 (s)	123 ± 85 b	46.5 ± 28.7 a	88.4 ± 1.4 a	58.0 ± 14.0 b	50.8 ± 14.0 a	5.0 ± 1.4 ab
K4 (s & b)	170 ± 101 b	50.3 ± 33.9 a	88.1 ± 0.6 a	55.6 ± 18.2 b	52.3 ± 13.9 a	4.2 ± 1.2 b
K5 (con)	303 ± 26 a	65.8 ± 31.6 a	87.8 ± 0.5 a	69.0 ± 14.0 a	56.1 ± 9.9 a	5.0 ± 1.2 a
$P_{Lilliefors}$	0.009	0.018	>0.200	>0.200	0.003	0.022
$P_{Shapiro-Wilk}$	0.021	0.009	0.233	0.192	0.100	0.025
P_{Levene}	0.003	0.392	0.046	0.249	0.035	0.508
Post-hoc	Median	Kruskal-Wallis	ANOVA	Tukey-B	ANOVA	Kruskal-Wallis

Different letters within a column indicate significant differences.

Funded by the European Union

Funded by the European Union under Grant Agreement No 101096056. Views and opinions expressed are however those of the author(s) only and do not necessarily reflect those of the European Union or CINEA. Neither the European Union nor the granting authority can be held responsible for them.

Table 33. Yield parameters of *C. annuum* cv. California Wonder: total fruit yield per plant, mean single fruit yield, fruit water content, fruit length and width, and fruit wall thickness (S, shading nets; b, CO_2Bags; con, control).

	Total yield [g]	Fruit fresh weight [g]	Fruit water content [%]	Fruit length [mm]	Fruit width [mm]	Thickness fruit wall [mm]
K3 (s)	93 ± 50 b	38.8 ± 28.3 b	86.9 ± 2.5 a	62.8 ± 16.7 ab	42.1 ± 9.0 b	4.0 ± 1.0 b
K4 (s & b)	133 ± 98 ab	36.8 ± 48.3 b	86.2 ± 2.4 a	56.3 ± 24.0 b	43.6 ± 11.6 b	3.1 ± 0.9 c
K5 (con)	189 ± 74 a	77.9 ± 53.0 a	87.1 ± 1.3 a	77.7 ± 24.6 a	53.0 ± 10.0 a	5.0 ± 0.9 a
$P_{Lilliefors}$	0.130	0.000	>0.200	0.182	>0.200	>0.200
$P_{Shapiro-Wilk}$	0.164	0.000	0.574	0.004	0.630	0.588
P_{Levene}	0.377	0.170	0.164	0.473	0.497	0.974
Post-hoc	Median	Kruskal-Wallis	ANOVA	Tukey-B	Tukey-B	Kruskal-Wallis

Different letters within a column indicate significant differences.

Table 34. Yield parameters of *C. annuum* cv. De Cayenne: total fruit yield per plant, mean single fruit yield, fruit water content, fruit length and width (S, shading nets; b, CO_2Bags; con, control).

	Total yield [g]	Fruit fresh weight [g]	Fruit water content [%]	Fruit length [mm]	Fruit width [mm]
K3 (s)	26.4 ± 24.6 b	6.2 ± 3.3 b	76.7 ± 3.7 a	69.3 ± 14.7 b	16.0 ± 4.4 a
K4 (s & b)	39.2 ± 32.0 b	6.7 ± 2.9 b	78.0 ± 3.5 a	69.5 ± 15.7 b	18.0 ± 4.5 a
K5 (con)	77.6 ± 17.7 a	8.4 ± 3.1 a	75.6 ± 1.7 a	81.0 ± 13.6 a	17.8 ± 3.4 a
$P_{Lilliefors}$	0.118	>0.200	0.124	0.011	>0.200
$P_{Shapiro-Wilk}$	0.031	0.018	0.194	0.004	0.038
P_{Levene}	0.374	0.828	0.241	0.275	0.020
Post-hoc	Tukey-B	Tukey-B	ANOVA	Kruskal-Wallis	ANOVA

Different letters within a column indicate significant differences.

Water consumption and water use efficiencies were calculated for each of the three cultivars and are as follows:

	Water consumption per yield	Water use efficiency (WUE)	WUE per area
- Bendigo chamber 3 (shading):	408 L/kg	2.45 g/L	9.82 g L^{-1} m^{-2}
- Bendigo chamber 4 (shading & CO_2):	294 L/kg	3.40 g/L	13.61 g L^{-1} m^{-2}
- Bendigo chamber 5 (control):	165 L/kg	6.05 g/L	24.21 g L^{-1} m^{-2}
- California Wonder cha. 3 (shading):	538 L/kg	1.86 g/L	7.45 g L^{-1} m^{-2}
- California Wonder cha. 4 (shading & CO_2):	377 L/kg	2.65 g/L	10.61 g L^{-1} m^{-2}
- California Wonder cha. 5 (control):	264 L/kg	3.78 g/L	15.13 g L^{-1} m^{-2}
- De Cayenne chamber 3 (shading):	1887 L/kg	0.53 g/L	2.11 g L^{-1} m^{-2}
- De Cayenne chamber 4 (shading & CO_2):	1282 L/kg	0.78 g/L	3.14 g L^{-1} m^{-2}
- De Cayenne chamber 5 (control):	645 L/kg	1.55 g/L	6.21 g L^{-1} m^{-2}

Funded by the European Union under Grant Agreement No 101096056. Views and opinions expressed are however those of the author(s) only and do not necessarily reflect those of the European Union or CINEA. Neither the European Union nor the granting authority can be held responsible for them.

It can be summarized for *Capsicum annuum* that in the "control" treatment fruit yield was about twice as high as in both shaded variants, and the application of CO_2Bags had only an insignificant positive effect on fruit yield. Water use efficiency was largest in the "control" treatments and cv. Bendigo performed best under the experimental conditions.

After harvesting, the fruits were examined in the laboratory to determine their marketability. Overall, it was found that the fruits in the shaded chambers (K4, K4) were not as ripe as those in the "control" chamber. In the case of the 'De Cayenne' variety, increased cracking of the fruit was observed, particularly in the "control" chamber. Cracks were not found in the two bell pepper varieties.

The first infestation of whiteflies and aphids was detected in the "control" chamber at the end of May, and in the following days they were found in all chambers. Daily visual inspections revealed that as the temperature rose, so did the pressure in all chambers. It was also noticeable that the 'De Cayenne' variety was significantly more infested than the other two varieties.

In all variants, flower buds were shed, with the 'De Cayenne' variety being particularly affected in the "control" chamber. It was also noticeable that significantly fewer flowers were formed in the shaded chambers than in the "control" chamber. Flower and fruit formation also began significantly later in the shaded chambers compared to the "control". Blossom end rot was observed on individual plants of both bell pepper varieties, 'Bendigo' and 'California Wonder', in all three trial variants.

3. Experiment *Lactuca sativa* cv. Teide 16/05/ - 17/07/2023

The experiment with lettuce was conducted only once, because the plants showed premature shooting despite selecting a cultivar that was said to tolerate elevated temperatures, which were on average about 27°C within the chambers. Atmospheric CO_2 concentrations did not differ significantly among chambers, but light intensity was about 50% less in the shaded variants (Table 35).

Table 35. Cultivation chamber parameter: Mean CO_2-concentration in the chambers, light intensity, temperature and humidity (S, shading nets; b, CO_2Bags; con, control).

	Atmospheric CO_2-conc. [µmol mol^{-1}]	PAR [µmol m^{-2} s^{-1}]	Day temperature [°C]	Night temperature [°C]	Relative humidity [%]
K3 (s)	456 ± 33 a	93 ± 38 b	27.0 ± 3.2 a	20.4 ± 3.0 b	59.3 ± 6.6 a
K4 (s & b)	458 ± 38 a	102 ± 36 b	27.0 ± 3.2 a	20.3 ± 3.0 c	53.2 ± 6.0 c
K5 (con)	471 ± 47 a	234 ± 82 a	26.0 ± 1.9 a	21.0 ± 2.4 a	57.2 ± 7.1 b
Post-hoc	Paired T-Tests & Bonferroni correction	Paired T-Tests & Bonferroni correction	Paired T-Tests & Bonferroni correction	Paired T-Tests & Bonferroni correction	Paired T-Tests & Bonferroni correction

Different letters within a column indicate significant differences.

Funded by the European Union

Funded by the European Union under Grant Agreement No 101096056. Views and opinions expressed are however those of the author(s) only and do not necessarily reflect those of the European Union or CINEA. Neither the European Union nor the granting authority can be held responsible for them.

Plant yield was comparatively low (Table 36), being highest in the "control" (K5) and the variant "shading & CO_2Bags" (K4). Noteworthy, the yield was distinctly smaller than that accepted as a minimum for greenhouse-produced lettuce (100 g). In the case of lettuce, the application of CO_2Bags was at least partly able to compensate for yield losses due to the 50% shading. However, this interpretation has to be considered with care, because the conditions, first of all temperature, were not suitable for lettuce cultivation.

Table 36. Growth parameter: plant height at harvest, yield per plant at harvest, and water content (S, shading; b, CO_2Bags; con, control).

	Plant height [cm]	Yield [g]	Water content [%]
K3 (s)	22.0 ± 1.8 a	29.7 ± 2.5 b	93.6 ± 0.5 a
K4 (s & b)	24.0 ± 3.4 a	34.0 ± 2.8 a	93.6 ± 0.5 a
K5 (con)	17.4 ± 1.6 b	37.7 ± 5.3 a	92.0 ± 0.8 b
$P_{Lilliefors}$	>0.200	0.107	0.000
$P_{Shapiro-Wilk}$	0.183	0.115	0.001
P_{Levene}	0.176	0.009	0.022
Post-hoc	Tukey	Tamhane	Median

Different letters within a column indicate significant differences.

Water consumption differed among the variants. It was 50 mL per day and container for the "control" and 30 mL per day and container for the shaded variants. The increased water requirement of the "control" is also reflected by the reduced water content of this variant (Table 34). Water consumption per yield was thus largest in the "control" (18.8 L kg^{-1}) followed by "shading" (14.5 L kg^{-1}) and least in the variant "shading & CO_2Bags" (12.6 L kg^{-1}). Water use efficiencies accounted for 79.0, 69.0 and 53.1 g L^{-1} for the variants "shading & CO_2Bags" (K4), "shading" (K3) and "control" (K5), respectively. If any conclusion can be drawn from this experiment, it is that the lettuce in variant "shading & CO_2Bags" with respect to plant height, yield and relative water content performed best under these elevated temperatures.

With regard to plant care measures, it should be briefly mentioned that on 26th June 2023, two-spotted ladybirds were introduced into all chambers to combat aphids.

4. Experiment *Cucumis sativus* L. cv. Snackgurke Hopeline F1 06/03/ - 29/05/2024

A single experiment with cucumber was realised at BOKU in order to compare the results from this locality with those of others, where this crop was investigated as well. In this experiment with CO_2Bags, the atmospheric CO_2 concentration was significantly higher in the chamber with "shading & CO_2Bags" (K4) on average by about 20 µmol mol^{-1} (Table 37). Light intensity was reduced by shading in this experiment by as much as 65% on average.

Funded by the European Union

Funded by the European Union under Grant Agreement No 101096056. Views and opinions expressed are however those of the author(s) only and do not necessarily reflect those of the European Union or CINEA. Neither the European Union nor the granting authority can be held responsible for them.

Table 37. Cultivation chamber parameter: Mean CO_2-concentration in the chambers, light intensity, temperature and humidity (S, shading nets; b, CO_2Bags; con, control).

	Atmospheric CO_2-conc. [µmol mol^{-1}]	PAR [µmol m^{-2} s^{-1}]	Day temperature [°C]	Night temperature [°C]	Relative humidity [%]
K3 (s)	439 ± 26 b	98 ± 49 b	22.4 ± 1.3 c	18.2 ± 1.7 a	39.0 ± 9.0 a
K4 (s & b)	455 ± 39 a	106 ± 55 b	22.5 ± 1.3 b	18.2 ± 1.7 a	40.4 ± 10.4 a
K5 (con)	435 ± 30 b	291 ± 187 a	22.6 ± 1.4 a	18.0 ± 1.8 b	38.6 ± 10.6 a
Post-hoc	Paired T-Tests & Bonferroni correction	Paired T-Tests & Bonferroni correction	Paired T-Tests & Bonferroni correction	Paired T-Tests & Bonferroni correction	Paired T-Tests & Bonferroni correction

Different letters within a column indicate significant differences.

Differences in fruit yield per plant were quite distinct, being highest in the "control" (K5), by about 50% reduced in the variant "shading & CO_2Bags" (K4) and by about 95% lower in the variant "shading" (K3). Single fruit mass was comparable between the shaded variants K3 and K4, but about 44% larger in the "control" treatment (K5). Unexpectedly, fruit water content was significantly larger in "control" fruits, which may be partly explained by the larger size of fruits (Table 38). Leaf water content, by contrast, was higher in the shaded variants (Table 38), which may be regarded as a common response to a shading environment that reduced temperature within the chamber (Table 37) and also of the leaf. Leaf mass was comparable between the variants "shading & CO_2Bags" (K4) and "control" (K5) and slightly smaller in the "shading" variant (K3). These results suggest that in cucumber photoassimilates are transferred to the leaves as a priority, next to the developing fruit, resulting in the observed distinct differences in fruit yield.

Table 38. Fruit yield per plant, mean fruit mass and water content, leaf fresh mass at harvest and leaf water content (S, shading; b, CO_2Bags; con, control).

	Plant yield [g]	Mean fruit mass [g]	Fruit water content [%]	Leaf mass [g]	Leaf water content [%]
K3 (s)	44.6 ± 37.3 c	66.9 ± 21.9 ab	93.7 ± 0.9 b	33.8 ± 17.5 b	81.2 ± a
K4 (s & b)	370.7 ± 31.5 b	60.1 ± 24.3 b	93.7 ± 0.4 b	49.2 ± 6.7 a	79.1 ± ab
K5 (con)	751.8 ± 37.5 a	92.0 ± 36.0 a	95.7 ± 0.4 a	48.9 ± 21.2 ab	71.4 ± b
$P_{Lilliefors}$	0.004	0.047	> 0.200	>0.200	0.000
$P_{Shapiro-Wilk}$	0.001	0.001	0.356	0.662	0.000
P_{Levene}	0.685	0.029	0.236	0.002	0.000
Post-hoc	Kruskal-Wallis	Median	Tukey-B	Tamhane	Median

Different letters within a column indicate significant differences.

Water consumption of *Cucumis sativus* L. cv. Snackgurke Hopeline was highest in the "control" (28.0 L per plant), followed by "shading & CO_2Bags" (13.9 L per plant) and "shading" (13.7 L per plant). Due to the very low fruit yield, water consumption per fruit yield was highest in "shading" (307 L kg^{-1}), whereas the

Funded by the European Union under Grant Agreement No 101096056. Views and opinions expressed are however those of the author(s) only and do not necessarily reflect those of the European Union or CINEA. Neither the European Union nor the granting authority can be held responsible for them.

Funded by the European Union

water consumption of the variants "shading & CO_2Bags" and "control" was comparable, 38 and 37 L kg^{-1}, respectively. Correspondingly, water use efficiencies were 3.3 g L^{-1} (16 g L^{-1} m^{-2}) in the "shading" variant, 26.6 g L^{-1} (128 g L^{-1} m^{-2}) in the "shading & CO_2Bags" variant and 26.9 g L^{-1} (129 g L^{-1} m^{-2}) in the "control".

Worthy of note, in May symptoms of leaf spot disease appeared in some plants of all varieties. These spots may be caused by various bacteria or fungi. At this late stage of fruit development, the infestation should not have affected the yield. However, it indicates a general weakening of the plants. Countermeasures were not taken.

5. Experiment *Capsicum annuum* L. cv. California Wonder 06/03/ - 31/08/2024: cultivation partly with shading nets partly with photovoltaic cells

The effect of shading by nets and by the PV system were compared in a single experiment. This was possible, because part of the chambers K3 and K4 were covered by PVs, while the remaining portion was covered by shading nets. It follows that apart from the light intensities, atmospheric CO_2 concentrations and temperature were similar under shading nets and PV within the same chamber.

With respect to the CO_2 concentration, differences occurred between the shaded chambers (K2 & K4) and the "control" variant (K5), which was significantly lower (Table 39). Light intensity was highest under "control" conditions, about 50% lower under the PV systems of chambers K3 and K4, and about 75% lower under shading nets in K3 and K4.

Table 39. Cultivation chamber parameter of the experiment 06/03/-31/03/2024: Mean CO_2-concentration in the chambers, light intensity, temperature and humidity (S, shading nets; b, CO_2Bags; con, control; PV, photovoltaic cell).

	Atmospheric CO_2-conc. [µmol mol^{-1}]	PAR [µmol m^{-2} s^{-1}]	Day temperature [°C]	Night temperature [°C]	Relative humidity [%]
K3 (s)	424 ± 24 a	87 ± 51 c	25.1 ± 2.8 b	21.0 ± 2.5 a	44.4 ± 10.4 a
K4 (s & b)	434 ± 48 a	92 ± 56 c	25.2 ± 2.9 a	21.0 ± 2.5 ab	44.0 ± 11.2 a
K5 (con)	410 ± 18 b	368 ± 199 a	25.1 ± 2.8 b	20.9 ± 2.5 b	42.2 ± 12.4 a
K3 (PV)	424 ± 24 a	182 ± 107 b	25.1 ± 2.8 b	21.0 ± 2.5 a	44.4 ± 10.4 a
K4 (PV & b)	434 ± 48 a	171 ± 104 b	25.2 ± 2.9 a	21.0 ± 2.5 ab	44.0 ± 11.2 a
Post-hoc	Paired T-Tests & Bonferroni correction	Paired T-Tests & Bonferroni correction	Paired T-Tests & Bonferroni correction	Paired T-Tests & Bonferroni correction	Paired T-Tests & Bonferroni correction

Different letters within a column indicate significant differences.

Plant height was only marginally affected, being smallest in the "control" (K5) and largest in chamber K3. Plants cultivated with CO_2Bags in chamber K4 were intermediate in height growth, suggesting that the application of CO_2Bags was able to compensate at least partly for the shading effects (Table 40). Leaf area was smallest in the "control" and "shading & CO_2Bags" variants and largest in chamber K3 under the PV

Funded by the European Union

Funded by the European Union under Grant Agreement No 101096056. Views and opinions expressed are however those of the author(s) only and do not necessarily reflect those of the European Union or CINEA. Neither the European Union nor the granting authority can be held responsible for them.

system. The other variants did not differ significantly from the extreme ones (Table 40). However, leaf fresh mass per plant did not differ among variants, which implies differences in the specific leaf area (unit: m^2 kg^{-1}) and leaf water content (Table 40). Total fruit yield was highest in the "control" (K5), smallest under shading (with and without CO_2Bags) and intermediate under PVs (with and without CO_2Bags), in this respect following PAR (Tables 39-40).

Table 40. Yield parameters of *C. annuum* cv. California Wonder: plant height, stem diameter at stem bottom, mean leaf area per plant, leaf fresh mass per plant, leaf water content and total fruit yield per plant (S, shading nets; b, CO_2Bags; con, control; PV, photovoltaic cell).

	Plant height [cm]	Stem diameter [cm]	Leaf area per plant [cm^2]	Leaf fresh mass per plant [g]	Water content of leaves [%]	Total fruit yield [g]
K3 (s)	133 ± 19 a	1.5 ± 0.2 ab	7069 ± 1414 ab	160 ± 42 a	88.0 ± 0.9 a	80 ± 64 b
K4 (s & b)	114 ± 14 ab	1.4 ± 0.3 b	5679 ± 1867 b	134 ± 49 a	86.9 ± 0.6 ab	153 ± 63 b
K5 (con)	98 ± 18 b	1.9 ± 0.2 a	6711 ± 1153 b	183 ± 31 a	82.6 ± 1.5 c	767 ± 151 a
K3 (PV)	169 ± 44 a	1.6 ± 0.2 ab	9679 ± 141 a	194 ± 2 a	85.3 ± 0.1 b	232 ± 47 ab
K4 (PV & b)	115 ± 13 ab	1.7 ± 0.1 ab	7639 ± 1498 ab	179 ± 21 a	85.4 ± 1.0 b	448 ± 70 ab
$P_{Lilliefors}$	>0.200	>0.200	>0.200	0.062	0.026	0.005
$P_{Shapiro-Wilk}$	0.195	0.830	0.320	0.092	0.060	0.005
P_{Levene}	0.029	0.730	0.279	0.271	0.068	0.101
Post-hoc	Tamhane	Tukey-B	Tukey-B	ANOVA	Tukey-B	Kruskal-Wallis

Different letters within a column indicate significant differences.

Single fresh fruit weight was largest under "control" conditions and in chamber K4 with CO_2Bags, irrespective of shading by nets or PV. By contrast, fruit water content was largest under shading (with and without CO_2Bags) and lower in the "control" variant and under PVs (with and without CO_2Bags). Fruit length, width, and wall thickness did not show differences related to the treatments (Table 41).

The relative allocation of photoassimilates into roots, stem, leaves and fruits (in %) is indicated in Figure 1., showing the highest percentage allocated to fruits in the variants "control" and "PV & CO_2Bags" in chamber K4. The least amount of assimilates transported to fruits was observed in the "shading" variant in K3, although this percentage was not significantly different from the remaining variants "PV" in chamber K3 and "shading & CO_2Bags" in chamber K4. The percentage allocated to leaves remained relatively stable. Only in the case of the "control" this percentage was significantly lower (Figure 117). The assimilate percentage allocated to stems was largest in the variants grown in chamber K3, which may reflect the promotion of height growth (Table 40) under low light intensities.

Funded by the European Union

Funded by the European Union under Grant Agreement No 101096056. Views and opinions expressed are however those of the author(s) only and do not necessarily reflect those of the European Union or CINEA. Neither the European Union nor the granting authority can be held responsible for them.

Table 41. Yield parameters fruit of *C. annuum* cv. California Wonder: Mean single fruit yield, fruit water content, fruit length and width, and fruit wall thickness (S, shading nets; b, CO_2Bags; con, control; PV, photovoltaic cell).

	Fruit fresh weight [g]	Fruit water content [%]	Fruit length [mm]	Fruit width [mm]	Thickness fruit wall [mm]
K3 (s)	44.5 ± 18.8 ab	93.7 ± 0.5 a	43.0 ± 12.7 a	57.2 ± 10.4 ab	6.2 ± 1.5 a
K4 (s & b)	63.1 ± 36.0 a	92.6 ± 0.8 ab	53.6 ± 18.2 a	63.3 ± 9.8 a	6.1 ± 1.4 ab
K5 (con)	54.2 ± 15.3 a	90.3 ± 1.2 c	52.1 ± 11.6 a	58.5 ± 6.3 ab	5.3 ± 0.7 ab
K3 (PV)	33.2 ± 16.5 b	90.3 ± 0.1 c	47.2 ± 11.3 a	50.7 ±9.0 b	4.2 ± 1.0 b
K4 (PV & b)	64.1 ± 35.9 a	91.2 ± 0.2 bc	58.1 ± 17.4 a	61.8 ± 11.2 ab	5.4 ± 1.3 ab
$P_{Lilliefors}$	0.000	>0.200	0.018	>0.200	0.019
$P_{Shapiro-Wilk}$	0.000	0.358	0.008	0.444	0.000
P_{Levene}	0.000	0.202	0.059	0.001	0.000
Post-hoc	Median	Tukey-B	Kruskal-Wallis	Tamhane	Median

Different letters within a column indicate significant differences.

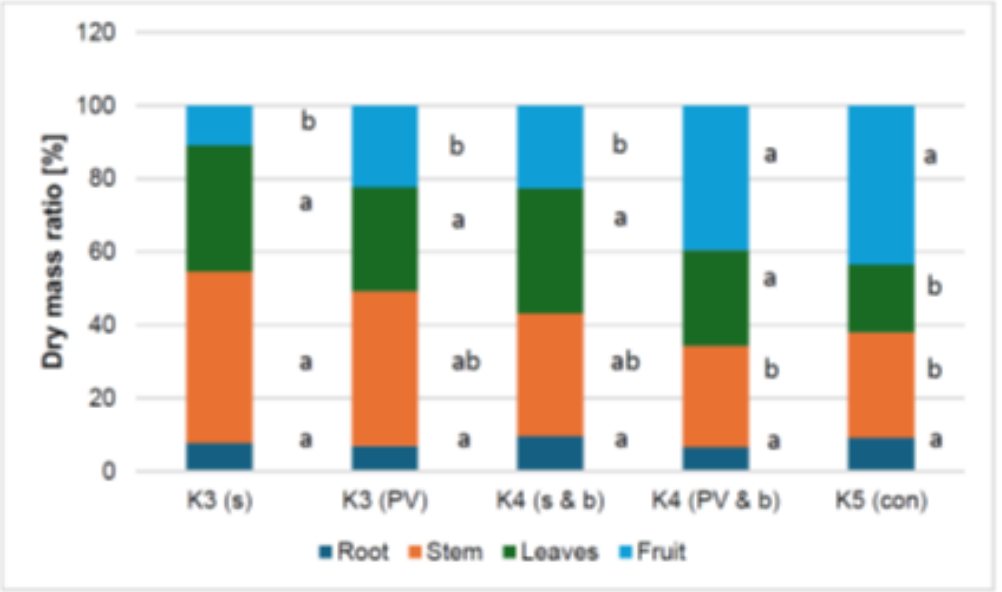

Figure 117. Dry mass ratios reflecting assimilate distribution within the plant. Different letters indicate significant differences for root, leaves, fruit by Tukey-B and for stem by Kruskal-Wallis tests (S, shading nets; b, CO_2Bags; con, control; PV, photovoltaic cell).

Harvest of the plants differed in time: Control plants were harvested after 118 days, the remaining variants after 131-132 days. The different harvest dates were selected in order to give the by nets or PVs shaded variants additional time for fruit growth and ripening.

Funded by the European Union

Funded by the European Union under Grant Agreement No 101096056. Views and opinions expressed are however those of the author(s) only and do not necessarily reflect those of the European Union or CINEA. Neither the European Union nor the granting authority can be held responsible for them.

Despite the shorter growth period of control plants, the accumulated water consumption was larger (66.9 L per plant) than in the remaining variants (Shading or PV in chamber K3: 47.9 L per plant; shading or PV with CO_2Bags in chamber K4: 47.2 L per plant). Water use efficiencies are thus as follows:

	Water consumption per yield	Water use efficiency	Water use efficiency per area
Shading	599 L/kg	1.67 g/L	5.34 g L^{-1} m^{-2}
CO_2 & Shading	308 L/kg	3.24 g/L	10.37 g L^{-1} m^{-2}
Control	87 L/kg	11.47 g/L	36.70 g L^{-1} m^{-2}
PV	206 L/kg	4.84 g/L	15.49 g L^{-1} m^{-2}
CO_2 & PV	105 L/kg	9.49 g/L	30.37 g L^{-1} m^{-2}

Table 42. Leaf area index (LAI, cm^2/cm^2), specific leaf area (SLA, m^2/kg), leaf weight ratio (LWR, %), leaf area ratio (LAR, m^2/kg), net assimilation rate (NAR, $kg/m^2/day$), absolute (AGR, kg/day) & relative growth rate (RGR, %/day) of 'California Wonder' (S, shading; b, CO_2Bags; con, control; PV, photovoltaic cell).

	LAI [cm^2 cm^{-2}]	SLA [m^2 kg^{-1}]	LWR [%]	LAR [m^2 kg^{-1}]	NAR [kg m^{-2} day^{-1}]	AGR [kg day^{-1}]	RGR [% day^{-1}]
K3 (s)	45.9	37.2	36.4	13.5	0.0011	0.0004	1.52
K4 (s & b)	36.9	32.5	32.7	10.6	0.0014	0.0004	1.52
K5 (con)	43.6	21.1	18.7	4.0	0.0043	0.0015	1.70
K3 (PV)	62.9	33.9	28.4	9.6	0.0016	0.0008	1.52
K4 (PV & b)	49.6	29.2	26.2	7.7	0.0020	0.0008	1.52

Different letters within a column indicate significant differences.

The results of the growth analyses revealed that net assimilation rates and absolute growth rates were largest in the "control" variant, followed by the two "PV" variants (with and without CO_2Bags), and smallest in the "shading nets" variants (with and without CO_2Bags). Interestingly, relative growth rates were similar for all variants, except the "control" treatment (Table 42), pointing to a well-balanced partitioning of assimilates between vegetative and generative growth, optimally adapted to the respective low light conditions.

In order to improve plant health and minimise the risk of infections, six yellow sticky traps (Substral) were placed between the bell pepper plants in each cabin at the start of the experiment. On 25th April 2024, predatory mites (*Neoseiulus californicus*) were applied as a preventive measure, with three sachets (Spical-Plus, Koppert) containing 100 individuals each being placed per cabin.

Due to a severe fungus gnat infestation, the number of yellow sticky traps per cabin was increased from six to twelve starting on 11th June 2024. In addition, two treatments with an azadirachtin-containing preparation (Trauermücken EX, Substral) were carried out to combat the larvae in the substrate. On 12th July 2024, all plants were treated with another azadirachtin-containing preparation (NeemAzal-T/S, Nufarm) after spider mites were found on the abaxial side of the leaves, especially in K4. The application

Funded by the European Union

Funded by the European Union under Grant Agreement No 101096056. Views and opinions expressed are however those of the author(s) only and do not necessarily reflect those of the European Union or CINEA. Neither the European Union nor the granting authority can be held responsible for them.

was carried out with a pressure sprayer to ensure even wetting. The treatments were carried out in the evening to avoid leaf burns from sunlight.

Due to a calcium deficiency, which manifested itself in the form of blossom end rot, particularly in K5, all plants were treated with calcium nitrate (Calcium-Plus-Spray, Hauert Manna) on 2nd August 2024. This treatment was also carried out in the evening to avoid leaf burn.

6. Experiment *Raphanus sativus* L. cv. Riesen von Aspern 06/03/ - 11/05/24 (shading) and 22/03/ - 16/05/24 (PV)

This experiment interprets the results of two subsequent cultivations of radish, where the first was realised under shading nets, the second under the recently installed PV system. As could be expected, light and temperature conditions differed slightly between both experiments depending on the time of year and differences in the experimental setup. Light intensity was reduced on average by about 65% due to the shading nets, whereas the effect of the PV system accounted for about 50% light reduction (Tables 43-44). Atmospheric CO_2 concentrations were about 20 µmol mol^{-1} higher in the chamber with CO_2Bags (K4).

Table 43. Cultivation chamber parameter: Mean CO_2-concentration in the chambers, light intensity, temperature and humidity under shading nets of the shading experiment 06/03/-22/04/24 (b, CO_2Bags; con, control; s, shading nets).

	Atmospheric CO_2-conc. [µmol mol^{-1}]	PAR [µmol m^{-2} s^{-1}]	Day temperature [°C]	Night temperature [°C]	Relative humidity [%]
K3 (s)	442 ± 26 b	51 ± 22 b	22.2 ± 1.5 a	17.5 ± 2.3 a	41.2 ± 11.0 a
K4 (s & b)	459 ± 38 a	63 ± 42 b	22.2 ± 1.5 a	17.5 ± 2.2 a	42.3 ± 13.1 a
K5 (con)	438 ± 30 b	173 ± 119 a	22.2 ± 1.6 a	17.3 ± 2.4 b	38.1 ± 10.4 a
Post-hoc	Paired T-Tests & Bonferroni correction	Paired T-Tests & Bonferroni correction	Paired T-Tests & Bonferroni correction	Paired T-Tests & Bonferroni correction	Paired T-Tests & Bonferroni correction

Different letters within a column indicate significant differences.

Total plant fresh mass differed significantly between the two experiments, being generally larger in the second experiment (Table 45). This was mainly due to tuber fresh mass and tuber size. In fact, almost no tubers were produced under shade in the first experiment. Remarkably, light intensity was on average larger for the “control” treatment in the first experiment than for the “PV-shaded” variants of the second, but yield remained significantly lower in the “control”, indicating that other parameters than light intensity must have contributed to the performance of radish in the first experiment.

Funded by the European Union

Funded by the European Union under Grant Agreement No 101096056. Views and opinions expressed are however those of the author(s) only and do not necessarily reflect those of the European Union or CINEA. Neither the European Union nor the granting authority can be held responsible for them.

Table 44. Cultivation chamber parameter: Mean CO_2-concentration in the chambers, light intensity, temperature and humidity under photovoltaic cells of the PV experiment 22/03/-16/05/24 (b, CO_2Bags; con, control; PV, photovoltaic system).

	Atmospheric CO_2-conc. [µmol mol^{-1}]	PAR [µmol m^{-2} s^{-1}]	Day temperature [°C]	Night temperature [°C]	Relative humidity [%]
K3 (PV)	439 ± 26 b	124 ± 71 b	22.7 ± 1.2 b	18.7 ± 0.9 a	35.7 ± 6.6 a
K4 (PV & b)	456 ± 38 a	137 ± 80 b	22.7 ± 1.2 b	18.7 ± 0.9 a	37.3 ± 8.7 a
K5 (con)	436 ± 29 b	251 ± 165 a	22.9 ± 1.4 a	18.6 ± 1.0 b	34.3 ± 6.3 a
Post-hoc	Paired T-Tests & Bonferroni correction	Paired T-Tests & Bonferroni correction	Paired T-Tests & Bonferroni correction	Paired T-Tests & Bonferroni correction	Paired T-Tests & Bonferroni correction

Tuber fresh mass (tuber yield) was consistently largest in the "control" variant. As radish leaves could also be consumed as a salad, though rarely in practice, it may be important to note that leaf fresh mass was consistently largest in the variants "shading & CO_2Bags" or "PV & CO_2Bags".

Table 45. Total plant, root, tuber, stem and leaf fresh mass per plant as well as tuber length and diameter under shading (prefix 1) and PV conditions (prefix 2; b, CO_2Bags; con, control; PV, photovoltaic system; s, shading nets).

	Total plant fresh mass [g]	Root fresh mass [g]	Tuber fresh mass [g]	Stem fresh mass [g]	Leaf fresh mass [g]	Tuber length [mm]	Tuber diameter [mm]
1-K3 (s)	6.9 ± 3.9 d	0.7 ± 1.0 a	0.1 ± 0.4 e	2.0 ± 1.1 a	4.1 ± 2.1 a	0.3 ± 0.5 c	0.2 ± 0.5 e
1-K4 (s & b)	8.6 ± 5.9 d	0.4 ± 0.5 b	0.5 ± 1.2 d	2.6 ± 1.7 a	5.2 ± 3.2 a	5.1 ± 10.8 b	2.1 ± 5.0 d
1-K5 (con)	12.2 ± 7.0 c	0.4 ± 0.9 b	7.8 ± 6.2 c	1.1 ± 0.5 c	3.0 ± 1.2 b	29.0 ± 17.0 a	18.8 ± 11.2 c
2-K3 (PV)	18.6 ± 5.8 b	0.2 ± 0.2 bc	14.1 ± 5.1 b	1.5 ± 0.4 b	2.9 ± 0.8 b	31.8 ± 4.4 a	31.4 ± 3.5 b
2-K4 (PV & b)	24.5 ± 5.6 ab	0.1 ± 0.1 c	15.3 ± 4.9 b	2.9 ± 0.9 a	6.1 ± 2.0 a	34.6 ± 4.0 a	29.4 ± 4.0 b
2-K5 (con)	28.8 ± 8.5 a	0.1 ± 0.1 c	24.1 ± 8.4 a	1.5 ± 0.5 b	3.2 ± 0.8 b	38.0 ± 4.6 a	37.0 ± 4.7 a
$P_{Lilliefors}$	0.000	0.000	0.000	0.000	0.000	0.000	0.000
$P_{Shapiro-Wilk}$	0.000	0.000	0.000	0.000	0.000	0.000	0.000
P_{Levene}	0.000	0.000	0.000	0.000	0.000	0.000	0.000
Post-hoc	Median	Median	Median	Median	Median	Median	Median

Different letters within a column indicate significant differences.

With respect to plant growth, it is important to note that in the case of the first experiment with shading nets, the control plants were harvested after 32 days, whereas the variants "shading" and "shading & CO_2Bags" were harvested after 50 and 52 days in order to allow further tuber growth. In the second experiment with PVs, all variants were harvested after 38 days.

Funded by the European Union

Funded by the European Union under Grant Agreement No 101096056. Views and opinions expressed are however those of the author(s) only and do not necessarily reflect those of the European Union or CINEA. Neither the European Union nor the granting authority can be held responsible for them.

In these experiments water consumption per tuber yield and water use efficiencies were as follows:

	Water consumption per tuber yield	Water use efficiency (WUE)	WUE per area
Shading	15 221 L/kg	0.1 g/L	0.1 g L^{-1} m^{-2}
CO_2 & Shading	2 460 L/kg	0.4 g/L	0.7 g L^{-1} m^{-2}
Control (22/04/)	117 L/kg	8.5 g/L	14.2 g L^{-1} m^{-2}
PV	90 L/kg	11.1 g/L	18.6 g L^{-1} m^{-2}
CO_2 & PV	84 L/kg	11.9 g/L	19.8 g L^{-1} m^{-2}
Control (16/05/)	54 L/kg	18.7 g/L	31.1 g L^{-1} m^{-2}

Discussion: In previous experiments, CO_2Bags were used to increase the atmospheric CO_2 concentration in one of the three greenhouse chambers. This approach was only successful to a limited extent: only in 4 out of 8 experimental approaches was the CO_2 concentration significantly increased, and even then, only by an average of 20 µmol mol^{-1}. Nevertheless, in around half of the trials, a significant increase in yield was achieved through the use of CO_2Bags compared to the shading variant without CO_2Bags: in basil (2x), cucumber (1x), lettuce (1x) and radish (1x). In contrast, the yield was not significantly increased for *Capsicum annuum* (4x) and radish (1x), although there was a clear tendency towards larger values in *Capsicum*. This indicates a positive effect of CO_2Bags, which could also be linked to the positive effect of ammonium as a foliar nitrogen fertiliser or a combination of slightly increased atmospheric CO_2 and ammonium levels. Further studies are needed to investigate this phenomenon. However, based on the yield increases observed to date, it is doubtful at this stage whether the cost/benefit ratio of CO_2Bags justifies their use in commercial greenhouse cultivation.

B. Experiments with CO_2 generated by mushroom cultivation and additional light

In this experimental part of the project, it was decided to lead CO_2 produced by growing mushrooms from another experiment into one of the experimental chambers in order to elevate the atmospheric CO_2 concentration considerably. In doing so, it was possible to increase the atmospheric CO_2 concentration in this chamber at plant height on average by 30 – 35%. A second goal of this experimental setup was the application of additional light, because previous experiments revealed that light intensity might have been a limiting factor.

1. Experiment Basil 30/01/ - 07/04/2025

When measuring the atmospheric CO_2 concentration at plant height, it became evident that the CO_2 concentrations around the plants below additional light were always lower, though not significantly, indicating the effect of a promoted photosynthesis in these plants (Table 46). Another effect of the experimental setup was the on average 3° C elevated day temperature in the chamber with the elevated CO_2 level (K4), which was the consequence of longer closed windows to maintain elevated CO_2 levels.

Funded by the European Union under Grant Agreement No 101096056. Views and opinions expressed are however those of the author(s) only and do not necessarily reflect those of the European Union or CINEA. Neither the European Union nor the granting authority can be held responsible for them.

Table 46. Cultivation chamber parameter: Mean CO_2-concentration in the chambers, light intensity, temperature and humidity under photovoltaic cells with or without additional light of the experiment 10/03/-07/04/25 (b, elevated CO_2; con, control; L, additional light; PV, photovoltaic cells).

	Atmospheric CO_2-conc. [µmol mol^{-1}]	PAR [µmol m^{-2} s^{-1}]	Day temperature [°C]	Night temperature [°C]	Relative humidity [%]
K3 (PV)	446 ± 30 b	94 ± 51 d	22.2 ± 1.7 b	18.4 ± 0.1 b	38.7 ± 14.7 a
K3 (PV, L)	439 ± 34 bc	133 ± 52 c			
K4 (PV, b)	592 ± 99 a	109 ± 60 d	25.6 ± 2.8 a	18.6 ± 0.3 a	36.3 ± 14.6 a
K4 (PV, b, L)	563 ± 73 a	155 ± 67 b			
K5 (con)	431 ± 25 c	214 ± 119 b	22.2 ± 1.8 b	18.4 ± 0.2 b	34.2 ± 14.3 a
K5 (con, L)	428 ± 28 c	252 ± 124 a			
Post-hoc	Paired T-Tests & Bonferroni correction	Paired T-Tests & Bonferroni correction	Paired T-Tests & Bonferroni correction	Paired T-Tests & Bonferroni correction	Paired T-Tests & Bonferroni correction

Different letters within a column indicate significant differences.

Total fresh and dry mass of basil plants was highest in the variant “PV & elevated CO_2 & additional light”, followed by the variants “control & additional light”, “control”, and “PV & additional light” indicating the relative importance of additional light over additional CO_2 in basil (Tables 47-48).

Table 47. Leaf, stem, root fresh mass (FM) and total fresh mass per pot (best 10 plants per pot harvested) at harvest in addition to the from leaf fresh mass calculated mean leaf area per plant (b, elevated CO_2; con, control; L, additional light; PV, photovoltaic cells).

	Leaves FM [g]	Stem FM [g]	Root FM [g]	Total FM [g]	Calculated mean leaf area per plant [cm^2]*
K3 (PV)	20.4 ± 8.0 b	9.0 ± 3.3 b	2.9 ± 1.0 b	32.3 ± 12.1 c	82.3 b
K3 (PV, L)	26.1 ± 10.3 ab	11.3 ± 5.0 ab	3.4 ± 1.4 b	40.8 ± 16.2 abc	105.3 ab
K4 (PV, b)	20.1 ± 5.6 b	9.9 ± 2.7 b	3.2 ± 1.1 b	33.2 ± 8.9 bc	81.1 b
K4 (PV, b, L)	31.3 ± 7.5 a	17.0 ± 4.6 a	5.4 ± 1.2 a	53.6 ± 12.9 a	126.3 a
K5 (con)	27.3 ± 7.2 ab	12.1 ± 3.1 ab	5.3 ± 1.6 a	44.7± 11.6 abc	110.2 ab
K5 (con, L)	28.4 ± 8.3 ab	13.0 ± 4.1 ab	6.9 ± 1.6 a	48.3 ± 13.5 ab	114.6 ab
$P_{Lilliefors}$	0.000	0.024	0.075	0.000	
$P_{Shapiro-Wilk}$	0.000	0.007	0.004	0.081	
P_{Levene}	0.202	0.063	0.383	0.147	
Post-hoc	Kruskal-Wallis	Kruskal-Wallis	Tukey	Kruskal-Wallis	Kruskal-Wallis

*f(x) = 4.0351 x; Different letters within a column indicate significant differences.

Funded by the European Union

Funded by the European Union under Grant Agreement No 101096056. Views and opinions expressed are however those of the author(s) only and do not necessarily reflect those of the European Union or CINEA. Neither the European Union nor the granting authority can be held responsible for them.

Table 48. Leaf, stem, root dry mass (DM) and total dry mass per pot (best 10 plants per pot harvested) at harvest (b, elevated CO_2; con, control; L, additional light; PV, photovoltaic cells).

	Leaves DM [g]	Stem DM [g]	Root DM [g]	Total DM [g]
K3 (PV)	1.43 ± 0.64 c	0.57 ± 0.26 c	0.47 ± 0.16 c	2.48 ± 1.05 c
K3 (PV, L)	2.14 ± 0.99 abc	0.84 ± 0.43 abc	0.58 ± 0.23 c	3.56 ± 1.59 bc
K4 (PV, b)	1.53 ± 0.50 bc	0.62 ± 0.22 c	0.50 ± 0.18 c	2.65 ± 0.87 c
K4 (PV, b, L)	3.08 ± 0.86 a	1.53 ± 0.49 a	1.04 ± 0.32 ab	5.66 ± 1.52 a
K5 (con)	2.28 ± 0.70 abc	0.93 ± 0.29 abc	0.97 ± 0.33 b	4.18 ± 1.25 abc
K5 (con, L)	2.54 ± 0.83 ab	1.11 ± 0.36 ab	1.32 ± 0.33 a	4.97 ± 1.38 ab
$P_{Lilliefors}$	0.004	0.046	0.071	0.001
$P_{Shapiro-Wilk}$	0.003	0.004	0.002	0.001
P_{Levene}	0.297	0.134	0.246	0.353
Post-hoc	Kruskal-Wallis	Kruskal-Wallis	Tukey	Kruskal-Wallis

Different letters within a column indicate significant differences.

With respect to the relative water content, it may be summarized that it was always lower when additional light was supplied. This effect was most distinct in the case of the leaves (Table 49). This observation might reflect a higher photosynthesis rate, because this would require a wider opening of the stomata to improve uptake of CO_2 from the surrounding air, which would in turn result in an increased loss of water into the atmosphere.

Table 49. Leaf, stem, root water content and total water content per plant at harvest (b, elevated CO_2; con, control; L, additional light; PV, photovoltaic cells).

	Leaves WC [%]	Stem WC [%]	Root WC [%]	Total WC [%]
K3 (PV)	93.1 ± 0.5 a	93.9 ± 0.7 a	83.8 ± 1.6 ab	92.5 ± 0.5 a
K3 (PV, L)	92.0 ± 0.8 bc	92.8 ± 0.8 ab	82.6 ± 1.8 abc	91.4 ± 0.6 ab
K4 (PV, b)	92.5 ± 0.6 ab	93.8 ± 0.8 a	84.5 ± 1.5 a	92.1 ± 0.7 a
K4 (PV, b, L)	90.3 ± 1.3 d	91.1 ± 1.8 b	81.0 ± 3.1 c	89.6 ± 1.2 c
K5 (con)	91.8 ± 0.8 bc	92.4 ± 1.3 ab	81.6 ± 2.8 bc	90.7 ± 0.9 b
K5 (con, L)	91.2 ± 0.9 cd	91.3 ± 1.8 b	80.8 ± 1.5 c	89.7 ± 1.1 c
$P_{Lilliefors}$	>0.200	0.030	>0.200	0.179
$P_{Shapiro-Wilk}$	0.006	0.000	0.343	0.006
P_{Levene}	0.075	0.157	0.102	0.128
Post-hoc	Tukey	Kruskal-Wallis	Tukey	Tukey

Different letters within a column indicate significant differences.

Funded by the European Union

Funded by the European Union under Grant Agreement No 101096056. Views and opinions expressed are however those of the author(s) only and do not necessarily reflect those of the European Union or CINEA. Neither the European Union nor the granting authority can be held responsible for them.

Table 50. Relative dry mass of leaves, stems, and roots at harvest (b, elevated CO_2; con, control; L, additional light; PV, photovoltaic cells).

	Relative leaf DM [%]	Relative stem DM [%]	Relative root DM [%]	Relative total DM [%]
K3 (PV)	57.4 ± 2.5 a	22.8 ± 1.6 b	19.9 ± 3.2 bc	100
K3 (PV, L)	59.6 ± 3.2 a	23.0 ± 2.4 b	17.4 ± 4.4 c	100
K4 (PV, b)	57.8 ± 2.5 a	23.4 ± 1.6 b	18.8 ± 3.2 bc	100
K4 (PV, b, L)	54.7 ± 4.9 ab	26.7 ± 3.5 a	18.6 ± 3.5 bc	100
K5 (con)	54.3 ± 4.2 ab	22.1 ± 1.2 b	23.6 ± 5-1 ab	100
K5 (con, L)	50.3 ± 4.8 b	22.1 ± 2.7 b	27.6 ± 5.8 a	100
$P_{Lilliefors}$	0.010	0.190	0.001	--
$P_{Shapiro-Wilk}$	0.001	0.000	0.002	--
P_{Levene}	0.036	0.058	0.074	--
Post-hoc	Median	Tukey	Kruskal-Wallis	--

Different letters within a column indicate significant differences.

The relative assimilate partitioning of basil plants turned out to be quite stable (Figure 118). If a trend were discernible, it would be a slight preference for the root over the shoot in the case of "control" variants, especially in the variant "control & additional light".

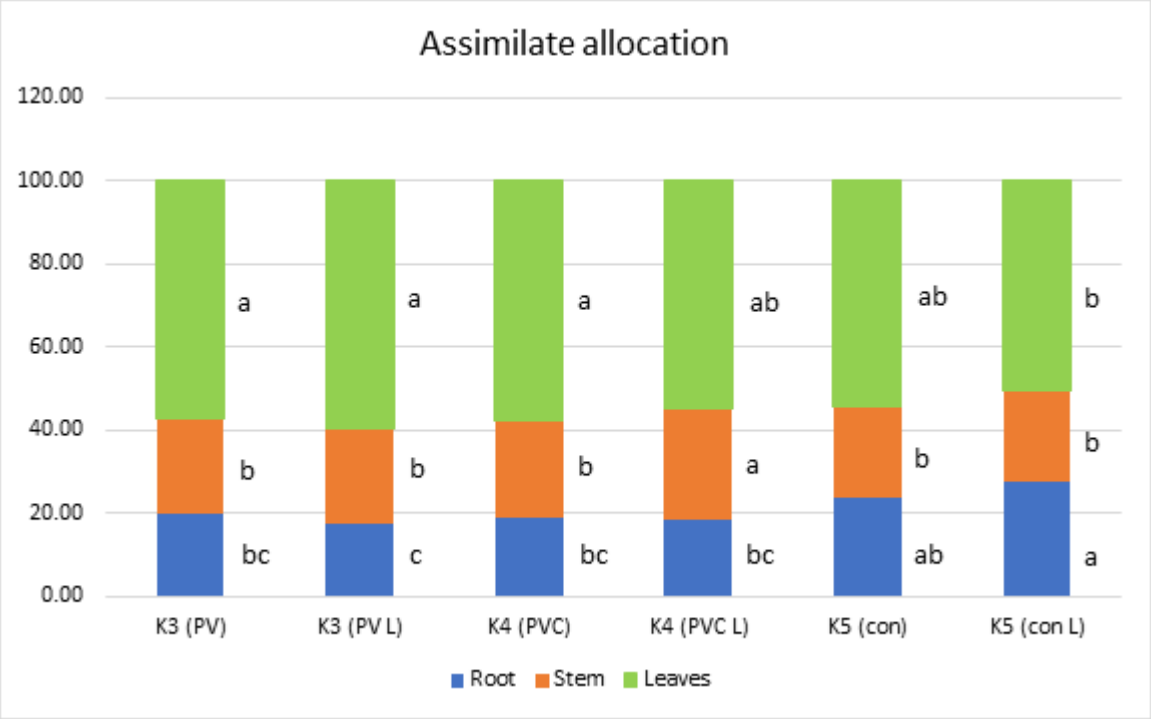

Figure 118. Dry mass ratios reflecting assimilate distribution within the basil plant. Different letters indicate significant differences per plant organ with the statistics indicated in Table 50 (con, control; L, additional light; PV, photovoltaic cells; PVC, photovoltaic cells & elevated CO_2).

Funded by the European Union

Funded by the European Union under Grant Agreement No 101096056. Views and opinions expressed are however those of the author(s) only and do not necessarily reflect those of the European Union or CINEA. Neither the European Union nor the granting authority can be held responsible for them.

The results of the water consumption per plant yield may be summarized as follows:

	Water consumption per plant yield	Water use efficiency (= WUE)	WUE per area
K3, PV	88.2 L/kg	11.3 g/L	217.6 g L^{-1} m^{-2}
K3L, PV & additional light	69.8 L/kg	14.3 g/L	274.9 g L^{-1} m^{-2}
K4, PV & CO_2	85.6 L/kg	11.7 g/L	224.3 g L^{-1} m^{-2}
K4L, PV & CO_2 & additional light	53.2 L/kg	18.8 g/L	361.1 g L^{-1} m^{-2}
K5, control	63.8 L/kg	15.7 g/L	301.1 g L^{-1} m^{-2}
K5L, control & additional light	59.0 L/kg	16.9 g/L	325.4 g L^{-1} m^{-2}

Water use efficiency was best in the case of the variant “PV & elevated CO_2 & additional light”, followed by both “control” variants and the variant “PV & additional light”. Both “PV” variants without additional light performed worse.

Table 51. Leaf area index (LAI, cm^2 cm^{-2}), specific leaf area (SLA, m^2 kg^{-1}), leaf weight ratio (LWR, %), leaf area ratio (LAR, m^2 kg^{-1}), net assimilation rate (NAR, kg m^{-1} day^{-1}), absolute (AGR, kg day^{-1}) & relative growth rate (RGR, % day^{-1}) of basil (b, CO_2Bags; co, control; L, additional light; PV, photovoltaic cells).

	LAI [cm^2 cm^{-2}]	SLA [m^2 kg^{-1}]	LWR [%]	LAR [m^2 kg^{-1}]	NAR [kg m^{-2} day^{-1}]	AGR [kg day^{-1}]	RGR [% day^{-1}]
K3 (PV)	0.47	37.0	71.3	26.4	0.0023	0.000012	5.98
K3 (PV, L)	0.57	54.2	59.8	32.4	0.0019	0.000011	6.07
K4 (PV, b)	0.44	49.1	61.7	30.3	0.0019	0.000009	5.82
K4 (PV, b, L)	0.60	33.2	58.4	19.4	0.0032	0.000021	6.29
K5 (co)	0.55	41.7	58.5	24.4	0.0025	0.000015	6.16
K5 (co, L)	0.57	35.0	57.5	20.1	0.0031	0.000019	6.24

A similar ranking was obtained from the absolute and relative growth rates of the basil plants (Table 51). Net assimilation rates could be arranged into two distinct groups being 0.02 and 0.03 kg m^{-2} day^{-1}, respectively. The first group consisted of the variants “PV”, “PV & additional light” and “PV & elevated CO_2”, whereas the second of the two “control” variants and the variant “PV & elevated CO_2 & additional light”. Obviously, the latter combination was able to compensate for the installation of the PV system.

The present experiment impressively demonstrated the importance of the available light intensity for basil. Only at a PAR above an average of 130-150 µmol m^{-2} s^{-1} did the increased atmospheric CO_2 concentration take effect and contributed to faster growth and thus higher yields. This calls into question the economic viability of a PV system, especially in latitudes with low solar radiation.

Funded by the European Union

Funded by the European Union under Grant Agreement No 101096056. Views and opinions expressed are however those of the author(s) only and do not necessarily reflect those of the European Union or CINEA. Neither the European Union nor the granting authority can be held responsible for them.

2. Experiment Radish 28/02/ - 15/04/2025

The radish experiment was performed under the same experimental conditions such as the above-mentioned basil experiment. The atmospheric CO_2 concentration was about 30 – 35% larger in the chamber K4 and the CO_2 levels were by 4 – 25 µmol mol^{-1} CO_2 lower in the plant stand (Table 52). Day temperature was on average by 5°C warmer in chamber K4.

Table 52. Cultivation chamber parameter: Mean CO_2-concentration in the chambers, light intensity, temperature and humidity under photovoltaic cells with or without additional light of the experiment 28/02/-15/04/25 (b, CO_2Bags; con, control; L, additional light; PV, photovoltaic cells).

	Atmospheric CO_2-conc. [µmol mol^{-1}]	PAR [µmol m^{-2} s^{-1}]	Day temperature [°C]	Night temperature [°C]	Relative humidity [%]
K3 (PV)	431 ± 19 b	133 ± 77 c	23.1 ± 2.1 b	18.4 ± 0.1 b	37.2 ± 14.8 a
K3 (PV, L)	423 ± 16 bc	167 ± 72 b			
K4 (PV, b)	574 ± 90 a	122 ± 70 c	28.4 ± 3.7 a	18.5 ± 0.2 a	35.0 ± 14.3 a
K4 (PV, b, L)	549 ± 61 a	173 ± 77 b			
K5 (con)	419 ± 11 bc	240 ± 127 b	22.8 ± 1.6 b	18.3 ± 0.2 c	33.1 ± 14.4 a
K5 (con, L)	415 ± 13 c	280 ± 123 a			
Post-hoc	Paired T-Tests & Bonferroni correction	Paired T-Tests & Bonferroni correction	Paired T-Tests & Bonferroni correction	Paired T-Tests & Bonferroni correction	Paired T-Tests & Bonferroni correction

Different letters within a column indicate significant differences.

Table 53. Leaf, tuber, root fresh mass (FM) per plant at harvest in addition to the from leaf FM calculated mean leaf area per plant (b, CO_2Bags; con, control; L, additional light; PV, photovoltaic cells).

	Leaves FM [g]	Tuber FM [g]	Root FM [g]	Calculated mean leaf area per plant [cm^2]*
K3 (PV)	11.5 ± 1.8 a	4.2 ± 1.4 c	0.29 ± 0.09 d	370.1 a
K3 (PV, L)	12.0 ± 0.7 a	20.2 ± 3.1 b	0.32 ± 0.09 cd	385.5 a
K4 (PV, b)	10.9 ± 1.6 a	2.9 ± 0.5 c	0.38 ± 0.08 cd	351.0 a
K4 (PV, b, L)	11.2 ± 1.4 a	16.7 ± 2.3 b	0.44 ± 0.08 bc	360.9 a
K5 (con)	11.2 ± 1.3 a	17.2 ± 1.6 b	0.53 ± 0.07 ab	361.9 a
K5 (con, L)	13.2 ± 2.1 a	30.8 ± 2.4 a	0.60 ± 0.13 a	426.8 a
$P_{Lilliefors}$	0.042	0.003	>0.200	
$P_{Shapiro-Wilk}$	0.007	0.001	0.214	
P_{Levene}	0.216	0.002	0.430	
Post-hoc	Kruskal-Wallis	Median	Tukey	Kruskal-Wallis

*f(x) = 32.239 x; Different letters within a column indicate significant differences.

Funded by the European Union under Grant Agreement No 101096056. Views and opinions expressed are however those of the author(s) only and do not necessarily reflect those of the European Union or CINEA. Neither the European Union nor the granting authority can be held responsible for them.

Funded by the European Union

Significant differences were detected in leaves' fresh mass, but with respect to leaves' dry mass, it tended to be larger in the variants exposed to additional light (Tables 53-54). Consequently, leaf water contents were lower in these variants (Table 54). A similar, even more distinct effect was detectable in tuber fresh and dry mass, as well as in its water content, with the exception of the "control" treatments (Tables 53-54).

Table 54. Leaf, tuber, and root dry mass (DM) and water content (WC) per plant at harvest (b, CO_2Bags; con, control; L, additional light; PV, photovoltaic cells).

	Leaves DM [g]	Tuber DM [g]	Root DM [g]	Leaves WC [%]	Tuber WC [%]	Root WC [%]
K3 (PV)	0.73 ± 0.17 ab	0.21 ± 0.05 c	0.06 ± 0.02 b	93.7 ± 0.6 ab	95.0 ± 0.5 a	80.5 ± 2.1 a
K3 (PV, L)	0.80 ± 0.10 a	1.14 ± 0.13 b	0.07 ± 0.02 b	93.3 ± 0.6 cd	94.4 ± 0.4 b	78.4 ± 2.1 a
K4 (PV, b)	0.63 ± 0.11 b	0.16 ± 0.04 c	0.07 ± 0.01 b	94.2 ± 0.3 a	94.6 ± 0.4 ab	81.3 ± 1.4 a
K4 (PV, b, L)	0.78 ± 0.10 ab	1.06 ± 0.13 b	0.08 ± 0.01 b	93.0 ± 0.8 cd	93.6 ± 0.6 c	80.8 ± 2.2 a
K5 (con)	0.70 ± 0.10 ab	0.98 ± 0.16 b	0.12 ± 0.03 a	93.7 ± 0.4 ab	94.4 ± 0.5 ab	77.7 ± 3.2 ab
K5 (con, L)	0.97 ± 0.21 a	1.67 ± 0.13 a	0.17 ± 0.05 a	92.7 ± 0.8 d	94.6 ± 0.2 ab	71.4 ± 2.6 b
$P_{Lilliefors}$	>0.200	0.000	0.000	0.178	>0.200	0.002
$P_{Shapiro-Wilk}$	0.003	0.000	0.000	0.021	0.018	0.001
P_{Levene}	0.039	0.003	0.013	0.099	0.551	0.049
Post-hoc	Tamhane	Median	Median	Tukey	Kruskal-Wallis	Median

Different letters within a column indicate significant differences.

Table 55. Relative dry mass (DM) of leaves, tubers, and roots at harvest as well as total relative dry mass (b, CO_2Bags; con, control; L, additional light; PV, photovoltaic cells).

	Relative leaf DM [%]	Relative tuber DM [%]	Relative root DM [%]	Relative total DM [%]
K3 (PV)	73.0 ± 3.7 a	21.0 ± 4.1 bc	6.0 ± 2.6 ab	100
K3 (PV, L)	39.8 ± 2.5 b	56.7 ± 3.0 a	3.5 ± 1.2 b	100
K4 (PV, b)	73.0 ± 2.1 a	18.7 ± 3.1 c	8.3 ± 1.5 a	100
K4 (PV, b, L)	40.6 ± 4.8 b	55.0 ± 5.0 a	4.4 ± 0.7 b	100
K5 (con)	39.3 ± 5.6 b	54.0 ± 4.8 ab	6.7 ± 1.5 a	100
K5 (con, L)	34.1 ± 4.4 b	59.6 ± 3.0 a	6.3 ± 2.1 ab	100
$P_{Lilliefors}$	0.000	0.000	0.025	--
$P_{Shapiro-Wilk}$	0.000	0.000	0.253	--
P_{Levene}	0.010	0.766	0.020	--
Post-hoc	Median	Kruskal-Wallis	Tamhane	--

Different letters within a column indicate significant differences.

Assimilate allocation towards root, tuber and leaf showed a very distinct pattern (Figure 119): In the case of the variants "PV" and "PV & CO_2", the largest percentage was translocated into the leaves, distinctly less into tuber development. In the case of additional light and in the case of the "control" treatments,

Funded by the European Union under Grant Agreement No 101096056. Views and opinions expressed are however those of the author(s) only and do not necessarily reflect those of the European Union or CINEA. Neither the European Union nor the granting authority can be held responsible for them.

the largest percentage was translocated into the tubers. In both adjustments for assimilate partitioning, the assimilate partitioning among root, tuber and leaf was comparatively stable.

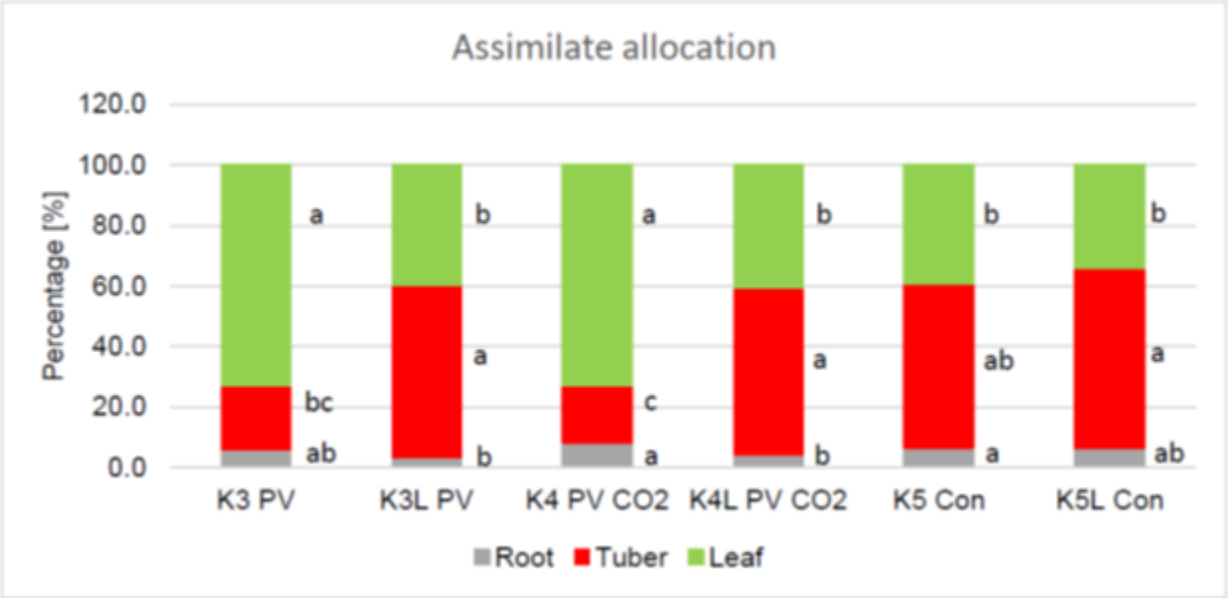

Figure 119. Dry mass ratios reflecting assimilate distribution within the radish plant. Different letters indicate significant differences per plant organ with the statistics indicated in Table 55 (con, control; L, additional light; PV, photovoltaic cells; PVC, photovoltaic cells & CO_2Bags).

The accumulated water consumptions per plant were 11.5 L per pot for the variants “PV” (K3), “PV & additional light” (K3L), and “PV & elevated CO_2” (K4) and 13.5 L per pot in the variants “PV & elevated CO_2 & additional light” (K4L), “control” (K5), and “control & additional light” (K5L). Further results for water consumption based on tuber yield and water use efficiency are as follows:

	Water consumption per plant yield	Water use efficiency (= WUE)	WUE per area
K3, PV	113.0 L/kg	8.8 g/L	44.3 g L^{-1} m^{-2}
K3L, PV & additional light	23.7 L/kg	42.3 g/L	211.3 g L^{-1} m^{-2}
K4, PV & CO_2	162.9 L/kg	6.1 g/L	30.7 g L^{-1} m^{-2}
K4L, PV & CO_2 & additional light	33.7 L/kg	29.7 g/L	148.4 g L^{-1} m^{-2}
K5, control	32.6 L/kg	30.6 g/L	153.2 g L^{-1} m^{-2}
K5L, control & additional light	18.3 L/kg	54.7 g/L	273.5 g L^{-1} m^{-2}

In the case of radish, water use efficiency was highest for “control & additional light” (K5L), followed by “PV & additional light” (K3L), and then closely together “control” (K5) and “PV & elevated CO_2 & additional light” (K4L), emphasising the significance of a sufficiently high light intensity and only a minor effect of additional CO_2.

Funded by the European Union under Grant Agreement No 101096056. Views and opinions expressed are however those of the author(s) only and do not necessarily reflect those of the European Union or CINEA. Neither the European Union nor the granting authority can be held responsible for them.

Table 56. Leaf area index (LAI, cm^2/cm^{-2}), specific leaf area (SLA, m^2/kg), leaf weight ratio (LWR, %), leaf area ratio (LAR, m^2/kg), net assimilation rate (NAR, kg/m/day), absolute (AGR, kg/day) & relative growth rate (RGR, %/day) of radish (b, CO_2Bags; co, control; L, additional light; PV, photovoltaic cells).

	LAI [$cm^2\ cm^{-2}$]	SLA [$m^2\ kg^{-1}$]	LWR [%]	LAR [$m^2\ kg^{-1}$]	NAR [$kg\ m^{-2}\ day^{-1}$]	AGR [$kg\ day^{-1}$]	RGR [$\%\ day^{-1}$]
K3 (PV)	0.19	50.9	73.3	37.3	0.0017	0.000033	6.41
K3 (PV, L)	0.19	48.3	39.8	19.2	0.0034	0.000068	6.52
K4 (PV, b)	0.19	55.7	73.1	40.7	0.0016	0.000029	6.36
K4 (PV, b, L)	0.19	46.1	40.6	18.7	0.0035	0.000065	6.50
K5 (con)	0.19	51.5	39.1	20.1	0.0032	0.000061	6.49
K5 (con, L)	0.19	44.2	34.4	15.2	0.0043	0.000096	6.57

Net assimilation rates (NAR), absolute growth rates (AGR) and relative growth rates (RGR) revealed quite different arrangements of the variants (Table 56): NAR was largest for “control & additional light” (K5L). Closely together followed the variants “PV & elevated CO_2 & additional light” (K4L), “PV & additional light” (K3L), and “control” (K5), while the variants “PV” (K3) and “PV & elevated CO_2” (K4) were far behind in the second-to-last and last place. A similar ranking was found for AGR, whereas RGRs were about comparable for all variants, being largest for “control & additional light” (K5L), followed by “PV & additional light” (K3L), “PV & elevated CO_2 & additional light” (K4L), “control” (K5), “PV” (K3) and “PV & elevated CO_2” (K4)

Discussion: The experiments with the combination of elevated atmospheric CO_2 concentrations and additional light reveal in the case of basil and radish unequivocally that sufficient light intensity is of fundamental importance and cannot be compensated for by additional CO_2. Only in the case a “certain” light level is achieved, adding CO_2 may have a positive effect on photosynthesis, yield and also water use efficiency.

Literature

Briggs, G. E., Kidd, F., West, C. (1920) A quantitative analysis of plant growth: Part II. Annals of Applied Biology 7 (2-3), 202–223. DOI: 10.1111/j.1744-7348.1920.tb05308.x

Chen, K., Hu, G., Keutgen, N., Janssens, M., Lenz, F. (1999) Effects of NaCl salinity and CO_2 enrichment on pepino (*Solanum muricatum* Ait.) I. Growth and yield. Scientia Horticulturae 81 (1), 25–41. DOI: 10.1016/S0304-4238(98)00264-7

Hunt, R. (2016) Growth analysis, individual plants. In: Encyclopedia of Applied Plant Sciences (Bd. 1, S. 421–429). DOI: 10.1016/B978-0-12-394807-6.00226-4

Shipley, B. (2006) Net assimilation rate, specific leaf area and leaf mass ratio: Which is most closely correlated with relative growth rate? A meta-analysis. Functional Ecology 20 (4), 565–574. DOI: 10.1111/j.1365-2435.2006.01135.x

Watson, D. J. (1947) Comparative physiological studies on the growth of field crops: I. Variation in net assimilation rate and leaf area between species and varieties, and within and between years. Annals of Botany 11 (1), 41–76. DOI: 10.1093/oxfordjournals.aob.a083148

Funded by the European Union

Funded by the European Union under Grant Agreement No 101096056. Views and opinions expressed are however those of the author(s) only and do not necessarily reflect those of the European Union or CINEA. Neither the European Union nor the granting authority can be held responsible for them.

Wilson, P. J., Thompson, K., Hodgson, J. G. (1999) Specific leaf area and leaf dry matter content as alternative predictors of plant strategies. New Phytologist 143 (1), 155–162. DOI: 10.1046/j.1469-8137.1999.00427.x

5.2.2 Kfar Kari

Four experiments were performed to evaluate the effects of photovoltaic coverage inside the greenhouse affecting plant growth and yield. In the first experiment, plants were planted in the ground. In all subsequent experiments, the growing system is shifted to soilless grow-bags full of coconut fibre coir (Pelemix) 100 cm long, 18 cm wide, and 13 cm high (23.4 litres), with 5 plants. Two integral drip pipes (16 mm diameter with 20 cm interval between 2.3 L/h drippers, Netafim) were passed into the grow-bases above the cocopeat surface. Four rows of growbags (15 per row, 60 per structure) were located above a spacer and polypropylene 30 cm channel (Mapal) for drainage collection.

The variables for the experiments are summarised in Table 57 and described below. In all experiments, the plants were planted from seedlings in 4 rows per greenhouse.

Table 57. Summary of experiments at Kfar Kari.

Treatments	Experiment 1	Experiment 2	Experiment 3	Experiment 4
Crop	Cucumber	Cucumber	Tomato	Capsicum
Season dates	June-July, 2024	January-April, 2025	June- , 2025	June- , 2025
Growbags		x	x	x
Control	x	x	x	x
PV (Tracking)	x	x	x	x
CO_2		x		
PV + CO_2 (Tracking)		x		

Measurements

Harvest

From the four rows of plants in the greenhouse, the two central rows were selected to avoid marginal effects from the greenhouse edges. In each of these rows, 2 replicates (comprising five consecutive plants) of each treatment were marked for measurement, each replicate consisted of five plants. Thus, 20 plants were sampled from each greenhouse.

At each harvest, fruits from the marked plots were harvested and weighed separately to track yield components (fruit number and weight by treatment).

Funded by the European Union under Grant Agreement No 101096056. Views and opinions expressed are however those of the author(s) only and do not necessarily reflect those of the European Union or CINEA. Neither the European Union nor the granting authority can be held responsible for them.

Growth, biomass, and fruit quality

At 3-4 timepoints throughout the season, 4 samples were randomly selected from the middle rows of each greenhouse for measurement of plant height (from the ground in cm) and stem diameter on the soil surface.

These same samples were then uprooted and divided into fractions (leaves, fruits, roots, and stems). The number of leaves, the total leaf area, and the number of fruits of each plant were recorded. Then leaves, fruits, stems, and roots of each plant were weighed before drying (10 days at 70 °C oven) and weighed again.

Furthermore, four groups of five fruits were collected from each greenhouse for assessment of external and internal fruit colour (1-5 scale), taste (1-5), and brix (%) tests.

Statistical analysis

GraphPad Prism 10.6.1 software was used for all statistical analysis. The statistical tests are elaborated below.

Results

Experiment 1

This experiment was conducted from June, 2024 to July, 2024. Cucumber seedlings (Kingstar, commercial variety) were transplanted in the ground in 4 greenhouses. All 4 greenhouses were used, with 2 replicates for each condition (PV panels vs. no PV panels).

Average fruit mass did not differ significantly between PV and non-PV greenhouses at any of the measured harvest dates (Figure 120a). The total yield in PV greenhouses (15.68 kg) reached 88.84 % of that measured in non-PV greenhouses (18.41 kg), indicating a slight reduction. However, this reduction was not significant by Mann-Whitney U test ($U = 19$, $p = 0.195$, two-tailed; Fig. 120b).

Funded by the European Union under Grant Agreement No 101096056. Views and opinions expressed are however those of the author(s) only and do not necessarily reflect those of the European Union or CINEA. Neither the European Union nor the granting authority can be held responsible for them.

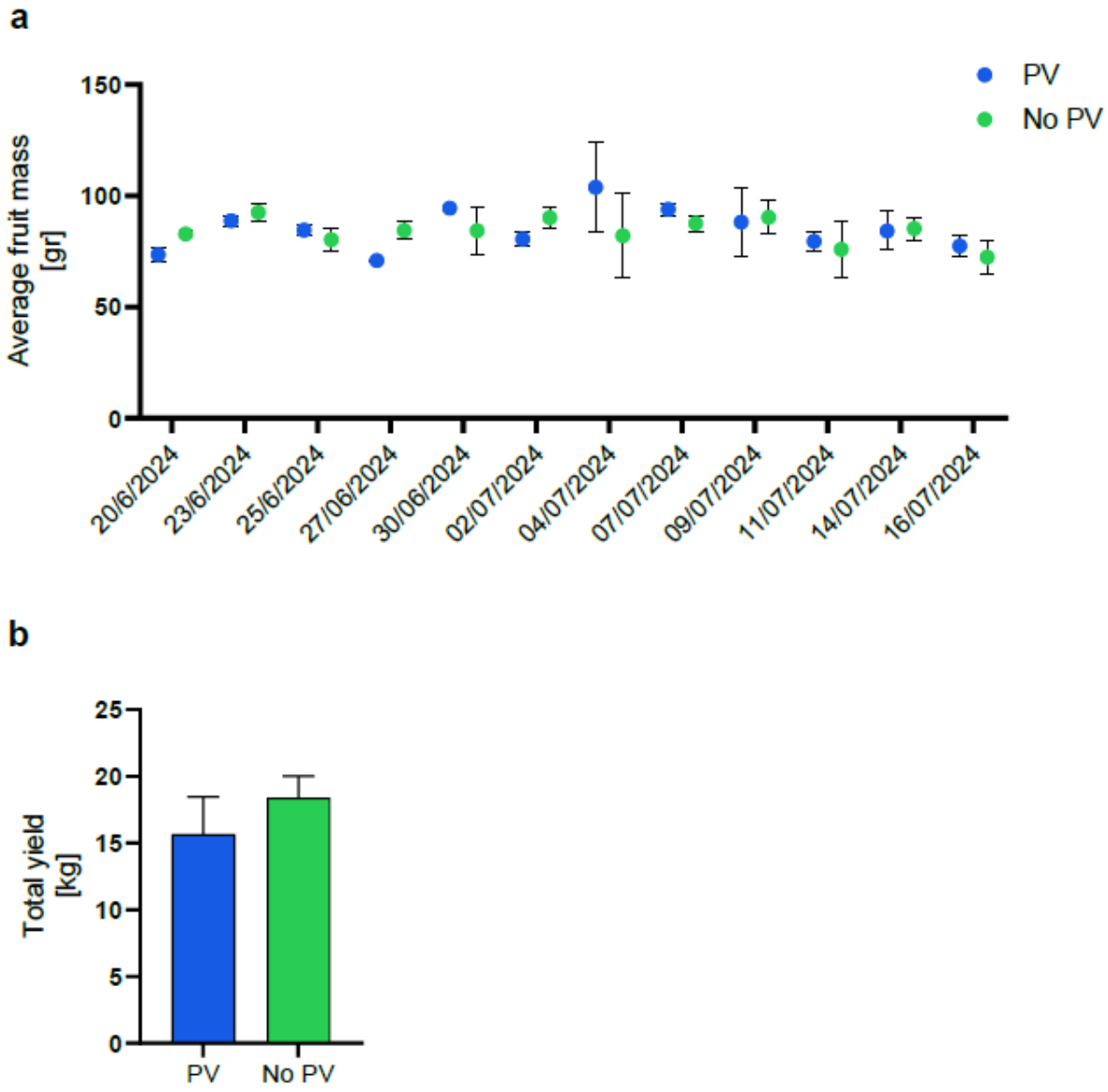

Figure 120. Average fruit mass over time for PV and No-PV greenhouses (a) and total yield (b) (*, $p \leq 0.05$; PV, photovoltaic panels).

In summary, PV installation did neither significantly affect fruit size nor total seasonal yield, suggesting that productivity under PV conditions was comparable to that of conventional greenhouses during the July 2024 season.

Funded by the European Union under Grant Agreement No 101096056. Views and opinions expressed are however those of the author(s) only and do not necessarily reflect those of the European Union or CINEA. Neither the European Union nor the granting authority can be held responsible for them.

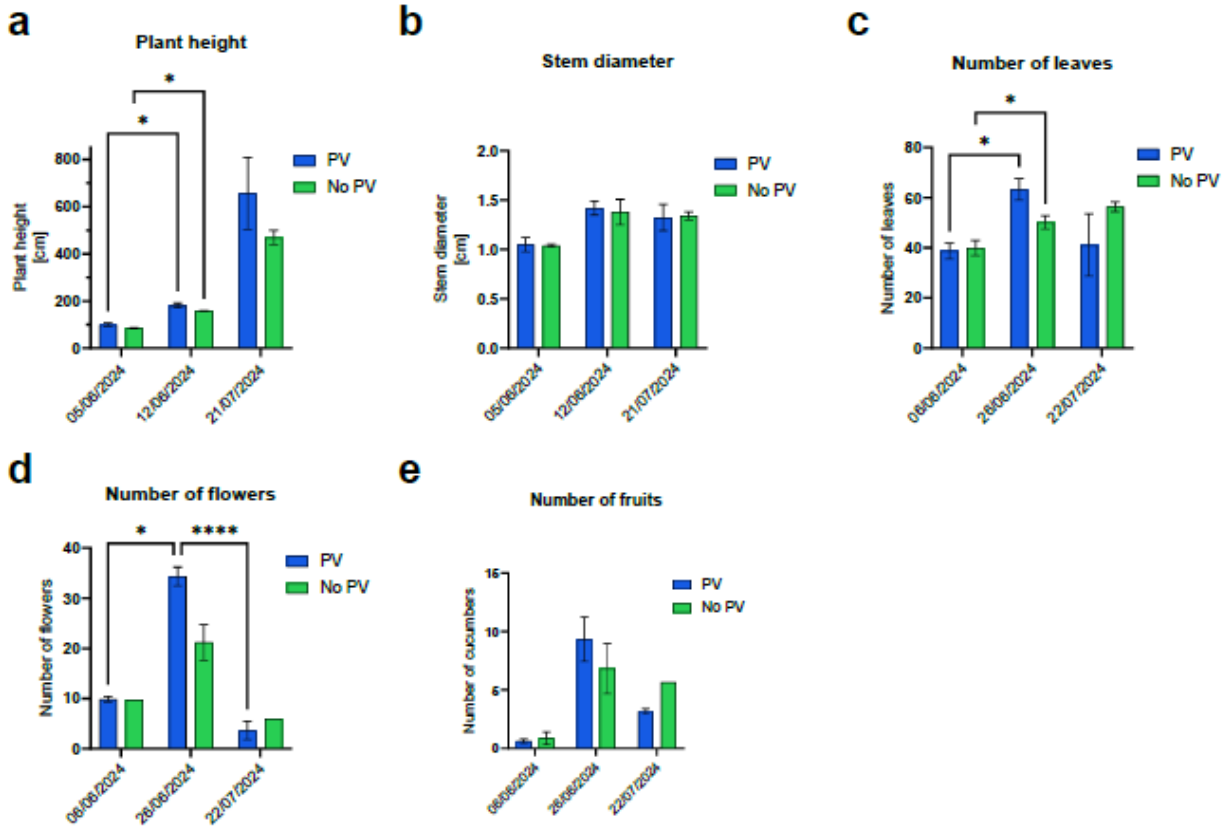

Figure 121. Plant height (a), stem diameter (b), number of leaves (c), number of flowers (d), and number of cucumber fruits (e) (*, $p \leq 0.05$; PV, with photovoltaic panels).

Plant height, leaf number, stem diameter, and flower count, were measured to indicate plant growth characteristics. Two-way ANOVA was conducted to determine statistical significance between the PV and no-PV and over time. Figure 121 shows that both groups had similar growth trends over time, indicating that PV installation did not significantly affect vegetative or reproductive development.

In summary, cucumber plants maintained normal, uniform growth under PV conditions, confirming that PV coverage is compatible with healthy crop development.

The fruit quality parameters external colour, internal colour, Brix, fruit bitterness are indicated in Figure 122. These were measured at 3 time-points, early in the season, mid-season, and at the end of the season. A two-way ANOVA was conducted to observe the differences between groups and over time.

Funded by the European Union under Grant Agreement No 101096056. Views and opinions expressed are however those of the author(s) only and do not necessarily reflect those of the European Union or CINEA. Neither the European Union nor the granting authority can be held responsible for them.

Funded by the European Union

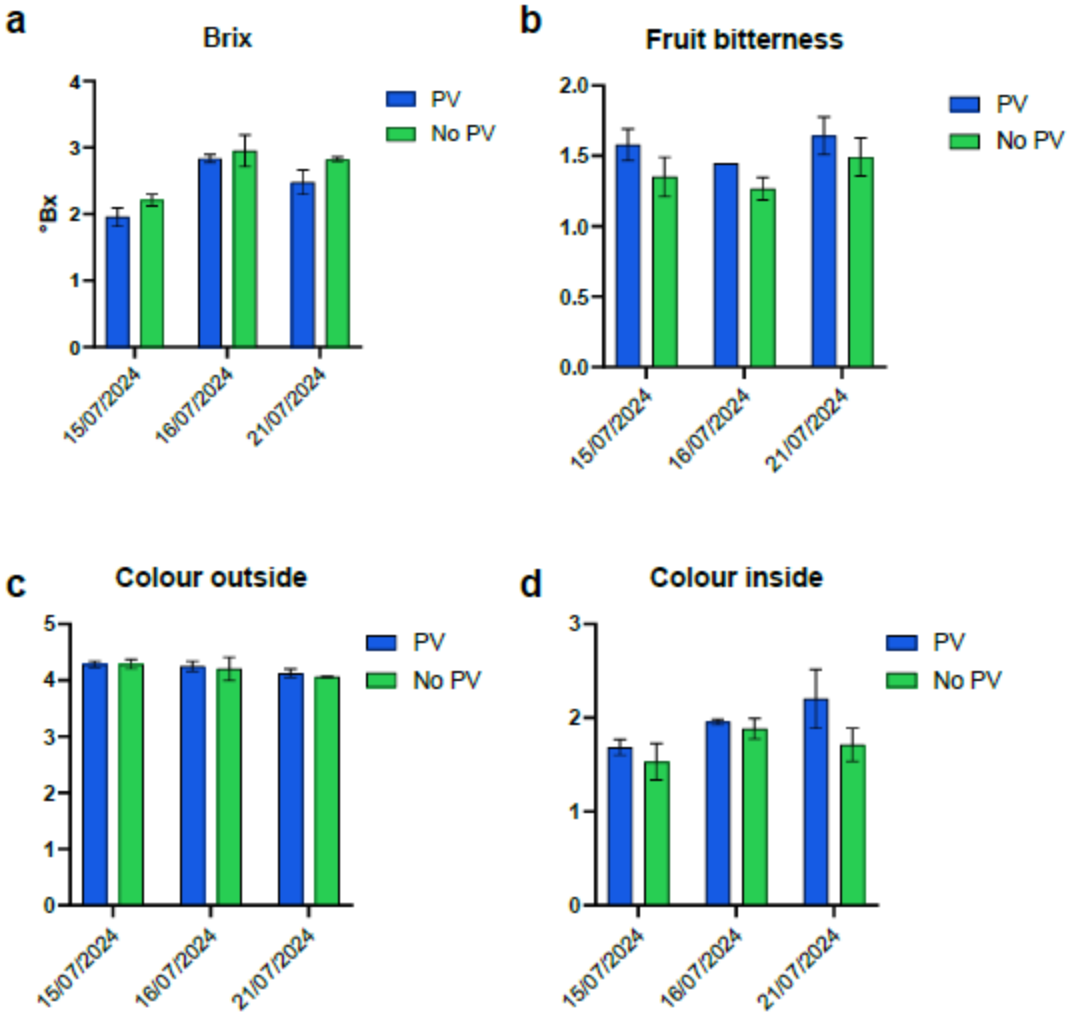

Figure 122. a. Brix measure of sugar content. b. Subjective assessment of cucumber bitterness (scale 1-5). c. Colour outside d. Colour inside the cucumber fruits (1-5 scale, grading done in comparison to colour guide; PV, with photovoltaic panels).

Statistically significant differences were not observed for colour, Brix (PV: 2.424 ± 0.4418; no PV: 2.662 ± 0.3957 for the whole season) and subjective bitterness scores (1-5 scale; PV: 1.558 ± 0.09874; no PV: 1.558 ± 0.09874 for the whole season).

In addition, external (PV: 4.218 ± 0.08544; no PV: 4.185 ± 0.1138 for the whole season) and internal (PV: 1.948 ± 0.2591; no PV: 1.709 ± 0.1764 for the whole season) colour ratings remained consistent between groups throughout the sampling dates, indicating uniform fruit appearance and ripeness.

In summary, fruit quality measures remained stable over time and were not significantly different between groups, indicating that PV conditions did not compromise fruit quality.

Funded by the European Union

Funded by the European Union under Grant Agreement No 101096056. Views and opinions expressed are however those of the author(s) only and do not necessarily reflect those of the European Union or CINEA. Neither the European Union nor the granting authority can be held responsible for them.

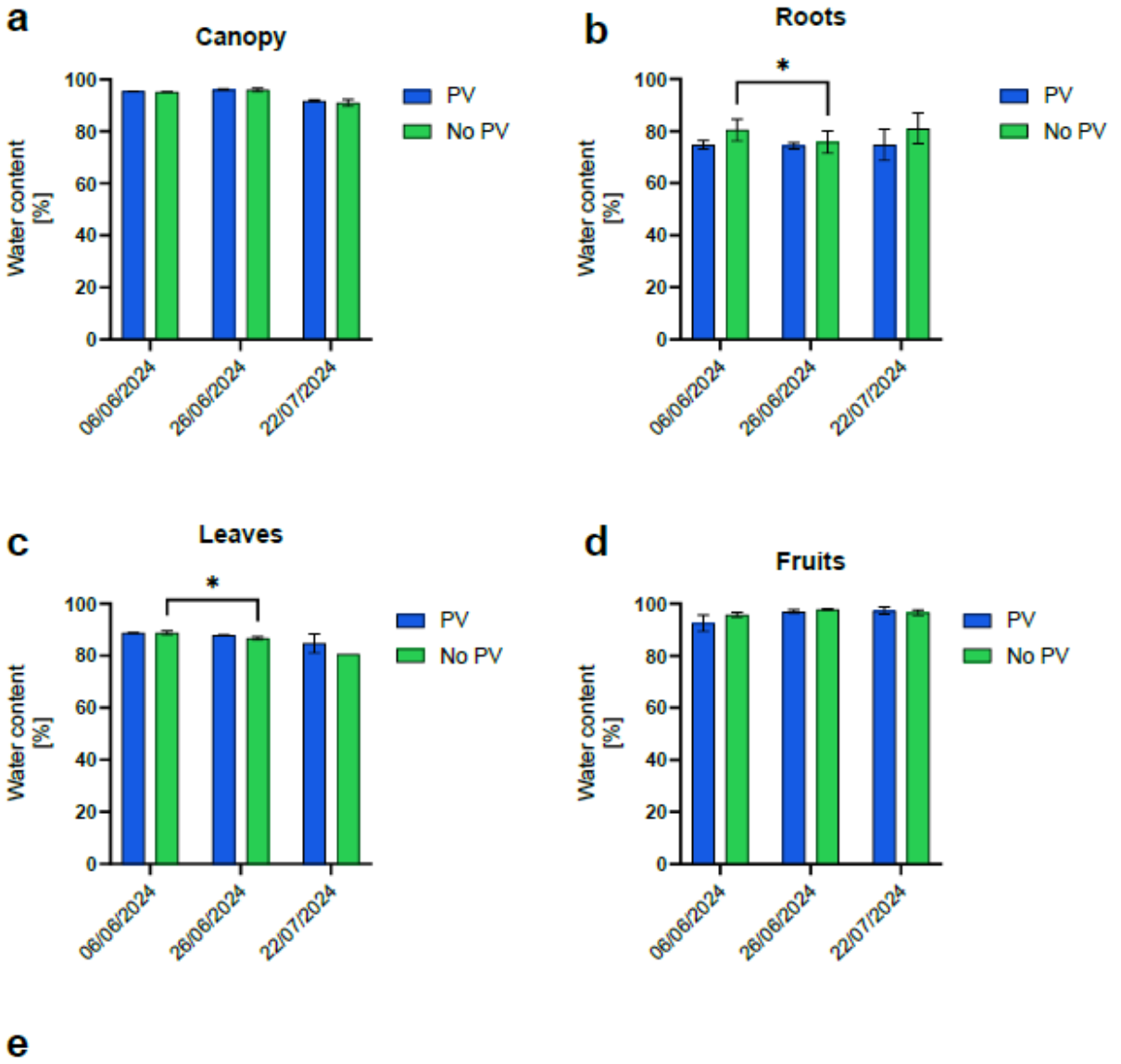

e

	Canopy [%]	Roots [%]	Leaves [%]	Fruits [%]
PV	94.4 ± 2.342	74.69 ± 0.2232	87.1 ± 2.102	95.65 ± 2.672
No PV	94.01 ± 2.671	79.13 ± 2.819	85.37 ± 4.216	96.73 ± 1.061

Figure 123. Relative water content of cucumber plants in (a) the canopy (stems and flowers), (b) roots, (c) leaves, and (d) cucumber fruits. e. Mean ± SD of the relative water content calculated over the whole season (*, $p \leq 0.05$; PV, with photovoltaic panels).

Funded by the European Union under Grant Agreement No 101096056. Views and opinions expressed are however those of the author(s) only and do not necessarily reflect those of the European Union or CINEA. Neither the European Union nor the granting authority can be held responsible for them.

Across all plant parts, significant differences were not observed in the water content of plants grown under PV panels versus those grown without (Figure 123). A two-way ANOVA was used to determine the differences between groups and over time.

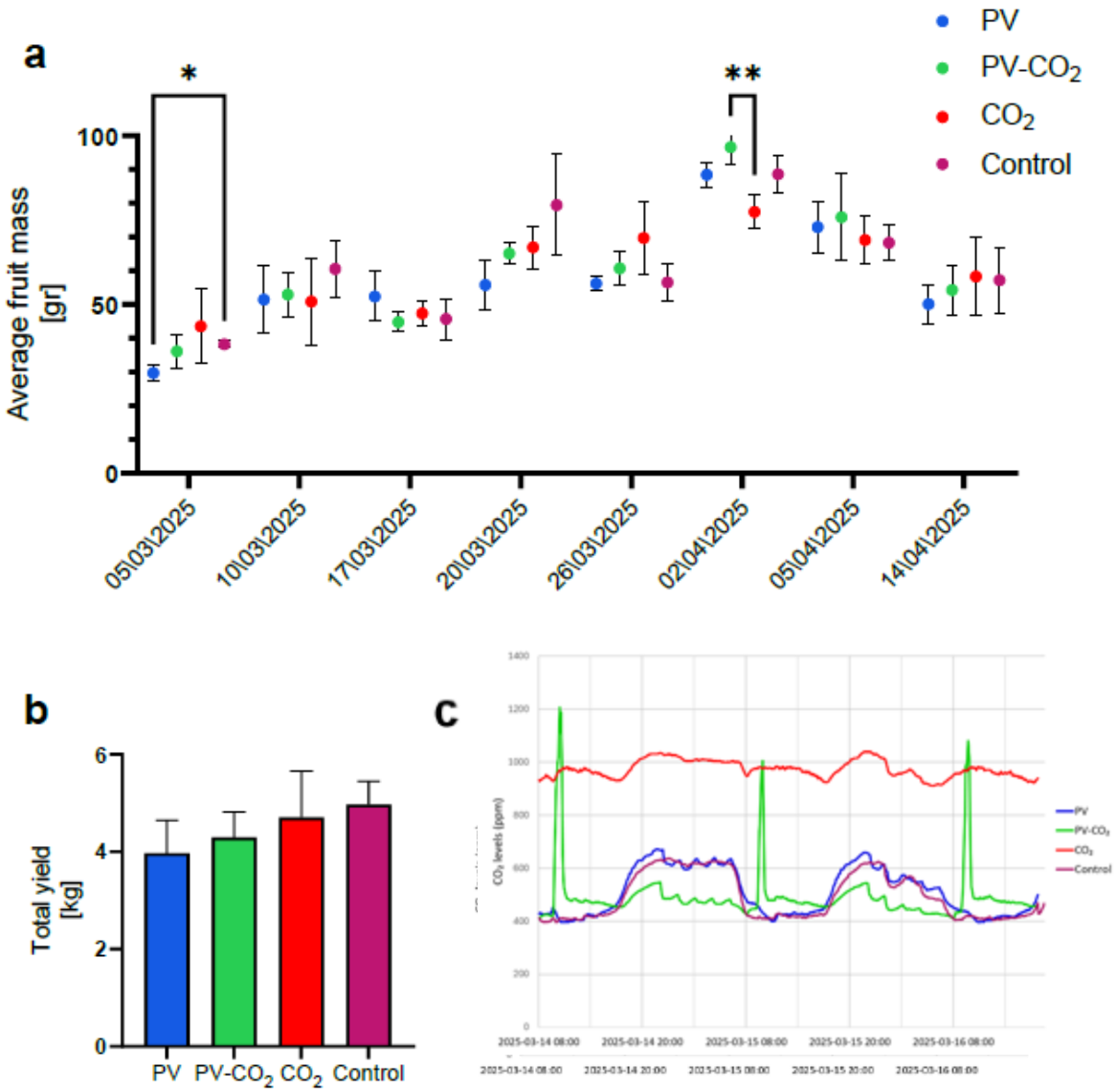

Figure 124. a. Average fruit mass for PV and No-PV greenhouses. b. Total yield. c. CO_2 levels in each greenhouse for 2-3 representative days (*, $p \leq 0.05$; **, $p \leq 0.01$; PV, with photovoltaic panels; PV-CO_2, with PV & CO_2 enrichment; CO_2, without PV but with CO_2; Control, neither PVs nor CO_2).

Funded by the European Union

Funded by the European Union under Grant Agreement No 101096056. Views and opinions expressed are however those of the author(s) only and do not necessarily reflect those of the European Union or CINEA. Neither the European Union nor the granting authority can be held responsible for them.

Experiment 2

Cucumber seedlings (Kingstar, commercial variety) were transplanted on January 22, 2025. Ventilators were added to all greenhouses. CO_2 from cylinders was distributed to the plants via repurposed drip pipes. CO_2 administration took place during daylight hours (8 am - 4 pm) until April, whereupon ventilation was limited to 7 - 9am due to ventilation requirements. There were 4 treatment groups: greenhouse with PV panels installed but no CO_2 enrichment (PV), greenhouse with PV and CO_2 enrichment (PV-CO_2), greenhouse without PVs but with CO_2 (CO_2) and a control greenhouse with neither PVs nor CO_2 enrichment (Control).

Average fruit mass varied over time among treatments (Figure 124a). Significant differences were observed on 05/03/2025 and 02/04/2025, but none of the treatment groups consistently outperformed the others. At other time points, average fruit mass values overlapped among all groups, showing similar growth patterns across the season. Mixed effects analysis (REML) was employed to determine a statistical significance.

Comparison of total yield per greenhouse was conducted via Friedman test (PV: median 3.88, IQR 1.26; PV–CO_2: median 4.18, IQR 0.98; CO_2: median 4.36, IQR 1.65; Control: median 4.94, IQR 0.88). Cumulative yield over the season did not differ significantly among treatments (Figure 124b), although the control greenhouses performed slightly better than those with PVs.

In general, productivity was not significantly affected by either PV coverage or CO_2 supplementation. The similarity in cumulative yield across treatments suggests that PV installation and moderate CO_2 enrichment are compatible with stable cucumber production, without detrimental effects on total output or fruit size across the growing period.

It is important to note that our greenhouses are not sealed environments, and therefore, there was free gaseous exchange with the external environment. As a result, it was very difficult to regulate CO_2 levels. Figure 124c shows the fluctuations of CO_2 levels within each greenhouse over 2-3 days mid-March. It is evident that, while the CO_2-treated greenhouse managed to maintain elevated levels of CO_2, the PV-CO_2 greenhouse did not. Rather, there were large spikes in CO_2 that rapidly reverted to normal levels. In spite of this, the CO_2-only greenhouse did not show an advantage over the other groups. Furthermore, CO_2 enrichment can be a costly endeavour, as can sealing the greenhouses for farmers who do not already have this setup, suggesting that this is not a financially justifiable option in a Mediterranean climate.

Funded by the European Union under Grant Agreement No 101096056. Views and opinions expressed are however those of the author(s) only and do not necessarily reflect those of the European Union or CINEA. Neither the European Union nor the granting authority can be held responsible for them.

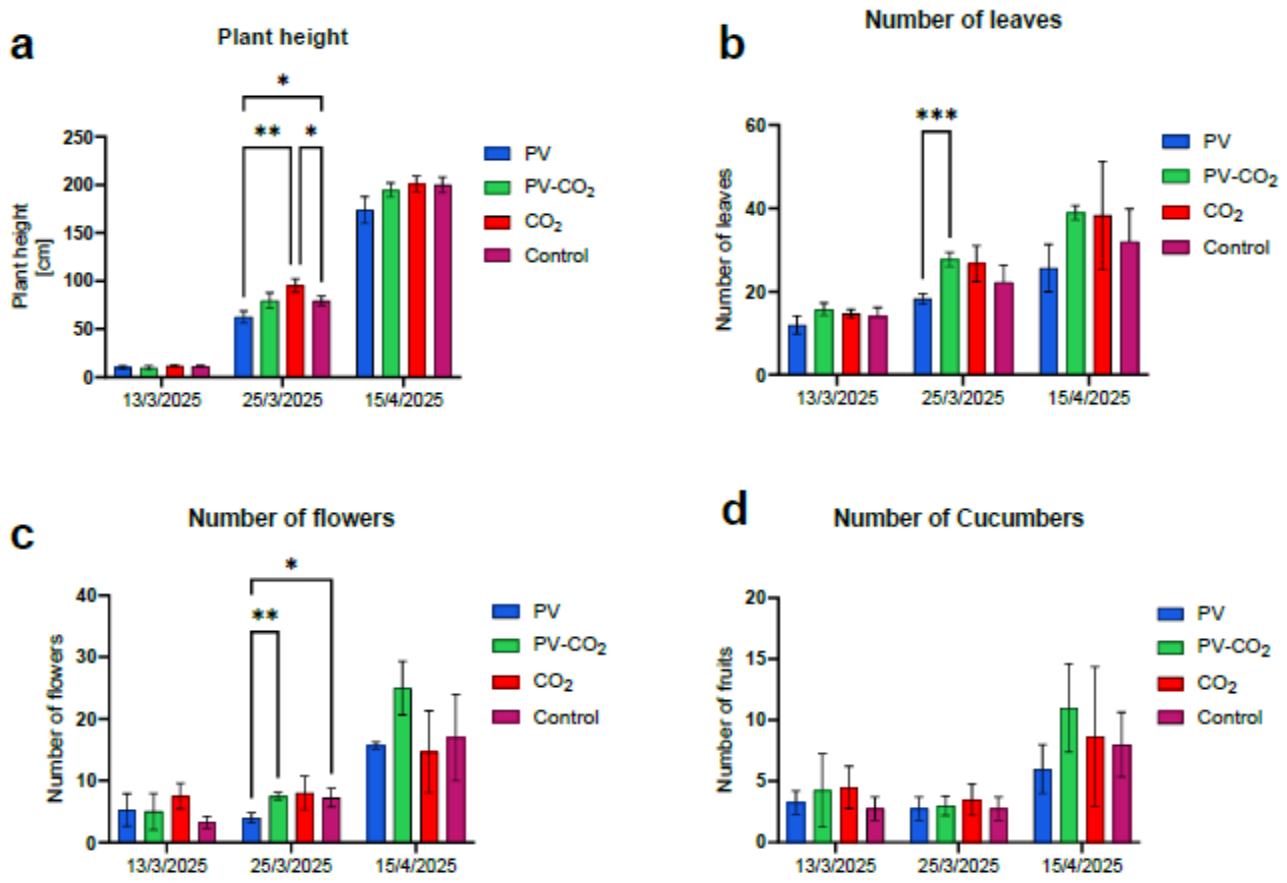

Figure 125. a. Plant height; b. stem diameter; c. number of leaves; d. number of flowers; e. number of fruits (*, $p \leq 0.05$; **, $p \leq 0.01$; ***, $p \leq 0.001$. PV, with photovoltaic panels; PV-CO_2, with PV & CO_2 enrichment; CO_2, without PV but with CO_2; Control, neither PVs nor CO_2).

Plant growth parameters were measured at the beginning of the season, mid-season, and at the end (Figure 125). At the early measurement (13/03/2025), all groups showed comparable plant height, leaf number, flower count, and fruit number. By mid-season, significant differences emerged, with CO_2 - treated plants were taller than the non-treated plants and produced more leaves and flowers. By the final measurement, these differences evened out to a certain extent. This indicates that CO_2 enrichment may pose an advantage early in the season, but these effects seem to be transient. The number of cucumbers did not differ significantly among treatments at any time point. Statistical testing was done via the mixed effects model (REML).

Funded by the European Union under Grant Agreement No 101096056. Views and opinions expressed are however those of the author(s) only and do not necessarily reflect those of the European Union or CINEA. Neither the European Union nor the granting authority can be held responsible for them.

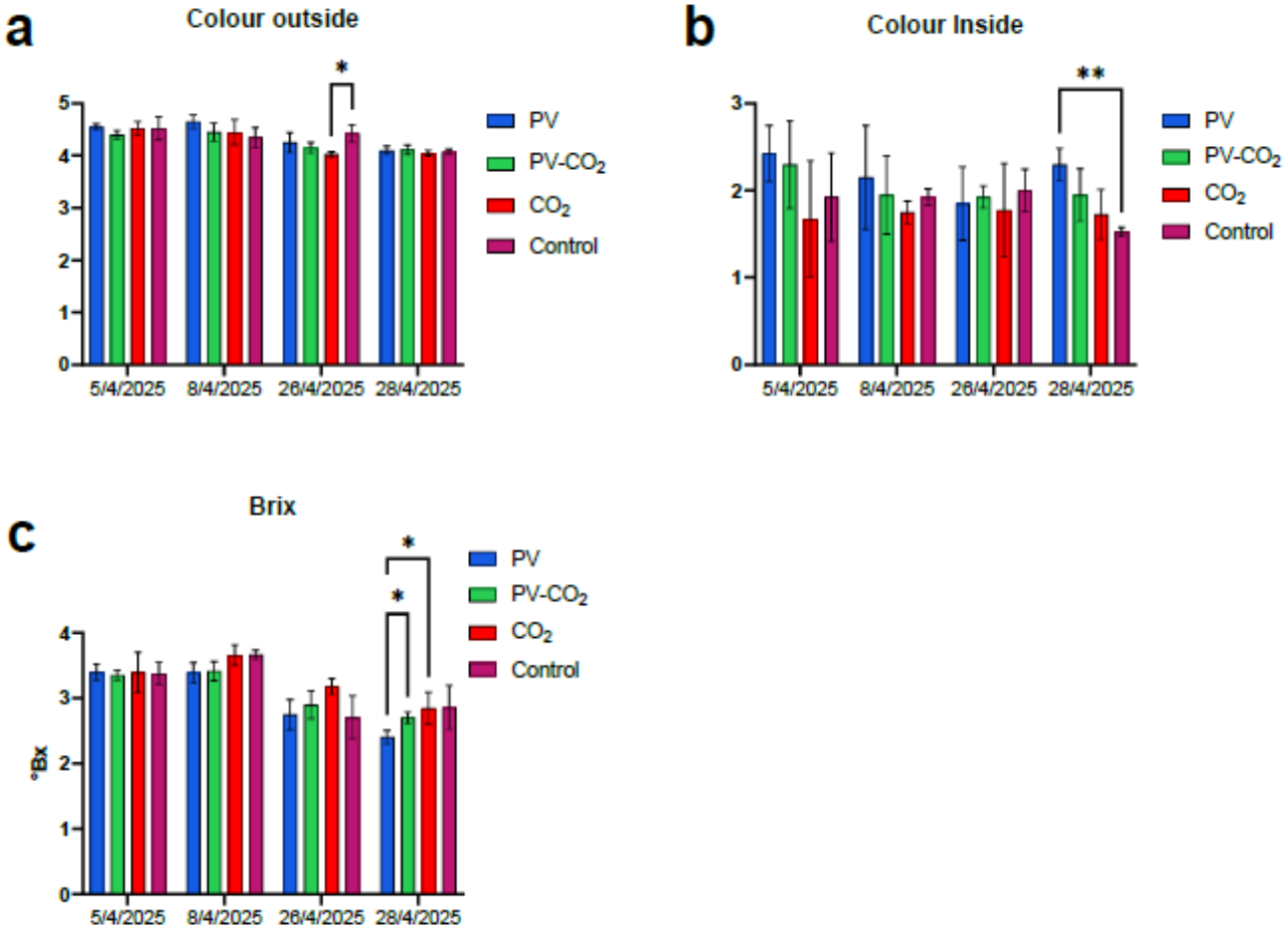

Figure 126. Colour outside (a) and inside (b) the cucumber fruits (1-5 scale, grading in comparison to colour guide). c. Sugar content of fruits by Brix (*, $p \leq 0.05$; **, $p \leq 0.01$. PV, with photovoltaic panels; PV-CO_2, with PV & CO_2 enrichment; CO_2, without PV but with CO_2; Control, neither PVs nor CO_2).

Two-way ANOVA was used to test differences in cucumber quality between groups and over time. For external and internal colour, the groups performed similarly with the exception of specific sampling dates, but no consistent effects were evident across the measurement period (Figure 126a, b). Plants in the CO_2-enriched greenhouse slightly outperformed the PV-incorporating greenhouses in Brix measurements, with the difference becoming significant at the final sampling.

Funded by the European Union under Grant Agreement No 101096056. Views and opinions expressed are however those of the author(s) only and do not necessarily reflect those of the European Union or CINEA. Neither the European Union nor the granting authority can be held responsible for them.

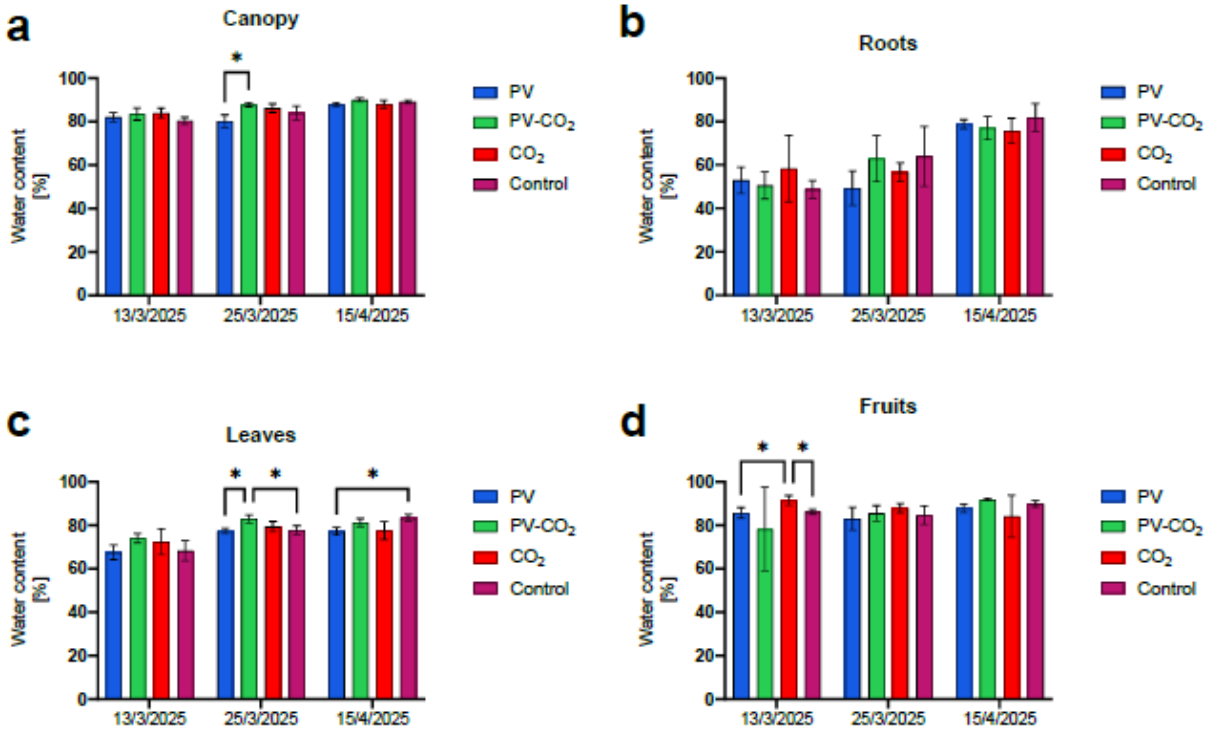

e

	Canopy [%]	Roots [%]	Leaves [%]	Fruits [%]
PV	83.4 ± 3.987	60.36 ± 16.08	74.05 ± 5.618	85.52 ± 2.466
PV-CO_2	87.11 ± 3.269	63.5 ± 13.24	79.4 ± 4.717	85.2 ± 6.82
CO_2	86.06 ± 2.009	63.6 ± 10.56	76.5 ± 3.548	87.79 ± 3.676
Control	84.5 ± 4.428	64.86 ± 16.56	76.47 ± 7.665	86.89 ± 2.697

Figure 127. Percentage of water in (a) the canopy (stems and flowers); (b) roots; (c) leaves; (d) fruits. e. Mean ± SD of these parameters calculated over the whole season (*p ≤ 0.05. PV, with photovoltaic panels; PV-CO_2, with PV & CO_2 enrichment; CO_2, without PV but with CO_2; Control, neither PVs nor CO_2).

Mixed-effects (REML) analysis revealed transient differences in water content between treatments (Figure 127), which does not seem to indicate an advantage to any particular treatment.

In all figures, only statistical differences between groups at each sampling are shown, statistically significant differences within groups over time are not shown but are available upon request.

Experiment 3

Bell pepper (*Capsicum annuum*, Top 103, commercial variety) seedlings were transplanted in growbags on June 30, 2024. CO_2 enrichment was not applicable in this experiment due to ventilation requirements; therefore, 2 greenhouses were used in this experiment, one containing sun-tracking PV modules and the other without (PV) and the other without (No PV). Shading nets were added to the greenhouse without PV installations, as per regional standard practices (30%).

Funded by the European Union

Funded by the European Union under Grant Agreement No 101096056. Views and opinions expressed are however those of the author(s) only and do not necessarily reflect those of the European Union or CINEA. Neither the European Union nor the granting authority can be held responsible for them.

Two-way ANOVA to assess differences between groups over time was used for all measurements other than cumulative yield, where a Mann-Whitney U test was employed. In the figures, only statistically significant differences between groups were indicated and discussed, not differences over time, those are available upon request.

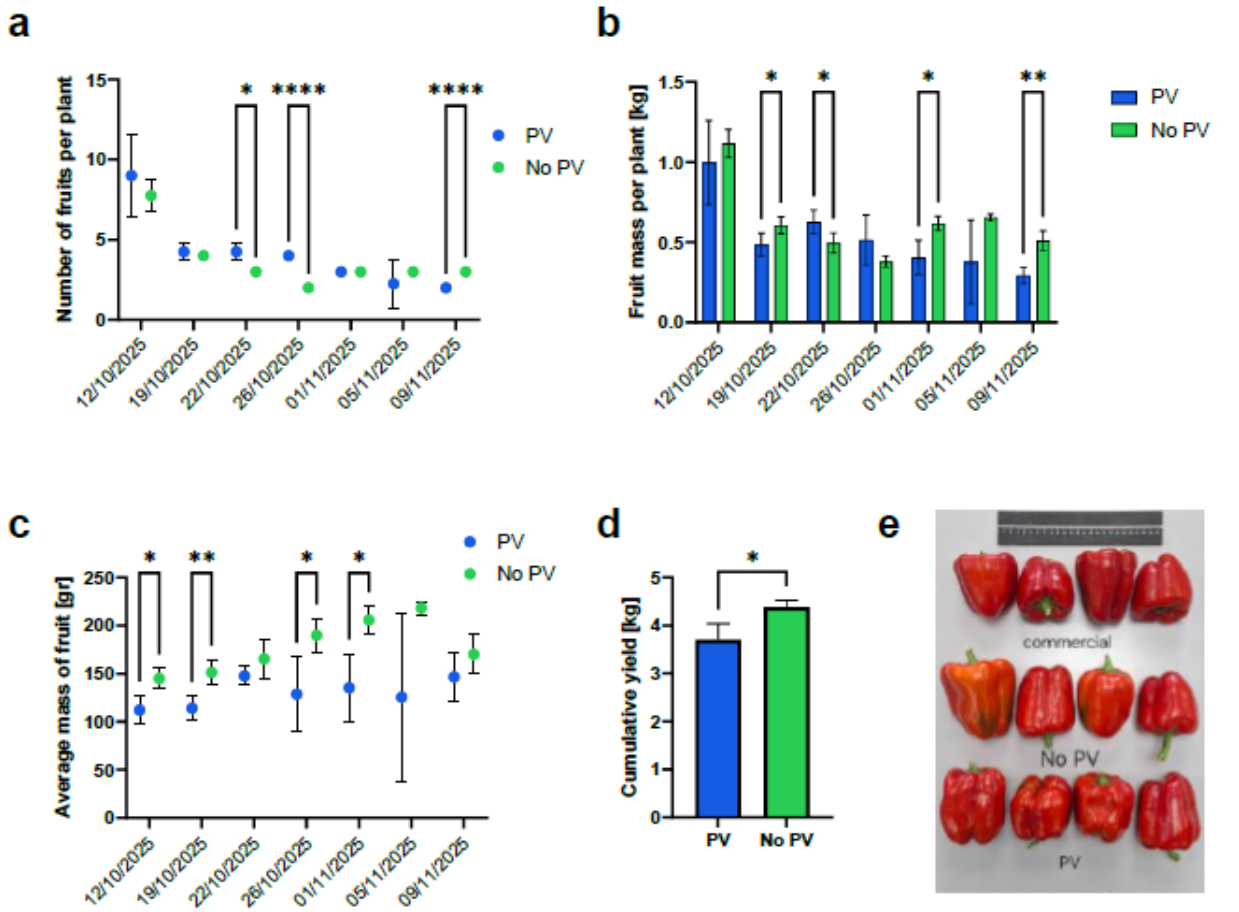

Figure 128. a. Average fruit mass over time for PV and No-PV greenhouses. b. Total fruit mass per plant per harvest. c. Average mass of individual fruits per harvest. d. Cumulative yield. e. qualitative comparison with commercial fruits (*, $p \leq 0.05$; **, $p \leq 0.01$; ****, $p \leq 0.0001$; PV, with photovoltaic panels).

Although the number of bell peppers harvested per plant under PV panels (4.12 ± 2.35) was generally comparable to and slightly higher than that of the control greenhouse (3.68 ± 1.89) (Figure 128a), the average mass of individual bell peppers and consequently the fruit mass per plant were higher in the control greenhouse (130 ± 14.21 gr and 0.53 ± 23 kg, respectively) than in the PV-greenhouse (177.90 ± 27.52 and 0.63 ± 0.24, respectively) (Figure 128b, c). Importantly, bell peppers were harvested once they achieved red colouring, rather than a certain size. Therefore, our results indicate that, under PV panels, bell peppers transitioned from green to red faster than without PV panels. Ultimately, the cumulative yield in the PV greenhouse (3.70 ± 0.34) was significantly, though moderately, lower than that of the No-PV greenhouse (4.38 ± 0.15), with a 16% decrease in the presence of PV panels (Figure 128d).

Funded by the European Union under Grant Agreement No 101096056. Views and opinions expressed are however those of the author(s) only and do not necessarily reflect those of the European Union or CINEA. Neither the European Union nor the granting authority can be held responsible for them.

Qualitatively, we compared the colour of similarly-sized bell peppers grown with PVs, without PVs, and those acquired from a commercial greenhouse (Figure 128e), while the colour of the fruits harvested from the PV greenhouse was comparable to the commercial bell peppers, the No-PV bell peppers tended to be slightly more orange in colour and contained traces of green.

Studies indicate that light and temperature can influence the maturation of bell peppers (Kader, 1997; Yoshida et al., 2014). It is possible that due to the PV panels being open for parts of the day, the bell peppers receive greater light exposure than the shaded greenhouse, thereby promoting fruit maturation. This opens the possibility to tailor the functionality of the PV panels in such a way that optimises the rate of maturation of bell peppers.

Experiment 4

Tomato (*Solanum lycopersicum,* Magi) seedlings were transplanted in growbags on June 30, 2024. This experiment is similar to Experiment 3, CO_2 enrichment was not applied, and there were 2 experimental groups in 2 greenhouses, one containing sun-tracking PV modules (PV) and the other without (No PV) Shading nets were added to the greenhouse without PV installations, as per regional standard practices.

Two-way ANOVA to assess differences between groups over time was used for all measurements other than cumulative yield, where a Mann-Whitney U test was employed. In the figures, only statistically significant differences between groups were indicated and discussed, not differences over time, those are available upon request.

Funded by the European Union under Grant Agreement No 101096056. Views and opinions expressed are however those of the author(s) only and do not necessarily reflect those of the European Union or CINEA. Neither the European Union nor the granting authority can be held responsible for them.

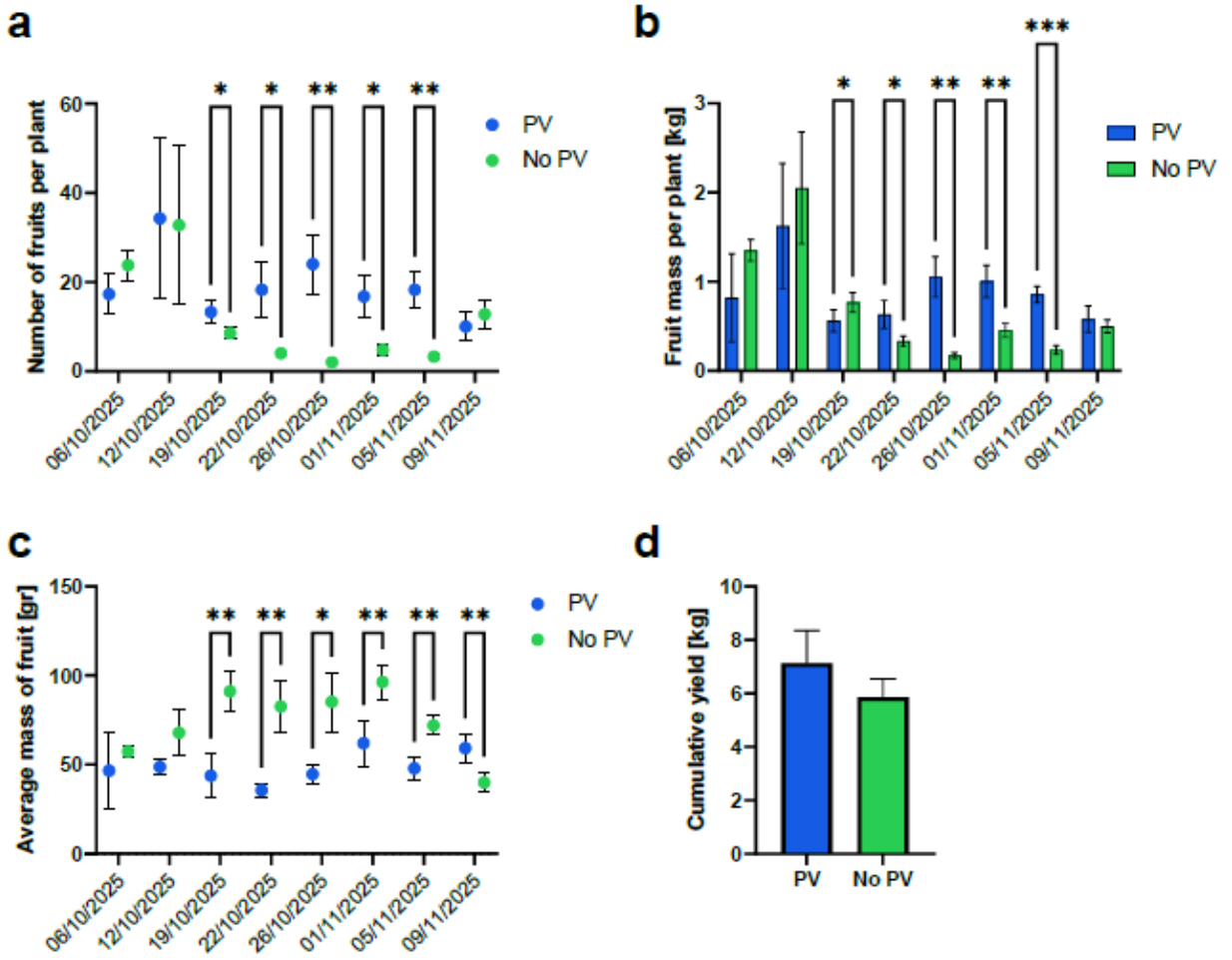

Figure 129. a. Average fruit mass over time for PV and No-PV greenhouses. b. Total mass of fruit harvested per plant per harvest. c. Average mass of individual tomatoes. d. Total seasonal yield (*, $p \leq 0.05$; **, $p \leq 0.01$; PV, with photovoltaic panels).

The PV-installed greenhouse consistently produced a larger number (19 ± 7.38) and fruit mass per plant (0.89 ± 0.35 kg) of tomatoes than the control greenhouse (11.47 ± 11.16 and 0.73 ± 0.65 kg, respectively) (Figure 129a,b). Interestingly, mid-season, the greenhouse without PVs produced heavier individual tomatoes (74.03 ± 18.76 gr) than the PV group (48.51 ± 8.51 gr), an effect that seemed to be reversed towards the end of the season (Figure 129c).

The cumulative yield under PV panels (7.13 ± 1.22 kg) was slightly, though not significantly, higher than the control (5.86 ± 0.68 kg) (Figure 129d) by 21.6%.

Of note, early in the season (pre-harvest), technical issues resulted in the PV greenhouse not receiving irrigation [SO1] and fertilisation for a short period of time. This might have caused stress in the tomato plants resulting in a larger amount of smaller tomato fruits.

Funded by the European Union under Grant Agreement No 101096056. Views and opinions expressed are however those of the author(s) only and do not necessarily reflect those of the European Union or CINEA. Neither the European Union nor the granting authority can be held responsible for them.

Literature

Yoshida, C. H. I. E., Takahashi, M. A. S. A. A. K. I., Iwasaki, Y. A. S. U. N. A. G. A., Furuno, S. H. I. N. S. U. K. E., Matsunaga, H. I. R. O. S. H. I., & Nagata, M. A. S. A. Y. A. S. U. (2014). Factors affecting color development in sweet pepper (*Capsicum annuum* L) fruit harvested at breaker stage of mature-green fruit.
Kader, A. A. (1997, August). Fruit maturity, ripening, and quality relationships. In *International Symposium Effect of Pre-& Postharvest factors in Fruit Storage 485* (pp. 203-208).

5.2.3 Watzkendorf & Berlin

At the greenhouse location in Watzkendorf Germany, two test cycles were realised. The focus was mainly put on crop performance, quality of fruits and the turnaround of the whole system. The test greenhouses have a similar area of 600 m² and are not separated. That is why the detailed analysis of CO_2-fertilization took place at Humboldt-University with organic matter produced and also used at Watzkendorf.

Besides multiple uses of the greenhouse over the year, the main test cycles were from May-October in 2024 and 2025. The winter period was used for cleaning the facility and an early radish crop in springtime.

Table 58. Cumulated results of the tomato variety 'Orama F1' on rootstock 'Maxifort F1'.

	Crop	Growth period	Overall Yield	Loss	Irrigation	Water per Yield	Turnover	Retail price
Unit					l	l/kg	€	€/kg
No PV	Tomato	May-October	4438,5	<1% in weight	48000	10,81	17.754,00 €	4,00 €
PV-shading	Tomato	Mai-October	3911,1	<1% in weight	48000	12,27	15.644,40 €	4,00 €

Table 1 - Tomato 2024

Quality of fruits and diseases of the plants have not been an issue in comparison between the two variants. The main problem was an infection of the whole greenhouse with mildew and white fly, which forced us to terminate cultivation of the crop to prevent a further propagation of the pest population that could harm the following crops. The crop cycle would have gone normally until the end of November.

The main difference between the two greenhouses was the growth rate of the plants and the rate of fruit ripening, as there was a significantly lower rate in the variant with PV-shading. That resulted in a lower total yield. As the ripening of fruits took time, we couldn't monitor a connection between times with lower or higher global radiation.

Table 59. Cumulated results of the Mini-cucumber 'Bettanis F1' on rootstock 'Becada F1' in 2025.

	Crop	Growth period	Overall Yield	Loss	Irrigation	Water per Yield	Turnover	Retail price
Unit			kg		l	l/kg	€	€/kg
No-PV	Cucumber	May-October	7928	<1% in weight	60000	7,57	25.766,00 €	3,25 €
PV-shading	Cucumber	May-October	7126	<1% in weight	60000	8,42	23.159,50 €	3,25 €

Table 2 – Cucumber 2025

Funded by the European Union

Funded by the European Union under Grant Agreement No 101096056. Views and opinions expressed are however those of the author(s) only and do not necessarily reflect those of the European Union or CINEA. Neither the European Union nor the granting authority can be held responsible for them.

Between the two trial greenhouses, the data showed a difference in growth rate and therefore the number of harvested cucumbers per plant resulted in a difference in total yield. The shaded cucumber crop had a lower number of burnt heads in times of high radiation but also a slower growth rate. A difference in mildew infection could not be observed. The better plant health (burnt heads) of the cucumbers in the PV-trial greenhouse couldn't compensate for the slower growth and therefore couldn't reach the total yield of the control greenhouse.

Discussion: Both years had a reduction of yield mostly due to shading by the panels. On average there was a financial loss of 2358.- € per year for the main crop in summer season in comparison to the control area. In Table 60 the costs for the installation of the PV system are shown. They sum up to 13.567.- € for the system with 12 KWp performance.

Table 60. Costs for the installation of the PV system.

Cost position	Total costs	Percentage of costs
Staff	4.637 €	34,18%
Inverter	4.163 €	30,68%
Steel pipes	2.153 €	15,87%
Holders & actuator	500 €	3,69%
Small parts	434 €	3,20%
Panels	1.680 €	12,38%

A normal depreciation for PV-systems in Germany would be linear over 20 years, for an indoor system in a greenhouse like that in Watzkendorf, it would take 15 years as depreciation time. The yearly write-off for a capital paid system (no credit) would sum up to 905.- € plus 100.- € yearly for maintenance and cleaning of the panels.

On the other hand, there is the electrical yield, yearly approximately 12,000 KWh that can be fed in the net or used by the company. At the moment, the feed-in tariff for a full feed-in system is at 10.45 ct/KWh. The purchase price for electricity above 10,000 kwh per year is at 27 ct/KWh. Therefore, a large percentage of self-produced electricity that is used in the company is more profitable than feeding in. The total financial gain of installing the system is 3,240.- € / year, whereas the total cost (yield lost + depreciation + maintenance) is about 3,363.- € / year, 4% higher than the gain.

Unfortunately, even the full use of 12,000 KWh, cannot compensate for the yield loss, maintenance and installation costs for the system in northern Germany/Watzkendorf. Due to the light conditions and the location, shading is just needed on some days from June to August and electrical yield is different to southern locations like Italy or Israel.

As the financial difference between costs and electrical plus vegetable yield is not immense, there are some options to optimize to get to an even outcome and benefit from the non-monetary benefits like independence of the electricity market and advantages in marketing by promoting renewables.

Funded by the European Union

Funded by the European Union under Grant Agreement No 101096056. Views and opinions expressed are however those of the author(s) only and do not necessarily reflect those of the European Union or CINEA. Neither the European Union nor the granting authority can be held responsible for them.

The biggest cost position is taken by staff for installation. There have been two engineers on site, who were needed to adjust the installation of the prototype and detect and correct bugs that are related to the early stage of development of the system. For a second system and with experience-based supervision, the costs for staff could easily be halved. Inverter prices in Germany have been halved over the last two years. The holders and actuators even have been adjusted and optimized and have been custom-built for the project's prototype. In Table 61 the costs for a market-ready system are shown, they can be reduced down to a sum of 9,494.69 € for the same size.

Table 61. The estimated costs for a market-ready system.

Cost position	Total costs	Percentage of costs
Staff	2.827 €	29,77%
Inverter	2.000 €	21,06%
Steel pipes	2.153 €	22,68%
Holders & actuator	400 €	4,21%
Small parts	434 €	4,57%
Panels	1.680 €	17,69%

This results in a lowered depreciation over ten years of 632.98 € per year plus 100.- € maintenance costs. Together with the yield loss due to shading in darker growing seasons, the additional costs add up to 3091.- € for 600 m², 12 KWp performance installed in 2025. Quantity effects like lower prices for pipes or larger inverters for larger systems are not noticed in this calculation.

Right now, Watzkendorf (Germany) is on the edge of profitability of the system in low light conditions. If some trends intensify, like the drop of PV-panel prices, durability of PV-systems, rising energy costs per KWh and increase of sunshine hours in the summertime, the profitability of an indoor PV-system will also rise in northern regions.

5.2.4 Hydroponic Greenhouse Cultivation at University of Thessaly

UTH conducted four experiments to evaluate the performance of the PV modules and CO_2 as mentioned in chapter 4.1.

Experiment A

Cucumber seedlings (*Cucumis sativus* cv. Columbia) were obtained in rockwool cubes (Grodan International, Netherlands). Three seedlings were transplanted on the rockwool slabs on September 12, 2024 resulting in a plant density of 1.8 plants m^{-2}. The experiment lasted a total of 91 days. In Experiment A, as shown in Table 18, four treatments were applied in four different greenhouse compartments. CO_2 enrichment started the 62th day after transplantation (DAT) and ended on DAT 91.

Funded by the European Union under Grant Agreement No 101096056. Views and opinions expressed are however those of the author(s) only and do not necessarily reflect those of the European Union or CINEA. Neither the European Union nor the granting authority can be held responsible for them.

Experiment B

Similarly, to Experiment A, Experiment B, included the same experimental design and treatments. The experiment was set from January 16 to April 3, 2025. The CO_2 enrichment started on DAT 0 and ended at DAT 55.

Experiment C

Experiment C was conducted from May 24 to June 12, 2025. In this experiment, cucumber seedlings were also used following the similar process to Experiment A & B. However, in this case, only three treatments were evaluated, as shown in Table 18, since during spring/summer periods the enrichment of a compartment with CO_2 is not feasible as natural ventilation is required. Therefore, in Experiment C, a solar-tracking and an opposite to solar-tracking approach were evaluated to assess their effect on plant growth and microclimate conditions.

Experiment D

Two different lettuce cultivars *Lactuca sativa* cv. Green Towers and *Lactuca sativa* cv. Sanguine were transplanted on rockwool slabs on September, 19, 2025. Three greenhouse compartments were used in this case. This experiment aimed at investigating the effect of solar-tracking PVs and fixed PVs on plant growth and microclimate alternations. Four plants were transplanted per slab. The plant density was the same for both cultivars and was 2.5 plants m^{-2}. The experiment lasted a total of 31 days.

Measurements

Experiments A, B, C

Measurements of plant growth characteristics such as plant height, number of leaves, and number of fruits were collected weekly from five randomly selected plants per treatment. In order to assess biomass accumulation and leaf area index (LAI), four destructive measurements were performed throughout the experiment. The first destructive measurement was conducted on Day 0, followed by additional measurements at monthly intervals. During each destructive measurement, the plants were separated into leaves, stems, and fruits to determine both fresh and dry biomass for each plant component as well as LAI. Dry biomass was determined after drying samples in a drying oven at 70°C. Leaf area per plant was quantified using the ImageJ software, and the LAI was calculated by multiplying the leaf area of a plant by the plant density.

The chlorophyll content index (CCI) was determined using an Opti-Science sensor, taking readings directly on the leaf surface (CCM 200, Opti-Science, Hudson, NH, USA). Leaf gas exchange measurements were conducted during the cultivation period in order to examine the effects of PV and CO_2 fertilization on plant photosynthesis, transpiration, and stomatal conductance. The measurements were conducted every two weeks throughout the cultivation period, using a portable photosynthesis instrument (LI-6400 XT, LI-COR, Lincoln, NE, USA). In Experiment A, a trial to assess the effect of CO_2 enrichment on plant physiological

Funded by the European Union

Funded by the European Union under Grant Agreement No 101096056. Views and opinions expressed are however those of the author(s) only and do not necessarily reflect those of the European Union or CINEA. Neither the European Union nor the granting authority can be held responsible for them.

parameters was performed. In total three measurements of the photosynthetic rate were taken; one before CO_2 enrichment, one during the enrichment, and one after the enrichment.

Experiment D

Similarly, to Experiments A, B, C, four destructive measurements were performed throughout the experimental session. Fresh and dry weight were also measured following the protocols reported in the previous experiments. In addition, the photochemical reflectance index (PRI) was measured with the handheld reflectance meter, PlantPen PRI120 (Photon Systems Instruments, Drásov, Czech Republic), which uses an internal dual-wavelength light source emitting 531 and 570 nm to provide the PRI values (Mourantian et al., 2025).

Calculations

Plant transpiration (L m^{-2}) was calculated by subtracting the total volumes of applied and drained nutrient solutions over the cultivation period by the cultivated area. Water use efficiency (WUE, kg m^{-3}) was calculated as the ratio of total fruit yield (kg m^{-2}) to total volume of the applied nutrient solution (m^3 m^{-2}). Similarly, fertiliser use efficiency (FUE) was determined by dividing total fruit yield (kg m^{-2}) by the total amount (kg m^{-2}) of fertilisers supplied to the crop. The daily light integral (DLI) represents the total flux of photosynthetically active radiation (PAR; 400–700 nm) received by a unit surface area of crop canopy over a 24-hour period, and is expressed in mol m^{-2} day^{-1}. For each treatment, weekly cumulative DLI was determined by integrating the daily values across consecutive seven-day intervals.

Effect of PVs on Plant growth

Table 62 summarizes plant growth characteristics across treatments and experimental periods. In Experiment A, plants grown under PV-Tracking and PV-Tracking + CO_2 showed significantly greater height (513.8 and 522.8 cm, respectively) compared with the non–PV-shaded control and CO_2 treatments. Leaf production followed a similar pattern, with PV-Tracking + CO_2 plants producing 6.2% more leaves than the non–PV-shaded treatments. In contrast, LAI responded primarily to CO_2 enrichment, with the CO_2 treatment exhibiting higher LAI by 18% than all other treatments, indicating enhanced canopy development.

In Experiment B, the synergistic effect of PV and CO_2 contributed to the record statistically higher stem elongation compared to the other treatments (246.3±3.53 cm), while the CO_2-only treatment consistently showed the lowest plant height. Leaf number differences were less pronounced. Plants of the CO_2 treatment produced significantly fewer leaves than the control but did not differ statistically from PV-Tracking or PV-Tracking + CO_2 treatments. Despite reduced height and leaf number, LAI in the CO_2 treatment was comparable to the other treatments.

Funded by the European Union under Grant Agreement No 101096056. Views and opinions expressed are however those of the author(s) only and do not necessarily reflect those of the European Union or CINEA. Neither the European Union nor the granting authority can be held responsible for them.

Table 62. Mean plant height (cm, ± SE), leaf count (per plant, ± SE), and LAI (m^2 m^{-2}, ± SE), during the three experimental periods.

	Treatments	Height [cm]	Leaf count [plant $^{-1}$]	LAI (m^2 m^{-2}]
Exp. A	CTRL	476.6±9.55 b	45.6±0.50 b	3.38±0.41b
	CO_2	481.0±12.63 b	45.6±0.74 b	4.19±0.06 a
	PV-Tracking	513.8±8.99 a	46.8±0.91 ab	3.41±0.05 b
	PV-Tracking + CO_2	522.8±11.23 a	48.6±0.67 a	3.54±0.09 b
Exp. B	CTRL	227.8±2.06 b	30.2±0.49 a	1.90±0.05 a
	CO_2	207.6±4.78 c	26.8±0.80 b	1.80±0.11a
	PV-Tracking	233.1±3.34 b	29.3±0.33 ab	1.97±0.10 a
	PV-Tracking + CO_2	246.3±3.53 a	29.6±0.50 ab	2.21±0.09 a
Exp. C	CTRL	361.4±4.66 b	44.2±0.37 a	2.91±0.21 b
	PV-Tracking	395.6±6.01 a	45.6±0.68 a	3.53±0.41 a
	PV-Opposite	376.2±3.84 b	45.4±1.08 a	3.48±0.62 a
Exp. D Green Towers	CTRL	-	39.3±0.48 a	-
	PV-Tracking	-	34.8±0.85 b	-
	PV-Fixed	-	35.3±1.11 b	-
Exp. D Sanguine	CTRL	-	23.0±1.35 a	-
	PV-Tracking	-	21.8±0.25 a	-
	PV-Fixed	-	21.2±0.80 a	-

Different letters (a, b, c) indicate statistically significant differences between treatments ($p < 0.05$).

In Experiment C, PV-Opposite plants exhibited significantly lower height, yet leaf number remained similar to the control and PV-Tracking treatments, while LAI matched only the PV-Tracking treatment. Notably, the PV-shaded treatments produced the highest LAI values overall.

Across the experimental periods, PV shading and CO_2 enrichment exhibited distinct influences on canopy development (Table 66). PV shading generally promoted stem elongation, with significantly taller plants recorded in PV-Tracking treatments across Experiments 1 and 3, and in the PV-Tracking + CO_2 treatment in Experiment 2. Leaf production increased only in Experiment 1, where PV-Tracking + CO_2 plants produced significantly more leaves than the non–PV-shaded treatments, while no consistent differences were observed in Experiments 2 and 3. CO_2 enrichment significantly enhanced LAI, particularly in Experiment 1, where the CO_2 treatment exhibited an ~18% increase compared with all other treatments. Similar trends, though less pronounced, were evident in Experiments 2 and 3, indicating that CO_2 fertilization primarily stimulated canopy expansion through greater leaf surface development in the fall/winter period rather than changes in height or leaf number.

Effect of PVs on Photosynthetic rate and chlorophyll content

Photosynthetic rate and SPAD values are presented in Table 63. In Experiment A, crop photosynthetic rates were uniform across treatments, ranging from 10.9 to 11.6 µmol CO_2 m^{-2} s^{-1}, with no statistically significant differences observed between treatments.

Funded by the European Union

Funded by the European Union under Grant Agreement No 101096056. Views and opinions expressed are however those of the author(s) only and do not necessarily reflect those of the European Union or CINEA. Neither the European Union nor the granting authority can be held responsible for them.

Table 63. Mean photosynthetic rate (µmol m^{-2} s^{-1}, ±SE) and SPAD values (± SE) for the three experimental periods.

	Treatments	Photosynthetic rate [µmol m^{-2} s^{-1}]	SPAD
Exp. A	CTRL	11.1±0.74 a	42.3±1.67 a
	CO_2	11.6±0.52 a	42.7±2.24 a
	PV-Tracking	10.9±0.60 a	42.3±2.64 a
	PV-Tracking + CO_2	11.4±0.82 a	42.8±3.84 a
Exp. B	CTRL	10.5±0.26 b	51.2±0.55 a
	CO_2	11.4±0.28 a	50.7±1.43 a
	PV-Tracking	10.6±0.27 b	50.1±1.17 a
	PV-Tracking + CO_2	11.0±0.38 ab	54.6±1.23 a
Exp. C	CTRL	12.4±0.83 a	47.2±0.55 a
	PV-Tracking	10.4±0.35 b	45.6±1.28 a
	PV-Opposite	11.9±0.45 ab	48.2±0.65 a

Different letters (a, b) indicate statistically significant differences between treatments ($p < 0.05$).

In Experiment B, CO_2 enrichment increased photosynthetic rates in both CO_2 and PV-Tracking + CO_2 treatments compared to the CTRL and PV-Tracking treatments. In Experiment C, solar tracking significantly reduced the average photosynthetic rate in PV-Tracking treatment compared to CTRL. In contrast, PV-Opposite treatment allowed higher photosynthetic rates (11.9 ± 0.45 µmol m^{-2} s^{-1}), close to those of CTRL treatment. SPAD values presented no significant differences among the different treatments and experimental periods.

Based on the results, the differences in photosynthetic activity did not affect the chlorophyll content of the plants under different light and CO_2 concentration conditions. Overall, shading from the PV modules reduced photosynthetic rates; however, CO_2 enrichment effectively mitigated this limitation, sustaining higher photosynthetic activity across the enriched treatments, highlighting the potential of CO_2 supplementation to overcome light limitations in PV-integrated greenhouse systems.

Table 64. Photosynthetic pigment concentrations (mg g^{-1} FW, ± SE) in leaves from Experiments A and B under different treatments.

	Treatments	Car [mg g^{-1}]	Chl a [mg g^{-1}]	Chl b [mg g^{-1}]	Chl tot [mg g^{-1}]	Chl a/b
Exp. A	CTRL	0.11±0.01a	0.39±0.03a	0.19±0.02a	0.57±0.05a	2.10±0.06a
	CO_2	0.12±0.00a	0.38±0.01a	0.18±0.01a	0.56±0.01a	2.13±0.04a
	PV-Tracking	0.12±0.01a	0.43±0.02a	0.22±0.01a	0.65±0.03a	1.91±0.10a
	PV-Tracking+CO_2	0.12±0.01a	0.41±0.03a	0.20±0.02a	0.61±0.04a	2.04±0.05a
Exp. B	CTRL	0.12±0.01a	0.41±0.02a	0.21±0.02a	0.62±0.04a	2.01±0.10a
	CO_2	0.11±0.00a	0.38±0.01a	0.18±0.01a	0.56±0.02a	2.13±0.12a
	PV-Tracking	0.12±0.01a	0.43±0.03a	0.21±0.02a	0.64±0.05a	2.00±0.05a
	PV-Tracking+CO_2	0.12±0.01a	0.42±0.03a	0.20±0.02a	0.62±0.05a	2.06±0.04a

Different letters within a column indicate significant differences at $p < 0.05$.

Funded by the European Union

Funded by the European Union under Grant Agreement No 101096056. Views and opinions expressed are however those of the author(s) only and do not necessarily reflect those of the European Union or CINEA. Neither the European Union nor the granting authority can be held responsible for them.

Table 64 reports photosynthetic pigment concentrations in leaves from Experiments A and B. For all treatments and both experiments, no statistical differences were detected in carotenoids, chlorophyll a, chlorophyll b, total chlorophyll, or chlorophyll a/b ratios. Pigment composition was therefore unaffected by either CO_2 enrichment, PV-Tracking, or their combination.

Table 65. Flavonoid, phenolic compounds, nitrate content, antioxidant capacity, and carbohydrate content (fructose and glucose) in leaves from Experiments A and B under different treatments.

	Treatments	Flavonoid [g kg^{-1}]	Phenols [mg g^{-1}]	Ant. capacity [mg g^{-1}]	Fructose [mg kg^{-1}]	Glucose [mg kg^{-1}]	Nitrates [mg g^{-1}]
Exp. A	CTRL	3.1 ± 0.58a	0.2 ± 0.02a	22.1 ± 2.33a	237.9 ± 15.09a	225.9 ± 9.71a	0.6 ± 0.05b
	CO_2	2.2 ± 0.63a	0.2 ± 0.02a	27.5 ± 2.21a	249.9 ± 17.04a	202.8 ± 9.61a	0.6 ± 0.05b
	PV-Tracking	2.0 ± 0.12a	0.2 ± 0.01a	21.7 ± 1.30a	247.3 ± 2.48a	207.6 ± 13.17a	0.6 ± 0.03b
	PV-Tracking+CO_2	2.2 ± 0.07a	0.2 ± 0.01a	22.1 ± 2.06a	228.7 ± 16.25a	211.1 ± 5.96a	0.8 ± 0.04a
Exp. B	CTRL	2.4 ± 0.22a	0.2 ± 0.01a	22.5 ± 0.69a	257.6 ± 1.30a	240.3 ± 9.63a	0.6 ± 0.03a
	CO_2	2.7 ± 0.22a	0.2 ± 0.01a	25.5 ± 1.49a	248.8 ± 7.54a	215.2 ± 23.64ab	0.7 ± 0.03a
	PV-Tracking	2.5 ± 0.12a	0.2 ± 0.01a	21.5 ± 1.76a	229.0 ± 8.44a	219.5 ± 8.55ab	0.7 ± 0.03a
	PV-Tracking+CO_2	2.3 ± 0.19a	0.2 ± 0.01a	21.3 ± 1.11a	222.1 ± 4.45a	197.3 ± 1.18b	0.9 ± 0.06a

Different letters within a column indicate significant differences at $p < 0.05$.

Table 65 shows data on flavonoids, phenolic compounds, antioxidant capacity, sugars, and nitrate content. Most parameters, including flavonoids, phenols, antioxidant capacity, and fructose, did not differ significantly among treatments in either experiment. In Experiment B, leaves of the PV-Tracking + CO_2 treatment accumulated significantly less glucose (197.3 ± 1.18 mg kg^{-1}) than the control treatment (240.3 ± 9.63 mg kg^{-1}).

The only parameter with consistent significant variation was nitrate content. In Experiment A, nitrate levels were higher under PV-Tracking + CO_2 (0.8 ± 0.04 mg g^{-1}) compared to all other treatments (0.6 mg g^{-1}). A complementary analysis examined the combined effect of the four treatments across both experiments. The results indicated that only the antioxidative capacity was affected, while all other parameters remained stable. Specifically, the treatment with CO_2 enrichment but without PV-Tracking showed the highest antioxidative capacity compared to the other treatments. The control treatment (no CO_2, no PVs) showed intermediate values, while the PV-Tracking treatments, with or without CO_2, remained lower. Overall, these findings suggest that elevated CO_2, together with increased sunlight exposure, enhanced leaf antioxidative capacity.

The photochemical reflectance index (PRI) showed distinct trends between the two lettuce cultivars evaluated (Figure 130). In the Green Tower cultivar, PRI values were positive across all treatments and sampling dates. No significant differences were observed among treatments at 5, 12, 26, and 31 days after treatment (DAT). However, at 26 DAT, the CTRL treatment exhibited a significantly lower PRI value compared to the PV-Tracking and PV_Fixed treatments. In contrast, PRI values for the Sanguine cultivar were negative throughout the experimental period. Similar to Green Tower, no significant differences were detected among treatments at 5, 12, 18, and 26 DAT. At DAT 31, however, the PRI value in the CTRL treatment was significantly lower than those in the PV_Tracking and PV_Fixed treatments.

Funded by the European Union

Funded by the European Union under Grant Agreement No 101096056. Views and opinions expressed are however those of the author(s) only and do not necessarily reflect those of the European Union or CINEA. Neither the European Union nor the granting authority can be held responsible for them.

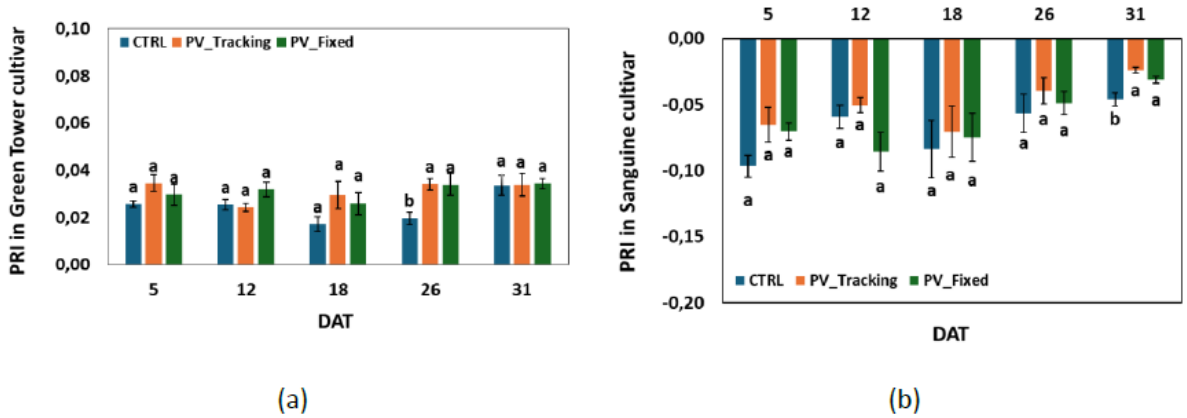

(a) (b)

Figure 130. Photochemical Reflectance Index (PRI) in 'Green Tower' and 'Sanguine' lettuce cultivars under CTRL, PV_Tracking, and PV_Fixed conditions at different days after transplantation (DAT).

Table 66. Mean total fresh biomass (g plant^{-1}), dry biomass (g plant^{-1}), and total yield (kg m^{-2}) (± SE) across treatments during the first, second, and third experimental periods.

	Treatments	Fresh biomass [g plant^{-1}]	Dry biomass [g plant^{-1}]	Total yield [kg m^{-2}]
Exp. A	CTRL	988.0±47.36 a	117.6±2.99 a	8.62±0.29 a
	CO_2	1092.0±30.58 a	119.4±3.80 a	8.92±0.43 a
	PV-Tracking	1008.6±17.85 a	108.2±1.09 b	8.30±0.20 a
	PV-Tracking + CO_2	1028.0±13.78 a	114.4±1.24 ab	8.89±0.72 a
Exp. B	CTRL	811.6±41.63 a	61.1±2.37 a	5.12±0.22 a
	CO_2	703.8±9.98 b	59.9±0.60 a	5.18±0.32 a
	PV-Tracking	769.4±31.70 ab	62.0±2.66 a	5.15±0.14 a
	PV-Tracking + CO_2	791.8±45.17 ab	66.2±4.08 a	5.68±0.25 a
Exp. C	CTRL	1516.0±85.96 a	133.1±7.44 a	5.86±0.11 a
	PV-Tracking	1612.8±40.71 a	136.3±4.48 a	5.55±0.10 a
	PV-Opposite	1447.4±60.26 a	130.5±5.77 a	5.43±0.53 a
Exp. D Green Towers	CTRL	615.9±18.38 a	20.4±0.64 a	1.53±0.05 a
	PV-Tracking	552.4±32.49 b	20.1±1.35 a	1.38±0.08 b
	PV-Fixed	497.1±20.93 b	19.4±0.68 a	1.24±0.05 b
Exp. D Sanguine	CTRL	253.7±13.52 a	9.4±0.91 a	0.58±0.06 a
	PV-Tracking	263.4±4.12 a	10.4± 0.39 a	0.66±0.01 a
	PV-Fixed	227.6±9.43 a	9.9± 0.56 a	0.57±0.02 a

Different letters (a, b) indicate statistically significant differences between treatments ($p < 0.05$).

Effect of PVs on Crop Yield

Across all three experimental periods, total yield did not differ significantly among treatments (Table 66). In Experiments A and B, CO_2-enriched treatments exhibited a non-significant trend toward higher productivity. In Experiment A, fresh biomass production was similar across treatments, although the PV-Tracking treatment exhibited a slight reduction in dry biomass. In Experiment B, plants under the CO_2

Funded by the European Union under Grant Agreement No 101096056. Views and opinions expressed are however those of the author(s) only and do not necessarily reflect those of the European Union or CINEA. Neither the European Union nor the granting authority can be held responsible for them.

Funded by the European Union

treatment produced the lowest fresh biomass, but this difference was not significant when expressed as dry biomass. In Experiment C, no significant differences among treatments were observed for any of the measured parameters.

Effect of PVs on Leaf tissue analysis

Despite the variations in treatment conditions, nutrient concentrations in cucumber leaves did not differ significantly during Experiment A, and B (Table 67). Despite the variations in treatment conditions, nutrient concentrations in cucumber leaves did not differ significantly during Experiment A, and B (Table 67). In general, nitrogen, phosphorus, and potassium levels remained consistent across all treatments. The only differences were observed for calcium in Experiment A. Calcium content in the PV-Tracking + CO_2 treatment was significantly lower compared to the other treatments.

Table 67. Mean concentrations of N, P, K, Ca, and Na (mg g^{-1} dry matter, ± SE) in cucumber leaf tissue across treatments during Experiment A, and B.

	Treatments	N [mg g^{-1}]	P [mg g^{-1}]	K [mg g^{-1}]	Ca [mg g^{-1}]
Exp. A	CTRL	52.1±1.52 a	6.8±0.58 a	24.2±1.52 a	19.2±1.52 ab
	CO_2	51.6±0.46 a	6.6±1.70 a	22.1±0.69 a	23.3±1.63 a
	PV-Tracking	51.3±0.28 a	6.1±2.09 a	23.3±1.51 a	19.2±0.71 ab
	PV-Tracking + CO_2	51.1±0.79 a	6.2±1.52 a	22.7±1.18 a	18.5±1.07 b
Exp. B	CTRL	45.4±1.48 a	7.3± 0.33 a	26.3±1.01 a	14.8±2.92 a
	CO_2	49.0±0.91 a	7.7±0.77 a	23.4±2.38 a	16.0±1.05 a
	PV-Tracking	47.8±1.19 a	8.9±0.83 a	28.5±1.91 a	15.6±1.30 a
	PV-Tracking + CO_2	49.0±0.60 a	9.5±1.06 a	28.1±1.96 a	14.5±0.84 a

Different letters (a, b) indicate statistically significant differences between treatments ($p < 0.05$).

Water and Fertiliser Use Efficiency

The shading effect of the PV modules, either alone or in combination with elevated CO_2 concentrations, had a significant impact on cumulative plant transpiration (Table 68). In Experiment A, crop water uptake under the CO_2 treatment was significantly higher than in the other treatments, followed by the CTRL treatment. Both PV-shaded treatments exhibited the lowest transpiration rates. In Experiment B, the PV-Tracking treatment recorded the lowest water uptake, whereas the PV-Tracking + CO_2 treatment showed values comparable to the CTRL and CO_2 treatments, highlighting a synergistic effect between PV shading and CO_2 enrichment. Water use efficiency did not differ significantly among the treatments during any experimental period, with exception of Experiment D. Fertilizer use efficiency was affected only in Experiment A and D. Specifically, in Experiment A the CTRL and CO_2 treatments achieved the highest FUE values (36.6 and 34.2 $kg \cdot kg^{-1}$, respectively), followed by the PV-Tracking + CO_2 treatment (30.7 $kg \cdot kg^{-1}$). The lowest FUE was observed in the PV-Tracking treatment. In Experiment D, FUE was decreased in the case of the PV-Fixed treatment only for the Green Towers cultivar.

Funded by the European Union under Grant Agreement No 101096056. Views and opinions expressed are however those of the author(s) only and do not necessarily reflect those of the European Union or CINEA. Neither the European Union nor the granting authority can be held responsible for them.

Table 68. Mean crop water uptake (L m^{-2}, ± SE), water use efficiency (WUE, kg m^{-3}, ± SE), and fertiliser use efficiency (FUE, kg kg^{-1}, ± SE) across treatments during the three experimental periods.

	Treatments	Water Uptake [L m^{-2}]	WUE [kg m^{-3}]	FUE [kg kg^{-1}]
Exp. A	CTRL	88.8±1.95 b	50.6±1.70 a	36.6±1.23 a
	CO_2	94.9±0.27 a	50.9±2.63 a	34.2±1.66 ab
	PV-Tracking	82.6±1.15 c	49.8±1.17 a	28.3±0.67 c
	PV-Tracking + CO_2	83.1±4.10 c	51.4±4.28 a	30.7±2.48 bc
Exp. B	CTRL	72.5±1.42 ab	46.6±1.98 a	37.7±1.65 a
	CO_2	74.8±1.24 a	48.4±3.47 a	39.9±2.49 a
	PV-Tracking	69.6±1.84 b	50.1±1.43 a	39.9±1.06 a
	PV-Tracking + CO_2	74.9±0.18 a	52.8±2.30 a	42.1±1.84 a
Exp. C	CTRL	74.0±1.04 a	56.1±0.97 a	37.7±0.69 a
	PV-Tracking	68.8±1.21 b	57.2±1.20 a	39.4±0.71 a
	PV-Opposite	69.1±0.94 b	54.1±5.31 a	36.7±3.59 a
Exp. D Green towers	CTRL	7.9±0.05 b	75.7±1.81 a	24.9±0.74 a
	PV-Tracking	8.1±0.96 b	70.0±1.38 a	22.4±1.32 ab
	PV-Fixed	12.7±0.33 a	61.1±2.21 b	20.2±0.85 b
Exp. D Sanguine	CTRL	7.9±0.05 b	28.5±0.95 b	9.4±0.97 a
	PV-Tracking	8.1±0.96 b	32.6±0.57 a	10.7±0.17 a
	PV-Fixed	12.7±0.33 a	29.4±1.35 ab	8.9±0.27 a

Different letters (a, b, c) indicate statistically significant differences between treatments ($p < 0.05$).

Electrical yield of the PV system in UTH greenhouse

The two inverters provide the ability to monitor and record the power produced by the two arrays through a website (https://kostal-solar-portal.com/plant/1084087/chart-data-dashboard) as shown in Figure 131. The website is available for all the REGACE consortium members while the weekly and monthly data sets are uploaded in the project repository. The system began operation from 9/12/2024.

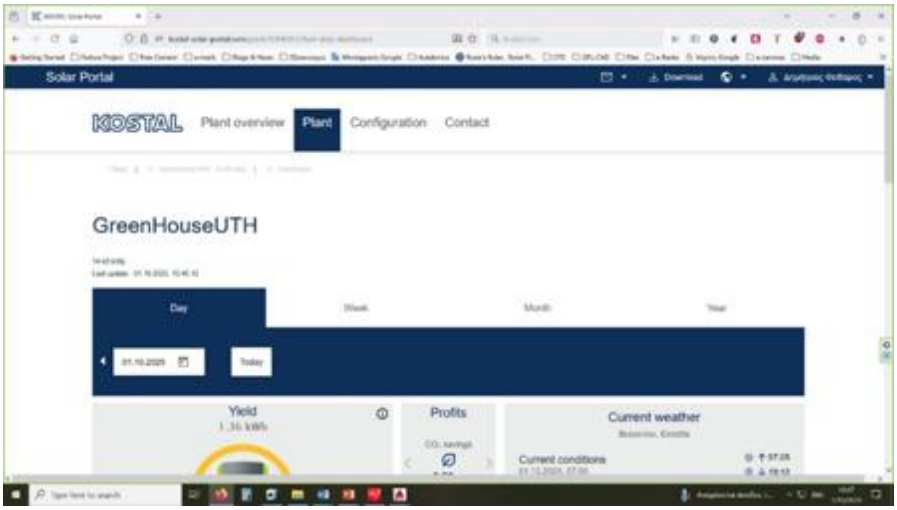

Figure 131. Inverter's website home page.

Funded by the European Union

Funded by the European Union under Grant Agreement No 101096056. Views and opinions expressed are however those of the author(s) only and do not necessarily reflect those of the European Union or CINEA. Neither the European Union nor the granting authority can be held responsible for them.

The data that may be retrieved are current daily yield and local weather conditions (Figure 132).

Figure 132. Current daily yield and local weather conditions.

-Time series data are available both graphically and as datasets for the daily power output of the entire system. For example, Figure 133 illustrates the daily power production for a cloudy and rainy day, September 30, 2025. Measurements were recorded at 10-minute intervals. The data can also be aggregated and provided on a weekly basis while maintaining the same temporal resolution. Figure 134 presents the monthly power production for September 2025.

Figure 133. Daily power production on a cloudy and rainy day, September 30, 2025.

Funded by the European Union

Funded by the European Union under Grant Agreement No 101096056. Views and opinions expressed are however those of the author(s) only and do not necessarily reflect those of the European Union or CINEA. Neither the European Union nor the granting authority can be held responsible for them.

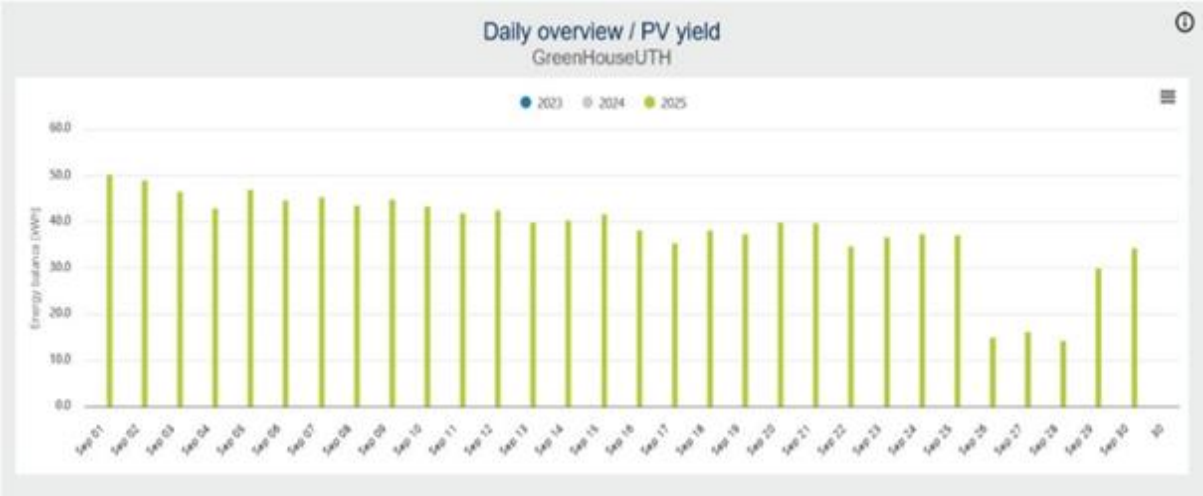

Figure 134. Monthly power production of the whole system in September 2025.

-Time series in terms of figure and data sets for yearly power production

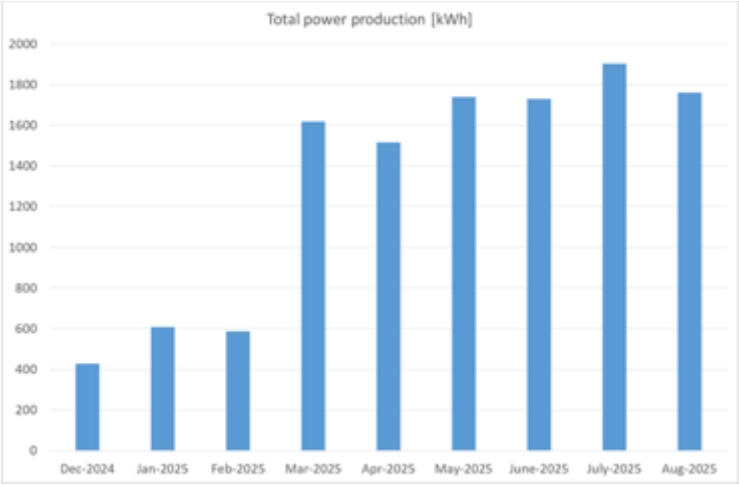

Figure 135. Yearly power production.

March was expected to exhibit lower power production compared to April, while June was anticipated to have higher production than July and August (Figure 135). However, no cultivation occurred during March, July, or August.

-Time series data are available both graphically and as datasets for daily or weekly power production at the inverter level (e.g., per compartment). Inverter 2 (serial number 1053511792092WF200002) corresponds to compartment 4, while inverter 1 (serial number 1053511792092WF60018) corresponds to compartment 3. Figure 136 presents the weekly power production for compartment 3, and Figure 137 shows the weekly power production for compartment 4 for the week of September 22–28, 2025, coinciding with the start of lettuce cultivation in the last experiment.

Funded by the European Union

Funded by the European Union under Grant Agreement No 101096056. Views and opinions expressed are however those of the author(s) only and do not necessarily reflect those of the European Union or CINEA. Neither the European Union nor the granting authority can be held responsible for them.

Figure 136. Weekly power production of compartment 3 – week from 22/9/2025 to 28/9/2025.

Figure 137. Weekly power production of compartment 4 – week from 22/9/2025 to 28/9/2025.

Since compartment 4 is equipped with a CO_2 enrichment system, the crop's light requirement is reduced. Consequently, under conditions of low available solar radiation, the PV array inclination is adjusted to maximize power production. It should also be noted that, in each case, two time series are provided: the string DC output and the inverter AC output. The AC output is generally lower due to the inverter efficiency and the loss of DC power produced under low solar radiation conditions, when the generated voltage is below the inverter's start-up DC voltage. However, in cases where no crop is present, the power production of the two compartments is comparable.

Funded by the European Union

Funded by the European Union under Grant Agreement No 101096056. Views and opinions expressed are however those of the author(s) only and do not necessarily reflect those of the European Union or CINEA. Neither the European Union nor the granting authority can be held responsible for them.

Figure 138. Weekly power production of compartment 3 – week from 18/8/2025 to 24/8/2025.

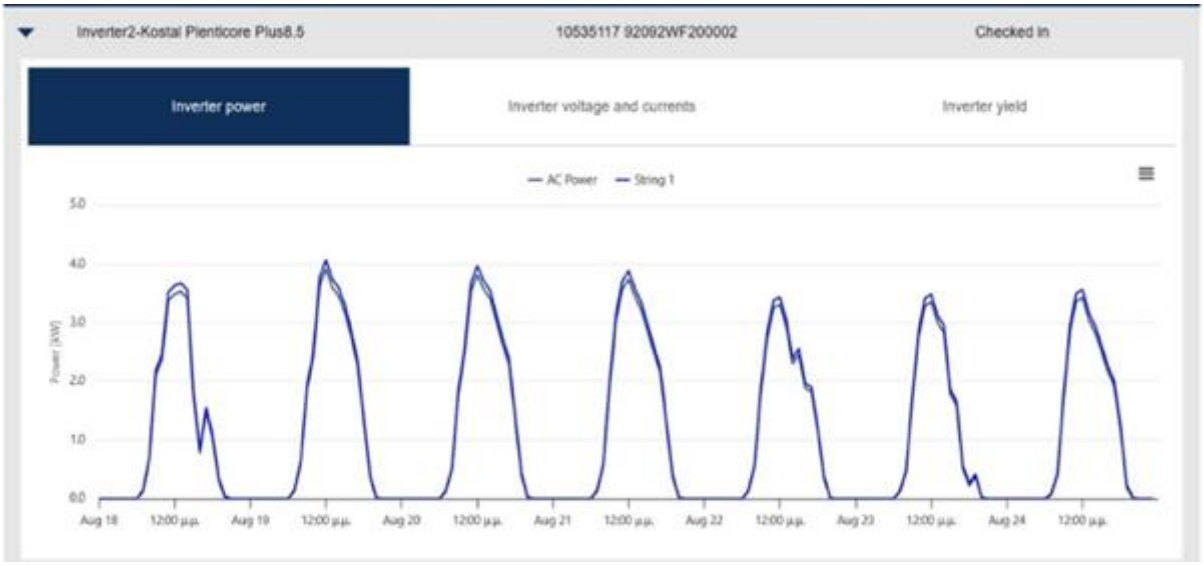

Figure 139. Weekly power production of compartment 4 – week from 18/8/2025 to 24/8/2025.

-Time series data are available both graphically and as datasets for inverter voltage and current on a daily or weekly basis, using a 10-minute time step. For example, Figure 140 presents the inverter voltage and current for compartment 3 for the week of August 18–24, 2025.

Funded by the European Union under Grant Agreement No 101096056. Views and opinions expressed are however those of the author(s) only and do not necessarily reflect those of the European Union or CINEA. Neither the European Union nor the granting authority can be held responsible for them.

Funded by the European Union

Figure 140. IV curve for inverter of compartment 3.

-Finally, daily, weekly, monthly, and yearly power production can be provided for each individual inverter, array, or compartment, as illustrated in Figures 141 and 142.

Figure 141. Compartment 4 weekly power production.

Funded by the European Union

Funded by the European Union under Grant Agreement No 101096056. Views and opinions expressed are however those of the author(s) only and do not necessarily reflect those of the European Union or CINEA. Neither the European Union nor the granting authority can be held responsible for them.

Figure 142. Compartment 3 monthly power production.

Total energy production during the experiment

Figure 143 presents the daily power production time series for the winter experiment (Experiment B, January 16 to April 3, 2025), while Figure 144 shows the power production time series at a 10-minute interval for Experiment C (April 25 to June 13, 2025). Both figures correspond to compartment 3.

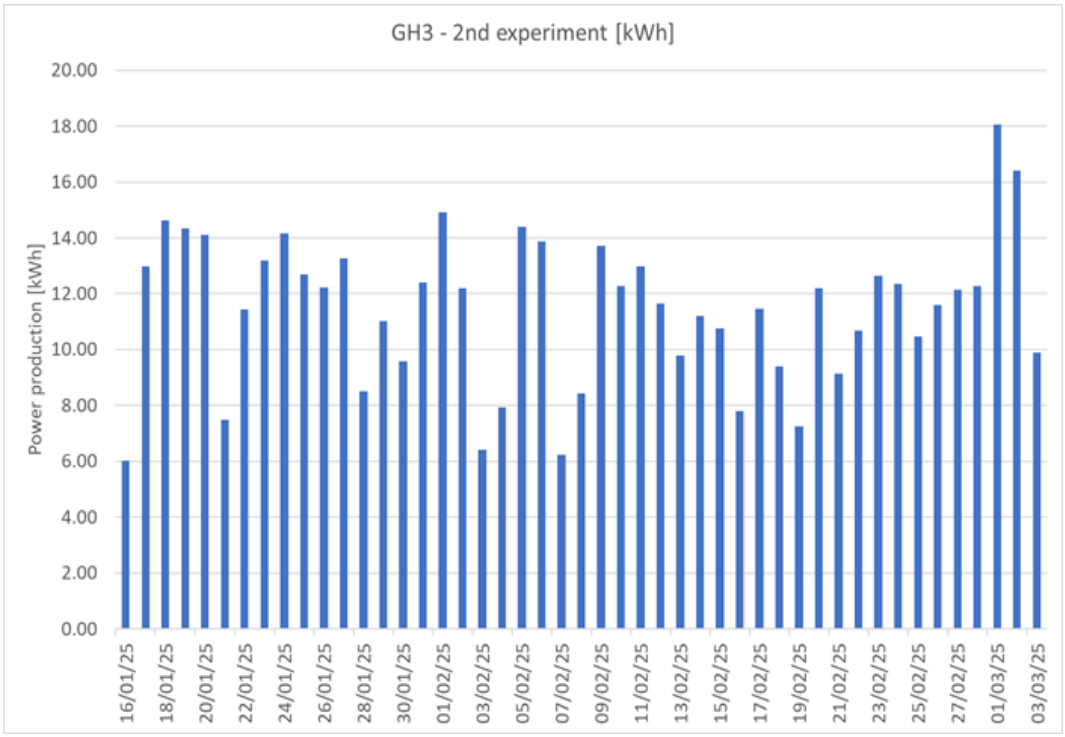

Figure 143. Daily power production during Experiment B.

Funded by the European Union under Grant Agreement No 101096056. Views and opinions expressed are however those of the author(s) only and do not necessarily reflect those of the European Union or CINEA. Neither the European Union nor the granting authority can be held responsible for them.

Funded by the European Union

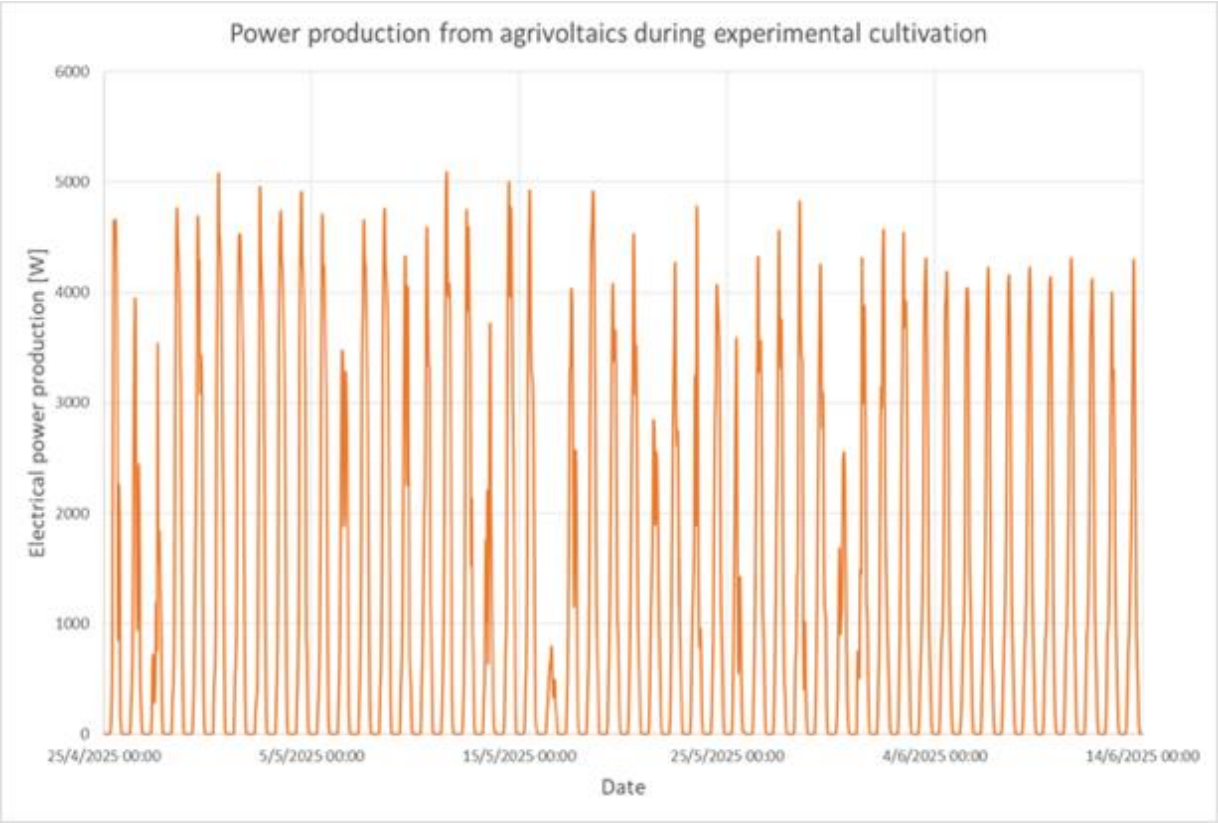

Figure 144. Time series of power production during Experiment C at 10 min time steps.

Table 69 presents the total energy produced during time intervals with and without cultivation for the two compartments.

Table 69. Total energy (kWh) produced for time intervals with and without cultivation.

Cultivation	From	To	Energy produced in compartment 3[kWh]	Energy produced in compartment 4 [kWh]
No	09/12/2024	15/01/2025	361.03	318.83
Cucumber (Exp. A)	16/01/2025	03/04/2025	1101.92	1059.8
No	04/04/2025	24/04/2025	563.15	532.66
Cucumber (Exp. B)	25/04/2025	13/06/2025	1388.93	1490.99
No	14/06/2025	31/08/2025	2245.36	2398.61

From Table 69, it is evident that as available solar radiation increases, the energy produced by the PV system also increases. Figure 145 illustrates the relationship between energy production and available radiation inside the greenhouse for a period without cultivation (April 4–24, 2025), while Figure 146 presents the same relationship for the period corresponding to Experiment C.

Funded by the European Union

Funded by the European Union under Grant Agreement No 101096056. Views and opinions expressed are however those of the author(s) only and do not necessarily reflect those of the European Union or CINEA. Neither the European Union nor the granting authority can be held responsible for them.

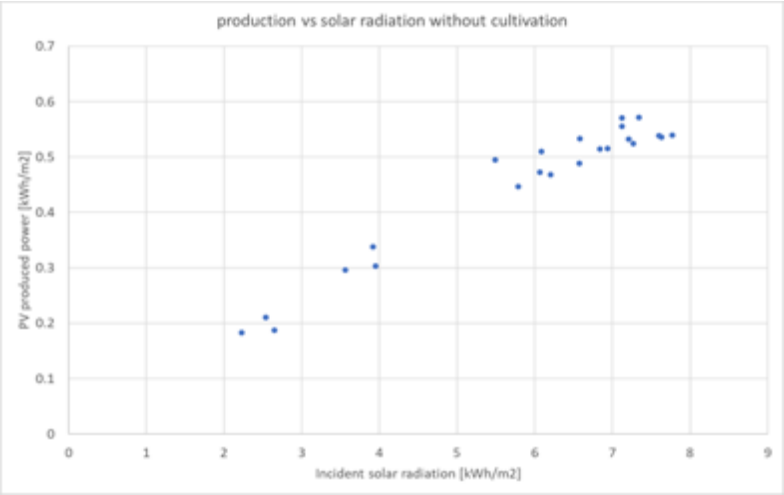

Figure 145. Energy dependence on available solar radiation without cultivation.

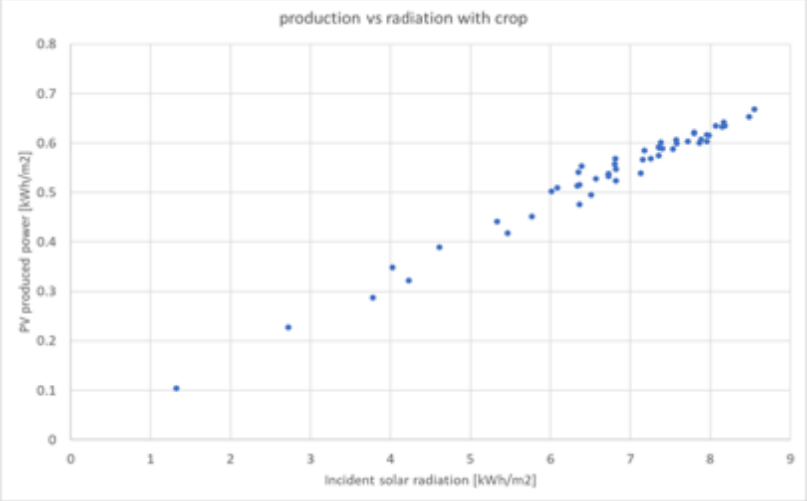

Figure 146. Energy dependence on available solar radiation with cultivation.

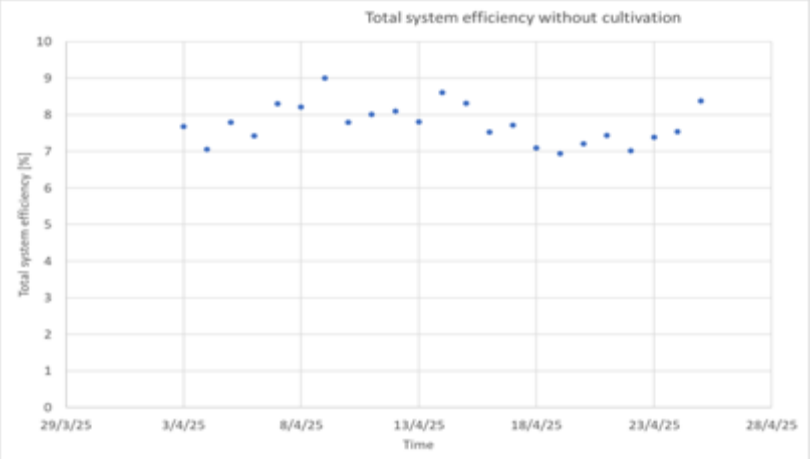

Figure 147. Total system efficiency against time without cultivation.

Funded by the European Union

Funded by the European Union under Grant Agreement No 101096056. Views and opinions expressed are however those of the author(s) only and do not necessarily reflect those of the European Union or CINEA. Neither the European Union nor the granting authority can be held responsible for them.

It is important to identify the response of the total system efficiency to the various factors affecting energy production. Since solar radiation inside the greenhouse and above the PV arrays is measured, the total efficiency coefficient, n_{tot} can be calculated on a daily basis as:

n_{tot} = (Daily solar energy above the PV array)/(Daily power production by the PV array)

This total efficiency coefficient accounts for multiple factors, including the PV cell efficiency, module efficiency, cable losses, inverter efficiency, optical transmittance of the greenhouse air, periods when the produced voltage is below the inverter's start-up voltage, and the effective operation of the bifacial PV characteristics. Figure 147 presents the total system efficiency over calendar time for a period without cultivation, while Figure 148 shows the total system efficiency during the third experiment with the cucumber crop.

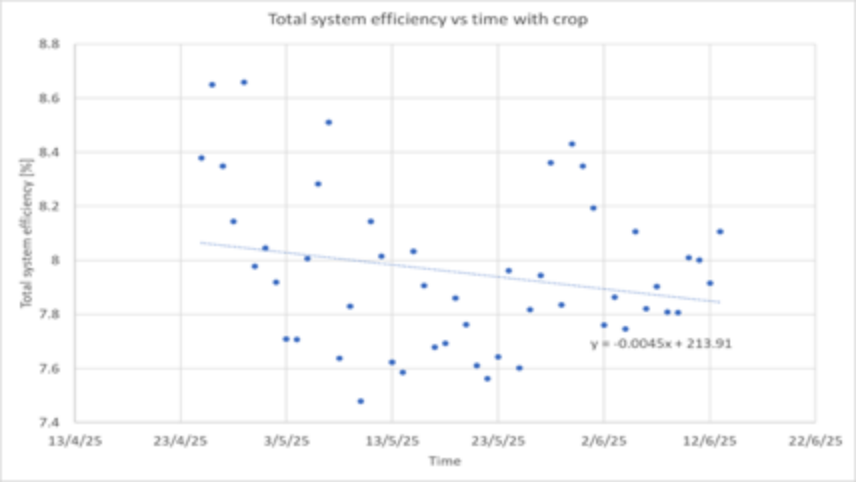

Figure 148. Total system efficiency against time with cultivation.

From Figure 147, it is evident that the system efficiency remains relatively constant over time, as expected. In contrast, Figure 148 clearly shows a reduction in system efficiency during the Experiment C, indicating that crop growth negatively affects overall system performance. This reduction can be attributed primarily to two factors: (a) as the crop develops, increased humidity reduces the optical transparency of the air inside the greenhouse, and (b) as the crop canopy grows, the reflected radiation from the greenhouse floor (covered by light-coloured geotextile) decreases, resulting in lower electricity production from the rear surface of the bifacial PV modules.

Literature

Mourantian, A., Chatzinikolaou, M., Feka, M., Levizou, E. (2025) Bioponics in Tomato Cultivation Toward Sustainable Farming: Evaluation of a Circular Tri-Trophic System Incorporating Aquaponics and Insects. Plants. 14. 10.3390/plants14182882.

Funded by the European Union

Funded by the European Union under Grant Agreement No 101096056. Views and opinions expressed are however those of the author(s) only and do not necessarily reflect those of the European Union or CINEA. Neither the European Union nor the granting authority can be held responsible for them.

5.2.5 Soil greenhouse crop analysis at FSC

Crop growth is evaluated by comparing the yield of plants grown under the PV system with those in the reference section, based on their weight at harvest.

The first planting cycle started on February 19th 2025, included lettuce and zucchini. The end of the harvest was on April 9th 2025 for lettuce and on May 12th 2025 for zucchini. The greenhouse was divided into four sections: two under the PV panels (PVW and PVE for West and East, respectively), and two in the open area (REFW and REFE). Lettuce was planted in PVW and REFW (13 rows of 12 plants each), and zucchini in PVE and REFE (7 rows of 5 plants each) (Figure 149).

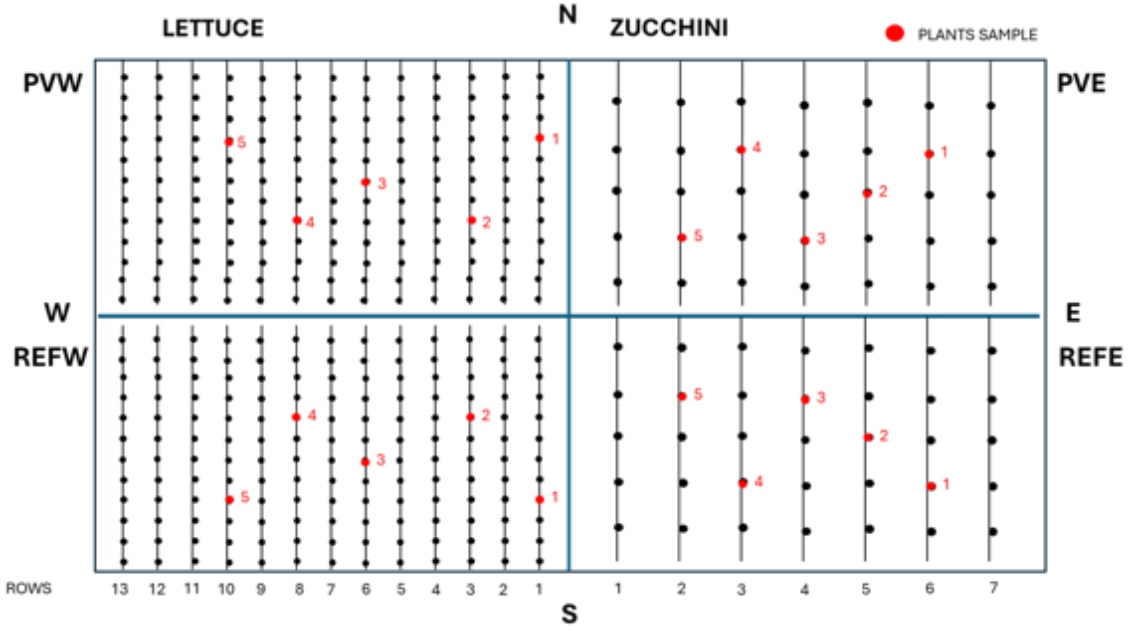

Figure 149. Layout and sample plants for the first cultivation cycle (February-May 2025).

The second planting cycle started on May 20th 2025, and included tomato and eggplant. The end of the harvest was on August 26th 2025 for tomatoes and on September 18th 2025 for eggplants. Eggplant was planted in PVW and REFW (7 rows of 5 plants each), and tomato in PVE and REFE (7 rows of 5 plants each) (Figure 150).

Funded by the European Union

Funded by the European Union under Grant Agreement No 101096056. Views and opinions expressed are however those of the author(s) only and do not necessarily reflect those of the European Union or CINEA. Neither the European Union nor the granting authority can be held responsible for them.

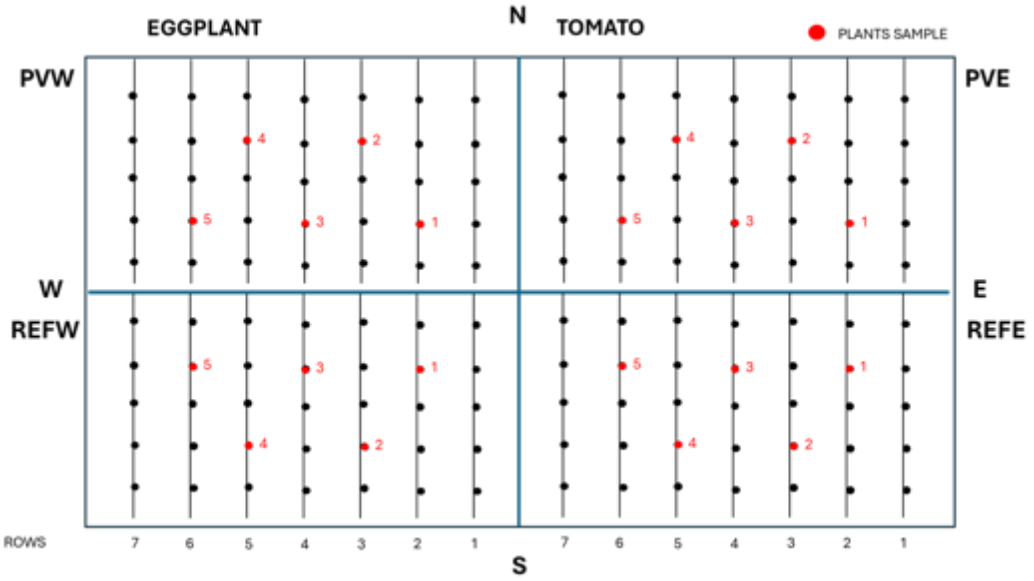

Figure 150. Layout and sample plants for the second cultivation cycle (June-August 2025).

Since the tomato life cycle proved to be shorter than that of the eggplant, it was decided to repeat a lettuce cultivation cycle (III Cycle), which ended on 2nd October. Figure 151 shows the lettuce crop alongside the eggplant crop, where 14 rows with 10 plants each can be observed.

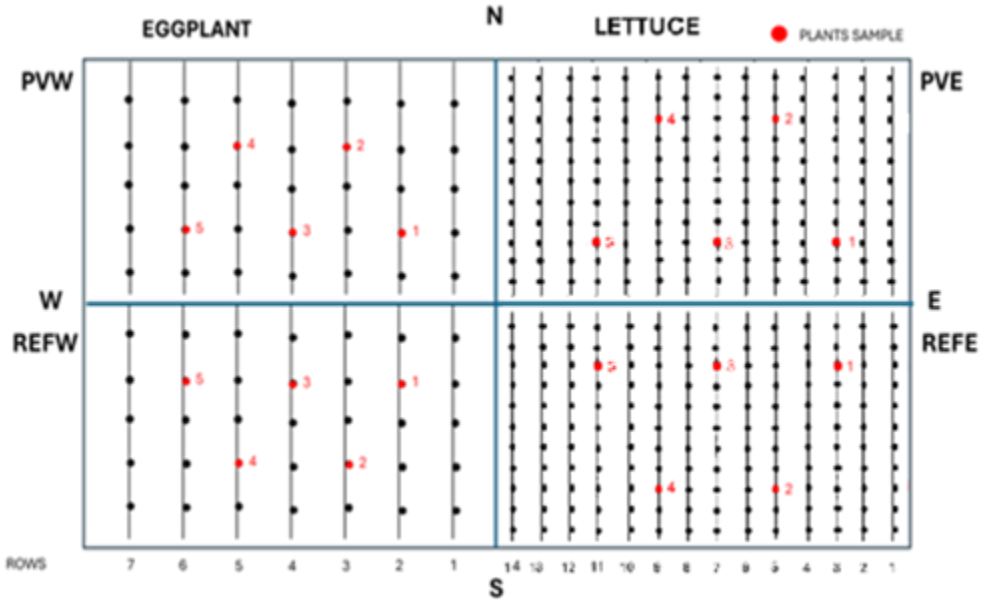

Figure 151. Layout and sample plants for the third cultivation cycle (August-October 2025).

In the following paragraph we will present the light and water resources and the crop yield for the 3 cultivation cycles.

Funded by the European Union

Funded by the European Union under Grant Agreement No 101096056. Views and opinions expressed are however those of the author(s) only and do not necessarily reflect those of the European Union or CINEA. Neither the European Union nor the granting authority can be held responsible for them.

Daily Light Integral (DLI)

Figures 152 and 153 illustrate the variations in Daily Light Integral (DLI) over time during the two production cycles. The optimal DLI ranges for the crops grown during each cycle have been included as shaded bands in the graphical representation. It is noteworthy that the DLI values for zucchini plants were almost consistently below the optimal range, whereas the situation was less critical for lettuce, whose optimal range is located at lower DLI levels. Furthermore, as expected, a clear increasing trend in DLI values is observed as the season progresses toward summer (Figure 151).

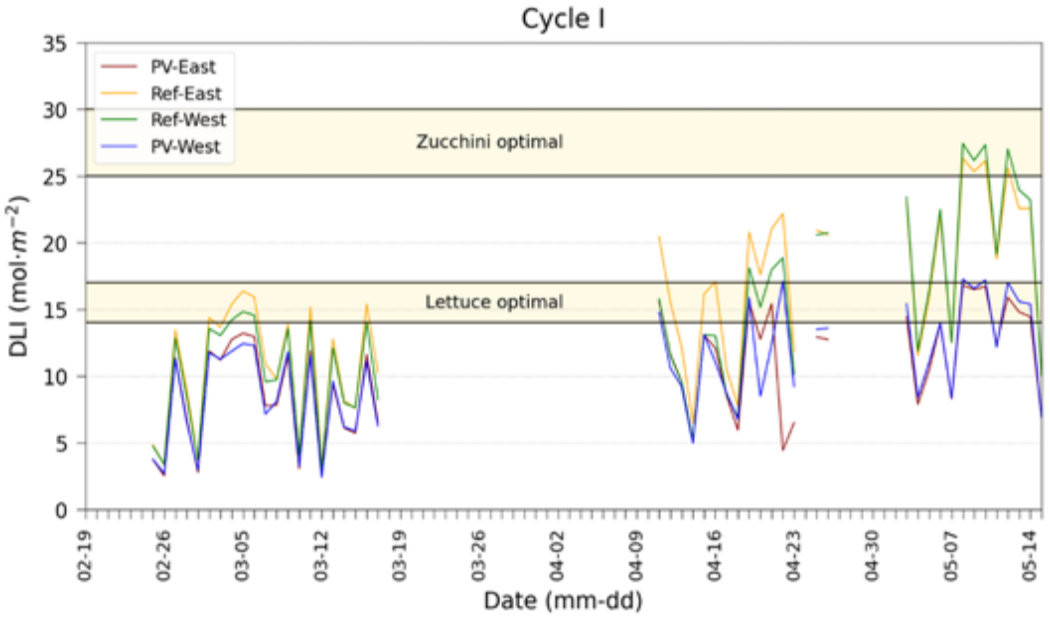

Figure 152. DLI for the first cultivation cycle (zucchini and lettuce).

Analysing the graph related to the second cultivation cycle, it is possible to observe that the trend is the opposite of the previous cycle. In this case, there is a decreasing trend in DLI starting from June. It is noteworthy that the optimal light ranges for the two crops show that eggplants consistently received more than sufficient light, even reaching optimal conditions underneath the photovoltaic panels. Conversely, tomatoes — characterized by higher light requirements — found their optimal placement outside the PV system, while under the panels, DLI levels remained below the lower threshold of their optimal range (Figure 153).

Funded by the European Union

Funded by the European Union under Grant Agreement No 101096056. Views and opinions expressed are however those of the author(s) only and do not necessarily reflect those of the European Union or CINEA. Neither the European Union nor the granting authority can be held responsible for them.

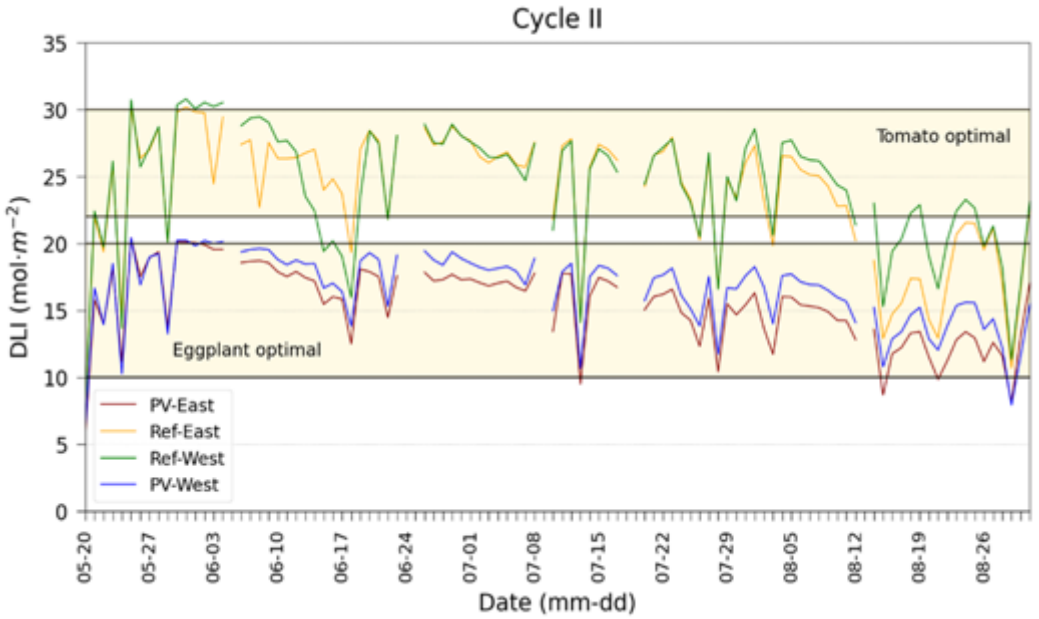

Figure 153. DLI for the second cultivation cycle (tomato and eggplant).

Finally, Figure 154 illustrates the trend of the DLI during the third cultivation cycle (lettuce). Unlike the previous two cycles, this time an alternation of optimal conditions can be observed: a) in the initial phase, the lettuce appears to benefit from the shading provided by the PV panels, and b) as the weeks progress, the optimal DLI for lettuce then seems to align more closely with the values measured outside the area covered by the panels.

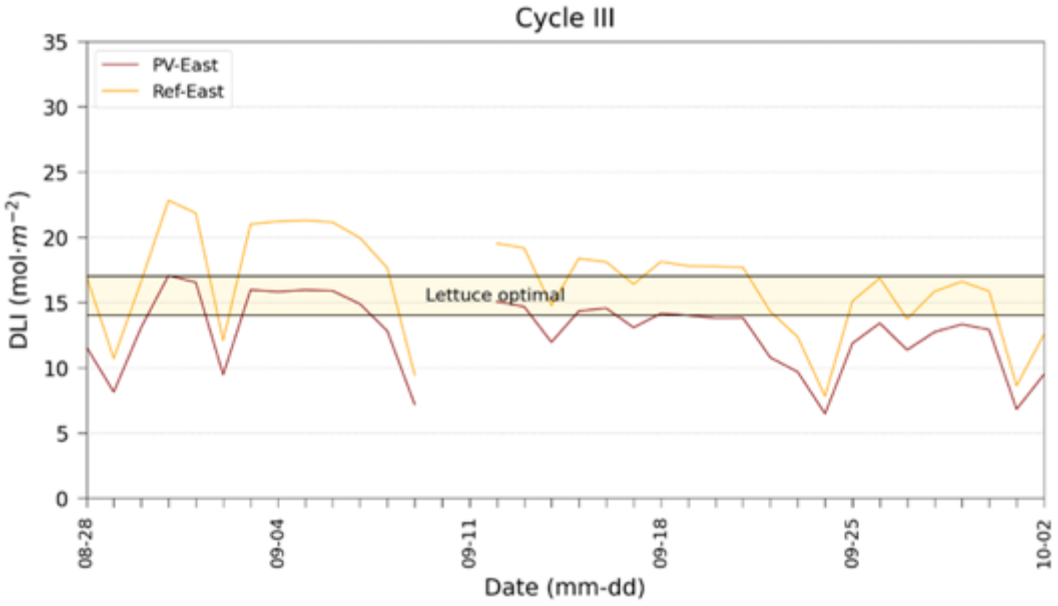

Figure 154. DLI for the third cultivation cycle (lettuce).

Funded by the European Union under Grant Agreement No 101096056. Views and opinions expressed are however those of the author(s) only and do not necessarily reflect those of the European Union or CINEA. Neither the European Union nor the granting authority can be held responsible for them.

Crop growth analysis

LAI measurements were performed using the AccuPAR PAR/LAI Ceptometer LP-80. Sampling was conducted by scanning the area between two rows and between two contiguous plants at two randomly selected points within each plot. Measurements were carried out during the central hours of the day, as prescribed by the measurement protocol, to minimize asymmetries in shadow projection relative to the row axes. The sampling was repeated over time, and at each subsequent sampling event, the two scanning areas were changed. Data from the most recent measurements (plant height, leaf count, canopy size, and LAI) were used to estimate crop growth. The means calculated from the five sampled plants, together with their corresponding standard errors (SE), and the results of the Welch's t-test assessing the significance of differences between the means of the two groups, are presented in Tables 70 and 71.

From the perspective of crop growth, there is insufficient evidence to conclude that the mean values of the two groups differ in terms of plant height, leaf count, or canopy size. The canopy size was calculated as the area of the rectangle enclosing the canopy of the plants under measurement.

Table 70. Mean plant height (cm, ± SE), leaf count (per plant, ± SE), and Canopy expansion (m^2 $plant^{-1}$, ± SE), during the two experimental periods.

	Plot	Crop	Height [cm]	Welch test[1]	Leaf count [plant $^{-1}$]	Welch test[1]
Cycle I	REFW	Lettuce	36.0±0.3	>	17.2±0.6	>
	PVW	Lettuce	35.8±2.0		18.0±1.2	
	REFE	Zucchini	68.6±3.7	>	15.4±0.2	>
	PVE	Zucchini	73.4±3.9		16.6±0.7	
Cycle II	REFW	Eggplant	89.2±6.4	>	*31.8±7.3	>
	PVW	Eggplant	100.8±9.1		*44.6±6.7	
	REFE	Tomato	247.4±6.1	>	*19.8±0.8	>
	PVE	Tomato	233.0±4.8		*20.6±0.7	

* Last data available on 23rd June 2025. [1] ">": p-value higher than 0.05, "<": p-value lower than 0.05

Table 71. Mean canopy expansion (m^2 $plant^{-1}$, ± SE) and LAI (m^2 m^{-2}, ± SE), during the two experimental periods.

	Plot	Crop	Canopy size [m^2 $plant^{-1}$]	Welch test[1]	LAI [m^2 m^{-2}]	Welch test[1]
Cycle I	REFW	Lettuce	0.170±0.008	>	-	
	PVW	Lettuce	0.152±0.014		-	
	REFE	Zucchini	2.498±0.075	>	-	
	PVE	Zucchini	2.307±0.117		-	
Cycle II	REFW	Eggplant	0.865±0.143	>	0.72±0.01	<
	PVW	Eggplant	0.836±0.079		1.77±0.02	
	REFE	Tomato	0.580±0.048	>	1.03±0.02	<
	PVE	Tomato	0.469±0.031		0.61±0.01	

[1] ">": p-value higher than 0.05, "<": p-value lower than 0.05

Funded by the European Union

Funded by the European Union under Grant Agreement No 101096056. Views and opinions expressed are however those of the author(s) only and do not necessarily reflect those of the European Union or CINEA. Neither the European Union nor the granting authority can be held responsible for them.

In contrast, the LAI measured during the second cultivation cycle indicates a difference in plant development between the reference plot and the plot located beneath the photovoltaic (PV) system. Specifically, eggplants exhibited greater growth under the PV panels, as also suggested by the DLI data, which showed optimal DLI values for eggplant growth directly beneath the PV installation. Conversely, tomato plants showed greater development in the area outside the PV system. In this case as well, the DLI values recorded in the two plots (reference and PV) are consistent with these experimental observations, since tomatoes require higher optimal DLI values, which were achieved only in the reference zone.

Crop yield

Crop yield was monitored throughout the entire production phase until the final harvest, by weighing the yield from each row separately. In addition, five plants per plot were randomly selected as sample plants in order to measure dry weight and other growth parameters useful for crop modelling. Table 72 reports total fresh yield per plot and mean fresh yield per square meter while Table 73 reports the mean fresh and dry weight of the plant samples.

Table 72. Total fresh yield per plot and mean fresh yield per m^2.

Cycle	Crop	Total fresh yield (kg)	Mean fresh yield ($kg \cdot m^{-2}$)
		PV – Ref.	PV – Ref.
I	Lettuce	101.27 – 115.99	2.70 – 3.10
	Zucchini	41.36 – 50.97	1.16 – 1.43
II	Eggplant	124.79 – 153.26	2.65 – 3.26
	Tomato	21.60 – 23.81	0.46 – 0.51
III	Lettuce	80.34 – 82.62	2.39 – 2.46

Fresh yield was consistently higher in the reference cultivation areas compared to the crops grown beneath the photovoltaic system. In particular, during the first cycle, lettuce — the crop least affected by potential light limitation — showed a 12.6% lower yield compared to its reference counterpart. In contrast, zucchini, which requires more stringent DLI levels, exhibited a 23.1% reduction in yield compared to its reference.

Table 73. Mean fresh and dry weight of the samples (±SE).

Cycle	Crop	Dry weight ($g \cdot plant^{-1}$)	Fresh weight ($g \cdot plant^{-1}$)
		PV – Ref.	PV – Ref.
I	Lettuce	40.83±4.9 – 40.87±2.6	750.4±108.0 – 839.0±46.1
	Zucchini	116.2±28 – 89.2±20	280.4±46.4 – 237.8±26.2
II	Eggplant	170.0±71.7 – 185.0±93.8	503.2±146.8 – 538.6±183.0
	Tomato	14.4±6.7 – 46.6±11.5	104.2±40.1 – 306.0±81.9
III	Lettuce	44.44±2.8 – 42.99±3.1	852.2±33.2 – 812.6±55.9

During the second production cycle, eggplant was the crop that consistently received a DLI above its optimal requirement, yet it produced 18.4% less yield compared to the reference. Lastly, tomato — which

Funded by the European Union under Grant Agreement No 101096056. Views and opinions expressed are however those of the author(s) only and do not necessarily reflect those of the European Union or CINEA. Neither the European Union nor the granting authority can be held responsible for them.

has a higher light requirement and may have experienced stress under the PV panels — showed a 9.8% reduction in yield. It is worth noting that the tomato crop suffered from water stress during the initial growth phase and experienced flower abortion (due to the presence of a net that hindered free movement of pollinators), which probably influenced the final results and prevented the crops from reaching their full productive potential. Examining the data from the third cycle, a difference of a marginal 2% can be observed between lettuce production beneath the PV panels and that outside their coverage.

Given the high standard error (SE) relative to the mean value, it is difficult to draw definitive conclusions — with the possible exception of lettuce, for which the dry weight appears to be consistent, thus cancelling out the reduction in fresh weight between the reference and PV zones in terms of biomass.

Figures 155-159 show the results for total fresh yield per row and the total fresh yield measured on individual sample plants. The figures confirm the generally higher productivity observed in the reference zones outside the PV panels.

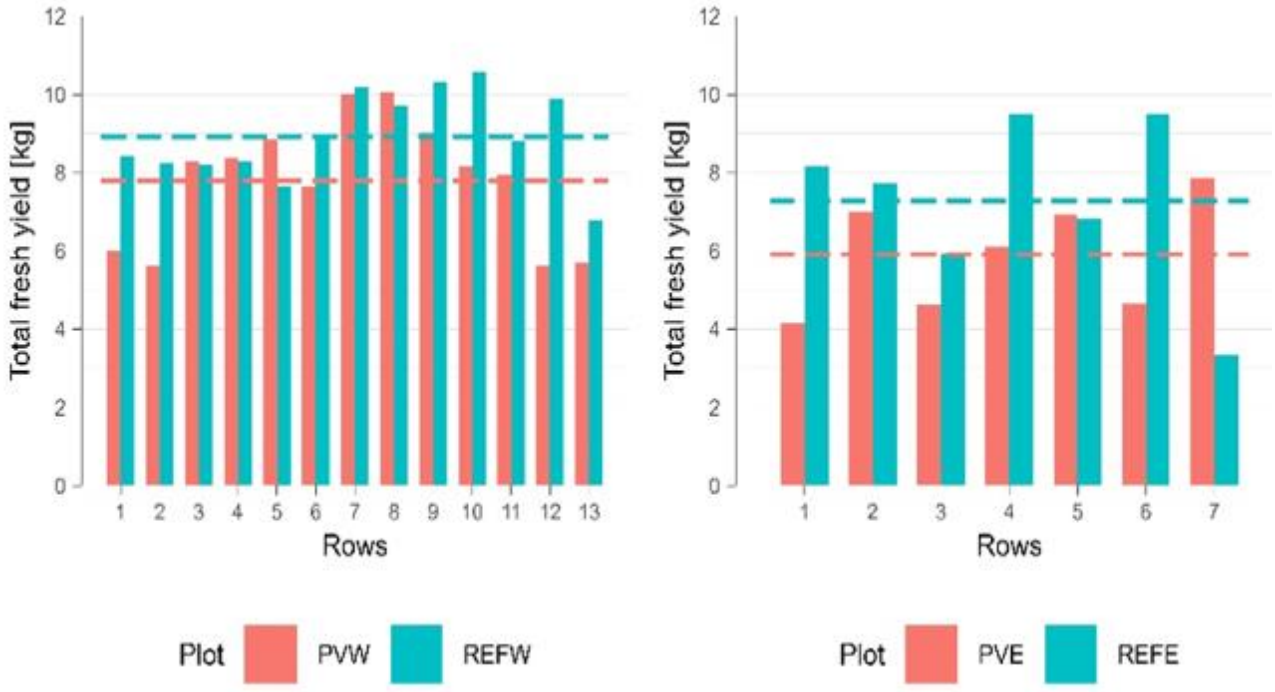

Figure 155. Cycle I - Total fresh yield per row: Lettuce (left), Zucchini (right).

Funded by the European Union under Grant Agreement No 101096056. Views and opinions expressed are however those of the author(s) only and do not necessarily reflect those of the European Union or CINEA. Neither the European Union nor the granting authority can be held responsible for them.

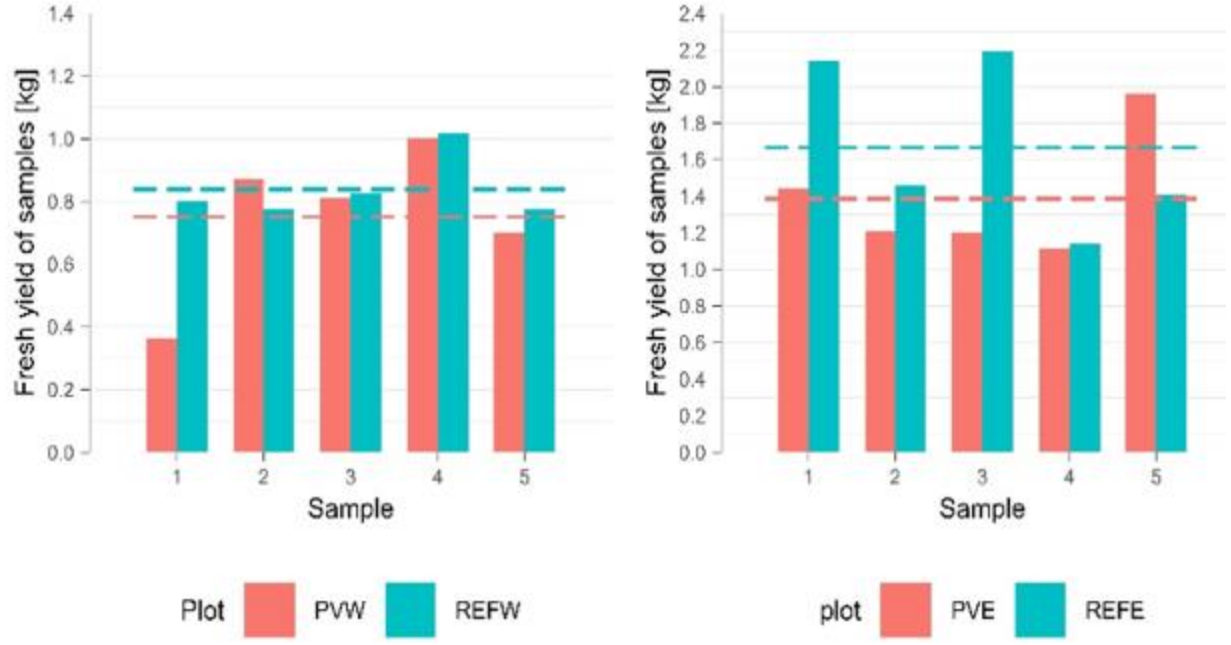

Figure 156. Cycle I - Total fresh yield of the samples: Lettuce (left), Zucchini (right).

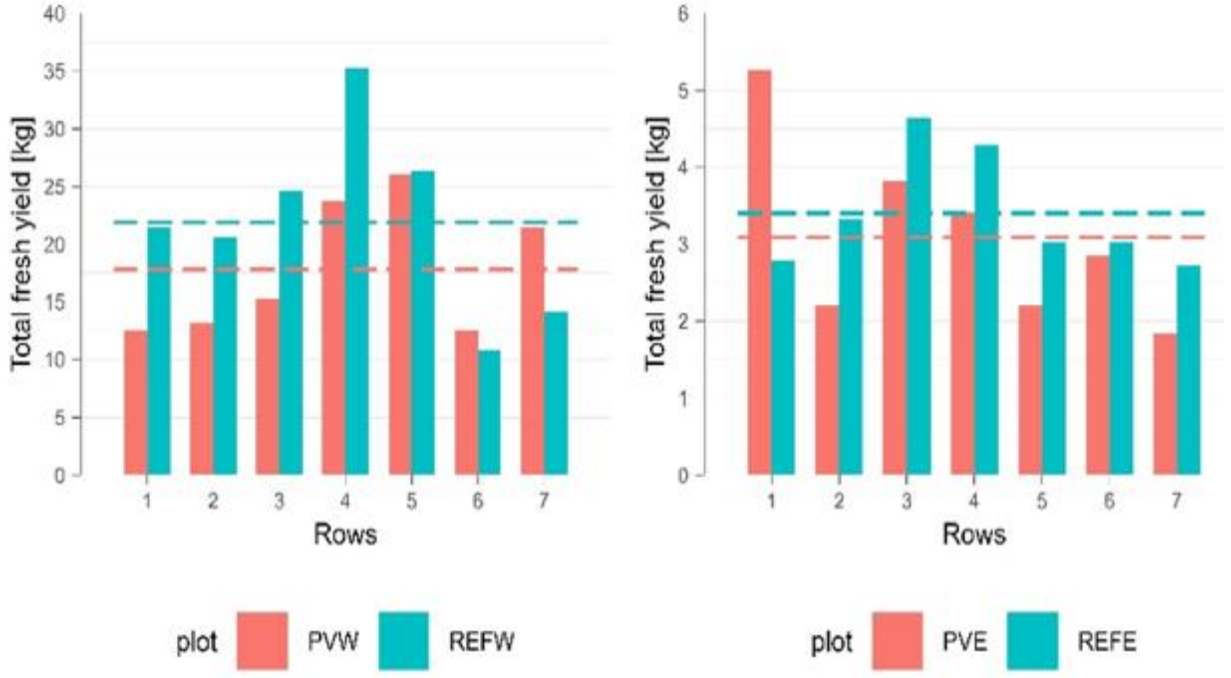

Figure 157. Cycle II - Total fresh yield per row: Eggplant (left), Tomato (right).

Funded by the European Union under Grant Agreement No 101096056. Views and opinions expressed are however those of the author(s) only and do not necessarily reflect those of the European Union or CINEA. Neither the European Union nor the granting authority can be held responsible for them.

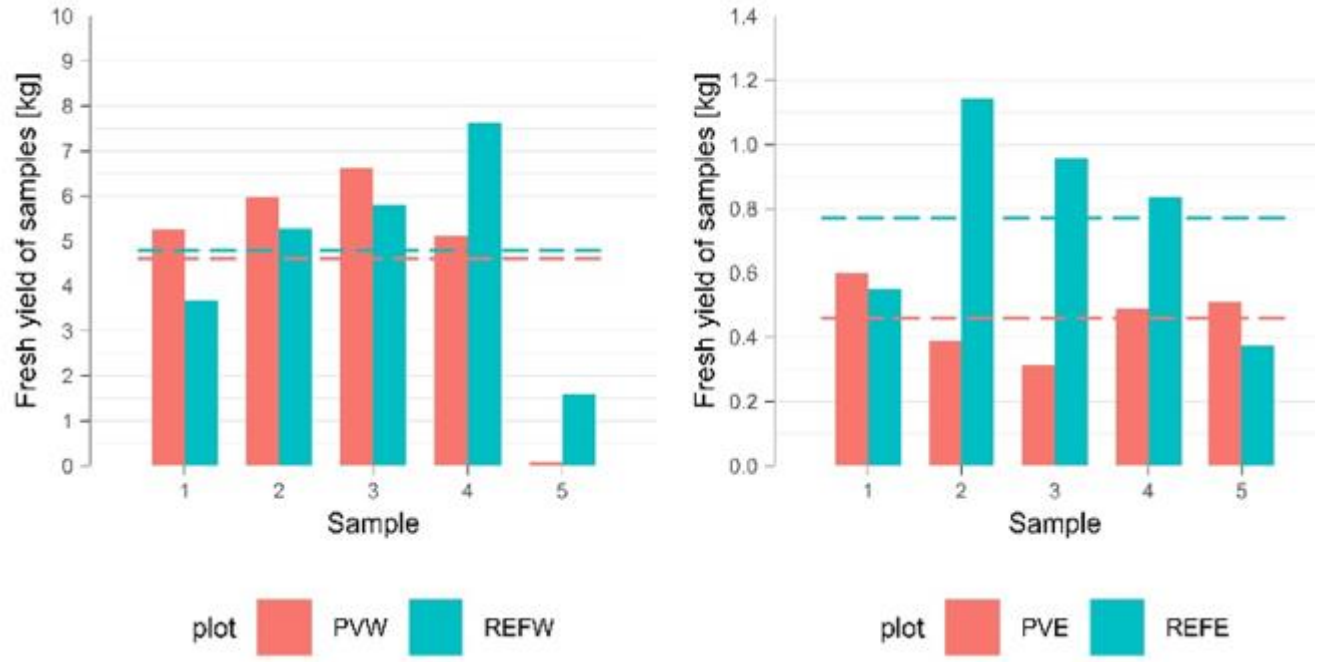

Figure 158. Cycle II - Total fresh yield of the samples: Eggplant (left), Tomato (right).

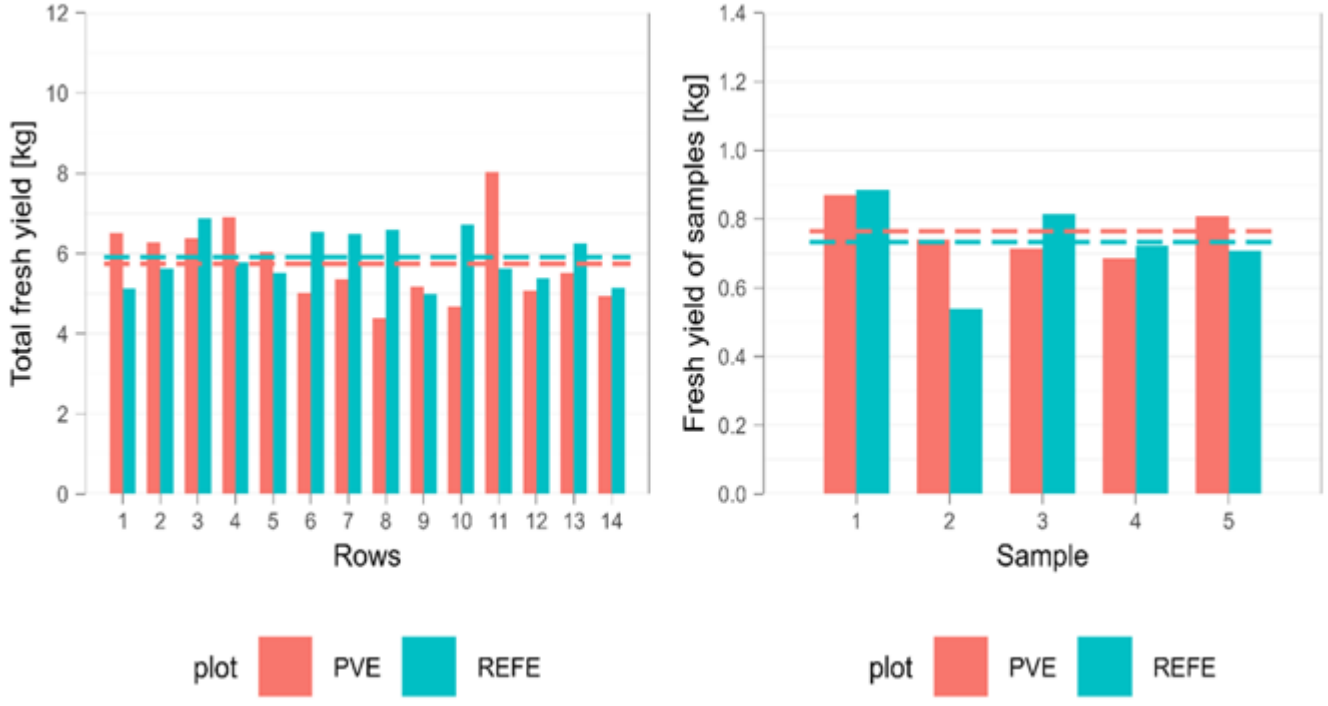

Figure 159. Cycle III (Lettuce) – total fresh yield left) per row and right) of the samples.

Funded by the European Union

Funded by the European Union under Grant Agreement No 101096056. Views and opinions expressed are however those of the author(s) only and do not necessarily reflect those of the European Union or CINEA. Neither the European Union nor the granting authority can be held responsible for them.

Water Consumption Analysis

The irrigation monitoring at FSC described above allows for an accurate assessment of the greenhouse's overall water consumption as well as that of each individual sector, enabling a comparative analysis of water use between the PV section and the reference area.

As an example, the following graph presents the monitoring results over a 5-day period from June 20 to 25, 2025 (Figure 160). The graph shows the temporal trend of water flow rate across the different sectors.

By comparing data from analogous sectors (in terms of duration and average flow rate during irrigation), for instance West PV versus West no-PV, a differentiated water consumption between the two can be observed. Similar results can also be noted in the sectors labelled EAST.

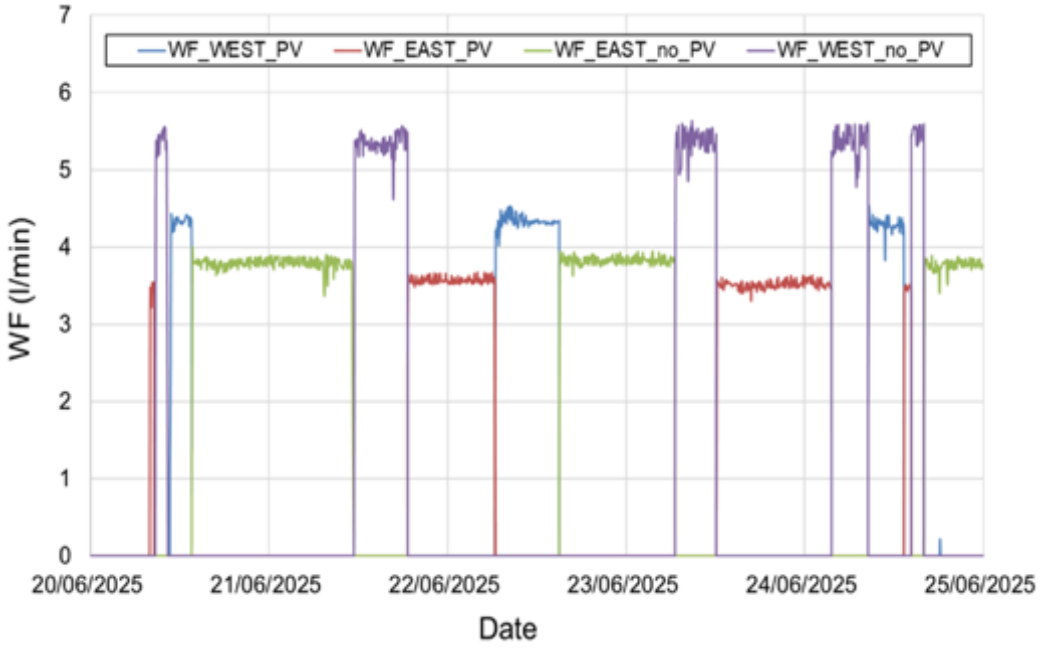

Figure 160. Irrigation data by sector.

Irrigation monitoring began on April 19, 2025. During this period, three cultivation cycles were carried out: the first with zucchini (April–May), the second with tomatoes and eggplants (May–August), and the third with lettuce (September).

Table 74. Water consumption per crop and percentage variation compared to the reference.

	PV (liter)	Ref (liter)	Δ (%)
Zucchini	8188	10154	-19.4
Tomato	181369	397450	-54.4
Eggplant	337036	286613	17.6
Lettuce	35190	42206	-16.6

Funded by the European Union

Funded by the European Union under Grant Agreement No 101096056. Views and opinions expressed are however those of the author(s) only and do not necessarily reflect those of the European Union or CINEA. Neither the European Union nor the granting authority can be held responsible for them.

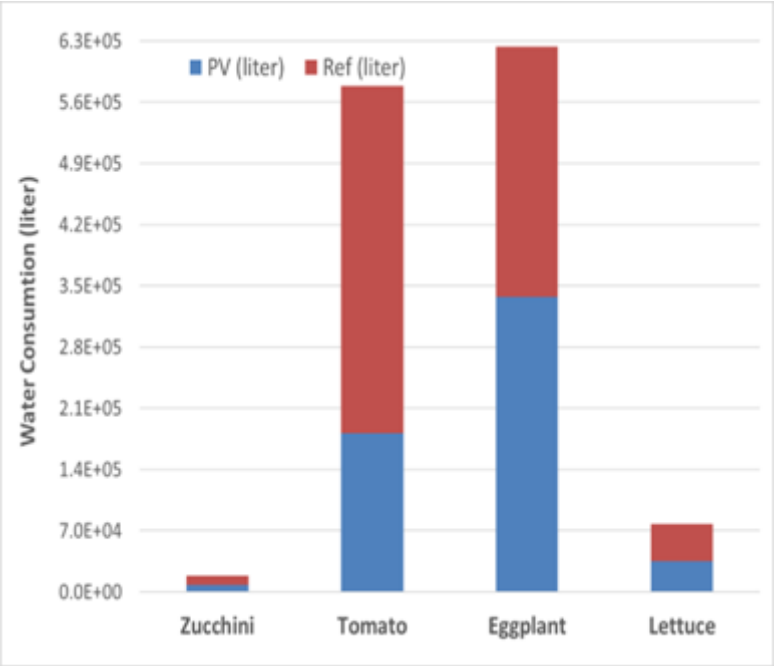

Figure 161. Water consumption per crop.

From the data reported in Table 74 and illustrated in Figure 161, it can be observed that all crops — except eggplants — benefited from the shading effect of the photovoltaic panels, resulting in a water consumption reduction between 15% and 55%.

Eggplants, on the other hand, consumed about 18% more water over the entire cultivation cycle. This is most likely due to the fact that eggplants were grown in the western section of the greenhouse, which receives more sunlight during the summer period.

Water Use Efficiency (WUE) was also calculated from crop yield data and recorded water consumption data, and the results are shown in Table 75. WUE was calculated as the ratio between the fresh weight per square meter for each sector and the total water supplied per square meter to the corresponding sector.

Table 75. Water Use Efficiency at FSC.

	WUE_PV (g/liter)	WUE_ref (g/liter)
Zucchini (1st cycle)	5.05	5.02
Tomato (2nd cycle)	0.12	0.06
Eggplant (2nd cycle)	0.37	0.53
Lettuce (3rd cycle)	2.28	1.96

Funded by the European Union

Funded by the European Union under Grant Agreement No 101096056. Views and opinions expressed are however those of the author(s) only and do not necessarily reflect those of the European Union or CINEA. Neither the European Union nor the granting authority can be held responsible for them.

Economic Analysis at FSC

The Italian pilot greenhouse (FSC) is connected to the grid for the sale of electricity. Thanks to this connection, it is possible to carry out economic analyses of the overall performance of the greenhouse, both in terms of electricity generation and plant production.

The data collected so far, although they do not represent a full year of observation, allow for a preliminary evaluation. Before presenting and analysing the data, a few premises must be made, as outlined below:

1. The photovoltaic yield extends from March to September (inclusive). Therefore, it was necessary to extrapolate data for the missing months, based on a typical yield for the area where the greenhouse is located, and to correct it with the measured values. In Figure 162 is shown the result of this extrapolation (light green the extrapolated values, green the measured one.)

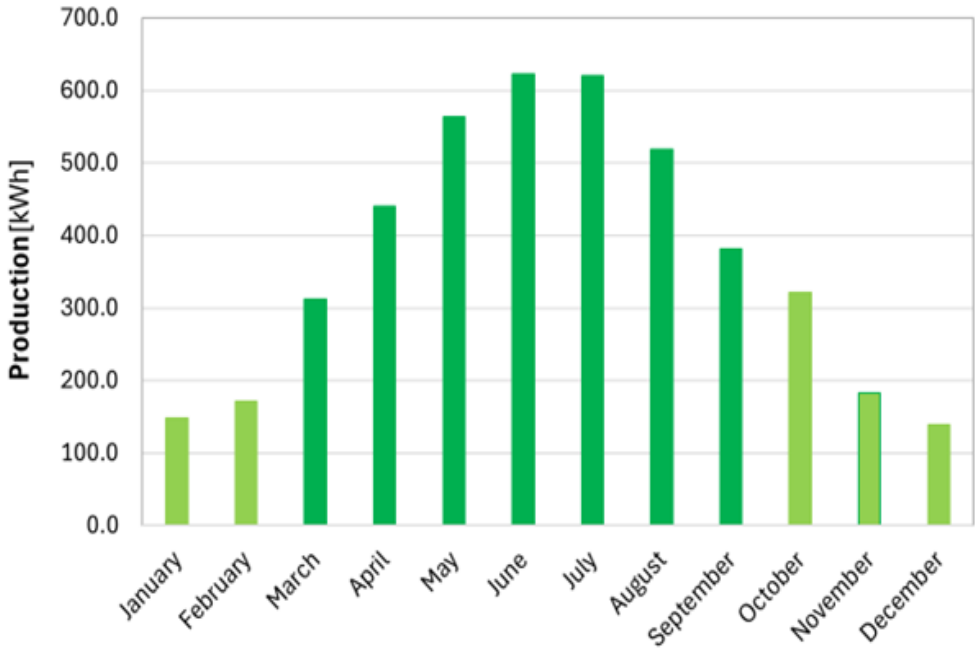

Figure 162. Extrapolated photovoltaic production for the entire year.

2. The economic analysis was based on two indicators: ROI (Return on Investment) and NPV (Net Present Value). ROI measures the efficiency and profitability of an investment, indicating the gain achieved relative to its initial cost. NPV, on the other hand, is a financial metric used to assess the profitability of an investment by discounting future cash flows to their present value. A positive NPV indicates a potentially profitable investment, while a negative NPV suggests that the investment may not be advantageous.
3. ROI and NPV were evaluated based on two scenarios of electricity use, Total self-consumption of the produced energy, and Grid exchange, through the Italian “Scambio sul Posto” contractual scheme.

Funded by the European Union

Funded by the European Union under Grant Agreement No 101096056. Views and opinions expressed are however those of the author(s) only and do not necessarily reflect those of the European Union or CINEA. Neither the European Union nor the granting authority can be held responsible for them.

4. Self-consumption was estimated, on average for the farm, based on electricity bills at about €0.30/kWh, including taxes but excluding fixed costs related to the POD (Point of Delivery).
5. The second tariff, €0.16/kWh, corresponds to one of the available rates in Italy for the sale of electricity.
6. Agricultural production data refers to the experimental results obtained within the greenhouse.
7. The selling prices of agricultural products (lettuce, eggplants, tomatoes, and zucchini) were provided by the fruit and vegetable market of the Province of Latina.

With these premises, we can proceed to the economic analysis of the Italian greenhouse.

The total cost of the photovoltaic system was estimated at approximately €3,740. This cost includes modules, inverter, mounting structure, electrical components, design, project management, testing, installation, and grid connection, all the costs are reported in Figure 163.

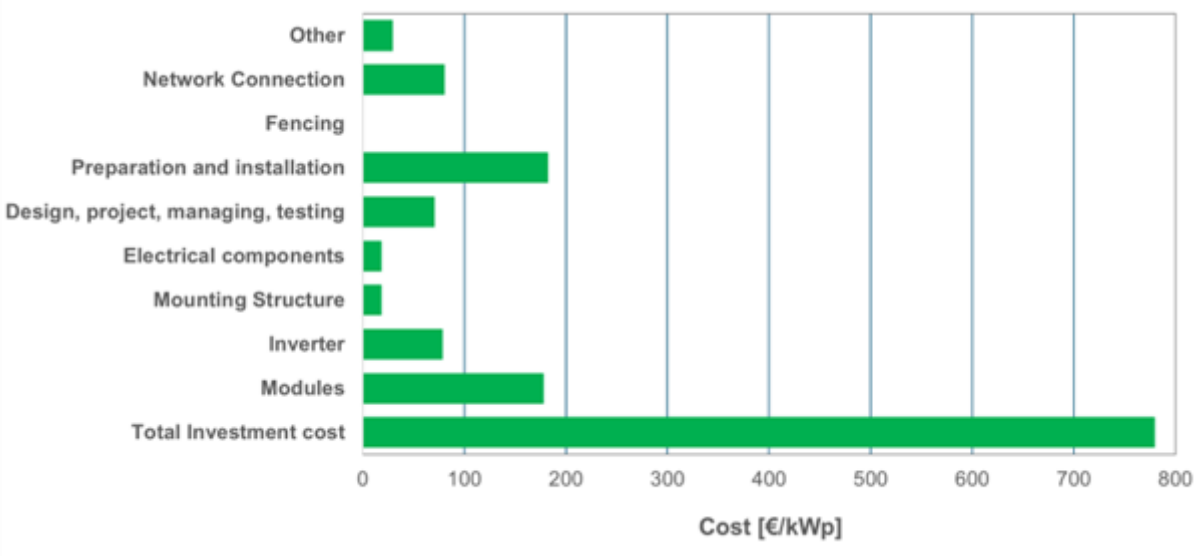

Figure 163. Average costs for REGACE installations 3.96 kWp per 100 m^2.

The total electricity production during the operational period (March–September) was 3,460 kWh, while the estimated annual production amounts to 4,423 kWh, according to Figure 162.

Table 76 summarizes the revenue for the two tariffs taken into account for the FSC and the Return of the Investment (ROI).

Table 76. ROI of the PV system in Italy.

	Self-Consumption	**"Scambio sul posto"**
Tariff [€/kWh]	0.30	0.16
Revenue [€]	1326.92	707.69
ROI (%)	35.47	18.92

Funded by the European Union

Funded by the European Union under Grant Agreement No 101096056. Views and opinions expressed are however those of the author(s) only and do not necessarily reflect those of the European Union or CINEA. Neither the European Union nor the granting authority can be held responsible for them.

It should be noted that in the case of self-consumption (Table 76), the corresponding "Revenue" value must be understood as the savings on electricity not purchased and therefore not paid for.

Even more interesting are the NPV results shown in table 77.

Table 77. NPV of the PV system in Italy.

	Self-Consumption	"Scambio sul posto"
Tariff [€/kWh]	0.30	0.16
Revenue [€]	1326.92	707.69
NPV (Year)	4	8

It can be observed that in the case of self-consumption, the NPV payback period is only four years, while under the "Scambio sul Posto" scheme, the value practically doubles. This means that profits are achieved from the fourth year in the self-consumption scenario, and after eight years with the second tariff.

Self-consumption is a feasible practice on the farm, as the main electricity demands are almost perfectly aligned with solar production.

The last analysis carried out is the combined evaluation of agricultural and electrical production. Table 78 shows the average selling prices per kilogram, and the production quantities in kilograms.

Table 78. Average selling price of products and crop production in kg.

	Ave Price [€/kg]	PV [kg]	No-PV [kg]	Δ [%]
Lettuce (1st cycle)	1	101.3	116	-12.7
Zucchini (1st cycle)	1	41.4	51	-18.8
Tomato (2nd cycle)	1.2	21.604	23.81	-9.3
Eggplant (2nd cycle)	0.9	124.788	153.284	-18.6
Lettuce (3rd cycle)	1	80.34	82.62	-2.8

Based on the data in Tables 78 the Net Revenue was calculated for the two tariff scenarios and presented in Table 79, although there is a decrease in plant production and consequently a reduction in revenues from the sale of agricultural products this does not significantly affect the income derived from the use or sale of electricity produced by the photovoltaic system.

Since the experimental period for crop cultivation was limited, it is not possible to recalculate the NPV and ROI by also considering the losses due to reduced agricultural production. However, it is reasonable to assume that the updated results would not differ substantially from those presented in Table 72.

Funded by the European Union

Funded by the European Union under Grant Agreement No 101096056. Views and opinions expressed are however those of the author(s) only and do not necessarily reflect those of the European Union or CINEA. Neither the European Union nor the granting authority can be held responsible for them.

Table 79. Net revenue of the Italian pilot greenhouse.

		PV [€]	No-PV [€]	Δ [€]	Energy Production [kWh]	Revenue [€]	Net Revenue [€]
Self-Consumption	Lettuce (1st cycle)	101.30	116.00	-14.7	376.22	112.87	98.17
	Zucchini (1st cycle)	41.40	51.00	-9.6	658.10	197.43	187.83
	Tomato (2nd cycle)	25.93	28.57	-2.6	881.29	264.39	261.74
	Eggplant (2nd cycle)	112.31	137.96	-25.6	881.29	264.39	238.74
	Lettuce (3rd cycle)	80.34	82.62	-2.3	190.64	57.19	54.91
Scambio sul Posto	Lettuce (1st cycle)	101.30	116.00	-14.7	376.22	60.20	45.50
	Zucchini (1st cycle)	41.40	51.00	-9.6	658.10	105.30	95.70
	Tomato (2nd cycle)	25.92	28.57	-2.6	881.29	141.01	138.36
	Eggplant (2nd cycle)	112.31	137.96	-25.6	881.29	141.01	115.36
	Lettuce (3rd cycle)	80.34	82.62	-2.3	190.64	30.50	28.22

5.3 Characterisation of produce quality

While the previous chapter focussed on crop performance, this chapter addresses the produce quality assessment of BOKU university. As such we regard first of all nutritive and health promoting compounds such as carbohydrates, organic acids, and carotenoids, as well as contaminants, first of all nitrate. Because this kind of chemical analysis (including the preparation and conservation of materials for transport) was only available for a few institutes, other parameters for the characterisation of produce quality such as sensory panel tests (by untrained panels) and proceeds from sale (if there were differences among the variants) were considered.

Samples from the second harvest at the end of each of the BOKU experiments were used for quality analysis of the harvested material. Freeze drying (Alpha 1-2 LDplus from Christ and Lyovapor™ L-250 from Büchi) was used as the drying method for the analysis of constituents. After freeze drying, the samples were weighed again to determine their water content. A coffee grinder from CASO Coffee & Kitchen Flavour (model SP-7437) was used to grind the freeze-dried samples. The samples were stored in a desiccator with drying beads from Carl Roth GmbH & Co. KG in a dark place until analysis.

Three different extracts were produced from the freeze-dried and ground samples using metaphosphoric acid, ethanol and water extraction. Metaphosphoric acid extraction was carried out to determine the ascorbic acid content according to Akhtar et al. (2010).

Ethanol extraction was required for the analysis of chlorophylls, carotenoids, total phenols, total flavonoids, anthocyanins, and antioxidant capacity. Chlorophyll and carotenoid contents were determined spectrophotometrically (Agilent Cary 60 UV-Vis) according to Sumanta et al. (2014) using ethanol. Total polyphenol content was determined colourimetrically using Folin-Ciocalteu reagent and

Funded by the European Union

Funded by the European Union under Grant Agreement No 101096056. Views and opinions expressed are however those of the author(s) only and do not necessarily reflect those of the European Union or CINEA. Neither the European Union nor the granting authority can be held responsible for them.

flavonoid content was determined spectrophotometrically, both according to Keutgen & Pawelzik (2007). The anthocyanin content was measured using the pH differential method according to Giusti & Wrolstad (2001). The antioxidant capacity of the samples was determined using the FRAP method modified according to Keutgen & Pawelzik (2007).

The water extraction was used to determine the nitrate, soluble sugar and organic acid content. Nitrate content was measured using a reagent mixture consisting of N-(1-Naphthyl)ethylenediamine dihydrochloride (NNED) solution, sulfanilic acid solution, and a vanadium (III) chloride solution following the preparation of a standard curve.

The soluble carbohydrates were determined by HPLC using a pre-column and the sugar column (Sigmaaldrich, LiChrospher 100 NH2 (5 µm) LiChroCart® 250-4). The eluents were 80% acetonitrile and 20% deionised water. Detection was performed using a refractive index detector (Agilent Technologies G7162A 1260 RID Serial No. DEAC901760).

The organic acids were determined in the same way as the carbohydrates. A pre-column (Hi-Plex H, 50 x 7.7 mm, 8 µm guard column) and a main column (Hi-Plex H, 300 x 7.7 mm, 8 µm HPLC column) were used for this purpose. The eluent was deionised water plus 555 µL/L H_2SO_4. The organic acids were detected using a UV detector (Agilent Technologies G7114A 1260 VWD Serial No. DEACX07920).

A. Experiments with CO_2Bags

1. Experiment Basil 17/05/ - 15/06/2023 and 06/02/ - 21/03/2024

In the first experiment on basil, the sensory panel test revealed different results for the 2023 and 2024 experiments. In both cases the controls received the best ranking, but in 2023 the variant “shading” was rated better than the variant “shading & CO_2Bags”, while in 2024 it was just the opposite (Table 80).

Table 80. Relative taste evaluation of basil leaves cultivated under “shading” (s), “shading & CO_2Bags” (s & b) and “control” conditions.

	K3 (s)	K4 (s & b)	K5 (con)
Taste exp. 2023			
Taste exp. 2024			

Photosynthetic leaf pigments revealed differences between the variants (Table 81): Total chlorophyll (Chl) content was generally largest in the variant “shading & CO_2Bags” (K4), followed by “shading” (K3), and least in the “control” (K5), whereby the differences between K3 and K5 were less distinct in 2024. The Chl

Funded by the European Union

Funded by the European Union under Grant Agreement No 101096056. Views and opinions expressed are however those of the author(s) only and do not necessarily reflect those of the European Union or CINEA. Neither the European Union nor the granting authority can be held responsible for them.

a/b ratio responded inconsistently. While both shaded variants had similar ratios, the "control" variants were significantly different. However, in 2023 the Chl a/b ratio of the "control" variants was significantly smaller, in 2024 larger than for the shaded variants. As for Chl content, carotenoid (Car) content was largest in the variant "shading & CO_2Bags" and smallest in the "control".

Table 81. Photosynthetic pigments of the experiments 17/05/-15/06/2023 (prefix 1) and 06/02/-21/03/2024 (prefix 2; S, shading; b, CO_2Bags; con, control).

	Car [g/kg]	Chl a [g/kg]	Chl b [g/kg]	Tot Chl [g/kg]	Chl a/b [--]
1-K3 (s)	0.22 ± 0.04 d	1.68 ± 0.34 c	1.29 ± 0.25 d	2.97 ± 0.59 d	1.30 ± 0.02 b
1-K4 (s & b)	0.49 ± 0.04 c	5.00 ± 0.56 a	3.79 ± 0.53 b	8.79 ± 1.09 ab	1.33 ± 0.06 ab
1-K5 (con)	0.07 ± 0.01 e	0.63 ± 0.07 d	0.57 ± 0.05 e	1.20 ± 0.13 e	1.09 ± 0.03 c
2-K3 (s)	1.51 ± 0.25 a	3.90 ± 0.71 b	3.39 ± 0.40 bc	7.28 ± 0.95 bc	1.15 ± 0.17 bc
2-K4 (s & b)	1.72 ± 0.14 a	5.52 ± 1.31 a	4.59 ± 1.00 a	10.11 ± 2.27 a	1.20 ± 0.11 bc
2-K5 (con)	0.88 ± 0.35 b	3.76 ± 0.54 b	2.91 ± 0.63 c	6.66 ± 0.99 c	1.32 ± 0.19 a
$P_{Lilliefors}$	0.002	>0.200	0.075	0.013	0.004
$P_{Shapiro-Wilk}$	0.001	0.008	0.001	0.002	0.000
P_{Levene}	0.021	0.007	0.106	0.027	0.015
Post-hoc	Median	Tamhane	Tukey-B	Median	Median

Different letters within a column indicate significant differences.

Table 82. Flavonoid, phenol, vitamin C and nitrate content as well as antioxidative capacity of basil leaves of the experiments 17/05/-15/06/2023 (prefix 1) and 06/02/-21/03/2024 (prefix 2; S, shading; b, CO_2Bags; con, control).

	Flavonoids [g/kg]	Phenols [g/kg]	Vit. C [g/kg]	Nitrate [mg/kg]	Antiox. capacity [mmol/g]
1-K3 (s)	13.4 ± 3.9 c	0.64 ± 0.07 bc	1.3 ± 0.2 b	0.05 ± 0.01 e	0.12 ± 0.02 c
1-K4 (s & b)	36.2 ± 7.4 b	0.89 ± 0.09 a	1.3 ± 0.5 b	0.09 ± 0.03 d	0.21 ± 0.02 a
1-K5 (con)	8.1 ± 3.9 c	0.48 ± 0.06 c	1.3 ± 0.3 b	0.06 ± 0.03 de	0.08 ± 0.02 d
2-K3 (s)	45.7 ± 5.7 ab	0.94 ± 0.10 a	1.2 ± 0.2 b	1.59 ± 0.78 b	0.17 ± 0.02 b
2-K4 (s & b)	49.0 ± 3.7 a	0.85 ± 0.05 ab	1.3 ± 0.2 b	3.73 ± 0.61 a	0.15 ± 0.02 b
2-K5 (con)	40.1 ± 4.2 b	0.88 ± 0.06 a	1.9 ± 0.2 a	0.50 ± 0.18 c	0.16 ± 0.02 b
$P_{Lilliefors}$	0.000	0.000	0.017	0.000	>0.200
$P_{Shapiro-Wilk}$	0.000	0.002	0.016	0.000	0.953
P_{Levene}	0.023	0.215	0.001	0.000	0.554
Post-hoc	Median	Kruskal-Wallis	Tukey-B	Median	Tukey-B

Different letters within a column indicate significant differences.

In 2023, antioxidative capacity was largest in the variant "shading & CO_2Bags" and smallest in the "control", whereas in 2024 significant differences were not observed (Table 82). A similar statistical

Funded by the European Union

Funded by the European Union under Grant Agreement No 101096056. Views and opinions expressed are however those of the author(s) only and do not necessarily reflect those of the European Union or CINEA. Neither the European Union nor the granting authority can be held responsible for them.

pattern was observed for phenol content, with reservations for flavonoid content, indicating that antioxidative capacity of basil leaves was mainly determined by phenolic compounds. Vitamin C content was stable, with the exception of the "control" variant in 2024 being largest (Table 82). Nitrate content differed distinctly among years, being very low in 2023. In 2024, nitrate content was largest in variant "shading & CO_2Bags" (K4), medium in "shading" (K3), and smallest in the "control" treatment (K5).

Flavour-relevant organic acids are compounds such as citric acid, malic acid, and tartaric acid, which are found in many foods and give them their characteristic sour taste (Table 83). While citric acid provides a clear, sour taste, malic acid has a softer character, and tartaric acid adds a sharp note reminiscent of grapes. Oxalic acid is an antinutritive substance as it binds to essential minerals like calcium, magnesium, and iron, forming insoluble compounds that prevent their absorption by the body. In small amounts it is present in many plants. Maleic acid itself has a gritty, chalky taste. Maleic acid plays diverse roles in plants, acting as a signaling molecule to recruit beneficial bacteria and inhibiting fungal pathogens like *Sclerotinia*. Fumaric acid has a sour, tart, fruity-sour taste that is long-lasting and persistent, often described as a very sharp acidity, being stronger than that of citric acid.

Table 83. Organic acids content of basil leaves of the experiments 17/05/-15/06/2023 (prefix 1) and 06/02/-21/03/2024 (prefix 2; S, shading; b, CO_2Bags; con, control).

	Oxalic acid [g/kg]	Citric acid [g/kg]	Tartaric acid [g/kg]	Maleic acid [g/kg]	Malic acid [g/kg]	Fumaric acid [mg/kg]
1-K3 (s)	2.62 ± 0.37 a	2.7 ± 5.4 b	7.16 ± 0.86 abc	0.82 ± 0.14 ab	11.6 ± 1.7 e	0.11 ± 0.11 b
1-K4 (s & b)	1.41 ± 0.22 b	1.4 ± 2.8 b	8.61 ± 1.26 ab	0.20 ± 0.07 c	17.9 ± 1.6 dc	0.15 ± 0.02 a
1-K5 (con)	2.02 ± 0.80 ab	14.7 ± 6.2 a	5.61 ± 2.31 c	0.60 ± 0.21 b	9.0 ± 5.4 e	0.01 ± 0.03 d
2-K3 (s)	1.41 ± 0.43 b	1.5 ± 0.9 b	7.68 ± 0.54 ab	0.57 ± 0.16 b	33.4 ± 7.7 a	0.26 ± 0.18 a
2-K4 (s & b)	1.81 ± 0.98 ab	2.2 ± 1.0 b	9.94 ± 2.54 a	0.01 ± 0.04 d	28.7 ± 4.1 abc	0.22 ± 0.15 a
2-K5 (con)	1.51 ± 0.42 a	10.4 ± 5.9 ab	6.67 ± 1.50 bc	0.96 ± 0.12 a	22.7 ± 4.5 bcd	0.07 ± 0.01 c
$P_{Lilliefors}$	>0.200	0.000	0.021	0.006	>0.200	0.000
$P_{Shapiro-Wilk}$	0.409	0.000	0.002	0.000	0.423	0.000
P_{Levene}	0.032	0.002	0.003	0.023	0.007	0.006
Post-hoc	Tamhane	Median	Median	Median	Tamhane	Kruskal-Wallis

Different letters within a column indicate significant differences.

To simplify interpretation, the annual effect was not taken into account (Table 84). The results indicate very low concentrations of citric acid in the shaded variants, which might have contributed to their worse taste. By contrast, malic and fumaric acid were highest under shade conditions. In fact, the latter three organic acids are part of the citrate cycle and the accumulation of either citric or malic and fumaric acid may indicate an adequate or undersupply with NADPH and ATP due to the shading conditions, leading to the consumption of citric acid and accumulation of malic and fumaric acid. Consistent differences in the antinutritive compound oxalic acid were not observed.

Funded by the European Union under Grant Agreement No 101096056. Views and opinions expressed are however those of the author(s) only and do not necessarily reflect those of the European Union or CINEA. Neither the European Union nor the granting authority can be held responsible for them.

Table 84. As is Table 83, but the effect of year is not considered.

	Oxalic acid [g/kg]	Citric acid [g/kg]	Tartaric acid [g/kg]	Maleic acid [g/kg]	Malic acid [g/kg]	Fumaric acid [mg/kg]
K3 (s)	1.96 ± 0.73 a	2.0 ± 3.5 b	7.45 ± 0.73 b	0.69 ± 0.20 a	23.6 ± 12.5 ab	0.19 ± 0.17 a
K4 (s & b)	1.61 ± 0.72 a	1.9 ± 2.0 b	9.34 ± 2.13 a	0.10 ± 0.11 b	23.9 ± 6.4 a	0.19 ± 0.12 a
K5 (con)	1.73 ± 0.65 a	13.0 ± 6.2 a	6.20 ± 1.93 b	0.80 ± 0.24 a	16.6 ± 8.5 b	0.04 ± 0.04 b
$P_{Lilliefors}$	>0.200	0.000	0.021	0.006	>0.200	0.000
$P_{Shapiro-Wilk}$	0.409	0.000	0.002	0.000	0.423	0.000
P_{Levene}	0.613	0.000	0.015	0.137	0.000	0.010
Post-hoc	ANOVA	Median	Median	Kruskal-Wallis	Tamhane	Median

Different letters within a column indicate significant differences.

Carbohydrate content was elevated in the variant "shading & CO_2Bags" (K4), especially in the case of glucose (Tables 85-86), which should result in a sweeter taste. Significant differences between the "shading" and "control" variants were not observed.

Table 85. Carbohydrate content of basil leaves of the experiments 17/05/-15/06/2023 (prefix 1) and 06/02/-21/03/2024 (prefix 2; S, shading; b, CO_2Bags; con, control).

	Glucose [mg/kg]	Fructose [mg/kg]	Sum [mg/kg]
1-K3 (s)	14.5 ± 5.2 d	12.8 ± 4.4 ab	27.3 ± 9.6 b
1-K4 (s & b)	37.1 ± 9.3 b	14.2 ± 2.5 a	51.3 ± 11.7 ab
1-K5 (con)	14.0 ± 4.5 d	13.9 ± 3.7 a	27.9 ± 8.2 b
2-K3 (s)	32.8 ± 10.9 bc	6.8 ± 1.8 b	39.7 ± 11.3 ab
2-K4 (s & b)	74.2 ± 16.2 a	13.3 ± 2.4 a	87.6 ± 17.1 a
2-K5 (con)	23.9 ± 4.6 c	7.8 ± 2.0 b	31.6 ± 5.4 b
$P_{Lilliefors}$	0.000	0.008	0.000
$P_{Shapiro-Wilk}$	0.000	0.006	0.000
P_{Levene}	0.035	0.168	0.209
Post-hoc	Median	Kruskal-Wallis	Kruskal-Wallis

Different letters within a column indicate significant differences.

In summary, the carbohydrates would favour the variant "shading & CO_2Bags" (K4), whereas organic acids would support the "control" (K5), not taking into account a balanced sugar-acid ratio. None of the variants is unequivocally preferable in terms of the phenolic components and vitamin C content, but the higher nitrate content tends to argue against the variant "shading & CO_2Bags" (K4). However, this criterion is offset by at least partially higher chlorophyll and carotenoid contents. This evaluation supports the result of the 2024 sensory panel test, but cannot explain why in 2023 the variant "shading" (K3) was rated superior to "shading & CO_2Bags" (K4).

Funded by the European Union under Grant Agreement No 101096056. Views and opinions expressed are however those of the author(s) only and do not necessarily reflect those of the European Union or CINEA. Neither the European Union nor the granting authority can be held responsible for them.

Funded by the European Union

Table 86. As is Table 6, but effect of year not considered).

	Glucose [mg/kg]	Fructose [mg/kg]	Sum [mg/kg]
K3 (s)	21.6 ± 11.9 b	10.5 ± 4.6 ab	32.1 ± 11.6 b
K4 (s & b)	57.5 ± 23.1 a	13.8 ± 2.5 a	71.3 ± 23.5 a
K5 (con)	20.0 ± 6.6 b	10.2 ± 4.1 b	30.2 ± 6.7 b
$P_{Lilliefors}$	0.000	0.008	0.000
$P_{Shapiro-Wilk}$	0.000	0.006	0.000
P_{Levene}	0.000	0.000	0.000
Post-hoc	Median	Median	Median

2. Experiment *Capsicum annuum* L. 23/03/ - 15/08/2023

Taste and visual appearance were rated by a sensory panel test, which revealed generally better results for the "control" variants of the three examined *Capsicum* cvs (Table 87). In the two bell pepper cvs Bendigo and California Wonder differences between the two shaded variants could not be detected, but in 'De Cayenne" pepper the shading variant (K3) was rated worst (Table 87).

Table 87. Relative visual and taste evaluations of fruits of *C. annuum* cvs Bendigo, California Wonder, and De Cayenne produced under "shading" (s), "shading & CO_2Bags" (s & b) and "control" conditions.

	K3 (s)	K4 (s & b)	K5 (con)
Taste & visual appearance cv. Bendigo			
Taste & visual appearance cv. California Wonder			
Taste & visual appearance cv. De Cayenne			

Table 88. Chlorophyll and carotenoid contents of fruits of cv. Bendigo in addition to Brix values of the fruit sap (S, shading; b, CO_2Bags; con, control).

	Car [g/kg]	Chl a [g/kg]	Chl b [g/kg]	Tot Chl [g/kg]	Chl a/b [--]	Brix [°]
K3 (s)	0.57 ± 0.12 a	0.52 ± 0.11 a	0.60 ± 0.09 a	1.12 ± 0.19 a	0.87 ± 0.05 a	4.5 ± 0.8 b
K4 (s & b)	0.56 ± 0.16 a	0.52 ± 0.14 a	0.59 ± 0.11 a	1.11 ± 0.25 a	0.87 ± 0.09 a	5.5 ± 1.4 ab
K5 (con)	0.31 ± 0.09 b	0.29 ± 0.08 b	0.43 ± 0.06 b	0.72 ± 0.14 b	0.67 ± 0.07 b	6.2 ± 0.7 a
$P_{Lilliefors}$	>0.200	>0.200	>0.200	>0.200	>0.200	> 0.200
$P_{Shapiro-Wilk}$	0.683	0.683	0.607	0.670	0.432	0.079
P_{Levene}	0.484	0.487	0.587	0.529	0.795	0.170
Post-hoc	Duncan	Duncan	Duncan	Duncan	Tukey	Tukey-B

Different letters within a column indicate significant differences.

Funded by the European Union

Funded by the European Union under Grant Agreement No 101096056. Views and opinions expressed are however those of the author(s) only and do not necessarily reflect those of the European Union or CINEA. Neither the European Union nor the granting authority can be held responsible for them.

The Chl content of pepper fruit is first of all a sign of the ripening stage. Lower Chl contents as in the case of the "control" variant in cvs. Bendigo indicates a delayed ripening of shaded plants (Table 88-90). By contrast, elevated carotenoid concentrations suggest a less advanced ripening process. Interestingly, the Brix value measured for the bell pepper varieties was less susceptible to ripening. Only in the case of 'Bendigo', a significant difference between the "control" (K5) and the "shading" variant (K3) was observed.

Table 89. Chlorophyll and carotenoid of fruits of cv. California Wonder in addition to Brix values of the fruit sap (S, shading; b, CO_2Bags; con, control).

	Car [g/kg]	Chl a [g/kg]	Chl b [g/kg]	Tot Chl [g/kg]	Chl a/b [--]	Brix [°]
K3 (s)	0.65 ± 0.18 a	0.60 ± 0.16 a	0.65 ± 0.13 a	1.25 ± 0.29 a	0.90 ± 0.07 a	5.0 ± 1.0 a
K4 (s & b)	0.66 ± 0.18 a	0.61 ± 0.16 a	0.66 ± 0.13 a	1.27 ± 0.29 a	0.91 ± 0.07 a	6.5 ± 1.2 a
K5 (con)	0.37 ± 0.23 a	0.36 ± 0.22 a	0.66 ± 0.50 a	1.01 ± 0.70 a	0.58 ± 0.19 a	6.1 ± 0.9 a
$P_{Lilliefors}$	>0.200	>0.200	0.193	>0.200	0.003	>0.200
$P_{Shapiro-Wilk}$	0.399	0.377	0.023	0.692	0.008	0.854
P_{Levene}	0.379	0.331	0.065	0.256	0.137	0.661
Post-hoc	ANOVA	Duncan	Duncan	Duncan	Kruskal-Wallis	ANOVA

Different letters within a column indicate significant differences.

Table 90. Chlorophyll and carotenoid in addition to Brix values of fruits of cv. De Cayenne (S, shading; b, CO_2Bags; con, control).

	Car [g/kg]	Chl a [g/kg]	Chl b [g/kg]	Tot Chl [g/kg]	Chl a/b [--]
K3 (s)	0.56 ± 0.30 a	0.52 ± 0.27 a	0.58 ± 0.21 a	1.10 ± 0.48 a	0.83 ± 0.26 a
K4 (s & b)	0.32 ± 0.31 a	0.30 ± 0.28 a	0.41 ± 0.20 a	0.71 ± 0.48 a	0.63 ± 0.26 a
K5 (con)	0.13 ± 0.00 a	0.13 ± 0.00 a	0.28 ± 0.00 a	0.41 ± 0.01 a	0.45 ± 0.01 a
$P_{Lilliefors}$	0.000	0.000	0.000	0.000	0.008
$P_{Shapiro-Wilk}$	0.001	0.001	0.001	0.001	0.002
P_{Levene}	0.484	0.487	0.587	0.529	0.795
Post-hoc	Kruskal-Wallis	Kruskal-Wallis	Kruskal-Wallis	Kruskal-Wallis	Kruskal-Wallis

Different letters within a column indicate significant differences.

Table 91. Flavonoid, phenol, and nitrate content as well as antioxidative capacity of fruits of cv. Bendigo (S, shading; b, CO_2Bags; con, control).

	Flavonoids [g/kg]	Phenols [g/kg]	Antiox. capacity [mmol/g]	Nitrate [g/kg]
K3 (s)	6.9 ± 2.3 a	0.41 ± 0.06 ab	0.06 ± 0.02 b	0.32 ± 0.22 a
K4 (s & b)	9.0 ± 3.5 a	0.33 ± 0.04 b	0.07 ± 0.05 b	0.54 ± 0.34 a
K5 (con)	11.2 ± 3.2 a	0.50 ± 0.04 a	0.14 ± 0.04 a	0.52 ± 0.26 a
$P_{Lilliefors}$	>0.200	>0.200	>0.200	>0.200
$P_{Shapiro-Wilk}$	0.260	0.497	0.619	0.333
P_{Levene}	0.790	0.665	0.214	0.779
Post-hoc	ANOVA	Tukey	Tukey	ANOVA

Different letters within a column indicate significant differences.

Funded by the European Union

Funded by the European Union under Grant Agreement No 101096056. Views and opinions expressed are however those of the author(s) only and do not necessarily reflect those of the European Union or CINEA. Neither the European Union nor the granting authority can be held responsible for them.

Flavonoid content tended to be highest in the "control" variant, while in the case of total phenol content differences could not be detected. Antioxidative capacity was highest in the "control" variant as well. Nitrate content did not differ significantly among variants (Tables 91-93).

Table 92. Flavonoid, phenol, and nitrate content as well as antioxidative capacity of fruits of cv. California Wonder (S, shading; b, CO_2Bags; con, control).

	Flavonoids [g/kg]	Phenols [g/kg]	Antiox. capacity [mmol/g]*	Nitrate [g/kg]
K3 (s)	6.3 ± 0.9 b	0.37 ± 0.06 a	0.04 ± 0.02 b	0.41 ± 0.48 a
K4 (s & b)	7.2 ± 1.3 b	0.36 ± 0.09 a	0.04 ± 0.01 b	0.79 ± 0.32 a
K5 (con)	11.2 ± 0.8 a	0.44 ± 0.12 a	0.15 ± 0.04 a	0.40 ± 0.13 a
$P_{Lilliefors}$	0.132	0.146	0.143	0.100
$P_{Shapiro-Wilk}$	0.111	0.238	0.078	0.111
P_{Levene}	0.399	0.199	0.535	0.193
Post-hoc	Tukey	ANOVA	Tukey	ANOVA

* Transformation: f(x) = ln(x); Different letters within a column indicate significant differences.

Table 93. Flavonoid, phenol, and nitrate content as well as antioxidative capacity of fruits of cv. De Cayenne (S, shading; b, CO_2Bags; con, control).

	Flavonoids [g/kg]	Phenols [g/kg]*	Antiox. capacity [mmol/g]	Nitrate [g/kg]
K3 (s)	9.4 ± 4.2 b	0.51 ± 0.31 a	0.07 ± 0.04 b	0.43 ± 0.35 a
K4 (s & b)	14.6 ± 3.5 ab	0.38 ± 0.09 a	0.09 ± 0.03 ab	0.41 ± 0.15 a
K5 (con)	18.8 ± 4.8 a	0.47 ± 0.04 a	0.13 ± 0.01 a	0.68 ± 0.38 a
$P_{Lilliefors}$	0.181	>0.200	0.099	>0.200
$P_{Shapiro-Wilk}$	0.404	0.183	0.037	0.498
P_{Levene}	0.865	0.096	0.188	0.152
Post-hoc	Tukey	ANOVA	Tukey	ANOVA

* Transformation: f(x) = ln(x); Different letters within a column indicate significant differences.

In summary, quality parameters examined in the three cvs of *Capsicum annuum* did not reveal distinct effects among the variants, but point towards a clear trend favouring the "control" variant (K5) over the variant "shading & CO_2Bags" (K4) over "shading" (K3).

3. Experiment *Capsicum annuum* L. cv. California Wonder from 23/03/ - 15/08/2023 and 06/03/ - 31/08/24: comparison of fruit quality parameters

The overall fruit quality of 'California Wonder' bell pepper was consistently rated by a sensory panel, being best in the "control" variant, while differences between the two shading variants could not be detected (Table 94).

Funded by the European Union

Funded by the European Union under Grant Agreement No 101096056. Views and opinions expressed are however those of the author(s) only and do not necessarily reflect those of the European Union or CINEA. Neither the European Union nor the granting authority can be held responsible for them.

Table 94. Relative visual and taste evaluations of fruits of *C. annuum* cv. California Wonder produced under "shading" (s), "shading & CO_2Bags" (s & b) and "control" conditions in the 2023 and 2024 experiments.

	K3 (s)	K4 (s & b)	K5 (con)
Taste & visual appearance 2023			
Taste & visual appearance 2024			

Table 95. Chlorophyll and carotenoid contents of fruits of cv. California Wonder of experiments 23/03/-15/08/2023 (prefix 1) and 06/03/-31/08/2024 (prefix 2; S, shading; b, CO_2Bags; con, control).

	Car [g/kg]	Chl a [g/kg]	Chl b [g/kg]	Tot Chl [g/kg]	Chl a/b [--]
1-K3 (s)	0.65 ± 0.18 a	0.60 ± 0.16 ab	0.65 ± 0.13 b	1.25 ± 0.29 ab	0.90 ± 0.07 a
1-K4 (s & b)	0.66 ± 0.18 a	0.61 ± 0.16 ab	0.66 ± 0.13 ab	1.27 ± 0.29 ab	0.91 ± 0.07 a
1-K5 (con)	0.37 ± 0.23 a	0.36 ± 0.22 b	0.66 ± 0.50 ab	1.01 ± 0.70 b	0.58 ± 0.19 b
2-K3 (s)	0.85 ± 0.15 a	0.88 ± 0.08 a	0.86 ± 0.07 a	1.74 ± 0.14 a	1.01 ± 0.02 a
2-K4 (s & b)	0.69 ± 0.17 a	0.80 ± 0.06 a	0.80 ± 0.05 a	1.59 ± 0.11 a	1.00 ± 0.02 a
2-K5 (con)	0.91 ± 0.34 a	0.58 ± 0.10 b	0.63 ± 0.10 b	1.20 ± 0.20 b	0.92 ± 0.05 a
$P_{Lilliefors}$	>0.200	0.003	0.062	0.005	0.000
$P_{Shapiro-Wilk}$	0.140	0.004	0.003	0.009	0.000
P_{Levene}	0.016	0.000	0.000	0.000	0.000
Post-hoc	Tamhane	Median	Tamhane	Median	Median

Different letters within a column indicate significant differences.

Table 96. Chlorophyll and carotenoid contents of fruits of cv. California Wonder of experiments 23/03/-15/08/2023 and 06/03/-31/08/2024, but not considering an effect of the year.

	Car [g/kg]	Chl a [g/kg]	Chl b [g/kg]	Tot Chl [g/kg]	Chl a/b [--]
K3 (s)	0.81 ± 0.17 a	0.83 ± 0.14 a	0.83 ± 0.11 a	1.66 ± 0.25 a	1.00 ± 0.05 a
K4 (s & b)	0.68 ± 0.16 a	0.77 ± 0.11 a	0.77 ± 0.09 a	1.54 ± 0.20 a	0.99 ± 0.05 a
K5 (con)	0.83 ± 0.37 a	0.54 ± 0.15 b	0.63 ± 0.20 b	1.17 ± 0.31 b	0.87 ± 0.15 b
$P_{Lilliefors}$	>0.200	0.003	0.062	0.005	0.000
$P_{Shapiro-Wilk}$	0.140	0.004	0.003	0.009	0.000
P_{Levene}	0.000	0.383	0.162	0.221	0.002
Post-hoc	ANOVA	Kruskal-Wallis	Tukey-B	Kruskal-Wallis	Median

Different letters within a column indicate significant differences.

Funded by the European Union

Funded by the European Union under Grant Agreement No 101096056. Views and opinions expressed are however those of the author(s) only and do not necessarily reflect those of the European Union or CINEA. Neither the European Union nor the granting authority can be held responsible for them.

Table 97. Flavonoid, phenol, and nitrate content as well as antioxidative capacity of fruits of cv. California Wonder of experiments 23/03/-15/08/2023 (prefix 1) and 06/03/-31/08/2024 (prefix 2; S, shading; b, CO_2Bags; con, control).

	Flavonoids [g/kg]	Phenols [g/kg]	Nitrate [g/kg]	Antiox. capacity [mmol/g]
1-K3 (s)	6.3 ± 0.9 cd	0.37 ± 0.06 a	0.41 ± 0.48 a	0.04 ± 0.02 ab
1-K4 (s & b)	7.2 ± 1.3 cd	0.36 ± 0.09 a	0.79 ± 0.32 a	0.04 ± 0.01 ab
1-K5 (con)	11.2 ± 0.8 ab	0.44 ± 0.12 a	0.40 ± 0.13 a	0.15 ± 0.04 a
2-K3 (s)	4.0 ± 2.2 d	0.66 ± 0.04 a	0.15 ± 0.08 a	0.03 ± 0.01 b
2-K4 (s & b)	8.9 ± 3.8 bc	0.68 ± 0.06 a	0.15 ± 0.07 ab	0.05 ± 0.01 a
2-K5 (con)	14.2 ± 4.7 a	0.72 ± 0.06 a	0.08 ± 0.07 b	0.09 ± 0.02 a
$P_{Lilliefors}$	0.074	0.000	0.000	0.004
$P_{Shapiro-Wilk}$	0.001	0.000	0.000	0.000
P_{Levene}	0.013	0.010	0.000	0.000
Post-hoc	Tamhane	Median	Median	Median

Table 98. Flavonoid, phenol, and nitrate content as well as antioxidative capacity of fruits of cv. California Wonder of experiments 23/03/-15/08/2023 and 06/03/-31/08/2024, but not considering an effect of the year.

	Flavonoids [g/kg]	Phenols [g/kg]	Nitrate [g/kg]	Antiox. capacity [mmol/g]
K3 (s)	4.4 ± 2.2 c	0.60 ± 0.12 b	0.20 ± 0.23 ab	0.03 ± 0.01 c
K4 (s & b)	8.6 ± 3.6 b	0.63 ± 0.14 ab	0.26 ± 0.29 a	0.05 ± 0.01 b
K5 (con)	13.7 ± 4.4 a	0.67 ± 0.13 a	0.13 ± 0.14 b	0.10 ± 0.03 a
$P_{Lilliefors}$	0.074	0.000	0.000	0.004
$P_{Shapiro-Wilk}$	0.001	0.000	0.000	0.000
P_{Levene}	0.020	0.813	0.155	0.000
Post-hoc	Tamhane	Kruskal-Wallis	Kruskal-Wallis	Median

Different letters within a column indicate significant differences.

The results of the chemical analyses (Tables 95-98) confirm the conclusions of the above experiment on different cvs of *Capsicum annuum*. However, the differences between the "control" variant (K5) and the shaded variants on the one hand and the differences between the variant "shading & CO_2Bags" (K4) and "shading" (K3) became more distinct, allowing a corresponding ranking.

4. Experiment *Lactuca sativa* cv. Teide 16/05/ - 17/07/2023

A sensory panel test was not conducted for this lettuce experiment, because lettuce did not achieve the quality that would have allowed its marketing. Nevertheless, the content of valuable compounds was examined.

Chl and Car contents did not differ significantly among the variants (Table 99).

Funded by the European Union

Funded by the European Union under Grant Agreement No 101096056. Views and opinions expressed are however those of the author(s) only and do not necessarily reflect those of the European Union or CINEA. Neither the European Union nor the granting authority can be held responsible for them.

Table 99. Chlorophyll and carotenoid content of leaves (S, shading; b, CO_2Bags; con, control).

	Car [mg/kg]	Chl a [g/kg]	Chl b [g/kg]	Tot Chl [g/kg]	Chl a/b [--]
K3 (s)	34.7 ± 6.3 a	308 ± 17 a	298 ± 11 a	606 ± 7 a	1.03 ± 0.10 a
K4 (s & b)	33.2 ± 9.6 a	321 ± 23 a	290 ± 14 a	612 ± 9 a	1.11 ± 0.13 a
K5 (con)	28.3 ± 9.8 a	305 ± 13 a	300 ± 8 a	605 ± 5 a	1.02 ± 0.07 a
$P_{Lilliefors}$	>0.200	>0.200	>0.200	>0.200	>0.200
$P_{Shapiro-Wilk}$	0.975	0.910	0.910	0.910	0.871
P_{Levene}	0.387	0.296	0.296	0.296	0.246
Post-hoc	ANOVA	ANOVA	ANOVA	ANOVA	ANOVA

Different letters within a column indicate significant differences.

In the case of the total phenol and flavonoid contents significant differences were not detected and antioxidative capacity was similar among the three variants as well (Table 100). Interestingly, the cultivar-typical anthocyanin compound could only be detected in the "control" variant exposed to the highest light intensity. Nitrate content was significantly elevated under shading conditions.

Table 100. Anthocyanin, flavonoid, phenol, and nitrate content as well as antioxidative capacity of leaves (S, shading; b, CO_2Bags; con, control).

	Anthocyanins [mg/kg]	Flavonoids [g/kg]	Phenols [g/kg]	Antiox. capacity [mmol/g]	Nitrate [mg/kg]
K3 (s)	n.d.	28.4 ± 6.5 a	0.36 ± 0.07 a	0.05 ± 0.01 a	87.0 ± 18.3 a
K4 (s & b)	n.d.	31.6 ± 8.7 a	0.37 ± 0.09 a	0.05 ± 0.02 a	60.2 ± 42.7 ab
K5 (con)	9 ± 18 b	25.8 ± 4.0 a	0.36 ± 0.06 a	0.05 ± 0.01 a	6.8 ± 7.6 b
$P_{Lilliefors}$	--	>0.200	>0.200	>0.200	0.000
$P_{Shapiro-Wilk}$	--	0.198	0.239	0.260	0.000
P_{Levene}	--	0.151	0.327	0.668	0.001
Post-hoc	--	ANOVA	ANOVA	ANOVA	Median

Different letters within a column indicate significant differences.

In summary, elevated nitrate contents and the lack of anthocyanins clearly indicate that the shaded variants developed lower quality than the "control".

5. Experiment *Cucumis sativus* L. cv. Snackgurke Hopeline F1 06/03/ - 29/05/2024

Taste evaluation of cucumber fruits by a sensory panel did not reveal any significant difference (Table 101).

Table 101. Relative taste evaluation of the cucumber fruits cultivated under "shading" (s), "shading & CO_2Bags" (s & b) and "control" conditions.

	K3 (s)	K4 (s & b)	K5 (con)
Taste			

Funded by the European Union

Funded by the European Union under Grant Agreement No 101096056. Views and opinions expressed are however those of the author(s) only and do not necessarily reflect those of the European Union or CINEA. Neither the European Union nor the granting authority can be held responsible for them.

Total Chl content was largest in the variant “shading” (K3), whereas the variants “control” (K5) and “shading & CO_2Bags” (K4) were characterised by smaller values. Noteworthy, the Chl a/b ratio was in tendency larger in fruits cultivated in the shade. Carotenoid content also as a consequence of shading (Table 102).

Table 102. Fruit pigment contents of cucumber fruits (S, shading; b, CO_2Bags; con, control).

	Car [g/kg]	Chl a [g/kg]	Chl b [g/kg]	Tot Chl [g/kg]	Chl a/b [--]
K3 (s)	0.09 ± 0.02 a	0.59 ± 0.05 a	0.38 ± 0.10 a	0.97 ± 0.09 a	1.65 ± 0.53 a
K4 (s & b)	0.07 ± 0.01 ab	0.43 ± 0.04 b	0.29 ± 0.08 a	0.72 ± 0.08 b	1.61 ± 0.48 a
K5 (con)	0.05 ± 0.02 b	0.43 ± 0.06 b	0.34 ± 0.08 a	0.76 ± 0.09 b	1.35 ± 0.38 a
$P_{Lilliefors}$	>0.200	>0.200	>0.200	>0.200	0.005
$P_{Shapiro-Wilk}$	0.913	0.226	0.452	0.445	0.007
P_{Levene}	0.480	0.571	0.182	0.480	0.055
Post-hoc	Tukey-B	Tukey-B	ANOVA	Tukey-B	Kruskal-Wallis

Different letters within a column indicate significant differences.

Total phenol and flavonoid content of fruits were not affected by the different cultivation environments (Table 103). Antioxidative capacity showed an unusual pattern, with the largest difference between the variants “shading” (K3) and “shading & CO_2Bags” (K4). Nitrate content was highest under “shading & CO_2Bags” (K4), followed by “shading” (K3) and “control” (K5).

Table 103. Table 103. Flavonoid, phenol, and nitrate content as well as antioxidative capacity of cucumber fruits (S, shading; b, CO_2Bags; con, control).

	Flavonoids [g/kg]	Phenols [g/kg]	Antiox. capacity [µmol/g]	Nitrate [g/kg]
K3 (s)	2.0 ± 0.1 a	0.22 ± 0.02 a	12.7 ± 0.4 a	0.21 ± 0.16 ab
K4 (s & b)	1.9 ± 0.1 a	0.27 ± 0.03 a	8.9 ± 1.1 b	0.56 ± 0.07 a
K5 (con)	2.0 ± 0.2 a	0.27 ± 0.03 a	10.9 ± 0.9 ab	0.01 ± 0.02 b
$P_{Lilliefors}$	>0.200	>0.200	>0.200	0.077
$P_{Shapiro-Wilk}$	0.076	0.621	0.601	0.024
P_{Levene}	0.360	0.807	0.451	0.006
Post-hoc	ANOVA	ANOVA	Tukey-B	Tamhane

Different letters within a column indicate significant differences.

The most frequent organic acids in cucumber fruits were succinic, malic, and fumaric acid, all being “later” components of the citrate cycles. Malic acid concentration rose under shading conditions, which is interpreted as a hint for a lack in ATP and NADPH. The antinutritive compound oxalic acid was especially frequent in the variant “shading & CO_2Bags” (K4), while the “control” treatment (K5) was characterised by the smallest concentration (Table 104).

Funded by the European Union

Funded by the European Union under Grant Agreement No 101096056. Views and opinions expressed are however those of the author(s) only and do not necessarily reflect those of the European Union or CINEA. Neither the European Union nor the granting authority can be held responsible for them.

Table 104. Organic acids of cucumber fruits (S, shading; b, CO_2Bags; con, control).

	Succinic acid [g/kg]	Malic acid [g/kg]	Fumaric acid [g/kg]	Oxalic acid [g/kg]	Trans-aconitic acid [g/kg]
K3 (s)	57.5 ± 2.2 a	58.1 ± 4.1 a	0.25 ± 0.03 b	0.15 ± 0.05 ab	0.009 ± 0.002 a
K4 (s & b)	57.8 ± 2.4 a	51.6 ± 1.7 a	0.48 ± 0.10 ab	0.22 ± 0.07 a	0.004 ± 0.001 a
K5 (con)	56.3 ± 1.3 a	27.9 ± 8.4 b	0.69 ± 0.23 a	0.10 ± 0.02 b	0.002 ± 0.001 b
$P_{Lilliefors}$	0.042	0.072	>0.200	>0.200	0.060
$P_{Shapiro-Wilk}$	0.106	0.172	0.481	0.165	0.119
P_{Levene}	0.030	0.117	0.220	0.190	0.036
Post-hoc	ANOVA	Tukey-B	Tukey-B	ANOVA	Tamhane

Different letters within a column indicate significant differences.

Carbohydrate content was largest in the "shading" variant (K3), while the variants "shading & CO_2Bags" (K4) and "control" (K5) were characterised by similar values (Table 105).

Table 105. Carbohydrate content of cucumber fruits.

	Glucose [mg/kg]	Fructose [mg/kg]
K3 (s)	288.8 ± 1.9 a	181.4 ± 3.8 a
K4 (s & b)	233.7 ± 4.6 b	145.6 ± 11.7 b
K5 (con)	249.7 ± 10.1 b	142.0 ± 10.5 b
$P_{Lilliefors}$	0.097	>0.200
$P_{Shapiro-Wilk}$	0.046	0.170
P_{Levene}	0.100	0.298
Post-hoc	Tukey-B	Tukey-B

Different letters within a column indicate significant differences.

The assessed quality parameters of cucumber fruits yielded partly contradictory results. While carbohydrate content seemed to favour the "shading" variant (K3), organic acids supported the "control" treatment (K5). Correspondingly, antioxidative capacity was best in K3, but nitrate content in K5. Taken together, it may not be surprising that the untrained sensory panel rated all fruits similarly well, however a trained panel might have identified subtle differences. Based on a weighting of the differences, the low nitrate and oxalic acid content would ultimately favour the "control" variant as having produced the preferable quality.

Funded by the European Union

Funded by the European Union under Grant Agreement No 101096056. Views and opinions expressed are however those of the author(s) only and do not necessarily reflect those of the European Union or CINEA. Neither the European Union nor the granting authority can be held responsible for them.

6. Experiment *Capsicum annuum* L. cv. California Wonder 06/03/ - 31/08/2024: cultivation partly with shading nets partly with photovoltaic cells

The results of the present sensory panel test followed the previous test for fruits of *Capsicum annuum* cv. California Wonder, indicating a slightly better performance of control fruits, which was mainly due to the somewhat advanced ripening stage (Table 106).

Table 106. Relative visual and taste evaluations of fruits of *C. annuum* cv. California Wonder produced under "shading by nets" (s), "shading by nets & CO_2Bags" (s & b), "control" (con), "shading by PV" (PV), and "shading by PV & CO_2Bags" (PV & b) conditions.

	K3 (s)	K4 (s & b)	K5 (con)	K3 (PV)	K4 (PV & b)
Taste & visual appearance 2024					

Car content of fruits did not differ among treatments, but in the case of fruit Chl content, fruits grown under shading nets were characterised by a higher content than under the PV system, while fruits from the "control" variant had the lowest Chl content (Table 107). This observation corresponds well with the higher percentage of green fruits in the shaded variants, despite the fact that these fruits were allowed an extended ripening period.

Table 107. Chlorophyll and carotenoid of fruits of cv. California Wonder (S, shading nets; b, CO_2Bags; con, control; PV, photovoltaic cell).

	Car [g/kg]	Chl a [g/kg]	Chl b [g/kg]	Tot Chl [g/kg]	Chl a/b [--]
K3 (s)	0.85 ± 0.15 a	0.88 ± 0.08 a	0.86 ± 0.07 a	1.74 ± 0.14 a	1.01 ± 0.02 a
K4 (s & b)	0.69 ± 0.17 a	0.80 ± 0.06 a	0.80 ± 0.05 ab	1.59 ± 0.11 ab	1.00 ± 0.02 a
K5 (con)	0.91 ± 0.34 a	0.58 ± 0.10 c	0.63 ± 0.10 c	1.20 ± 0.20 d	0.92 ± 0.05 b
K3 (PV)	0.77 ± 0.16 a	0.66 ± 0.06 bc	0.71 ± 0.07 b	1.38 ± 0.12 c	0.93 ± 0.07 ab
K4 (PV & b)	1.19 ± 0.21 a	0.70 ± 0.09 b	0.75 ± 0.12 b	1.46 ± 0.20 bc	0.94 ± 0.06 ab
$P_{Lilliefors}$	>0.200	0.051	>0.200	0.050	0.012
$P_{Shapiro-Wilk}$	0.072	0.128	0.078	0.097	0.000
P_{Levene}	0.009	0.330	0.096	0.161	0.004
Post-hoc	Tamhane	Tukey-B	Tukey-B	Tukey-B	Tukey-B

Different letters within a column indicate significant differences.

Flavonoid content was highest in the "control" variant and the variant "shading by PV & CO_2Bags" (PV & b), followed by "shading by PV" (PV), and "shading by nets & CO_2Bags" (s & b). The lowest concentration was found in the variant "shading by nets" (s), indicating first that flavonoid content is highly light dependent and second that the application of CO_2Bags was able to enhance flavonoid content (Table 108). Total phenol content and antioxidative capacity followed in principle flavonoid content, but the effects

Funded by the European Union under Grant Agreement No 101096056. Views and opinions expressed are however those of the author(s) only and do not necessarily reflect those of the European Union or CINEA. Neither the European Union nor the granting authority can be held responsible for them.

were less statistically significant. Vitamin C content was stable (Table 108). Nitrate content was elevated under shading conditions and especially under shading nets.

Table 108. Flavonoid, phenol, vitamin C, and nitrate content as well as antioxidative capacity of fruits of cv. California Wonder (S, shading nets; b, CO_2Bags; con, control; PV, photovoltaic cell).

	Flavonoids [g/kg]	Phenols [g/kg]	Vit. C [g/kg]	Nitrate [g/kg]*	Antiox. capacity [mmol/g]
K3 (s)	4.0 ± 2.2 c	0.66 ± 0.04 b	6.0 ± 0.7 a	0.15 ± 0.08 a	0.03 ± 0.01 c
K4 (s & b)	8.9 ± 3.8 b	0.68 ± 0.06 ab	6.2 ± 0.6 a	0.15 ± 0.07 a	0.05 ± 0.01 b
K5 (con)	14.2 ± 4.7 a	0.72 ± 0.06 a	6.1 ± 0.8 a	0.08 ± 0.07 ab	0.09 ± 0.02 a
K3 (PV)	8.8 ± 3.6 b	0.68 ± 0.07 ab	6.3 ± 0.3 a	0.09 ± 0.05 ab	0.06 ± 0.01 b
K4 (PV & b)	13.3 ± 2.2 a	0.71 ± 0.04 a	6.5 ± 0.7 a	0.06 ± 0.01 b	0.07 ± 0.01 ab
$P_{Lilliefors}$	>0.200	>0.200	>0.200	>0.200	>0.200
$P_{Shapiro-Wilk}$	0.013	0.088	0.113	0.191	0.023
P_{Levene}	0.052	0.268	0.158	0.153	0.009
Post-hoc	Tukey-B	Duncan	ANOVA	Tukey-B	Tamhane

* Transformation: f(x) = (x)^0.5; Different letters within a column indicate significant differences.

Organic acids content was fairly stable in the fruits of 'California Wonder' and a consistent trend related to the treatments could not be identified (Table 109).

Table 109. Organic acids of fruits of cv. California Wonder (S, shading nets; b, CO_2Bags; con, control; PV, photovoltaic cell).

	Succinic acid [g/kg]	Malic acid [g/kg]	Citric acid [g/kg]	Oxalic acid [g/kg]	Fumaric acid [g/kg]	Trans-aconitic acid [mg/kg]
K3 (s)	61.7 ± 14.3 a	34.1 ± 16.3 ab	12.9 ± 2.8 a	0.57 ± 0.31 a	0.05 ± 0.04 a	0.04 ± 0.02 a
K4 (s & b)	70.0 ± 11.8 a	41.4 ± 15.5 a	12.4 ± 5.2 a	0.66 ± 0.27 a	0.07 ± 0.05 a	0.02 ± 0.01 a
K5 (con)	72.7 ± 24.5 a	36.2 ± 12.0 ab	13.8 ± 6.4 a	0.75 ± 0.38 a	0.10 ± 0.05 a	0.03 ± 0.01 a
K3 (PV)	49.8 ± 8.0 a	23.5 ± 9.4 b	12.5 ± 4.9 a	0.45 ± 0.16 a	0.03 ± 0.04 a	0.03 ± 0.00 a
K4 (PV & b)	55.6 ± 6.7 a	24.4 ± 3.7 b	17.8 ± 3.5 a	0.22 ± 0.09 a	0.02 ± 0.01 a	0.04 ± 0.01 a
$P_{Lilliefors}$	0.029	0.085	>0.200	0.029	0.002	>0.200
$P_{Shapiro-Wilk}$	0.039	0.007	0.385	0.009	0.001	0.171
P_{Levene}	0.000	0.056	0.054	0.028	0.039	0.313
Post-hoc	Median	Tukey-B	ANOVA	Median	Median	ANOVA

Different letters within a column indicate significant differences.

Fruit carbohydrate measurements did not reveal significant differences among the variants (Table 110).

Funded by the European Union

Funded by the European Union under Grant Agreement No 101096056. Views and opinions expressed are however those of the author(s) only and do not necessarily reflect those of the European Union or CINEA. Neither the European Union nor the granting authority can be held responsible for them.

Table 110. Carbohydrate content of fruits of cv. California Wonder.

	Glucose [g/kg]	Fructose [g/kg]	Sucrose [g/kg]
K3 (s)	221.9 ± 10.0 a	182.0 ± 7.8 a	13.4 ± 2.7 a
K4 (s & b)	232.1 ± 9.6 a	197.8 ± 5.8 a	7.9 ± 1.3 a
K5 (con)	231.7 ± 9.2 a	191.7 ± 7.1 a	7.4 ± 0.9 a
K3 (PV)	221.6 ± 23.5 a	191.7 ± 5.2 a	8.7 ± 2.2 a
K4 (PV & b)	223.1 ± 25.0 a	206.8 ± 10.5 a	10.3 ± 1.4 a
$P_{Lilliefors}$	0.197	0.039	0.000
$P_{Shapiro-Wilk}$	0.001	0.002	0.000
P_{Levene}	0.914	0.333	0.023
Post-hoc	ANOVA	Kruskal-Wallis	Median

Different letters within a column indicate significant differences.

In summary, differences in fruit quality were minor. Taste relevant compounds such as carbohydrates and organic acids did not differ among treatments. “Control” fruits performed best or second with respect to antioxidative capacity, total phenol, flavonoid, and nitrate content, but in this respect the variant “shading by PV & CO_2Bags” (PV & b) performed rather similarly. The fact that the “control” fruits were rated superior to the latter variant by the sensory panel may thus be related to the visual appearance, as the shaded fruits contained more Chl and were assessed as less ripe.

7. Experiment *Raphanus sativus* L. cv. Riesen von Aspern 06/03/ - 11/05/24 (shading nets) and 22/03/ - 16/05/24 (PV)

The evaluation of leaves and tubers by an untrained panel revealed similar results for leaves and tubers (Table 111). However, while in the first experiment with shading nets a slight but consistent difference between the variants “shading by nets” (s) and “shading by nets & CO_2Bags” (s & b) was reported, in the second experiment a corresponding difference between the variants “shading by PV” (PV), and “shading by PV & CO_2Bags” (PV & b) was not observed.

Table 111. Relative visual and taste evaluations of radish leaves and tubers produced under “shading by nets” (s), “shading by nets & CO_2Bags” (s & b), “control” (con), “shading by PV” (PV), and “shading by PV & CO_2Bags” (PV & b) conditions in two subsequent experiments (prefix 1 or 2).

	1-K3 (s)	1-K4 (s & b)	1-K5 (con)	2-K3 (PV)	2-K4 (PV & b)	2-K5 (con)
Taste & visual appearance, tubers						
Taste & visual appearance, leaves						

Funded by the European Union

Funded by the European Union under Grant Agreement No 101096056. Views and opinions expressed are however those of the author(s) only and do not necessarily reflect those of the European Union or CINEA. Neither the European Union nor the granting authority can be held responsible for them.

Not only tubers, also leaves of radish can be consumed, which is why their quality was evaluated for this experiment as well. In the first experiment differences in Chl content indicated a higher content under shading by nets when compared to the "control" (Table 112). In the second experiment with PVs, differences were almost insignificant, indicating however a trend towards larger values in the variant "shading by PV & CO_2Bags" (PV & b). Because the light intensity below the PV system was between that of controls and the net-shaded variants, it may be speculated that the effect of a higher Chl content as a consequence of a lower light intensity should also occur in the case of the PV variants, however less distinct. Car content turned out to be comparatively stable, but was significantly higher in the variant "shading by PV & CO_2Bags" (PV & b).

Table 112. Chlorophyll and carotenoid of leaves of radish plants under shading by nets (prefix 1) and PV conditions (prefix 2; b, CO_2Bags; con, control; PV, photovoltaic system; s, shading nets).

	Car [g/kg]	Chl a [g/kg]	Chl b [g/kg]	Tot Chl [g/kg]	Chl a/b [--]
1-K3 (s)	0.38 ± 0.13 b	5.60 ± 1.05 ab	5.17 ± 1.33 a	10.77 ± 2.13 a	1.12 ± 0.22 b
1-K4 (s & b)	0.25 ± 0.16 b	5.87 ± 0.28 a	5.92 ± 0.51 a	11.79 ± 0.37 a	1.00 ± 0.14 b
1-K5 (con)	0.41 ± 0.09 b	2.78 ± 0.25 bc	1.94 ± 0.13 b	4.72 ± 0.38 b	1.43 ± 0.05 a
2-K3 (PV)	0.35 ± 0.14 b	2.42 ± 0.48 ab	1.64 ± 0.33 b	4.06 ± 0.81 b	1.48 ± 0.02 a
2-K4 (PV & b)	0.64 ± 0.12 a	3.88 ± 0.88 abc	2.66 ± 0.44 ab	6.54 ± 1.32 ab	1.50 ± 0.02 a
2-K5 (con)	0.36 ± 0.10 b	1.93 ± 0.21 c	1.30 ± 0.10 b	3.23 ± 0.30 b	1.52 ± 0.02 a
$P_{Lilliefors}$	>0.200	0.001	0.000	0.000	0.000
$P_{Shapiro-Wilk}$	0.500	0.002	0.000	0.000	0.000
P_{Levene}	0.767	0.017	0.000	0.000	0.000
Post-hoc	Tukey-B	Median	Median	Median	Median

Different letters within a column indicate significant differences.

Antioxidative capacity, flavonoid, total phenol, and also nitrate content were always highest in the variants "shading by nets" (s) and "shading by nets & CO_2Bags" (s & b; Table 113).

Citric acid content was highest in the control treatments and smallest in the variants "shading by nets" (s) and "shading by nets & CO_2Bags" (s & b), suggesting a corresponding rating for leaf taste, because citric acid is associated with a positive perception. Oxalic acid, an antinutritive, showed the opposite tendency (Table 114).

Funded by the European Union

Funded by the European Union under Grant Agreement No 101096056. Views and opinions expressed are however those of the author(s) only and do not necessarily reflect those of the European Union or CINEA. Neither the European Union nor the granting authority can be held responsible for them.

Table 113. Flavonoid, phenol, and nitrate content as well as antioxidative capacity of radish leaves under shading by nets (prefix 1) and PV conditions (prefix 2; b, CO_2Bags; con, control; PV, photovoltaic system; s, shading nets; n.d., not detected).

	Flavonoids [g/kg]	Phenols [g/kg]	Nitrate [g/kg]	Antiox. capacity [mmol/g]
1-K3 (s)	53.2 ± 9.8 a	0.32 ± 0.06 a	0.41 ± 0.12 a	0.07 ± 0.01 a
1-K4 (s & b)	55.7 ± 3.2 a	0.33 ± 0.06 a	0.21 ± 0.21 ab	0.08 ± 0.01 a
1-K5 (con)	18.2 ± 1.5 b	0.24 ± 0.16 ab	0.03 ± 0.03 b	0.04 ± 0.00 b
2-K3 (PV)	16.8 ± 2.8 b	0.12 ± 0.06 b	0.02 ± 0.03 b	0.04 ± 0.01 b
2-K4 (PV & b)	23.5 ± 2.2 a	0.16 ± 0.03 ab	0.05 ± 0.06 b	0.05 ± 0.00 a
2-K5 (con)	15.0 ± 1.4 b	0.12 ± 0.02 b	n.d.	0.03 ± 0.01 b
$P_{Lilliefors}$	0.000	0.047	0.000	0.015
$P_{Shapiro-Wilk}$	0.000	0.010	0.000	0.004
P_{Levene}	0.000	0.122	0.000	0.005
Post-hoc	Median	Kruskal-Wallis	Median	Median

Different letters within a column indicate significant differences.

Table 114. Organic acids of radish leaves under shading by nets (prefix 1) and PV conditions (prefix 2; b, CO_2Bags; con, control; PV, photovoltaic system; s, shading nets).

	Malic acid [g/kg]	Citric acid [g/kg]	Oxalic acid [g/kg]	Fumaric acid [g/kg]
1-K3 (s)	28.5 ± 14.1 ab	12.0 ± 3.7 c	0.92 ± 0.15 a	0.10 ± 0.04 b
1-K4 (s & b)	20.7 ± 14.8 ab	7.0 ± 2.7 c	0.61 ± 0.21 ab	0.11 ± 0.06 b
1-K5 (con)	29.4 ± 6.1 ab	38.5 ± 8.8 a	0.08 ± 0.03 c	0.20 ± 0.05 ab
2-K3 (PV)	34.5 ± 4.8 a	42.7 ± 6.4 a	0.07 ± 0.01 c	0.22 ± 0.04 ab
2-K4 (PV & b)	36.6 ± 1.3 a	22.9 ± 7.0 b	0.10 ± 0.04 abc	0.39 ± 0.09 a
2-K5 (con)	20.6 ± 3.7 b	34.6 ± 6.5 a	0.07 ± 0.03 c	0.20 ± 0.02 ab
$P_{Lilliefors}$	0.086	0.090	0.000	0.036
$P_{Shapiro-Wilk}$	0.179	0.009	0.000	0.013
P_{Levene}	0.003	0.698	0.000	0.184
Post-hoc	Tamhane	Tukey-B	Median	Kruskal-Wallis

Different letters within a column indicate significant differences.

Carbohydrate contents tended to be highest in the variants “control”, “shading by nets & CO_2Bags” (s & b), and “shading by PV & CO_2Bags” (PV & b). In the case of fructose, the highest values were found in the variant “shading by nets & CO_2Bags” (s & b). These results indicate that CO_2Bags were able to compensate for a reduced light intensity with respect to leaf carbohydrate content (Table 115).

Funded by the European Union

Funded by the European Union under Grant Agreement No 101096056. Views and opinions expressed are however those of the author(s) only and do not necessarily reflect those of the European Union or CINEA. Neither the European Union nor the granting authority can be held responsible for them.

Table 115. Carbohydrate content of radish leaves under shading nets (prefix 1) and PV conditions (prefix 2; b, CO_2Bags; con, control; PV, photovoltaic system; s, shading nets).

	Glucose [g/kg]	Fructose [g/kg]	Sucrose [g/kg]	Sum [g/kg]
1-K3 (s)	21.8 ± 8.6 c	8.4 ± 2.5 b	0.14 ± 0.40 a	30.4 ± 13.7 c
1-K4 (s & b)	29.7 ± 4.5 bc	25.8 ± 7.2 a	0.28 ± 0.79 a	55.9 ± 11.2 ab
1-K5 (con)	36.3 ± 9.5 b	14.3 ± 1.8 ab	0.59 ± 1.25 a	51.2 ± 6.9 ab
2-K3 (PV)	36.6 ± 4.8 b	11.3 ± 3.2 ab	0.10 ± 0.14 a	48.0 ± 7.1 b
2-K4 (PV & b)	51.0 ± 6.7 a	18.7 ± 5.0 a	0.01 ± 0.03 a	69.7 ± 11.1 a
2-K5 (con)	41.4 ± 6.7 ab	10.8 ± 2.6 ab	0.09 ± 0.14 a	52.3 ± 8.6 ab
$P_{Lilliefors}$	>0.200	0.041	0.000	>0.200
$P_{Shapiro-Wilk}$	0.969	0.007	0.000	0.444
P_{Levene}	0.766	0.009	0.094	0.446
Post-hoc	Tukey-B	Median	Kruskal-Wallis	Tukey-B

Different letters within a column indicate significant differences.

Neither antioxidative capacity, nor anthocyanin, flavonoid or total phenol contents of tubers differed significantly among the variants (Table 116). Nitrate contents were comparable, with a significant difference detected between the two “control” treatments.

Table 116. Anthocyanin, flavonoid, phenol, and nitrate content as well as antioxidative capacity of radish tubers under shading nets (prefix 1) and PV conditions (prefix 2; b, CO_2Bags; con, control; PV, photovoltaic system; s, shading nets).

	Anthocyanins [g/kg]	Flavonoids [g/kg]	Phenols [g/kg]	Nitrate [g/kg]	Antiox. capacity [mmol/g]
1-K3 (s)	109.2 ± 43.7 a	1.6 ± 1.6 a	0.25 ± 0.09 a	0.12 ± 0.03 ab	0.01 ± 0.00 a
1-K4 (s & b)	120.5 ± 30.7 a	1.8 ± 0.2 a	0.32 ± 0.05 a	0.10 ± 0.01 ab	0.01 ± 0.00 a
1-K5 (con)	128.5 ± 69.1 a	1.5 ± 0.7 a	0.24 ± 0.13 a	0.23 ± 0.19 a	0.01 ± 0.00 a
2-K3 (PV)	95.0 ± 70.5 a	1.1 ± 1.1 a	0.08 ± 0.06 a	0.13 ± 0.05 ab	0.01 ± 0.01 a
2-K4 (PV & b)	69.3 ± 34.3 a	1.2 ± 1.4 a	0.05 ± 0.03 a	0.20 ± 0.08 a	0.01 ± 0.00 a
2-K5 (con)	92.7 ± 16.3 a	2.1 ± 1.4 a	0.05 ± 0.03 a	0.09 ± 0.01 b	0.01 ± 0.01 a
$P_{Lilliefors}$	0.023	>0.200	0.004	0.000	0.007
$P_{Shapiro-Wilk}$	0.065	0.063	0.005	0.000	0.009
P_{Levene}	0.641	0.019	0.002	0.000	0.045
Post-hoc	Tukey	ANOVA	Median	Median	Median

Different letters within a column indicate significant differences.

Tubers’ organic acids were fairly stable (Table 117). In the second experiment with PVs, fumaric acid content was elevated in variant “shading by PV & CO_2Bags” (PV & b).

Funded by the European Union under Grant Agreement No 101096056. Views and opinions expressed are however those of the author(s) only and do not necessarily reflect those of the European Union or CINEA. Neither the European Union nor the granting authority can be held responsible for them.

Table 117. Organic acids of radish tubers under shading nets (prefix 1) and PV conditions (prefix 2; b, CO_2Bags; con, control; PV, photovoltaic system; s, shading nets.

	Malic acid [g/kg]	Citric acid [g/kg]	Fumaric acid [g/kg]	Oxalic acid [g/kg]
1-K3 (s)	24.7 ± 10.0 a	5.10 ± 0.22 a	0.37 ± 0.05 ab	0.10 ± 0.04 a
1-K4 (s & b)	22.7 ± 4.4 a	5.41 ± 0.33 a	0.37 ± 0.12 ab	0.09 ± 0.01 ab
1-K5 (con)	24.6 ± 5.2 a	5.37 ± 0.31 a	0.38 ± 0.12 ab	0.09 ± 0.01 ab
2-K3 (PV)	24.0 ± 4.6 a	5.28 ± 2.47 a	0.36 ± 0.12 b	0.05 ± 0.03 b
2-K4 (PV & b)	21.2 ± 3.1 a	1.59 ± 0.61 a	0.55 ± 0.08 a	0.05 ± 0.01 b
2-K5 (con)	20.2 ± 1.9 a	5.27 ± 2.43 a	0.28 ± 0.08 b	0.06 ± 0.02 ab
$P_{Lilliefors}$	0.170	0.001	>0.200	0.122
$P_{Shapiro-Wilk}$	0.080	0.026	0.747	0.018
P_{Levene}	0.057	0.002	0.461	0.067
Post-hoc	ANOVA	Median	Tukey	Tukey

Different letters within a column indicate significant differences.

Carbohydrate content of tubers did not show significant differences in the first experiment with shading nets, but in the second with PVs carbohydrate content was largest in the variant “shading by PV & CO_2Bags” (PV & b) and smallest in the “control” (Table 118).

Table 118. Carbohydrate content of radish tubers under shading nets (prefix 1) and PV conditions (prefix 2; b, CO_2Bags; con, control; PV, photovoltaic system; s, shading nets).

	Glucose [g/kg]	Fructose [g/kg]	Sucrose [g/kg]	Sum [g/kg]
1-K3 (s)	111.2 ± 41.9 ab	56.5 ± 15.2 b	43.7 ± 16.1 a	211.5 ± 67.5 ab
1-K4 (s & b)	114.3 ± 28.2 ab	50.5 ± 10.5 b	45.7 ± 21.5 a	210.6 ± 27.3 ab
1-K5 (con)	105.6 ± 30.8 b	53.1 ± 23.9 b	34.7 ± 9.6 a	193.4 ± 49.4 b
2-K3 (PV)	117.3 ± 47.9 ab	64.3 ± 25.5 b	49.0 ± 4.7 a	230.7 ± 74.5 ab
2-K4 (PV & b)	177.2 ± 26.6 a	101.4 ± 16.4 a	34.8 ± 5.8 a	313.4 ± 36.0 a
2-K5 (con)	85.9 ± 33.8 b	41.2 ± 21.0 b	48.2 ± 7.2 a	175.2 ± 60.0 b
$P_{Lilliefors}$	0.069	0.191	>0.200	>0.200
$P_{Shapiro-Wilk}$	0.292	0.430	0.063	0.458
P_{Levene}	0.866	0.360	0.258	0.513
Post-hoc	Tukey-B	Tukey-B	ANOVA	Tukey-B

Different letters within a column indicate significant differences.

In summary, quality parameters of radish tubers were rather similar. Thus, the differences rated by the sensory panel can only be explained by the distinctly smaller size of the tubers, especially in the first experiment (see above). In the case of the leaves, the important factor represented light intensity. Generally, quality parameters were highest in the “control” and lowest in the variants with shading by nets. Interestingly, the addition of CO_2Bags had a positive effect on leaf carbohydrate content. The results of the chemical analysis of the leaves is in accordance with the rating of the sensory panel.

Funded by the European Union

Funded by the European Union under Grant Agreement No 101096056. Views and opinions expressed are however those of the author(s) only and do not necessarily reflect those of the European Union or CINEA. Neither the European Union nor the granting authority can be held responsible for them.

B. Experiments with CO_2 generated by fungus cultivation and additional light

1. Experiment Basil 30/01/ - 07/04/2025

The untrained sensory panel detected slight differences in taste, less in visual appearance that resulted in rating the control plants and the variant "PV & elevated CO_2 & additional light" best and the remaining variants second (Table 119).

Table 119. Relative visual and taste evaluations of basil leaves cultivated under shading by PVs (PV), shading & elevated CO_2 (PV & b) and "control" conditions (con), with (L) or without additional light.

	K3 (PV)	K3 (PV & L)	K4 (PV & b)	K4 (PV & b & L)	K5 (con)	K5 (con & L)
Taste & visual appearance						

Differences in leaf Chl contents were small but distinct among the variants. An increasing trend from the "control" variants towards the "PV-shaded" became obvious and additional light also lowered Chl contents. Trends in Car content followed Chl content (Table 120).

Table 120. Chlorophyll and carotenoid content of basil leaves (b, elevated CO_2; con, control; L, additional light; PV, photovoltaic cells).

	Car [g/kg]	Chl a [g/kg]	Chl b [g/kg]	Tot Chl [g/kg]	Chl a/b [--]
K3 (PV)	1.62 ± 0.38 a	6.00 ± 1.35 a	4.21 ± 0.93 ab	10.21 ± 2.27 a	1.43 ± 0.06 bc
K3 (PV L)	1.40 ± 0.10 ab	5.19 ± 0.98 ab	3.51 ± 0.68 abc	8.71 ± 1.64 ab	1.48 ± 0.09 ab
K4 (PV, b)	1.66 ± 0.43 a	6.40 ± 1.45 a	4.61 ± 1.02 a	11.01 ± 2.47 a	1.39 ± 0.04 c
K4 (PV, b, L)	1.41 ± 0.27 ab	4.86 ± 0.97 ab	3.47 ± 0.77 abc	8.32 ± 1.73 ab	1.41 ± 0.08 bc
K5 (con)	1.28 ± 0.28 b	5.09 ± 0.97 ab	3.36 ± 0.70 bc	8.45 ± 1.67 ab	1.52 ± 0.04 a
K5 (con L)	1.06 ± 0.07 c	4.74 ± 0.49 b	3.15 ± 0.33 c	7.89 ± 0.81 b	1.51 ± 0.06 a
$P_{Lilliefors}$	0.000	0.002	0.006	0.016	>0.200
$P_{Shapiro-Wilk}$	0.000	0.000	0.002	0.001	0.003
P_{Levene}	0.001	0.106	0.062	0.083	0.538
Post-hoc	Median	Kruskal-Wallis	Kruskal-Wallis	Kruskal-Wallis	Tukey

Different letters within a column indicate significant differences.

Data on Chl fluorescence were added in Table 121, because this measurement allowed to assess the stress level of leaves. A value of Fv/Fm below 0.8 is generally considered as indicative of stress. In the present experiment the results would suggest a moderate stress in the "control" variants and the variants with "PV & elevated CO_2" with or without additional light.

Funded by the European Union

Funded by the European Union under Grant Agreement No 101096056. Views and opinions expressed are however those of the author(s) only and do not necessarily reflect those of the European Union or CINEA. Neither the European Union nor the granting authority can be held responsible for them.

Table 121. Chlorophyll fluorescence of basils leaves as stress indicators (b, elevated CO_2; con, control; L, additional light; PV, photovoltaic cells).

	F0 [relative unit]	Fm [relative unit]	Fv/Fm [relative unit]	PI_{Abs} [relative unit]
K3 (PV)	6788 ± 468 a	34111 ± 2587 a	0.801 ± 0.007 a	1.82 ± 0.23 a
K3 (PV L)	6110 ± 457 b	30620 ± 2130 bc	0.800 ± 0.009 a	2.00 ± 0.24 a
K4 (PV, b)	6704 ± 415 a	32365 ± 2305 ab	0.792 ± 0.014 ab	1.70 ± 0.35 a
K4 (PV, b, L)	6010 ± 395 b	29357 ± 1907 c	0.795 ± 0.013 ab	1.87 ± 0.55 a
K5 (con)	6130 ± 489 b	28828 ± 3447 c	0.786 ± 0.015 b	1.68 ± 0.52 a
K5 (con L)	6110 ± 432 b	28752 ± 2760 c	0.792 ± 0.011 ab	2.06 ± 0.43 a
$P_{Lilliefors}$	>0.200	>0.200	0.004	>0.200
$P_{Shapiro-Wilk}$	0.351	0.158	0.031	0.120
P_{Levene}	0.973	0.586	0.114	0.012
Post-hoc	Tukey-B	Tukey-B	Kruskal-Wallis	ANOVA

Different letters within a column indicate significant differences.

Antioxidative capacity, flavonoid, total phenol and vitamin C contents were higher under elevated light levels, whereas nitrate content rose with decreasing light intensity (Table 122). This indicates a better produce quality under elevated light levels.

Table 122. Flavonoid, phenol, vitamin C, and nitrate content as well as antioxidative capacity of basil leaves (b, elevated CO_2; con, control; L, additional light; PV, photovoltaic cells).

	Flavonoids [g/kg]	Phenols [g/kg]	Vit. C [g/kg]	Antiox. capacity [µmol/g]	Nitrate [g/kg]
K3 (PV)	59.3 ± 9.1 b	0.73 ± 0.09 d	2.1 ± 1.2 b	69.9 ± 10.4 b	0.57 ± 0.46 ab
K3 (PV L)	67.2 ± 9.9 ab	0.88 ± 0.09 ab	4.8 ± 0.8 a	92.6 ± 9.5 ab	0.52 ± 0.30 ab
K4 (PV, b)	59.5 ± 4.0 b	0.75 ± 0.05 cd	3.1 ± 1.0 b	97.0 ± 5.9 a	0.85 ± 0.46 a
K4 (PV, b, L)	59.3 ± 5.4 b	0.81 ± 0.09 bcd	4.7 ± 2.0 a	102.4 ± 13.3 a	0.22 ± 0.12 b
K5 (con)	65.8 ± 8.0 ab	0.85 ± 0.06 abc	4.6 ± 1.1 a	97.7 ± 7.8 a	0.25 ± 0.17 b
K5 (con L)	71.9 ± 10.3 a	0.92 ± 0.14 a	5.2 ± 1.6 a	104.6 ± 12.4 a	0.27 ± 0.20 ab
$P_{Lilliefors}$	>0.200	>0.200	>0.200	0.043	0.000
$P_{Shapiro-Wilk}$	0.011	0.011	0.395	0.044	0.000
P_{Levene}	0.160	0.176	0.103	0.196	0.000
Post-hoc	Tukey-B	Tukey-B	Tukey-B	Kruskal-Wallis	Median

Different letters within a column indicate significant differences.

Organic acids content was almost unaffected by the different light and CO_2 levels (Table 123). However maleic acid content tended to be largest at higher light intensities. The taste of maleic acid is rather considered as unfavourable.

Funded by the European Union under Grant Agreement No 101096056. Views and opinions expressed are however those of the author(s) only and do not necessarily reflect those of the European Union or CINEA. Neither the European Union nor the granting authority can be held responsible for them.

Table 123. Organic acids content of basil leaves (b, elevated CO_2; con, control; L, additional light; PV, photovoltaic cells).

	Malic acid [g/kg]	Tartaric acid [g/kg]	Citric acid [g/kg]	Oxalic acid [g/kg]	Maleic acid [g/kg]	Fumaric acid [g/kg]
K3 (PV)	29.6 ± 19.6 a	15.0 ± 5.8 a	1.41 ± 1.04 ab	0.64 ± 0.51 a	0.06 ± 0.10 b	0.35 ± 0.25 a
K3 (PV L)	18.4 ± 12.1 a	11.6 ± 5.5 a	2.67 ± 2.90 ab	0.93 ± 0.63 a	0.29 ± 0.31 ab	0.23 ± 0.24 a
K4 (PV, b)	24.9 ± 14.5 a	14.8 ± 5.1 a	1.15 ± 0.35 b	1.15 ± 1.00 a	0.17 ± 0.04 ab	0.28 ± 0.27 a
K4 (PV, b, L)	21.5 ± 9.2 a	15.9 ± 6.8 a	3.71 ± 3.03 ab	1.01 ± 0.21 a	0.52 ± 0.28 ab	0.19 ± 0.19 a
K5 (con)	18.3 ± 13.1 a	14.6 ± 5.8 a	2.87 ± 1.32 ab	1.50 ± 1.14 a	0.38 ± 0.30 ab	0.10 ± 0.08 a
K5 (con L)	16.2 ± 11.7 a	12.4 ± 4.7 a	4.80 ± 2.41 a	0.65 ± 0.44 a	0.74 ± 0.44 a	0.14 ± 0.08 a
$P_{Lilliefors}$	0.062	0.019	0.001	0.000	0.018	0.000
$P_{Shapiro-Wilk}$	0.007	0.024	0.000	0.000	0.013	0.000
P_{Levene}	0.334	0.912	0.300	0.002	0.104	0.003
Post-hoc	ANOVA	Kruskal-Wallis	Kruskal-Wallis	Median	Kruskal-Wallis	Median

Different letters within a column indicate significant differences.

Significant differences in carbohydrate content were not detected, but a trend towards smaller concentrations at lower light intensities became obvious. Elevated atmospheric CO_2 concentrations promoted carbohydrate content in tendency and were thus able to compensate for the effect of a lower light intensity (Table 124).

Table 124. Carbohydrate content of basil leaves (b, elevated CO_2; con, control; L, additional light; PV, photovoltaic cells; n.d., not detected).

	Glucose [g/kg]	Fructose [g/kg]	Sucrose [g/kg]	Sum [g/kg]
K3 (PV)	7.47 ± 5.28 a	1.84 ± 0.93 a	n.d.	9.31 ± 4.98 a
K3 (PV L)	4.36 ± 1.81 a	1.74 ± 1.10 a	n.d.	6.10 ± 2.55 a
K4 (PV, b)	9.88 ± 5.96 a	2.21 ± 1.62 a	n.d.	12.09 ± 6.54 a
K4 (PV, b, L)	9.31 ± 3.63 a	1.72 ± 1.04 a	n.d.	11.03 ± 4.19 a
K5 (con)	9.71 ± 7.57 a	1.02 ± 0.70 a	n.d.	10.73 ± 7.73 a
K5 (con L)	9.35 ± 3.34 a	1.58 ± 1.10 a	1.14 ± 2.54	11.57 ± 5.13 a
$P_{Lilliefors}$	0.005	0.016	--	0.071
$P_{Shapiro-Wilk}$	0.007	0.001	--	0.028
P_{Levene}	0.000	0.019	--	0.000
Post-hoc	Median	Median	--	ANOVA

Different letters within a column indicate significant differences.

In summary, the present results impressively demonstrate the importance of light for the quality of basil. However, they also show that increased atmospheric CO_2 levels can have a positive effect on quality, particularly on the carbohydrate content in the leaves.

Funded by the European Union under Grant Agreement No 101096056. Views and opinions expressed are however those of the author(s) only and do not necessarily reflect those of the European Union or CINEA. Neither the European Union nor the granting authority can be held responsible for them.

2. Experiment Radish 28/02/ - 15/04/2025

The sensory panel test revealed for both leaves and tubers a similar rating (Table 125). Although the rating implies a distinct difference between the two light variants cultivated in chambers K3 and K4, the transition is rather fluent. The different rating for the variants in K3 and K4 might also reflect the visual appearance of the entire plants, as the panellists were allowed to select and harvest the plants from the growth containers.

Table 125. Relative visual & taste evaluations of radish leaves & tubers cultivated under shading by PVs (PV), shading & elevated CO_2 (PV & b) & control conditions (con), with (L) or without additional light.

	K3 (PV)	K3 (PV & L)	K4 (PV & b)	K4 (PV & b & L)	K5 (con)	K5 (con & L)
Taste & visual appearance; leaves	👎	👍	👎	👍	👍	👍
Taste & visual appearance; tubers	👎	👍	👎	👍	👍	👍

Leaf Chl content followed a difficult to interpret pattern. There was a tendency that additional light within a chamber was associated with a slightly lower leaf Chl content, however, this light response is not confirmed when the "control" variants are compared with the "PV" ones (Table 126). Car content positively correlated with light intensities.

Table 126. Chlorophyll and carotenoid content of radish leaves (b, elevated CO_2; con, control; L, additional light; PV, photovoltaic cells).

	Car [g/kg]	Chl a [g/kg]	Chl b [g/kg]	Tot Chl [g/kg]	Chl a/b [--]
K3 (PV)	0.86 ± 0.07 c	5.69 ± 0.40 ab	2.89 ± 0.40 ab	8.58 ± 0.69 ab	2.00 ± 0.27 c
K3 (PV L)	1.23 ± 0.05 a	5.34 ± 0.28 b	2.12 ± 0.26 c	7.46 ± 0.47 c	2.55 ± 0.26 a
K4 (PV, b)	1.06 ± 0.12 b	5.67 ± 0.26 ab	2.56 ± 0.30 abc	8.23 ± 0.48 b	2.23 ± 0.23 abc
K4 (PV, b, L)	1.22 ± 0.10 ab	5.46 ± 0.37 b	2.43 ± 0.45 bc	7.89 ± 0.66 bc	2.30 ± 0.37 abc
K5 (con)	1.22 ± 0.28 ab	6.13 ± 0.46 a	3.01 ± 0.47 a	9.14 ± 0.49 a	2.08 ± 0.37 bc
K5 (con L)	1.33 ± 0.20 a	6.09 ± 0.42 a	2.44 ± 0.33 bc	8.53 ± 0.35 ab	2.54 ± 0.42 ab
$P_{Lilliefors}$	>0.200	0.168	>0.200	>0.200	>0.200
$P_{Shapiro-Wilk}$	0.459	0.353	0.181	0.479	0.956
P_{Levene}	0.003	0.529	0.652	0.536	0.592
Post-hoc	Tamhane	Tukey	Tukey	Tukey	Tukey

Different letters within a column indicate significant differences.

Leaf flavonoid and total phenol contents did not differ significantly among variants, but antioxidative capacity was generally lower in leaves of plants cultivated under the PV system (Table 127). Nitrate content was highest in the low light variants "PV" (K3), "PV & additional light" (K3), and "PV & elevated CO_2".

Funded by the European Union

Funded by the European Union under Grant Agreement No 101096056. Views and opinions expressed are however those of the author(s) only and do not necessarily reflect those of the European Union or CINEA. Neither the European Union nor the granting authority can be held responsible for them.

Table 127. Flavonoid, phenol, and nitrate content as well as antioxidative capacity of radish leaves (b, elevated CO_2; con, control; L, additional light; PV, photovoltaic cells).

	Flavonoids [g/kg]	Phenols [g/kg]	Antiox. capacity [µmol/g]	Nitrate [g/kg]
K3 (PV)	24.6 ± 5.3 a	0.33 ± 0.03 ab	88.1 ± 15.1 bc	1.39 ± 0.75 a
K3 (PV L)	19.3 ± 1.8 a	0.31 ± 0.02 b	81.0 ± 9.7 c	1.07 ± 0.39 a
K4 (PV, b)	20.8 ± 2.1 a	0.32 ± 0.02 ab	76.6 ± 6.6 c	1.44 ± 0.35 a
K4 (PV, b, L)	21.9 ± 6.1 a	0.33 ± 0.04 ab	84.7 ± 7.6 bc	0.36 ± 0.23 c
K5 (con)	23.1 ± 2.2 a	0.34 ± 0.05 ab	105.4 ± 8.3 a	0.42 ± 0.17 bc
K5 (con L)	21.5 ± 1.3 a	0.35 ± 0.03 a	97.9 ± 6.7 ab	0.98 ± 0.42 ab
$P_{Lilliefors}$	0.047	0.018	>0.200	0.066
$P_{Shapiro-Wilk}$	0.001	0.010	0.265	0.013
P_{Levene}	0.003	0.102	0.142	0.001
Post-hoc	Median	Kruskal-Wallis	Tukey	Tamhane

Different letters within a column indicate significant differences.

Leaf citric acid content was elevated in the shaded variants of chamber K3 “PV” and “PV & additional light”. Oxalic acid content was highest in both control variants, altogether with respect to quality favouring the lower light intensity without elevated CO_2 (Table 128).

Table 128. Organic acids content of radish leaves (b, elevated CO_2; con, control; L, additional light; PV, photovoltaic cells).

	Malic acid [g/kg]	Citric acid [g/kg]	Oxalic acid [g/kg]	Fumaric acid [g/kg]
K3 (PV)	100.6 ± 12.9 a	36.5 ± 9.7 a	6.23 ± 2.48 ab	0.36 ± 0.05 a
K3 (PV L)	90.3 ± 20.2 a	34.4 ± 5.6 ab	5.45 ± 1.83 b	0.32 ± 0.06 ab
K4 (PV, b)	59.8 ± 13.7 a	18.3 ± 3.2 c	11.76 ± 2.66 a	0.27 ± 0.05 b
K4 (PV, b, L)	88.3 ± 11.0 a	26.4 ± 5.3 bc	4.19 ± 2.37 b	0.31 ± 0.05 ab
K5 (con)	57.8 ± 35.2 a	18.0 ± 8.6 c	16.44 ± 7.85 a	0.30 ± 0.06 ab
K5 (con L)	81.0 ± 29.8 a	23.4 ± 7.4 c	10.99 ± 4.72 a	0.33 ± 0.03 ab
$P_{Lilliefors}$	>0.200	>0.200	0.000	>0.200
$P_{Shapiro-Wilk}$	0.080	0.128	0.000	0.136
P_{Levene}	0.000	0.051	0.000	0.420
Post-hoc	Tamhane	Tukey	Median	Tukey

Different letters within a column indicate significant differences.

The observed differences in leaf carbohydrate content are small, but the trend favoured the “control” variants (K5) and the “PV” variants with elevated CO_2 “PV & elevated CO_2” and “PV & elevated CO_2 & light”, suggesting a positive effect of both, additional light and elevated atmospheric CO_2 levels (Table 129).

Funded by the European Union

Funded by the European Union under Grant Agreement No 101096056. Views and opinions expressed are however those of the author(s) only and do not necessarily reflect those of the European Union or CINEA. Neither the European Union nor the granting authority can be held responsible for them.

Table 129. Carbohydrate content of radish leaves (b, elevated CO_2; con, control; L, additional light; PV, photovoltaic cells; n.d., not detected).

	Glucose [g/kg]	Fructose [g/kg]	Sucrose [g/kg]	Sum [g/kg]
K3 (PV)	27.5 ± 6.6 b	18.7 ± 4.7 ab	n.d.	46.1 ± 9.0 b
K3 (PV L)	25.5 ± 4.7 b	19.8 ± 5.7 ab	n.d.	45.3 ± 8.1 b
K4 (PV, b)	31.9 ± 7.6 ab	18.0 ± 5.7 b	n.d.	49.9 ± 12.2 b
K4 (PV, b, L)	34.2 ± 13.7 ab	16.8 ± 8.6 b	2.1 ± 2.1 a	53.2 ± 22.6 ab
K5 (con)	36.2 ± 9.6 ab	24.1 ± 4.6 ab	n.d.	60.3 ± 13.8 ab
K5 (con L)	40.8 ± 7.4 a	27.6 ± 8.0 a	1.5 ± 1.8 a	69.9 ± 11.9 a
$P_{Lilliefors}$	>0.200	>0.200	--	0.050
$P_{Shapiro-Wilk}$	0.313	0.490	--	0.052
P_{Levene}	0.095	0.442	--	0.105
Post-hoc	Tukey	Tukey	T-Test	Tukey

Different letters within a column indicate significant differences.

With respect to tuber quality, neither antioxidative capacity nor anthocyanin, flavonoid, and total phenol contents indicated a trend attributable to the treatment parameters (Table 130). Nitrate content was elevated only in the variant “PV without additional light” (K3), but the difference was not significant.

Table 130. Anthocyanin, flavonoid, phenol, and nitrate content as well as antioxidative capacity of radish tubers (b, elevated CO_2; con, control; L, additional light; PV, photovoltaic cells).

	Anthocyanins [g/kg]	Flavonoids [g/kg]	Phenols [g/kg]	Antiox. capacity [µmol/g]	Nitrate [g/kg]
K3 (PV)	3.19 ± 0.90 a	1.49 ± 0.72 a	0.21 ± 0.02 ab	12.7 ± 1.7 abc	0.84 ± 0.64 a
K3 (PV L)	2.13 ± 0.42 ab	2.02 ± 1.85 a	0.23 ± 0.02 a	17.1 ± 1.9 a	0.60 ± 0.53 a
K4 (PV, b)	2.22 ± 0.52 ab	2.98 ± 0.85 a	0.20 ± 0.01 b	10.7 ± 1.5 c	0.60 ± 0.40 a
K4 (PV, b, L)	1.80 ± 0.22 b	2.44 ± 1.81 a	0.21 ± 0.02 ab	11.9 ± 1.6 bc	0.38 ± 0.06 a
K5 (con)	1.63 ± 0.40 b	1.87 ± 0.76 a	0.20 ± 0.01 b	14.5 ± 2.5 ab	0.61 ± 0.32 a
K5 (con L)	2.10 ± 0.49 ab	2.37 ± 1.46 a	0.20 ± 0.02 ab	11.7 ± 2.1 bc	0.30 ± 0.09 a
$P_{Lilliefors}$	0.009	0.054	0.079	0.005	0.000
$P_{Shapiro-Wilk}$	0.000	0.000	0.027	0.026	0.000
P_{Levene}	0.072	0.153	0.048	0.580	0.000
Post-hoc	Kruskal-Wallis	ANOVA	Tamhane	Kruskal-Wallis	Median

Different letters within a column indicate significant differences.

As in the case of the leaves, citric acid content tended to be elevated under shade conditions such as realised in chambers K3 and K4. The antinutritive oxalic acid content was highest in the variants “PV” (K3) and “PV & elevated CO_2” (K4), supporting additional light (Table 131). An unequivocal recommendation based on the organic acid content thus cannot be given.

Funded by the European Union under Grant Agreement No 101096056. Views and opinions expressed are however those of the author(s) only and do not necessarily reflect those of the European Union or CINEA. Neither the European Union nor the granting authority can be held responsible for them.

Table 131. Organic acids content of radish tubers (b, elevated CO_2; con, control; L, additional light; PV, photovoltaic cells).

	Malic acid [g/kg]	Tartaric acid [g/kg]	Citric acid [g/kg]	Oxalic acid [g/kg]	Fumaric acid [g/kg]
K3 (PV)	58.6 ± 12.0 a	2.92 ± 0.86 ab	2.74 ± 1.59 a	10.21 ± 3.17 a	1.26 ± 0.36 a
K3 (PV L)	61.5 ± 4.8 a	3.43 ± 0.91 a	2.90 ± 2.88 a	1.30 ± 1.12 c	1.40 ± 0.33 a
K4 (PV, b)	57.7 ± 14.6 a	2.19 ± 0.53 b	2.02 ± 0.67 ab	5.19 ± 2.11 b	1.26 ± 0.45 a
K4 (PV, b, L)	56.4 ± 10.7 a	2.13 ± 0.71 b	2.30 ± 1.48 a	0.52 ± 0.14 c	1.28 ± 0.20 a
K5 (con)	55.2 ± 11.8 a	2.48 ± 0.55 ab	1.30 ± 0.34 b	0.56 ± 0.19 c	1.57 ± 0.64 a
K5 (con L)	58.6 ± 10.6 a	1.77 ± 0.67 b	1.04 ± 0.31 b	0.77 ± 0.32 c	1.58 ± 0.52 a
$P_{Lilliefors}$	>0.200	0.020	0.000	0.000	0.013
$P_{Shapiro-Wilk}$	0.129	0.023	0.000	0.000	0.001
P_{Levene}	0.149	0.448	0.000	0.002	0.046
Post-hoc	ANOVA	Kruskal-Wallis	Median	Median	Median

Different letters within a column indicate significant differences.

Carbohydrate content of tubers was clearly light-dependent (Table 132). The content was lowest in the variants cultivated below the PV system and not supported by additional CO_2 in the atmosphere.

Table 132. Carbohydrate content of radish tubers (b, elevated CO_2; con, control; L, additional light; PV, photovoltaic cells).

	Glucose [g/kg]	Fructose [g/kg]	Sucrose [g/kg]	Sum [g/kg]
K3 (PV)	80.0 ± 15.2 bc	70.2 ± 11.1 b	6.3 ± 2.1 b	156.4 ± 22.2 bc
K3 (PV L)	132.8 ± 13.7 a	128.9 ± 9.0 a	6.5 ± 1.7 b	268.2 ± 19.6 a
K4 (PV, b)	76.7 ± 13.3 c	51.1 ± 8.8 c	6.4 ± 3.4 b	134.2 ± 20.4 c
K4 (PV, b, L)	116.2 ± 17.7 ab	99.2 ± 19.9 a	14.2 ± 3.2 a	230.9 ± 35.7 ab
K5 (con)	112.7 ± 21.7 ab	108.1 ± 19.5 a	5.0 ± 1.0 b	225.8 ± 40.1 ab
K5 (con L)	119.4 ± 16.8 a	118.6 ± 22.2 a	8.4 ± 3.0 ab	246.4 ± 38.6 a
$P_{Lilliefors}$	0.021	0.003	0.001	0.001
$P_{Shapiro-Wilk}$	0.021	0.005	0.000	0.002
P_{Levene}	0.226	0.012	0.052	0.074
Post-hoc	Kruskal-Wallis	Median	Kruskal-Wallis	Kruskal-Wallis

Different letters within a column indicate significant differences.

In summary, the results of the chemical analyses confirmed that additional light is positive for the taste and flavour of radish leaves and tubers, explaining also the results of the sensory panel. The present results suggest that carbohydrate content influenced the perception of the panellists most, because it was correlated best with the panel results. Antioxidative capacity, anthocyanin, flavonoid, and total phenol contents were less important parameters for radish quality and nitrate content was generally lower under elevated light levels. By contrast, for organic acids lower light intensities seemed to be advantageous, especially for leaves. Considering, however, yield parameters, it is out of question that an adequate light level, if necessary, with additional illumination, should be recommended for radish cultivation.

Funded by the European Union

Funded by the European Union under Grant Agreement No 101096056. Views and opinions expressed are however those of the author(s) only and do not necessarily reflect those of the European Union or CINEA. Neither the European Union nor the granting authority can be held responsible for them.

Discussion: All of the experiments indicated that an elevated light intensity is positive for produce quality. However, differences existed between the investigated crops with respect to the required light intensity. The supply of CO_2Bags or the addition of extra CO_2 in order to maintain distinctly elevated atmospheric CO_2 levels in the chambers were able to compensate for some of the negative effects of a limiting light intensity, especially with respect to the carbohydrate content, but ultimately were unable to completely substitute the required light intensity. In the case of CO_2Bags, there was a tendency towards higher nitrate levels in some of the crops.

Literature

Akhtar, H.M.N., Rahman, S.M.M., Muslim, T. (2010) Comparative study of the content of vitamin C in fresh fruits and different types of food prepared from them. Dhaka Univ. J. Sci, 58 (1), 55–57. https://journal.library.du.ac.bd/index.php/dujs/article/view/448

Giusti, M.M., Wrolstad, R.E. (2001) Characterization and measurement of anthocyanins by UV-visible spectroscopy. Current Protocols in Food Analytical Chemistry, F1.2.1-F1.2.13. DOI: 10.1002/0471142913.faf0102s00

Keutgen, A.J., Pawelzik, E. (2007) Modifications of strawberry fruit antioxidant pools and fruit quality under NaCl stress. Journal of Agricultural and Food Chemistry 55 (10), 4066-4072. DOI:10.1021/jf070010k

Sumanta, N., Haque, C.I., Nishika, J. Suprakash, R. (2014) Spectrophotometric analysis of chlorophylls and carotenoids from commonly grown fern species by using various extracting solvents. Research Journal of Chemical Sciences, 4 (9), 63-69.

6 Water use efficiency of crops cultivated in the greenhouses

6.1 Determination of water use efficiency for fully closed recirculating irrigation systems

Two experiments at HU Berlin with *Lactuca sativa* cv. Binex did not reveal differences in growth and yield among the variants ‘control’, ‘light shade’, ‘medium shade’ and ‘heavy shade’, resulting in similar water use efficiencies of 17.34 g and 5.22 g fresh mass per liter, respectively (see chapter 7.2.1). In the case of *Lycopersicon esculentum* 'Avalantino F1', the plants showed significant differences in the biomass and fruit development, whereby the general reduction in biomass and fruit yield followed the increasing shade level. The general water use efficiency was calculated at 18.28 kg per m^{-3} fertilizer solution.

6.2 Determination of water consumption per yield unit depending on the use of PV modules and comparison with photosynthetic water use efficiency

In the BOKU experiments, water use efficiency was calculated as yield [g] per water consumed [L]. The results are summarised in Tables 133 and 134, where Table 133 refers to the experiments with CO_2Bags and Table 134 refers to those with elevated atmospheric CO_2 concentrations achieved by adding mushroom-produced CO_2 into the greenhouse chamber (K4). When CO_2Bags were used, water use

Funded by the European Union under Grant Agreement No 101096056. Views and opinions expressed are however those of the author(s) only and do not necessarily reflect those of the European Union or CINEA. Neither the European Union nor the granting authority can be held responsible for them.

efficiency was highest in the variant "shading by nets & CO_2Bags" in basil and lettuce, whereas in *Capsicum annuum* and radish it was largest in the "control" treatment. For cucumber, water use efficiencies of the "control" and "shading by nets & CO_2Bags" variants were comparable. These results indicate that an unequivocal response of plants does not exist, but may be species-dependent. Noteworthy, in the case of basil and lettuce, yield is determined by leaf mass production and it is well documented that allocation of photoassimilates into leaf production relative to generative or storage organs is supported under shading conditions in order to promote photosynthesis. It is also well known that water consumption under shading is less and also the current experiments indicate that water use efficiency of basil and lettuce under shading conditions without CO_2Bags is (slightly) higher than in the "control" variant. In the case of fruits (*Capsicum annuum*) and tubers (radish) it is thus not surprising that water use efficiency was largest under "control" conditions, as the yield-relevant compounds were simply not produced under low light intensities as impressively indicated in the radish experiment between 06/03/ and 11/05/2024. In this respect, the cucumber experiment represented a remarkable exception, as water used efficiencies in chambers K4 and K5 were similar. Yield under shading conditions was half the amount of the control variant, and water consumption as well.

Table 133. Water use efficiencies calculated as yield [g] per water consumed [L] in the experiments performed by BOKU with shading nets (s) or under PV systems (PV) with or without CO_2Bags (S, shading; b, CO_2-bags; con, control; PV, photovoltaic system).

	K3 (s) [g L^{-1}]	K4 (s & b) [g L^{-1}]	K5 (con) [g L^{-1}]	K3 (PV) [g L^{-1}]	K4 (PV & b) [g L^{-1}]	Remarks
Basil 23/03/ - 15/06/2023	1.80	**2.43**	1.73			
Basil 02/01/ - 21/03/2024	3.08	**4.79**	2.83			
Capsicum 23/03/ - 15/08/2023	2.45 1.86 0.53	3.40 2.65 0.78	**6.05** **3.78** **1.55**			cv. Bendigo cv. California Wonder cv. De Cayenne
Lactuca 16/05/ - 17/07/2023	69.0	**79.0**	53.1			
Cucumis 06/03/ - 29/05/2024	3.26	**26.6**	**26.9**			
Capsicum 06/03/ - 31/08/2024	1.67	3.24	**11.5**	4.84	9.49	
Radish 06/03/ - 11/05/2024	0.06	0.41	**8.50**			
Radish 22/03/ - 16/05/2024			**18.7**	11.1	11.9	

The experiments with elevated CO_2 concentrations and additional light showed a comparable but not identical pattern (Table 134) as indicated in the experiments summarized in Table 133. In the case of basil, the variant "shading by PV & elevated CO_2 & light" performed with respect to water use efficiency best, but considering only the treatments without additional light, water use efficiency of the "control" variant

Funded by the European Union

Funded by the European Union under Grant Agreement No 101096056. Views and opinions expressed are however those of the author(s) only and do not necessarily reflect those of the European Union or CINEA. Neither the European Union nor the granting authority can be held responsible for them.

was better than that of the variant "shading by PV & elevated CO_2", indicating that the ratio of the effects of additional light and additional CO_2 may be decisive. In the case of radish, it was obviously the "control" variants that performed best.

Table 134. Water use efficiencies calculated as yield [g] per water consumed [L] in the BOKU experiments under PV systems (PV) with or without elevated atmospheric CO_2 concentrations, and with or without additional light (b, additional CO_2; con, control; L, additional light; PV, photovoltaic cells).

	K3 (PV) [g L^{-1}]	K3 (PV & L) [g L^{-1}]	K4 (PV & b) [g L^{-1}]	K4 (PV & b & L) [g L^{-1}]	K5 (con) [g L^{-1}]	K5 (con & L) [g L^{-1}]
Basil 30/01/ - 07/04/2025	11.3	14.3	11.7	**18.8**	15.7	16.9
Radish 22/03/ - 16/05/2024	8.8	42.3	6.1	29.7	30.6	**54.7**

It may be added that in the experiments performed at the UTH (Greece) water use efficiency was not significantly affected in cucumber, while in the lettuce experiment the response remined unclear (Table 68). Similarly, at FSC (Italy) water use efficiency under the PV system was similar when compared to the control in the case of zucchini, whereas it was higher in the case of the control treatment in tomato and eggplant, but in the lettuce experiment WUE of the shaded variant was larger (Table 75). At Watzkendorf (Germany) WUE was always larger under PV shading in the case of tomato and cucumber (Tables 58-59), altogether suggesting that the crop- or even cultivar-specific requirements in combination with the local environment conditions do not allow a general conclusion to predict optimal WUE.

At BOKU university, photosynthetic water use efficiency was assessed for the two basil experiments (23/03/ - 15/06/2023 and 02/01/ - 21/03/2024) as well. Gas exchange parameters were measured under different conditions:

- An atmospheric CO_2 concentration of c. 400 µmol mol^{-1} and a light intensity of c. 100 µmol m^{-2} s^{-1} PAR
- An atmospheric CO_2 concentration of c. 400 µmol mol^{-1} and a light intensity of c. 500 µmol m^{-2} s^{-1} PAR
- An atmospheric CO_2 concentration of c. 600 µmol mol^{-1} and a light intensity of c. 500 µmol m^{-2} s^{-1} PAR

The first conditions resemble those in the greenhouse chambers, especially with respect to the average light intensity. With respect to the atmospheric CO_2 concentrations, it should be kept in mind that the CO_2Bags did not result in a distinct increase, at best in a slight increase of up to 20 µmol mol^{-1}. The second set of measurements were undertaken under an elevated light intensity, which could have been achieved short-term during the day. The conditions of the third set of measurements examined the plants' response to elevated atmospheric CO_2 concentrations.

The results of the first set of measurements are summarised in Tables 135–138, where the 2023 (Tables 135–136) and 2024 experiments (Tables 137–138) were analysed separately. With respect to water use

Funded by the European Union

Funded by the European Union under Grant Agreement No 101096056. Views and opinions expressed are however those of the author(s) only and do not necessarily reflect those of the European Union or CINEA. Neither the European Union nor the granting authority can be held responsible for them.

efficiency, differences were not detected in 2023, but in 2024 leaves of the variant "shading" without additional CO_2 performed best. These results differ from the water used efficiencies calculated as the ratio yield per water consumed, where "shading & CO_2Bags" performed best.

Table 135. Photosynthesis parameters of the 2023 basil experiment measured at c. 400 µmol mol^{-1} CO_2 and 100 µmol m^{-2} s^{-1} PAR (s, shading; b, CO_2Bags; con, control).

	CO_2 [µmol mol^{-1}]	PAR [µmol m^{-2} s^{-1}]	Photosynthesis [µmol CO_2 m^{-2} s^{-1}]	Transpiration [mmol H_2O m^{-2} s^{-1}]
K3 (s)	394 ± 7	99 ± 0	1.8 ± 0.8 a	0.45 ± 0.17 a
K4 (s & b)	392 ± 12	99 ± 0	2.0 ± 0.7 a	0.42 ± 0.10 a
K5 (con)	393 ± 8	99 ± 0	1.5 ± 0.4 a	0.31 ± 0.11 a
$P_{Lilliefors}$			> 0.200	> 0.200
$P_{Shapiro-Wilk}$			0.491	0.516
P_{Levene}			0.322	0.569
Post-hoc			ANOVA	ANOVA

Table 136. Photosynthesis parameters of the 2023 basil experiment measured at c. 400 µmol mol^{-1} CO_2 and 100 µmol m^{-2} s^{-1} PAR (s, shading; b, CO_2Bags; con, control).

	Stomatal conductance [mmol H_2O m^{-2} s^{-1}]	Leaf internal CO_2 concentration [µmol mol^{-1}]	Water use efficiency [µmol CO_2 m^{-2} s^{-1}/mmol H_2O m^{-2} s^{-1}]
K3 (s)	21.1 ± 8.9 a	231 ± 63 a	4.3 ± 1.8 a
K4 (s & b)	20.8 ± 6.4 a	198 ± 44 a	4.7 ± 0.7 a
K5 (con)	13.9 ± 5.7 a	190 ± 62 a	5.2 ± 1.5 a
$P_{Lilliefors}$	> 0.200	> 0.200	> 0.200
$P_{Shapiro-Wilk}$	0.462	0.536	0.467
P_{Levene}	0.603	0.528	0.130
Post-hoc	ANOVA	ANOVA	ANOVA

Table 137. Photosynthesis parameters of the 2024 basil experiment measured at c. 400 µmol mol^{-1} CO_2 and 100 µmol m^{-2} s^{-1} PAR (s, shading; b, CO_2Bags; con, control).

	CO_2 [µmol mol^{-1}]	PAR [µmol m^{-2} s^{-1}]	Photosynthesis [µmol CO_2 m^{-2} s^{-1}]	Transpiration [mmol H_2O m^{-2} s^{-1}]
K3 (s)	400 ± 0	99 ± 0	2.1 ± 0.4 a	0.61 ± 0.25 a
K4 (s & b)	400 ± 0	99 ± 1	2.1 ± 0.8 a	0.80 ± 0.32 a
K5 (con)	400 ± 0	100 ± 1	1.7 ± 0.5 a	0.70 ± 0.17 a
$P_{Lilliefors}$			> 0.200	> 0.200
$P_{Shapiro-Wilk}$			0.886	0.273
P_{Levene}			0.098	0.289
Post-hoc			ANOVA	ANOVA

Funded by the European Union

Funded by the European Union under Grant Agreement No 101096056. Views and opinions expressed are however those of the author(s) only and do not necessarily reflect those of the European Union or CINEA. Neither the European Union nor the granting authority can be held responsible for them.

Table 138. Photosynthesis parameters of the 2024 basil experiment measured at c. 400 µmol mol^{-1} CO_2 and 100 µmol m^{-2} s^{-1} PAR (s, shading; b, CO_2Bags; con, control).

	Stomatal conductance [mmol H_2O m^{-2} s^{-1}]	Leaf internal CO_2 concentration [µmol mol^{-1}]	Water use efficiency [µmol CO_2 m^{-2} s^{-1}/mmol H_2O m^{-2} s^{-1}]
K3 (s)	26.6 ± 11.6 a	241 ± 42 b	3.9 ± 1.3 a
K4 (s & b)	36.5 ± 16.2 a	286 ± 25 a	2.7 ± 0.7 b
K5 (con)	28.6 ± 7.9 a	285 ± 33 ab	2.5 ± 0.8 b
$P_{Lilliefors}$	> 0.200	0.007	0.088
$P_{Shapiro-Wilk}$	0.108	0.007	0.008
P_{Levene}	0.070	0.201	0.083
Post-hoc	ANOVA	Kruskal-Wallis	ANOVA

In the second set of measurements, photosynthetic water use efficiency was highest in 2023 in the variant "shading & CO_2Bags", but the mean value was not significantly different from the "control" (Tables 139-140). The variant "shading" performed least. In 2024 significant differences of the water use efficiency among the variants could not be detected (Tables 141-142). The varying annual results make it difficult to interpret the findings.

Table 139. Photosynthesis parameters of the 2023 basil experiment measured at c. 400 µmol mol^{-1} CO_2 and 500 µmol m^{-2} s^{-1} PAR (s, shading; b, CO_2Bags; con, control).

	CO_2 [µmol mol^{-1}]	PAR [µmol m^{-2} s^{-1}]	Photosynthesis [µmol CO_2 m^{-2} s^{-1}]	Transpiration [mmol H_2O m^{-2} s^{-1}]
K3 (s)	394 ± 9	502 ± 2	3.6 ± 0.9 b	0.82 ± 0.24 a
K4 (s & b)	391 ± 11	501 ± 1	6.1 ± 1.2 a	0.75 ± 0.18 ab
K5 (con)	394 ± 9	501 ± 2	3.4 ± 0.9 b	0.51 ± 0.18 b
$P_{Lilliefors}$			0.084	> 0.200
$P_{Shapiro-Wilk}$			0.240	0.491
P_{Levene}			0.936	0.639
Post-hoc			Tukey-B	Tukey-B

Table 140. Photosynthesis parameters of the 2023 basil experiment measured at c. 400 µmol mol^{-1} CO_2 and 500 µmol m^{-2} s^{-1} PAR (s, shading; b, CO_2Bags; con, control).

	Stomatal conductance [mmol H_2O m^{-2} s^{-1}]	Leaf internal CO_2 concentration [µmol mol^{-1}]	Water use efficiency [µmol CO_2 m^{-2} s^{-1}/mmol H_2O m^{-2} s^{-1}]
K3 (s)	39.5 ± 11.8 a	218 ± 60 a	4.8 ± 1.7 b
K4 (s & b)	38.0 ± 11.0 a	41 ± 12 b	9.6 ± 1.8 a
K5 (con)	23.1 ± 8.8 b	115 ± 99 ab	7.4 ± 2.7 ab
$P_{Lilliefors}$	> 0.200	0.040	> 0.200
$P_{Shapiro-Wilk}$	0.697	0.033	0.373
P_{Levene}	0.775	0.088	0.530
Post-hoc	Tukey-B	Kruskal-Wallis	Tukey-B

Funded by the European Union

Funded by the European Union under Grant Agreement No 101096056. Views and opinions expressed are however those of the author(s) only and do not necessarily reflect those of the European Union or CINEA. Neither the European Union nor the granting authority can be held responsible for them.

Table 141. Photosynthesis parameters of the 2024 basil experiment measured at c. 400 µmol mol^{-1} CO_2 and 500 µmol m^{-2} s^{-1} PAR (s, shading; b, CO_2Bags; con, control).

	CO_2 [µmol mol^{-1}]	PAR [µmol m^{-2} s^{-1}]	Photosynthesis [µmol CO_2 m^{-2} s^{-1}]	Transpiration [mmol H_2O m^{-2} s^{-1}]
K3 (s)	400 ± 0	500 ± 8	5.1 ± 0.6 a	0.96 ± 0.22 a
K4 (s & b)	400 ± 0	500 ± 7	5.8 ± 0.7 a	1.15 ± 0.18 a
K5 (con)	400 ± 0	499 ± 7	5.0 ± 1.4 a	1.03 ± 0.18 a
$P_{Lilliefors}$			> 0.200	> 0.200
$P_{Shapiro-Wilk}$			0.618	0.355
P_{Levene}			0.029	0.465
Post-hoc			ANOVA	ANOVA

Table 142. Photosynthesis parameters of the 2024 basil experiment measured at c. 400 µmol mol^{-1} CO_2 and 500 µmol m^{-2} s^{-1} PAR (s, shading; b, CO_2Bags; con, control).

	Stomatal conductance [mmol H_2O m^{-2} s^{-1}]	Leaf internal CO_2 concentration [µmol mol^{-1}]	Water use efficiency [µmol CO_2 m^{-2} s^{-1}/mmol H_2O m^{-2} s^{-1}]
K3 (s)	42.5 ± 10.2 a	182 ± 32 a	5.4 ± 0.8 a
K4 (s & b)	52.2 ± 10.9 a	194 ± 39 a	5.2 ± 1.0 a
K5 (con)	42.6 ± 8.3 a	189 ± 49 a	4.9 ± 1.1 a
$P_{Lilliefors}$	> 0.200	0.159	> 0.200
$P_{Shapiro-Wilk}$	0.683	0.513	0.849
P_{Levene}	0.246	0.368	0.304
Post-hoc	ANOVA	ANOVA	ANOVA

In the case of the third set of measurements, the 2023 results showed a clear trend with respect to photosynthetic water use efficiency (Tables 143-146): the "control" variant performed best, followed by "shading & CO_2Bags", and the variant "shading" performed least. In 2024 the variant "shading & CO_2Bags" was characterised by the highest photosynthetic water use efficiency, the variant "shading" was intermediate and the "control" treatment performed least. Again, these results do not allow a reliable interpretation.

Table 143. Photosynthesis parameters of the 2023 basil experiment measured at c. 600 µmol mol^{-1} CO_2 and 500 µmol m^{-2} s^{-1} PAR (s, shading; b, CO_2Bags; con, control).

	CO_2 [µmol mol^{-1}]	PAR [µmol m^{-2} s^{-1}]	Photosynthesis [µmol CO_2 m^{-2} s^{-1}]	Transpiration [mmol H_2O m^{-2} s^{-1}]
K3 (s)	589 ± 16	503 ± 2	6.3 ± 0.9 b	1.03 ± 0.22 b
K4 (s & b)	583 ± 24	503 ± 1	10.1 ± 0.9 a	1.33 ± 0.25 a
K5 (con)	595 ± 11	501 ± 3	6.5 ± 1.0 b	0.58 ± 0.15 c
$P_{Lilliefors}$			0.088	> 0.200
$P_{Shapiro-Wilk}$			0.036	0.389
P_{Levene}			0.975	0.118
Post-hoc			Tukey-B	Tukey-B

Funded by the European Union

Funded by the European Union under Grant Agreement No 101096056. Views and opinions expressed are however those of the author(s) only and do not necessarily reflect those of the European Union or CINEA. Neither the European Union nor the granting authority can be held responsible for them.

Table 144. Photosynthesis parameters of the 2023 basil experiment measured at c. 600 µmol mol^{-1} CO_2 and 500 µmol m^{-2} s^{-1} PAR (s, shading; b, CO_2Bags; con, control).

	Stomatal conductance [mmol H_2O m^{-2} s^{-1}]	Leaf internal CO_2 concentration [µmol mol^{-1}]	Water use efficiency [µmol CO_2 m^{-2} s^{-1}/mmol H_2O m^{-2} s^{-1}]
K3 (s)	50.6 ± 11.9 b	352 ± 46 a	6.3 ± 1.0 c
K4 (s & b)	66.8 ± 17.2 a	265 ± 58 b	8.8 ± 1.7 b
K5 (con)	26.5 ± 7.9 c	163 ± 77 c	11.5 ± 1.8 a
$P_{Lilliefors}$	> 0.200	> 0.200	> 0.200
$P_{Shapiro-Wilk}$	0.225	0.315	0.271
P_{Levene}	0.190	0.560	0.271
Post-hoc	Tukey-B	Tukey-B	Tukey-B

Table 145. Photosynthesis parameters of the 2024 basil experiment measured at c. 600 µmol mol^{-1} CO_2 and 500 µmol m^{-2} s^{-1} PAR (s, shading; b, CO_2Bags; con, control).

	CO_2 [µmol mol^{-1}]	PAR [µmol m^{-2} s^{-1}]	Photosynthesis [µmol CO_2 m^{-2} s^{-1}]	Transpiration [mmol H_2O m^{-2} s^{-1}]
K3 (s)	600 ± 0	498 ± 6	8.0 ± 0.8 b	1.09 ± 0.33 b
K4 (s & b)	600 ± 0	502 ± 6	9.8 ± 1.8 a	1.15 ± 0.31 b
K5 (con)	600 ± 0	496 ± 5	9.8 ± 2.0 a	1.56 ± 0.41 a
$P_{Lilliefors}$			0.033	> 0.200
$P_{Shapiro-Wilk}$			0.117	0.198
P_{Levene}			0.051	0.756
Post-hoc			Tukey-B	Tukey-B

Table 146. Photosynthesis parameters of the 2024 basil experiment measured at c. 600 µmol mol^{-1} CO_2 and 500 µmol m^{-2} s^{-1} PAR (s, shading; b, CO_2Bags; con, control).

	Stomatal conductance [mmol H_2O m^{-2} s^{-1}]	Leaf internal CO_2 concentration [µmol mol^{-1}]	Water use efficiency [µmol CO_2 m^{-2} s^{-1}/mmol H_2O m^{-2} s^{-1}]
K3 (s)	48.8 ± 15.8 a	290 ± 66 a	7.6 ± 1.6 ab
K4 (s & b)	51.3 ± 15.0 a	244 ± 69 a	8.8 ± 1.8 a
K5 (con)	67.4 ± 19.6 a	314 ± 83 a	6.6 ± 1.9 b
$P_{Lilliefors}$	> 0.200	0.006	> 0.200
$P_{Shapiro-Wilk}$	0.285	0.071	0.413
P_{Levene}	0.644	0.939	0.738
Post-hoc	ANOVA	ANOVA	Tukey-B

Discussion: The photosynthetic water use efficiency measurements did not reveal clear results. Here, we focus with the interpretation onto the measurements that were performed under the conditions normally present in the chambers, which are summarised in Tables 135-138. Photosynthetic water use efficiencies were not different in 2023 and in 2024 it was largest under shaded conditions without additional CO_2. These data allow us to conclude that they do not reflect the water use efficiency calculated based on water consumption and yield. For the farmer, however, the latter calculation is of practical relevance,

Funded by the European Union

Funded by the European Union under Grant Agreement No 101096056. Views and opinions expressed are however those of the author(s) only and do not necessarily reflect those of the European Union or CINEA. Neither the European Union nor the granting authority can be held responsible for them.

whereas photosynthetic water use efficiency is not, as it did not relate water investment costs to the income or the profit generated by the plant produce.

7 CO_2-enrichment as compensation possibility

7.1 Preliminary experiments under different CO_2-, light- and temperature-conditions in phytoboxes

At Humboldt University, the PV modules were installed in a well-insulated solar collector greenhouse equipped with a finned tube cooling system installed under the roof. In addition to the cooling system, double energy screens were installed under the roof and on the sides. The cooling system enables closed operation (no ventilation openings) and thus a longer CO_2 enrichment time compared to conventional greenhouses. Next to it is a reference greenhouse with the same floor space, but without a cooling system and with only one energy screen under the roof (Figures 164-165). The following conclusions refer to the comparison of these two greenhouses.

Light distribution measurements were taken before installing the PV elements in the collector greenhouse. Due to the shadow effect of the double energy screens (east-west shadow) and the finned tubes for cooling (north-south shadow) in the collector greenhouse, there was an 11% reduction in light in the case of direct solar radiation under cloudless skies (Dannehl et al., 2012), of which, according to Schuch (2014), around 5% was attributable to the ribbed pipes and 6% to the double screen packages.

Figure 164. Experimental greenhouses at Humboldt University in Berlin; on the left, the collector greenhouse with technical cooling and maximum thermal insulation before the installation of PV elements; on the right, an identical reference greenhouse with conventional equipment.

Funded by the European Union

Funded by the European Union under Grant Agreement No 101096056. Views and opinions expressed are however those of the author(s) only and do not necessarily reflect those of the European Union or CINEA. Neither the European Union nor the granting authority can be held responsible for them.

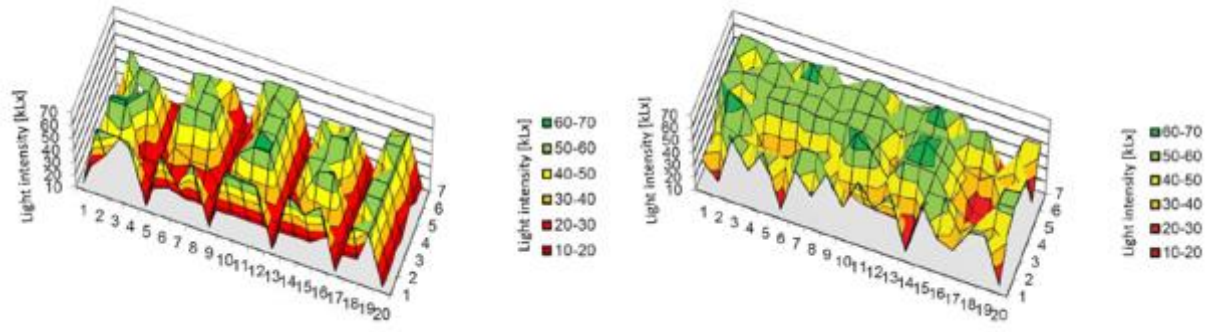

Figure 165. Differences between light intensities and light distribution between the two experimental greenhouses before installation of the PV panels in the collector greenhouse (left image).

The reference house showed that, on April 2nd and April 3rd, higher CO_2 concentrations due to cooling in the collector house (with a ventilation opening of 0%) led to approximately 25% higher photosynthesis rates (Figure 166). On April 4th, when outdoor temperatures were lower, ventilation in the reference house could also remain largely closed. Consequently, photosynthesis exceeded that of the collector house in the morning and afternoon at the same CO_2 levels, due to the higher light transmission in the reference house.

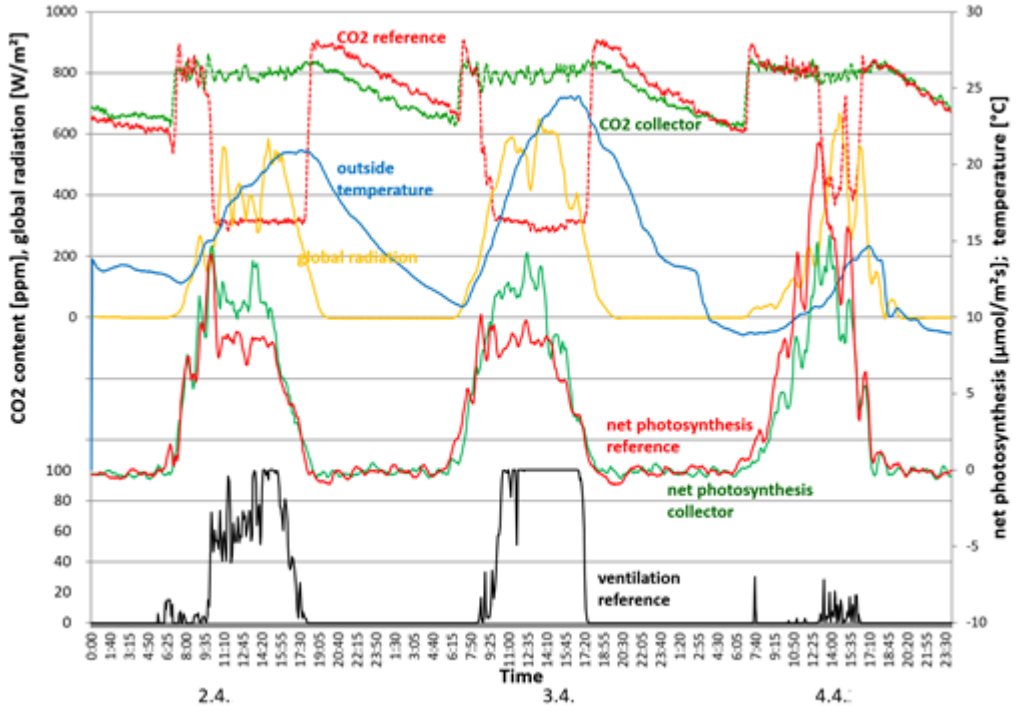

Figure 166. Comparative measurements in the two experimental greenhouses with tomatoes grown hydroponically under high radiation (first two days) and moderate radiation and lower outside temperature (third day of the experiment).

Funded by the European Union under Grant Agreement No 101096056. Views and opinions expressed are however those of the author(s) only and do not necessarily reflect those of the European Union or CINEA. Neither the European Union nor the granting authority can be held responsible for them.

Funded by the European Union

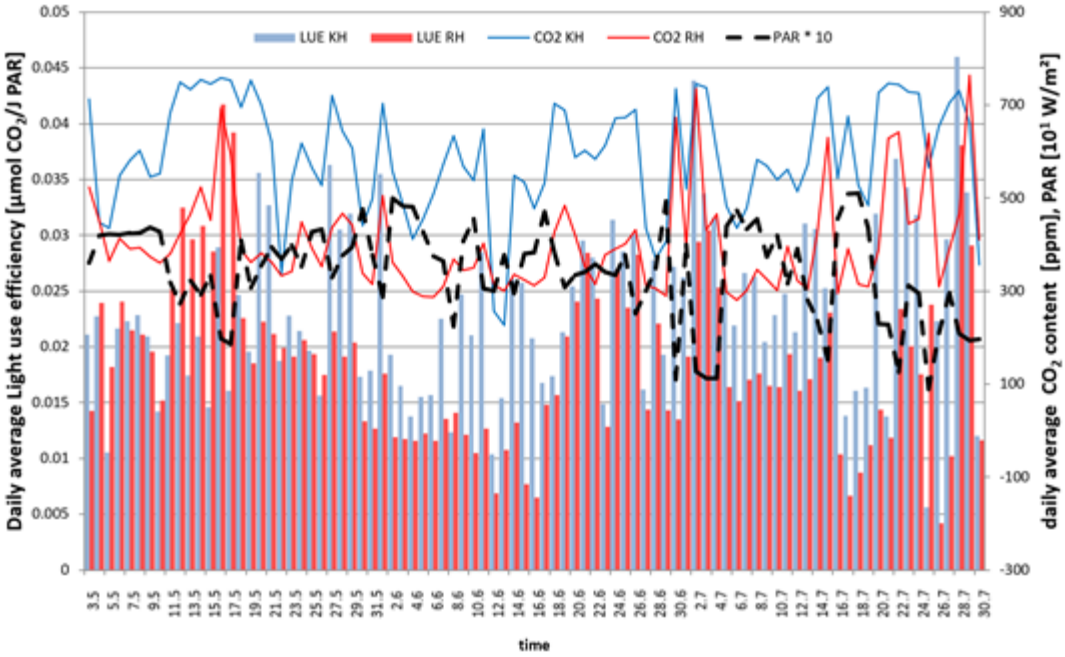

Figure 167. Comparison of light use efficiency (LUE) (bars) and CO_2 concentrations (lines) under different microclimate and PAR conditions (black dotted line) in the collector (blue) and reference greenhouse (red) over an entire summer period.

Continuous measurements of light use efficiency (LUE) (ratio of photosynthesis to photosynthetically active radiation, PAR) show that the situations described in Figure 167 are typical for the entire cultivation period in summer. From May 9 to May 17, moderate outdoor temperatures prevailed. Ventilation in both houses was mostly closed, resulting in similar CO_2 concentrations in both greenhouses. The advantage of higher light intensity in the reference house meant that the LUE values of the reference house were higher than those of the collector house.

Except in May, the CO_2 concentrations differ significantly. The light use efficiency of the reference house increases when the average PAR value is low. The reason for this can be seen in the smaller ventilation openings in both houses and in the greater increase in photosynthesis at lower PAR values.

Funded by the European Union

Funded by the European Union under Grant Agreement No 101096056. Views and opinions expressed are however those of the author(s) only and do not necessarily reflect those of the European Union or CINEA. Neither the European Union nor the granting authority can be held responsible for them.

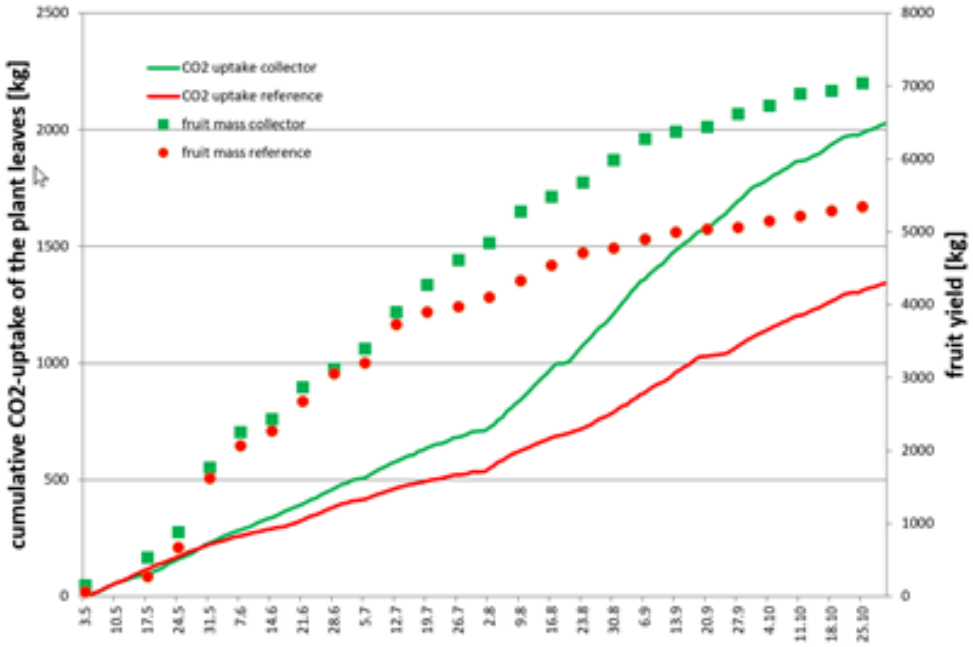

Figure 168. Net CO_2 uptake of leaves continuously measured with two gas exchange measurement systems and fruit yield of tomato in the collector (green) and reference greenhouse (red).

From the beginning of June onwards, the situation shown in Figure 167 results in differences in the net photosynthetic CO_2 uptake of the tomato leaves. Five weeks later, the resulting differences in the fruit yield of the tomato plants become apparent. During the cultivation period, a 23% increase in yield was achieved.

Conclusion: In terms of plant yield, the reduction in light intensity in the greenhouse can be compensated for by increased CO_2 concentrations. To achieve this, the closed greenhouse concept must be implemented. A key requirement is an efficient cooling system that largely prevents the ventilation from opening in response to high solar radiation and provides automated CO_2 enrichment throughout the day.

Literature

Dannehl, D., Huber, C., Rocksch, T., Huyskens-Keil, S., Schmidt, U. (2012) Interactions between changing climate conditions in a semi-closed greenhouse and plant development, fruit yield, and health-promoting plant compounds of tomatoes, Scientia Horticulturae, 138, 235-243.

Schuch, I., Dannehl, D., Rocksch, T., Schmidt, U. (2014) Energieeffizienz des Solarkollektorgewächshauses mit Wärmespeicher - ein Resümee aus 5 Jahren ZINEG-Projektarbeit. DGG-Proceedings, Vol. 4, Oct. 2014, No. 3, p. 1-5. DOI: 10.5288/dgg-pr-04-03-is-2014.

Funded by the European Union

Funded by the European Union under Grant Agreement No 101096056. Views and opinions expressed are however those of the author(s) only and do not necessarily reflect those of the European Union or CINEA. Neither the European Union nor the granting authority can be held responsible for them.

7.2 Experiments on the effect of CO_2-enrichment under PV modules in the greenhouses

7.2.1 CO_2-enrichment by application from CO_2-cylinders

At Humboldt University, the PV modules were installed in a well-insulated solar collector greenhouse equipped with a finned tube cooling system installed under the roof. In addition to the cooling system, double energy screens were installed under the roof and on the sides. The Greenhouse is a north-south oriented Venlo-type with an area of 307.2 m^2 (≈ 266.24 m^2 plant growing space). The growing space is equipped with 12 hydroponic drip irrigation channels. For CO_2 enrichment, a system with technical CO_2 is used. The PV system was completed and installed in summer 2024. Given these circumstances the original crop plan had been adjusted accordingly.

The PV-modules are installed in a pitchfork formation with a gradually increasing shade with a calculated light reduction of 21.6%, 16.2% and 10.8% (Figure 169).

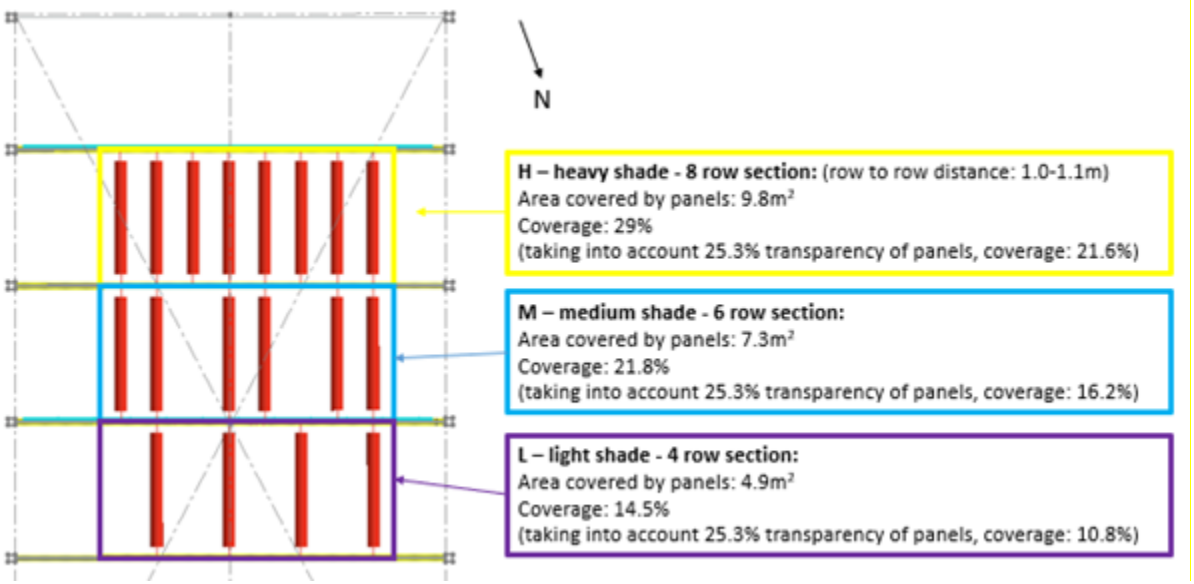

Figure 169. Arrangement of PV modules in the greenhouse; each red rectangle corresponds to two coupled PV modules.

The grow channels were classified in different sectors, corresponding to the shading based on light measurements after the installation was completed. Figure 170 shows the light distribution (20/08/24) in the greenhouse after PV-panel installation, with PV modules in horizontal orientation. Five sector classifications were formed (C_1 = Control, L = light shading, M = medium shade, H = heavy shade, C_2 = Control 2).

Funded by the European Union

Funded by the European Union under Grant Agreement No 101096056. Views and opinions expressed are however those of the author(s) only and do not necessarily reflect those of the European Union or CINEA. Neither the European Union nor the granting authority can be held responsible for them.

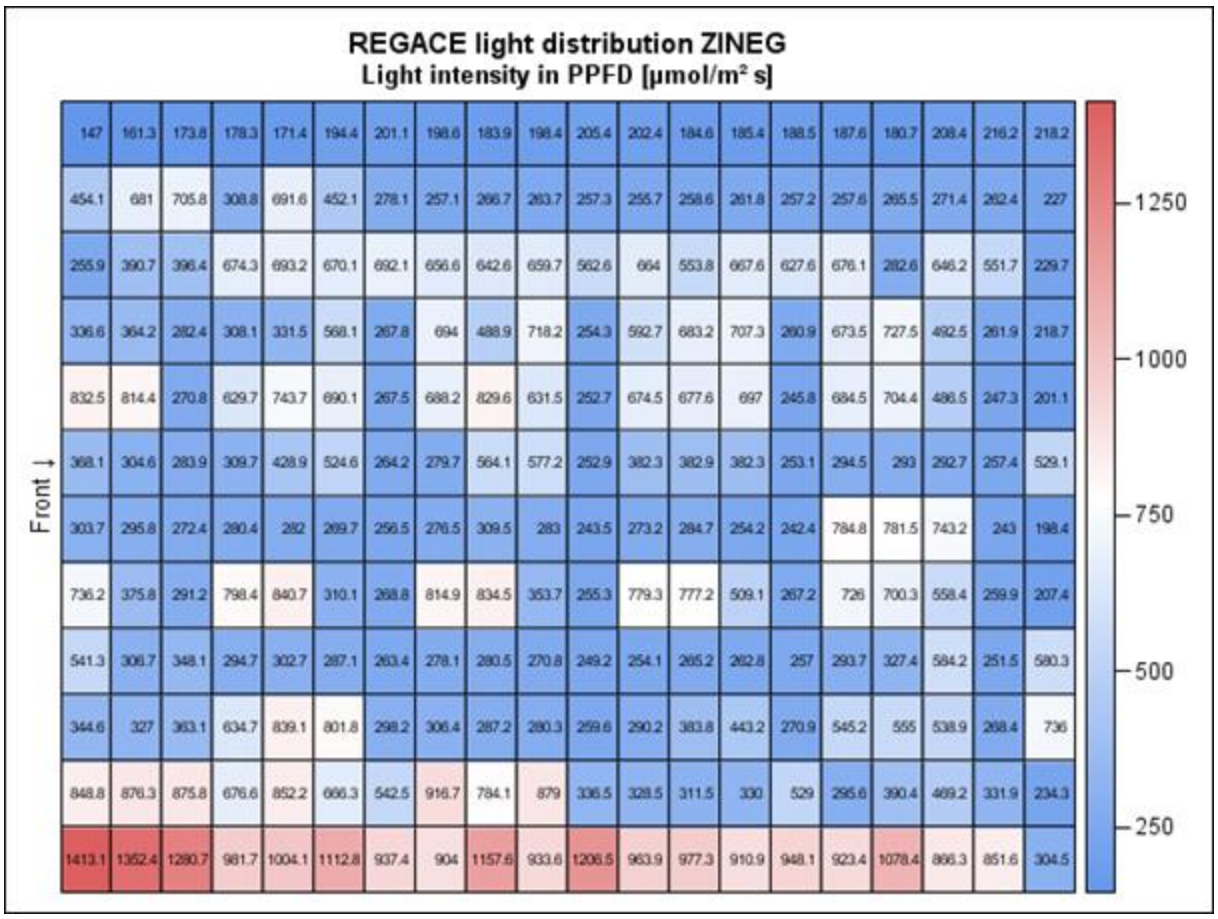

Figure 170. Heatmap of light intensity in ZINEG after installation of the PV-modules (20/08/24).

A. Experiments in Greenhouses

1. Experiment with *Lactuca sativa* cv. Binex 24/07/ - 15/10/2024

The experiments with lettuce were conducted with a lower capacity (9 hydroponic channels, 88.4 m^2 growing space). The area of sector C_1 was not used. Plants were sown 24/07/2024 and transplanted 20/08/2024 into the greenhouse. Harvest took place on 15/10/2024. CO_2 enrichment was not actively used, since the initial shading impact of the PV-Panels was the focus of this experiment. Cultivation parameters (mean values) in the ZINEG greenhouse during the experiment are shown in Table 147.

Funded by the European Union under Grant Agreement No 101096056. Views and opinions expressed are however those of the author(s) only and do not necessarily reflect those of the European Union or CINEA. Neither the European Union nor the granting authority can be held responsible for them.

Table 147. Mean values with standard deviation of CO_2 concentration in the atmosphere, temperature, relative humidity, vapor concentration deficit, and light intensity during greenhouse cultivation of the experiment 20/08–15/10/24.

Atmospheric CO_2-conc. [ppm]	346.90 ± 57.33
Temperature greenhouse [°C]	22.9 ± 5.44
Temperature weather station [°C]	17.87 ± 6.24
Rel. humidity greenhouse [%]	55.11 ± 17.11
Rel. humidity weather station [%]	67.17 ± 25.07
Vapor concentration deficit [g kg^{-2}]	8.95 ± 6.24
Global Irradiation [W m^{-2}]	172.86 ± 248.48
Photosynthetic active radiation [µmol m^{-2} s^{-1}]	288.26 ± 384.39

The plants showed a homogenous growth and for this variety typical colouration over all sectors. On a few single plants a light aphid infestation was observed. The data suggests that there is no significant difference in the collected grow parameter (Table 148).

Table 148. Mean values and standard deviations per sector of plant height at harvest, plant width at harvest, fresh mass of harvested leaf, dry mass of leaf and percent dry matter leaf (C: Control, L: light shade, M: medium shade, H: heavy shade).

	Height [cm]	Width [cm]	Fresh mass [g]	Dry mass [g]	Dry matter [%]
C	16.99 ± 1.73 a	26.25 ± 2.08 a	120.68 ± 33.52 a	8.28 ± 1.40 a	7.06 ± 0.86 a
L	16.37 ± 1.62 a	27.10 ± 2.08 a	120.80 ± 29.91 a	8.09 ± 1.62 a	7.01 ± 1.36 a
M	16.37 ± 1.66 a	26.71 ± 1.96 a	120.95 ± 29.92 a	8.02 ± 2.21 a	6.51 ± 0.40 a
H	16.67 ± 1.96 a	26.80 ± 2.08 a	122.76 ± 31.21 a	8.35 ± 1.68 a	6.58 ± 0.51 a
$P_{Shapiro-Wilk}$	< 0.0001	< 0.0001	0.0119	0.7017	< 0.0001
Post-hoc	Kruskal-Wallis	Kruskal-Wallis	Kruskal-Wallis	Tukey-Kramer	Kruskal-Wallis

Different letters within a column indicate significant differences

A total yield of 43.22 kg fresh weight over all sectors was recorded. This would result in a yield of 488.98 g m^{-2} (88.4 m^2 growing space used). However, this growing space includes a working area for scissor lifts in between the irrigation channels. Adjusting these results in a more practical approach for the actual surface area for the plants (16 plants per m^2) this would result in a surface area of 22.5 m^2 of growing space with a yield of 1.92 kg m^{-2}. A total of 2492.8 L of fertilizer solution was consumed, resulting in a water use efficiency of 17.34 g fresh weight per liter.

2. Experiment with *Lactuca sativa* cv. Binex 16/09/24 – 27/01/2025

The experiment was conducted similar to experiment 1 (9 hydroponic channels, 88.4 m^2 growing space, sector C_1 was not used). Plants were sown out 16/09/24 and transplanted into the greenhouse 31/10/24. The same growth media bags from experiment 1 were used. The plants were harvested 27/01/25.

Funded by the European Union

Funded by the European Union under Grant Agreement No 101096056. Views and opinions expressed are however those of the author(s) only and do not necessarily reflect those of the European Union or CINEA. Neither the European Union nor the granting authority can be held responsible for them.

Table 149. Mean values with standard deviation of CO_2 concentration in the atmosphere, temperature, relative humidity, vapor concentration deficit, and light intensity during greenhouse cultivation of the experiment 16/09/24–27/01/25.

Atmospheric CO_2-conc. [ppm]	473.77 ± 42.64
Temperature greenhouse [°C]	17.08 ± 1.61
Temperature weather station [°C]	4.56 ± 3.53
Humidity greenhouse [%]	53.47 ± 7.14
Humidity weather station [%]	85.88 ± 18.99
Vapor concentration deficit [g kg^{-2}]	5.60 ± 1.10
Global Irradiation [W m^{-2}]	22.67 ± 53.16
PAR PPFD [µmol m^{-2} s^{-1}]	41.62 ± 83.37

A slow growth and development of the plant was noticed. In general, the growth parameters were below the expectations, none of the plants reached a marketable fresh weight (Table 150). Except for the height there were no significant differences in the growth parameters observed, with the heavy shaded area showing the lowest height.

Table 150. Mean values and standard deviations per sector of plant height at harvest, plant width at harvest, fresh mass of harvested leaf, dry mass of leaf and percent dry matter leaf (C: Control, L: light shade, M: medium shade, H: heavy shade).

	Height [cm]	Width [cm]	Fresh mass [g]	Dry mass [g]	Dry matter [%]
C	10.40 ± 1.03 ab	20.39 ± 2.90 a	16.50 ± 6.80 a	0.79 ± 0.33 a	5.27 ± 0.29 a
L	10.76 ± 1.19 a	20.76 ± 2.84 a	17.92 ± 7.39 a	0.94 ± 0.29 a	5.15 ± 0.32 a
M	10.77 ± 1.23 a	21.00 ± 2.90 a	17.76 ± 7.27 a	0.78 ± 0.33 a	5.18 ± 0.28 a
H	10.29 ± 0.99 b	20.48 ± 2.91 a	17.85 ± 7.80 a	0.91 ± 0.40 a	5.28 ± 0.29 a
$P_{Shapiro-Wilk}$	< 0.0001	< 0.0001	0.0580	0.4780	< 0.3506
Post-hoc	Kruskal-Wallis	Kruskal-Wallis	Kruskal-Wallis	Tukey-Kramer	Tukey-Kramer

Different letters within a column indicate significant differences

A total yield of 6102.1 g fresh weight (69.0 g m^{-2}; 88.4 m^2 growing space, including workspace area) over all sectors was harvested. Adjusted for a more practical approach without workspace area this would result in a yield of 271.2 g m^{-2}. A total of 1168 L was used, resulting in a water use efficiency of 5.22 g per liter.

3. Experiment with *Lycopersicon esculentum* 'Avalantino F1' 05/02/25-30/06/25

For the tomato experiment the greenhouse was used at full capacity (12 irrigation channels, 266.24 m^2 growing space, 480 plants). The plants were cultivated under practical conditions, fruit clusters were reduced to 8 fruits per panicle with 16 to 18 leaves per plant. Beneficial organisms were used, when damage thresholds were exceeded, pesticides were applied. All five sectors were used, in sector L (light shade) additionally a phytomonitor was installed to record photometric data. A phytomonitor is a device to measure CO_2 and vapor gas exchange on selected leaves in the upper canopy. The cultivation parameters during the experiment are shown in Table 151. Collected biomass during cultivation care and

Funded by the European Union

Funded by the European Union under Grant Agreement No 101096056. Views and opinions expressed are however those of the author(s) only and do not necessarily reflect those of the European Union or CINEA. Neither the European Union nor the granting authority can be held responsible for them.

harvested fruits were weighed and recorded per sector. For the evaluation the outer rows were not included.

Table 151. Mean values with standard deviation of CO_2 concentration in the atmosphere, temperature, relative humidity, photometric data, and light intensity in ZINEG during the cucumber experiment 05/02/25–30/06/25.

Greenhouse CO_2-conc. [ppm]	634.59 ± 102.93
Atmospheric CO_2-conc. [ppm]	403.45 ± 69.27
Temperature greenhouse [°C]	23.22 ± 2.97
Temperature weather station [°C]	12.85 ± 6.35
Humidity greenhouse [%]	70.05 ± 13.60
Humidity weather station [%]	64.46 ± 27.26
Leaf temperature [°C]	21.27 ± 2.87
Transpiration [mg m^{-2} s^{-1}]	8.11 ± 10.06
Photosynthesis [µmol m^{-2} s^{-1}]	1.95 ± 3.80
Stomatal conductance [m s^{-1}]	31.62 ± 939.52
Vapor concentration deficit [g kg^{-2}]	5.41 ± 3.18
Global Irradiation [W m^{-2}]	188.11 ± 255.88
PAR PPFD [µmol m^{-2} s^{-1}]	310.19 ± 413.89

The plants showed an even growth and development. A few pests and diseases were observed, mainly tomato rust mite and two different fungus infections. Pesticides were applied accordingly and heavy damaged plants were removed. The plants showed significant differences in the biomass and fruit development between the sectors (Table 152). Both of the control sectors showed the highest produced biomass and fruit yield. For the other sector a general reduction in mean biomass and mean fruit mass was observed with increasing shading level.

Table 152. Mean values and standard deviations per sector of plant and fruit biomass and fruit per plant (C_1: Control 1, L: light shade, M: medium shade, H: heavy shade, C_2: Control 2).

	Biomass per Plant [g]	Fruit per plant [g]
C_1	783.40 ± 139.61 a	3803.3 ± 286.73 a
L	665.30 ± 93.70 ab	3155.9 ± 225.21 c
M	653.52 ± 96.15 ab	3137.9 ± 346.95 bc
H	627.29 ± 90.19 b	2929.1 ± 182.65 c
C_2	714.80 ± 100.38 a	3458.7 ± 153.62 ab
$P_{Shapiro-Wilk}$	0.0063	0.0809
Post-hoc	Kruskal-Wallis	Kruskal-Wallis

Different letters within a column indicate significant differences

A total of 1663 kg tomato fruits (6.25 kg m^{-2}, 266.24 m^2 growing space) for all sectors was harvested (including outer rows). A volume of 91.02 m^3 of fertilizer solution was consumed, resulting in a water use efficiency of 18.28 kg m^{-3}. Figure 171 shows the collected drainage of selected grow bags and global irradiation 28/04/25 until 15/04/25. Differences in drainage volume depending on the shading levels by PV modules were not observed.

Funded by the European Union

Funded by the European Union under Grant Agreement No 101096056. Views and opinions expressed are however those of the author(s) only and do not necessarily reflect those of the European Union or CINEA. Neither the European Union nor the granting authority can be held responsible for them.

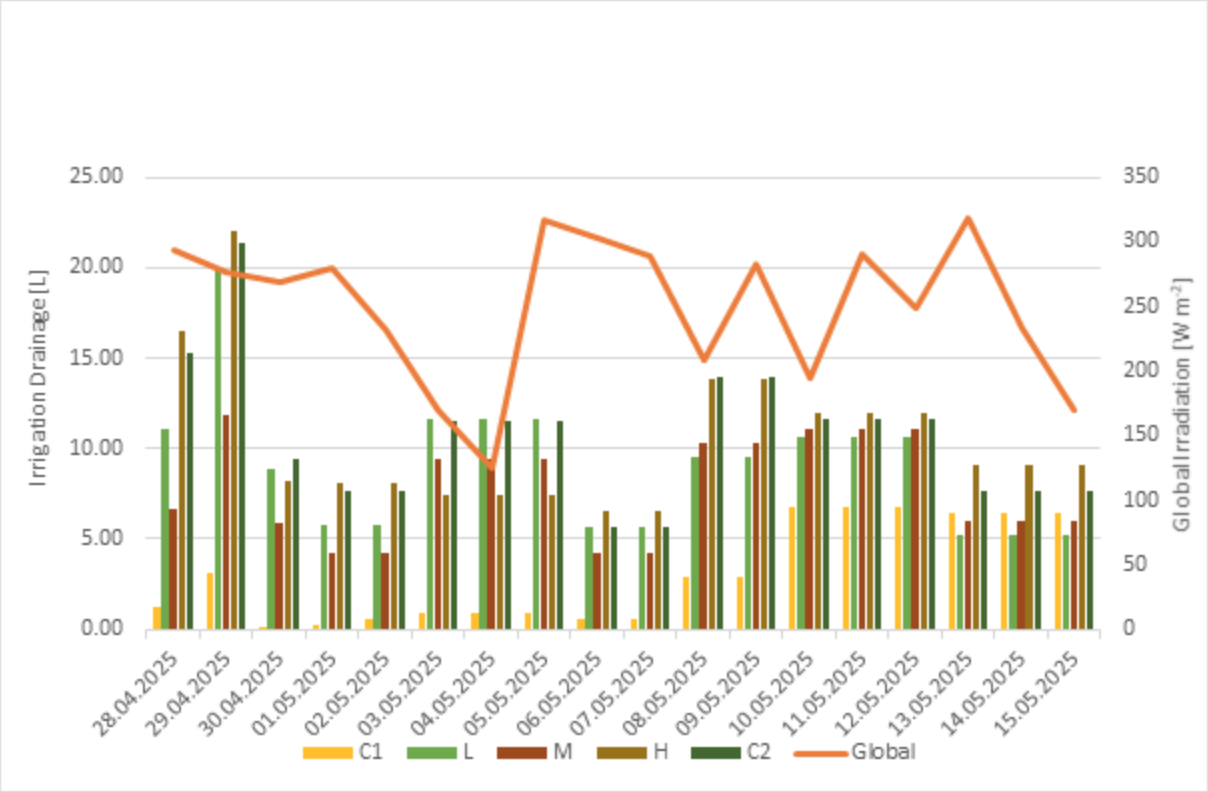

Figure 171. Drainage volume at different PV shading levels and daily mean value of global radiation.

4. Experiment with *Cucumis sativa* cv. 'Cordoba F1' 28/07/25 – 13/10/25

In the cucumber trial the greenhouse was used at full capacity (12 irrigation channels, 266.24 m^2 grow space, 480 plants). The plants were cultivated under practical conditions, the aimed harvest fresh weight was 320–380 g per fruit. Beneficial organisms were used, when damage thresholds were exceeded, pesticides were applied. All five sectors were used.

Comparative measurements were taken between 04/09/25 – 13/10/25 using two phytomonitors in two different sectors (L, light shade and M, medium shade) with different shading conditions by PV-panels in a cucumber canopy. Phytomonitors are gas exchange measuring devices that record CO_2 and water vapor gas exchange on ten randomly selected leaves in the upper canopy.

The two systems were set up to observe these areas covered with PV-panels, taking into account the altitude angle and PAR in September 2025 (Figure 172). Measurement data was recorded continuously for 40 days, in total 11.520 data series with a measurement interval of five minutes.

Funded by the European Union under Grant Agreement No 101096056. Views and opinions expressed are however those of the author(s) only and do not necessarily reflect those of the European Union or CINEA. Neither the European Union nor the granting authority can be held responsible for them.

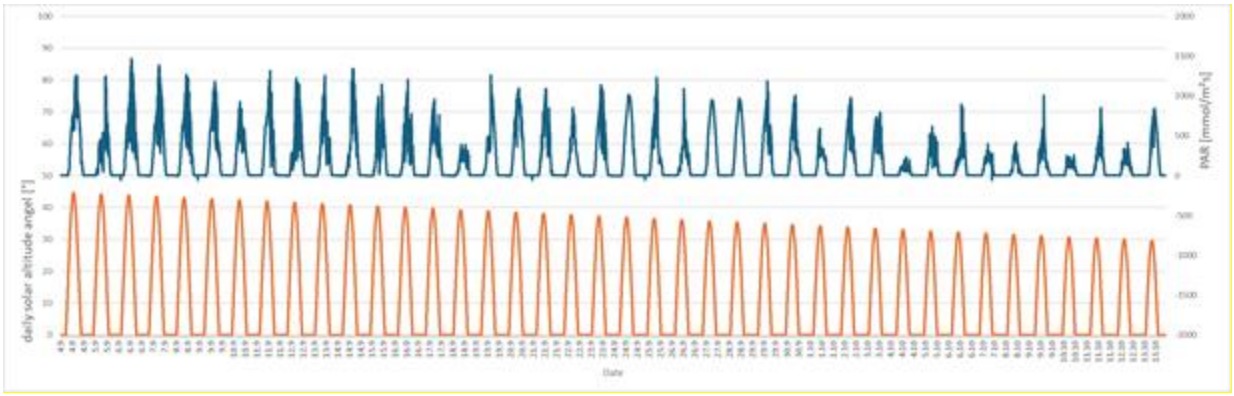

Figure 172. Progression of daily solar altitude angle (orange) and photosynthetic active radiation PAR (blue) during measurement period 04/09/25 – 13/10/25.

The data of the two phytomonitor systems was compared to evaluate the difference in photosynthesis and transpiration between two of the sectors (L, light shade and M, medium shade). The Figures 173 and 174. show the difference in photosynthesis sums and transpiration totals, respectively. The plants in the medium shaded area showed an increase in the reduction of photosynthesis from an initial 10 % to 25%. The changing altitude angles and decreasing global radiation (Figure 172) are most likely the cause. In contrast, transpiration in the medium sector was initially 20 % lower, but as the angle of the sun decreased, it approached the transpiration level of the light shaded sector (L).

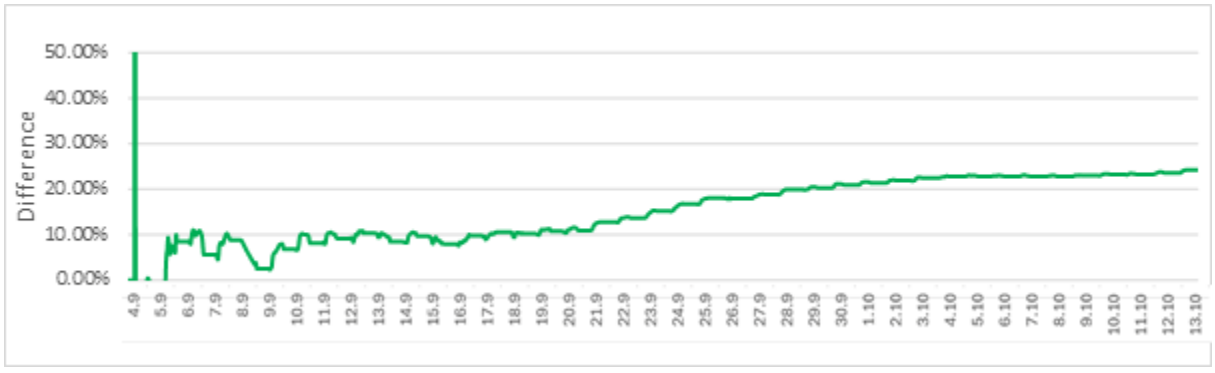

Figure 173. Percentage difference between the photosynthesis sums of medium and light shaded cucumber plants.

Funded by the European Union

Funded by the European Union under Grant Agreement No 101096056. Views and opinions expressed are however those of the author(s) only and do not necessarily reflect those of the European Union or CINEA. Neither the European Union nor the granting authority can be held responsible for them.

Figure 174. Percentage difference between the transpiration of medium and light shaded cucumber plants.

In Figure 176 the phytometric data on the cucumber plants for light and medium shaded sectors is compared over the course of a single day (25/09/25, sunny day/ no clouds). In the top the difference in photosynthesis is shown, the medium shaded plants (green) showed a lower but similar photosynthesis rate than the light shaded plants (red). In contrast the transpiration rate (middle) is comparable. This can be attributed to different radiation conditions. The stomatal conductance values of the leaves in the two different sectors, which were also recorded, did not differ in the same way as photosynthesis, which suggests an abiotic influence due to different light conditions. On days with light or heavy cloud cover, however, the differences in photosynthesis were less pronounced, resulting in a reduction in photosynthesis of 10 to 25% over the entire measurement period.

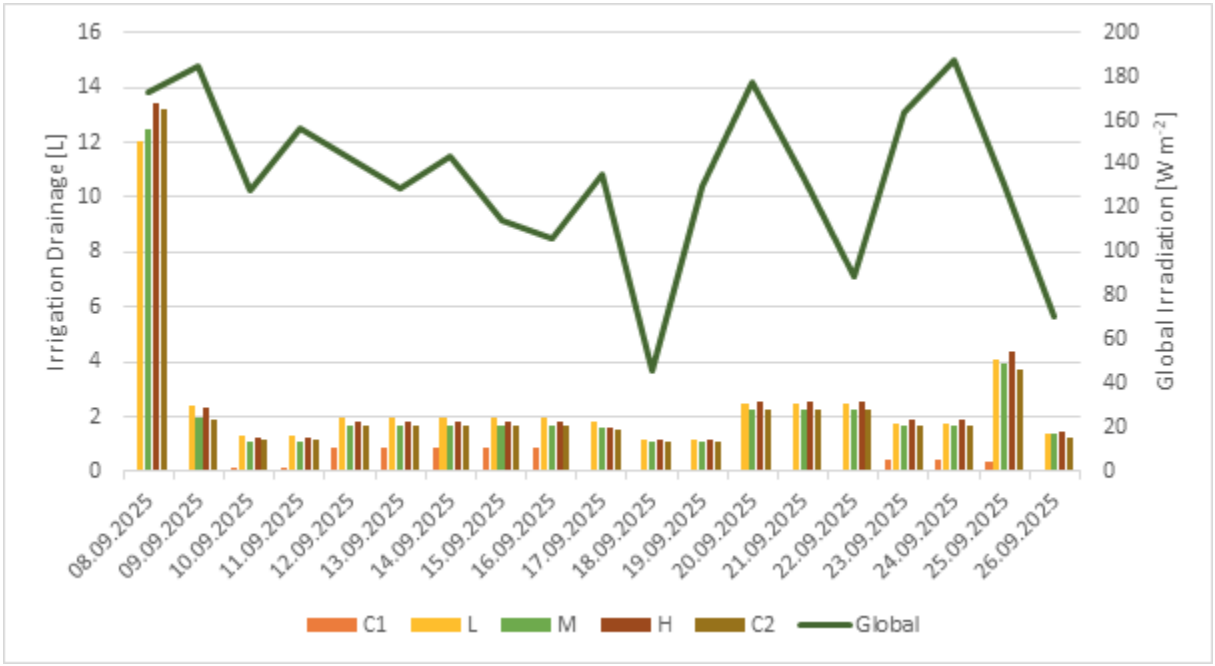

Figure 175. Drainage volume at different PV shading levels and global radiation in the greenhouse (unshaded).

Funded by the European Union

Funded by the European Union under Grant Agreement No 101096056. Views and opinions expressed are however those of the author(s) only and do not necessarily reflect those of the European Union or CINEA. Neither the European Union nor the granting authority can be held responsible for them.

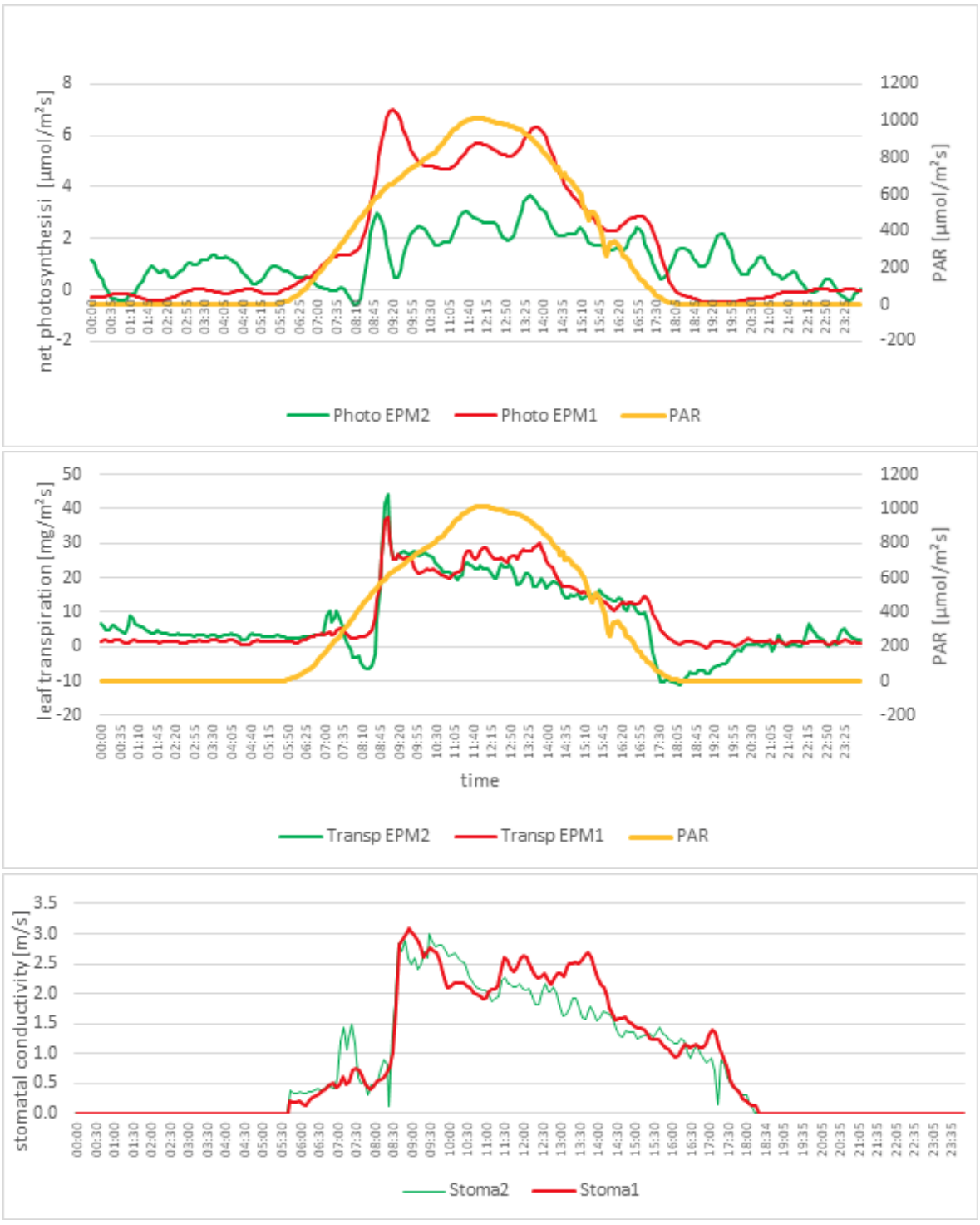

Figure 176. Phytometric data of cucumber plants for the 25/09/25 under different shading conditions (red: light shade, sector L; green: medium shade, sector M). Top - difference in photosynthesis; middle - difference in transpiration; bottom - difference in stomatal conductivity.

Funded by the European Union under Grant Agreement No 101096056. Views and opinions expressed are however those of the author(s) only and do not necessarily reflect those of the European Union or CINEA. Neither the European Union nor the granting authority can be held responsible for them.

Table 153. Mean values with standard deviation of CO_2 concentration in the atmosphere, temperature, relative humidity, photometric data, and light intensity during the cucumber experiment 28/07–13/10/25.

Greenhouse CO_2-conc. [ppm]	604.24 ± 82.82
Atmospheric CO_2-conc. [ppm]	365.39 ± 62.51
Temperature greenhouse [°C]	23.84 ± 2.68
Temperature weather station [°C]	16.42 ± 5.65
Humidity greenhouse [%]	63.68 ± 12.66
Humidity weather station [%]	72.16 ± 25.43
Leaf temperature [°C]	20.03 ± 3.28
Transpiration [mg m^{-2} s^{-1}]	9.95 ± 14.18
Photosynthesis [µmol m^{-2} s^{-1}]	1.85 ± 3.03
Stomatal conductance [m s^{-1}]	16.33 ± 392.89
Vapor concentration deficit [g kg^{-2}]	6.84 ± 3.38
Global Irradiation [W m^{-2}]	140.96 ± 216.63
PAR PPFD [µmol m^{-2} s^{-1}]	219.91 ± 329.60

The cultivation parameters are shown in Table 153. In general, the plants developed well. Multiple times they were treated against powdery mildew and spider mite. A few single plants in an outer row showed symptoms of downy mildew and were removed immediately. The recorded biomass and harvested fruit per plant are shown in Table 154, however, the two outer rows were not included in the evaluation. Significant differences among the sectors in biomass per plant were not detected. In fruit numbers and fresh weight, the control sectors showed the highest values. For the other sectors the number of fruits and fruit fresh weight per plant were reduced with increasing shading. The heavily shaded area showed the lowest yield of all sectors.

Table 154. Mean values and standard deviations per sector of plant and fruit biomass and fruit per plant (C_1: Control 1, L: light shade, M: medium shade, H: heavy shade, C_2: Control 2).

	Biomass per Plant [g]	Number of fruits per plant	Fruit mass per plant [g]
C_1	438.4 ± 14.2 a	9.2 ± 0.38 a	3687.5 ± 250.8 a
L	465.7 ± 9.2 a	8.6 ± 0.52 ab	3332.2 ± 317.2 a
M	477.7 ± 17.0 a	8.33 ± 0.73 ab	3224.1 ± 350.7 a
H	459.3 ± 22.7 a	8.18 ± 0.69 b	3235.7 ± 317.1 a
C_2	493.3 ± 14.5 a	8.78 ± 0.73 ab	3478.9 ± 342.1 a
$P_{Shapiro-Wilk}$	0.0871	0.0062	0.072
Post-hoc	Kruskal-Wallis	Kruskal-Wallis	Kruskal-Wallis

Different letters within a column indicate significant differences

A total amount of 16.89 dt (6.35 kg m^{-2}, 266.24 m^2 growing space) cucumber was harvested. The average single fruit weight was 398.47 g (4241 fruits in total), which is above the aimed harvest fresh weight. One contributing factor were alternating harvesting dates and also weekends, when the harvest was suspended. A total amount of 35.05 m^3 of fertilizer solution was consumed, resulting in a water use efficiency of 48.25 kg m^3.

Funded by the European Union

Funded by the European Union under Grant Agreement No 101096056. Views and opinions expressed are however those of the author(s) only and do not necessarily reflect those of the European Union or CINEA. Neither the European Union nor the granting authority can be held responsible for them.

B. Experiments in Phytotrons

1. Experiment with *Lactuca sativa* cv. Saturdaii 16/10/23 – 15/01/24

The aim of the experiment was to investigate the chamber effect of the phytotrons to determine the amount of influence for the following experiments. No additional CO_2 enrichment was utilized. The plants were sown out 16/10/23 and moved into the chambers at 27/11/2023. Harvest was done 15/01/24. The growth parameters during the experiment are listed in Table 155.

Table 155. Mean values and standard deviations of light intensity in PPFD, relative humidity and temperature for the experiment with *Lactuca sativa* cv. Saturdaii.

	CO_2-conc. [ppm]	PPFD [µmol m^{-2} s^{-1}]	Rel. Humidity [%]	Temperature [°C]
Chamber 1	429.61 ± 109.95	68.50 ± 94.51	63.73 ± 1.86	20.34 ± 0.12
Chamber 2	506.31 ± 123.80	72.49 ± 100.93	63.21 ± 1.77	19.92 ± 0.19
Chamber 3	430.17 ± 87.43	71.94 ± 100.06	66.14 ± 1.81	20.01 ± 0.16

Table 156. Growth parameters mean values and standard deviations per chamber: Recorded biomass and harvested fruit per plant.

Table 156. Mean values & standard deviations of growth parameters for *Lactuca sativa* cv. Saturdaii.

	Chamber 1	Chamber 2	Chamber 3	$P_{Shapiro-Wilk}$
Height [cm]	13.38 ± 0.92 a	13.23 ± 0.85 a	13.55 ± 0.86 a	0.0237
Width [cm]	31.93 ± 0.96 a	30.95 ± 0.67 b	31.70 ± 3.50 a	< 0.0001
Fresh mass leaf [g]	94.99 ± 14.03 a	93.48 ± 12.61 a	100.47 ± 24.52 a	0.0833
Dry mass leaf [g]	4.65 ± 0.62 a	4.63 ± 0.66 a	4.38 ± 0.92 a	0.6614
Percent dry matter leaf [%]	4.91 ± 0.32 a	4.95 ± 0.18 a	4.48 ± 0.76 b	< 0.0001
Fresh mass root [g]	6.55 ± 0.60 a	6.85 ± 1.06 a	5.91 ± 0.88 a	0.8775
Dry mass root [g]	0.33 ± 0.02 a	0.32 ± 0.05 a	0.31 ± 0.03 a	0.1084
Percent dry matter root [%]	5.08 ± 0.33 ab	4.74 ± 0.19 b	5.56 ± 0.37 a	0.3777

Different letters within a row indicate significant differences

The plants showed a uniform growth and development and for most of the growth parameters significant differences were not observed (Table 156). Exceptions are the width, where chamber 2 showed a significantly lower width than the other chambers. The percent dry matter of the leaves was the lowest in chamber 3 and it was significantly different from the other two chambers. In the percent dry matter of the roots significant differences were observed, with chamber 2 showing the lowest mean values followed by chamber 1 and chamber 3. It was concluded that the chambers work similarly and that the chamber effects should not impose a significant impactful on future experiments.

2. Experiment with *Lactuca sativa* cv. Concentrus 28/11/23-07/03/24

In the experiment the influence of CO_2-enrichment on the development and growth of salad was investigated. In three growth chambers different CO_2 concentrations were set. Chamber 1 with 400 ppm

Funded by the European Union

Funded by the European Union under Grant Agreement No 101096056. Views and opinions expressed are however those of the author(s) only and do not necessarily reflect those of the European Union or CINEA. Neither the European Union nor the granting authority can be held responsible for them.

CO_2, Chamber 2 600 ppm CO_2 and Chamber 3 with 800 ppm CO_2. The plants were sown out 28/11/23, transplanted into pots 10/01/24 and moved into the chambers 02/02/2024. The plants were harvested on 07/03/2024. Table 157. shows the cultivation parameter during the experiment. The low light intensity in chamber 3 is a result of overhanging leaves over the light sensor inside the chamber.

Table 157. Mean values and standard deviations of CO_2 concentration, light intensity in PPFD, relative humidity and temperature for the experiment with *Lactuca sativa* cv. Concentrus.

	CO_2-conc. [ppm]	PPFD [µmol m^{-2} s^{-1}]	Rel. Humidity [%]	Temperature [°C]
Chamber 1	504.11 ± 88.63	70.46 ± 121.77	61.89 ± 2.41	18.61 ± 2.05
Chamber 2	648.82 ± 96.52	71.99 ± 128.14	62.25 ± 1.68	18.05 ± 2.11
Chamber 3	787.62 ± 100.23	52.94 ± 112.18	64.77 ± 1.71	18.13 ± 2.09

The plants showed an even growth and development in the beginning. Over time a subjective faster growth in chamber 3 was observed. In addition, some plants showed symptoms of tip burn. Significant differences in the percentage of dry matter of the leaves were not observed (Table 158), however the fresh and dry mass of the leaves was significantly different. In general, the plants showed a gradient in correspondence with the increased CO_2 levels. The highest mean values were observed in chamber 3 followed by chamber 2 and chamber 1.

Table 158. Mean values & standard deviations of growth parameters for *Lactuca sativa* 'Concentrus'.

	Height [cm]	Fresh mass leaf [g]	Dry mass leaf [g]	Dry matter [%]
Chamber 1	27.65 ± 2.50 a	283.21 ± 44.83 b	11.71 ± 1.78 b	4.24 ± 0.44 a
Chamber 2	26.65 ± 2.03 ab	288.35 ± 40.90 ab	13.28 ± 1.79 ab	4.62 ± 0.57 a
Chamber 3	26.00 ± 1.03 b	319.88 ± 46.41 a	13.74 ± 1.97 a	4.32 ± 0.52 a
$P_{Shapiro\text{-}Wilk}$	< 0.0001	0.9703	0.5292	< 0.0001
Post-hoc	Kruskal-Wallis	Tukey-Kramer	Tukey-Kramer	Kruskal-Wallis

Different letters within a column indicate significant differences

The water use efficiency was calculated for each chamber and increased with the level of CO_2 enrichment with values of 66.16 g L^{-1}, 70.16 g $L^{-1}$and 74.22 g L^{-1} respectively.

3. Experiment with *Lactuca sativa* cv. Concentrus 07/03/2024–02/05/2024

The experiment was conducted similar to the previous experiment with cv. Concentrus. A few adjustments were made to improve the methodology. Plants were sown out 07/03/2024 and moved into the chambers at 20/03/2024. The same CO_2 concentrations were set. Chamber 1 with 400 ppm CO_2, Chamber 2 600 ppm CO_2 and Chamber 3 with 800 ppm CO_2. The cultivation parameters during the experiment are shown in Table 159. The low light intensity is a result of overlapping leaves on the low mounted light sensor. On 15/04/24 the CO_2 sensors in the chambers did not respond to the system, the mean values shown, are those recorded before sensor failure.

Funded by the European Union

Funded by the European Union under Grant Agreement No 101096056. Views and opinions expressed are however those of the author(s) only and do not necessarily reflect those of the European Union or CINEA. Neither the European Union nor the granting authority can be held responsible for them.

Table 159. Mean values and standard deviations of CO_2 concentration, light intensity in PPFD, relative humidity and temperature for the experiment with *Lactuca sativa* cv. Concentrus.

	CO_2-conc. [ppm]	PPFD [µmol m^{-2} s^{-1}]	Rel. Humidity [%]	Temperature [°C]
Chamber 1	460.92 ± 70.73	34.20 ± 81.58	61.75 ± 3.65	17.44 ± 1.92
Chamber 2	644.29 ± 170.89	30.50 ± 78.92	61.81 ± 3.51	16.93 ± 1.94
Chamber 3	742.86 ± 158.59	32.79 ± 87.01	63.02 ± 4.84	17.10 ± 1.96

For the plants an even development and growth was observed. The growth parameters (Table 160) did not reveal a significant difference in the percentage of dry matter of the leaves, this matches with the results from the previous experiment. A similar trend in the dry mass of the leaves was observed, where the CO_2 enrichment resulted in a higher dry mass of the leaves. However, in the fresh mass chamber 2 the mean value was significantly lower.

Table 160. Mean values & standard deviations of growth parameters for *Lactuca sativa* 'Concentrus'.

	Fresh mass leaf [g]	Dry mass leaf [g]	Dry matter [%]
Chamber 1	304.39 ± 45.76 ab	11.64 ± 1.69 a	2.73 ± 1.85 a
Chamber 2	285.86 ± 46.84 b	13.90 ± 2.06 b	3.42 ± 2.37 a
Chamber 3	329.15 ± 44.36 a	14.11 ± 2.32 b	2.74 ± 2.11 a
$P_{Shapiro-Wilk}$	0.5069	0.7236	< 0.0001
Post-hoc	Tukey-Kramer	Tukey-Kramer	Kruskal-Wallis

Different letters within a column indicate significant differences

The water use efficiency was calculated for each chamber. In contrast to the previous results, chamber 1 showed the highest water use efficiency of 72.30 g L^{-1}. Followed by chamber 3 with 65.36 g L^{-1} and chamber 2 with 62.83 g L^{-1}, where the lowest water efficiency was observed.

4. Experiment with *Raphanus sativus* 'Riesen von Aspern' 26/08/25 – 08/10/25

Three experiments with *Raphanus sativus* were realised between 12/05/25 and 08/10/25, due to time constraints only one of them is shown here.

The aim of the experiment was to test for a compensation by CO_2 enrichment in combination with lower light levels. Chamber 1 was assigned as the control chamber with an average light intensity of 161 µmol m^{-2} s^{-1} and CO_2 concentration of 400 ppm. In chamber 2, CO_2 concentration was increased to 800 ppm with an average light intensity of 161 µmol m^{-2} s^{-1}. Chamber 3 should simulate the shading of PV-modules by decreasing the light intensity by 15 % to 137 µmol m^{-2} s^{-1}. To compensate for the light loss the CO_2 concentration was increased to 800 ppm. The plants were sown out on 26/08/2025 and moved into the chambers on 09/09/25. Harvest took place on 08/10/25. Table 161 shows the cultivation parameter during the experiment. The CO_2 concentration in chamber 1 was continuously high in the first few days, a plausible cause is the organic processing of the peat based growing medium by microorganism and the subsequent release of CO_2.

Funded by the European Union

Funded by the European Union under Grant Agreement No 101096056. Views and opinions expressed are however those of the author(s) only and do not necessarily reflect those of the European Union or CINEA. Neither the European Union nor the granting authority can be held responsible for them.

Table 161. Mean values and standard deviations of CO_2 concentration, light intensity in PPFD per day, relative humidity and temperature of *Raphanus sativus* 'Riesen von Aspern'.

	CO_2-conc. [ppm]	PPFD [µmol m^{-2} s^{-1}]	Rel. Humidity [%]	Temperature [°C]
Chamber 1	633.48 ± 206.70	101.50 ± 104.93	65.34 ± 2.44	22.71 ± 1.78
Chamber 2	836.34 ± 66.60	106.20 ± 109.00	64.28 ± 2.07	22.34 ± 1.78
Chamber 3	715.26 ± 132.80	84.15 ± 84.82	66.12 ± 2.10	22.54 ± 1.77

At harvest, significant differences among the variants in terms of the number of leaves, leaf area and plant width did not occur. Plant height and the fresh and dry mass of the leaves remained significantly lower at a CO_2 target value of 400 ppm than at a CO_2 target value of 800 ppm (Table 162). The differences among the variants in terms of the fresh mass of the bulbs are particularly striking. Increasing the CO_2 concentration under the same light conditions led to a doubling of bulb fresh mass. Even with a 15% reduction in light, a 55% increase in yield was achieved compared to the variant with a lower CO_2 concentration. In contrast, there were no differences in terms of the percentage of dry matter of bulbs.

Table 162. Mean values and standard deviations of growth parameters for *Raphanus sativus* 'Riesen von Aspern'.

	Chamber 1	Chamber 2	Chamber 3	$P_{Shapiro-Wilk}$	Post-Hoc
Height [cm]	20.33 ± 3.75 a	22.11 ± 3.15 b	22.69 ± 3.80 b	0.0710	Kruskal-Wallis
Width [cm]	32.50 ± 4.74 a	30.94 ± 4.56 a	32.69 ± 4.93 a	0.6186	Tukey-Kramer
Leaf number	8.06 ± 0.95 a	8.25 ± 0.81 a	8.31 ± 0.92 a	< 0.0001	Kruskal-Wallis
Leaf Surface [cm^2]	755.75 ± 177.48 a	806.43 ± 165.91 a	795.16 ± 217.32 a	0.1946	Tukey-Kramer
Fresh mass leaf [g]	30.69 ± 8.04 b	35.51 ± 10.64 a	35.89 ± 9.03 a	0.0580	Kruskal-Wallis
Dry mass leaf [g]	1.71 ± 0.41 b	2.19 ± 0.45 a	2.09 ± 0.49 a	0.2284	Tukey-Kramer
Percent dry matter leaf [%]	5.63 ± 0.45 b	6.05 ± 0.71 a	5.76 ± 0.60 b	0.0016	Kruskal-Wallis
Bulb Diameter [cm]	4.44 ± 0.57 b	5.62 ± 0.57 a	5.39 ± 0.67 a	0.0485	Kruskal-Wallis
Fresh mass bulb [g]	46.86 ± 16.23 c	97.10 ± 26.95 a	72.93 ± 27.75 b	0.0078	Kruskal-Wallis
Dry mass bulb [g]	1.12 ± 0.42 c	2.29 ± 0.89 a	1.79 ± 0.70 b	< 0.0001	Kruskal-Wallis
Percent dry matter bulb [%]	2.52 ± 0.91 a	2.46 ± 0.92 a	2.76 ± 1.24 a	0.0001	Kruskal-Wallis

Different letters within a row indicate significant differences

There were also differences between the variants in terms of water use efficiency. It was lowest in Chamber 1 (CO2 target value of 400 ppm) at 25.18 g/l, followed by Chamber 3 at 40.51 g/l. The highest water use efficiency was achieved in Chamber 2 at 44.24 g/l.

7.2.2 CO_2-enrichment by transfer mulch

At the Watzkendorf organic farm (BW), CO_2 enrichment is achieved by spreading transfer mulch. The transfer mulch consists of a mixture of various grasses and rye straw. Before cultivation in spring, approximately 5 kg/m² of transfer mulch is placed on the soil of the greenhouses and not tilled into the soil. The effect of CO_2 release was recorded in 2024 and 2025 via CO_2 measurements in the greenhouse.

After spreading the transfer mulch, very high CO_2 concentrations of up to 10.000 ppm were measured for a short period of time. During the cultivation period for cucumbers and tomatoes, elevated CO_2 concentrations were measured over a period of more than two months. However, the increase occurred at night in combination with respiration (Figures 177-178). As a rule, the CO_2 concentration dropped

Funded by the European Union

Funded by the European Union under Grant Agreement No 101096056. Views and opinions expressed are however those of the author(s) only and do not necessarily reflect those of the European Union or CINEA. Neither the European Union nor the granting authority can be held responsible for them.

rapidly with the onset of photosynthetic activity, but never reached concentrations below 400 ppm. This shows that continuous CO_2 fertilisation with transfer mulch is possible.

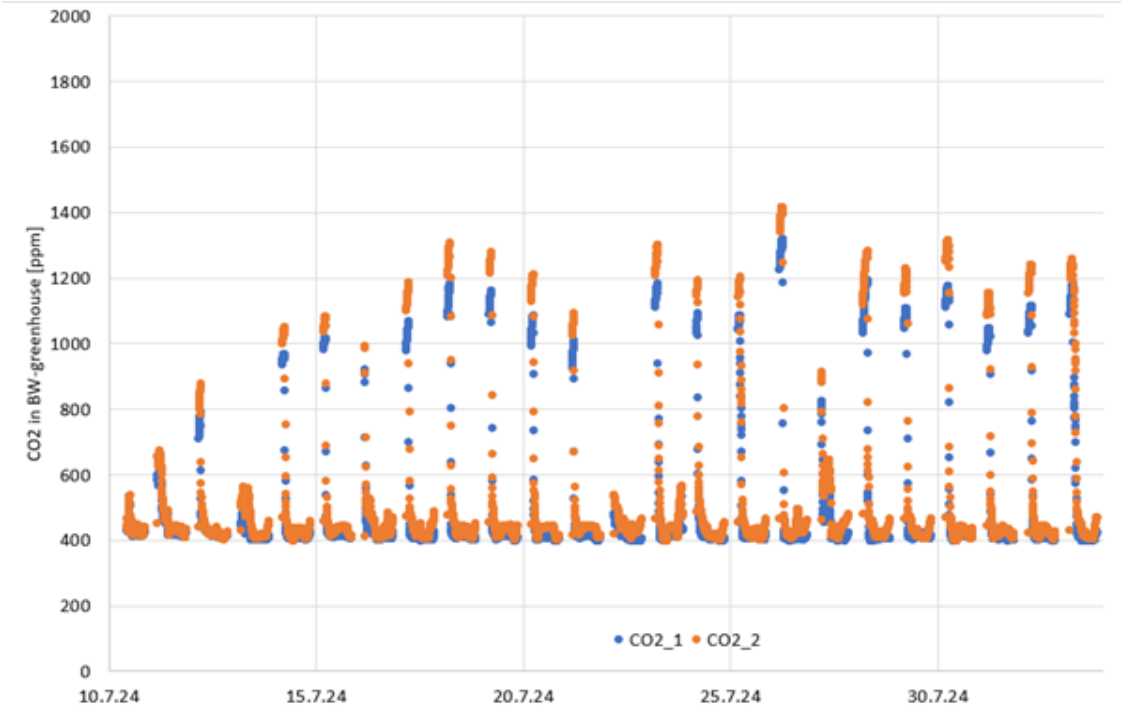

Figure 177. CO_2 concentrations in the Watzkendorf-greenhouse after applying transfer mulch 2024.

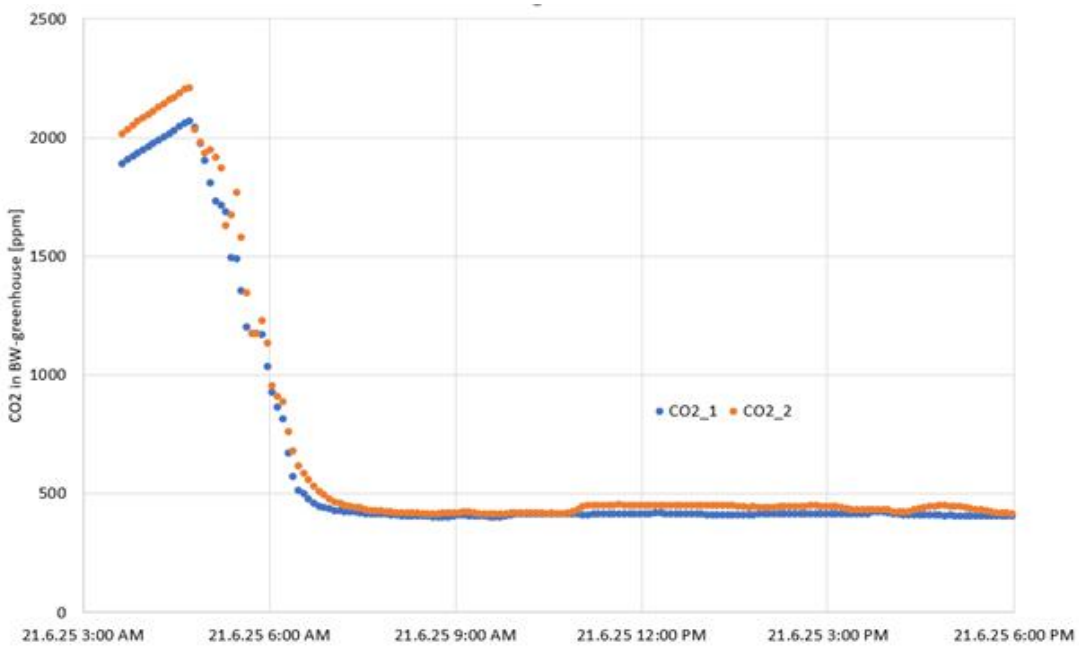

Figure 178. Typical daily course of CO_2 concentration during the cultivation period of cucumbers after application of transfer mulch in Watzkendorf 2025.

Funded by the European Union under Grant Agreement No 101096056. Views and opinions expressed are however those of the author(s) only and do not necessarily reflect those of the European Union or CINEA. Neither the European Union nor the granting authority can be held responsible for them.

Funded by the European Union

The potential CO_2 release of the transfer mulch was quantified in 2025 using a system for measuring potential soil respiration. Here, material samples are incubated over a longer period of time. This also allows the dynamics of CO_2 release to be recorded (Figure 179).

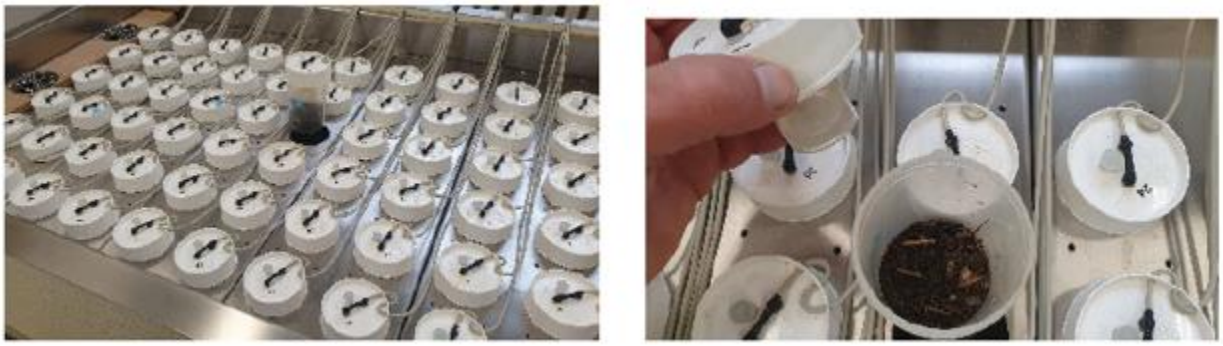

Figure 179. Unit for measuring CO_2-emission (left) and transfer mulch sample and KOH-solution for CO_2 absorption (right).

The carbon content of the transfer mulch was determined prior to the incubation experiment. The C_t content was 44.9%. With a sample weight of 2 g, this corresponds to 898 mg of carbon. After a period of 35 days, CO_2 releases of between 561 and 683 mg were detected in a total of 20 samples (Figure 180).

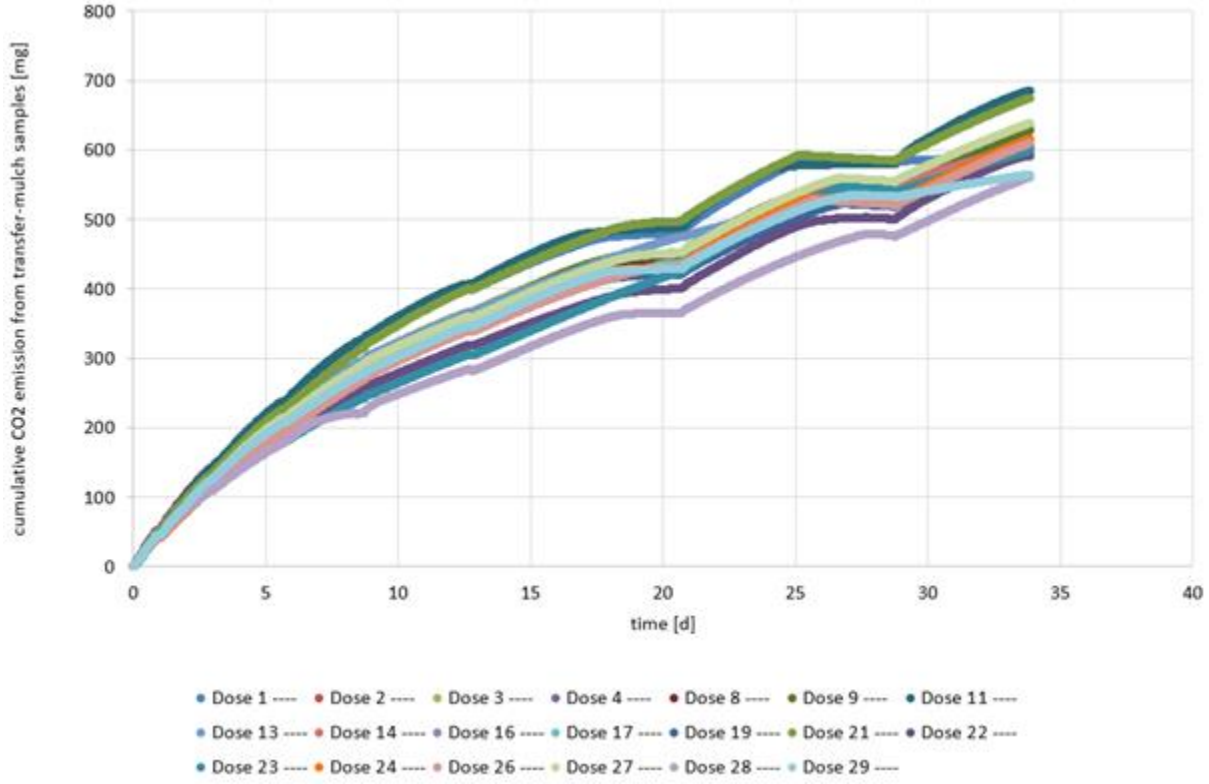

Figure 180. Cumulative CO_2 emissions from 20 transfer mulch samples (each sample weight 2 g).

Funded by the European Union under Grant Agreement No 101096056. Views and opinions expressed are however those of the author(s) only and do not necessarily reflect those of the European Union or CINEA. Neither the European Union nor the granting authority can be held responsible for them.

Based on the transfer application rate of 5 kg/m² and the mean value of the measurements, CO_2 emissions in the greenhouse of 1459 g/m² were calculated for a period of 35 days. This corresponds to 44% of the carbon contained in the transfer mulch (Figure 181).

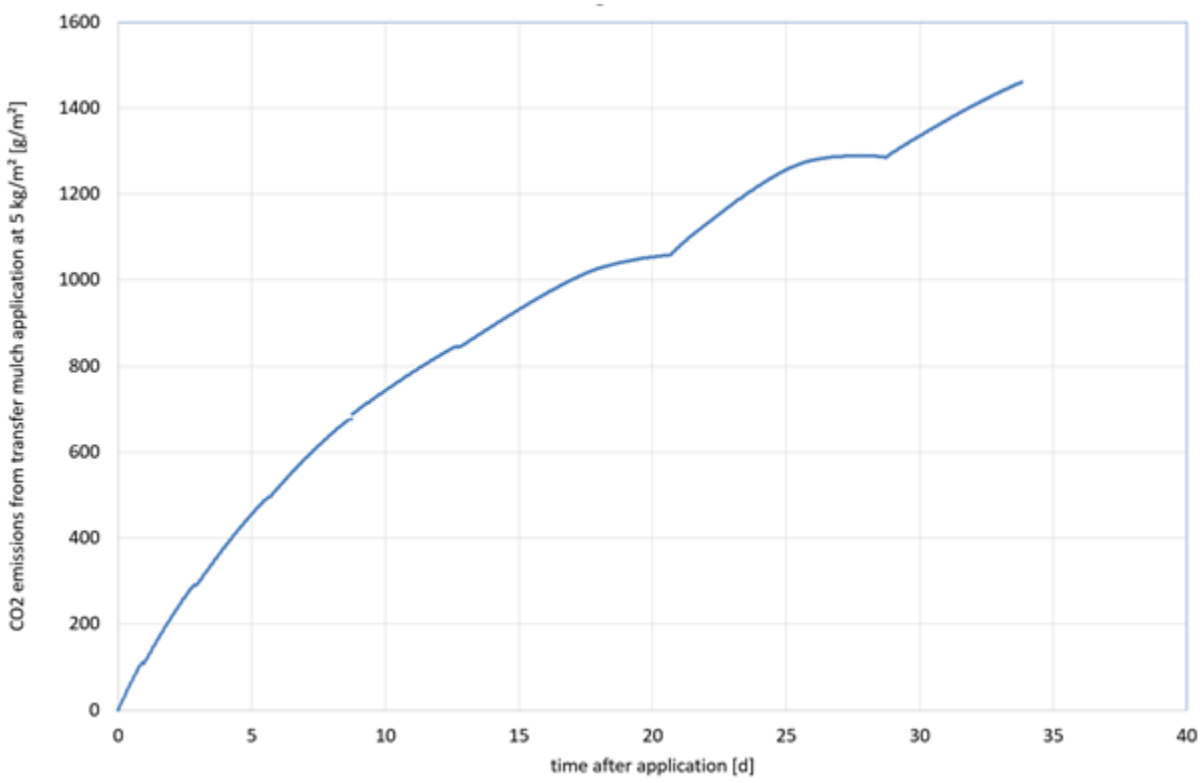

Figure 181. Calculated CO_2 emissions in the greenhouse with a transfer mulch application of 5 kg/m².

The determined CO_2 release of 1.4 kg/m² was compared with CO_2 enrichment using technical CO_2 in Berlin. There, approximately 3.2 g/m² per hour is applied during CO_2 enrichment. With 8 hours of CO_2 enrichment per day, 896 g/m² of CO_2 is applied in 35 days. With the transfer mulch in Watzkendorf (1459 g/m²), 63% more CO_2 is released than with enrichment using technical CO_2 in Berlin. It should be noted, however, that CO_2 emissions in Watzkendorf are a continuous process and difficult to control. As a result, high enrichment rates occurred mainly at night.

Funded by the European Union

Funded by the European Union under Grant Agreement No 101096056. Views and opinions expressed are however those of the author(s) only and do not necessarily reflect those of the European Union or CINEA. Neither the European Union nor the granting authority can be held responsible for them.

7.2.3 CO_2-enrichment by CO_2Bags

As already mentioned in chapter 5.2.1, the CO_2Bags of the company CO2BAG®Finland CO2 Products Oy did not raise the chamber's CO_2 concentration distinctly. The measurements indicate a range from no increase at all up to an increase of c. 20 µmol mol^{-1} CO_2. Nevertheless, the bags had a more or less distinct positive effect on growth and yield, although it remains unclear whether this effect was due to the additional CO_2 released, the released NH_3 acting as a foliar fertiliser, or both together.

7.2.4 CO_2 enrichment by mushroom cultivation

The strategy to enrich the CO_2 concentration by leading CO_2 from a mushroom cultivation into the greenhouse chamber at BOKU was successful and enabled to increase CO_2 levels on average by 127-156 µmol mol^{-1} depending on mushroom activity. The effect of significantly higher CO_2 concentrations to compensate for lower light intensity was very small in basil and radish. Light was obviously far more important for quality and yield formation.

7.3 Gas exchange measurements on basil leaves at different CO_2 and light conditions

At BOKU, light and A/Ci-curves were measured for selected plants of the two basil experiments performed in 2023 and 2024. It was intended to elucidate how the growing conditions in the three chambers "control" (K5), "shading & CO_2Bags" (K4) and "shading" affected the properties of the photosynthetic system.

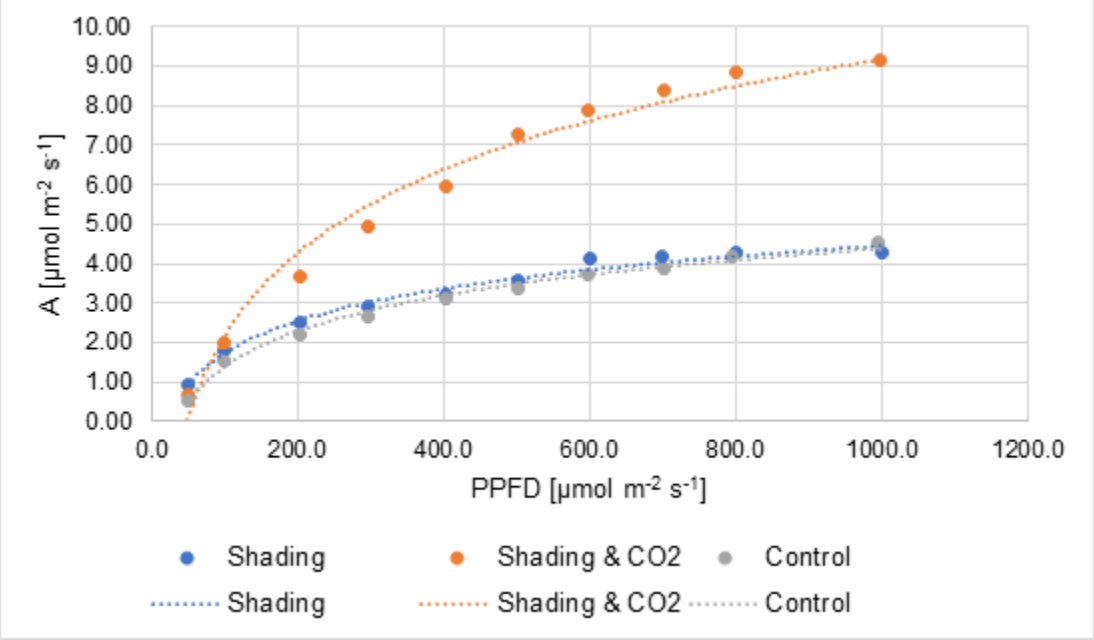

Figure 182. Light curve of basil leaves measured between 20th June and 18th July 2023.

Funded by the European Union under Grant Agreement No 101096056. Views and opinions expressed are however those of the author(s) only and do not necessarily reflect those of the European Union or CINEA. Neither the European Union nor the granting authority can be held responsible for them.

The light curves calculated from the mean values of c. 10 measurements each are given in Figures 182-183. It is immediately obvious that the results from both years differ distinctly. However, in both years, the curves of the plants of the two variants “shading” and “control” were comparable, while the curve of the plants of the variant “shading & CO_2Bags” showed larger values at higher light intensities. In 2024 this difference was less distinct.

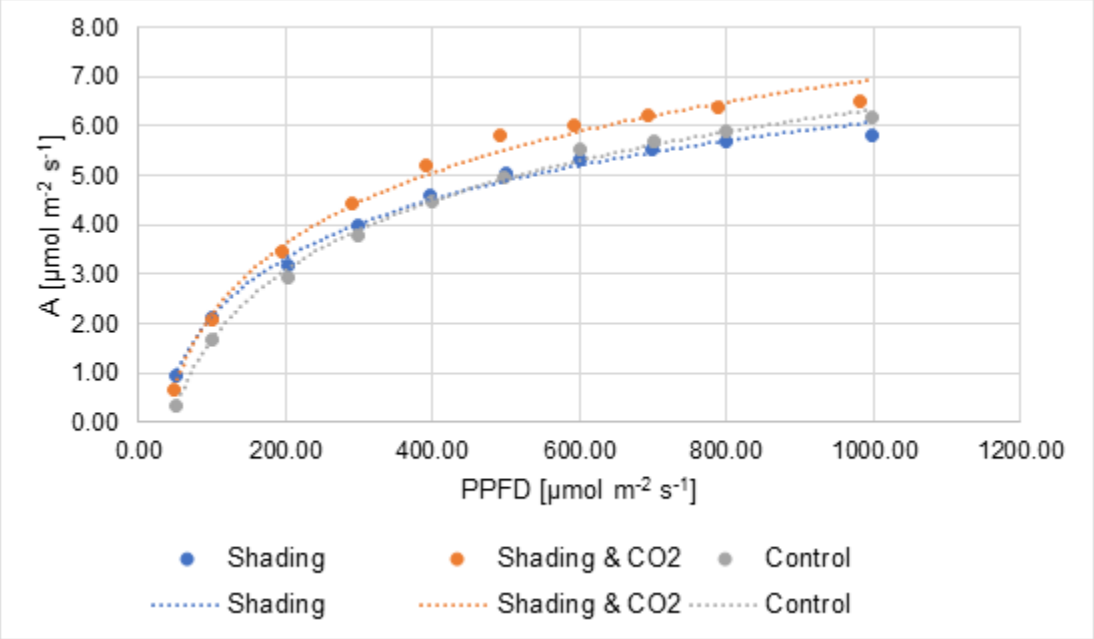

Figure 183. Light curve of basil leaves measured between 26th February and 15th April 2024.

The response of the photosynthetic apparatus is best characterised by the light compensation point (the light intensity when CO_2 assimilation starts), light use efficiency (the slope of the linear part of the graph at low light intensities), and the maximum photosynthesis calculated for a light intensity of 1000 µmol m^{-2} s^{-1} PAR (Table 163). Light compensation points were consistently smaller in the shaded variants “shading” and “shading & CO_2Bags”, indicating that these variants effectively adapted to the limited light availability. Light use efficiency did not show distinct differences, but for Amax of the variant “shading & CO_2Bags” a distinctly higher value is noted. The significantly higher values for Amax for this variant could be related to a higher Rubisco activity (see below).

Funded by the European Union

Funded by the European Union under Grant Agreement No 101096056. Views and opinions expressed are however those of the author(s) only and do not necessarily reflect those of the European Union or CINEA. Neither the European Union nor the granting authority can be held responsible for them.

Table 163. Parameters of the light-curves in 2023 and 2024 (Amax, maximum photosynthesis at a light intensity of 1000 µmol m^{-2} s^{-1} PAR; s, shading; b, CO_2Bags; con, control).

	Light compensation point 2023 [µmol m^{-2} s^{-1}]	Light compensation point 2024 [µmol m^{-2} s^{-1}]	Light use efficiency 2023 [--]	Light use efficiency 2024 [--]	Amax 2023 [µmol CO_2 m^{-2} s^{-1}]	Amax 2024 [µmol CO_2 m^{-2} s^{-1}]
K3 (s)	22.8	28.6	0.018	0.024	4.3	5.7
K4 (s & b)	23.9	26.4	0.019	0.029	9.1	6.5
K5 (con)	33.7	37.3	0.020	0.027	4.5	6.2

The A/Ci-curves calculated from the mean values of c. 10 measurements each are given in Figures 184-185. In both years the curves revealed a similar trend: “Shading” variants represented the lower curves, “control” treatments the medium, and the variant “shading & CO_2Bags” the upper curves.

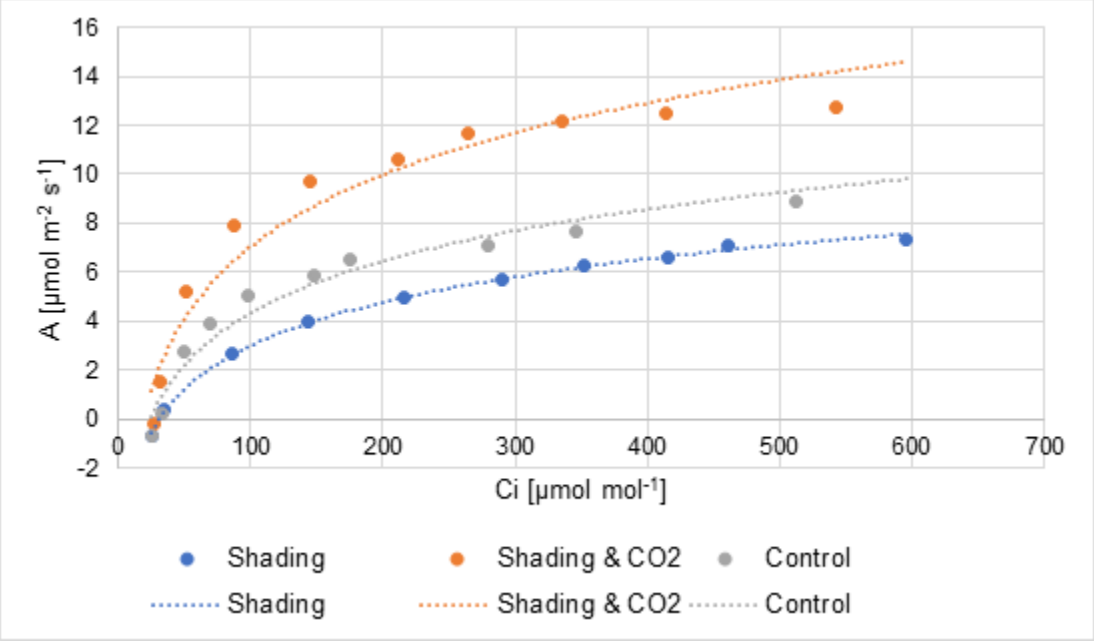

Figure 184. A/Ci-curve of basil leaves measured between 20th June and 18th July 2023.

Funded by the European Union

Funded by the European Union under Grant Agreement No 101096056. Views and opinions expressed are however those of the author(s) only and do not necessarily reflect those of the European Union or CINEA. Neither the European Union nor the granting authority can be held responsible for them.

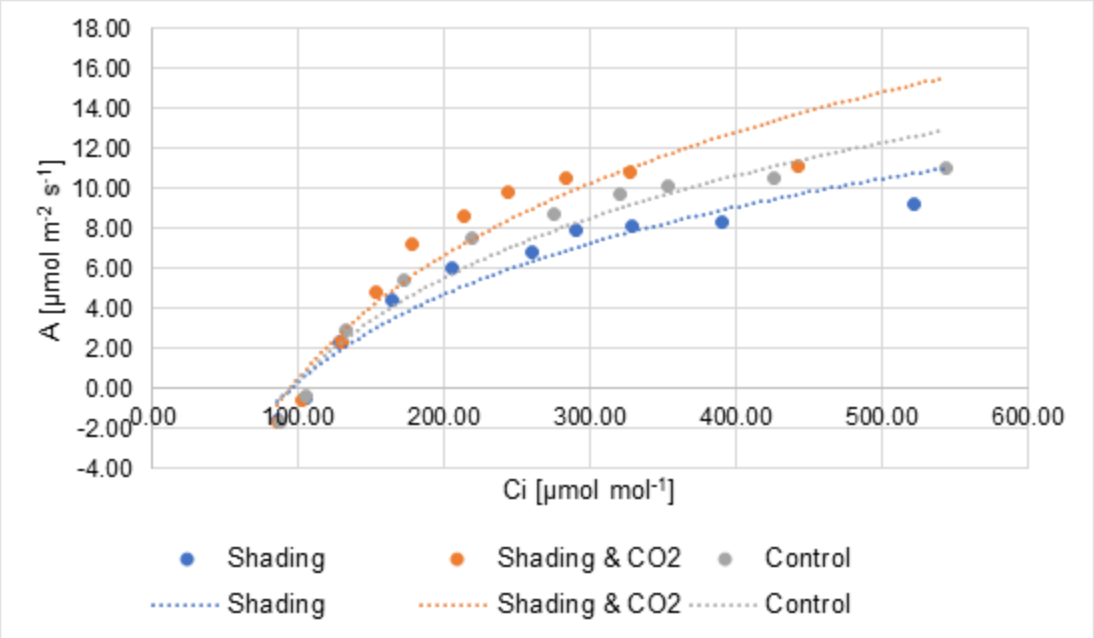

Figure 185. A/Ci-curve of basil leaves measured between 26th February and 15th April 2024.

The CO_2 compensation point was similar for all treatments (Table 164), proving that the CO_2Bags did not increase the CO_2 concentrations considerably. Worthy of note is the difference in absolute values between 2023 and 2024. As a matter of fact, this difference marks the range typical for C3-plants and indicates differences in the experimental environment between the years that cannot further be specified. For 2023, differences in carboxylation efficiency are distinct and the variant "shading & CO_2Bags" performed best, suggesting a distinctly higher Rubisco activity and/or concentration in this variant. For 2024 the ranking of the variants corresponded well to that of 2023, but the value for the variant "shading & CO_2Bags" was not that outstanding. The differences in Amax probably reflect differences in the leaf Chl content or other compounds characterising the efficiency of the light reactions of photosynthesis.

Table 164. Parameters of the A/Ci-curves in 2023 and 2024 (Amax, maximum photosynthesis at a leaf internal CO_2 concentration (Ci) of 800 µmol mol^{-1}; s, shading; b, CO_2Bags; con, control).

	CO_2 compensation point 2023 [µmol m^{-2} s^{-1}]	CO_2 compensation point 2024 [µmol m^{-2} s^{-1}]	Carboxylation efficiency 2023 [--]	Carboxylation efficiency 2024 [--]	Amax 2023 [µmol CO_2 m^{-2} s^{-1}]	Amax 2024 [µmol CO_2 m^{-2} s^{-1}]
K3 (s)	30.9	106.4	0.116	0.053	7.7	11.1
K4 (s & b)	27.5	106.9	0.218	0.095	13.2	12.3
K5 (con)	30.6	106.1	0.140	0.070	8.1	12.3

In summary, the light and A/Ci-curves characterise well the acclimation of the photosynthetic system to the environmental conditions in the chambers. The light compensation point proves the acclimation of the shaded plants in the chambers K3 and K4 to the lower light intensities. A clear acclimation to elevated

Funded by the European Union

Funded by the European Union under Grant Agreement No 101096056. Views and opinions expressed are however those of the author(s) only and do not necessarily reflect those of the European Union or CINEA. Neither the European Union nor the granting authority can be held responsible for them.

CO_2 levels in the chambers could not be deduced from the measurements. However, the leaf Chl concentrations of the 2023 experiments suggest a slight nitrogen deficiency, which might have been compensated for by ammonium hydrogen carbonate (NH_4HCO_3) in the CO_2Bags in chamber K4. In 2024, hints for a nitrogen deficiency as indicated by leaf Chl content were not found and, consequently, differences in the photosynthetic properties of the leaves were not as distinct as in 2023. In fact, values of Amax in Table 164 of 7.7 and 8.1 µmol CO_2 m^{-2} s^{-1} may accompany nitrogen deficiency, whereas values of Amax between 11.1 and 13.2 µmol CO_2 m^{-2} s^{-1} may indicate an adequate nitrogen status.

8 Additional lighting as compensation possibility

In the experiment performed in 2025 with basil and radish at BOKU, it became clear that additional light had a rather positive effect on yield and quality formation. The question arose, which criteria could be used to decide about the supplementation of artificial light. BOKU addressed this problem by taking the 2024 measured light and A/Ci-curves of basil leaves to create a three-dimensional diagram for basil in order to estimate when elevated atmospheric CO_2 concentrations can be expected to promote photosynthesis, which is the basis of crop growth and yield (Figure 186).

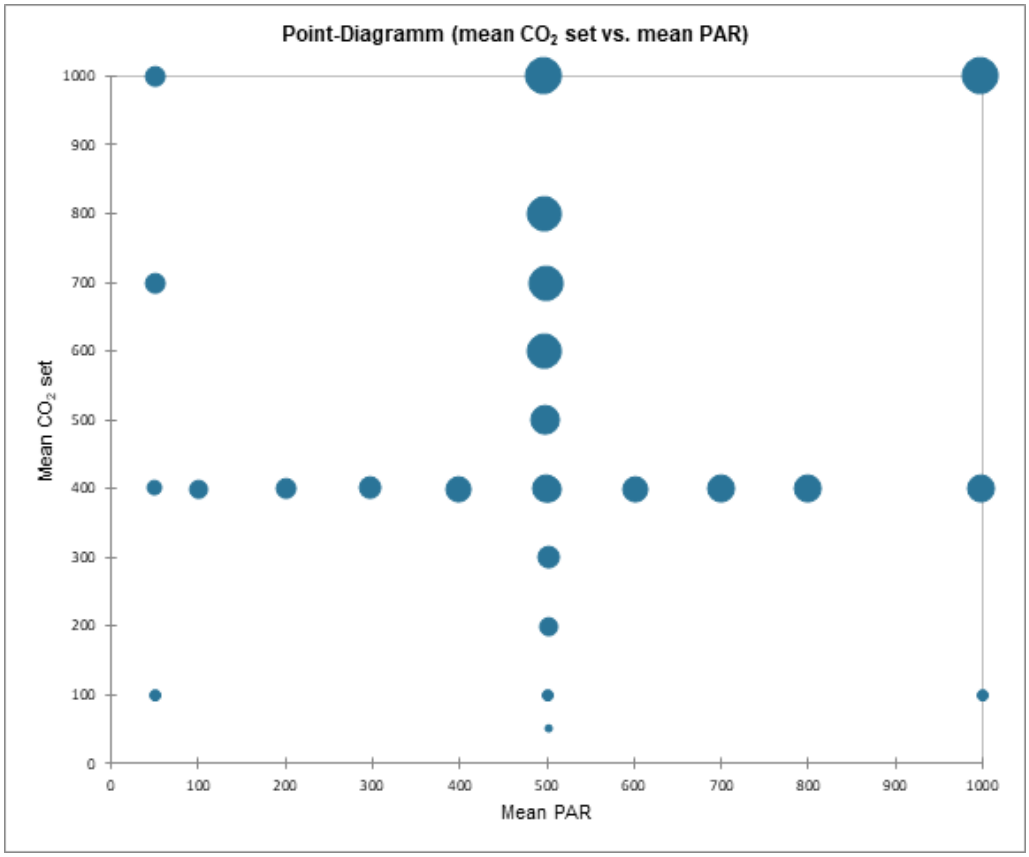

Figure 186. Interactive effect of atmospheric CO_2 concentration and light intensity of photosynthesis. The size of the points represents a measure of net photosynthesis rate.

Funded by the European Union under Grant Agreement No 101096056. Views and opinions expressed are however those of the author(s) only and do not necessarily reflect those of the European Union or CINEA. Neither the European Union nor the granting authority can be held responsible for them.

Funded by the European Union

As indicated in Figure 186, atmospheric CO_2 concentrations above 600 µmol mol^{-1} did not promote photosynthesis. Correspondingly, light intensities above c. 700 µmol m^{-2} s^{-1} PAR did not enhance photosynthesis. However, an increase of light intensity e.g. from 50 to 200 µmol m^{-2} s^{-1} PAR was found to be as effective as an increase of atmospheric CO_2 concentrations from 400 to 700 µmol mol^{-1} at 50 µmol m^{-2} s^{-1} PAR. In practice, it will obviously be necessary to test selected crops and/or varieties individually and, based on the average naturally available light intensity on site, to check whether the CO_2 enrichment strategy or the additional light strategy is more cost-effective, depending on the cost development for an additional supply of CO_2 and light.

9 Conclusions

The results of the bifacial PV characterization have so far shown a consistently higher yield for the bifacial panels compared to the monofacial counterparts, which confirms the working hypothesis. The performance ratio was consistently > 0.8 for all modules tested, even surpassing 0.9 in several instances. The 75W-rated modules performed slightly better than the 105W ones. In terms of degradation and ageing, the preliminary results suggest a minor impact, with power at Standard Test Conditions and Bifacial Standard Test Conditions remaining fairly stable up to now.

The results of this study revealed that the integration of photovoltaic modules into existing greenhouse structures can be technically feasible and energetically viable. However, successful implementation requires site-specific planning that takes local climatic conditions into account. The geometry and orientation of the greenhouse, as well as the covering material, also influence energy yield and efficiency. Dynamic sun-tracking systems that consider both the greenhouse geometry and the microclimate within the greenhouse further optimize energy yield. Furthermore, effective albedo management, such as the use of reflective ground coverings, can increase the energy output of bifacial PV systems by 15–20%. Particularly in the southern, warmer locations of this study, cooling or heat-dissipating layers, which result in lower temperatures of the PV panels, can improve their efficiency, as lower temperatures contribute to higher voltage stability and reduced degradation rates. The present results indicate that, with appropriate optimization of conditions, semi-transparent bifacial panels have the potential to generate clean energy without significantly impairing crop growth, yield formation, and yield quality, provided crop plants are carefully selected and adapted to the growing conditions. The observed investment costs and energy yields of the participants UTH, FSC and AZS, which have focused also on agricultural practice, serve as a basis for further optimization for commercial use. Thus, the following results demonstrate that agricultural profitability can be maintained in PV-equipped greenhouses.

A comparative analysis between tracking and fixed PV modules installed inside and outside the greenhouse confirmed the performance advantage of sun-tracking systems. The energy harvested was increased by 15–20% in the greenhouse environment and by 20–25% in the open-field system. This lower gain is due to light scattering, spectral filtering, and shading by the greenhouse structure and the polyethylene cover.

Funded by the European Union under Grant Agreement No 101096056. Views and opinions expressed are however those of the author(s) only and do not necessarily reflect those of the European Union or CINEA. Neither the European Union nor the granting authority can be held responsible for them.

The fill factor (FF) remained more stable in tracking systems, consistent with findings from other studies, which reported lower FF variability due to better alignment with sunlight. In contrast, fixed modules exhibited midday FF drops, likely caused by suboptimal angles and heat accumulation.

The temperature behaviour of the module was primarily governed by incident irradiance rather than ambient air temperature. Tracking modules consistently operated at slightly higher temperatures (*c*. 5-8 °C difference), which, although beneficial for energy yield, may accelerate long-term degradation. These findings support previous recommendations for thermal management solutions in tracking systems to enhance reliability.

The performance ratio (PR) of the tracking system in July was 0.65, considering a bifaciality factor of 0.7. This value is below the typical range of 0.80–0.90 for open-field systems, mainly due to reduced irradiance, spectral diffusion, and elevated temperatures inside the greenhouse. Such results are in line with expectations for agrivoltaic environments using diffusive polyethylene covers. Literature also suggests that using spectral-selective or adaptive cover materials can improve both PV and crop performance by optimizing wavelength transmission.

Overall, these findings strengthen the understanding of agrivoltaic performance under greenhouse conditions, emphasizing that while tracking remains advantageous, its relative benefit is moderated by the optical and thermal properties of the greenhouse environment. The study demonstrates that greenhouse agrivoltaic systems are technically viable and energy-efficient, with measurable benefits in dual-use energy-agriculture applications.

However, across all sites, the combined results demonstrate that PV integration within greenhouse systems inevitably reduces light availability (typically by 25–40%), while its influence on thermal and humidity parameters remains limited when supported by automated climate management. In order to assess these effects under practical conditions, cultivation studies under practical conditions were performed in Israel, Greece, Italy, and Germany.

The results regarding yield formation and yield quality are evaluated hereinafter with respect to the individual experimental locations. In the case of Israel (Kfar Qara), cucumber plants were cultivated. A key finding was that shading by the PV tracking system did not significantly affect either fruit size or total yield during the growing season. However, a tendency towards a lower yield was observed in one instance. The additional application of atmospheric CO_2 had temporary effects on plant growth. CO_2-treated plants were taller than the non-treated plants and produced more leaves and flowers. Plants in the CO_2-enriched greenhouse slightly outperformed the PV-integrated greenhouses in Brix measurements, with the difference becoming significant at the final sampling, indicating a higher sugar content and thus an improvement in the quality of the cucumber fruits. However, yield was not increased.

In Greece (Volos), cucumber and lettuce were cultivated hydroponically. In two experiments with cucumbers, an increase in CO_2 concentrations of 70-100 ppm showed a non-significant trend toward a higher yield, which correlated with a generally higher photosynthetic rate. Shading by the PV tracking

Funded by the European Union

Funded by the European Union under Grant Agreement No 101096056. Views and opinions expressed are however those of the author(s) only and do not necessarily reflect those of the European Union or CINEA. Neither the European Union nor the granting authority can be held responsible for them.

system resulted in increased plant growth and a higher number of leaves. This plant response is typical of a mild light deficiency. By contrast, in the case of lettuce, fewer leaves were observed under PV tracking in one of the two varieties studied. No clear effects were found regarding water use efficiency. Shading resulted in lower yields in only one case for lettuce.

At the Italian test site FSC Circeo, the fresh yield of lettuce, zucchini, tomato, and eggplant was consistently lower beneath the photovoltaic system. Furthermore, shading had a positive effect on water consumption for lettuce, zucchini, and tomato, but not for eggplant.

At Watzkendorf (Germany), the northernmost location, the yields of tomatoes and cucumbers were approximately 10% less under the PV tracking system. Additional CO_2 was generated at that location using transfer mulch in both the control and the PV variant. Thus, it was impossible to determine whether the increased CO_2 concentration could at least partially compensate for the yield reduction at lower light intensities.

At the four locations mentioned, the experiments were conducted under practical conditions. From the south to the north, a clear trend was observed. While there were not any significant yield losses in the south (Israel and Greece), yields under the PV tracking systems were distinctly lower in Italy and northern Germany. Elevated atmospheric CO_2 concentration increased yields, if at all, only marginally, affecting vegetative plant growth and, in some cases, yield quality. Shading sometimes had rather a positive effect on water use efficiency.

The studies at Humboldt University Berlin (Germany) and BOKU (Austria) took advantage of their additional resources to study the effects of shading on produce quality and elevated atmospheric CO_2 concentrations as a compensation strategy to counter low light intensity, but did not primarily focus on yield maximisation under market conditions. The results obtained at the BOKU greenhouse are characterized by the low light intensities specific to the location, so that light intensity became limiting and the yield was generally highest in the control group. Therefore, CO_2 enrichment is the focus of the discussion for the BOKU experimental results. Two concepts were implemented: CO_2 enrichment using CO_2Bags and CO_2 produced by parallel mushroom cultivation. The use of CO_2Bags was only able to significantly increase the atmospheric CO_2 concentration in 4 out of 8 experiments. Nevertheless, predominantly higher yields were observed, either significantly or as a trend. It remains unclear whether these effects are actually due to CO_2 or to additional foliar fertilisation with ammonium, or both. With regard to quality, the observation made in Israel was confirmed, namely that an increased CO_2 concentration can potentially have a positive effect on carbohydrate content. Ultimately, however, not all quality reductions caused by insufficient light were compensated for.

At Humboldt University in Berlin, the effects of transfer mulch on CO_2 levels in Watzkendorf were investigated, among other things. Although CO_2 concentrations at Watzkendorf were only elevated during the night, their calculations showed that more CO_2 was released by transfer mulch than by the controlled release of technical CO_2. However, it was pointed out that CO_2 enrichment – regardless of the CO_2 source – can only be effective if the greenhouse is sealed, so that the CO_2 cannot escape into the surrounding

Funded by the European Union

Funded by the European Union under Grant Agreement No 101096056. Views and opinions expressed are however those of the author(s) only and do not necessarily reflect those of the European Union or CINEA. Neither the European Union nor the granting authority can be held responsible for them.

environment in larger quantities. Since many greenhouses regulate their temperature by exchanging air with the outside air, it follows that the supplementation of extra CO_2 is only feasible in a suitably closed greenhouse - and when the outside temperatures are low enough to keep the greenhouse closed. This is more likely to be the case in mid-latitudes during the winter months, when solar radiation is also relatively low. Nevertheless, based on the results of phytotron experiments in Berlin under controlled conditions, it should be emphasized that elevated atmospheric CO_2 concentrations are indeed capable of compensating for lower light intensities and increasing water use efficiency.

With regard to the experiments conducted under practical conditions, water use efficiency did not show a consistent pattern. On the one hand, increased atmospheric CO_2 concentrations did lead to improved water utilization, but on the other hand, there were also numerous examples where the water use efficiency of the control variant was the best. The yield component was decisive here: If yield formation was too severely impaired by shading, and consequently the assimilate distribution was shifted at the costs of the yield component, even an increased CO_2 concentration, which generally leads to a lower transpiration rate, could not sustainably and positively influence water use efficiency.

In summary, the results of the project suggest that PV tracking systems represent a positive, innovative development and can generate additional energy without significantly reducing yield. The further south the location, the less negative impact shading has on yield production. For a cost-benefit analysis, however, local conditions must be considered, and new developments, such as energy storage options, must be included in the calculations. A preliminary calculation for the northernmost location in Germany (Watzkendorf) suggests that the system may indeed operate profitably in future even in the mid-latitudes. Whether CO_2 enrichment is worthwhile is questionable for southern regions. However, where it is already used during the winter months and consequently the requirements for airtightness and greenhouse climate control are met, it is an adequate measure to further optimize yield. These findings collectively validate the technical feasibility of agrivoltaic greenhouse integration under diverse climatic conditions in Europe. They highlight the potential of adaptive PV technologies such as solar tracking and semi-transparent modules to enhance energy generation while maintaining suitable microclimates for horticultural production.

Funded by the European Union under Grant Agreement No 101096056. Views and opinions expressed are however those of the author(s) only and do not necessarily reflect those of the European Union or CINEA. Neither the European Union nor the granting authority can be held responsible for them.